Nonlinear Interaction of Piles-Soil-Raft during Consolidation

Rongchang Yang

A Thesis

in

The Department

of

Building, Civil & Environmental Engineering

Presented in Partial Fulfillment of the Requirements

for the Degree of Doctor of Philosophy at

Concordia University

Montreal, Quebec, Canada

March 2007

Your file Votre référence
ISBN: 978-0-494-30130-2
Our file Notre référence
ISBN: 978-0-494-30130-2

ABSTRACT

Nonlinear Interaction of Piles-Soil-Raft During Consolidation

Rongchang Yang, Ph.D. Candidate

Concordia University, 2007

In the literature the analysis of piles-soil-cap interaction received little attention from the geotechnical engineering community. This is mainly due to the complexity of the problem and the difficulties involved in experimental and analytical modelling. This thesis presents highly sophisticated analytical and numerical models to investigate the problem stated and incorporating the pore water pressure dissipation, which takes place during the consolidation process for the plane-strain, axi-symmetrical and three dimensional cases. Furthermore, the theories developed estimate the nonlinear load-settlement relationship of pile-soil-raft interactive foundation, the proportions of loads carried by the raft and piles, the increasing process of the ultimate bearing capacity of piles and the effective stress changes which take place in the soil mass.

Evaluation of piles–soil–caps interaction during pore water pressure dissipation and the consolidation process may positively impact on the foundation settlement and the load sharing mechanism. The interaction is a nonlinear operation which involves the piles in the group, soil surrounding the piles, piles' cap (raft), and excess pore-water pressure (EPWP) in the soil.

In the literature, due to the complexity of the problem stated, the role of the pore water pressure was ignored and accordingly, the raft will share the foundation load when the

piles reach the ultimate load. Under this condition, the sharing ratio of the soil-piles load does not change during consolidation and further overestimates the contribution of the raft to the total load.

This thesis presents a nonlinear method of analysis to evaluate the load sharing ratio during the consolidation process and accordingly as a result of the pore water pressure dissipation. The proposed analysis establishes the load-sharing ratio as a function of the load level and load location on the raft. The initial pore water pressure distribution after pile driving was also investigated. It was noted that the pore pressure generated during driving is not only due to cavity expansion but also due to an increase in mean total stress caused by the skin friction along the pile's shaft and on the pile tip. Furthermore, the pore pressure generated by the residual forces is relatively small and can be neglected. The analysis of strength-stress relationship shows that the excess pore pressure generated during pile driving increases almost linearly with depth, which confirms field measurements. Furthermore, fractures in soil during pile driving make the excess pore pressure fall to a stable level equivalent to the effective overburden pressure. This becomes a major factor, which should be considered in the estimation of the excess pore pressure generated within the pile group.

Analytical models are developed to simulate the cases of pore pressure dissipation for plan-strain, axi-symmetrical and rectangle-area problems with only horizontal permeating, and 3-D dissipation problem for uniform soil. Moreover, the numerical inversion of Laplace transform to find solution of pore-pressure dissipation in layered soil is presented. The changing process of the ultimate bearing capacity of pile foundations due to the interaction process is presented. The proposed theories are practical and easy

to use. Furthermore, charts for the consolidation level for a pile group and pile length are also given in this thesis.

The simplified and convenient interaction analysis methods established in this thesis were validated using the results obtained by a sophisticated numerical model. This method is capable to estimate the load-settlement curves of pile-soil-raft nonlinear interactions and accordingly, the variations of load sharing proportions.

Key words: piles–soil–raft interaction, pore-water pressure, initial distribution models, nonlinear analyses, consolidation process, numerical methods, effective stress analysis

To My Family:

My Wife Bing Xian Lin,

My Daughter Muen Yang,

And My Mother Fudi Yang

And

To The Soul of My Father

ACKNOWLEDGMENTS

I wish to express my sincere gratitude to Professor Adel M. Hanna, my supervisor, for his encouragement and his drive for excellence. He has provided valuable guidance which made this research work carried out. Without his continuously financial and academic support, it would not be possible to finish such a large project.

Special thanks are due to Mr. Hani Keria, Oscar A. Pekau, A. Bagchi, Ahmad Elhakeem and Ayadata T. of the Building, Civil and Environmental Engineering, Concordia University, for their interest, suggestion and advice for this research work.

Many thanks also to Mr. François Carrière and Sylvain Belanger, for their useful suggestion and consultation on the use of the computation software.

I can never thank enough my wife, Bing X. Lin, for bearing the tough student life with me, for her continuous encouragement and sacrifice, and for her endless love. I want to thank our daughter, Muen, who always has given me true love, happiness and strength throughout the course of my graduate studies; without their love I couldn't have done it.

Last but not least, I wish to express my sincere gratitude to my mother for her kindness, love, understanding and support during my life in Canada.

TABLE OF CONTENTS

LIST OF FIGURES

page

CHAPTER 1

CHAPTER 2

CHAPTER 3

CHAPTER 5

CHAPTER 6

CHAPTER 7

CHAPTER 8

LIST OF TABLES

LIST OF SYMBOLS

The following symbols are used in the thesis:

A= area of raft

A_f = Skempton pore-pressure coefficient A at failure

A_g= total section area of the pile group

A_p= the section area of pile

a = radius of pile

a_{av} = average coefficient of settlement of soil in area of load

ac = width of foundation column

B = width of foundation (or raft), = 2b

B_0= the distance between a edge pile and another edge pile that is opposite to center axle

b = half of foundation width;

side length of section of square pile

BEM = Boundary Element Method

C_c = compression index of soil

C_h, C_v = horizontal, vertical consolidation coefficients, respectively

C_p , C_c = coefficients of the ultimate resistance to the soil sliding around a pile

C_s = swelling index of soil

c = soil cohesion;

C_{v3} =3-D consolidation coefficient of soil

c_{mn} = parameter of m, n term of series

c_u = undrained shear strength of soil

D, D_f = depth of embedment form ground surface to foundation level

D_r = relative density

d = diameter of pile;

the depth of raft bottom

$d_{eq}=\sqrt{(4A_g/\pi)}=1.13\sqrt{A_g}$, equivalent diameter of the pile group

E = deformation modulus of soil

$E_{eq}=E_s+(E_p-E_s)(A_p/A_g)$, the equivalent modulus of of the pile group

E_p = elastic modulus of pile

E_s = deformation modulus of soil

$E_{s1\text{-}2}$ = compression modulus of soil between pressure 100~200KPa (1~2Kg/cm^2)

E_{sc} = drained deformation modulus of soil

E_u = undrained elastic (immediate) deformation modulus of soil

E_{ur} = unload-reload elastic modulus of soil

e = base of natural logarithms (=2.71828182845904523536028747135 27);

e_s = void ratio of soil

EPWP = Excess Pore Water Pressure

F_s = safety factors of subsoil

F_t = *total safety factor* of pile-and-soil system

F.E. = finite elements

FEM = Finite Elements Method

FLM = Finite Layer Method

$\{F_B\}$ = load of cap element

f_s = ultimate friction stress of pile (shape factors)

f_b = ultimate bearing capacity of pile base

G_b, G_l, G_{av} = Shear modulus of soil at pile base,

Gs = specific gravity of soil

GSDT = Generalized shear-displacement theory

H_c, H_q, H_γ = incremental bearing capacity coefficients effected by soil cohesion, depth of raft, and width of raft, respectively

h_k = thickness of the k-th layer of the layered soil;

$= \frac{k\pi}{R_z}$ for permeating bottom, or $= \frac{(1+2k)\pi}{2R_z}$ for impermeating bottom boundary

I_P, I_L = respectively, plastic index and liquid index of soil

i = imaginary number ($=\sqrt{-1}$)

i_k = hydraulic gradient of the k-th layer of soil

J

J_0, J_1, J_2 = Order 0, 1, 2 Bessel functions of the first kind (column), respectively

j_0, j_1 = Order 0, 1 Bessel functions of the second kind (sphere), respectively

K_h, K_v = hydraulic conductivity of the soil in horizontal, vertical directions, respectively

K_0 = rest earth pressure coefficient

K_{pr} = complex stiffness of piles and raft

K_r = stiffness of raft

K_p = stiffness of group piles

k_1 = the pile-head stiffness of a single pile

$[\mathbf{K_p}]$ = pile stiffness matrix

L, ℓ = length of pile

l = distance from 0 point to the point that initial excess pore pressure is zero

M = substitution used for integration

N = substitution used for integration

N_c, N_q, N_γ = ultimate bearing capacity coefficients of soil

n = number of piles;

numerical term of series

n_b = number of cap load elements

n_p = number of pile load elements.

OCR = overconsolidation ratio

P = resultant force acting on surface

P_0 = the design load

P_1 = the load carried by the raft corresponding to allowed settlement S_a

P_{su} = ultimate shaft resistance of all pile

P_t, P_b = forces of pile top and pile base, respectively

$P_u = U \Sigma f_{si} \Delta l_i + f_b A_b$, Ultimate bearing capacity of a single pile (UBCP)

$P_{ut} = P_u(t)$, UBCP at some time t after pile driving

P_{ui} = the initial UBCP estimated by dynamic penetration resistance (due to thixotropic residual strength) during pile driving

$P_{u0} = P_u(0)$, a theoretical static UBCP at the exact time that driving ends

p = perimeter of pile section

$p_o = \xi_s q_a - \gamma D$, additional pressure on the bottom of raft

p_r = pressure on the bottom of raft

p.w.p = pore water pressure

Q = total load of both upper structure and foundation

Q_r = total load beard by soil

Q_p = total load beard by piles

Q_u = total ultimate bearing load capacity of both piles and soil under raft

Q(z) = unit permeatability in soil at depth z

q = using-in-design pressure of soil under raft

$q_a = q_{ur}/F_s$, allow bearing capacity of soil

q_u = ultimate bearing capacity of soil

q_{ur} = Ultimate bearing capacity of soil under raft

Δq_u = increment of soil bearing capacity for piles' resisting to the soil sliding around piles

$\hat{q}_o$ = a variable after Laplace transform and finite Fourier series transform

R = the range radius of plastic field;

boundary range of excess pore pressure.

R_s = ratio of the settlement of pile group to that of single pile

R_x, R_y, R_z = boundary range of excess pore pressure, respectively in x, y, and z direction

r = radical or polar coordinate

r_0 = radius of pile shaft

r_b = radius of pile base

r_c = an equivalent radius calculated from the area of raft associated with each pile

S = piles' center space;

the settlement of foundation

S_A, S_B = settlement at point A, B in foundation

S_a = allowed settlement

S_b =settlement of the soil at pile base

ΔS_{SL} = compressive displacement of the soil between the top and the base of pile

ΔS_{PE} =elastic deformation of the pile body

{S} = the displacement of the soil under raft and around piles

$\{S_B\}$ = the settlement and load of cap element

$\{S_p\}$ = the displacement of piles

SAM = Simplified analytical methods

SDT = Shear-displacement theory

{ΔS} = displacement difference between calculating point and cap bottom, i.e. pile head

s = piles' center space

δ =deformation of pile-end punching into soil at the pile base

$[\delta_s]$, δ_{sij} = the soil flexibility matrix, and its coefficients

T = $C_h t/R_x^2$, or $C_h t/R^2$,

time factor of excess pore water pressure dissipation or consolidation of soil

t = time length from the date of driven pile to considering date

U = consolidation degree of soil;

perimeter/circumference of pile

UBC=Ultimate Bearing Capacity

UBCP= Ultimate Bearing Capacity of Pile

UBCS= Ultimate Bearing Capacity of Soil

u = pore pressure in soil

u_0 = initial pore pressure in soil

u_{00}, u_{0b}, u_{0m} = initial excess pore pressure at z = 0, b_z, and l_z, respectively

Δu_m = maximum excess pore pressure

w (%) = moisture content of soil

x, y = coordinates of x, y axle

z = soil depth from surface, coordinates of z axle

Δ = increment

$\Phi = \sigma_z+\sigma_r+\sigma_\theta$, total sum of stresses σ_z, σ_r, σ_θ

Γ_{11}, Γ_{12}, Γ_{21}, Γ_{22} = four elements of metrix [Γ]

[Λ] = metrix [Λ]

Π = multiplication sign for all the numbers in a range expressed by subscript multiply with one another.

Θ =

Σ = summation sign to add all the numbers in a range expressed by subscript.

$\because$ = cause, due to

$\therefore$ = hence, or therefore

α = failure angle between failure plan and horizontal surface

α_b = the ratios of pile-base load to pile–head load

α_{bu} = the ratios of pile-base load to pile–head load near to plastic or ultimate state

$\alpha_f = 0.707(3A_f\text{-}1)$ = Henkel's pore-pressure coefficient at failure

α_m = numerical values which makes order 0 Bessel functions of the first kind $J_0(\alpha_m) = 0$ (positive zeroes)

α_{rp} = interactive factor of pile to raft

β = another Henkel's pore-pressure coefficient at failure

$\chi = \Delta\sigma_h'/\Delta u \approx 0.5+\mu$

δ = deformation of pile-end punching into soil at the pile base;

$[\delta^{SS}]_{nb\times np}$, $[\delta^{SP}]_{nb\times np}$, $[\delta^{PS}]_{np\times nb}$ and $[\delta^{PP}]_{np\times np}$ = respectively interactive flexible coefficient matrixs of soil—soil, soil—pile, pile—soil as well pile—pile element points

ε_z, ε_r, ε_θ = strains in vertical (z), radial (r), and angle (θ) directions

ϕ = initial friction angle of soil

γ = soil unit weight;

shear strain

γ_0 = average effective unit weight of soil above the bottom of foundation

γ_B = effective unit weight of soil under the bottom of foundation

γ_f = unit weight of foundation

$\eta = r_b/r_o$, ratio of underream for underreamed piles

η_g = pile-group efficiency coefficient

$\eta_r = 1+\Delta q_{ur}/q_{ur}$ increment factor caused by pile's resisting action on soil moving laterally

$l=\ell$ = length of pile

φ = initial friction angle of soil

$\lambda = E_p/ G_l$, pile-soil stiffness ratio

$\lambda = Qs/Q \approx \xi_s q_a A/Q = \xi_s \psi$, the proportion of load carried by the raft

μ, ν, ν_s = Poisson's Ratio of soil

$\mu\, l = (l/r_o)\sqrt{(2/\zeta\lambda)}$, measure of pile compressibility

π= pi (= 3.14159265359)

θ = angle coordinate

$\rho = G_{av}/G_l$, variation of soil modulus with depth;

$= \sqrt{r^2 + (z-D)^2}$, distance between calculated point and pile tip, polar coordinate;

$= r/r_0$.

σ = normal stress

σ_x, σ_y, σ_z = stresses in x, y, and z (vertical) directions, respectively

σ_z, σ_r, σ_θ = stresses in vertical (z), radial (r), and angle (θ) directions, respectively

$\sigma(z) = \sigma_r(z) + \sigma_p(z)$, vertical additional stresses at depth z

$\sigma_r(z)$ = additional stress caused by raft additional pressure p_o,

$\sigma_p(z)$ ------additional stress caused by all pile load Q_p

σ'_{vo} = initial vertical effective stress in soil

τ = shear stress

τ_e = shear stress at limit elastic shear strain of soil around pile.

τ_f = shear strength of soil, ultimate unit frictional resistance of pile shaft.

τ_{rz} = shear stress in r = C (a constant) or z = C plan

ω = range radian of each pile around the center of circle raft

$\xi = G_l/G_b$ =ratio of shear modulus of soil at end-bearing for end-bearing piles

$\xi_s = q/q_a = qF_s/q_{ur}$, *Utilization ratio* of soil bearing capacity

ξ_p = raft-effect factor

$\psi = q_aA/Q = q_uA/(F_sQ)$, *Satisfaction degree* of natural soil bearing capacity

$\psi_1(x)=u(x,0)$, $\psi_2(x)=u(x, y,0)$, $\psi_3(x)=u(x, y, z,0)$, initial distribution of pore pressure

$\zeta = \ln(r_m/r_o) = \ln\{\langle 0.25+\xi[2.5\rho(1-\upsilon_s)-0.25]\rangle 1/r_o\}$, measure of influence radius of pile

ζ = complex parameter in the procedure of Laplace transform and finite Fourier series transform

∂ = partial derivative

$\int$ = integral

∞ = infinite value

$\hat{F} = \tilde{\bar{F}} = \square\ (F) = \square\ [\square\ (F)] = \square\ [\square\ (F)]$ = the compositive transform by Laplace transform $\square$ ( ) and finite Fourier series transform $\square$ ( )

$\bar{F} = \square$ (F) = finite Fourier series transform

$\tilde{F} = \square$ (F) = Laplace transform

sh( ), ch( ) = hyperbolic sine and cosine function, respectively

$[A]_k$, $[B]_k$, $[\Gamma]$, $[\Lambda]$ = matrix

CHAPTER 1

INTRODUCTION

1.1 Preface

Building design has two main components: (1) the design of the superstructure and (2) the design of foundations. The superstructure is assumed to produce predetermined column and wall loads that the foundations are required to carry. The applied loads cause foundation settlements; the non-uniform settlements of the foundation's elements cause secondary internal forces in the structure's components, due to the inevitable interaction between the structure and the foundation. Secondary settlements may also occur due to the interaction between the foundation, its various elements and the surrounding soils.

One of the outstanding unsolved problems is the non-linear interaction among the piles, the soil and the cap (piles-soil-cap). This can be achieved only if the load-deformation characteristics of beams, columns, walls and the surrounding soil during the loading process are known. However, this mechanism is a very complex one and, in practice, engineers have developed simplified theories and empirical formulae, which tend to be over-conservative. The secondary internal forces experiences by the structure's components, caused by non-uniform displacement of the foundation, can lead to their failure. In order to avoid such situations, designers have empirically increased the thickness of the foundation's raft and increased the stiffness of the subsoil system (pile-soil) by increasing the number and length of piles, which produce over-conservative designs.

Engineers often assume that the differential settlement between foundation's elements is relatively small, the foundation is rigid, and the secondary internal forces in components of the upper structure are accordingly quite small and that they can be dealt with using an adequate factor of safety.

Piles embedded in soil provide reinforcement to the soil, increase its load-bearing capacity and modify its deformation behavior, similar to the reinforcement of concrete. Piles are also one of the oldest traditional foundation forms used to overcome the difficulties of building on soft soils and they have been widely used and various types have been developed for use in building and civil engineering projects.

The understanding of the interaction between the pile foundation and the surrounding soil has recently been greatly advanced. Under permitting ground conditions, load sharing effects of the interaction of piles–soil–cap can be applied to improve the economy of design. The increasing demand of reliable prediction of a pile design's behavior has stimulated more sophisticated research into the piles-soil-cap interaction, which is the subject of this research study.

While a sufficiently accurate analysis of the effects of reinforcement can be obtained in concrete, the extended-continuum nature of the embedded piles in soil makes the analysis of the reinforcement effect much more difficult. This can be explained by the fact that the behaviors of piles, soil and cap are non-linear interactions, which include soil nonlinear stress-strain characterization, pile shaft, base ultimate strength theories and pile-soil

interaction theory. This is difficult at best, as soil is a compounded geological body that is not uniformly distributed and is not ideally elastic-plastic on a stress-strain relationship except for dilatation/shrink behavior, which is associated with a pore water pressure increase caused by shearing. Furthermore, the components of the piles, cap and soil (including pore-water pressure) involved in the mechanism can influence each other, such as:

(1) Weakening the friction of the upper part of the pile's shaft, due to the displacement difference of the pile-soil caused by the cap (a direct effect of the cap's load on both the soil under the cap and around the piles).

(2) Enhancing the pile's shaft friction strength and the bearing capacity of the pile base, due to an increase in effective normal stress caused by the load applied on the soil both under the cap and around the piles.

(3) Increasing action on the soil capacity due to the resistance of the piles to the soil sliding around the pile.

Additionally, the pore-water pressure development in the soil, due to pile driving and pile interaction, and its dissipation with time is regarded as a complex mechanism besides the fact that geotechnical parameters and in-situ stress state may change due to pile installation and continue to change afterward with time.

1.2 Research Objectives

This thesis will review pertinent literature on the subject matter, develop a model for piles-soil-cap interaction and develop the mathematical formulations to simulate the interaction's complex mechanism.

In order to achieve the above mentioned objectives, the following steps will be followed:

1- To conduct and report a literature review related to the subject of the thesis;
2- To develop a mathematical model to simulate the initial pore-water pressure developed in the surrounding soil mass during the driving of piles and its dissipation with time;
3- To derive the analytical or numerical model to predict the excess pore-water pressure dissipation with time in uniform and layered soils;
4- To develop numerical models to analyze the piles–soil–cap non-linear interaction before, during driving and over a period of time;
5- To validate the results using the existing available results in the literature;
6- To propose a simple and practical method that predicts the influence of excess pore-water pressure dissipation on the behavior of piles-soil-cap interactions.

1.3 Scope (Organization) of the thesis

This thesis is composed of the following chapters:

Chapter 1 gives an introduction of importance of considering pile-soil-cap interaction in design; background of the interaction, and the objective of this thesis.

Chapter 2 reviews the previous literature on reported tests and observations of pile group and piled foundations, the methods of simplified, approximate computer-based and more rigorous numerical analyses, and effects of EPWP (excess pore-water pressure) in the interaction.

Chapter 3 sets up a numerical model for analyzing pile-soil-raft system in a Hybrid method combining the finite layer method with the generalized shear-displacement theory without consolidation factor, runs tests for validation, analyzes some cases and presents general conclusions.

Chapter 4 presents the investigation of the excess pore pressure caused during driving single pile and afterward with a theoretical calculation method based on existing observations and experience, and gives methods for estimating the initial pore pressure distribution due to driving group piles and case analysis.

Chapter 5 presents analytical solutions of pore-water pressure dissipation for plane-strain, axi-symmetrical and rectangle-area problems with only horizontal permeating, and 3-D dissipation problem for uniform soil, establishes numerical Laplace-Fourier integral transform and its inversion method calculating pore-water pressure dissipation for layered soil.

Chapter 6 investigates the changes in the effective stresses in the soil around the pile due to pore pressure dissipation and the interaction, and presents the formulations for estimating the ultimate bearing capacity of piles (UBCP) in the system.

Chapter 7 presents the theory for predicting settlement of the system; which is divided into four parts: two immediate settlements from raft-bottom pressure and from pile-top load and two consolidation settlements caused by remnant EPWP of driving and by raft-bottom pressure.

Chapter 8 presents the analyses of two case histories: one is to estimate the increment of the UBC of a single pile due to the dissipation of EPWP from pile driving, another is to analyze the changes of the loads shared by piles and raft and further the settlement in the

pile-soil-raft interaction, presenting comparative analyses of the results produced by different methods with or without EPWP effects, due to the driving and raft-bottom pressure. In this analysis, the methods developed in Chapter 6 and 7 are used, and accordingly important conclusions are drawn.

Chapter 9 presents the contributions and conclusions on pile-soil-cap interaction drawn from this study and recommendations for future research.

CHAPTER 2

LITERATURE REVIEW

2.1 Model Tests and Empirical

The first to discuss pile group interaction is on group efficiency and group settlement action before 1950'. It has been recognized that for some time that the ultimate load borne by a group is not simply that of a single pile multiplied by the number of piles in the group (Sooysmith, 1896). Press (1933) test on piles in pairs in sand, and Swiger (1941) a row of three piles, also in sand. Masters (1943) gave the results of full-scale loading test on a few groups in clay. According to Bolin (1941), Feld (1943), Seiler & Keeney (1944), Converse-Labarre formula gives the efficiency of a pile group from the spacing and layout, based on the idea that adjacent piles interfere to an extent which is dependent on their spacing. Skempton (1952, 1953) discussed the settlement ratio of pile groups in sand, taking a series of examples from practice for which data were available.

Since 1957 activity in pile group studies has increased considerably. Zeevaert (1957) presented a study on compensated friction-pile foundations. Model tests have been carried out to determine group efficiency factors in homogeneous sand (Whitaker 1957; Fleming 1958; Kezdi 1960). Furthermore, both Whitaker (1960) and Saffery and Tate (1961) investigated the case of pile-group-cap foundation. Sowers et al. (1961) and Hanna (1963) studied the case of free-standing pile groups in clays. A summary of some of these tests was presented by de Mello (1969), and the load distribution on piles in a

group was given by Whitaker (1970). More reports on settlement-reducing piled foundations appeared at the end of the 1980s. Afterward, some field measured and experimental data were reported (Lin et al, 1989; Tong et al, 1989; Nan, 1991; and Sommer, 1993).

2.1.1 Model Tests

Whitaker (1957) reported that the capacity of a pile group in clay is always less than the product of the total individual piles capacity, whereas that of sand was usually more. He also indicated the existence of two types of failure: (1) the failure of individual piles within the pile group and (2) the block failure of the pile group. For a given length and a given number of piles in a group, there was a critical value of spacing at which the failure mechanism changed from block failure to individual pile failure. For spacing near to the critical value, failure was in the form of vertical slip planes around the perimeter of the block; For wider spacing, the piles individually penetrated the soil.

Fleming (1958) examined the case of square pile groups in dry sand. His findings confirmed the general trends of the small-scale field tests reported by Kezdi (1957). That is, the types and characters of soil and pile spacing control the group's efficiency. For a foundation of a given size, increasing the number of the piles does not increase the total ultimate capacity of the group when piles are spaced below the critical value.

Hanna (1963) conducted model tests on pile groups which confirmed Whitaker's findings (1957). Furthermore, he indicated that the settlement of a group of piles can be much

greater than the settlement of an individual pile, which is caused by the pile-pile interaction, and accordingly, larger factor of safety for the design of a single pile is required in order to control group settlement.

Cooke et al (1979) presented a series of field tests performed on instrumented rows of two and three tubular steel piles installed at close spacing in London Clay. However, this investigation failed to assign in the nonlinear state near to the ultimate load. The comparison results show that the calculated value of the interaction using the elastic theory is relatively higher than the measured values.

Liu et al (1994) reported that the behaviors of shaft resistance, base resistance and soil reaction beneath the cap of pile groups vary with pile spacing, arrangement and the ratio of pile length over cap breadth. Test results indicated that the cap-pile-soil interaction lead to a reduction in the shaft resistance and an increase in base resistance. Furthermore, the soil reaction beneath the cap increased with both increasing pile spacing and load. Under working load (less than half of the pile's ultimate bearing capacity), the efficiency of the pile group in soft soil usually reaches an approximate value close to or greater than 1. The low-set cap effect reduces the upper pile's shaft resistance, increases the base resistance. And its load-settlement curve shows a gradual drop rather than the steep drop seen in the curve of high-rise caps.

Horikoshi & Randolph (1996) performed centrifuge tests of model piled raft foundations in order to examine the role of a small centered pile group in reducing the settlement of

the raft. The results showed that a small low-set cap increased the total bearing capacity significantly due to the load transfer to the soil through the cap. These results differ from those of the elastic numerical analysis conducted by Butterfield & Banerjee (1971a).

2.1.2 Field Measured Data and Case Histories

Zeevaert (1957) described the design and performance of a compensated friction pile foundation that reduced the settlement of buildings on the highly compressible volcanic clay in Mexico City. The settlement observations and subsoil investigation revealed that the settlement was much smaller as compared to the estimated settlement for the same foundation without piles. A great economy was achieved because the friction piles carried only a fraction of the building's total load. Moreover, since the piles were designed without support from deep strata, the undesirable feature of sidewalks settling away from buildings, caused by the well known ground surface subsidence of Mexico City, was eliminated.

Lin Bai et al. (1989) reported their experience with piled foundation in Shanghai and Wenzhou, China. Through observations of the coordinated deformation between piles and soil beneath the cap, they suggested that the dualistic simultaneous equations are suitable for solving the settlement for sparse piled foundation.

Tong et al. (1989) presented the following results based on their observations:

1) Up to 70% of the load is transferred from the top of a pile in a group to its base. This is about twice the value that can be transferred to an isolated pile. In the case of half

the ultimate pile bearing capacity, the shaft friction developed in the pile group is only 45-60% of that of an isolated pile.

2) Even in a conventionally designed piled raft, about 88% of the building load is supported by the piles, and the remaining (about 12%) by the soil beneath the cap.
3) The contribution of the reaction pressure at the bottom of the cap is of a saddle shape, that is, it is larger near the corners and edges and smaller near the inside of the cap. Similarly, the largest observed loads of the top, shaft and base of the piles occur on the corner piles, the second on the side piles, and the smallest on the inner piles.
4) In the case that a building's total load (minus the buoyant force of water on the foundation) does not exceed the ultimate bearing capacity of the pile group, the settlement of the short-pile foundation is mainly caused by the compression deformation of soil under the pile base, and the effect of the punch deformation of the piles of low-set cap is quite smaller.

Nan (1991) reported the case of a seven-story building supported by a sparse piled raft. When the spacing between piles was 7 to 8 times the pile's diameter, it was found that piles shared 47% of the total load at 70 to 90 % of the ultimate load and that the raft shared 53% of the total load. The foundation settlement was 6 to 10mm at the time of construction completion and 12mm after two years.

Sommer (1993) reported the case of the 256 m high *Messe-Turm*, Europe's tallest high-rise building, which rests on a piled raft foundation on Frankfurt clay. He describes both the "locked stresses" after the excavation and the negative skin friction due to the

compression of the raft subgrade by the "wet-load" of the concrete. He also indicates that piles shared 61 to 75 % of the total load when near the ultimate load of the piles, while the designer indicated that the piles would share 33% and that the raft would share 67% of the total load. The percentage of the load actually carried by the piles is twice that of the design value used or the working load of the piles, which is half of the ultimate bearing capacity (UBC) of the pile group.

2.2 Simplified Design and Analysis Methods

With the exception of Zeevaert's design and study of compensated frictional pile foundations (1957), many engineering practices emerged after the 1980s for spare pile foundations, settlement-reducing piled foundations, and foundations designed according to the concept of piles-soil-raft interaction. In other words, analysis methods for the piles–soil–cap interaction appeared afterward. Randolph (1983, 1994) developed very convenient approximate equations to determine the stiffness of a piled-raft system and the load-sharing between the piles and the raft. Poulos (1991, 1994) developed the strip-on-springs and the plate-on-springs approaches. Zai (1992) presented a simple formula which verifies the stability and settlement of piles-soil systems. Burland (1995) developed a useful simplified design process, in which the piles act as settlement reducers and develop their full geotechnical capacity at the design load. Yang and Zai (1995, 1996) presented formula that estimate the increments of the soil's ultimate bearing capacity under sparse pile foundation for the resistance of piles to soil sliding around them.

Randolph (1983, 1994) developed approximate equations to estimate the stiffness of a piled-raft system and the load-sharing between the piles and the raft. The equation for the overall stiffness of the piles and the raft, K_{pr}, is:

$$K_{pr} = \frac{K_p + (1 - 2\alpha_{rp})K_r}{1 - \alpha_{rp}^2 (K_r / K_p)} \qquad (2\text{-}1)$$

The equation to determine the load proportion carried by the raft is:

$$\lambda = \frac{Q_r}{Q_r + Q_p} = \frac{(1 - \alpha_{rp})K_r}{K_p + (1 - 2\alpha_{rp})K_r} \qquad (2\text{-}2)$$

where:

K_r = stiffness of raft

K_p = stiffness of group piles

α_{rp} = interaction factor of piles to raft.

The raft stiffness K_r can be estimated via elastic theory, such as, for example, the solutions of Fraser and Wardle (1976) and Mayne and Poulos (1999). The pile group stiffness K_p can also be estimated using elastic theory, such as those described by Poulos and Davis (1980), Fleming et al (1992) and Poulos (1989).

$$K_r \approx 2.25 G_s B/(1 - \nu_s) \qquad \text{(from Poulos \& Davis 1974)} \qquad (2\text{-}3)$$

$$K_p \approx k_1 \cdot n^{1-e}; \qquad \text{(Fleming et al 1992)} \qquad (2\text{-}4)$$

where, k_1 is the pile-head stiffness of a single pile; n is the total number of piles; the exponent e lies between 0.4 and 0.6 for most pile groups, determined by the given charts on page 193 of Fleming et al (1992).

The pile-raft interaction factor α_{rp} can be estimated as follows:

$$\alpha_{rp} \approx 1 - \frac{\ln(r_c / r_o)}{\varsigma} \qquad (2\text{-}5)$$

Where r_c is an equivalent radius, calculated from the raft area associated with each pile. Clancy & Randolph (1996) performed a more rigorous analysis on the subject matter and reported that as the group size increases, the value of α_{rp} tends toward a constant value of about 0.8, i.e.:

$$K_{pr} = \frac{1 - 0.6(K_r / K_p)}{1 - 0.64(K_r / K_p)} K_p \qquad (2\text{-}6)$$

$$\lambda = Q_r/Q = \frac{P_r}{P_r + P_p} = \frac{0.2}{1 - 0.8(K_r / K_p)} \frac{K_r}{K_p} \qquad (2\text{-}7)$$

It should be noticed herein that the above formulae produce reasonable results only in the elastic state of the pile-soil system whereas they produce an overestimate for a system in the elastic-plastic state because of the pile-soil nonlinear relationship.

For the case where piles are designed to act as settlement reducers and allowed to develop their full geotechnical capacity at the design load, Burland (1995) developed the following simplified design procedure for pile-raft systems:

1) Estimate the total long-term load-settlement relationship for the raft without piles (see Fig. 2-1). The design load P_o gives a total settlement S_o.
2) Assume an acceptable settlement S_a, which should include a margin of safety.
3) P_1 is the load carried by the raft corresponding to S_a.

4) The excess load $Po–P_1$ is assumed to be carried by the settlement-reducing piles. The shaft resistance of these piles will be fully mobilized and therefore no factor of safety is applied. However, Burland suggests that a mobilization factor of about 0.9 should be applied for a "conservative best estimate" of ultimate shaft resistance, P_{su}.

On this basis, the number of piles required can be estimated as follows:

$$n = (P_o–P_1)/(0.9P_{su}) \qquad (2\text{-}8)$$

Furthermore, if the piles are located below columns that carry a load in excess of the group capacity, P_{su}, the piled raft may be analyzed as a raft with reduced column loads. The column's reduced load Q_r is calculated as:

$$Q_r=Q-0.9P_{su} \qquad (2\text{-}9)$$

Where, Q = total column load.

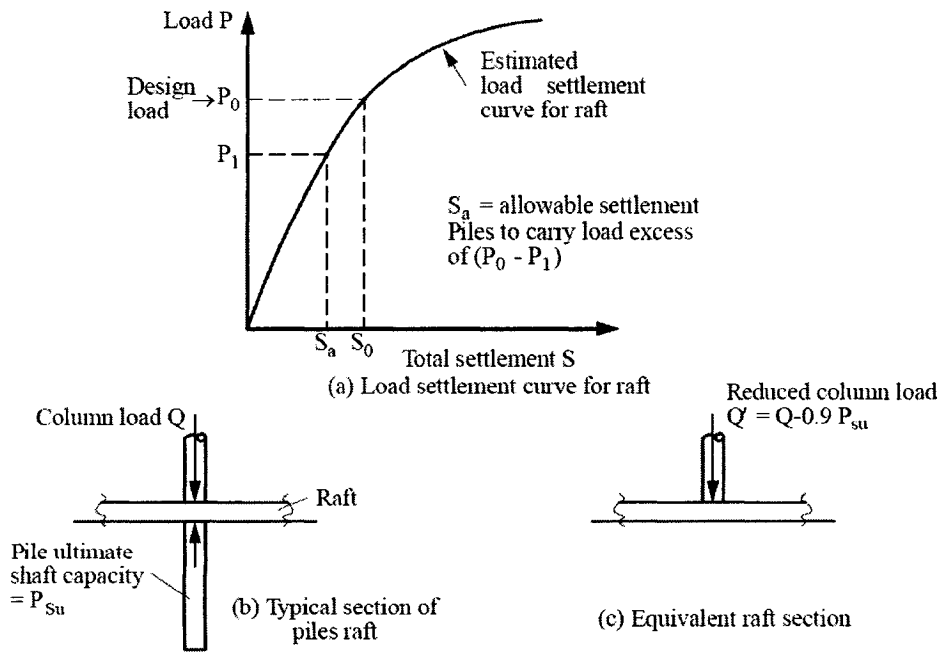

Fig. 2-1 Burland's Simplified Design Approach (Burland 1995)

It should be noted that the above method neglects many other factors, such as the additional settlement caused by the pile load, similar to the method suggested by Zai (1992), for the case where the center spacing between piles is quite large, S> 8d. Moreover, Burland's method does not consider the change of the bearing capacity of both soil and piles due to the changing pore pressure in the soil

Zai (1992) presented a simple formula to check the stability of the piles-soil system. The said formula was modified by Zai & Yang (1994), as follows:

$$F_t=\frac{Q_u}{Q}=\frac{\eta_r q_u A+\eta_g n P_u}{Q}=1.111+(\eta_r F_s-1.111\xi_s)\psi \qquad (2\text{-}10)$$

Where,

F_t = safety factor of the piles-soil system;

Q = total load of both upper structure and foundation;

Q_u = total ultimate bearing load capacity of both piles and soil under raft;

η_r = increment factor for soil capacity for the lateral movement of pile.

$\eta_r=1+\Delta q_{ur}/q_{ur}=1.1\sim1.3$ (Yang 1995);

η_g is the group coefficient (for piles' with a center spacing, S> 6d (d=pile's diameter) or in the case of a pile load P equal or close to P_u, $\eta_g \approx 1.$;

n_p is number of piles in the group;

P_u is the capacity of a single pile;

$\xi_s=q/q_a=qF_s/q_{ur}$, is a ratio of soil bearing capacity;

q uses the in-design pressure of soil under raft;

$q_a = q_{ur}/F_s$ (F_s is soil factor of safety), is the allowed bearing capacity of soil;

q_{ur} is ultimate bearing capacity of soil under raft;

F_s is the safety factor of a soil's bearing capacity for swallow foundation;

$\psi = q_aA/Q = q_{ur}A/(F_sQ)$ represents satisfaction degree of the soil bearing capacity;

$q \leq q_a$;

A is area of raft.

The formula (2.2-10) is actually simplified to the following form:

$$F_t = \eta_g/\xi_p + (\eta_r F_s - \xi_s \eta_g/\xi_p)\psi \qquad (2\text{-}11)$$

where, ξ_p is the factor that accounts for the effect of the cap on the capacity of the group.

From Equation (2-11), setting ξ_p=0.9 (recommended by Zai 1992 and Burland 1995) and η_g=1.0 yields the relationship between F_t and ξ_s as well as ψ, e.g., (2-10) as shown in Table 2.1.

It can be noted from Table 2.1 that when $\eta_r F_s = 2.5$, the satisfaction degree of soil bearing load $\psi = q_aA/Q > 0.5$ and the utilization ratio of soil bearing capacity $\xi_s = q/q_a < 0.6$. The total safety factor of a pile-soil system can be satisfied if $F_t > 2$. When $\eta_r F_s$ increases, the satisfaction degree of soil bearing load will decrease and the utilization ratio of soil bearing capacity will increase.

The *s*atisfaction degree of soil bearing capacity, ψ, can be determined at the design stage. By selecting the utilization ratio of soil bearing capacity ξ_s from Table 2.1, the sharing ratio of soil-bearing loads (the proportion of load carried by the raft), λ can be calculated as follows:

$$\lambda = \xi_s \psi \qquad (2\text{-}12)$$

The number of piles can be then determined using the following equation:

$$n_p = (1 - \xi_s \psi) \frac{Q}{\xi_p P_u} \qquad (2\text{-}13)$$

Knowing λ and n_p, the settlement of the entire piles-soil system can be checked for the following cases:

(1) When the piles' center spacing S> 8d, the compression of the soil between the pile top and the pile base ΔS_{SL} is >95% of the total settlement of foundation (Zai 1992), therefore, the effect of piles can be neglected. The settlement is then calculated assuming the pressure on the bottom of the raft $p_o = \xi_s q_a - \gamma D$ to be p_r and using elastic theory formula or the method proposed by Das (1999).

(2) For a general case, the individual settlements caused by the raft pressure p_o and by the piles' load can be calculated using the following:

$$Q_p = \xi_p n P_u = (1 - \xi_s \psi)\, Q = \xi_p n\, (U \Sigma f_{si} \Delta l_i + f_b A_b) \qquad (2\text{-}14)$$

Table 2-1 Safety factor of pile-soil system

F_t value when $\eta_r F_s$=2.5 (from Zai, 1992)

ξ_s \ ψ	0.1	0.2	0.3	0.4	0.5	0.6	0.7	0.8	0.9	1
0.1	1.35	1.59	1.83	2.07	2.31	2.54	2.78	3.02	3.26	3.50
0.2	1.34	1.57	1.79	2.02	2.25	2.48	2.71	2.93	3.16	3.39
0.3	1.33	1.54	1.76	1.98	2.19	2.41	2.63	2.84	3.06	3.28
0.4	1.32	1.52	1.73	1.93	2.14	2.34	2.55	2.76	2.96	3.17
0.5	1.31	1.50	1.69	1.89	2.08	2.28	2.47	2.67	2.86	3.06
0.6	1.29	1.48	1.66	1.84	2.03	2.21	2.39	2.58	2.76	2.94
0.7	1.28	1.46	1.63	1.80	1.97	2.14	2.32	2.49	2.66	2.83
0.8	1.27	1.43	1.59	1.76	1.92	2.08	2.24	2.40	2.56	2.72
0.9	1.26	1.41	1.56	1.71	1.86	2.01	2.16	2.31	2.46	2.61
1	1.25	1.39	1.53	1.67	1.81	1.94	2.08	2.22	2.36	2.50

F_t value when $\eta_r F_s$=3.0 (by equation 2-22)

ξ_s \ ψ	0.1	0.2	0.3	0.4	0.5	0.6	0.7	0.8	0.9	1
0.1	1.40	1.69	1.98	2.27	2.56	2.84	3.13	3.42	3.71	4.00
0.2	1.39	1.67	1.94	2.22	2.50	2.78	3.06	3.33	3.61	3.89
0.3	1.38	1.64	1.91	2.18	2.44	2.71	2.98	3.24	3.51	3.78
0.4	1.37	1.62	1.88	2.13	2.39	2.64	2.90	3.16	3.41	3.67
0.5	1.36	1.60	1.84	2.09	2.33	2.58	2.82	3.07	3.31	3.56
0.6	1.34	1.58	1.81	2.04	2.28	2.51	2.74	2.98	3.21	3.44
0.7	1.33	1.56	1.78	2.00	2.22	2.44	2.67	2.89	3.11	3.33
0.8	1.32	1.53	1.74	1.96	2.17	2.38	2.59	2.80	3.01	3.22
0.9	1.31	1.51	1.71	1.91	2.11	2.31	2.51	2.71	2.91	3.11
1	1.30	1.49	1.68	1.87	2.06	2.24	2.43	2.62	2.81	3.00

F_t value when $\eta_r F_s$=3.5 (by equation 2-22)

ξ_s \ ψ	0.1	0.2	0.3	0.4	0.5	0.6	0.7	0.8	0.9	1
0.1	1.45	1.79	2.13	2.47	2.81	3.14	3.48	3.82	4.16	4.50
0.2	1.44	1.77	2.09	2.42	2.75	3.08	3.41	3.73	4.06	4.39
0.3	1.43	1.74	2.06	2.38	2.69	3.01	3.33	3.64	3.96	4.28
0.4	1.42	1.72	2.03	2.33	2.64	2.94	3.25	3.56	3.86	4.17
0.5	1.41	1.70	1.99	2.29	2.58	2.88	3.17	3.47	3.76	4.06
0.6	1.39	1.68	1.96	2.24	2.53	2.81	3.09	3.38	3.66	3.94
0.7	1.38	1.66	1.93	2.20	2.47	2.74	3.02	3.29	3.56	3.83
0.8	1.37	1.63	1.89	2.16	2.42	2.68	2.94	3.20	3.46	3.72
0.9	1.36	1.61	1.86	2.11	2.36	2.61	2.86	3.11	3.36	3.61
1	1.35	1.59	1.83	2.07	2.31	2.54	2.78	3.02	3.26	3.50

In order to obtain the total settlements, one must sum the individual settlements calculated with the above equation. Otherwise, the additional vertical stresses $\sigma(z)$ can be calculated at different depths under a given point on raft, as

$$\sigma(z) = \sigma_r(z) + \sigma_p(z) \qquad (2\text{-}15)$$

Where,

$\sigma_r(z)$ is the additional stress caused by p_o, and

$\sigma_p(z)$ is the additional stress caused by Q_p, which can be determined according to Geddes (1966).

One should then add up the settlements of the stratified layers, based on one-dimensional consolidation settlement equation (Das 1999)

The total safety factor method based on equation (2-11) considers many factors, including the increment factor of soil bearing capacity caused by a pile's resisting action on laterally moving soil, which can be determined by equations (2-17) or (2-24), and also including the decreasing effect factor of a cap on the pile's ultimate bearing capacity, to be defined in Chapter 3 as per equations (3-21) to (3-23).

An increment of soil ultimate bearing capacity for shaft resistance, Δq_u, can be determined (Yang & Zai 1995, 1996) as follows:

$$\Delta q_u = (H_q \cdot \gamma_o D + H_\gamma \cdot \gamma_B B/2 + H_c \cdot c)d/S \qquad (2\text{-}17)$$

where,

d = diameter of circle pile-group or the width of a square group;

S = space between piles' centers;

B = width of strip foundation (or raft);

H_q, $H\gamma$, and H_c are determined by the following formulae:

$$\left.\begin{aligned} H_q &= C_p K_o T(\xi^2 - \eta^2)/\sin^2\alpha \\ H\gamma &= 2/3 \cdot C_p K_o T(\xi^3 - \eta^3)/\sin^3\alpha \\ H_c &= C_c\, T(\xi^2 - \eta^2)/\sin^2\alpha \end{aligned}\right\} \qquad (2\text{-}18)$$

and

$$\left.\begin{aligned} \xi &= \cos\varepsilon \cdot e^{(\alpha-\varepsilon)tg\varphi} \\ \eta &= (1-R_b)\cos\alpha, \qquad R_b = B_o/B \\ K_o &\approx 1-\sin\varphi \\ T &= 1/(1+K_a/tg^2\alpha), \qquad K_a = tg^2(45°-\varphi/2) \\ \alpha &= (\pi/4 - \varphi/2)(1+m_s),\ m_s \approx 0.5 \end{aligned}\right\} \qquad (2\text{-}19)$$

B_0 is the distance between two edge piles, or two times the distance between an edge pile and the center axis of the group (or the raft).

ε: can be calculated according to following iterative formula:

$$\varepsilon = \arcsin[(1-B_o/B)\sin\alpha \cdot e^{-(\alpha-\varepsilon)\cdot tg\varphi}] \qquad (2\text{-}20)$$

C_p and C_c are coefficients of the ultimate resistance to the soil sliding around a pile (Zhu and Shen, 1990).

$$C_p = \begin{cases} C_{Pb} = \dfrac{e^{(\pi/2-\varphi)tg\varphi}}{1-\sin\varphi} - \dfrac{e^{-(\pi/2+\varphi)tg\varphi}}{1+\sin\varphi} + 2tg\varphi & (square\ \ pile) \\ C_{PC} = e^{(\pi/2-\varphi)tg\varphi}\left[\dfrac{3tg\varphi\sin\mu + (2tg^2\varphi - 1)\cos\mu}{4tg^2\varphi + 1} + \dfrac{\cos\mu}{1+\sin\varphi}\right] & \\ + e^{-(\pi/2+\varphi)tg\varphi}\left[\dfrac{3tg\varphi\cos\mu - (2tg^2\varphi - 1)\sin\mu}{4tg^2\varphi + 1} - \dfrac{\sin\mu}{1+\sin\varphi}\right] & (circular\ \ pile) \end{cases} \quad (2\text{-}21)$$

Where, $\mu = \pi/4 - \varphi/2$;

$$C_c = \begin{cases} C_P / tg\varphi & (for\ \ \varphi \neq 0,\ \ ) \\ 4\sqrt{2} & (for\ \ \varphi = 0,\ \ circular\ \ pile) \\ 4 + \pi & (for\ \ \varphi = 0,\ \ square\ \ pile) \end{cases} \quad (2\text{-}22)$$

and $\lambda_c = C_{PC}/C_{Pb} \approx 0.80$ (when $\varphi = 0 \sim 40°$) (2-23)

For circular foundations, Δq_u can be determined using the following formula (Yang & Zai 1996)

$$\Delta q_u = (H_q \cdot \gamma_o D + H_\gamma \cdot \gamma_B B/2 + H_c \cdot c) T_\omega d/S \quad (2\text{-}24)$$

where, $S = \omega B/2$, $\omega = 2\pi/n$; n is the number of piles around circular raft center;

$$T_\omega = \frac{1 + \dfrac{\omega^2}{24}\left(2^{Ka} - 1\right)}{1 + \dfrac{\omega^2}{24}\dfrac{1+\sin\varphi}{2-\sin\varphi}} \quad (2\text{-}25)$$

$T_\omega = 0.92 \sim 1.05$ when $\omega = 0 \sim 90°$ and $\varphi = 0 \sim 35°$.

H_q, H_γ and H_c are same as given in formula (2-18); however, the parameters are changed to the following form:

$$T = 3/[2^{Ka}(1 + K_o/tg^2\alpha)] \quad (2\text{-}26)$$

$$\alpha = \pi/4 \quad (2\text{-}27)$$

ε can be calculated according to the following iterative formula, which is different from equation (2-13):

$$\varepsilon = \arcsin[(1-B_0/B)\sin(\pi/4)\cdot e^{-(\pi/4-\varepsilon)\cdot tg(\varphi/2)}] \qquad (2\text{-}28)$$

2.3 Approximate Computer-Based Analyses

The approximate computer-based methods include the following two broad approaches: the "strip on springs" approach and the "plate on springs" approach.

2.3.1 Strip-on-springs approach

A typical method in this category is that presented by Poulos (1991), in which a section of the raft is represented by a series of strip footings and the supporting piles by springs, as shown in Fig. 2-2. An approximate allowance is made for all four components of the interaction (raft-raft, pile-pile, raft-pile, and pile-raft). The effects of the parts of the raft located outside of the strip section are taken into account by computing the free field soil movements due to these parts and the interaction of these parts within the strip section.

This method has been shown to give settlement which is in reasonable agreement with more complete methods of analysis. However, it does have some significant limitations, as it does not consider torsional moments within the raft and it does not provide consistent settlement at a point when strips in two directions both acting through that point are analyzed. The method was also used by Zai (1992) and Katzenbach et al (1998).

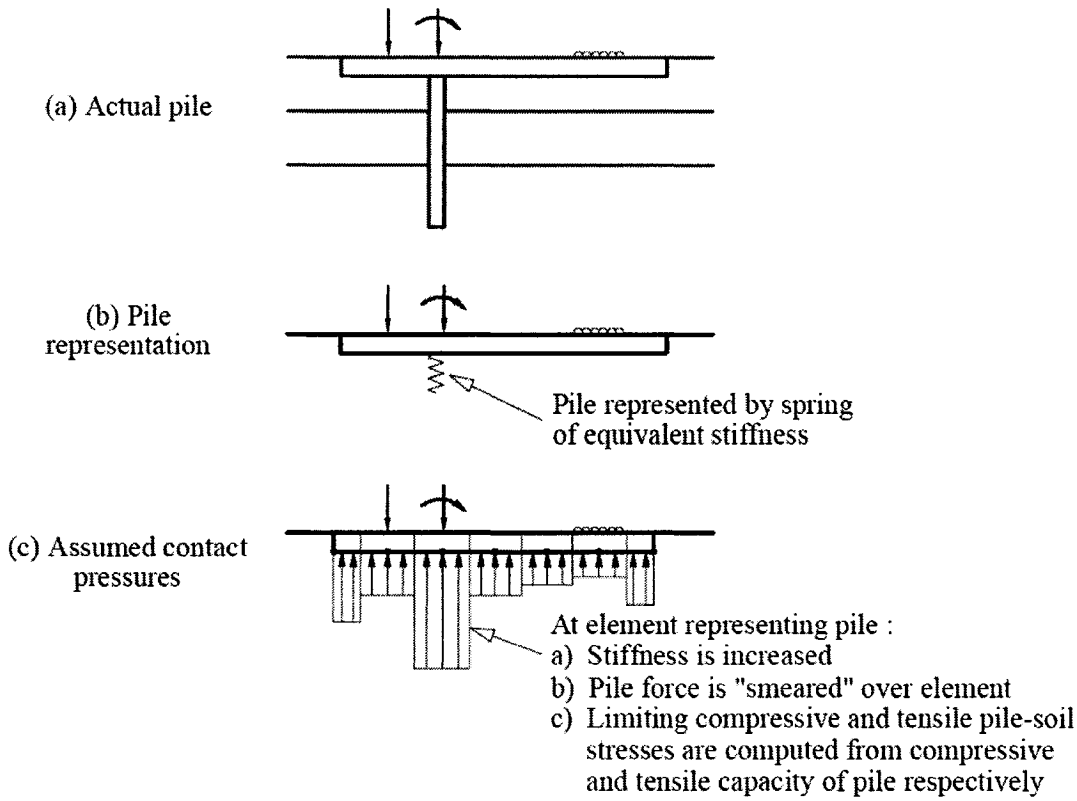

Fig.2-2 Strip-on-springs approach (Poulos, 1991)

2.3.2 Plate-on-springs approach

In this approach, the raft is represented by an elastic plate, the soil by an elastic continuum and the piles are modeled as interacting springs, similar to those employed in the program for piled strip. The method is restricted to the analysis of the foundation's elastic response.

Some early approaches within this category, e.g. Hongladaromp et al (1973), neglected some of the interactions and hence gave values too large for pile-raft stiffness, as revealed by the studies of Brown and Wiesner (1975). Poulos (1994) employed a finite difference method for the plate and allowed for various interactions via approximate elastic

solutions. Allowance was also made for the effects of piles reaching their ultimate capacity, the development of bearing capacity failure below the raft, and the presence of free-field vertical movements acting on the foundation system (Clancy & Randolph, 1993; Poulos, 1994; Viggiani, 1998; Anagnastopoulos & Georgiadis,1998).

2.4. More Rigorous Numerical Analysis

In the analysis of the piles–soil–cap interaction, the soil flexibility matrix piles and the cap stiffness matrices can be determined on the based of discrete elements of raft and piles. The latter two stiffness matrices can be formulated by the elastic theory.

2.4.1 Soil flexibility matrix

The soil flexibility matrix, i.e., $[\delta_s]$,

$$\{S\} = [\delta s] \cdot \{F\} \qquad (2\text{-}29)$$

Where,

$\{S\}$ is the displacement of the soil under the raft and around the piles;

$\{F\}$ is the raft-load and pile-fictitious soil tractions.

The matrix coefficients δ_{sij} can be established by the following methods:

1) Finite element method (FEM)

In FEM, a variety of nonlinear or elastic-plastic constitutive soil models can be utilized, and factors such as soil non-homogeneity and anisotropy can be taken into consideration (e.g., Desai 1974; Ottaviani 1975; Chow 1987; Lee et al 2002). Undoubtedly, the FEM is

considered as one of the most powerful approaches for analyses of the behaviors of pile groups. The technique can also simulate the complete history of the pile construction procedure, i.e. the processes of pile-group installation, dissipation of pore water following the installation, the reconsolidation of soil, etc. Such analyses are invaluable in leading to a better understanding of the behaviors and mechanism of groups of pile–soil–cap interactions. However, it is rather unlikely that FEM will readily be applied to the problems of a large pile group because of the complexity of the pile-group–soil–cap system and its high computational requirements. Another problem of FEM is the volumetric locking behavior in the analysis of ultimate state. Fig. 2-3 shows that Node A is fixed by the requirement of volume-preservation, or limited by the requirement of dilatant's /contracting plastic flow. The volumetric locking of 8-node elements is similar as that of 3-node elements (Fig. 2-4). The limitation of 8-node elements on foundation ultimate analysis is shown in Fig. 2-5, which results in overestimating the bearing capacity coefficient.

Volumetric locking must be taken into account during the development of numerical models. Currently, three-dimensional FEM for large pile group are mainly limited to elastic problems.

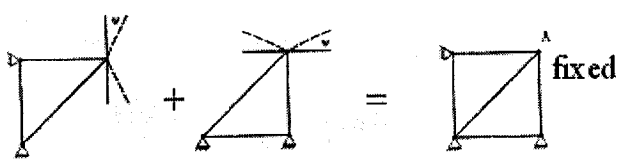

Fig.2-3 Volumetric Locking of 3-Node Element

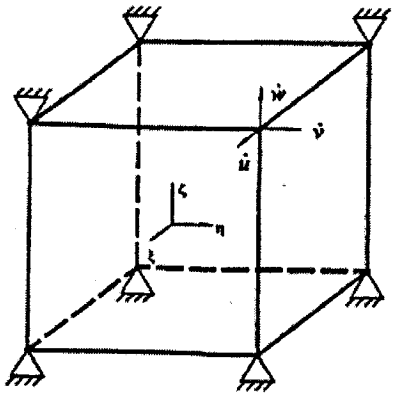

(a)The types of elements

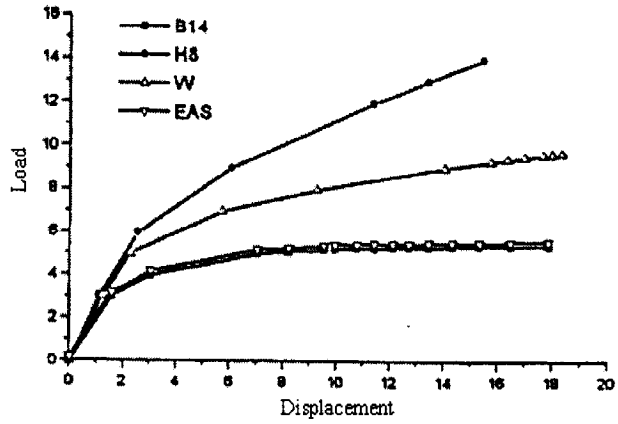

(b) Load-displacement curves of element

H8-----8-node brick element;
B14----14-node brick;

W------ Wilson's incompatible element
EAS------ Enhanced Assumed strain element

Fig. 2-4Volumetric locking of 8-Node Element (Yang et al 2000)

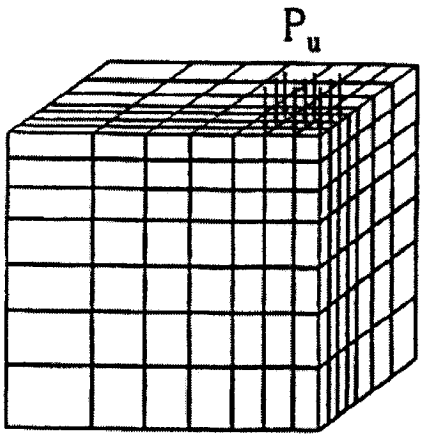

(a) Model of bearing capacity calculation of a square footing

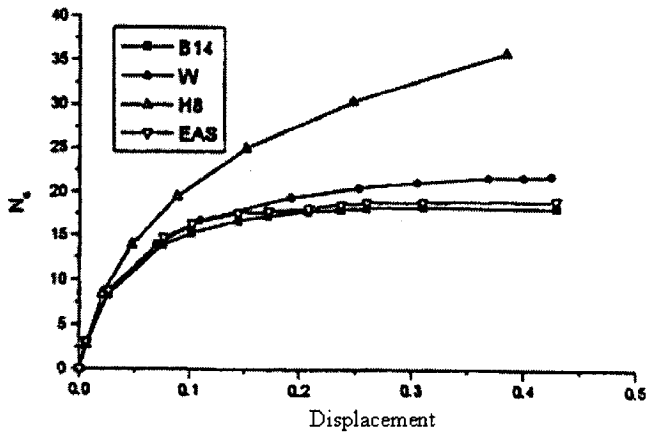

(b) Bearing capacity coefficient- displacement curves of the square footing

Fig. 2-5 Effect of Volumetric Locking on Foundation Ultimate Analysis (Yang et al 2000)

2) Boundary element method (BEM)

BEM is based on Mindlin's elastic theoretical solution as the kernel function to capture soil mass responses. That is, the soil displacements are obtained by using Mondlin's equation for the displacements within a soil mass caused by loading within the mass. Details of the complete analysis are given by Butterfield & Banerjee (1971a, 1971b), Banerjee (1978), Banerjee & Davis (1977), Poulos & Davies (1980); Lee et al (1990) and Mandolini & Viggiani (1997). If conditions at the pile-soil interface remain elastic and no slip occurs, the movements of the pile and the adjacent soil must be equal. Since BEM is based on the elastic theoretical solution, the method is strictly applicable only to the case of an ideal soil and cannot be used in nonlinear, non-homogenous and anisotropic mediums, which is its main shortcoming.

3) Finite Layer Method (FLM)

In FLM, non-homogenous and cross-anisotropic layered mediums can be taken into consideration. This was considered as the greatest advantage of this method, because natural geological soils often appear as cross-anisotropic layers, and soil displacement fields are represented by the product of complex polynomial and series-expansion functions, e.g., (i) discrete Fourier series (Zhang & Zhao et al 1981, 1982; Zai 1989; Lai & Booker 1989); (ii) Hankel transform, i.e., Bessel functions of first kind series (Small & Booker 1986; Lee & Small 1990). The former functions can respectively be used (i) to analyze a rectangular load area and (ii) to analyze a circular load area. However, FLM is not applicable to nonlinear materials, since it is based on the assumption of ideal elastic layered soil.

4) Simplified analytical methods (SAM):

(a) Transfer-Function Method (TFM)

TFM, or the so-called t-z curves method, uses the load-transfer function to describe the pile-soil deformation behavior (Coyle & Reese 1966; Kraft et al. 1981), shown in Table 2-2. This category is actually Winkler's idealization of soil, i.e., coefficients $\delta ij=0$ at i=j, only $\delta ii \neq 0$, which means that the method cannot consider the interaction of pile-pile or pile-raft; but it is attractive due to its flexibility, enabling non-linear analyses and non-homogeneous soil conditions.

(b) Shear-displacement theory (SDT)

SDT assumes that the distribution of the displacement and shear stress in the soil around the pile can be idealized as a concentric cylinder, i.e. $\tau(r) = \tau_0 r_0/r$, (Cooke 1974, 1979 and 1980). These assumptions were further validated by a finite-element-method analysis performed by Randolph & Wroth (1978). In this analysis, the vertical displacement of the soil, S_z caused by the shaft shear stress τ_z can be derived as a logarithmic relationship with the radial distance away from the pile shaft in the elastic medium, i.e. $S_z = \frac{r_o \tau_z}{G} \ln\left(\frac{r_m}{r_0}\right) = C_s \tau_z$ (see Table 2.2). This relationship has been widely applied to analyze the pile-pile interaction (e.g., Randolph & Wroth 1979, Chow 1986; Lee 1993; Guo & Randolph 1999; Lee & Xiao 2001; Shen & The 2002), assuming the relationship to be in a nonlinear medium (as shown in Table 2.2). Those linear and nonlinear relationships form some of the so-called t-z theory curves. The above simplified methods can only be used to analyze single piles, or at most to capture the responses of soil mass

around other piles at same depth, but not to calculate the interaction between pile shaft and pile end or cap bottom.

(c) Generalized shear-displacement theory (GSDT)

In GSDT, the shear-displacement theory is extended to derive the elastic displacement field and the plastic shear displacement in soils around the pile's shaft (Zai & Yang 1993a, 1993b; Yang & Zai 1994); accordingly, the soil elastic and plastic deformations are separated. The former deformation can be directly obtained from the elastic solution or FEM's results, which involves the interaction between any two points on the piles or the raft.

5) Combination methods (Hybrid methods)

Hybrid methods are developed to analyze the pile-group interaction, e.g., a combination of the elastic shear-displacement method (SDT) with nonlinear transfer function (Lee & Xiao 2001) can be used to analyze the behavior of piles with high-set caps but cannot analyze the interaction of pile--raft; a combination of BEM and Koyasu's transfer function (Meng 1999); a combination of FEM and Koyasu's function (Lee et al 2002). The above did not involve pile-raft interactions. Actually, the combination of BEM (or FLM) with z-t curves can be use to analyze pile-raft nonlinear interactions (Zai & Yang 1993a, 1993b; Yang & Zai 1994). Hybrid methods overcome the volumetric locking problem of FEM in the analysis of ultimate state, the restriction in nonlinear analysis of BEM and FLM, TFM's failure to consider the interaction of pile-pile or pile-raft, and the

shortcoming of SDT(or GSDT)'s, which does not allow for the calculation of the interaction between pile shaft and pile end or cap bottom.

According to hybrid methods, the elastic-plastic flexibility coefficients to analyze pile-group interaction are set such that $\delta_{ij}(i \neq j)$ is for elastic resolution (modified) and δ_{ii} is for non-linear resolution:

$$\{\Delta S_p\} = [\delta_{ep}] \cdot \{\Delta F_p\}; \qquad (2\text{-}30)$$

$$\delta_{epij} = \delta_{eij} \qquad (i \neq j); \qquad (2\text{-}30a)$$

$$\delta_{epii} = \delta_{eii} + \delta_{pii} \qquad (i = j) \qquad (2\text{-}30b)$$

Where

δ_{epij} = elastic-plastic flexibility coefficients

δ_{eij} = elastic flexibility coefficient from the resolution of elastic theory or FEM, BEM, FLM

δ_{pii} = plastic flexibility coefficient from GSDT

δ_{epii} can be obtained directly from TFM too (Yang and Zai, 1994).

Moreover, actual soil is not a completely elastic medium and cannot bear extensive stress. It behaves partly as a Winkler model (or Winkler foundation, Das 1999), so the elastic solution overestimates the pilegroup–soil–pilecap interaction. It can be seen from the deficiency between the experimental pile-soil interaction coefficient (Cooke at el 1980) and the computed data (Poulos & Davis 1980) as Fig. 2-6.

Table 2-2 Load Transfer Functions of pile shaft (t-z curves)

From	Based on τ--γ relationship	Transfer function (τ_0 -- S relationship)	Notation
Kezdi.A(1957)	Field pile test data	$\tau_0 = K\gamma z \operatorname{tg}\phi \left[1-\exp\left(\frac{-RS}{S_u - S}\right)\right]$	K----coeffient of lateral pressure R----coeffient τ_0----shear stress on pile
Koyasu (1956)	Field pile test data	$\tau_0 = S/C_s \le \tau_u$	τ_u----ultimate shear stress
Gardner(1975)	Field pile test data	$\tau_0 = A\cdot S/(1/K+S/\tau_u)$	K, A----emperimental constant
Vijayvergiva (1977)	Field pile test data	$\tau_0 = \tau_{max}(2\sqrt{S/S_u}$ --$S/S_u)$	S_u----critical displacement
Desai etc(1987)	Field pile test data	$\tau_0 = \frac{(K_o - K_f)S}{\left(1+\left\lvert(K_o-K_f)S/P_f\right\rvert^m\right)^{1/m}} + K_f S$	Ko---initial spring modulus K_f----final spring modulus P_f----yield load m----index of curve
Lee & Xiao (2001)	Lab test Data	$S = \frac{a\tau_0}{1-b\tau_0} + C_s\tau_0$, $Cs = \frac{r_o}{G}\ln\left(r_m/r_o\right)$	a,b----test coefficients G----Soil shear modulus
Cooke (1974,1979)	$\gamma = \tau/G$	$S = \frac{r_o\tau_0}{G}\ln\left(r_m/r_o\right) = C_s\tau_0$	r_o---- radius of pile r_m----radial distance from pile centre
Randolph(1977) Kraft etc (1981)	$\gamma = \frac{\tau}{G_i\left(1-\frac{\tau\cdot R_f}{\tau_f}\right)}$	$S = \frac{\tau_0 r_o}{G_i}\ln\left(\frac{r_m/r_o - (\tau_0 R_f)/\tau_f}{1-(\tau_0 R_f)/\tau_f}\right)$	G_i---initial shear modulus τ_f----failure shear stress R_f---failure ratio
Chow(1986)	$\Delta\gamma = \frac{\Delta\tau}{G_i\left(1-\frac{\tau\cdot R_f}{\tau_f}\right)^2}$	$\Delta S = \frac{\Delta\tau_0 r_0}{G_i}\left\{\ln\left(\frac{\lambda-\beta}{1-\beta}\right) + \frac{\beta(\lambda-1)}{(\lambda-\beta)(1-\beta)}\right\}$	$\lambda = r_m/r_0$; $\beta = \tau R_f/\tau_f$
Naggar &Novak (1994)	$\frac{\gamma}{\gamma_f} = \frac{\eta}{1-\eta}$ $\gamma_f = \tau_f/G_s$, $\eta = \tau/\tau_f$	$S = \frac{r_o\tau}{G_s}\ln\left(\frac{r_m/r_0 - \eta_0}{1-\eta_0}\right)$	G_s---initial tangent shear Modulus $\eta_0 = \tau_0/\tau_f$
Richwien & Wang(1999)	$\gamma = B\tau^m$, $B = \gamma_f/\tau_f^m$	$S = B\frac{(r_0\tau_0)^m}{m-1}\frac{1}{r_0^{m-1}}$	m----material constant
Zai & Yang (1993a,b)	Stepwise linear model $\Delta\gamma^e = \Delta\tau/G_e$, at $\tau \le \tau_e$ $\Delta\gamma^p = \Delta\tau/G_{p1}$, at $\tau_e < \tau \le \tau_2$ $\Delta\gamma^p = \Delta\tau/G_{p2}$, at $\tau_2 < \tau \le \tau_f$	at $\tau_e < \tau \le \tau_2$, $\Delta S_p = \frac{r_o\Delta\tau_0}{G_{p1}}\left[\ln\left(\frac{\tau}{\tau_e}\right)+1\right]$; at $\tau_2 < \tau \le \tau_f$, $\Delta S_p =$ $= r_o\tau_0\left\{\frac{1}{G_{p1}}\ln\left(\frac{\tau_2}{\tau_e}\right) + \frac{1}{G_{p2}}\left[\ln\left(\frac{\tau_0}{\tau_2}\right)+1\right]\right\}$	G_e---elastic shear modulus τ_e----critical shear stress at elastic phase τ_2----critical shear stress at 1st plastic phase τ_f---- failure shear stress G_{p1}, G_{p2}----shear modulus at 1st & 2nd plastic phases
Yang & Zai (1994)	$\gamma^e = \tau/G_e$; $\gamma^p = \frac{\tau}{G_0\left(1-\frac{R_f\tau}{\tau_f}\right)} - \frac{\tau}{G_e}$	$\Delta S_p = \frac{r_o\Delta\tau_0}{G_0}\left\{\ln\left(\frac{1-\lambda}{1-\beta}\right) + \frac{\beta}{1-\beta} - \frac{\lambda}{1-\lambda}\left[\ln\left(\frac{\tau_0}{\tau_e}\right)+1\right]\right\}$	G_e---elastic shear modulus; R_f----shear failure ratio; $\lambda = R_f\tau_e/\tau_f$; $G_0 = G_e/(1-\lambda)$; $\beta = R_f\tau_0/\tau_f$;

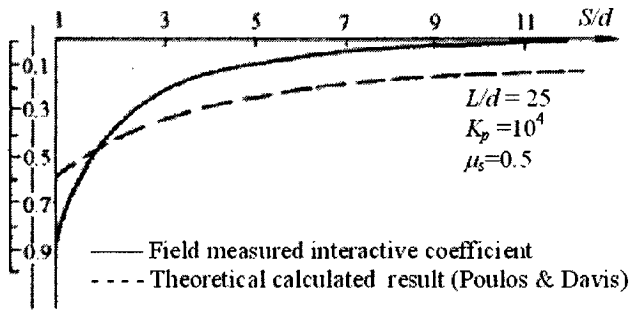

Fig 2-6 Theoretical Curve vs. Experimental Curve

2.4.2 Pile Stiffness Matrix and Treatment Methods

In the three-dimensional finite element method (FEM), piles are separated into cubic element bodies, but in BEM or FLM, piles can be separated into discrete one-dimensional element raps under vertical load. There are two methods to establish one-dimension piles' stiffness (or flexible) matrix.

A. Directly establishing pile stiffness matrix

The pile stiffness matrix, $[K_p]$, is based on Bernoulli-Euler's beam theory and is easily available in literature (Poulos & davis 1980; Smith & Griffith 1988):

$$[K_p]\ \{S_p\}=\{P\} - \{F_P\} \qquad (2\text{-}31)$$

Where, $\{S_p\}$ is $\{P\}=\{P_0,0,0,.....0\}_n^T$, P_0 is the load at the pile head; $\{F_P\}$ is the pile-fictitious soil traction, i.e., some parts of $\{F\}$.

B. Directly establishing pile flexibility matrix

The pile flexibility matrix, $[\delta_p^{-1}]$, is defined by the following equation:

$$\{\Delta s\}= [\delta_p^{-1}] \cdot \{F_P\} \qquad (2\text{-}32)$$

Where{Δs} is the displacement difference between a calculating point and the cap bottom, i.e. pile head, and $[\delta_p^1] \neq [K_p]^{-1}$. If S_B is the settlement of the cap bottom or pile head, $\{S_p\} = S_B - \{\Delta s\}$. This means that equation (2-32) can be directly added to (2-29), but equation (2-31) cannot. The $[\delta_p^1]$ can be derived by adding displacement differences between two conjoint sections of pile from pile head to calculating points, which is shown by Lee & Xiao (2001).

C. **Variation approach**

Another discrete treatment of pile is the variation approach (Shen et al, 1997, 1999, 2000, 2001), which sets

$$S_{zi} = \sum_{j=1}^{k1} \beta_{ij} (1 - z_i / \ell)^{j-1} \qquad (2\text{-}33)$$

and

$$\tau_{zi} = \sum_{j=1}^{k2} \alpha_{ij} (z_i / \ell)^{j-1}, \; i=1,2,\ldots,n_p; \qquad (2\text{-}34)$$

Where ℓ is the pile length and n_p is the number of piles.

This approach allows the pile to be divided into sections, i.e., k_1 or k_2 is 3 or 4, and it can give better precision. This approach has not been used in nonlinear or elastic-plastic medium cases.

2.5 Effects of Pore-water Pressure on Pile-soil-raft Interaction

As indicated above, the behavior of pile-soil-raft interaction is greatly influenced by the pore-water pressure and its dissipation in soil with time. To clarify this influence, the initial contribution and dissipation of the excess pore-water pressure (EPWP) during the

whole process from the end of pile driving to the completion of consolidation after construction of supper structure, should be considered.

2.5.1 Pore pressure developments during driving

A number of measurements of the excess pore pressure developed in a soil because of pile driving have been performed (Bjerrum et al. 1958; Bjerrum & Johannessen,1960; Milligan et al. 1962; Lambe & Horn, 1965; Lo & Stermac, 1965; Orrje & Broms, 1967; Hanna,1967; Koizumi & Ito,1967; D'Appolonia & Lambe,1971).The results of the measurements of pore pressure at the pile face in many of these papers have revealed common results such as the excess pore pressure's decrease which may become equal to or even greater than the effective overburden stress. However, the induced excess pore pressure decreases rapidly with distance from the pile (Fig. 2-7).

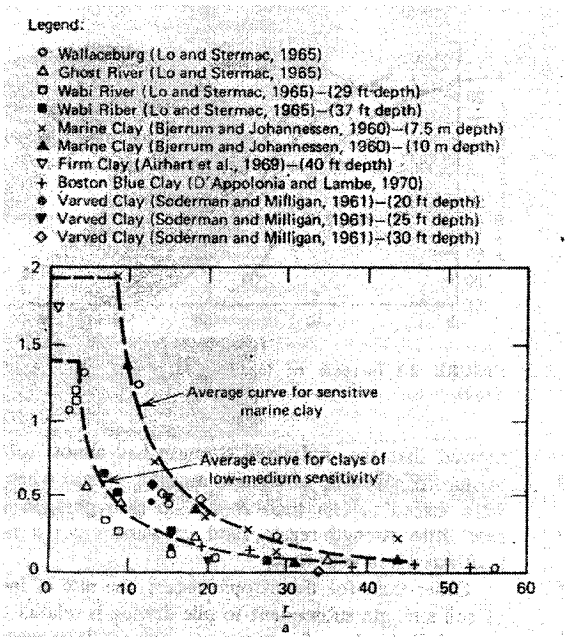

Fig.2-7Excess Pore Pressure Decreases with Distance from the Pile (Poulos & Davis, 1990)

Lo & Stermac (1965) derived an expression of the maximum pore pressure distribution near the pile surface, based on the hydraulic failure (crack) of a radial zone of soil around the pile:

$$\Delta u_m = \left[1 - K_0 + \left(\frac{\Delta u}{p'}\right)_m\right]\sigma'_{v0} \qquad (2\text{-}35)$$

where K_0 is the coefficient of earth pressure at rest in the intact clay; $(\Delta u/p')_m$ is the ratio of excess pore pressure to the initial consolidation pressure p' measured in a conventional consolidated-undrained triaxial test and generally assumes values in the order of 0.6-0.8.

D'Appolonia & Lambe (1971) derived another form of Lo & Stermac's expression, namely,

$$\frac{\Delta u_m}{\sigma'_{v0}} = \left[(1 - K_0) + \frac{2c_u}{\sigma'_{v0}}\right]A_f \qquad (2\text{-}36)$$

Where

Δu_m = maximum excess pore pressure;

K_o = in-situ coefficient of earth pressure at rest,

c_u = undrained shear strength,

A_f = pore-pressure coefficient A at failure;

σ'_{vo} = initial effective vertical stress in soil.

Based on theories of expansion of spherical and cylindrical cavities in ideal elastic-plastic soils with Mohr-Coulomb yield criterion, Vesic (1972) suggested the following:

In the plastic field: $$\frac{\Delta u}{c_u} = 2Ln\left(\frac{R}{r}\right) + 0.817\alpha_f \qquad (2\text{-}37)$$

In the elastic field:

$$\frac{\Delta u}{c_u} = 0.817\alpha_f \left(\frac{R}{r}\right)^2 \tag{2-38}$$

and

$$R = r_0 \sqrt{\frac{E}{2(1+\mu)c_u}} \tag{2-39}$$

Where R is the radius of the plastic field; r_0 is radius of pile; α_f is Henkel's pore-pressure coefficient at failure, and $\alpha_f = 0.707(3A_f\text{-}1)$.

Carter et al (1979) and Randolph and Wroth (1979) presented the following expression for soil with the Modified Cam-clay model (generated excess pore water pressure is equal to the increase in mean total stress):

$$\Delta u = 2c_u Ln\left(\frac{R}{r}\right) \tag{2-40a}$$

However the model of Eq. (2-40) has two shortcomings: one is no account taken of pore pressure generated due to pure shear; another is inability to link soil strength and its change with the current effective stress state and stress history of the soil. For the work hardening soil model, the value of the mean effective stress changes during shearing. Randolph et al (1979) presented the following expression

$$\Delta u = 2c_u Ln\left(\frac{R}{r}\right) + (p'_i - p'_f), \quad r_0 \le r \le R \tag{2-40}$$

Where p_i' and p_f' are the mean effective stresses around the pile before and after pile driving respectively.

Poulos & Davis (1980) suggested the following procedure as a rapid and practical means of estimating the excess pore-pressure distribution

$$\Delta u = \Delta u_m \left(\frac{R}{r}\right)^2 \qquad (2\text{-}41)$$

Where R = 3*a* to 4*a* for normal clays or 8*a* for sensitive clays (*a* is the pile radius); Δu_m is estimated by equation (2-35), and equation (2-41) is of the same form as (2-40).

Tang (1990) proposed the following uniform expression for the initial excess pore-pressure based on field data,

$$\Delta u = \frac{\Delta u_m}{Ln(\omega)} Ln\left(\frac{\omega r_0}{r}\right) \qquad (2\text{-}42)$$

in which ω is the extended radius coefficient. It should be noted that beyond $r/r_0 = \omega$, the excess pore pressures are virtually negligible.

Yao & Wu (1997) suggested that the soil is an ideal elastoplastic body which obeys the Mohr Coulomb failure criterion; and that when the soil is in limit equilibrium state during pile driving, the horizontal radial stress is the maximum lateral stress increment produced by driving.

Thus, they determined the initial excess pore-pressure expression as:

Plastic area ($r \leq R_p$): $$\Delta u_p = \Delta \sigma_r A = \left[(1 - K_0)\gamma' h + 2c_u\right] A \qquad (2\text{-}43)$$

Elastic area ($r \geq R_p$): $$\Delta u_e = \Delta u_p \left(\frac{r}{R_p}\right) \qquad (2\text{-}44)$$

Luo (1997) assumed that tangential stress in a soil around a pile is equal to the radial stress at the end of driving and that the undrained shear strength of the soil increases linearly with depth. Based on the Mohr-Coulomb failure criterion and Henkel's formula,

an approximate formula to predict the excess pore pressure was obtained:

$$\Delta u = (1 - K_0 + 2Am)\gamma' h \frac{\ln\left(\frac{\omega r_0}{r}\right)}{\ln\left(\frac{\omega r_0}{R_p}\right)} \tag{2-45}$$

Where m is the linearly increasing factor of the undrained shear strength of the soil, $m = \Delta c_u/\Delta z$.

Chen (1999), basing himself on the field data and the limit equilibrium theory, assumed that both the pile lateral pressure and the friction resistance increase linearly with depth. Their distribution is shown in Fig. 2-8 and the expressions are as follows:

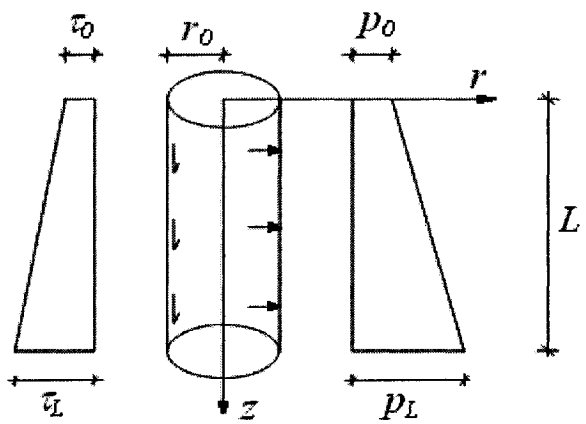

Fig. 2-8 Calculation Model (Chen 1999)

$$p_z = p_0 + \frac{p_L - p_0}{L} z = p_0 + K_p \gamma' z \tag{2-46}$$

$$\tau_{rz} = -\tau_0 - \frac{\tau_L - \tau_0}{L} z = -(c_a + K_p \gamma' z \tan\varphi) \tag{2-47}$$

Where:

p_0, p_L ---- lateral pressures respectively at pile top and pile tip;

τ_0, τ_z ---- frictional stresses respectively at pile top and pile tip;

c_a, φ ---- cohesion and friction angle in pile-soil contacted surface;

K_p ---- soil passive earth pressure coefficient.

Thus, a three dimensional analytic solution is obtained, namely:

Plastic area ($r \leq R_p$):

$$\Delta u = \frac{1}{3}\left[2\left(2c - K_p \gamma' r_0 \tan\varphi\right)\ln\frac{R_p}{r} + \frac{c_a}{r}z\right] + 0.817\alpha_f c \qquad (2\text{-}48)$$

Elastic area ($r \geq R_p$):

$$\Delta u = 0.817\alpha \cdot c \cdot \left(\frac{r_0}{r}\right)^2 \qquad (2\text{-}49)$$

The $\Delta u(r)$ curves obtained from equations (2-48) and (2-49) are not continuous. In fact, the value of Δu in elastic area by Eq (2-49) is quite small; therefore Chen (1999) suggested that Eq. (2-48) can be approximately used in whole area. Modifications to the formulae (2-48) and (2-49) based on the results of the model test were obtained:

$$\Delta u = \frac{1}{3\ln\omega}\left\{\left[2\left(2c_u - K_p \gamma' r_0 \tan\phi\right)\ln\frac{R_p}{r_0} + c_a\frac{z}{r_0}\right] + 2.45\alpha_f c_u\right\}\ln\frac{\omega r_0}{r} \qquad (2\text{-}50)$$

According to the experience of Bjerrum & Andersen (1972), a state where $\Delta u_m > \sigma'_{vo}$ is maintained for a very short time (five minutes) in normally consolidated soil. This is due to the action of hydraulic fracturing in soil under high pore pressure leading to negative

total effective stress in soil; e.g., $K_o\sigma'_{vo} + \Delta\sigma_\theta \leq 0$ or $\sigma'_v + \Delta\sigma_v \leq 0$, changing into situation of $\Delta u_m \leq \sigma'_{vo}$.

The field data of statically driven piles in the Shanghai Subway Project (Chen, 1999) demonstrated that $\Delta u_m = (1.1\sim1.4)\sigma'_{vo}$, as well as a stable value for $\Delta u_m \approx 1.1\sigma'_{vo}$.

For pile groups, the pore pressure distributions around individual piles may be superimposed but the pore pressure cannot exceed Δu_m, as found by Lo & Stermac (1965).

Azzouz and Morrison (1988), Masood and Mitchell (1993), Lunne et al(1986), Kalsarud and Haugen (1985), and Huntsman & Mitchell (1986) respectively measured stresses and excess pore-pressure around piles by using PLSC (Piezo-Lateral Stress Cell) and CPT (Cone Penetration Test) and found that stresses and excess pore-pressure linearly increase with depth.

2.5.2 Dissipation of Excess Pore Pressure after Driving

Soderberg (1962) proposed a relatively simple solution for estimating the rate of dissipation of excess pore pressures around a driven pile. It is assumed that dissipation occurs radially only; the vertical dissipation that may occur near the top of the pile can be ignored. The relevant equation of consolidation then becomes

$$\frac{\partial u}{\partial t} = C_h\left(\frac{\partial^2 u}{\partial r^2} + \frac{1}{r}\frac{\partial u}{\partial r}\right) \qquad (2\text{-}51)$$

The above equation (2-51) may readily be written in finite differential form (Gibson & Lumb, 1953), and can be solved by other numerical methods.

Poulos & Davis (1980) compared the theoretical results produced by equation (2-51) with an empirical relationship suggested by Radugin (1969). They reported that there is some difference between the shapes of the curves, but they are generally in sufficient agreement to suggest that the simple consolidation analysis may provide a reasonable estimate of the rate of increase of load capacity.

More rigorous analysis of the stress change, excess pore pressures and subsequent consolidation around a single driven pile in clay has been presented by Wroth et al. (1979).

Based on a mechanical model for soil re-consolidation after pile driving (Esrig et al, 1977), a simple analytical solution for single pile is presented (Tang 1985, Zhu & Tang 1986):

$$u(\rho,t)=\begin{cases}\dfrac{2u_m}{Ln(\omega)}\displaystyle\sum_{i=1}^{\infty}\frac{J_0(\alpha_i\rho/\omega)}{\alpha_i^2 J_1^2(\alpha_i)}Exp\left[-\frac{3(1-\mu)}{1+\mu}\left(\frac{\alpha_i}{\omega}\right)^2 T\right] & m=1\\ \dfrac{2u_m}{Ln(\omega)}\displaystyle\sum_{i=1}^{\infty}(1-\cos\lambda_i)j_0\left(\lambda_i\frac{\rho}{\omega}\right)Exp\left[-\frac{3(1-\mu)}{1+\mu}\left(\frac{\lambda_i}{\omega}\right)^2 T\right] & m=2\end{cases} \qquad (2\text{-}50)$$

where, J_0 and j_0 respectively are the cylindrical and the spherical Bessel functions of the first kind; α_i and λ_i respectively are the i-th values of infinitely many positive zeros solutions, $x=\alpha_i$, $y=\lambda_i$, $i=1,2,\ldots$, of equations $J_0(x)=0$ and $j_0(y)=0$, and $\lambda_1 = i\pi$ *because of* $j_0(y)$

$= \sin(y)/y$; $\rho = r/r_o$, $T = C \cdot t/r_o^2$ (where $C=\frac{kE}{3\gamma_w(1-2\mu)}$), $\omega = R/r_o$; $m = 1$ for axisymmetrical problems, m = 2 for sphere-symmetrical problem.

2.6 Discussion

From the previous research, field tests and case studies, some useful findings for foundation design can be reported, although they tend to be rather conservative with respect to both design and calculations. The main advantages of the sparse piles and raft systems include the reduction of the number of piles and the use of the soil bearing capacity up to its maximum, the gradual development of settlement, and the increase of pile bearing capacity when excess pore-water pressure dissipates in the soil.

The analysis of the piles-soil-cap interaction is meaningful for the improvement of theory and practice on the design of foundation engineering. However, there are several complex problems in performing the analysis, especially in evaluating the excess pore-water pressure dissipation in soil around a group of piles and its influence on the settlement and the bearing-load behaviour of the pile group-soil-cap system.

The mechanism of the pile-soil-cap system is interactive (including pore-water pressure); i.e. they are affected by each other, such as, (1) the weakening action on the friction of the pile shaft (upper part of piles) due to the limitation of displacement difference of pile-soil caused by the cap (actually, by the cap's load acting on the soil under the cap and around the piles), (2) the enhancing action on the friction strength of the pile shaft's and

the bearing capacity of the pile base due to increase in the effective normal stress caused by a load acting on the soil under the cap, around the piles and other piles, and (3) the increasing action on vertical soil's ultimate bearing capacity due to the resistance to soil sliding around a pile; hence, it requires quite a big capacity, computer speed and high computational technology. This is especially the case for the mechanism of the pore-water pressure change during the pile group driving and over time.

2.7 Background of Pile–Soil–Cap Interaction

The facts presented in Fig. 2.9 show the principle of pile-soil-raft interaction design, that is, only if pile load reaches or is near to ultimate bearing load, the pressure of raft bottom will share a great load.

In Fig. 2.9(a), the piles carry loads in the elastic state, usually under half the load of the piles' ultimate bearing capacity. The settlement difference between the pile and the soil around the pile is very small. For soil settlement to reach the same value of pile settlement, only a small surface pressure on the soil is required. This phenomenon has been demonstrated in numerical analysis of elastic media by Butterfield and Banerjee (1971a, 1971b).

It is therefore not necessary, in a regular design of pile foundations, to consider that the soil around the piles shares the load of the upper structure.

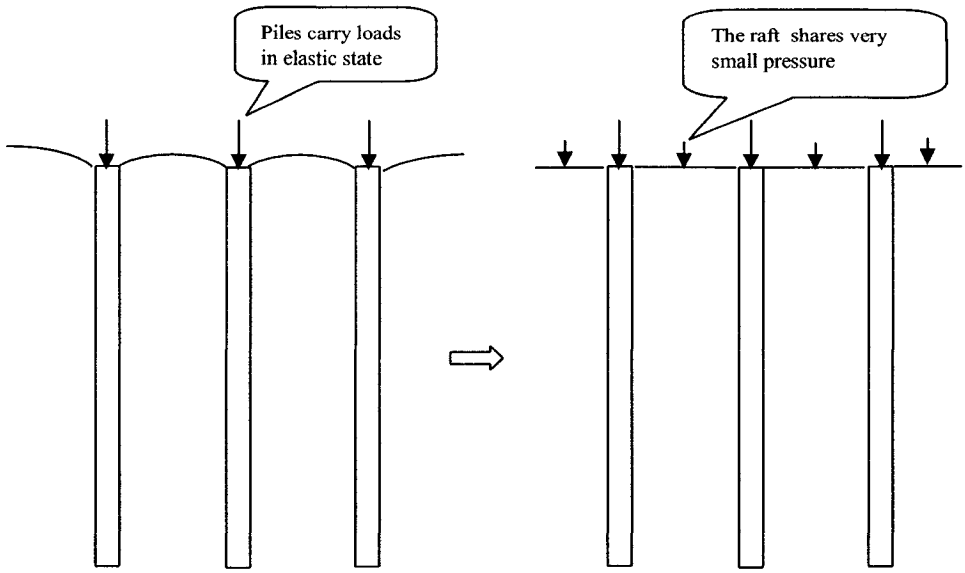

a) Working loads applied on piles equal to half the ultimate bearing capacity (Elastic state)

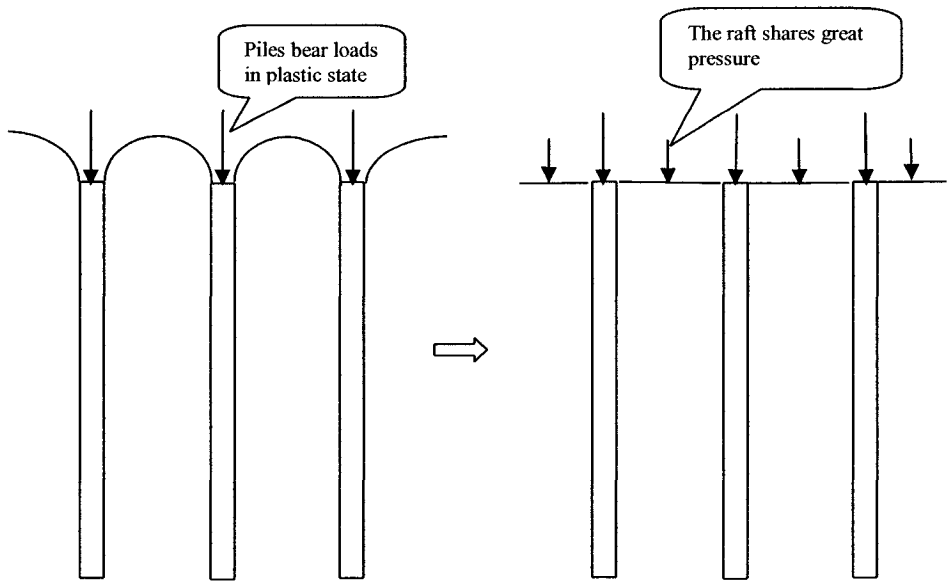

b) Working load applied on piles almost reaching ultimate bearing capacity (Plastic state)

Fig. 2-9 Relationship between the Bearing Load of Piles and Soil

In Fig. 2.9(b), the piles carry loads in the plastic state (the piles' load is near the value of the ultimate bearing capacity of the piles). In imaging case of a high-set cap, the settlement difference between the pile and the soil around the pile is quite big, thus in the case of the low-set cap, a great surface pressure on the soil is required for the soil settlement to reach the same value of pile settlement needs. The surface pressure on the soil is provided by interactive raft in case of low-set cap. Only in this state does the pile-soil-raft interaction design have engineering meaning.

The following approximate theoretical analysis also describes the pile-soil-raft interaction design principle. From Fig. 2.10, the settlement on the pile at point A is:

$$S_A=\Delta S_{PE} + \delta + S_b \qquad (2\text{-}51)$$

where S_A = the settlement at point A on the pile;

ΔS_{PE} = the elastic compressive deformation of the pile body between the top and the base of pile;

δ = the deformation of pile-end punching into soil at the pile base;

S_b = the settlement of the soil at pile base.

At the bottom of the raft, the settlement at point B is given by:

$$S_B = \Delta S_{SL} + S_b \qquad (2\text{-}52)$$

Where ΔS_{SL} is the compressive deformation of the soil between the top and the base of the pile

When the settlement at point A is equal to that of point B (e.g., $S_A = S_B$), the following relationship is obtained:

$$\square\Delta S_{SL} = \Delta S_{PE} + \delta \qquad (2\text{-}53)$$

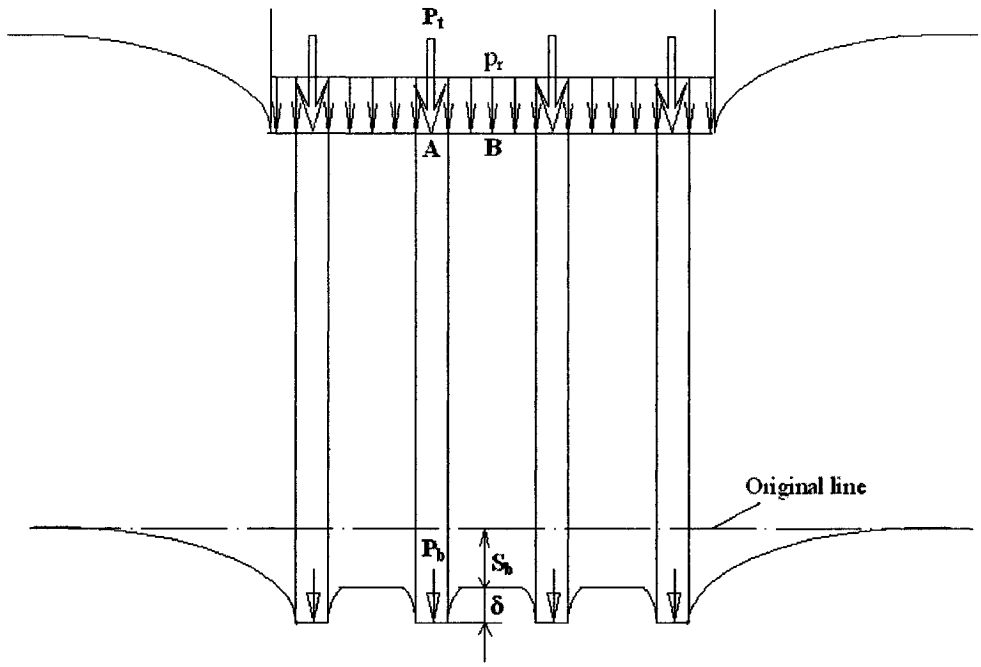

Fig.2-10 Loads and Settlements of Pile-Soil-Cap System

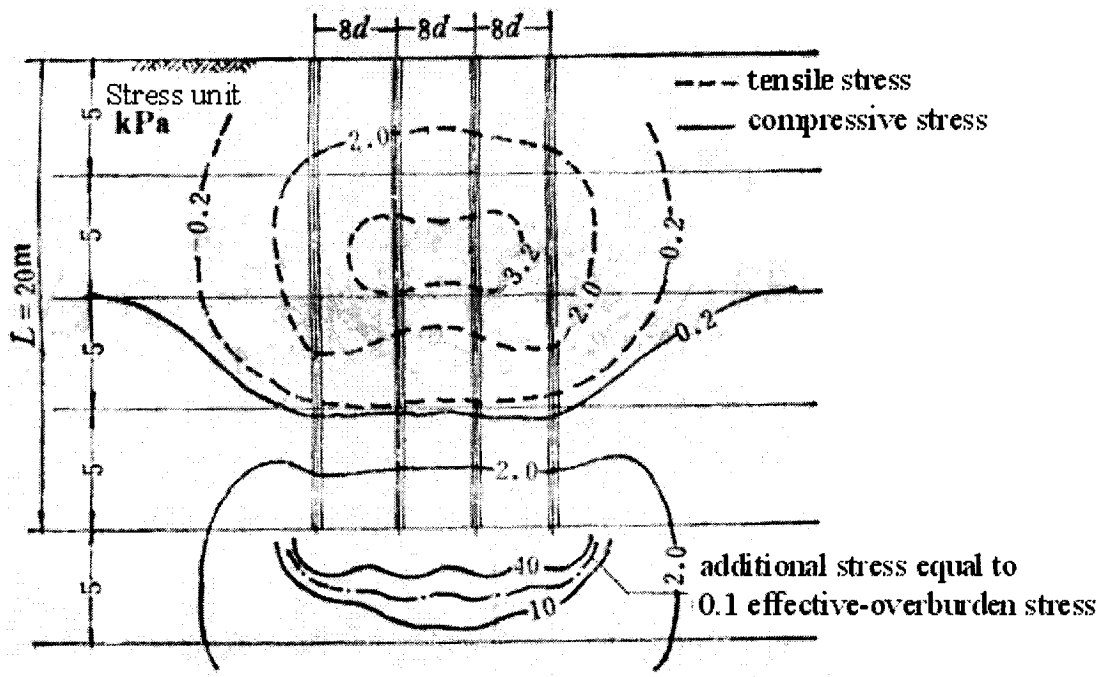

Fig. 2-11 Additional vertical stress caused by piles (from Zai & Zai 1993)

The elastic deformation of the pile body ΔS_{PE} is very small. Likewise, it can also be proved that δ is also very small in the elastic phase of the pile load–settlement. Therefore, the compressive deformation of the soil under the raft ΔS_{SL} is quite small. Moreover, ΔS_{SL} is mainly created by the pressure p_r on the bottom of raft, which is due to the pile-shaft frictional stress and the pile-base pressure that cause negative (or tensile) additional stresses on most of the pile's depth and cause very small compression (shown in Fig. 2-11).

$$p_r \approx \frac{E_s}{\alpha_{av}(1-\upsilon_s^2)} \frac{\Delta S_{SL}}{B} \tag{2-54}$$

Where E_s is elastic modulus of soil, υ_s is Poisson's ratio of soil.

Equation (2-54) proves that p_r is small, because ΔS_{SL} is quite small, in the elastic level of piles' load–settlement. According to Fleming et al. (1992), the following relationships exist in the elastic phase between ΔS_{PE}, δ, ΔS_{SL}, the forces of the pile top, P_t, and the pile base, P_b, and the pressure of the raft's bottom, p_r,:

$$\delta = \frac{1-\upsilon_b}{4G_b} \frac{P_b}{r_b} \quad \text{(Timoshenko \& Goodier, 1970)} \tag{2-55}$$

$$\Delta S_{PE} = \frac{1}{2}(P_t + P_b) \cdot \frac{\ell}{E_p A_p} \tag{2-56}$$

$$\Delta S_{SL} = a_{av} \cdot \frac{1-\upsilon_s^2}{E_{s1}} B \cdot p_r \tag{2-57}$$

$$\frac{P_b}{P_t} = \frac{\dfrac{4\eta}{(1-\upsilon_b)\xi} \cdot \dfrac{1}{ch(\mu \cdot \ell)}}{\dfrac{4\eta}{(1-\upsilon_b)\xi} + \dfrac{2\pi\rho}{\zeta} \cdot \dfrac{th(\mu \cdot \ell)}{\mu \cdot \ell} \cdot \dfrac{\ell}{r_o}} = \alpha \tag{2-58}$$

$$S_b = \frac{1-\upsilon_b}{4G_b}\frac{\alpha' \cdot Q}{\sqrt{4BL/\pi}} \qquad (2\text{-}59)$$

Where $\eta = r_b/r_0$ (ratio of under-ream radius, for under-reamed piles)

$\xi = G_l / G_b$ (ratio of end-bearing modulus, for end-bearing piles)

$\rho = G_{av} / G_l$ (variation of soil modulus with depth)

$\lambda = E_p / G_l$ (pile-soil stiffness ratio)

$\zeta = \ln (r_m/r_o)$ (measure of radius of influence of pile)

$\mu l = (l / r_o)\sqrt{(2/\zeta\lambda)}$ (measure of pile compressibility)

It should be noted that r_b and r_0 are the radii of the base of the under-reamed piles and of the shaft respectively. The variation with depth of the soil's shear modulus is idealized as being linear Gibson's soil by the following relationship: $G=G_0+mz$, where z is the depth. There is also a possibility of a sharp rise in the value of G_b for levels below that of the pile base, that is for

$G_{av}=G|_{z=l/2}=G_{l/2}$;

$G_l = G|_{z=l/2}$;

$r_m = \{0.25+\xi[2.5\rho(1-\upsilon_s)-0.25]\}l$ (Randolph & Wroth 1978);

υ_s and υ_b are Poisson's ratios of soil for depths where $z \leq l$ and for levels below that of the pile base respectively;

α' is the α value calculated with an equivalent larger pile (pier), which has an equivalent modulus $E_{eq}= E_s+(E_p-E_s)(A_p/A_g)$ and an equivalent diameter $d_{eq} =\sqrt{(4A_g/\pi)} =1.13\sqrt{A_g}$, where A_g is area of the pile group and $r_o= d_{eq}/2$ (as per Randolph 1994);

l is the length of piles; and

B, L are breadth and length of the section of the equivalent pile (pier).

The following two examples will be used to depict the reasons why an analysis of pile-soil-raft interaction is nonlinear and piles-soil relationship is in the plastic state.

Example 1

A 6 m × 6 m raft uses 4 × 4 piles with pile length L = 20 m, pile section area A_p = 0.4 m ×0.4 m = 0.16 m^2 (equivalent diameter d_{eq} = 0.45135 m), pile modulus E_p = 28 000 MPa and the following soil parameters: $G_{av} = G_l$ = 12 MPa, υ_s = 0.35 (E_s = 32.4 Mpa), G_b = 40 Mpa, υ_{sb} = 0.25 (E_{sb} = 100). Therefore, $\eta = 1$, $\xi = G_l / G_b = 0.30$, $\lambda = E_p/G_l = 2333$, $\rho = G_{av}/G_l = 1$ and $\zeta = \ln (r_m/r_o) = 4.4$. From equations (1-1) to (1-8), one obtains a value for α= 0.078 (=7.8%) in the elastic state.

Assuming a pile working load P_t = 800KN, then $P_b = \alpha P_t$ = 62 kN. Using equations (2-55) and (2-56), it is found that δ = 1.30 mm and ΔS_{PE} = 1.925 mm. From equation (2-53), it is found that $\Delta S_{SL} = \delta + \Delta S_{PE}$ = 3.225 mm. Finally, using equation (2-57), it is determined that $p_r = \dfrac{\Delta S_{SL} E_s}{B(1-\upsilon_s^2)a_{av}}$ = 20.456 kPa (real value $p_r' = p_r A_r/(A_r - n_p A_p) = 1.076 p_r$; where p_r is the idealized value of raft bottom pressure without piles). Therefore, $Q_p = 16P_t$ = 12800 kN; $Q_r = A_r p_r$ = 736.4 kN and $Q_r/(Q_p+Q_r)$ = 5.44%, which is very small.

If large pile bearing loads are allowed to develop in the plastic phase, the value of δ will greatly increase and that of p_r can also become quite large.

Example 2

Assuming a 4-pile load P_t of 1600 kN (which is close to the ultimate bearing capacity) for the case presented in Example1, $\alpha \rightarrow 0.2$, $P_b \rightarrow 0.2 \times 1600$ kN = 320 kN (where $\sigma_b = P_b/A_p = 2000$ kPa), then $\Delta S_{PE} = 4.29$ mm; supposing $\delta = 2$ cm = 20 mm yield $\Delta S_{SL} = \delta + \Delta S_{PE} = 24.29$ mm. Although pile-soil relationship is in yield state, raft-soil is still in elastic state. Using equation (2-57), $p_r = 154.1$ kPa, which is about 7.5 times the value obtained in Example 1. $Q_p = n_p \cdot P_t = 6400$ kN and $Q_r = A_r \cdot p_r = 5547.6$ kN and so $Q_r / (Q_p + Q_r) = 0.46 = 46\%$, which is approximately 11.7 times the value obtained in Example 1.

The comparison of the above examples, seen in Table 2-3, shows that in cases where the pile load reaches up to near ultimate bearing load, the pressure of raft bottom will share greater loads than that in the elastic state, such as under half the ultimate bearing load of the piles. Therefore, any analysis of pile-soil-raft interaction has to be in a nonlinear or plastic state.

Table 2-3 Comparison of examples in elastic state and in plastic state

Example1 (pile in elastic state)	Example 2 (pile in plastic state)
$n_p = 16$ $P_t = P_u/2 = 800$ kN	$n_p = 4$ $P_t = P_u = 1600$KN
$\alpha = 7.8\%$ (equation 1-8) $P_b = \alpha P_t = 62$ kN	$\alpha = 0.2$ (ultimate state) $P_b = \alpha P_t = 320$KN ($\sigma_b = q_u = 2$MPa)
$\delta = 1.30$ mm $\Delta S_{PE} = 1.925$ mm $\Delta S_{SL} = \delta + \Delta S_{PE} = 3.225$ mm $S_b = 3.391$ mm $S_1 = \Delta S_{SL} + S_b = 6.62$mm	$\delta = 20$mm $\Delta S_{PE} = 4.29$mm $\Delta S_{SL} = \delta + \Delta S_{PE} = 24.29$mm $S_b = 2.380$mm $S_2 = \Delta S_{SL} + S_b = 26.67$mm
$Q_p = 16P_t = 12\,800$ kN; $p_{r1} = 20.5$ kPa $Q_r = 736$ kN $Q = Q_p + Q_r = 13536$KN $\lambda_1 = Q_r/Q = 5.44\%$	$Q_p = 4P_t = 6400$KN; $p_{r2} = 154.1$KPa $Q_r = 5548$KN $Q = Q_p + Q_r = 11948$KN $\lambda_2 = Q_r/Q = 0.46 = 46\%$
$S_2/S_1 = 4.03$ $p_{r2}/p_{r1} = 7.5$ $\lambda_2/\lambda_1 = 11.7$	

2.8 Prospective of this research

Based on the analysis of the piles-soil-cap interaction, the literature review related to the analyses of the pile-soil-cap, the nonlinear interaction and the governing factors, it can be seen that the current methods of analysis and design does not include the excess pore-water pressure dissipation and, accordingly, its influence on pile group-soil-cap interactive system. The objective of this study, therefore, is to develop an analysis method that incorporates the following considerations, mainly:

1) Excess pore-water pressure dissipation in pile-soil-raft system
2) The increase of the soil shear strength with soil consolidation
3) The increase of soil deformation modulus with soil consolidation
4) The rate of raft sharing load decrease and pile sharing load increase with soil consolidation
5) Foundation settlement associated with the excess pore-water pressure dissipation

CHAPTER 3

ANALYSIS OF PILE-SOIL-RAFT SYSTEM

WITHOUT CONSOLIDATION FACTOR

3.1 General

In this chapter, a numerical model is developed to examine the mechanism of nonlinear pile-soil-raft interaction. Analyses are performed for the cases of (1) a single pile, (2) a one-pile raft, (3) a nine-pile high-set raft and (4) a nine-pile low-set raft, based on the previously described Hybrid method of FLM and GSDT, which combines the finite layer method (FLM) with generalized shear-displacement theory (GSDT). The evaluation of the pore water pressure (p.w.p.) dissipation and the correspondingly analysis of the pile-soil-raft nonlinear interaction in the state of p.w.p dissipation will be presented in Chapters 7 and Chapter 8.

3.2 The Basic Equation of a Piles-Soil-Cap Interactive System

(a) Interactive flexibility coefficient matrices

The soil flexibility matrix, i.e., $[\delta_s]$,

$$\{S\} = [\delta s] \cdot \{F\} \tag{3-1}$$

Equation (3-1) is converted into equation (3-2)

$$\begin{bmatrix} \delta^{SS} & \delta^{SP} \\ \delta^{PS} & \delta^{PP} \end{bmatrix} \cdot \begin{Bmatrix} F_B \\ F_P \end{Bmatrix} = \begin{Bmatrix} S_B \\ S_P \end{Bmatrix} \tag{3-2}$$

where, $\{S_B\}$ and $\{F_B\}$ are the settlement and load of cap element respectively; $\{S_P\}$ and $\{F_P\}$ are the settlement and load of pile element, respectively; $[\delta^{SS}]_{nb\times np}$, $[\delta^{SP}]_{nb\times np}$, $[\delta^{PS}]_{np\times nb}$ and

$[\delta^{PP}]_{np\times np}$ are respectively the interactive flexibility coefficient matrices of soil—soil, soil—pile, pile—soil and pile—pile element points; n_b is the number of cap load elements, n_p is the number of pile load elements. They can be established by the above FEM, BEM or FLM based on elastic theory. The flexibility coefficient δ_{ii}^{PP} can be added to plastic displacement coefficients, based on the generalized shear-displacement theory, to analyze pile-soil-raft nonlinear interaction (Zai & Yang 1993a, 1993b; Yang & Zai 1994).

Because actual soil is not elastic and cannot bear tensile stress, partly like the Winkler model, the elastic solution overestimates piles–soil–cap interactions, as shown in Fig. 2-6. Based on the figure, the modified factor of pile-pile or pile-soil settlement interactive factor can be obtained

$$f_{sp} = \alpha^{-r/d} \qquad (3\text{ -}2a)$$

in which, $\alpha = 1.11$ when $r_m = 12d$. The curve obtained from equation (3-2a) is illustrated in Fig. 3.1.

Same, the soil-soil settlement interactive coefficient should be modified as

$$f_{ss} = \beta^{-\frac{r}{\sqrt{A}}} \qquad (3\text{-}2b)$$

Where: $\beta = 1.5$, $B = \sqrt{A}$, the curve obtained from equation (3-2b) is shown in Fig. 3.2.

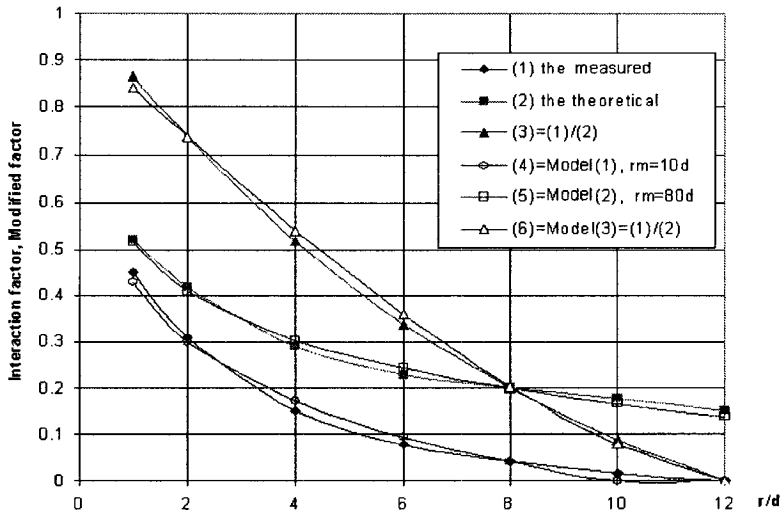

(1) The measured from Cooke at el (1980);
(2) The elastic theoretical solution from Poulos & Davis (1980);
(4) Interaction factor α= 0.56[1-ln(2r/d)/ln(24)] for modeling (1);
(5) Interaction factor α= 0.62[1-ln(2r/d)/ln(80)] for modeling (2);
(6) Modified factor f_{sp} = $0.95(1-r/d/24)^{1.4}$ for modeling (3)=(1)/(2);

Fig. 3-1 Interaction factor α_{sp} and Modified factor f_{sp}

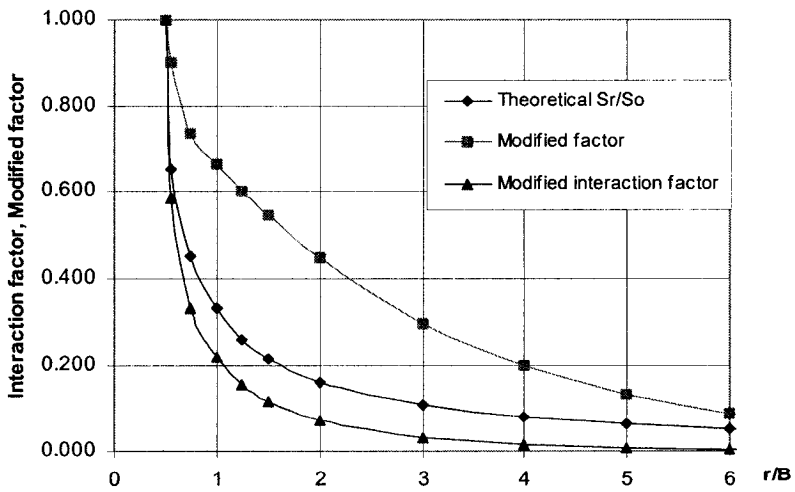

Fig.3-2 Interaction factor α_{ss} and Modified factor f_{ss}

(b) Basic Equations for Interaction Analysis

Finding the inverse of the flexibility matrix of equation (3.1), i.e. $[\delta_S]^{-1}=[K_S]$, one obtains

$$\begin{bmatrix} K^{SS} & K^{SP} \\ K^{PS} & K^{PP} \end{bmatrix} \cdot \begin{Bmatrix} S_B \\ S_P \end{Bmatrix} = \begin{Bmatrix} F_B \\ F_P \end{Bmatrix} \qquad (3\text{-}3)$$

Extending $[K_P]$ of equation (2.31) with zeros into the same number of element as equation (3-3), and then adding extended equation (2.31) to equation (3-3) yields equation (3-4):

$$\begin{bmatrix} \underline{K}^{SS} & \underline{K}^{SP} \\ \underline{K}^{PS} & \underline{K}^{PP} \end{bmatrix} \cdot \begin{Bmatrix} S_B \\ S_P \end{Bmatrix} = \begin{Bmatrix} \underline{F}_B \\ 0 \end{Bmatrix} \qquad (3\text{-}4)$$

i.e, $$[K_{sp}] \cdot \{S\} = \{F\} \qquad (3\text{-}4')$$

Where, $\{\underline{F_B}\} = \{F_{\underline{B}}\}+\{P\}$, which is compound forces of the load of the cap element and the load at the pile head. Separating (3-4), the equation is transformed as follows:

$$[\underline{K}^{SS}]\cdot\{S_B\} + [\underline{K}^{SP}]\cdot\{S_P\} = \{\underline{F_B}\} \qquad (3\text{-}5a)$$

$$[\underline{K}^{PS}]\cdot\{S_B\} + [\underline{K}^{PP}]\cdot\{S_P\} = \{0\} \qquad (3\text{-}5b)$$

Equation (3-6) is obtained from (3-5b):

$$\{S_P\} = -[\underline{K}^{PP}]^{-1}\cdot[\underline{K}^{PS}]\cdot\{S_B\} \qquad (3\text{-}6)$$

Substituting equation (3-6) into (3-5), one obtains

$$\{\underline{F_B}\} =([\underline{K}^{SS}] - [\underline{K}^{PS}]\cdot[\underline{K}^{PP}]^{-1}\cdot[\underline{K}^{PS}])\cdot\{S_B\} \qquad (3\text{-}7)$$

Setting $[K]= [\underline{K}^{SS}] - [\underline{K}^{SP}]\cdot[\underline{K}^{PP}]^{-1}\cdot[\underline{K}^{PS}]$, equation (3-7) becomes

$$[K]\cdot\{S_B\} = \{\underline{F_B}\} \qquad (3\text{-}7b)$$

Separating equation (3-4) into (3-7) is known as the sub-structure method.

(c) Basic Equations for a flexible piled raft

The stiffness matrix of a cap is $[K_B]$,

$$[K_B]\cdot\{\underline{S_B}\} = \{\underline{T_B}\} \qquad (3\text{-}8)$$

where $\{\underline{T_B}\}$ includes the compounded loads of the upper structure and $\{\underline{T_B}\} = \{\underline{T_1}, \underline{T_2}, \ldots, \underline{T_{nb}}\}^T$, ($\{\underline{T_i}\} = \{\underline{Q_i}, M_{\theta xi}, M_{\theta yi}\}^T$, i = 1,2,...,nb), and $\{\underline{Q_i}\} = \{Q_i\} - \{\underline{F_B}\}$. Q_i, $M_{\theta xi}$ and $M_{\theta yi}$ are the force; the cap element node's rotating moments for the X-axis and the Y-axis respectively.

$\{\underline{S_B}\} = \{S_i, \theta_{xi}, \theta_{yi}\}$, where S_i is just an element of $\{S_B\}$, and θ_{xi} and θ_{yi} respectively are the rotary angles rotating in the X and Y axis.

Therefore, $[K]_{nb\times nb}$ of equation (3-7b) is extended into $[K']_{(3nb)\times(3nb)}$, and then added to equation (3-8), forming

$$[\underline{K_B}]\cdot\{\underline{S_B}\} = \{T_B\} \qquad (3\text{-}9)$$

Where $[\underline{K_B}] = [K_B] + [K']$; in $\{T_B\}$, $\{T_i\} = \{Q_i, M_{\theta xi}, M_{\theta yi}\}^T$, so that $\{T_B\}$ does not include $\{\underline{F_B}\}$.

From equation (3-9), we get a solution for $\{\underline{S_B}\}$. $\{\underline{S_B}\}$ can be used to find the internal forces of the cap; $\{S_B\}$ belonging to $\{\underline{S_B}\}$ is substituted into equation (3-6) to get the pile element settlement $\{S_P\}$; $\{S_B\}$ and $\{S_P\}$ are then substituted into (3-4) to obtain $\{F_B\}$ and $\{F_P\}$, which are the loads on the soil under the raft and around piles respectively.

Non-linear or elastic-plastic interactive solutions should adopt the stepwise–increment calculation method.

(d) Basic Equations for a rigid piled raft

It is necessary again to find the inverse of the stiffness matrix [K] of equation (3-7b), i.e., $[\delta] = [K]^{-1}$, and by introducing the condition for a rigid raft, the basic interactive equation is expressed as follows,

$$\begin{bmatrix} [\delta] & -[A'] \\ [A] & 0 \end{bmatrix} \cdot \begin{Bmatrix} \underline{F}_B \\ V \end{Bmatrix} = \begin{Bmatrix} 0 \\ M \end{Bmatrix} \qquad (3\text{-}10)$$

in which, $[A] = \begin{bmatrix} 1 & 1 & \cdots & \cdots & 1 \\ x_1 & x_2 & \cdots & \cdots & x_{nb} \\ y_1 & y_2 & \cdots & \cdots & y_{nb} \end{bmatrix}$; x_i, y_i, $i = 1 \sim nb$, are node coordinates of cap elements; $\{V\} = \{S_0, \theta_x, \theta_y\}^T$, w_0 is the vertical displacement of the coordinates' origin; θ_x, θ_y are the respective X and Y direction gradients (angles of inclination) of the cap; $\{M\} = \{Q_0, M_x, M_y\}^T$, the external load Q_0, the moments rotating the X-axis and Y-axis. By solving equation (3-10), one gets the solution for $\{\underline{F}_B\}$ and $\{V\}$. The settlement for each point of the cap can be expressed as:

$$S_{Bi} = S_0 + \theta_x \cdot x_i + \theta_y \cdot y_i \quad (i=1 \sim nb) \qquad (3\text{-}11)$$

Substituting $\{S_B\}$ into equation (3-6), we get the settlement of the pile node $\{S_P\}$. Substituting $\{S_B\}$ and $\{S_P\}$ into equation (3-4), we get loads of cap and pile element point, i.e., $\{F_B\}$ and $\{F_P\}$. Loads acting on pile heads can be found by $\{\underline{F}_B\} - \{F_B\}$.

The above can also be achieved by finding the inverse of the stiffness matrix [K] of equation (3-5) (i.e., $[\delta]=[K_{sp}]^{-1}$), or by adding equation (2.32) to (3-1) (i.e., $[\delta]=[\delta s]+[\delta_p{}^1]$), and applying the condition for a rigid raft, one directly gets $\{S_B\}$ and $\{S_P\}$. Equation (3-10) in this case becomes (nb+np+3)×(nb+np+3), requiring more initial computer storage space.

3.3 Running Tests for Validations

Selecting the Hybrid methods, my existing program was modified and executed according to the previously mentioned FLM and GSDT. Now this program can just analyze piles-soil-raft nonlinear interactions without considering the influence of pore pressure and its dissipation. The running tests involved responses for a load action on a plate without a pile, on a rigid pile, and on a compressible pile. Those responses may be validated by comparison with existing theoretical solutions or actual experience.

Test 1

A point force Q=1000KN acting on a 1.0 m ×1.0 m square plate on soil with an elastic modulus E_s = 2500 Kpa (i.e., $G = \frac{E_s}{2(1+\mu)}$ = 1000Kpa), a Poisson's ratio μ = 0.25, and a soil thickness (bottom depth) H = 50m. According to elastic theory on half-infinite spaces, the plate settlement is defined as being:

$$S = \frac{\pi}{4}\frac{1-\mu^2}{E_s} D \cdot p = \frac{1-\mu}{2 \cdot G}\frac{Q}{D} \qquad (3\text{-}18)$$

Where D is the diameter of the circular plate, $D = \sqrt{\frac{4}{\pi}\text{Area}} = 1.1284\sqrt{\text{Area}}$, p is the average load area, Q is the point force, where Q = p×Area. Then, D = 1.1284 × √(1) = 1.1284 m. According to equation (3-18),

$$S = \frac{1-0.25}{2\times 1000} \times \frac{1000}{1.128} = 0.3324 \text{ m}$$

The computed settlement result is of 0.3078 m, which is fairly close to 0.3324 m (a portion of the difference can be attributed to the difference between the half-infinite

space theory and the finite compressible layer theory), shown in Table 3-1, basically proves that the program is feasible.

Test 2

Q = 1000 kN acting on a rigid pile, its length L= 20 m, its section b×b= 0.4 m × 0.4 m, (equivalent diameter d = 4 × b/π = 0.5093 m for the circumference, and d' = 1.1284 × b = 0.45136 m for an area section). The soil around the pile is the same as in Test 1. According to Poulos & Davis (1980), the pile's settlement is defined by:

$$S=\frac{P}{E_s d}I \qquad (3\text{-}19)$$

Where, $I = I_0 R_K R_H R_b R_v$, of whom the meaning and value of each component is given in pages 87 to 89 of Poulos & Davis (1980). For *l*/d = 20/0.5 = 40, $I_0 = 0.043$, $R_K = R_b = 1.0$, $R_H = 0.84$, $R_v = 0.92$ when Poisson's ratio $\mu = 0.25$. Then, $I = I_0 R_K R_H R_b R_v = 0.043 \times 0.84 \times 0.92 = 0.04047$. Thus, $S = \frac{1000}{2500 \times 0.51} \times 0.04047 = 0.03174$ m. The computed result is 0.03034, which is very close to 0.3174 (Table 3.1). Therefore the program is good.

The following two figures in Fig.3-3 are respectively the axial force P_z and the shear stress τ_z (t in the figure) with changing depth z. From these figures, one can see that shear stress on the rigid pile is developed from the lower part of the pile shaft.

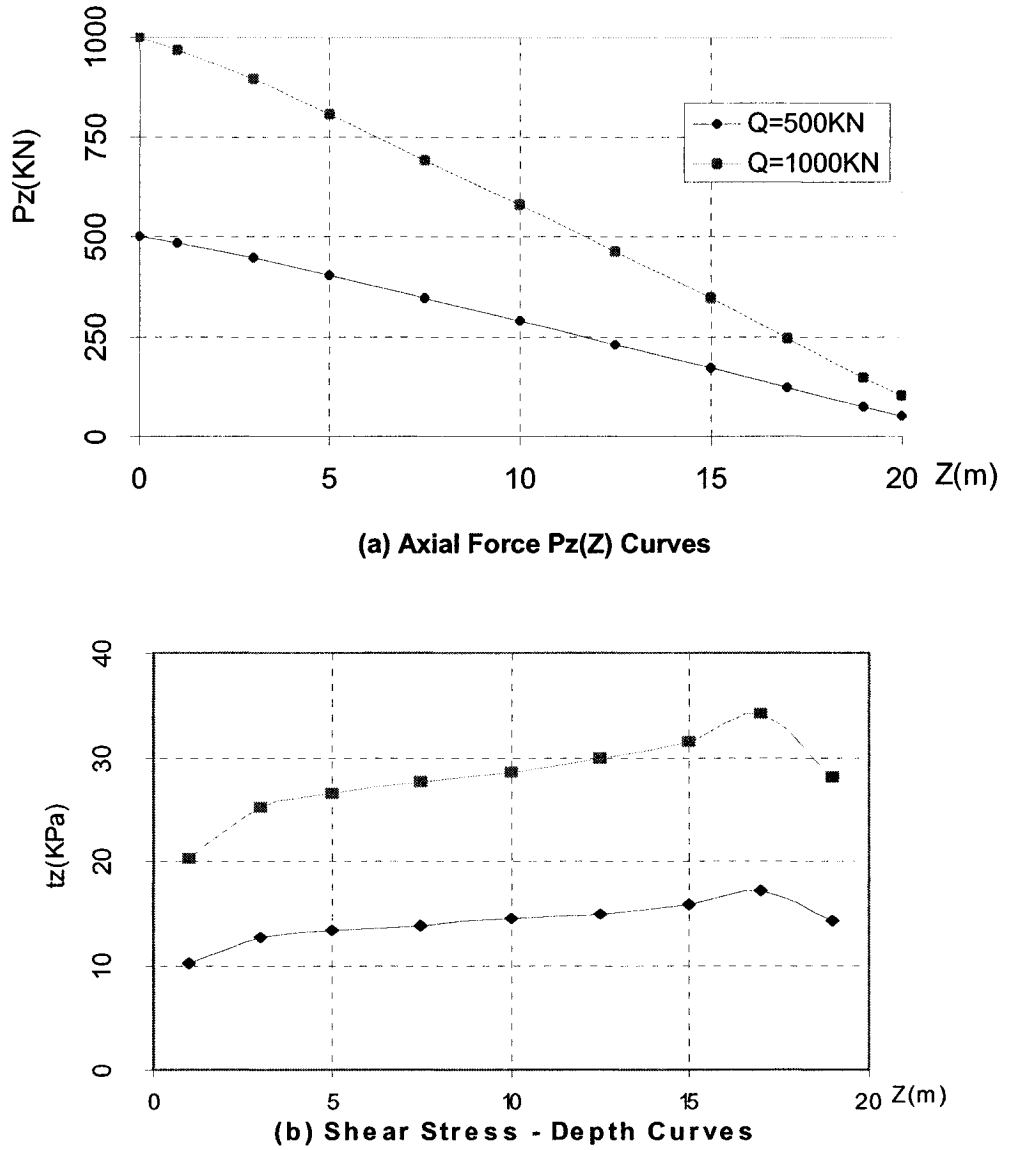

Fig. 3-3 $P_z(z)$ &$\tau_z(z)$ Curves (rigid pile)

Test 3

The pile in Test 3 was set as being compressible, with an elastic modulus of the pile E_p = 250Mpa (i.e., the ratio of modulus K = E_p / E_s= 1000). As per Poulos & Davis (1980), R_K ≈ 1.28, I = 0.04047×1.28 = 0.05180, then S ≈ 0.3174×1.28 = 0.04063 m.

The computed settlement, as a result of it, is 0.04024 m, which is close to 0.04063 m (shown in Table 3.1). The program is therefore also accepted.

The axial force $P_z(z)$ and shear stress $\tau_z(z)$ in the compressible pile case differs from those in incompressible pile cases, shown in Fig. 3-4. A comparison of Fig. 3-3 and Fig. 3-4 demonstrates that the shear stress on a rigid pile (Test 3) develops from the lower part of a pile shaft; while that on a high compressible pile develops from the upper part of the pile (shown in Fig. 3-4). A similar phenomenon is seen for a rigid pile from the result of a low compressible pile, as shown in Fig. 3-7(c) for Case 2, in which the pile elastic modulus is quite high, E_p = 22Gpa, so that Fig. 3-4 is close to behavior of rigid pile.

Table 3-1 Comparison of the computed and the theoretical values

	The calculated (finite compressible layer)	The theoretical (half-infinite space theory)
Test 1 a 1.0×1.0m^2 square plate	S=0.3078m	S=0.3324m
Test 2 a rigid pile with 20×0.4^2 m^3	S=0.03034m	S=0.03174 m
Test 3 a compressible pile with 20×0.4^2 m^3	S=0.04024m	S=0.04063m

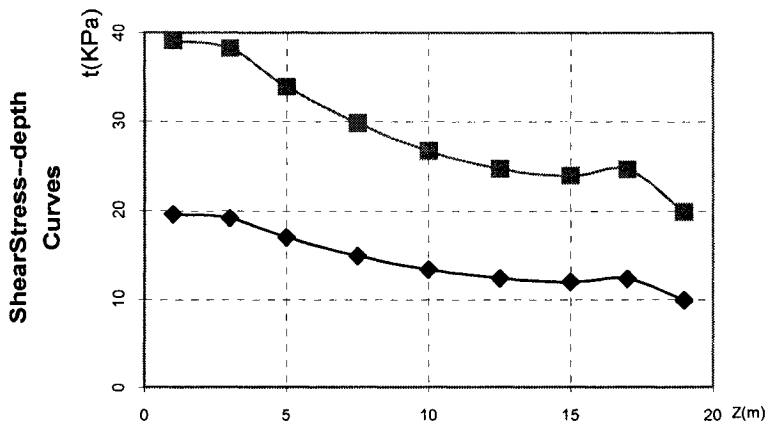

(a) Shear stress – depth curves $\tau_z(z)$

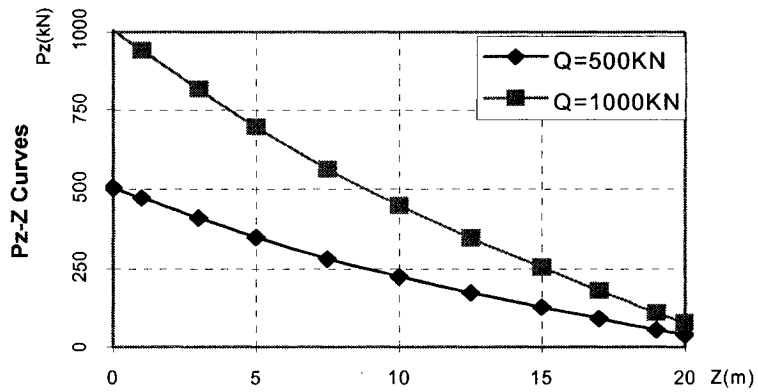

(b) Axial force of pile $P_z(z)$

Fig. 3-4 $P_z(z)$ &$\tau_z(z)$ Curves (elastic pile)

Test 4

Q= 4900KN, the rigid plate is 7 m×7 m, with the same soil conditions as in Test 1. The acting pressure distribution on the bottom of the plate is observed and is found to be in agreement with the actual case, shown in Fig. 3-5.

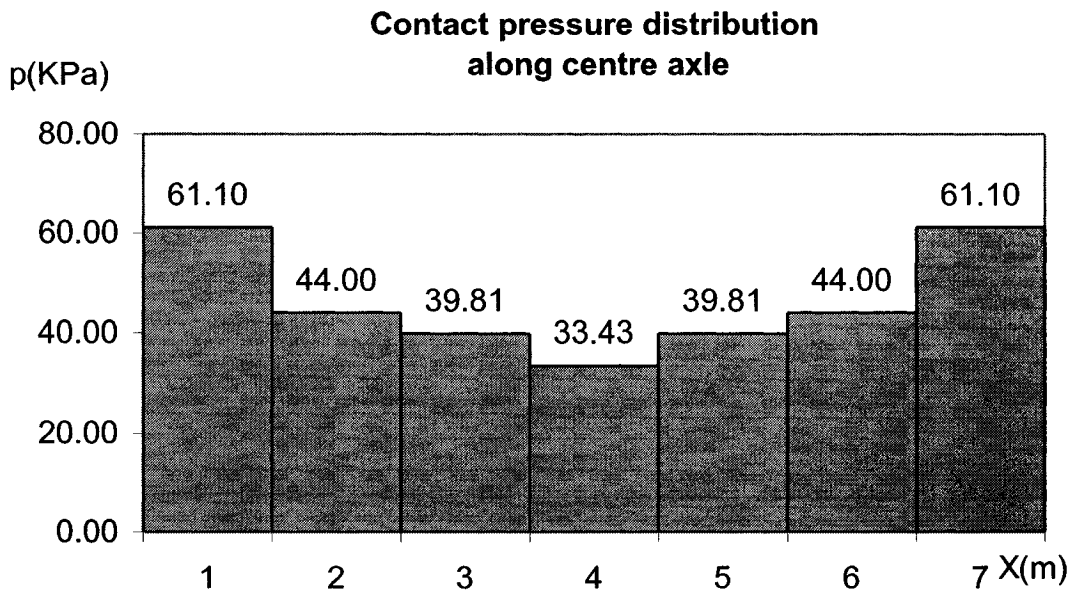

Fig. 3-5 The Computed Distribution of the Pressure on the Bottom of Raft

Test 5

In order to examine the calculated displacement coefficient of soil along different distances r, one sets one unit load acting on a square area, calculates the displacement at each point away from the centre of the load area as shown in Fig. 3-6. The soil elastic modulus Es and Poisson's ratio are the same as in Test1. The calculated range length of the finite layer, i.e., Lg is taken 40m and 60m; the maximum of the distance of the affected point r_{ij} is 19m. The result is shown in Fig. 3-7 (a, b).

From the figures, several regularities are found. First, when the distance of the affected point r_{ij} is close to half the calculating range length of the finite layer, i.e., Lg/2, the coefficient value will be underestimated. Therefore, in general, Lg must be larger than

two times the furthest distance of the affecting point and an unstable value which can take two to four times the square root of the load area, i.e. Lg > 2 ×[r_{max} + (1to2)× $\sqrt{Area}$]. Second, when Nr, selected maximum number of the finite Fourier series, is small, the coefficient value of the furthest affected point will be a wave along the distance; from Fig.3-7(a), the wave appears at a distance of 5× $\sqrt{Area}$. The larger the distance r is, the wavier the coefficient. Although the coefficient value wave is very small, it also causes larger pressure waves on the bottom of raft. Third, the Nr keeping from coefficient wave is related with Lg. At Lg equal to 40 $\sqrt{Area}$, the coefficient value creates a wave if Nr is 20, but not if Nr is 40. If Lg is equal to 60 $\sqrt{Area}$, the coefficient value creates waves if Nr is 40, but not if Nr is 60; i.e. large Lg needs large Nr to escape from coefficient wave. However, large Nr increases the computing time of computer. Therefore, when one applies FLM while adopting the Fourier series and calculates the interaction of raft and soil, it is necessary and very important to try to run the program and determine the calculating range length Lg and the number of Fourier series Nr. Fourth, when the affected distance r_{ij} is more than 12× $\sqrt{Area}$, the affected coefficient of settlement can be taken as being zero.

In the past, one could only take the approach where Nr = 10 to 15 because of the available computers' speeds, which often causes the wave values of the computed pressures on the bottom of raft to be along different place of the axis.

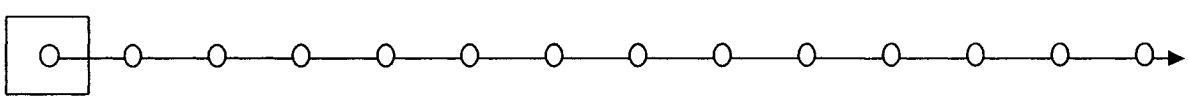

Fig. 3-6 Calculation Points Measured from the Loading Area Centre

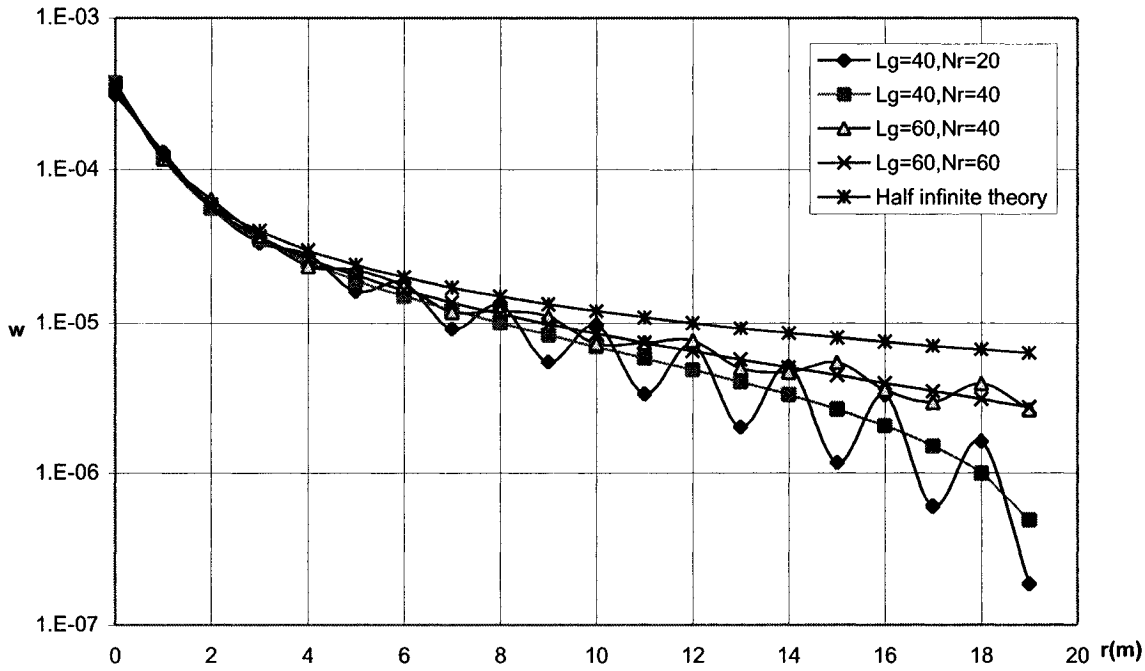

Fig. 3-7(a) The calculated displacement coefficients move along different distance

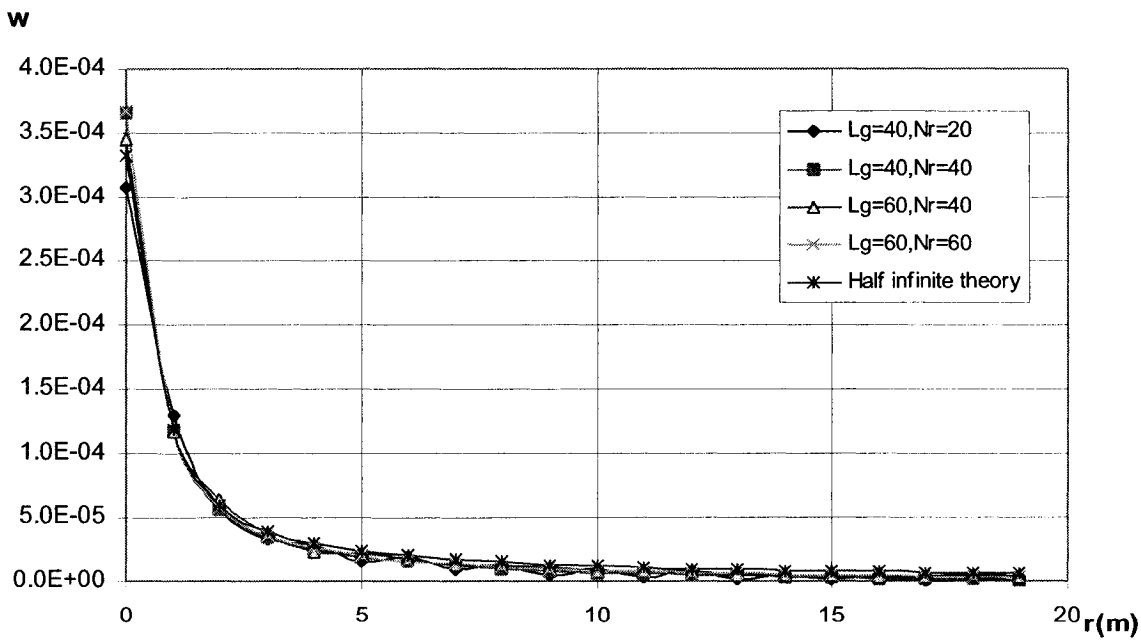

Fig. 3-7(b) The relationship between displacement coefficient and distance

3.4 Cases Analysis and Inference

The following presents the various numerical investigations that were carried out on piled raft models in order to explore the raft effect of pile-soil-raft interaction on settlement, load sharing, development of pile bearing capacity, etc.

Case 1

In this case, a rigid raft having dimensions of B×B= 2.40 m × 2.40 m; the pile is the same as that of Test 4 in Section 3.3, and so B/d ≈ 4.71 (or B/b = 6.0).

The objective of this case is to examine how much the load will be shared by the raft. The total load Q (a point force acting on the center of the raft) was set to 1000 kN. Upon running the program, a settlement result of S = 0.2856 m was obtained, which represents a decrease of 16.81% compared with a pile without a cap or with a high-set cap; the load shared by the raft is p_r = 25.91(KPa), i.e., Q_r = 149.24 kN, 14.92% of the total load. The axial force $P_z(z)$ and the shear stress $\tau_z(z)$ in the compressible pile case differ from those in incompressible pile, as shown in Fig. 3-8.

From Fig. 3-8, one can see that the decreasing effect of raft on a pile extends up to a depth that is larger than the width of the raft in an elastic state. However, in non-linear or plastic states, it was seen that the depth of the raft-decreasing effect has a limit which is at a= depth equivalent to the raft width in Cases 2 and 4.

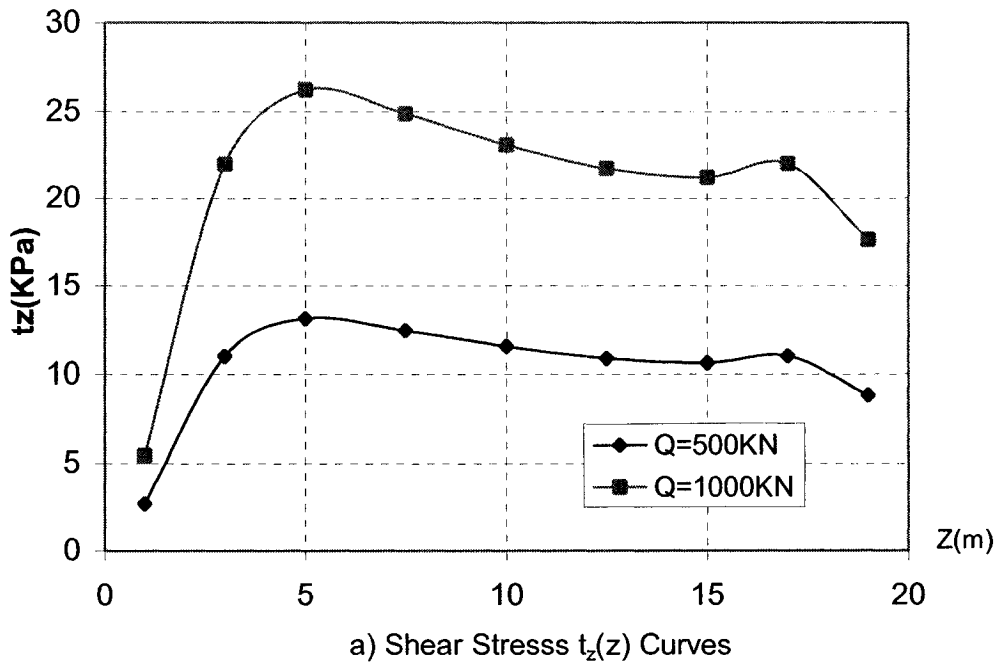

a) Shear Stresss $t_z(z)$ Curves

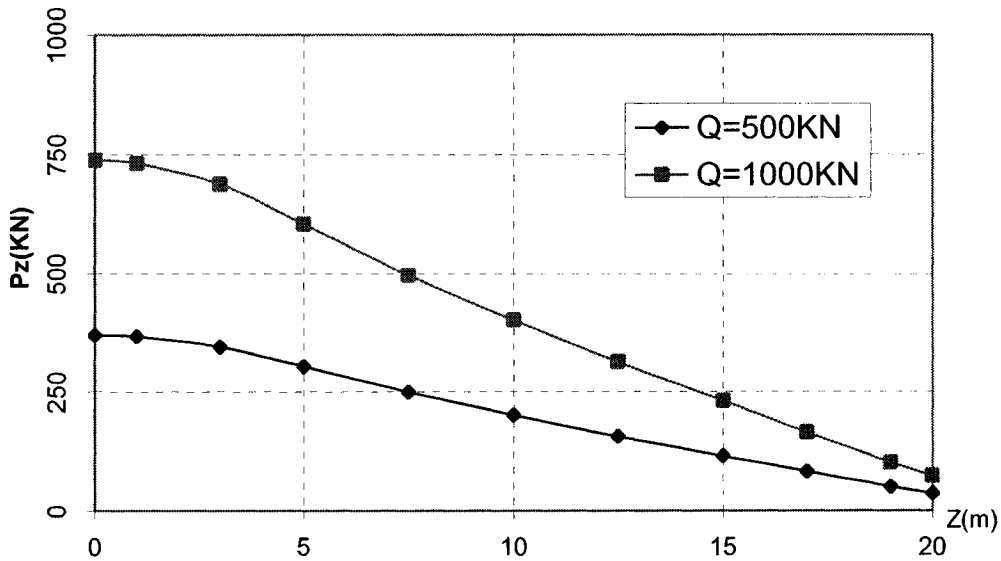

b) Pile Axial Force $P_z(z)$ Curves (pile under raft)

Fig. 3-8 $P_z(z)$, $\tau_z(z)$ Curves (a pile under raft)

Case 2

All of the tests performed within the scope of this case aimed at trying to calculate the non-linear interaction of pile-soil. First, a program run was performed for a single pile, which is a reinforced concrete pile, L×b×b = 20×0.4×0.4 m^3, its elastic modulus E_p = 22 GPa.

***Soil conditions*:**

Soft soil is found from 0.0 m to 20.0 m, E_s=2.5 MPa, with a soil shear strength τ_f = 40 kPa and a linear-elastic critical shear stress τ_e=20 kPa.

At depths ranging from 20.0 m to 50.0m, better soil is found with E_s = 5 MPa, a pile base ultimate bearing capacity σ_{bf} = 1000 kPa, the linear-elastic critical pile-base stress σ_{be} = 450 kPa. The total ultimate bearing capacity of the pile P_u = 1440 kN.

The modeling relationship between the shaft shear stress and the plastic displacement is adopted from the model of Yang & Zai (1994).

Upon running the program, the following results were obtained:

1) Load-settlement nonlinear curve shown in Fig. 3-9 (a)
2) Pile axial force $P_z(z)$ and shear stress on shaft $\tau_z(z)$ curves shown in Fig. 3-9 (b, c)

From the above results, it can seen be that some of the shear stress' contribution in the elastic state is similar to that of a rigid pile, whose shear stress develops from the lower part of the pile shaft. Even in load-settlements in a nonlinear state, shear stress from the lower to the upper part of the pile is almost a uniform contribution. This surmises that the form of the load-settlement nonlinear curve of a pile that is almost rigid might be similar to that of the

shear stress t-z curves, which are shown in Table 2.2. In fact, Chin (1972) once considered truly rigid piles to estimate the ultimate bearing capacity (UBC) of piles; upon this basis, Fleming (1992) adopted the assumption of a rigid pile to establish the load-settlement relationship of a pile. All of the obtained results were in agreement with the test data.

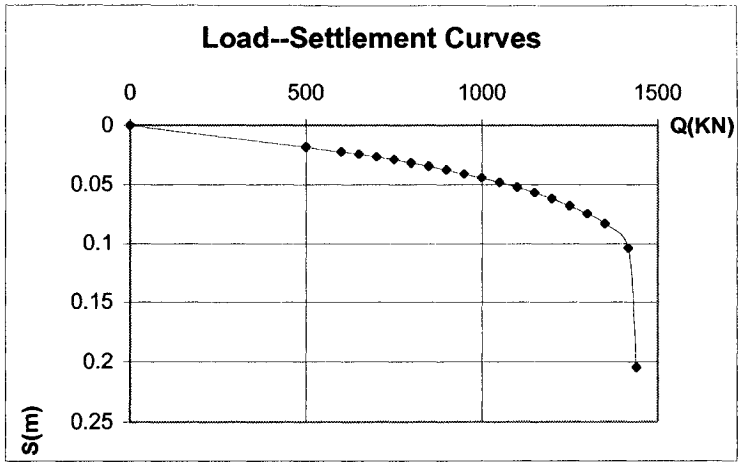

(a) Nonlinear Load-Settlement Curves

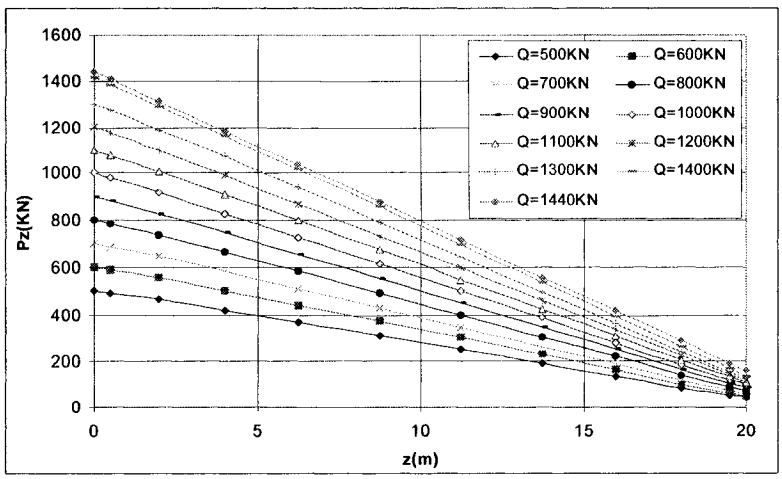

(b) Axial Force $P_z(z)$ Curves

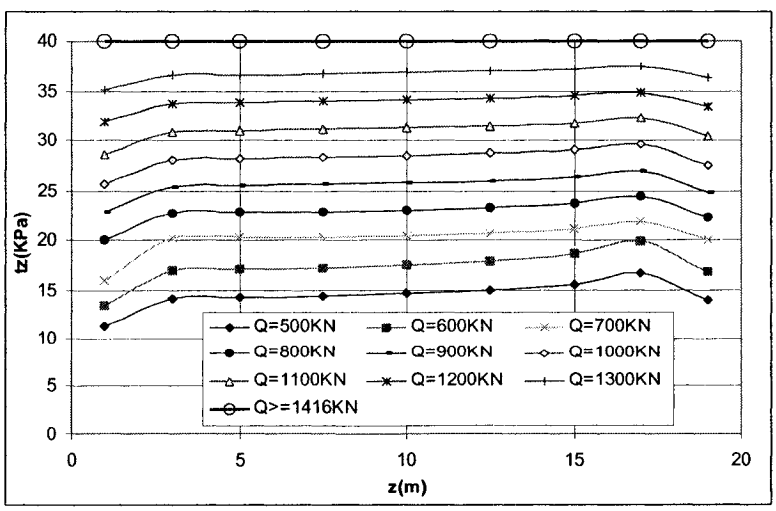

(c) Shear stress $\tau_z(z)$ Curves

Fig. 3-9 Results of Non-linear Interaction of Pile—Soil (Single pile)

Case 3

A piled raft has dimensions B×B = 3.2 m × 3.2 m. The pile and soil conditions are the same as those of Case 2. That is B/b = 3.2/0.4 = 8, B/d ≈ 6.28. The calculated results are the following:

1) The load-settlement curve shown in Fig. 3-10 (a).
2) The pile axial force $P_z(z)$ and the shear stress on the shaft $\tau_z(z)$ curves shown in Fig. 3-10(b, c).
3) The pile-head load versus the pile-end settlement and the total settlement curves seen in Fig. 3-10(d) and Fig. 3-10(e).
4) The pile-end load (P_b) - the total load (Q), as well as the total settlement (S) curves shown in Fig. 3-10(f, j).
5) The pile shaft load ($P_{sh} = P_o - P_b$) develops with total load(Q), as well as the total settlement (S) curves shown in Fig. 3-10(g, k);
6) The load of the raft, Qs, as well as the raft load percentage (hs = Qs/Q, %) developed with total load Q, as seen in Fig. 3-10(h, i)

From the figures mentioned above the following observations can be made:

1) For high-cap foundations (case 2), the settlement development with bearing load will suddenly drop at ultimate state when the load of the pile reaches or exceeds the failure load, shown in Fig. 3-10(1); whereas for low-caps (case 3), settlement gradually develops, even when the load on the pile head is close to, reaches or exceeds the ultimate value of the pile bearing capacity, because the cap bears the

excess load increase close to or after reaching the ultimate state, shown in Fig. 3-10(1).

2) In the elastic phase of the load-settlement relationship of a pile-soil system, the raft's decreasing action on the shear stress (frictional) development of the upper part of the pile shaft is evident. This decreasing action obviously weakens as the load on the pile develops close to failure or ultimate, shown Fig. 3-10(c) $\tau(z)$ curves. In this case, the raft's decreasing factor $\xi_p = P_0/P_u = 1400/1440 = 0.9722 \approx 1$ due to the small width of the raft.

3) The affecting depth of the decreasing action $z_r \approx B$; the reducing value of pile's final bearing capacity for a raft's decreasing action, $\Delta P_{ub}=P_u-P_0\approx \frac{1}{3}\tau_f z_r$ (estimated by frictional stress $\tau(z)$ are $f(z^2)$ curves in the ultimate state). In the case where $\Delta P_{ub} \approx 40 \times 3.2/3 = 42.7$KN, the estimate agrees with the numerical modeling value from, and near 40KN, the numerical result. The raft's decreasing factor $\xi_p = P_0/P_u \approx (P_u-\Delta P_{ub})/P_u = 1397/1440 = 0.9701$, near the modeled value of 0.9722.

4) The sharing ratio of the raft's bearing load $\lambda_s = Qs/Q$ is constant. In the elastic phase, it varies with the development of the elastic-plastic state of the load-settlement of a pile-soil system, and finally it increases up to a constant incremental rate at the pile's ultimate state so long as the load-settlement relationship of the raft-soil system is still in the elastic state, as shown in Fig. 3-10(h, i).

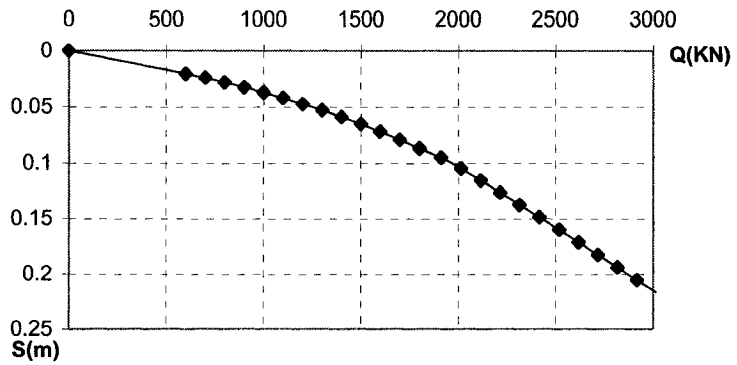

(a) Total Load-Settlement Relationship

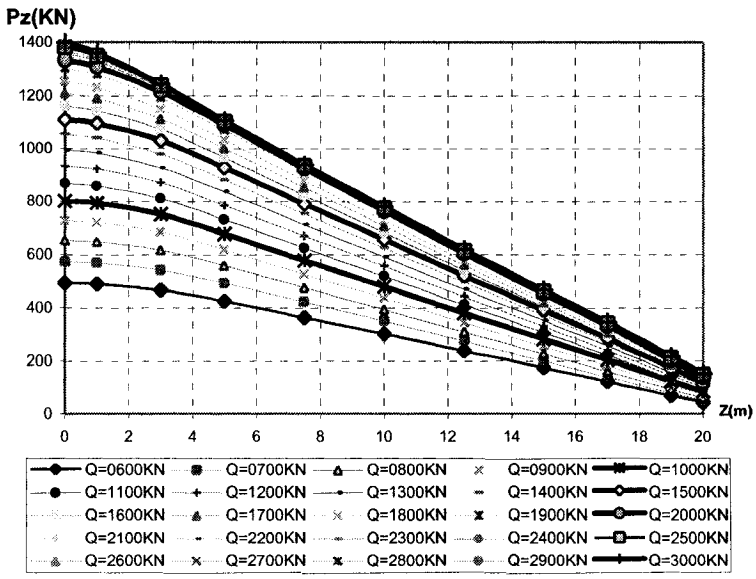

(b) Axial Force $P_z(z)$ Curves

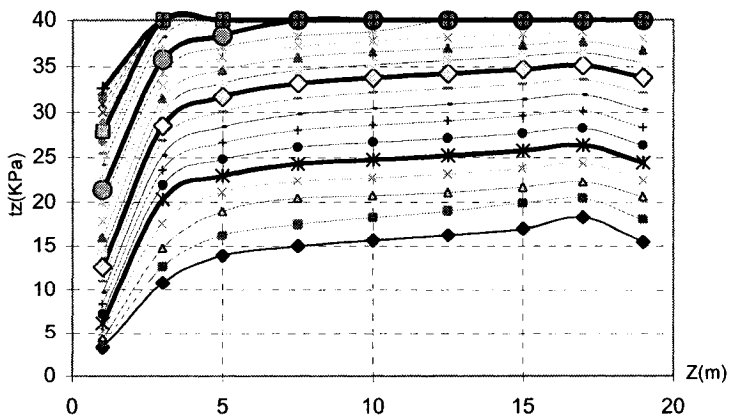

(c) Shear Stress $\tau_z(Z)$ Curves [Legend in (b)]

Fig. 3-10 (a~c) Calculated Loads, Settlements and Stresses of a Raft with a Pile (Case 2)

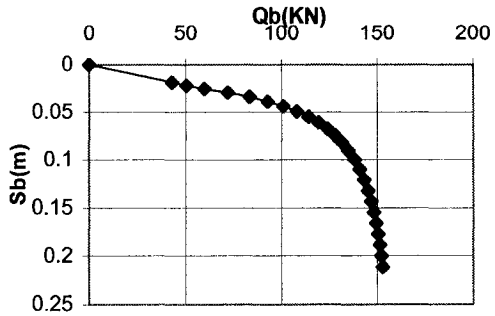

(d) Settlement-Load Curves of Pile End

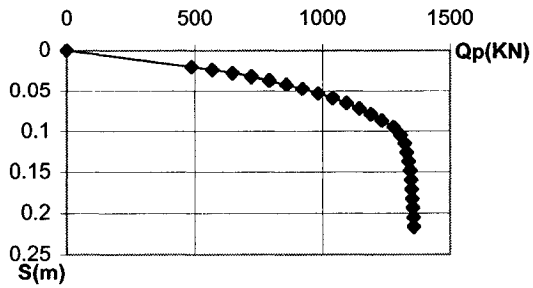

(e) Settlement-Load Curves of Pile Head

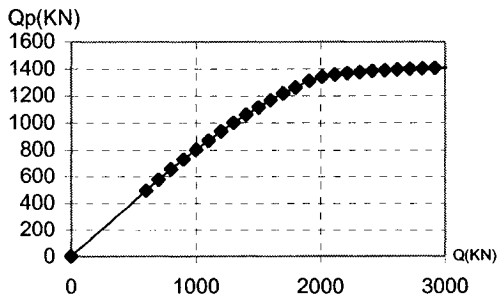

(f) Q-Q_p Curves

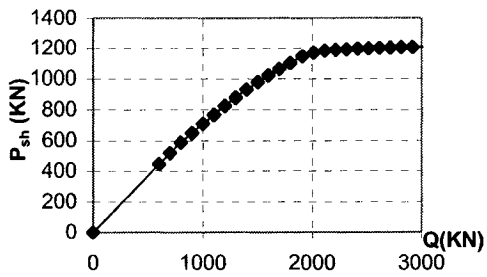

(g) Q—P_{sh}(=P_o-P_b) Curves

Fig. 3-10 (d~g) Calculated Loads, Settlements and Stresses of a Raft with a Pile (Case 2)

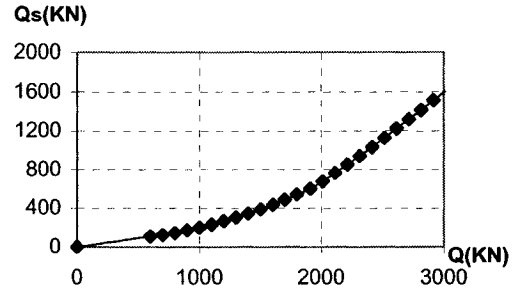

(h) Q-Qs Curves

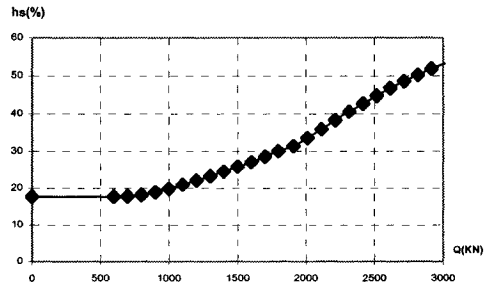

(i) Q-η_s(%) Curves

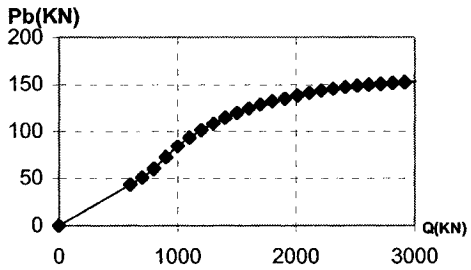

(j) Pile-end load—total load curves

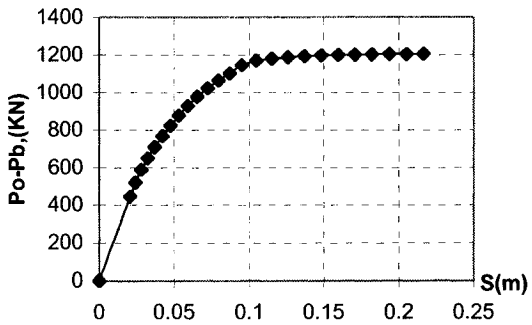

(k) S—P_{sh}(=P_o-P_b) Curves

Fig. 3-10(h~k) Calculated Loads, Settlements and Stresses of a Raft with a Pile (Case 2)

Case 4

A high raft (i.e. the bottom of a raft that does not come into contact with the soil) with 9 piles at a spacing of s = 2.4m. The raft has dimensions B×B = 7.6 m×7.6 m. The piles and soil condition are the as same as those of Test 7 or 8, i.e. s/b = 6. The total ultimate bearing Load $Q_u=9P_u=12.96$MN.

The calculated results are:

1) The total load-settlement curve as seen in Fig. 3-11(a).
2) The load of pile head - the total load curve shown in Fig. 3-11(b).
3) The pile-base load - the total load curve as seen in Fig. 3-11(c).
4) The pile shaft load ($P_{sh} = P_o-P_b$) develops with the total settlement (S) as shown in Fig. 3-11(d).
5) The ratio of the pile-base load to pile–head load, i.e. α_f, develops with the total settlement shown in Fig. 3-11(e).
6) Axial force Pz(Z) and shear stress on shaft τz(Z) curves of corner, edge and centre piles shown in Fig. 3-11(f~k).

From Fig. 3-11(e), it can be seen that the ratios of pile-base load to pile–head load vary according to their location on the raft, even in the elastic phase. However in engineering design, engineers often take the ratio as a constant which is not reasonable.

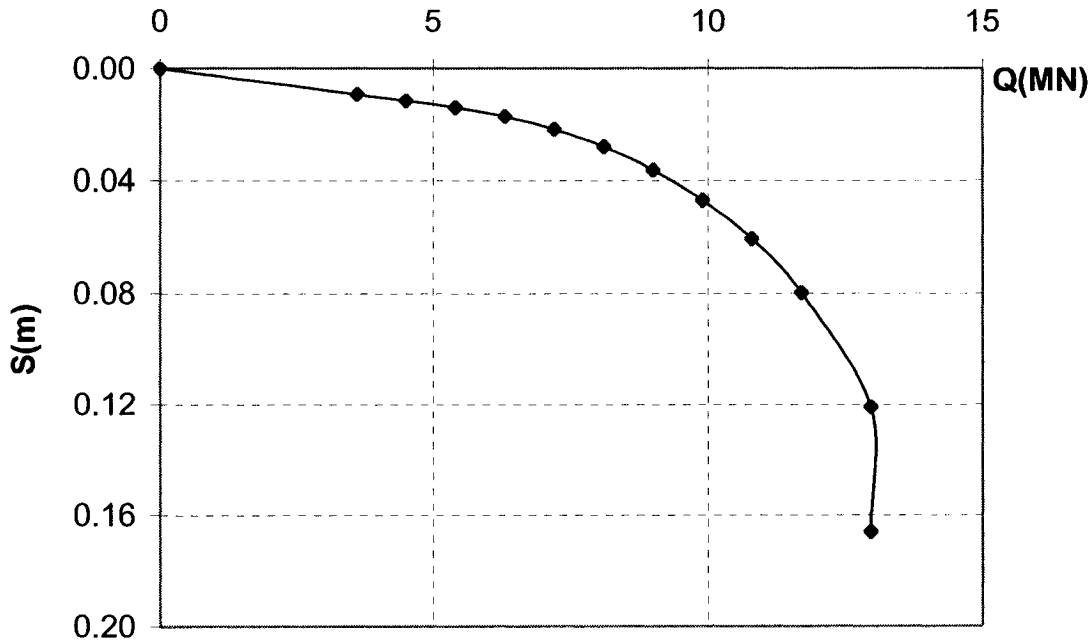

(a) Load--Settlement curve

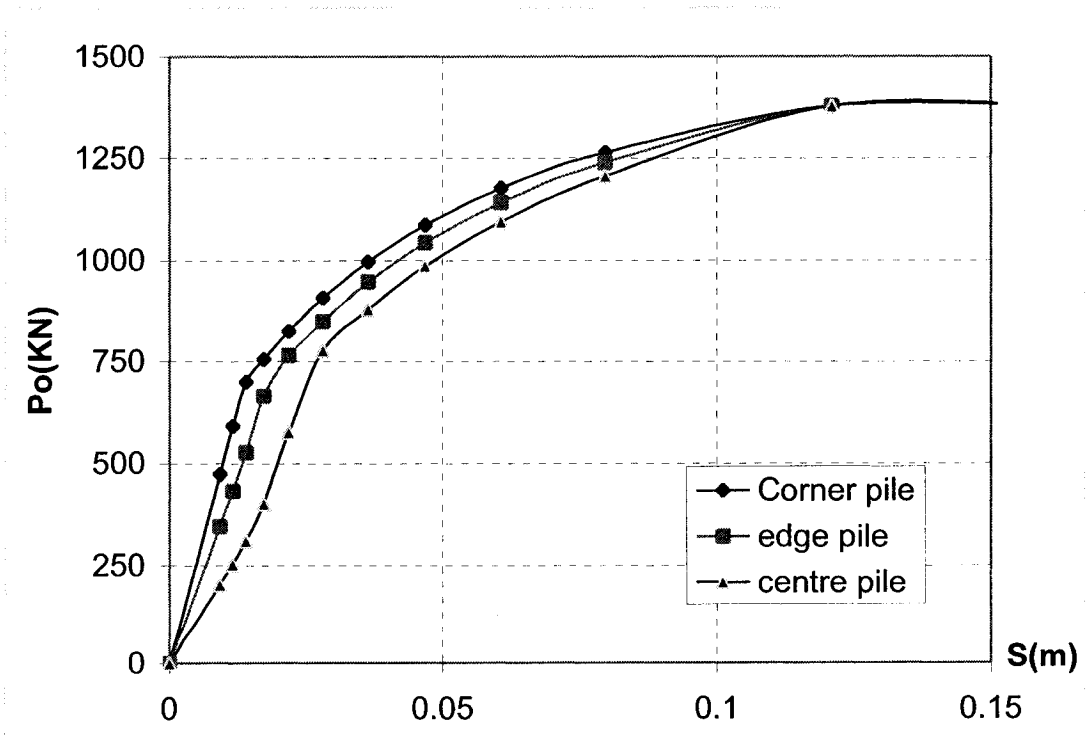

(b) Pile-head Load—Settlement Curves

Fig. 3-11(a, b) Calculated Loads, Settlements and Stresses for High Raft with 9 Piles

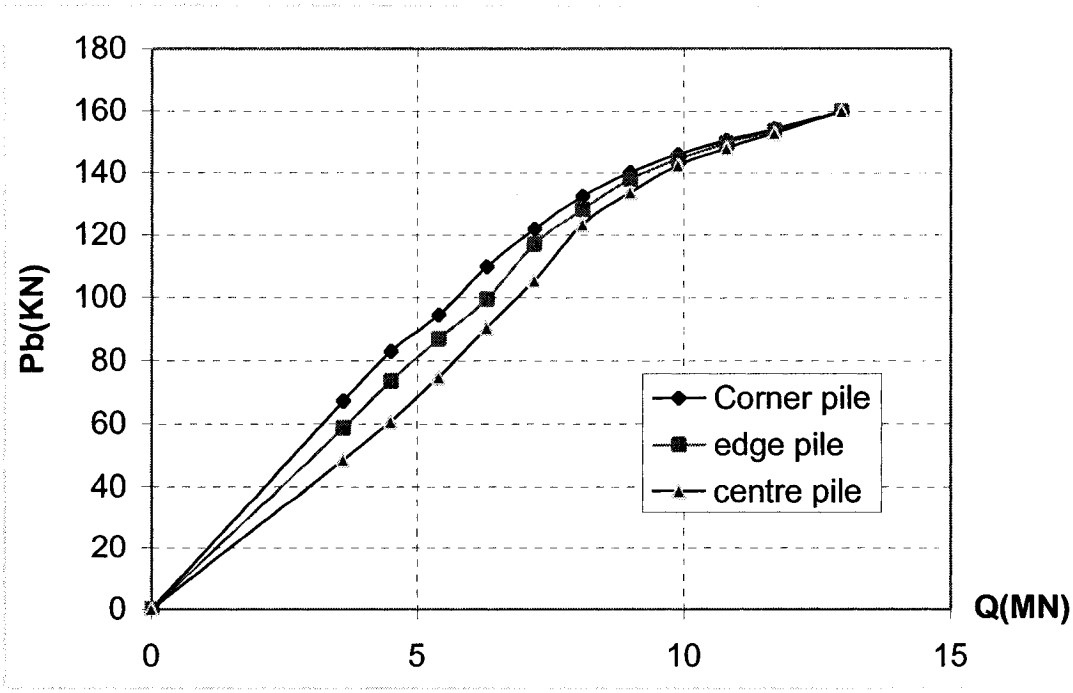

(c) Pile-base Load--Total Load Curves

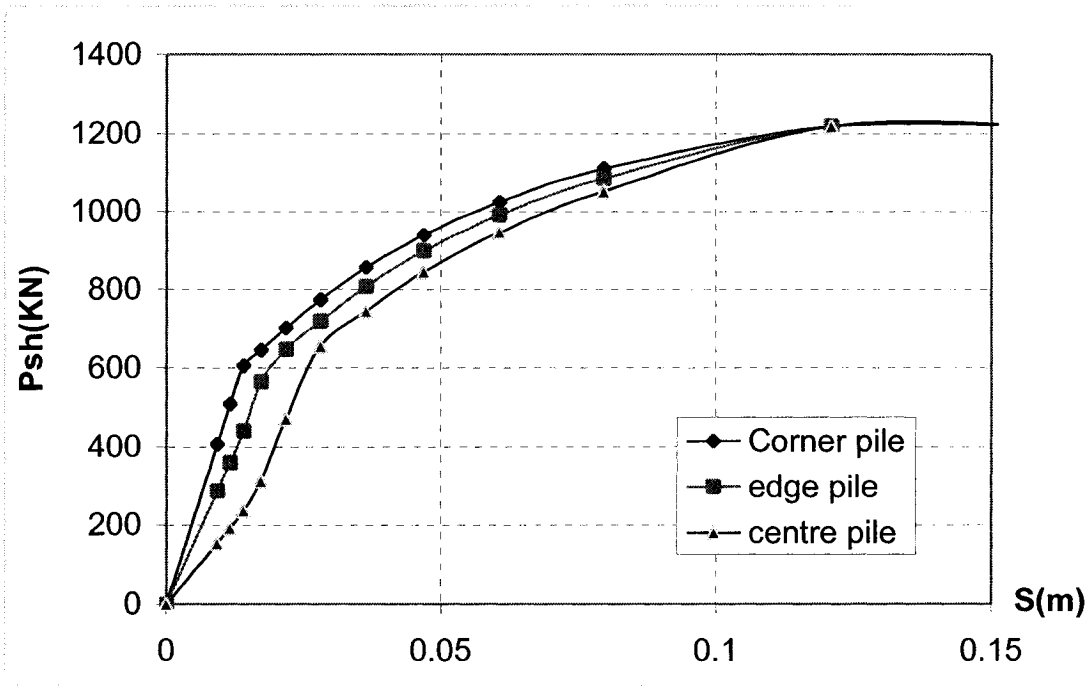

(d) Pile-shaft Load—Settlement Curves

Fig. 3-11(c, d) Calculated Loads, Settlements and Stresses for High Raft with 9 Piles

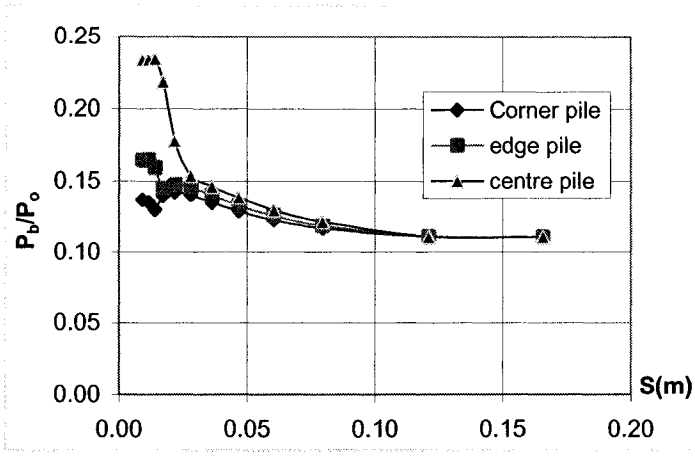

(e) α_b (P_b/P_o) develops with S

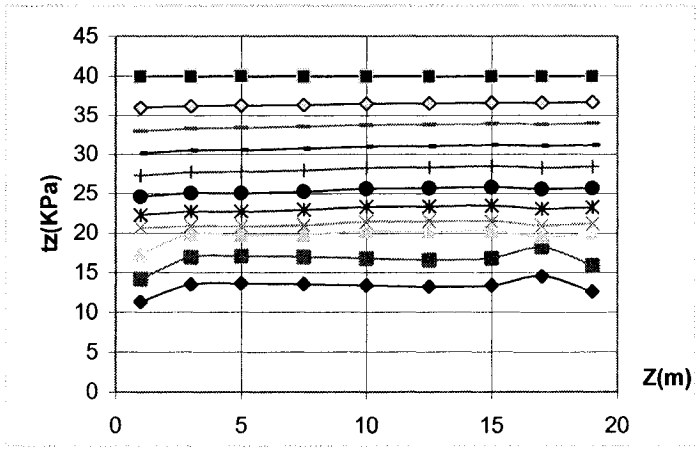

(f) Shear Stress $t_z(z)$ Curves (Corner Pile)

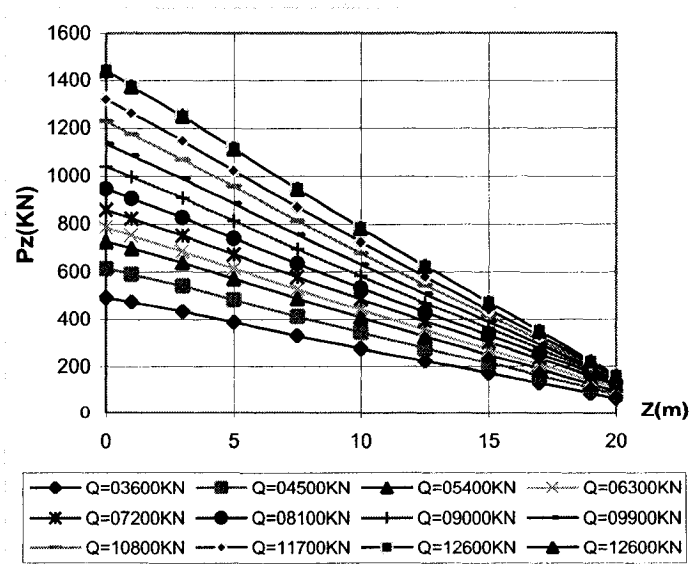

(g) Corner pile $P_z(z)$ Curves

Fig. 3-11(e~g) Calculated Loads, Settlements and Stresses for High Raft with 9 Piles

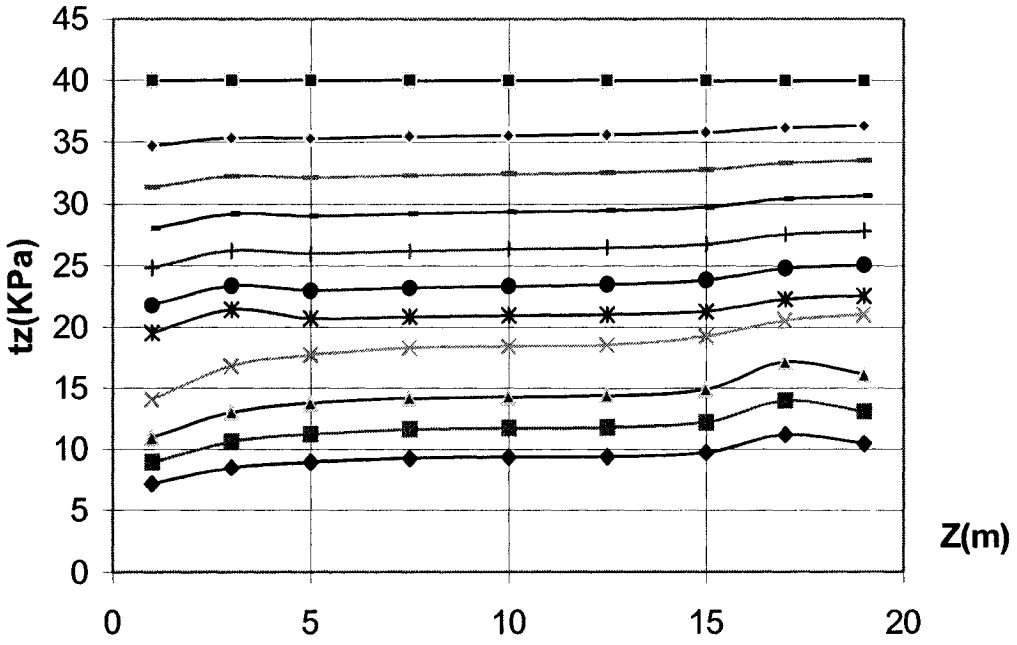

(h) Edge Pile tz(Z) Curves

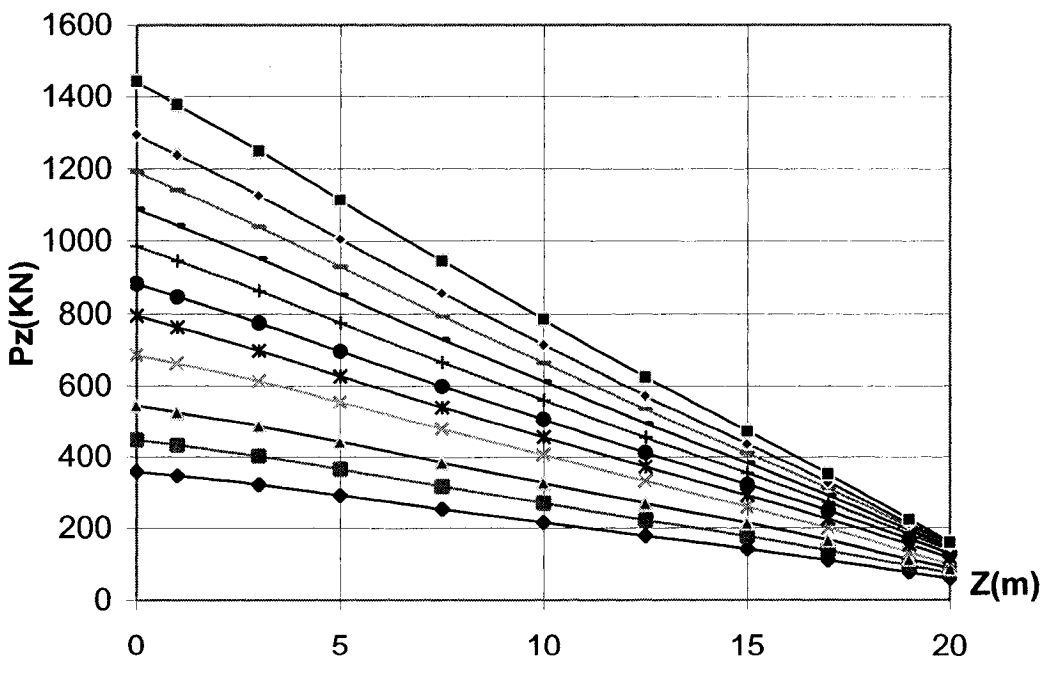

(i) Edge Pile Pz(Z) Curves

Fig. 3-11(h, i) The Calculated Loads, Settlements and Stresses for High Raft with 9 Piles
[legend is in Fig.3-11(g)]

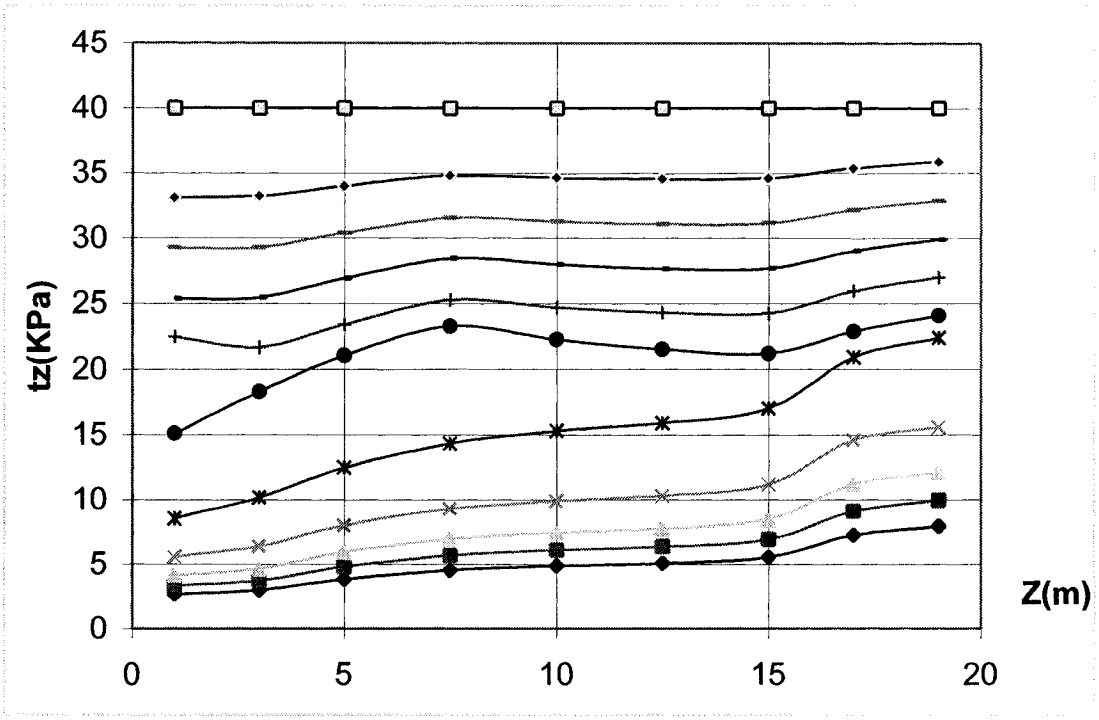

(j) Centre Pile Shear Stress tz(Z) Curves

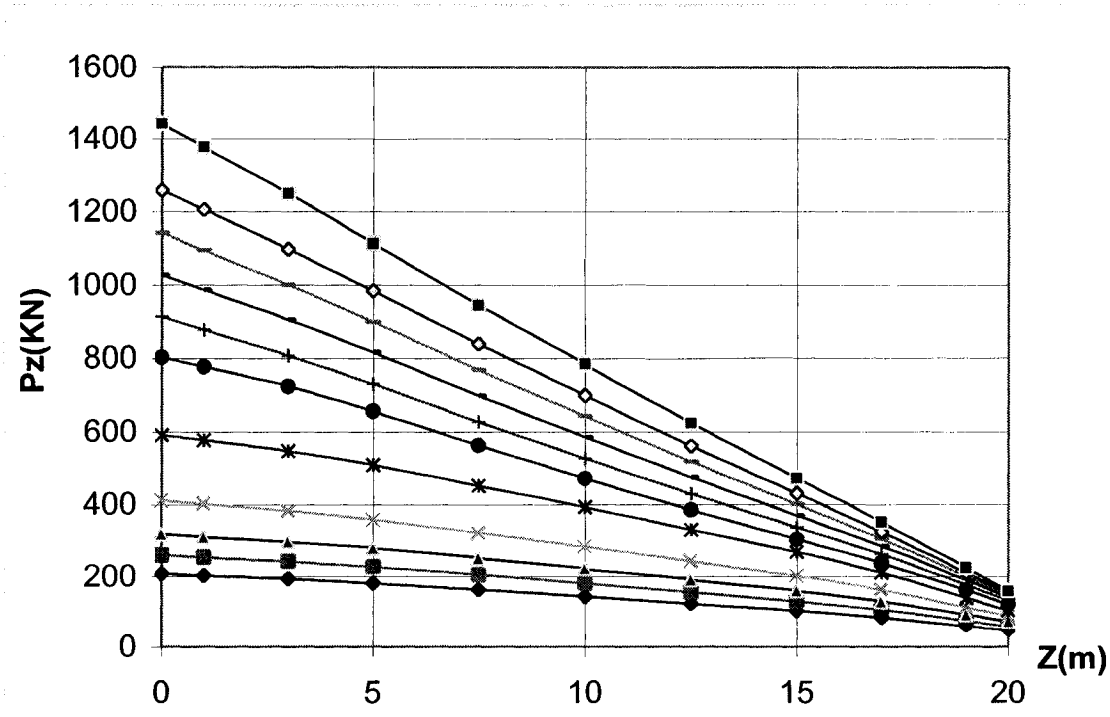

(k) Centre Pile Pz(Z) & tz(Z) Curves

Fig. 3-11(j,k) Calculated Loads, Settlements and Stresses for High Raft with 9 Piles
[Legend is in Fig.3-11(g)]

Case 5

A low raft (i.e. the bottom of the raft comes into contact with the soil) with 9 piles. The raft is the same as that in Case 4. The piles and soil conditions are the same as those of Cases 2 and 3, i.e., raft B × B = 7.6 m × 7.6 m; pile space s/b = 2.4/0.4 = 6.

The calculated results are as follows:

1) The load-Settlement curve shown in Fig. 3-12(a).
2) The load of the raft, Q_s, as well as the raft load percentage ($\lambda = h_s = Q_s/Q$, %), developing with the total load Q shown in Fig. 3-12(b, c).
3) The load of pile head - the total settlement curve shown in Fig. 3-12(d).
4) The pile-base load - the total settlement curve shown in Fig. 3-12(e).
5) The pile-shaft load ($P_{sh} = P_0 - P_b$) develops with the total settlement (S), shown in Fig. 3-12 (f).
6) The ratio of the pile-base load to the pile–head load, i.e. α_f, varies with the total settlement in Fig. 3-12 (g).
7) The axial force $P_z(z)$ and shear stress on the shaft $\tau_z(z)$ curves of corner, edge and centre piles shown in Fig. 3-12 (h to m).

From the above figures, the following conclusions can be drawn:

1) Just as for the comparison between Cases 2 and 3, comparing the settlement behaviour of high-raft pile group of Case 4, shown in Fig. 3-11 (a), when the pile-head load is close to its ultimate value, shown in Fig. 3-12(d), the settlement development with total load Q does not drop suddenly but drops gradually, as

seen in Fig. 3-12 (a). The advantage of considering a raft's action on load sharing of the upper structure is clear.

2) The load shared by the raft and its sharing ratio to total load Q behave in the same manner as observed for Case 3, this may be due to their both having the same raft sharing area ratio, i.e. B/b in Case 3 is equal to S/b in Case 5 (S is the space between pile-center to pile center).

3) Comparing Fig. 3-11 (e) with Fig. 3-12 (g), one can see that the ratios of pile-base load to pile–head load in elastic state are affected not only by their location on the raft, but also by the raft's width. However when the load of piles is near to plastic or ultimate state, the ratios tend to a stable theoretical value,

$$\alpha_{bu} = P_{bu}/P_{0u} = \sigma_{bf} A_b/[\xi_p(\sigma_{bf} A_b+\tau_f pL)]$$

$$= \frac{\sigma_{bf}}{4\tau_f}\cdot\frac{b}{L}\Bigg/\left[\xi_p\left(1+\frac{\sigma_{bf}}{4\tau_f}\cdot\frac{b}{L}\right)\right] \qquad (3\text{-}20)$$

In the case, the value $\alpha_{bu} = 0.125/[0.94(1+0.125)]=0.118$.

4) The action for a decreasing raft frictional stress of a pile's shaft is greater than that of Case 3 (small raft case). This is due to the width of the raft being larger than that of Case 3. In the elastic phase, the action even causes the upper part of the centre pile to demonstrate negative frictional stress, as shown in Fig. 3-12(*l*). However, in the non-linear phase, the action gets smaller with the development of settlement.

5) The raft-effect factors of a pile are ξ_p =0.903 for a center pile, 0.944 for corner and/or edge piles, and their average $\overline{\xi_p}$ =0.939. They are close to a value of 0.9, which is recommended by Zai 1992 and Burland 1995. One should be aware that

the program discussed within this research paper does not consider the shear strength increment caused by an increased normal stress on a pile's shaft due to the pressure of the raft's bottom. Otherwise, according to Katzenbach(1998), ξ_p will be much greater than 1.

6) From Fig. 3-12 (h to m), one sees the decreasing effect of the cap on the pile's UBC, which reaches its limit in the range where the depth is equal to the cap width for center piles, e.g., $z_f \approx B = 7.6$ m, whereas for edge piles and corner piles, the range depth is of about 0.75 the cap width, e.g., $z_f \approx 0.75B = 5.7$ m.

According to the following definition,

$$\xi_p = 1-\Delta P_{ur}/P_u \qquad (3\text{-}21)$$

ΔP_{ur} is the value of the pile's total frictional force decrement caused by the effect of the cap; P_u is the UBC of a single pile that is not affected by decreasing cap's effect. Thus,

$$\Delta P_{ur} \approx 0.33\tau_f pB \text{ (for center piles)} \qquad (3\text{-}22a)$$

$$\Delta P_{ur} \approx 0.25\tau_f pB \text{ (for edge or corner piles)} \qquad (3\text{-}22b)$$

Where the value of τ_f is taken as $\tau_f(z)|_{z=B}$ for center piles and $\tau_f(z)|_{z=0.75B}$ for edge or corner piles, p is perimeter of pile section

In Case 2, only for center piles, $\Delta P_{ur} \approx 0.33\tau_f pB = 0.33\times40\times1.6\times3.2 = 67.6$ kN, and $\xi_p = 1-\Delta P_{ur}/P_u = 1-68/1440 = 0.95$, which is close to the calculated value of 0.97.

In Case 4, for center piles, $\Delta P_{ur} \approx 0.33\tau_f pB = 0.33\times40\times1.6\times7.6=160.5$ kN, and $\xi_p = 1-\Delta P_{ur}/P_u = 1-160.5/1440 = 0.89$ (which is extremely close to 0.90); for edge or

corner piles $\Delta P_{ur} \approx 0.25\tau_f UB = 0.25\times40\times1.6\times7.6 = 121.6$ kN, $\xi_p = 1-\Delta P_{ur}/P_u = 1-122/1440 = 0.92$ which is close to 0.94.

The above two cases show that the estimates provided by equations (3-21) and (3-22) for the raft-effect factor of piles, ξ_p, are feasible.

In the case of uniform soil, $P_u = \sigma_{bf}A_b+\tau_f pL$ (L = length of pile),

$$\xi_p = 1-\Delta P_{ur}/P_u = 1-\frac{0.33B/L}{1+\frac{\sigma_{bf}}{\tau_f}\frac{b}{4L}} \quad \text{(for center piles)} \qquad (3\text{-}23a)$$

$$\xi_p = 1-\Delta P_{ur}/P_u = 1-\frac{0.25B/L}{1+\frac{\sigma_{bf}}{\tau_f}\frac{b}{4L}} \quad \text{(for edge or corner piles)} \qquad (3\text{-}23b)$$

Theoretically, $\sigma_{bf}/c_u \approx \sigma_{bf}/\tau_f = 9$. But actually, usual $\sigma_{bf}/\tau_f = 12\sim25$ (Meng, 1999). Therefore, $\frac{\sigma_{bf}}{\tau_f}\frac{b}{4L} \approx (3\sim6)b/L$. When $L/b \geq 30\sim60$, $\frac{\sigma_{bf}}{\tau_f}\frac{b}{4L} \approx (3\sim6)b/L \leq 0.1$, then $\xi_p = 1-(0.25\sim0.33)B/L$ (3-23c)

From equations (3-23), it can be noted that the raft-decreasing-effect factor of the pile, ξ_p, is actually a function of B/L, e.g., the ratio of the cap width over the pile length. Hence, taking ξ_p to be 0.9, the value recommended by Zai 1992 or Burland 1995, does not take into account the factor, and it is not reasonable for some cases, such as small caps and long piles, or big caps and short piles.

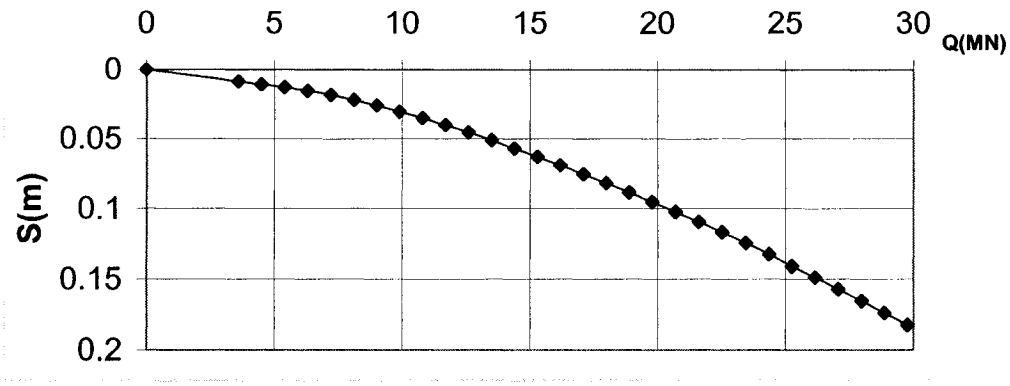

(a) Total Load--Settlement curve

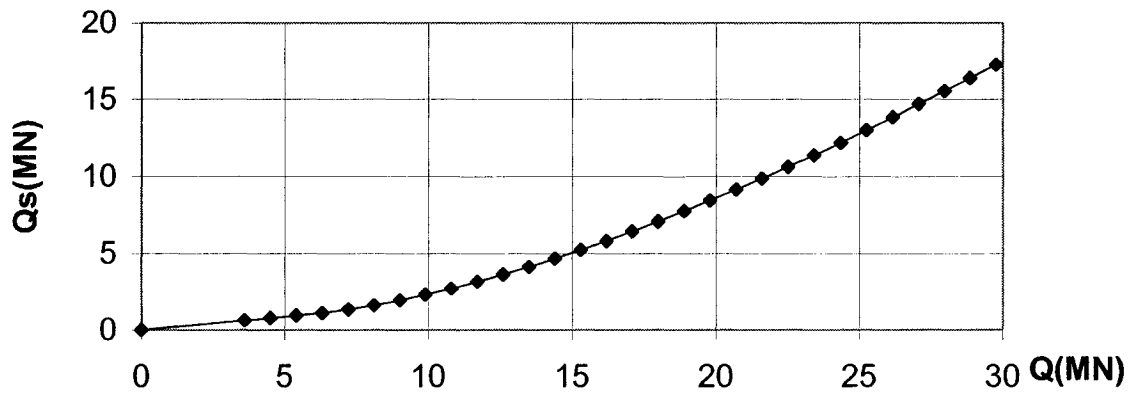

(b) Raft's load—total load relationship

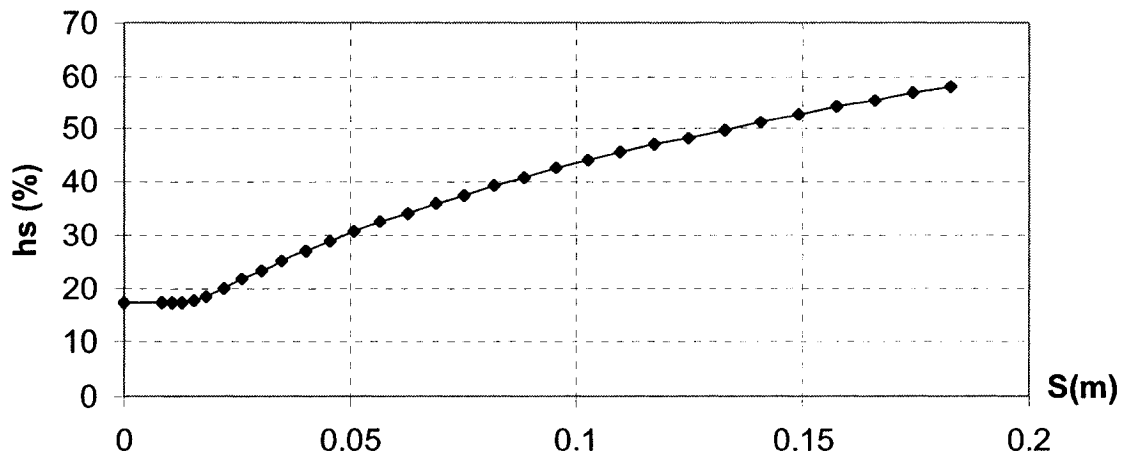

(c) Raft's Load Percentage hs (Qs/Q) with Settlement

Fig. 3-12 Calculated Loads and Settlements for Low Raft with 9 Piles

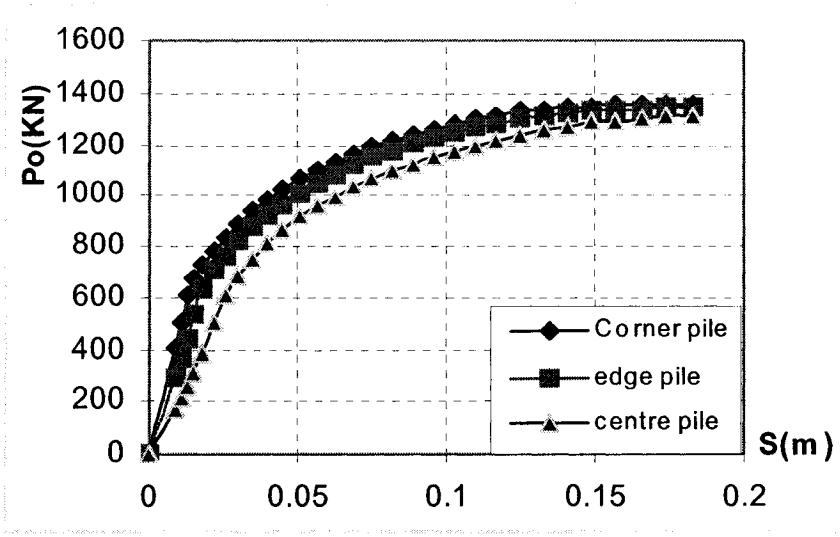

(d) Pile-Head Load—Settlement Curve

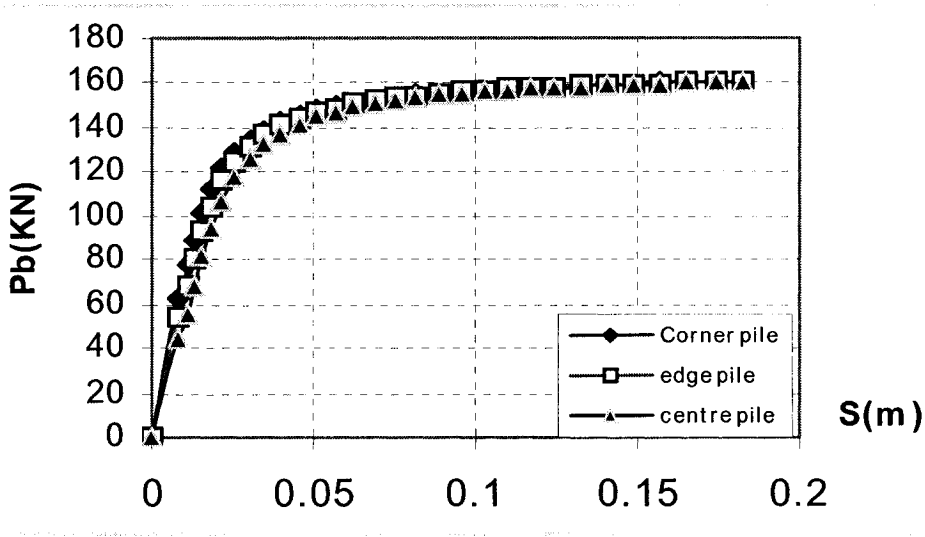

(e) Pile-Base Load—Settlement Curve

Fig. 3-12 Calculated Loads and Settlements for Low Raft with 9 Piles

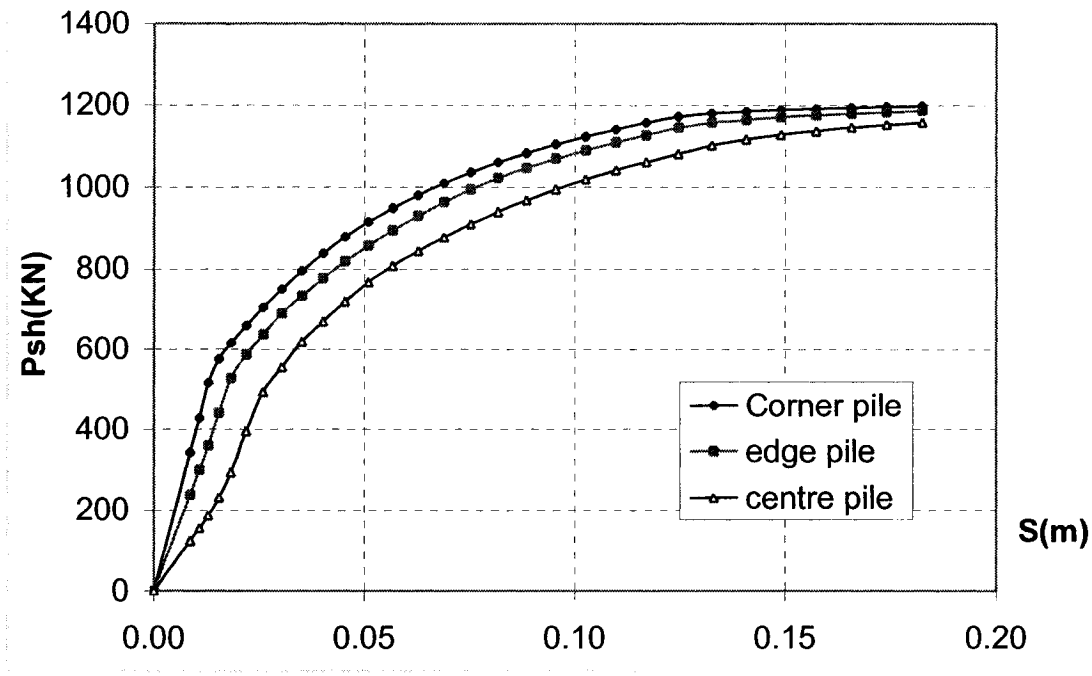

(f) Pile-Shaft Load—Settlement Curve

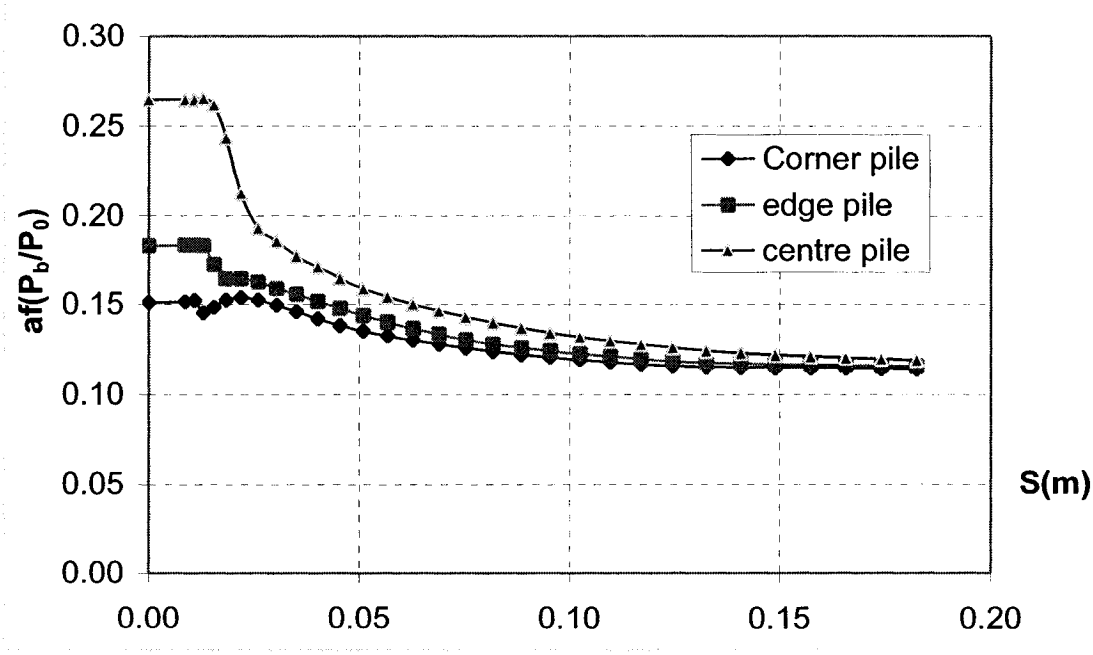

(g) Pile-Base Load Ratios' Developing with Settlement

Fig. 3-12 Calculated Loads and Settlements for Low Raft with 9 Piles

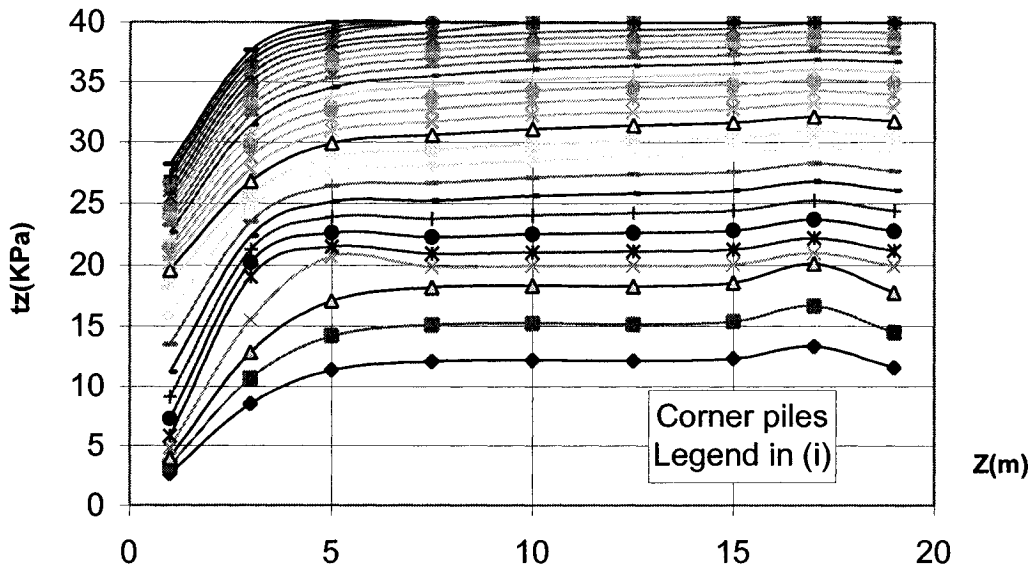

(h) Shear Stress $\tau_z(Z)$ Curves of Corner Piles [legend is in Fig.3-12(i)]

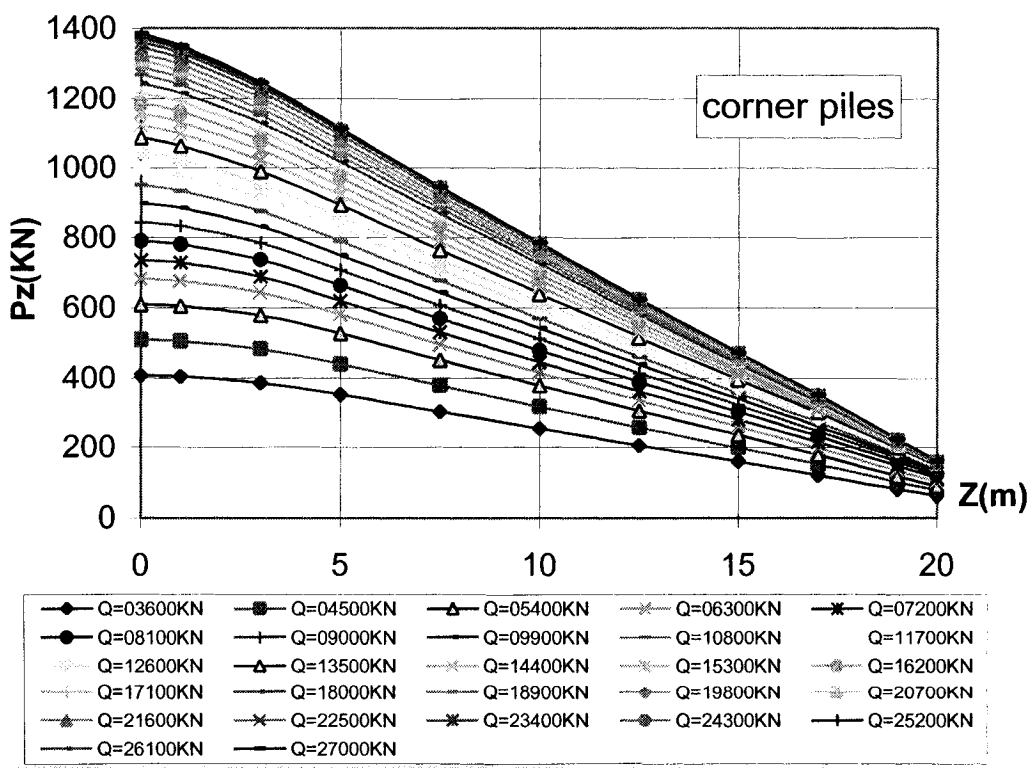

(i) Axial Force $P_z(Z)$ Curves of Corner Piles

Fig. 3-12 Calculated Loads and Settlements for Low Raft with 9 Piles

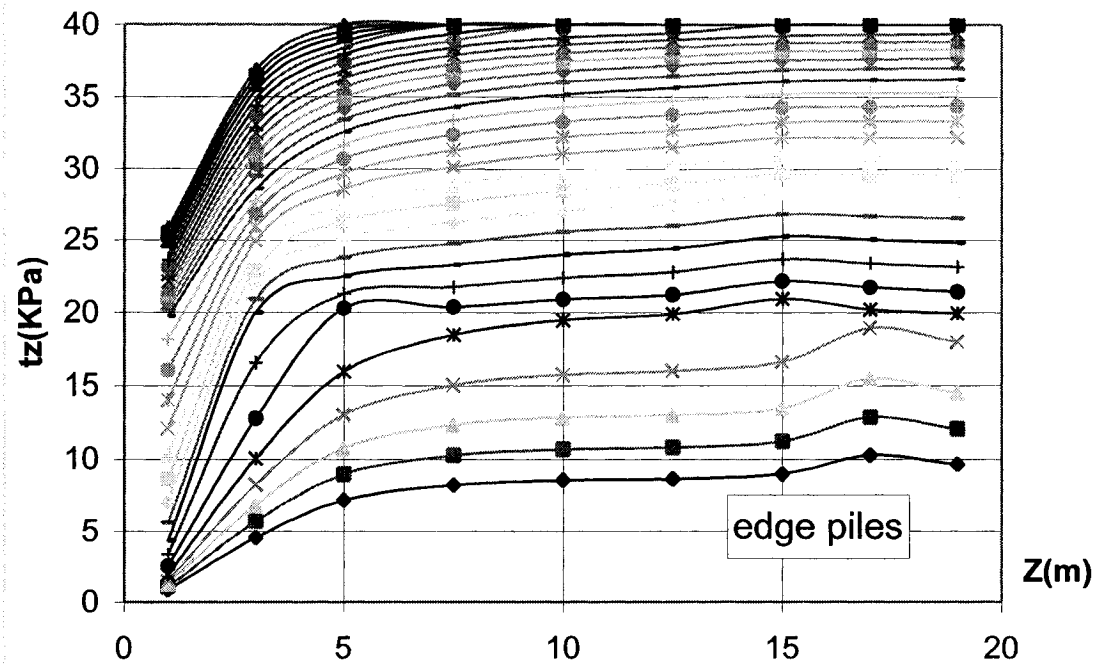

(j) Shear Stress $\tau_z(z)$ Curves of Edge Piles [legend is in Fig.3-12(i)]

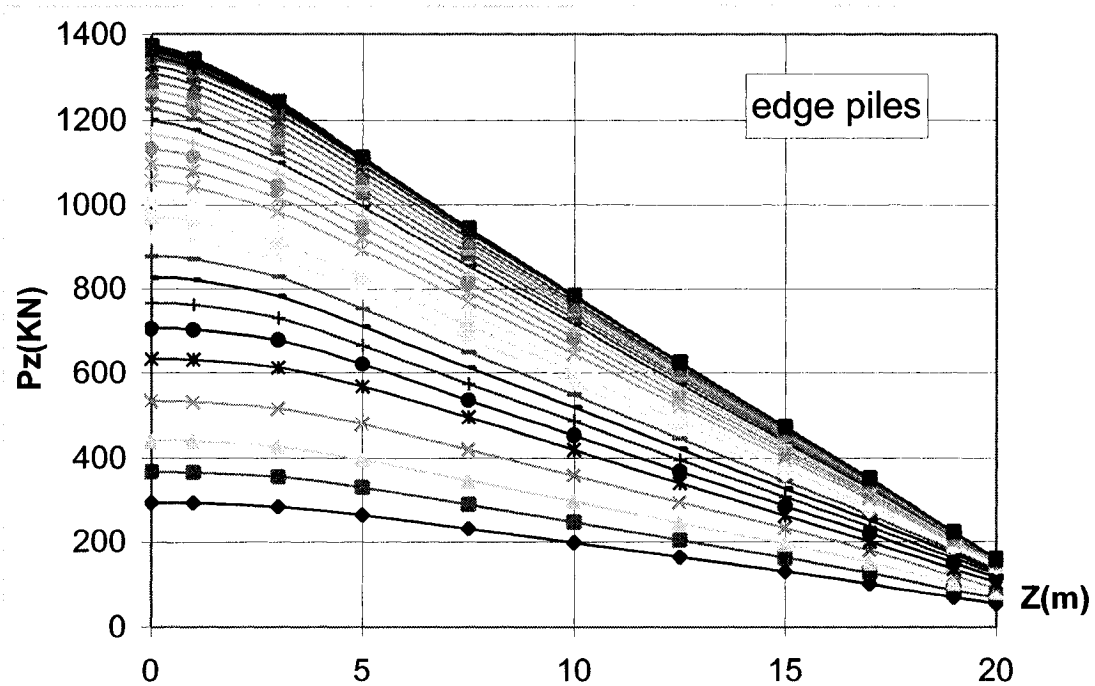

(k) Axial Force Pz(Z) Curves of Edge Piles [legend is in Fig.3-12(i)]

Fig. 3-12 Calculated Loads and Settlements for Low Raft with 9 Piles

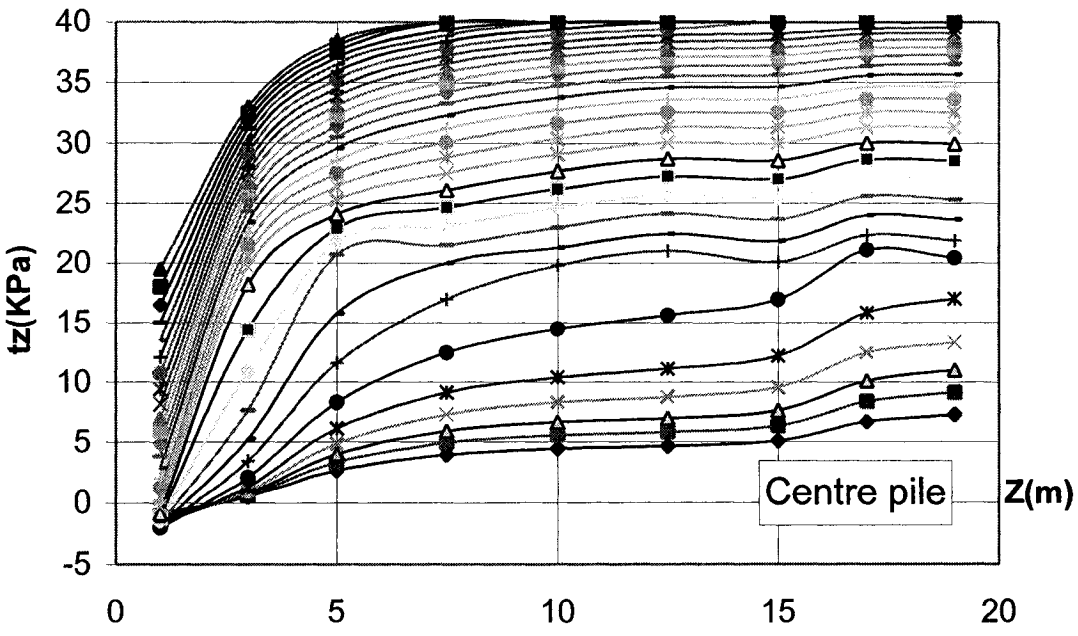

(*l*) Shear Stress $\tau_z(z)$ Curves of Centre Pile [legend is in Fig.3-12(i)]

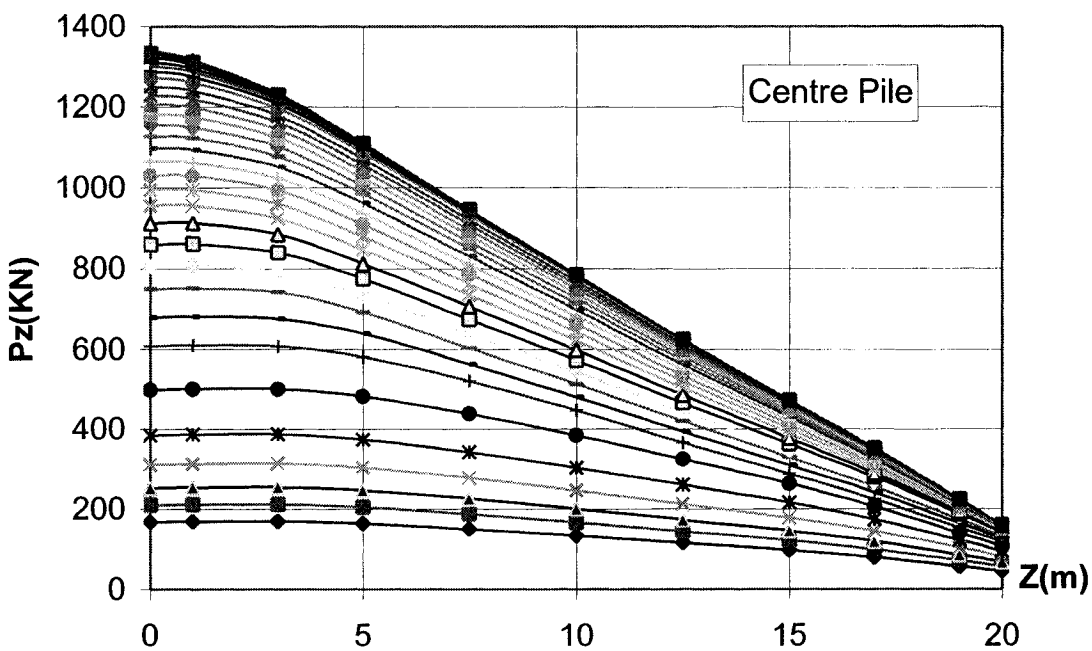

(m) Axial Force $P_z(z)$ Curves of Centre Pile [legend is in Fig.3-12(i)]

Fig. 3-12 Calculated Loads and Settlements for Low Raft with 9 Piles

3.5 Discussions

When FLM adopting the Fourier series and calculating the interaction of raft and soil, larger Lg (calculating range length) needs larger Nr (selected maximum number of the finite Fourier series) to escape from coefficient wave. Because large Nr increases run time of computer, it is necessary and very important to try to run the program and determine the calculating range length Lg and the number of Fourier series Nr.

For high-cap foundations (case 2), the settlement developed with bearing load will sharply increases at ultimate state when the load of the pile is up to or exceeds the failure load; whereas for low-caps (case 3), settlement is gradually developed even when the load on the pile head is close to, reach or exceeds the ultimate value of the pile bearing capacity, because caps bear the excess load increases close to reaching or after reaching ultimate state.

In the elastic phase of the load-settlement relationship of a pile-soil system, the raft's decreasing action on shear stress (frictional) development on the upper part of the pile's shaft is evident, and it also obviously weakens as the load on the pile develops at or close to failure or ultimate bearing capacity.

The decreasing effect of a cap on a pile's UBC is limited in the range of the depth that is equal to the cap width of the center pile, e.g., $z_f \approx B$, whereas for edge piles and corner piles, the range depth is of about 0.75 of the cap width, e.g. $z_f \approx 0.75B$. The reducing value of a pile's final bearing capacity for a raft's decreasing action, $\Delta P_{ub} = P_u - P_0 \approx \frac{1}{3}\tau_f z_f$,

is estimated by frictional stress $\tau(z) \approx f(z^2)$ curves in ultimate state. The factor of the decreasing effect of a cap on a pile's UBC, $\xi_p = 1-\Delta P_{ur}/P_u$, can be estimated by equations (3-21) to (3-23).

CHAPTER 4

PORE PRESSURE CAUSED BY DRIVING PILE GROUPS

4.1 Initial Distribution of Pore Pressure Developed During Driving

The Excess pore water pressure (EPWP) induced during the procedure of single pile driving is different from the EPWP distribution at the end of pile driving. This difference is attributed to a decrease in the shaft's resistant frictional stress and the base resistant force of the pile, which seem to disappear upon load removal of the pile top at the end of pile driving, which is accompanied by some residual pile tip resistance and negative frictional stress of the pile shaft, as shown in Fig.4-1. However, the excess pore pressure data measured during the procedure of single pile driving is useful in clarifying the stable initial excess pore pressure distribution caused by pile driving after its completion.

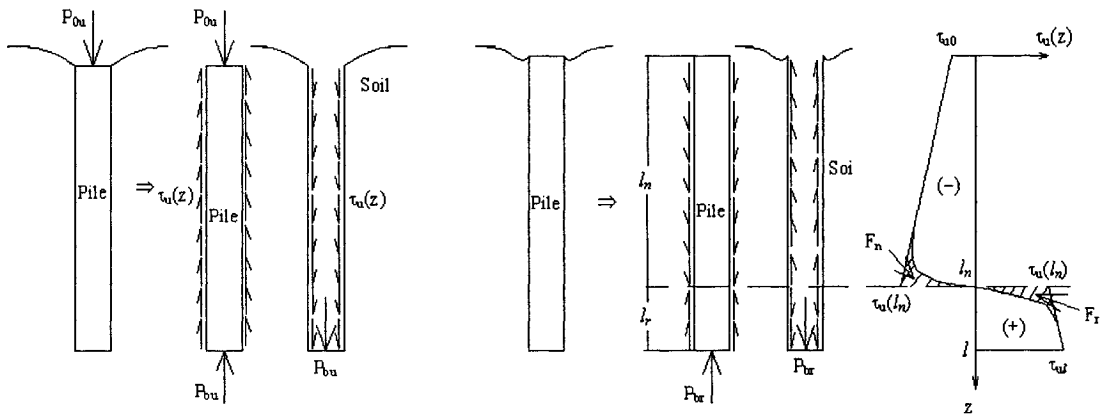

(a) Loading during pile penetration (b) After unloading and pile penetration

Fig. 4-1 Stress State of Pile and Soil during Pile Driving and After Unloading

4.2 Excess Pore Pressure Induced during Single Pile Driving

Roy et al (1981) gave the field pore pressure observed from various cells fixed on a pile during its penetration. The interpretation of the field data usually is the theory of expansion of spherical and cylindrical cavities in ideal elastic-plastic soil possessing both cohesion and friction as presented by Vesic (1972). That is, the generated pore pressure around the pile tip, Δu_t, is the result of the expansion of a nearly spherical cavity in the intact clay and it may be estimated from the theoretical solution for spherical cavity expansion:

$$\frac{\Delta u}{c_u} = 4Ln\left(\frac{R_p}{\rho}\right) + 0.94\alpha_f \qquad (4\text{-}1)$$

$$\frac{R_p}{r_0} = \sqrt[3]{\frac{E}{2(1+\mu_u)\cdot c_u}} \qquad (4\text{-}1')$$

in which R_p is the extent radius of the plastic zone around the pile axle, ρ is the radius from pile tip to calculating point, $\rho = \sqrt{r^2 + (z-D)^2}$, z is depth of calculating point, D is depth of pile into soil, r_0 is the radius of the pile and α_f is Henkel's pore pressure parameter (Henkel 1959).

The pore pressure maintained along the pile wall during the pile penetration, Δu_s, is much less than Δu_t, and may be estimated from the cylindrical cavity expansion theory, whose provided parameters should account for the effect of clay destructuration resulting from pile penetration.

$$\frac{\Delta u}{c_u} = 2Ln\left(\frac{R_p}{r}\right) + 0.817\alpha_f \qquad (4\text{-}2)$$

$$\frac{R_p}{r_0} = \sqrt{\frac{E}{2(1+\mu_u)\cdot c_u}} \qquad (4\text{-}2')$$

An estimate of Δu_s can be made from the solution proposed by Lo and Stermac (1965), which is based on the assumption that the pore pressure increase is caused by two phenomena: (1) an increase in mean total stress ($\Delta u_{s1} = (1\text{-}K_0)\sigma_{v0}'$) and (2) the shearing of the soil due to large strains around the pile ($\Delta u_{s2} = (\Delta u/p')_m \cdot \sigma_{v0}'$). Consequently, the driving pore pressure Δu_s in normally consolidated clays may obtained from $\Delta u_s = [1\text{-}K_0 + (\Delta u/p')]\cdot\sigma_{v0}'$. Its modification to account for the eventual pre-consolidation of the clay should be rewritten as

$$\Delta u_s = (1\text{-}K_0)\sigma_{v0}' + (\Delta u/p')_m \cdot \sigma_p' \qquad (4\text{-}3)$$

where K_0 is the coefficient of earth pressure at rest in intact clay, σ_{v0}' is the vertical effective stress, $(\Delta u/p')_m$ is the ratio of excess pore pressure to the initial consolidation pressure p', that was measured in a conventional consolidated-undrained tri-axial test and generally assumes values in the order of 0.6-0.8 and finally σ_p' is the pre-consolidation pressure.

Although the pore pressure computed from Equation (4-3) agrees remarkably well with the observation from Roy's field test, the interpretation mechanism of equation (4-3) is not clear.

When compared with Lo and Stermac's assumption (1965), equations (4-1) and (4-2) neglect the increase in mean total stress caused by shear stress on the interface between

the pile and soil that is maintained along the pile wall during penetration. This factor can be taken into account using the formulae developed by both Mindlin (1936) and Gedds (1953, 1966) and modifying Vesic's cavity expansion theory application.

The increase in mean total stress is defined by the following equation $\Delta\Phi = \Delta\sigma_z+\Delta\sigma_r+\Delta\sigma_\theta$, where $\Delta\sigma_z$, $\Delta\sigma_r$ and $\Delta\sigma_\theta$ and $\Delta\tau_{rz}$ are caused by a point load P_b applied at the pile tip, uniform skin friction along the pile (total load P_u) and linear variation of skin friction (total load P_t), shown in Fig. A-1 in Appendix A.

$$\left.\begin{aligned}
\Delta\sigma_z &= I_{z\text{-}b}\,P_b + I_{z\text{-}u}\,P_u + I_{z\text{-}t}\,P_t \\
\Delta\sigma_r &= I_{r\text{-}b}\,P_b + I_{r\text{-}u}\,P_u + I_{r\text{-}t}\,P_t \\
\Delta\sigma_\theta &= I_{\theta\text{-}b}\,P_b + I_{\theta\text{-}u}\,P_u + I_{\theta\text{-}t}\,P_t \\
\Delta\tau_{rz} &= I_{\tau\text{-}b}\,P_b + I_{\tau\text{-}u}\,P_u + I_{\tau\text{-}t}\,P_t
\end{aligned}\right\} \qquad (4\text{-}4)$$

in which, $I_{z\text{-}b}$, $I_{z\text{-}u}$, $I_{z\text{-}t}$, $I_{r\text{-}b}$, $I_{r\text{-}u}$, $I_{r\text{-}t}$, $I_{\theta\text{-}b}$, $I_{\theta\text{-}u}$, $I_{\theta\text{-}t}$, and $I_{\tau\text{-}b}$, $I_{\tau\text{-}u}$, $I_{\tau\text{-}t}$ all are stress coefficients expressed in dimensionless form and whose definitions can be obtained from Geddes (1966) in Appendix I.

Therefore, based on Lo and Stermac's assumption (1965), the pore pressure increase caused by the increase in mean total stress can be expressed as

$$\Delta u_1 = \beta\Delta\Phi(r,z;\,D)/3 = (\Delta\sigma_z+\Delta\sigma_r+\Delta\sigma_\theta)/3$$

$$= (I_{z\text{-}b}+I_{r\text{-}b}+I_{0\text{-}b})P_b/3 + (I_{z\text{-}u}+I_{r\text{-}u}+I_{0\text{-}u})P_u/3 + (I_{z\text{-}t}+I_{r\text{-}t}+I_{0\text{-}t})P_t/3 \qquad (4\text{-}5)$$

The second part of the pore pressure increase, caused by the shearing of the soil due to large strains around the pile, should be expressed by Equations (4-1) or (4-2):

Near the pile tip, D = z~z+10 r_0, $\Delta u_{2D} = \Delta u_{s2} = c_u\left[4Ln\left(\frac{R_p}{\rho}\right) + 0.94\alpha_f\right]$ (4-6)

Along the pile, for D ≤ z-10r_0, $\Delta u_{2S} = \Delta u_{s2} = c_u\left[2Ln\left(\frac{R_p}{r}\right) + 0.817\alpha_f\right]$ (4-7)

one can assume D = z-10r_0 ~ z,

$$\Delta u_2 = \Delta u_{2D}\,[1. - (z - D) / (10r_0)] \quad (4\text{-}8)$$

and for D < z-10r_0 , $\Delta u_2 = 0$

Therefore, $$\Delta u = \beta\Delta\Phi(r,z; D)/3 + \Delta u_2(r,z;D) \quad (4\text{-}9)$$

From Roy's data, intact clay exhibits an E_u/c_u ratio in the order of 900, whereas clay which has been remolded or "destructured" during cavity expansion at the pile-tip level, Leroueil et al (1979) report a reduction in the order of 50% for E_u/c_u and of 30% for c_u, and the following pore pressure parameters: β=1, α_f=0.35 (obtained from a CIU test). According to in situ vane strengths, taking c_u=5+3*z (kPa), and the point resistance and skin friction measured during the driving of piles, P_u = 0, P_t = 6.5 kN and P_b = 3.67 + 1.67*z (kN).

Fig. 4-2 is calculated from equation (4-9) and the measures from Roy *et al* (1981) for different measured depths z and the same radius distance r=0.3m.

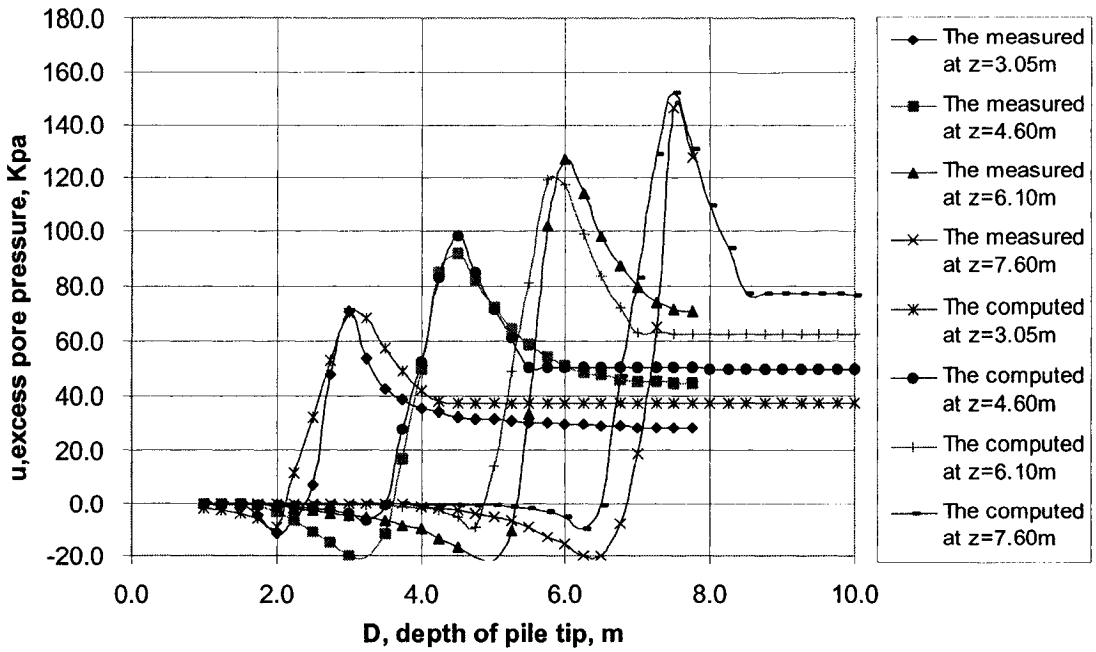

Fig. 4-2 The measured from Roy et al (1981) and the calculated by this thesis

Fig. 4-3 is a comparison of the pore pressure observed by Roy et al (1981) and the values computed using the method presented in this paper for two depths, z = 3.05m and z = 6.10m, and different radius distances surrounding the pile (pile tests 3 and 4). The comparison in the figure indicates that it is reasonable to use Equation (4-5) to displace the experimental term $(1-K_0)\sigma_{v0}'$ found in Equation (4-3) based on Lo and Stermac's assumption (1965).

Therefore, it can be accepted that the stable initial excess pore pressure distribution with radial distance, caused by pile driving and remaining after the end of pile driving (after having removed the load on the pile top), can be expressed by Vesic's pore expansion theory, namely equations (4-1) and (4-2), if the effect of residual resistance of pile after driving is not considered.

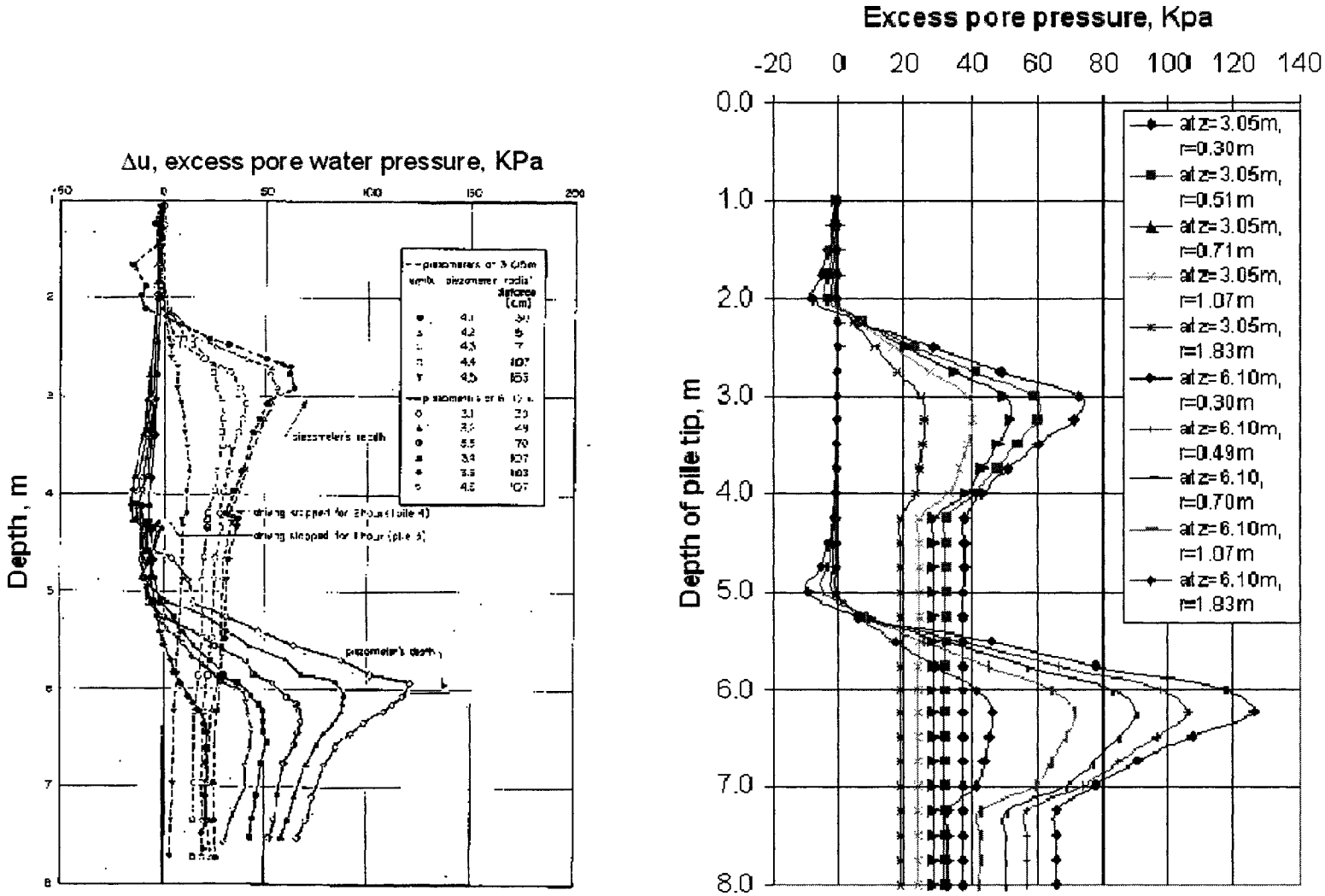

(a) Pore pressure measured by Roy (1981)

(b) Pore pressure calculated by present method

Fig. 4-3 Comparison of the pore pressure values observed by Roy(1981) and the computed values using presented method

4.3 Effect of Pile Residual Resistance on the Pore Pressure

The stable initial excess pore pressure distribution following the end of pile driving is possibly affected by the residual toe resistance and shaft resistance of the pile. Presently, research on residual resistance of pile driving force is limited to sand, since residual resistance of pile driving in clay is thought to be quite small. Actually, even if one considers a pile's residual force, one finds that the residual force's influence on the initial excess pore pressure distribution caused by driving is not large. This is because both the shaft's frictional resistance and the tip resistance of the pile is small when the soil around pile is disturbed during pile penetration.

(a) Effect of residual force

In Fig. 4-1(b), the total shaft residual force P_n and the total residual resistance of lower part P_r are defined as follows:

$$P_n = \int_{z=0}^{l_n} (\tau_{u0} + \alpha_\tau z)dz - F_n = \tau_{u0} l_n + \frac{1}{2}\alpha_\tau l_n^2 - F_n$$

$$P_r = \int_{z=l_n}^{l} (\tau_{u0} + \alpha_\tau z)dz - F_r + P_{br} = \tau_{u0}(l - l_n) + \frac{1}{2}\alpha_\tau (l^2 - l_n^2) - F_r + P_{br}$$

Due to the effect of equilibrium forces, $P_n = P_r$; $F_n \approx F_r$; and $P_{br} \le P_{bu}$, thus,

$$\tau_{u0} l_n + \frac{1}{2}\alpha_\tau l_n^2 - F_n \le \tau_{u0}(l - l_n) + \frac{1}{2}\alpha_\tau (l^2 - l_n^2) - F_r + P_{br}$$

When $P_{bu} \le P_{su} = \tau_{u0} l + \alpha_\tau l^2 / 2$, $F_n \approx F_r$; and $P_{br} = P_{bu}$

$$2\tau_{u0} l_n + \alpha_\tau l_n^2 = \tau_{u0} l + \frac{1}{2}\alpha_\tau l^2 + P_{bu} \qquad (4\text{-}10)$$

If $\alpha_\tau > 0$, $$l_n = \sqrt{\left(\frac{\tau_{u0}}{\alpha_\tau}\right)^2 + \frac{\tau_{u0} l}{\alpha_\tau} + \frac{l^2}{2} + \frac{P_{bu}}{\alpha_\tau}} - \frac{\tau_{u0}}{\alpha_\tau} \quad (4\text{-}11)$$

If $\alpha_\tau = 0$, $$l_n = \frac{1}{2}\left(l + \frac{P_{bu}}{\tau_{u0}}\right) \quad (4\text{-}12)$$

Equations (4-11, 12) are correct only when $P_{bu} \le P_{su} = \tau_{u0} l + \alpha_\tau l^2 / 2$, namely the case of a mainly frictional pile.

When $P_{bu} > \tau_{u0} l + \alpha_\tau l^2 / 2$, which is a case of a mainly end-bearing pile,

$$l_n = l, \text{ and } P_{br} = P_{su} = \tau_{u0} l + \alpha_\tau l^2 / 2 < P_{bu} \quad (4\text{-}13)$$

(b) Case calculation

Pile length l = 20 m, pile section b × b = 0.4 m × 0.4 m, disturbed soil τ_{u0} = 20 kPa, α_τ = 2.2 kPa/m, $P_{bu} = q_{bu} A_b = 1000 \times 0.16 = 160$ kPa.

Equivalent radus of pile $r_0 = \sqrt{\frac{A_p}{\pi}} = \frac{b}{\sqrt{\pi}} = 0.5642 \times 0.4 = 0.2257$ m

$P_{bu} < P_{su} = \tau_{u0} l + \alpha_\tau l^2 / 2 = 20 \times 20 + 2.2 \times 20^2 / 2 = 840$kN

Using (4-11), l_n = 14.09 m

The increase in mean total stress

$$\Delta\sigma_m = [\Delta\Phi(r,z; l) - 2\Delta\Phi(r,z; l_n)]/3$$

$$= (I_{z\text{-}b} + I_{r\text{-}b} + I_{\theta\text{-}b})_l P_{bu}/3 + (I_{z\text{-}u} + I_{r\text{-}u} + I_{\theta\text{-}u})_l \tau_{u0} l/3 + (I_{z\text{-}t} + I_{r\text{-}t} + I_{\theta\text{-}t})_l \alpha_\tau l^2/6$$

$$-(I_{z\text{-}u} + I_{r\text{-}u} + I_{\theta\text{-}u})_{ln} \tau_{u0} l_n/3 - (I_{z\text{-}t} + I_{r\text{-}t} + I_{\theta\text{-}t})_{ln} \alpha_\tau l_n^2/6$$

The result of $\Delta\sigma_m(r, z)$, shown in Fig. 4-4, demonstrates that $\Delta\sigma_m$ is small when it is caused by residual forces; it is of the order of 10 kPa for pore pressure caused by cavity expansion.

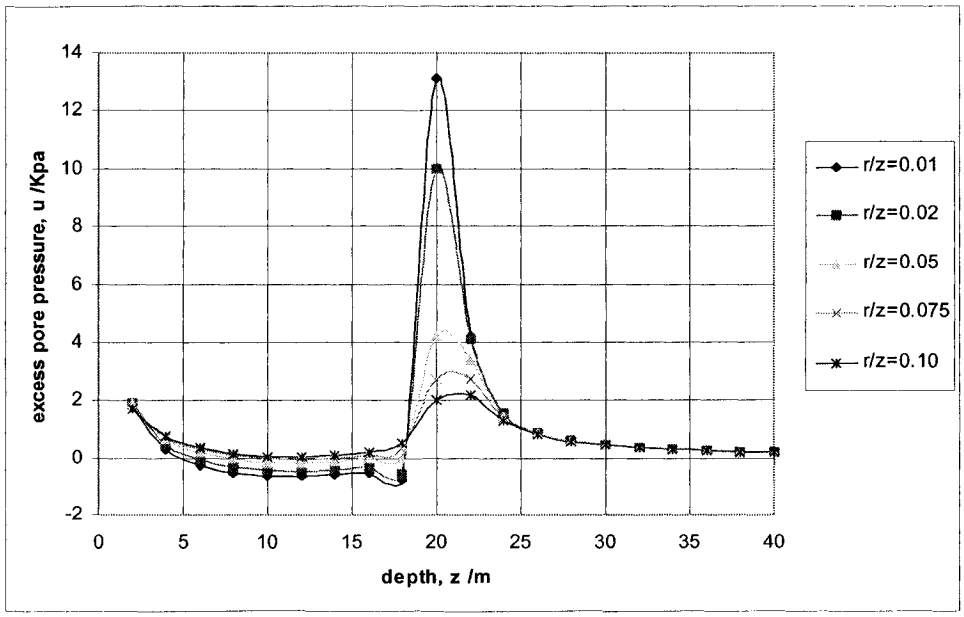

Fig. 4-4 $\Delta\sigma_m$ caused by residual forces

(c) Forms for Expressing the Initial Excess Pore Pressure

Fig.4-5 is a comparison among different expression forms, equations (2-37) to (2-49), for excess pore pressure caused by pile penetration, both theoretical and experimental. The comparison illustrates that there are some differences between the different expressions for excess pore pressure and between its mathematical expression and its measured value. It is therefore important to determine the mathematical expression of the initial excess pore pressure based on the measured or test results. Fig.4-5 also shows that the uniform formula (2-42) is the best better fit when compared to measured values. Another suitable form is the exponential model, defined as follows:

$$\frac{\Delta u}{\Delta u_m} = \exp\left[-\alpha\left(\frac{r}{r_0} - 1\right)\right] \tag{4-14}$$

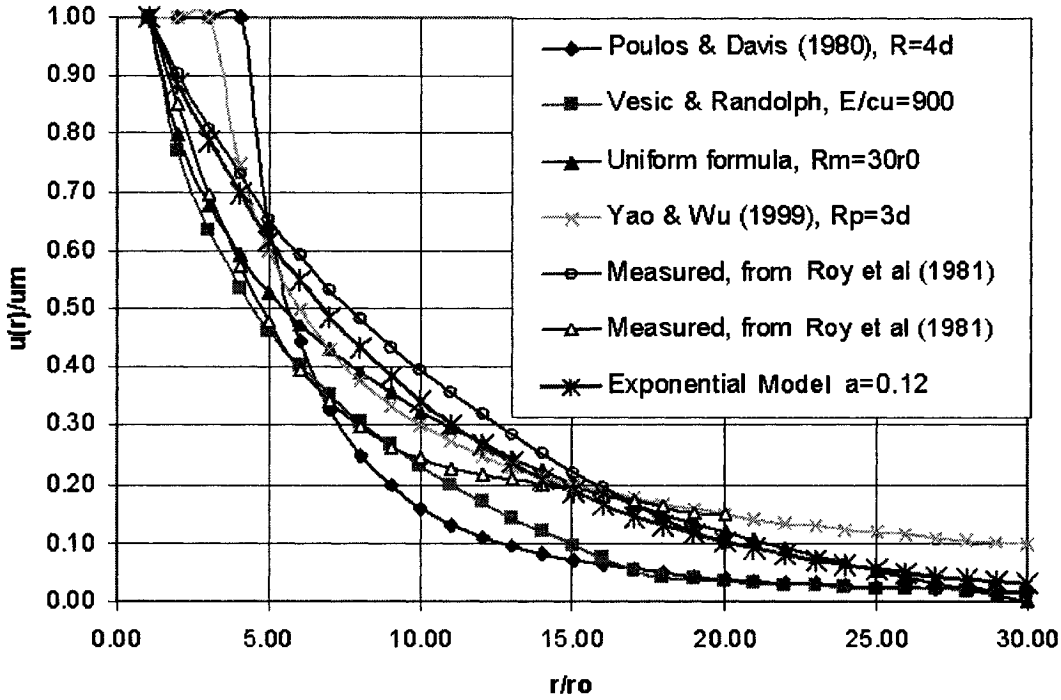

Fig. 4-5 Different Initial Pore Pressure Distribution Expression

4.4 Initial Excess Pore Pressure Distribution with Depth

The pore pressure in a plastic field can be expressed by (Vesic 1972 and Randolph et al 1979):

$$\frac{\Delta u}{c_u} = 2Ln\left(\frac{R_p}{r}\right) + 0.817\alpha_f \tag{4-15}$$

in which, $\frac{R_p}{r_0} = \sqrt{I_r} = \sqrt{\frac{E}{2(1+\mu_u)\cdot c_u}} = \sqrt{\frac{E}{3c_u}}$ (r_0 is the pile radius).

For normally consolidated clay, many experimental relationships exist between c_u and σ_v', such as the following: Skempton (1957) where $\frac{c_u}{p_o}=0.11+0.0037PI$ (p_0 is effective vertical overburden pressure σ_v'); Chandler (1988) determined $\frac{c_u}{p_c}=0.11+0.0037PI$ (p_c is pre-consolidated pressure; for normally consolidated clay, $p_c=p_0=\sigma_v$'), Mesri (1989) defined $\frac{c_u}{p_c}=0.22$ and finally Bjerrum and Simons (1960) found $\frac{c_u}{p_c}=f(LI)$.

It is now necessary to set up the relationship between $\frac{c_u}{\sigma'_{v0}}$ and the soil's effective inner frictional angle φ' for normally consolidated soil according to three different paths.

(a) Laboratory consolidation test model

Stress path: from initial confining stress $\sigma'_0=(\sigma'_{10}+\sigma'_{30})/2=(\sigma'_{h0}+\sigma'_{v0})/2$ to failure. In Fig. 4-6, $u_f=A_f(\Delta\sigma_1+\Delta\sigma_3)_f=2A_fc_u$; $\sigma'_A=\sigma'_0+c_u-u_f=\sigma'_0+(1-2A_f)c_u$

$$\therefore \quad \frac{c_u}{\sigma'_A}=\frac{c_u}{\sigma'_0+(1-2A_f)c_u}=tg\alpha'=Sin\varphi'$$

or
$$c_u=\frac{Sin\varphi'}{1-(1-2A_f)Sin\varphi'}\cdot\sigma'_0 \qquad (4\text{-}16)$$

Where σ'_0 is the initial consolidated stress (effective confining pressure), one can take $\sigma'_0=\frac{1+2K_0}{3}\sigma'_{vo}$ for soil around the driven pile and $\sigma'_v=q+\gamma d_w+\gamma' z$. The long-term surface load q=10 ~ 20 kPa usually for the site at street level. d_w is the depth of the underground water level, γ is the unit weight above water level and γ' is the unit weight below the water level, $\gamma'=\gamma-\gamma_w$.

Therefore

$$c_u = \frac{Sin\varphi'}{1-(1-2A_f)Sin\varphi'} \cdot \frac{1+2K_0}{3}\sigma'_v \qquad (4\text{-}17)$$

$$\Delta u = \frac{1+2K_0}{3} \cdot \frac{Sin\varphi'}{1-(1-2A_f)Sin\varphi'}\left[2Ln\left(\frac{R_p}{r}\right)+0.817\alpha_f\right]\cdot(q+\gamma_w d_w+\gamma' z) \qquad (4\text{-}17a)$$

(b) K_0 consolidation test model

Stress path: from initial consolidated stress (σ'_{h0},σ'_{v0}) to failure.

In Fig. 4-7, line K'_0 is the initial consolidated line; line K'_f is the failure line.

$K'_0 = (1-K_0)/(1+K_0)$; $\sigma_0 = \sigma_{v0}(1+K_0)/2$; $\tau_0 = K'_0\sigma_0 = \sigma_{v0}(1-K_0)/2$; $\Delta\sigma_1/2 = c_u - K'_0\sigma_0$;

$$u_f = A_f(\Delta\sigma_1 - \Delta\sigma_3)_f = A_f\Delta\sigma_{1f} = 2A_f(c_u - K'_0\sigma_0);$$

$$\sigma_A = \sigma_0 + \frac{\Delta\sigma_1}{2} - u_f = \sigma_0 + \frac{\Delta\sigma_1}{2} - A_f\Delta\sigma_1 = \sigma_0 + \left(\frac{1}{2}-A_f\right)\Delta\sigma_1$$

$$= \sigma_0 + \left(\frac{1}{2}-A_f\right)\cdot 2(c_u - K'_0\sigma_0) = [1-(1-2A_f)K'_0]\sigma_0 + (1-2A_f)c_u$$

$$\frac{c_u}{\sigma_A} = \frac{c_u}{[1+(1-2A_f)K'_0]\sigma_0 + (1-2A_f)c_u} = tg\alpha' = Sin\varphi'$$

$$\therefore \quad c_u = \frac{1-(1-2A_f)K'_0}{1-(1-2A_f)Sin\varphi'}Sin\varphi'\cdot\sigma_0$$

$$\text{Or} \quad c_u = \frac{1-(1-2A_f)K'_0}{1-(1-2A_f)Sin\varphi'}Sin\varphi'\cdot\frac{1+K_0}{2}\sigma'_{v0} \qquad (4\text{-}18)$$

Thus,

$$\Delta u = \frac{1+K_0}{2} \cdot \frac{[1-(1-2A_f)K_0']Sin\varphi'}{1-(1-2A_f)Sin\varphi'}\left[2Ln\left(\frac{R_p}{r}\right)+0.817\alpha_f\right]\cdot(q+\gamma_w d_w+\gamma' z) \qquad (4\text{-}18a)$$

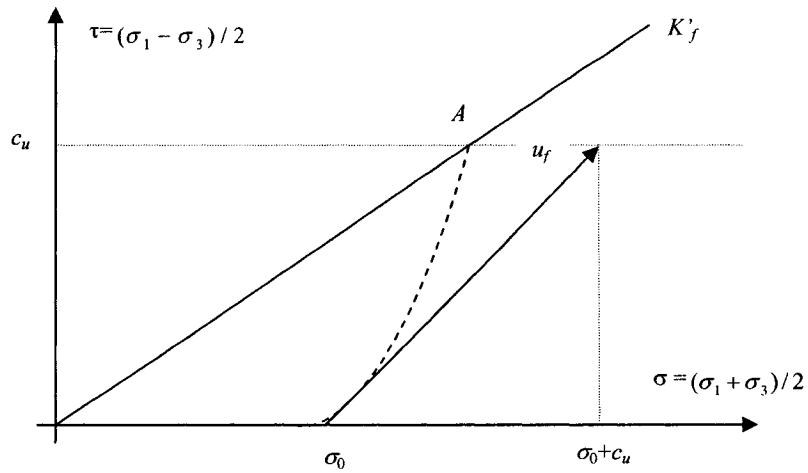

Fig4-6 stress and pore-pressure path A

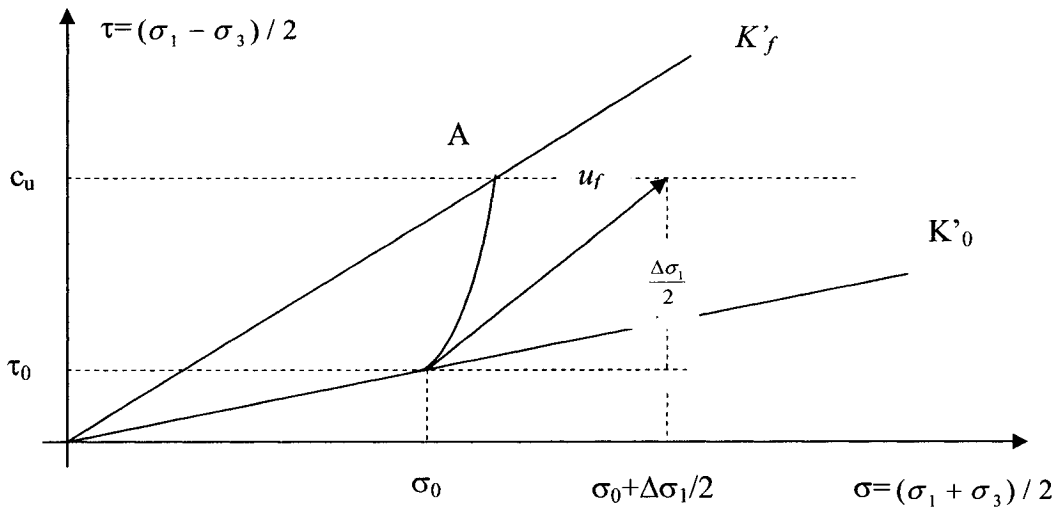

Fig. 4-7 stress and pore-pressure path B

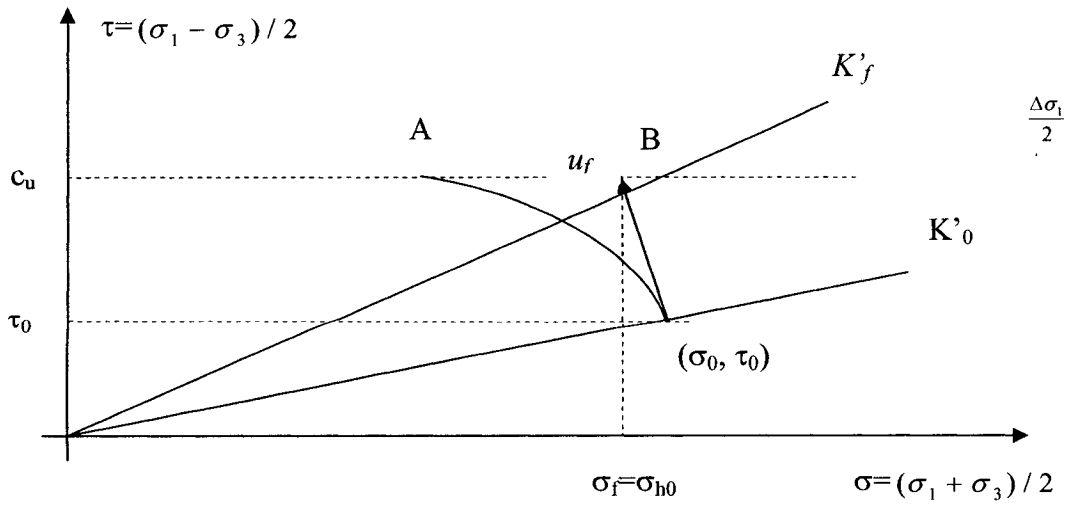

Fig. 4-8 Stress and Pore-pressure Path C

(c) Column expansion failure model

Stress path: from initial consolidated stress (σ'_{h0},σ'_{v0}) to column expansion failure.

In Fig. 4-8, the initial consolidated stress is $\sigma'_0 = \sigma'_{v0}(1+K_0)/2$ and $\tau_0 = K'_0\sigma'_0 = \sigma'_{v0}(1-K_0)/2$; According to Vesis (1972), the failure state stress is $\sigma_{1f} = \sigma_{rf} = \sigma'_{h0}+\Delta\sigma_r = \sigma'_{h0}+2c_uLn(R_p/r)+c_u$, $\sigma_{3f} = \sigma_{rf} = \sigma'_{h0}+\Delta\sigma_\theta = \sigma_{h0}+2c_uLn(R_p/r) - c_u$; $\Delta\sigma_1 = \Delta\sigma_r = 2c_uLn(R_p/r) + c_u$, $\Delta\sigma_3 = \Delta\sigma_\theta = 2c_uLn(R_p/r) - c_u$; $\sigma_f = (\sigma_1+\sigma_3)_f/2 = K_0\sigma'_{v0}+2c_uLn(R_p/r)$; $(\Delta\sigma_1-\Delta\sigma_3)_f = \Delta\sigma_r-\Delta\sigma_\theta = 2c_u$; $u_f = 2c_uLn(R_p/r)+0.817\alpha_f c_u$;

$\therefore \sigma'_A = \sigma_f - u_f = K_0\sigma_{v0}-0.817\alpha_f c_u$;

Thus, $$\frac{c_u}{\sigma_A} = \frac{c_u}{K_0\sigma_{v0} - 0.817\alpha_f c_u} = tg\alpha' = Sin\varphi'$$

$$c_u = \frac{K_0 Sin\varphi'}{1+0.817\alpha_f Sin\varphi'}\sigma_{v0} \qquad (4\text{-}19)$$

or $$\Delta u = \frac{K_0 Sin\varphi'}{1+0.817\alpha_f Sin\varphi'}\left[2Ln\left(\frac{R_p}{r}\right)+0.817\alpha_f\right]\cdot(q+\gamma_w d_w+\gamma' z) \qquad (4\text{-}19a)$$

However, because $\sigma'_A < \sigma'_0$, e.g., this is in over-consolidated state, line K'_f does not intersect at A but at B. It leads under-estimate of c_u and Δu.

Assuming $\sigma'_B \approx \sigma'_0 = \sigma'_{v0}(1+K_0)/2$,

Thus, $$\frac{c_u}{\sigma'_B} = \frac{2c_u}{(K_0+1)\sigma'_{v0}} = tg\alpha' = Sin\varphi'$$

$$c_u = (K_0+1)\sigma'_{v0}Sin\varphi'/2 \qquad (4\text{-}19')$$

$$\Delta u = \frac{(K_0+1)}{2}Sin\varphi'\left[2Ln\left(\frac{R_p}{r}\right)+0.817\alpha_f\right]\cdot(q+\gamma_w d_w+\gamma' z) \qquad (4\text{-}19b)$$

Table 4-1 Properties of deposits within the soil of #3 Subway of Shanghai City

Soil and No.	Thick (m)	W (%)	γ_{sat} (KN/m^2)	e_0	S_r	E_{s1-2} (Mpa)	φ' (°)
(1) Sandy Silt	7.5	31.8	18.9	0.88	0.98	3.8	28
(2) Mucky Clay	5.1	64.4	17.1	1.49	0.99	3.0	27
(3) Silt	11.6	43.3	17.8	1.21	0.98	3.2	28
(4) Silty Clay	4.3	23.8	20.0	0.69	0.98	3.5	31
(5) Silty Sand	8.1	28.8	19.0	0.83	0.99	3.7	32

Now checking formulae (4-17a) to (4-19a) using the field measured data from penetrating pile test #3 on the Shanghai City Subway in China (Chen 1999), with a square pile section of 0.45 m × 0.45 m, made of reinforced concrete and having a length of 30 m. The groundwater table $d_w \approx 1.0$ m below ground level. Deposits of soil layer are shown in Table 4-1. The pore-pressure meter is 0.8m away from the pile's axis. The depths of the measured points are 3.75m, 10.01m, 18.4m, 26.35m, 30.00 m.

The following are the average values of the various soil parameters: $\overline{\gamma'}$ = 8.33 kN/m^2, $\overline{\varphi'}$ = 29°, $\overline{E_{s1-2}}$ = 3.44 MPa, $\overline{c_u}$ = 20 kPa and A_f=0.9.

Empirically, taking Poisson's ratio μ = 0.3; K_0 = 1-*Sin*φ'=0.5152, K'_0 = $(1-K_0)/(1+K_0)$ =0.32. The equivalent radius of the pile $r_0 = \sqrt{b^2/\pi} = b/\sqrt{\pi}$ = 0.5642b = 0.2539m. Theoretically, the soil's elastic modulus is defines as being $E = \left(1-\frac{2\mu^2}{1-\mu}\right)E_{s1-2}$ but this is usually not correct. For soft clays, it is known that $E > \approx E_{s1-2}$. Therefore, one

can assume that E ≈ (1.1~1.2) $\overline{E_{s1-2}}$ = (1.1~1.2)×3.44 = 3.78~ 4.13 MPa. α_f = 0.707(3A_f-1) = 1.202. (e.g. r = 0.8 m). The long-term surface load q ≈ 20 kPa.

Hence,

$$\frac{R_p}{r_0} = \sqrt{I_r} = \sqrt{\frac{E}{2(1+\mu_u)\overline{c_u}}} = \sqrt{\frac{(3.78 \sim 4.13)\times 10^3}{2\times(1+0.5)\times 20}} = 7.94\sim 8.4 \approx 8.2;$$

$$\frac{R_p}{r} = \frac{R_p}{r_0}\frac{r_0}{r} = (7.94\sim 8.4)\times 0.254/0.8 = 2.52\sim 2.667 \approx 2.6$$

Using (4-17a),

$$\Delta u = \frac{1+2K_0}{3}\cdot\frac{Sin\varphi'}{1-(1-2A_f)Sin\varphi'}\left[2Ln\left(\frac{R_p}{r}\right)+0.817\alpha_f\right]\cdot(q+\gamma_w d_w+\gamma' z)$$

$$\approx 0.6768\times 0.3493\times 2.893057\times(29.86+8.33z) = 22.86+7.53z \text{ (KPa)}$$

Using (4-18a),

$$\Delta u = \frac{1+K_0}{2}\cdot\frac{[1-(1-2A_f)K_0']Sin\varphi'}{1-(1-2A_f)Sin\varphi'}\left[2Ln\left(\frac{R_p}{r}\right)+0.817\alpha_f\right]\cdot(q+\gamma_w d_w+\gamma' z)$$

$$\approx 0.7576\times 0.43875\times 2.893057\times(29.86+8.33z) = 28.7+8.01z \text{ (kPa)}$$

Using (4-19a),

$$\Delta u = \frac{K_0 Sin\varphi'}{1+0.817\alpha_f Sin\varphi'}\left[2Ln\left(\frac{R_p}{r}\right)+0.817\alpha_f\right]\cdot(q+\gamma_w d_w+\gamma' z)$$

$$\approx 0.16921\times 2.893057\times(29.86+8.33z) = 14.62+4.08z \text{ (kPa). It is too small.}$$

Using (4-19b),

$$\Delta u = \frac{(K_0+1)}{2}Sin\varphi'\left[2Ln\left(\frac{R_p}{r}\right)+0.817\alpha_f\right]\cdot(q+\gamma_w d_w+\gamma' z)$$

$$= 0.3673\times 2.893057\times(29.86+8.33z) = 31.73+8.85z \text{ (kPa).}$$

Comparing the above three estimate equations with field measured data shows that the estimate for pore pressure generated during pile driving using Equation (4-18a) is acceptable, as shown in Fig. 4-9, whereas the use of Equation (4-17a) gives an slight under-estimate, Equation (4-19a) yields an half under-estimate, and Equation (4-19b) yields an over-estimate. Only the calculated value for the pile tip differs from the measured one, and so one should use 3-D spherical expansion theory for this point, that is:

$$\Delta u = c_u\left[4Ln\left(\frac{R_p}{r}\right)+0.94\alpha_f\right] \qquad (4\text{-}20)$$

Here R_p differs with R in (4-15) or (4-17a~19a),

$\frac{R_p}{r_0}=\sqrt[3]{I_r}=\sqrt[3]{\frac{E}{2(1+\mu_u)\tau_f}}=\sqrt[3]{\frac{G}{\tau_f}}=\sqrt[3]{\frac{G}{c+q'\tan\varphi}}$. E/τ_f=500~1000; Taking E/τ_f= 900 for silty sand;

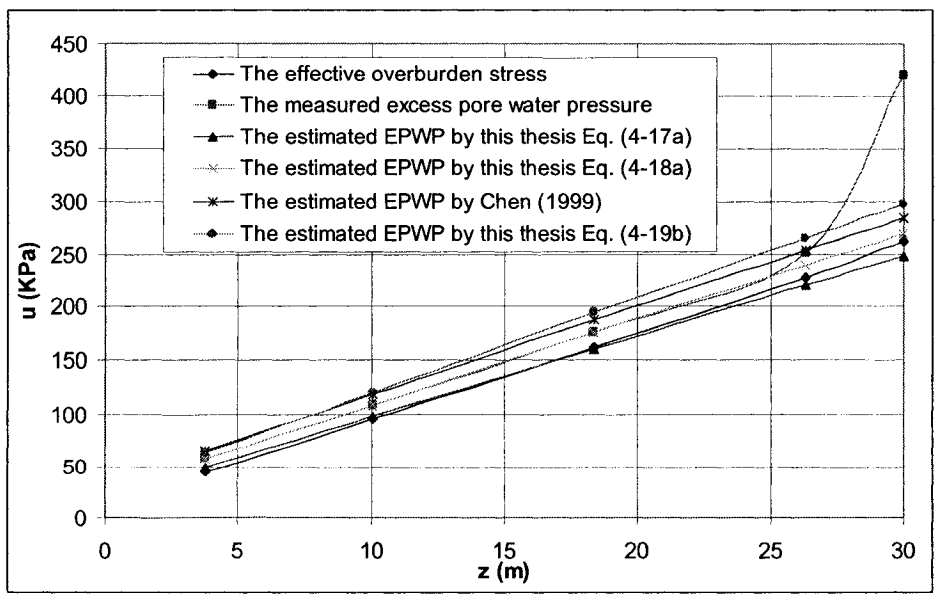

Fig. 4-9 Measured and Predicted Excess Pore Pressures with Depth

$$\frac{R_p}{r_0} = \sqrt[3]{\frac{E}{3\tau_f}} = \sqrt[3]{\frac{900}{3}} = 6.694; \quad \frac{R_p}{r} = \frac{R_p}{r_0}\frac{r_0}{r} = 6.694 \times 0.254/0.8 = 2.1253$$

Using (4-17),

$$\Delta u = \frac{1+2K_0}{3}\frac{Sin\varphi'}{1-(1-2A_f)Sin\varphi'}\left[4Ln\left(\frac{R_p}{r}\right)+0.94\alpha_f\right]\cdot(q+\gamma_w d_w+\gamma' z)$$

$$\approx 0.6768\times0.3493\times4.14\times280 = 274 \text{ kPa};$$

which is much smaller than the measured value of 419 kPa

Using (4-18),

$$\Delta u = \frac{1+K_0}{2}\cdot\frac{[1-(1-2A_f)K_0']Sin\varphi'}{1-(1-2A_f)Sin\varphi'}\left[4Ln\left(\frac{R_p}{r}\right)+0.94\alpha_f\right]\cdot(q+\gamma_w d_w+\gamma' z)$$

$$= 0.7576\times0.43875\times4.14\times280 = 385 \text{ kPa};$$

which is more near to the measured value 419 kPa.

Using (4-19),

$$\Delta u = \frac{1+K_0}{2}\cdot Sin\varphi'\left[4Ln\left(\frac{R_p}{r}\right)+0.94\alpha_f\right]\cdot(q+\gamma_w d_w+\gamma' z)$$

$$=0.3673\times4.14\times280 = 426\text{KPa};$$

which is slightly higher that the measured value 419 kPa.

This shows that equations (4-18) and (4-19) can be used to estimate additional pore pressure from pile driving at the pile tip. Equation (4-18b) is simply Wroth et al's method (1979).

Some field measured data, seen in Fig. 4-10, also show that the excess pore pressure generated by pile driving increases almost linearly with depth.

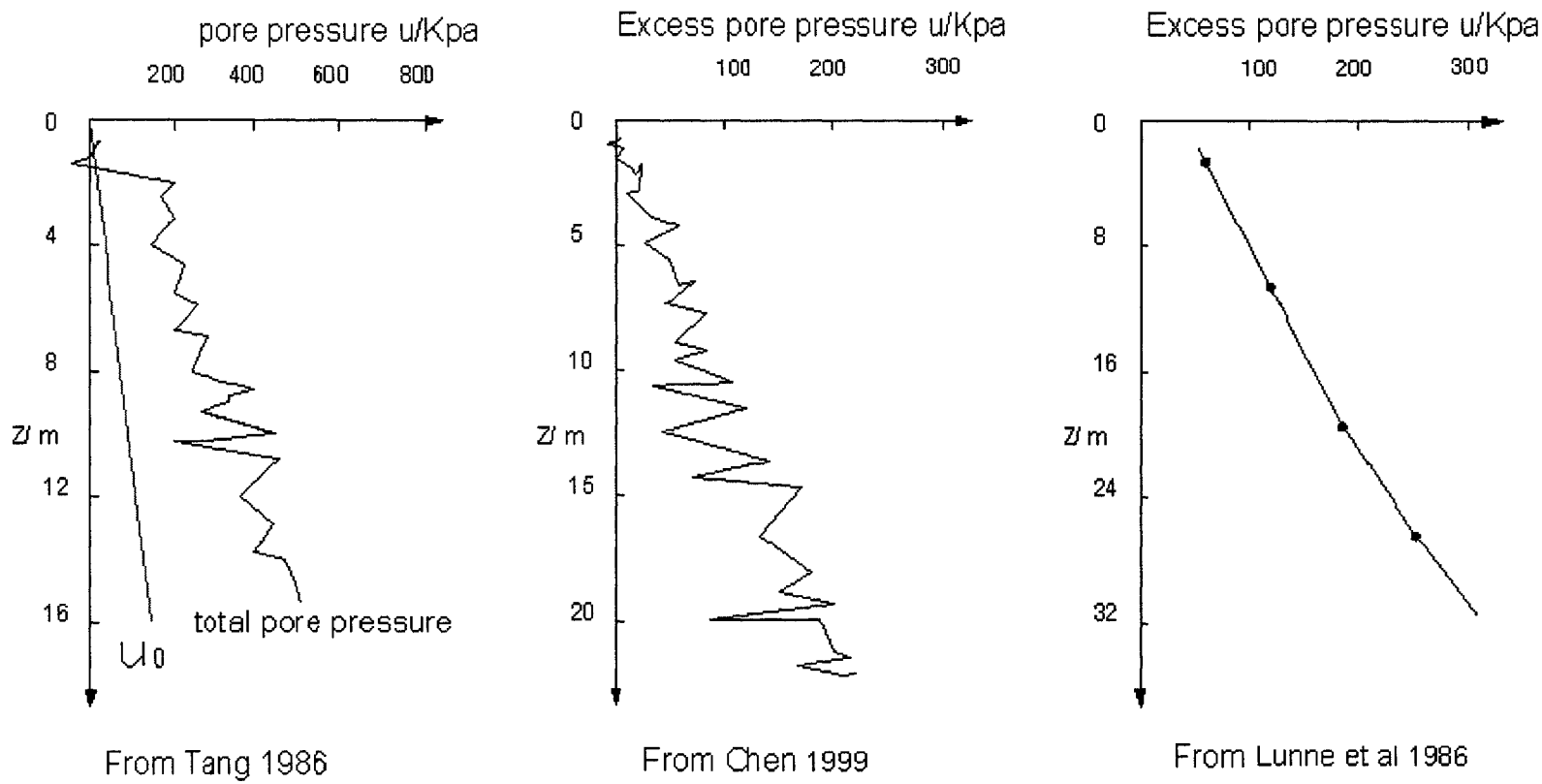

Fig. 4-10 Field Measured Excess Pore-Pressure Linearly Increase With Depth

Similarly, Azzouz et al (1988), Maqsood et al (1994), Lunne (1986), Kalsarud and Haugen(1985) all measured stresses and excess pore-pressure around piles using Piezo-Lateral Stress Cells (PLSC) and Cone Penetration Tests (CPT) and found that stresses and excess pore-pressure increase linearly with depth.

4.5 Initial Pore Pressure Distribution Due to Group Piles Driving

The initial distribution of excess pore water pressure (EPWP) from the group pile driving can be estimated based on the distribution of EPWP due to single pile driving.

4.5.1 Method of Estimation

According to the fundamental research and observations on excess pore pressure caused by the group pile construction (Tang 1990; Yang, Wu and Fi 1996; Zheng et al 1998; Mu 1998), the following general rules can be established:

(1) Zheng et al (1998) proved through the centrifugal model test that excess pore water pressure produced in soil differs according to the order of pile driving; it is larger for piles driven from the outside edges and corners to the inside (center). Regardless of the pile driving order, excess pore pressure finally tends to reach a similar stable value.

(2) In the internal piles of the pile group, excess pore pressure near the center pile is obviously larger than that of the side piles; in the exterior piles of the pile group, excess pore pressure distribution, similar to that of single piles, decreases rapidly with the distance from side piles.

(3) During construction, excess pore pressure in the pile group has a tendency to gradually increase, but it is limited by one maximum value. Much of the measured data

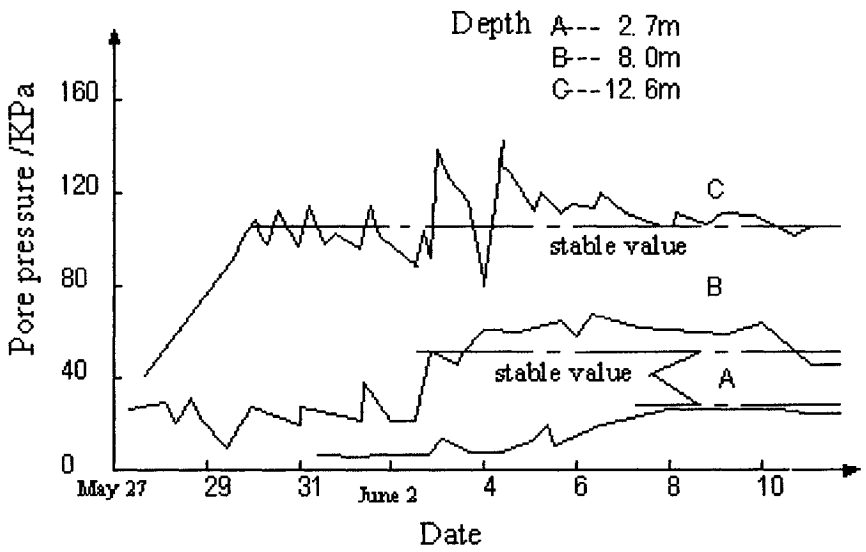

Fig. 4-11 Pore Pressure Change at Different Depths during Driving Procedure (From Tang 1990)

indicates that the instantaneous maximum excess pore pressure may reach (1.5~2.0)γ'h and may even reach up to (3~4)γ'h. However, some time (5-10 days) after the end of pile driving, the pore pressure value at the same depth tends to finally stabilize.

(4) With increasing depth, the stabilized value of excess pore pressure increases and approaches that of the effective overburden pressure σ'_v ($\approx \gamma'h$). Because effective stress increments in soil are a function of pore pressure and effective tangential stress, σ'_θ, can possibly be negative. When a negative effective tangential stress surpasses the extent of the soil's strength, vertical and horizontal fractures may appear in the direction that reduces effective stresses, such as the appearance of hydraulic cracks. Once the excess pore pressure drops to be of the order of the effective overburden pressure σ'_v, the fractures close, and the excess pore pressure is stable, as shown in Fig. 4-11.

There are some methods that one can use to pre-estimate the initial excess pore pressure caused by driving group piles:

(a) Equivalent-pile method

In case of the number of piles is more than 3 - 4, excess pore pressure on the inside of the pile group tends to reach a definite maximum value, the conception of an equivalent pile can be used to estimate some of the excess pore pressure's influence, caused by the driving of a group pile, on a pile outside of the pile group. The principles of the method are the equal total section area and the invariable shape-centre position of piles shown in Fig. 4-12. Thus, group piles are assumed to be an equivalent pile, and excess pore pressure of a pile group can be calculated by the means of the computational method and processes of a single pile. The method should not be used to estimate the value at internal points of the pile group.

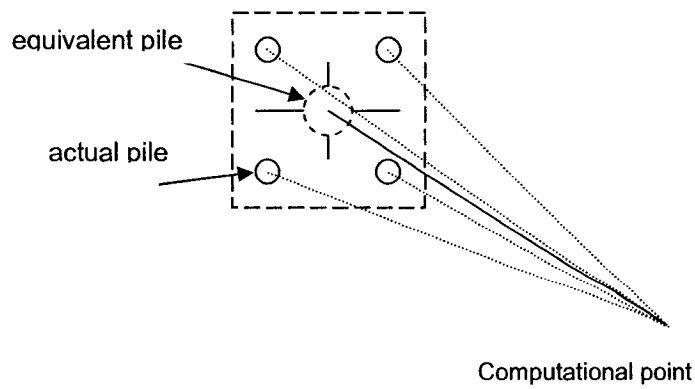

Fig. 4-12 Equivalent-pile Method

(b) Superposition method:

The excess pore pressure on the inside of the pile group, $u_g(t)$, is equal to the sum of all the values individually caused by each pile,

$$u_g(t) = Min\left\{\sum_i^n u_i(r_i, t-t_i),\quad \Delta u_m\right\} \tag{4-21}$$

in which,

$u_g(t)$--- excess pore pressure from the construction of group piles at a given time and location;

u_i ---- excess pore pressure at the calculation point from the i-th pile; equation $u_i(r_i, t)$ is defined in chapter 5.

t, ----the computation time, where t_i is the time at which the i-th single pile enters the soil ($t \geq t_i$);

h ---- depth of the calculation point

For a more general case, neglecting the construction procedure and time factor, the initial excess pore pressure can be estimated by using the following formulae:

Using Poulos & Davis's formula (2-41),

$$u_G = \sum_i^n u_i(r_i,0) = \Delta u_m R^2 \sum_{i=1}^n \frac{1}{r_i^2} \tag{4-22}$$

Using uniform formula (2-42)

$$u_G = \sum_i^n u_i(r_i,0) = \frac{\Delta u_m}{Ln\omega}\sum_{i=1}^n Ln\left(\frac{\omega r_0}{r_i}\right) = \frac{\Delta u_m}{Ln\omega}\left[nLn(\omega r_0) - \sum_i^n Ln(r_i)\right]$$

$$= \frac{\Delta u_m}{Ln\omega} Ln\left[\frac{(\omega r_0)^n}{r_1 r_2 \cdots r_n}\right] \qquad (r_i \le \omega r_0) \qquad (4\text{-}23)$$

A case of four piles with pile-pile space S is considered, shown in Fig. 4-13, where the construction procedure and time factor are neglected. Thus, the initial excess pore pressures from the driving of the four piles at points A and B are estimated.

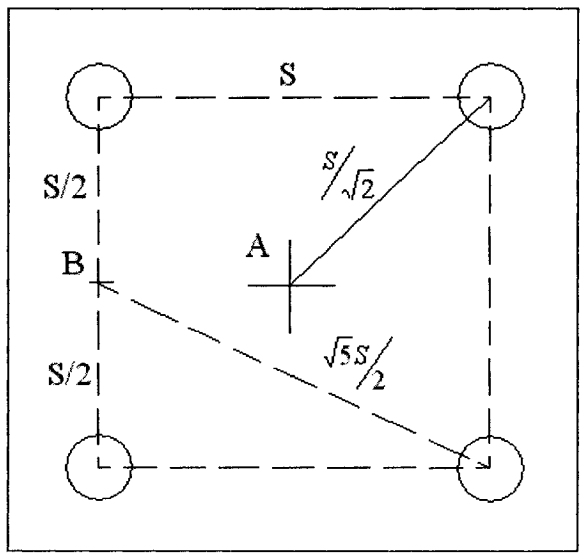

Fig. 4-13 Superimposition Method for Four Piles

Using Poulos & Davis's formula (2-41) and (4-21),

$$u_A = \sum_i^4 u_i(r_i,0) = 4\Delta u_m \left(\frac{R}{S/\sqrt{2}}\right)^2$$

$$= 8\Delta u_m \left(\frac{R}{S}\right)^2 \le \Delta u_m \qquad \Rightarrow \ S \ge S_c = 2\sqrt{2}R = 2.83R \qquad (4\text{-}24)$$

If R = 4~8, then

$$S \geq S_c = (11.3\sim22.6)\, r_0 = (5.7\sim11.3)d \qquad (4\text{-}24')$$

(d is the diameter of the pile).

$$u_B = \sum_i^4 u_i(r_i,0) = 2\Delta u_m\left(\frac{R}{S/2}\right)^2 + 2\Delta u_m\left(\frac{R}{\sqrt{5}S/2}\right)^2$$

$$= 9.6\Delta u_m\left(\frac{R}{S}\right)^2 \leq \Delta u_m$$

$$\Rightarrow S \geq S_c = 3.10R = (12.4\sim24.8)\, r_0 = (6.2\sim12.4)\, d \qquad (4\text{-}25)$$

Using Tang's formula (2-42) and (4-23),

$$u_A = \sum_i^4 u_i(r_i,0) = 4\frac{\Delta u_m}{Ln(\omega)} Ln\left(\frac{\omega r_0}{S/\sqrt{2}}\right)$$

$$= 4\frac{\Delta u_m}{Ln(\omega)} Ln\left(\sqrt{2}\omega\frac{r_0}{S}\right) \leq \Delta u_m$$

$$\Rightarrow S \geq S_c = \sqrt{2}\omega^{3/4} r_0 \qquad (4\text{-}26)$$

If ω = 20~30, then

$$S \geq S_c = (13.4\sim18.1)\, r_0 = (6.7\sim9.1)d \qquad (4\text{-}26')$$

$$u_B = \sum_i^4 u_i(r_i,0) = 2\frac{\Delta u_m}{Ln(\omega)} Ln\left(\frac{\omega r_0}{S/2}\right) + 2\frac{\Delta u_m}{Ln(\omega)} Ln\left(\frac{\omega r_0}{S\sqrt{5}/2}\right)$$

$$= 4\frac{\Delta u_m}{Ln(\omega)} Ln\left(\frac{\omega r_0}{S/2}\right) - 2\frac{\Delta u_m}{Ln(\omega)} Ln\left(\sqrt{5}\right) \leq \Delta u_m$$

$$\Rightarrow S \geq S_c = \frac{2}{\sqrt[4]{5\omega}}\omega r_0 = \frac{2\omega^{0.75}}{5^{0.25}} r_0 = (12.6\sim17.2)\, r_0 = (6.3\sim8.6)d \qquad (4\text{-}27)$$

According to equations (4-24) to (4-27), when the number of piles is ≥ 4 and S ≤ (6~12)d, for a general pile group situation for, the initial excess pore pressure reaches Δu_m.

Similarly, for cases of three (Fig. 4-14) and nine piles (Fig.4-15), one can observe some similar results, as shown in Table 4-2.

It should be noted that when using Equation (4-23), one must check if r_i is larger than ωr_0. If $r_i > \omega r_0$ then one should take $r_i = \omega r_0$. For example, the calculation for the critical pile space S_c for $u_G=\Delta u_m$ for a 9 piles case is shown in Fig.4-15.

$$u_A = \frac{\Delta u_m}{Ln\omega} Ln\left[\frac{(\omega r_0)^9}{\left(\frac{1}{\sqrt{2}}S\right)^4\left(\sqrt{\frac{5}{2}}S\right)^4\left(\frac{3}{2}S\right)}\right] = \frac{\Delta u_m}{Ln\omega}\left[Ln\left(\frac{\omega r_0}{S}\right)^9 - Ln\frac{75}{32}\right] \le \Delta u_m$$

$$\Rightarrow\ S \ge S_c = \left(\frac{32}{75}\right)^{\frac{1}{9}} \omega^{\frac{8}{9}} r_0 = 0.9097\omega^{\frac{8}{9}} r_0 = (13.04\sim 18.70)r_0$$

But, $r_{A5} = r_{A6} = r_{A7} = r_{A8} = \sqrt{5/2}\ S = 1.5811S = 1.5811\times 13.04\ r_0 = 20.62\ r_0 > \omega r_0$ (ω=20)

or $r_{A5} = r_{A6} = r_{A7} = r_{A8} = 1.5811S = 1.5811\times 18.70\ r_0 = 29.57\ r_0 < \omega r_0$ (ω=30)

Hence, when $\omega = 20$, set $r_{A5}\sim r_{A9} = \omega r_0$, the case is as the same as the case of 4 piles; when ω=30, set $r_{A9} = \omega r_0$, then

$$u_A = \frac{\Delta u_m}{Ln\omega} Ln\left[\frac{(\omega r_0)^8}{\left(\frac{1}{\sqrt{2}}S\right)^4\left(\sqrt{\frac{5}{2}}S\right)^4}\right] = \frac{\Delta u_m}{Ln\omega}\left[Ln\left(\frac{\omega r_0}{S}\right)^8 - Ln25\right] \le \Delta u_m$$

$$\Rightarrow\ S \ge S_c = \sqrt{2}25^{-\frac{1}{8}} \omega^{\frac{7}{8}} r_0 = 0.9457\omega^{\frac{8}{9}} r_0 = 18.5\ r_0$$

For point B, we may find that only $r_{B6}\sim r_{B9} > \omega r_0$ (ω=20~30). Hence,

$$u_B = \frac{\Delta u_m}{Ln\omega} Ln\left[\frac{(\omega r_0)^5}{\left(\frac{1}{2}S\right)^2\left(\sqrt{\frac{5}{2}}S\right)^2\left(\frac{3}{2}S\right)}\right] = \frac{\Delta u_m}{Ln\omega}\left[Ln\left(\frac{2\omega r_0}{S}\right)^5 - Ln(15)\right] \le \Delta u_m$$

$$\Rightarrow\ S \ge S_c = 2\times 15^{-\frac{1}{5}} \omega^{\frac{4}{5}} r_0 = 1.1636\omega^{\frac{4}{5}} r_0 = (12.8\sim 17.7)r_0 \quad \text{(shown in Table 4.2)}$$

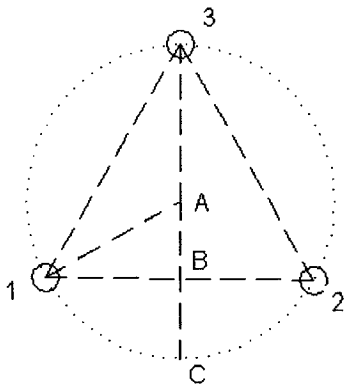

Fig. 4-14 Superimposition method for three piles

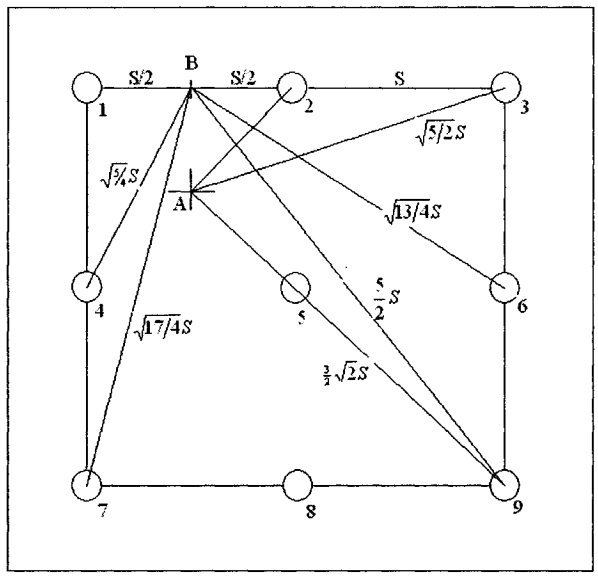

Fig. 4-15 Superimposition Method for nine piles

Table 4-2 Critical pile spacing S_c when $u_G=\Delta u_m$

Cases		Poulos & Divis fomula R=(3~8)r_0	Uniform fomula ω = 20~30
3 piles	Point A	S_c=3.0 R =(9.0~24.0) r0 =(4.5~12.0)d	$S_c=\sqrt{3}\omega^{2/3}r_0$ = (12.8~16.7)r0 =(6.4~8.4)d
	Point B	S_c=3.06 R =(9.2~24.5) r_0 =(4.6~12.3)d	S_c=1.6654 $\omega^{2/3}r_0$ = (12.3~16.1)r_0 =(6.1~8.0)d
	Point C	S_c=2.83 R =(8.5~22.6) r_0 =(4.3~11.3)d	S_c=1.3747 $\omega^{2/3}r_0$ = (10.1~13.3)r_0 =(5.0~6.6)d
4 piles	Point A	S_c=2.60 R =(7.8~20.8) r_0 =(3.9~10.4)d	$S_c=\sqrt{2}\omega^{3/4}r_0$ = (13.4~18.1)r_0 =(6.7~9.1)d
	Point B	S_c= 3.10 R =(9.3~24.8) r_0 =(4.7~12.4)d	$S_c=2\times5^{-0.25}\omega^{0.75}r_0$ =(12.6~17.2) r_0 =(6.3~8.6)d
9 piles	Point A	S_c= 3.13 R =(9.4~25.0) r_0 =(4.7~12.5)d	$S_c=\sqrt{2}\omega^{3/4}r_0\sim0.9457\omega^{7/8}r_0$ =(13.4~18.5) r_0 =(6.7~9.3)d
	Point B	S_c=3.31 R =(9.9~26.5) r_0 =(5.0~13.4)d	S_c=1.1636 $\omega^{2/3}r_0$ =(12.8~17.7) r_0 =(6.4~8.9)d

The critical pile spacing S_c of cases more than 9 piles should be slightly bigger than that of 9-pile case and thus can be theoretically determined for the 9 piles case, shown in Table 4-2. In the case where $S \leq S_c$, EPWP one should always take $u_G = \Delta u_m$.

4.5.2 Estimation of the Initial Pore-Pressure Distribution for Group Piles

Case: A 9-pile group, with pile d = 0.4 m (radius $r_0 = 0.2$m) and pile space S = (3~10)d is shown in Fig. 4-16.

The result according to formula (4-22) and R = 4d (= $8r_0$), shown in Fig. 4-17, indicate that there seems to be little influence from pile spacing on the distribution of excess pore water pressure (EPWP). Comparatively, the result obtained according to the equivalent-pile method is close to the result of formula (4-22) when S/d = 3. The equivalent-pile method does not consider the influence of pile space on the distribution of EPWP.

The result according to the formula (4-23) and $\omega = 30$ is shown in Fig. 4-18.

The result according to the formula (4-2) and $R_p/r_0 = 8$ is shown in Fig. 4-19

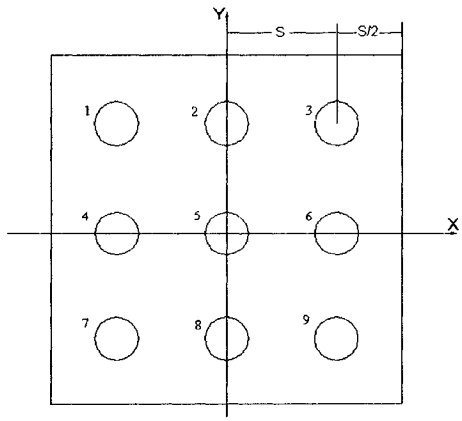

Fig. 4-16 Position of the piles in the group

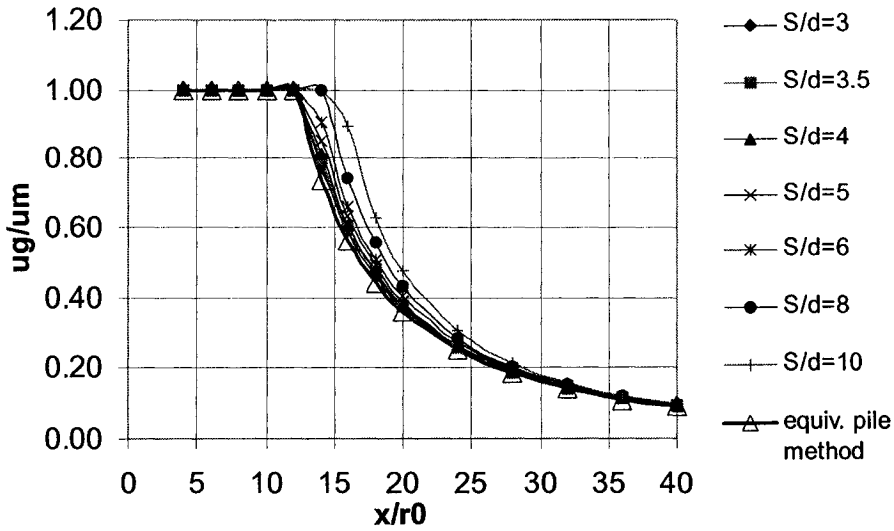

Fig. 4-17 Distribution of EPWP corresponding to different pile spacing, from equation (4-22)

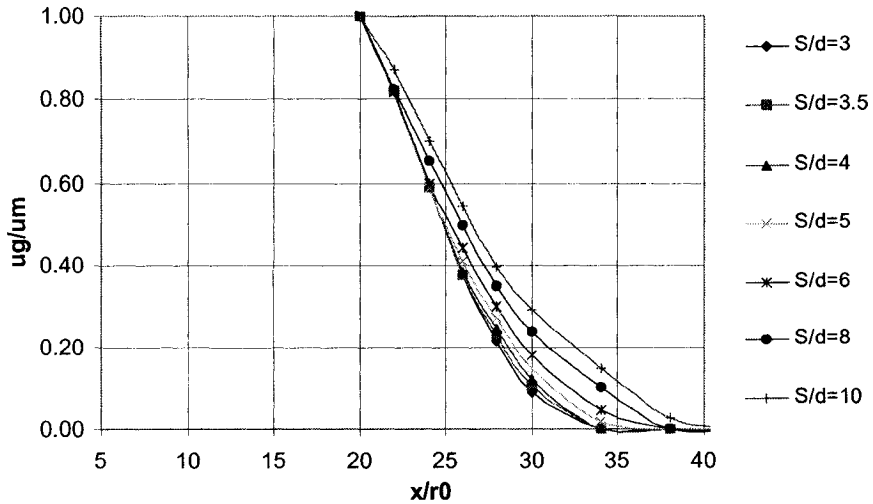

Fig. 4-18 Distribution of EPWP corresponding to different pile spacing, from equation (4-23)

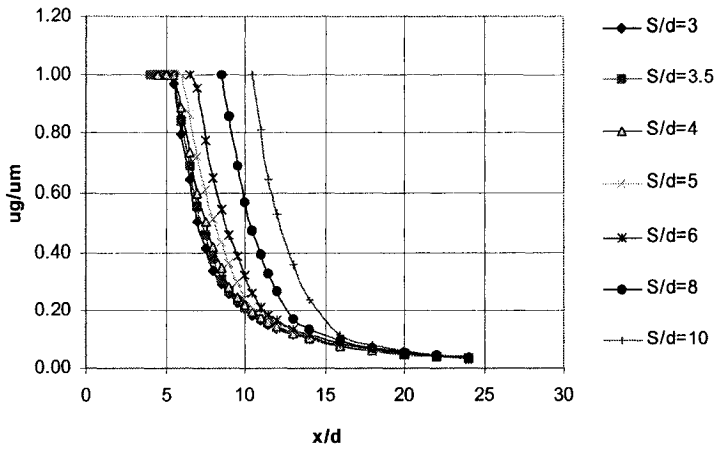

Fig. 4-19 Distribution of EPWP corresponding to different pile spacing, from equation (4-2)

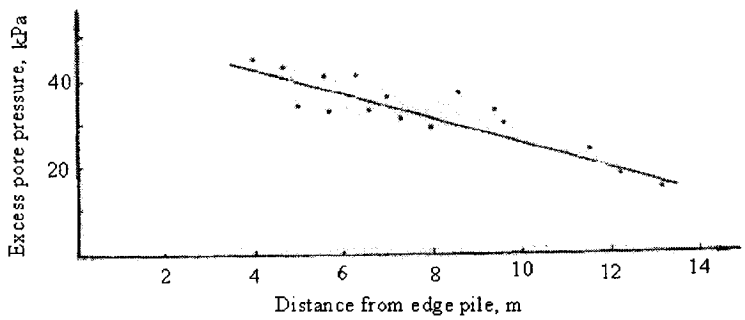

Fig. 4-20 Excess pore pressure caused by group piles (Tang 1990)

From Fig. 4-18&19, it is possible to simplify the distribution of EPWP into a linear variation with horizontal distance x. Also, the measured data from Tang (1990) prove this, as seen in Fig. 4-20.

4.6 Discussion

The pore pressure generated during single pile driving is not only due to cavity expansion but also partly due to an increase in mean total stress caused by skin friction along the pile and the point load P_b at the pile tip. The effect on the pore pressure caused by residual forces is small and can be neglected.

An approximate analysis of strength-stress relationship and field measured data shows that the excess pore pressure generated by pile driving increases almost linearly with depth.

Hydraulic fractures in soil during pile driving make the excess pore pressure fall to a stable level in the order of the effective overburden pressure σ'_v. This becomes a factor that is considered in the calculation of excess pore pressure on the inside of a pile group.

According to case calculation and some field data, the distribution of EPWP due to pile group with horizontal distance can be simplified into a linear variation.

CHAPTER 5

ANALYSIS OF PORE-WATER PRESSURE DISSIPATION

5.1 General

In this chapter solutions are developed for the dissipation and consolidation of excess pore water pressure (EPWP). This is based on the assumption that the effect of the piles on water permeating is ignored. First, analytical solutions for uniform soils are considered. These solutions apply in cases for plane strain problems, axi-symmetrical strain problems, rectangular area problems (only with water permeating horizontally), and 3-D dissipation problems. For layered soil, the use of the Finite Layer Method on Biot's Consolidation Theory don't give a stable results, and it has been found that the model easily caused data to diverge and that it could not converge to a stable value in a given time-increment. Instead, a study was conducted to find the numerical inversion of Laplace-Fourier integral transforms and an arithmetic method.

5.2 Analytical Solution of Pore-Pressure Dissipation in Uniform Soil

There are various problems, such as plane strain problems, axi-symmetrical strain problems, rectangular area problems (only water permeating horizontally), and 3-D dissipation problems, that any solution must address.

5.2.1 Plane Problem of Horizontal Dissipation

For plane-strain problems, the p.w.p dissipation or consolidation of a soil can be expressed mathematically (ignoring the effect of the piles):

$$\frac{\partial u}{\partial t} = C_h \frac{\partial^2 u}{\partial x^2} \tag{5-1}$$

$$u(x,0) = \psi(x) = \begin{cases} u_0 & (0 \le |x| \le b) \\ u_0 \dfrac{l-x}{l-b} & (b \le |x| \le l) \\ 0 & (|x| \ge l) \end{cases} \tag{5-1a}$$

The form of $\psi(x)$ is shown in Fig. 5-1.

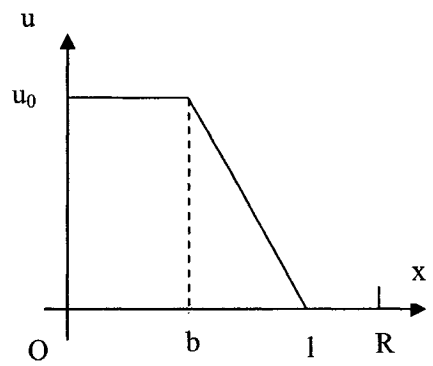

Fig. 5-1 $u(x,0)$ form

There are two boundary conditions at $|x| = R$:

a) Impermeable boundary condition:

$$\partial u/\partial x \,|_{x=0} = 0,\ \partial u/\partial x \,|_{|x|=R} = 0 \tag{5-1b}$$

b) Permeable boundary condition:

$$\partial u/\partial x \,|_{x=0} = 0,\ u \,|_{|x|=R} = 0 \tag{5-1c}$$

Where b is the contribution distance of the initial maximum p.w.p u_m, l is the range distance of the initial p.w.p contribution u = 0, R is the effective distance of finite p.w.p $u|_{t=\infty}$.

The solution of the above plane problem for impermeable boundary condition Eq. (5-1b) **(Appendix B-1)** is:

$$u(x,t) = u_0 \frac{l+b}{2R} + u_0 \sum_{n=1}^{\infty} \frac{2}{(n\pi)^2} \frac{R}{l-b} \left(\cos \frac{n\pi b}{R} - \cos \frac{n\pi l}{R} \right) \cos \left(\frac{n\pi x}{R} \right) \exp \left(- C_h \frac{n^2 \pi^2}{R^2} t \right)$$

(5-2)

When $R = l$, $a_n = \frac{2u_0}{(n\pi)^2} \frac{l}{l-b} \left(\cos \frac{n\pi b}{l} - \cos n\pi \right)$

$$\mathrm{u(x,t)} = u_0 \frac{1}{2} \left(1 + \frac{b}{l} \right) + u_0 \sum_{n=1}^{\infty} \frac{2l}{n^2 \pi^2 (l-b)} \left(\cos \frac{n\pi b}{l} - \cos n\pi \right) \cos \left(\frac{n\pi x}{l} \right) e^{-C_h \frac{n^2 \pi^2}{l^2} t}$$

(5-2a)

When b = l, $a_n = \frac{2u_0}{n\pi} \sin \frac{n\pi b}{R}$

$$\mathrm{u(x,t)} = u_0 \frac{1}{2} \left(1 + \frac{b}{l} \right) + u_0 \sum_{n=1}^{\infty} \frac{2u_0}{n\pi} \sin \frac{n\pi b}{R} \cdot \cos \left(\frac{n\pi x}{l} \right) e^{-C_h \frac{n^2 \pi^2}{l^2} t} \qquad \text{(5-2b)}$$

Noticing that $\mathrm{u(x,t)} \rightarrow u_0 \frac{l+b}{2R}$ when $t \rightarrow \infty$, it is known that the permeable boundary condition at $x = R_x$ does not agree with the actual situation of geotechnical engineering. Therefore, only the permeable boundary condition in the horizontal direction was used.

The solution to the above plane problem for permeable boundary conditions Eq. (5-1c) **(Appendix B-2)** is

$$u(x,t) = u_0 \sum_{n=0}^{\infty} c_n \cos \left(\frac{(\frac{1}{2}+n)\pi x}{R} \right) \cdot \exp \left(- C_h \frac{(\frac{1}{2}+n)^2 \pi^2}{R^2} t \right) \qquad \text{(5-3)}$$

Where, $c_n = \frac{2}{(\frac{1}{2}+n)^2 \pi^2} \frac{R}{l-b} \left(\cos \frac{(\frac{1}{2}+n)\pi b}{R} - \cos \frac{(\frac{1}{2}+n)\pi l}{R} \right)$ (5-3a)

If l = b, $$c_n = \frac{2u_0}{(1/2+n)\pi}\sin\frac{(1/2+n)\pi b}{R}$$

$$u(x,t) = u_0\sum_{n=1}^{\infty}\frac{2}{(1/2+n)\pi}Sin\frac{(1/2+n)\pi b}{R}Cos\left(\frac{(1/2+n)\pi x}{R}\right)Exp\left(-C_h\frac{(1/2+n)^2\pi^2}{R^2}t\right)$$

(5-3b)

Case1: l/R = 0.5, b/R = 0.2, x = 0, the consolidation degree U = $(u_0-u)/u_0$ from (5-3) is shown on Fig. 5-2, Fig. 5-3.

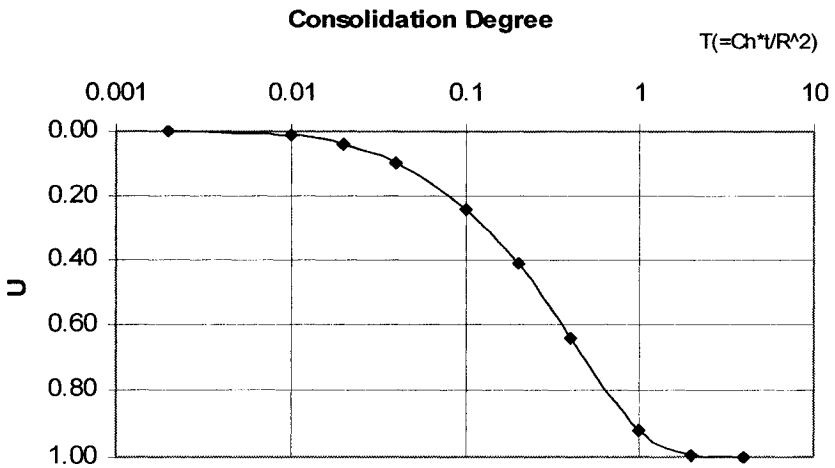

Fig. 5-2 Consolidation degree U –Time factor T Curve by Eq. (5-3) When x=0

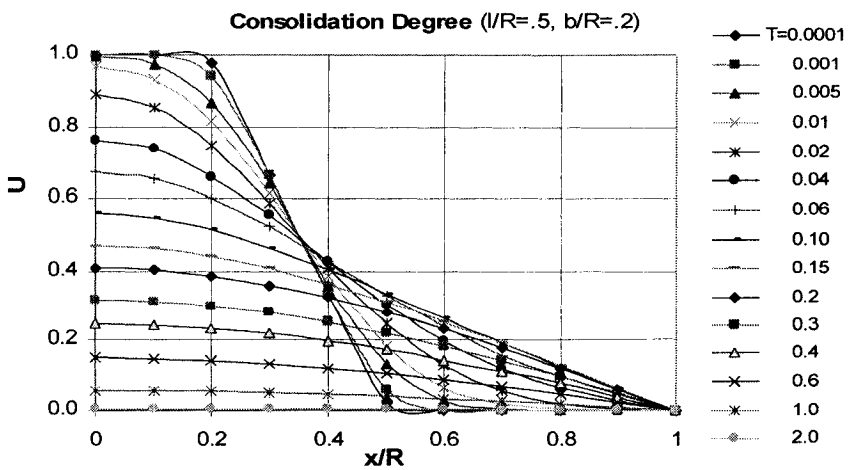

Fig 5-3 Consolidation-degree distribution under Time-factors (Case 1)

Case2: l/R = 1.0, b/R = 0.2, x = 0. The consolidation degree U = $(u_0-u)/u_0$, u from Eq. (5-3), is shown on Fig. 5-4

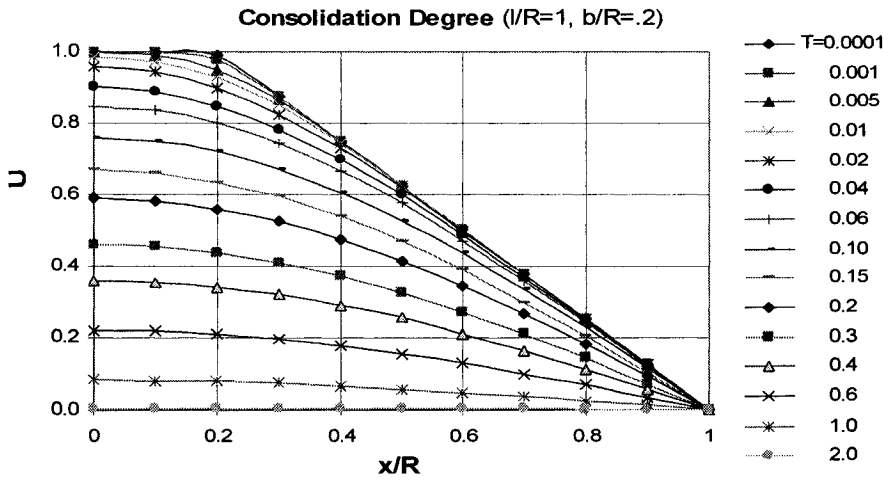

Fig. 5-4 Consolidation-degree distributions under different Time-factors at initial pore pressure (Case2)

5.2.2 Axi-symmetrical (Circle Area) Problem of Horizontal Dissipation

For axisymmetrical strain problem, p.w.p dissipation or consolidation of soil can be expressed mathematically:

$$\frac{\partial u}{\partial t} = C_h\left(\frac{\partial^2 u}{\partial r^2} + \frac{1}{r}\frac{\partial u}{\partial r}\right) \qquad (5\text{-}4)$$

$$u(x,0) = \omega(r) = \begin{cases} u_0 & (0 \le r \le b) \\ u_0 \dfrac{l^2 - r^2}{l^2 - b^2} & (b \le r \le l) \\ 0 & (l \le r \le R) \end{cases} \qquad (5\text{-}4a)$$

$$\partial u/\partial r\,|_{r=0} = 0,\ u\,|_{r=R} = 0 \qquad (5\text{-}4b)$$

In (5-4a), the use of $u_0 \frac{l^2 - r^2}{l^2 - b^2}$ (b<r≤ l), shown in Fig. 5-5(a), to replace $u_0 \frac{l-r}{l-b}$ is made to simplify the solution.

Another initial pore pressure distribution form, shown in Fig. 5-5(b), is mathematically depicted by the following expression

$$u(r,0) = \omega(r) = \begin{cases} u_0 & (0 \le r \le b) \\ u_0 \dfrac{Ln(l/r)}{Ln(l/b)} & (b \le r \le l) \\ 0 & (l \le r \le R) \end{cases} \qquad (5\text{-}4a')$$

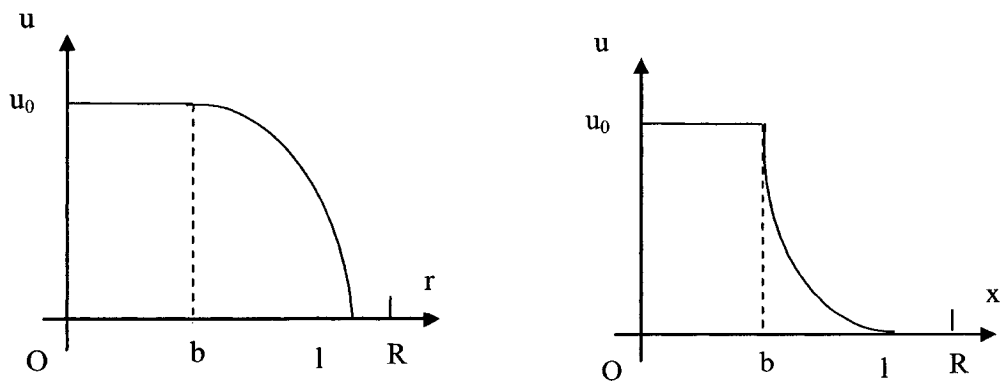

a) u(r,0) Form 1 b) u(r,0) Form 2

Fig. 5-5 u(r,0) Form

The solution of the above axisymmetrical problem for the first initial pore pressure distribution equation (5-4a) or Fig. 5-5a (Appendix B- 3) is given as following,

$$u(r,t) = u_0 \sum_{m=1}^{\infty} \frac{4\left[l^2 J_2(\frac{\alpha_m}{R} l) - b^2 J_2(\frac{\alpha_m}{R} b)\right]}{\alpha_m^2 (l^2 - b^2) J_1^2(\alpha_m)} J_0\left(\frac{\alpha_m}{R} r\right) \exp\left(-C_h \frac{\alpha_m^2}{R^2} t\right) \qquad (5\text{-}5)$$

Where α_m is the m-th value of infinitely many positive zeros solutions, x = α_m, m =1,2,..., of equation J_0 (x)=0; J_0, J_1 and J_2 respectively are 0, 1 and 2 order Bessel functions of the first kind. J_2 can be expressed in terms of J_0 and J_1:

$$J_2(x) = \frac{2J_1(x)}{x} - J_0(x)$$

The solution of the axisymmetrical problem for the second initial pore pressure distribution form Eq. (5-4a') or Fig. 5-5b (Appendix B- 3) is presented,

$$u(r,t) = u_0 \sum_{m=1}^{\infty} \frac{2\left[J_0(\frac{\alpha_m}{R}b) - J_0(\frac{\alpha_m}{R}l)\right]}{\alpha_m^2 J_1^2(\alpha_m) \cdot Ln(1/b)} J_0\left(\frac{\alpha_m}{R}r\right) \exp\left(-C_h \frac{\alpha_m^2}{R^2} t\right) \qquad (5\text{-}6)$$

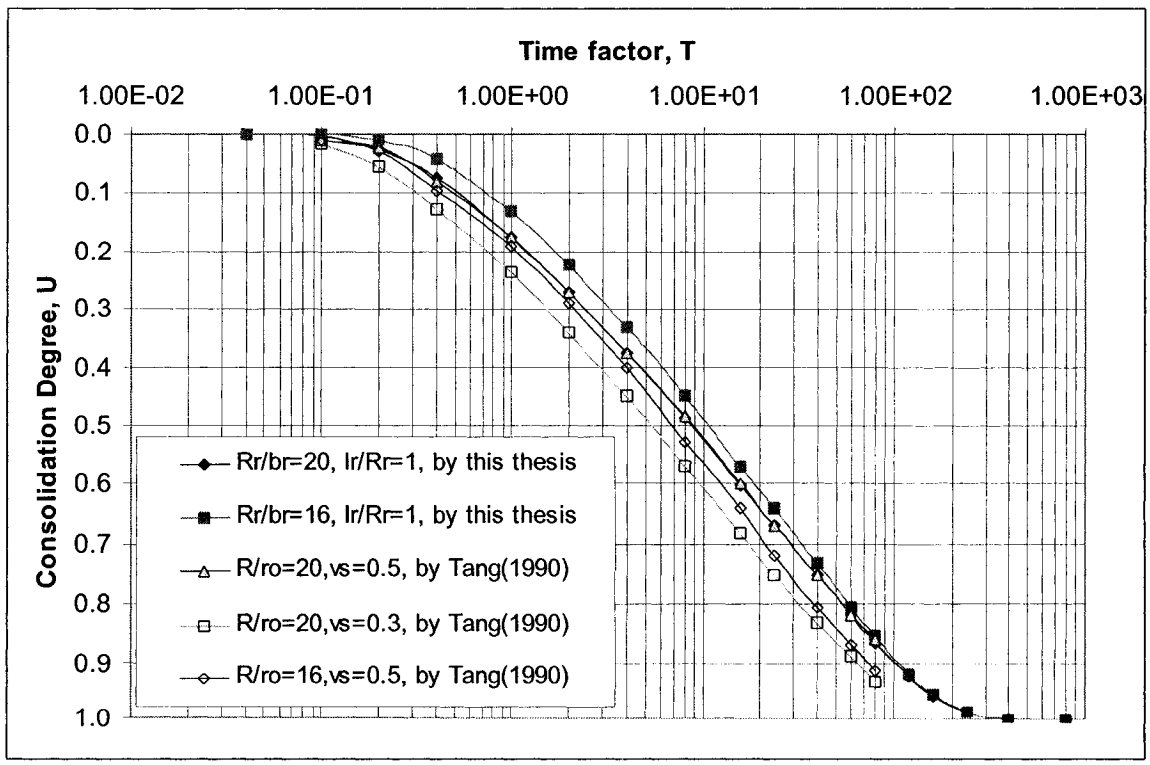

Fig. 5-6 Comparison between theResults of Equation (5-6) of Present Work and Tang (1990)'s Solution

Fig. 5-6 makes a comparison of the solution obtained from Equation (5-6) with that of Tang (1990). When $\omega = R/r_0 = 20$ and soil Poisson's ratio $v_s = 0.5$, the curve from this thesis' equation (5-6) is based on Terzaghi–Rendulic's theory which is almost completely coincident to the curve produced by Tang (1990)'s formula Eq. (2-50) which is based on Biot's consolidation theory. This shows that Terzaghi–Rendulic's consolidation theory is a special case of Biot's consolidation theory when the soil's Poisson ratio $v_s = 0.5$. This fact has been well known (Sills, 1975).

Case3: The initial pore pressure distribution form according to Eq. (5-4a) or Fig. 5-5(a), with l/R = 0.5, b/R = 0.2, r = 0, the consolidation degree $U = (u_0-u)/u_0$ from Eq. (5-5) is shown on Fig. 5-7 and Fig. 5-8, in which $T = C_h t/R^2$.

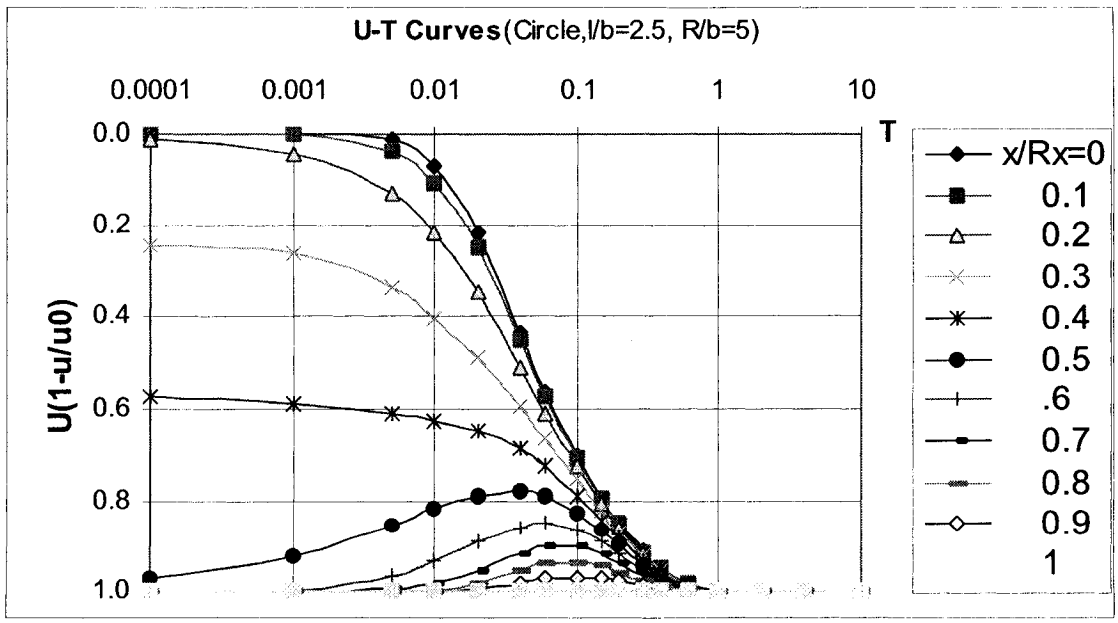

Fig. 5-7 Pore pressure dissipation with time factor under the first initial pore pressure distribution form

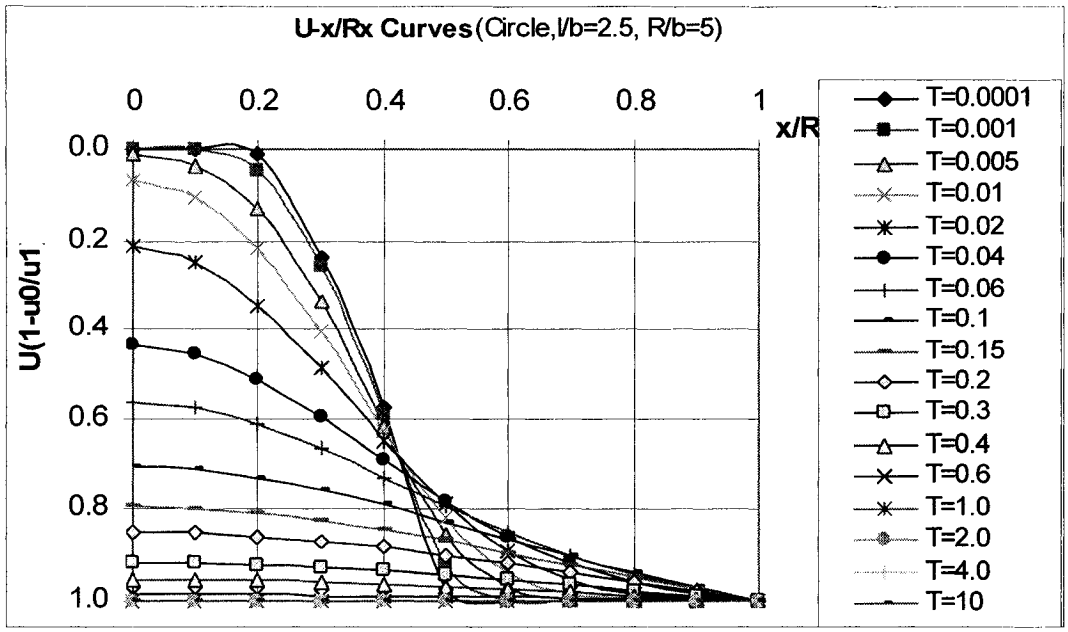

Fig. 5-8 Pore pressure contribution with time factor
under the first initial pore pressure distribution form

Case4: The initial pore pressure distribution form in this case is according to equation (5-4a') or Fig. 5-5(b). l/R=0.5, b/R=0.2, r=0, the consolidation degree $U=(u_0-u_t)/u_0$ from Equation (5-6) is shown on Fig. 5-9 and Fig. 5-10

From Cases 3 and 4, we know that the effect of initial pore pressure distribution on after pore pressure distribution with an increase in time is not great.

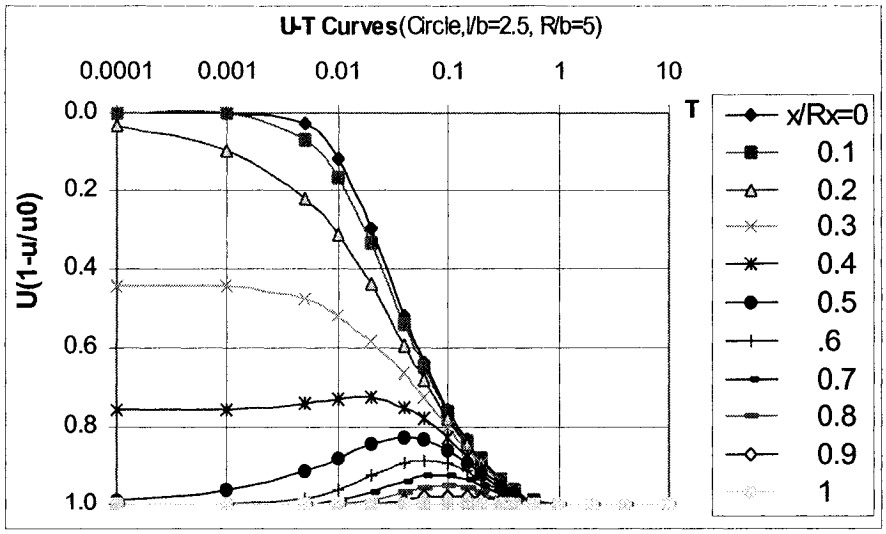

Fig. 5-9 Pore pressure-time curves at a place x/R_x under the second initial pore pressure distribution form

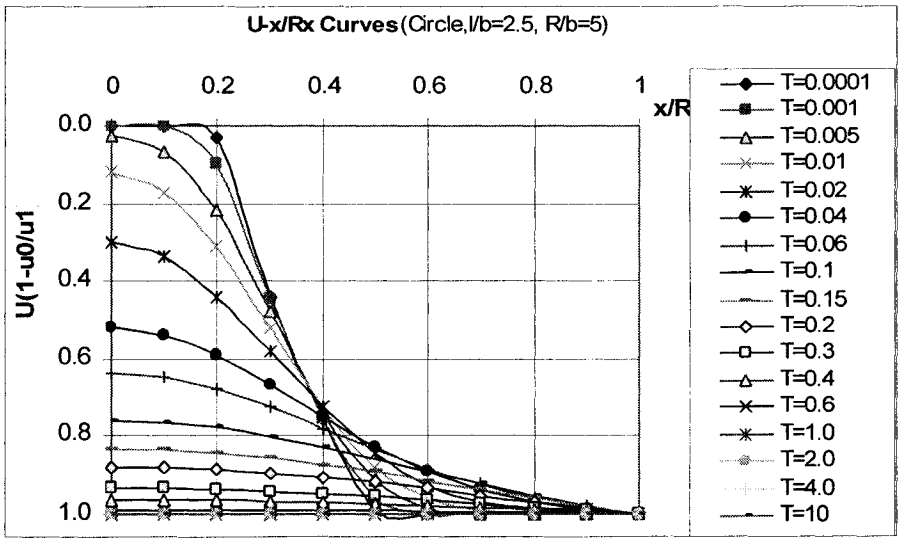

Fig. 5-10 Pore pressure contribution variation with time factor under the second initial pore pressure distribution form

5.2.3 Rectangle Area Problem of Horizontal Dissipation

For rectangular area, the p.w.p dissipation or consolidation of soil can be expressed mathematically by:

$$\frac{\partial u}{\partial t} = C_h\left(\frac{\partial^2 u}{\partial x^2} + \frac{\partial^2 u}{\partial y^2}\right) \tag{5-7}$$

$u(x,y,0) = u_0\psi_2(x,y)$,

in which,

$$\psi_2(x,y) = \begin{cases} 1 & (A_1 : |x| \le b_x, |y| \le b_y) \\ \dfrac{l_x - x}{l_x - b_x} & (A_2 : b_x \le x \le l_x, |y| \le b_y + \eta(x - b_x)) \\ \dfrac{l_y - y}{l_y - b_y} & (A_2 : b_y \le y \le l_y, |x| \le b_x + \dfrac{1}{\eta}(y - b_y)) \\ 0 & (A_4 : l_x \le x \le R_x, l_y \le y \le R_y) \end{cases}, \quad (\eta = \frac{l_y - b_y}{l_x - b_x}), \tag{5-7a}$$

$$\partial u/\partial x\,|_{x=0} = 0,\ u\,|_{x=Rx} = 0 \tag{5-7b}$$

$$\partial u/\partial y\,|_{y=0} = 0,\ u\,|_{y=Ry} = 0 \tag{5-7c}$$

The form of function $\psi_2(x,y)$ is shown in Fig. 5-11.

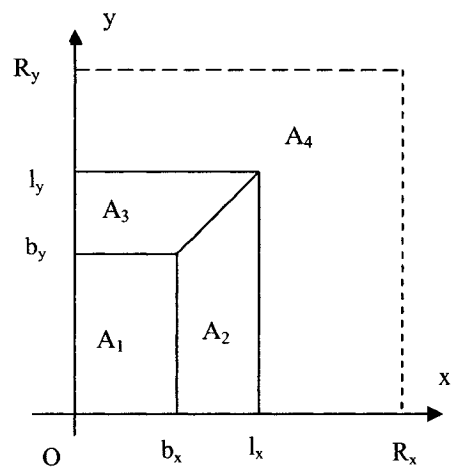

Fig. 5-11 Rectangular Area of Initial Pore Pressure Contribution

The solution to the above problem (the effect of the piles being ignored (**Appendix B- 4**) is given by following

$$u(x,y,t) = u_0 \sum_{m=1}^{\infty}\sum_{n=1}^{\infty} c_{mn} Cos\frac{(1/2+m)\pi x}{R_x}\cdot Cos\frac{(1/2+n)\pi y}{R_y}\cdot \exp\left(-\mu_{mn}\pi^2\frac{C_h}{R_x^2}t\right) \qquad (5\text{-}8)$$

Where, $$\mu_{mn} = (1/2+m)^2 + (1/2+n)^2\left(R_x/R_y\right)^2 \qquad (5\text{-}9)$$

$$c_{mn} = \frac{2}{(1/2+m)(1/2+n)\pi^2}\left[\frac{Sin(B_y+B_x)-Sin(L_y+L_x)}{D_y+D_x} - \frac{Sin(B_y-B_x)-Sin(L_y-L_x)}{D_y-D_x}\right]$$

(When $D_y \neq D_x$) (5-10)

$$\text{or } c_{mn} = \frac{2}{2(1/2+m)(1/2+m)\pi^2}\left[Cos(B_y-B_x) - \frac{Sin(L_y+L_x)-Sin(B_y+B_x)}{D_y+D_x}\right]$$

(When $D_y = D_x$) (5-11)

or

$$c_{mn} = \frac{4}{(1/2+m)(1/2+m)\pi^2} SinB_x \cdot SinB_y \qquad \text{(when } l_x=b_x \text{ \& } l_y=b_y\text{)} \qquad (5\text{-}12)$$

and

$$B_x = \frac{(1/2+m)\pi}{R_x}b_x; \quad B_y = \frac{(1/2+n)\pi}{R_y}b_y; \quad L_x = \frac{(1/2+m)\pi}{R_x}l_x; \quad L_y = \frac{(1/2+n)\pi}{R_y}l_y;$$

$$D_x = L_x - B_x = \frac{(1/2+m)\pi}{R_x}(l_x - b_x); \qquad D_y = L_y - B_y = \frac{(1/2+n)\pi}{R_y}(l_y - b_y);$$

In Equations (5-1) to (5-8), setting t= time length from the date of pile driving to the computation date, we can determine the p.w.p that was caused by pile driving and what remains.

Case5: Rectangular area problem of p.w.p horizontal dissipation, by/bx = 10 (close to strip shape), lx/bx = 2.5, Rx/bx = 5, η = 1.0, (bx/Rx = 0.2, lx/Rx = 0.5, by/Ry = 0.7143, ly/Ry = 0.8214, Rx/Ry = 0.3571). The calculated U-T curves and U-x/Rx curves are shown in Fig. 5-12 and Fig. 5-13 (consolidation degree $U=(u_0-u_t)/u_0$).

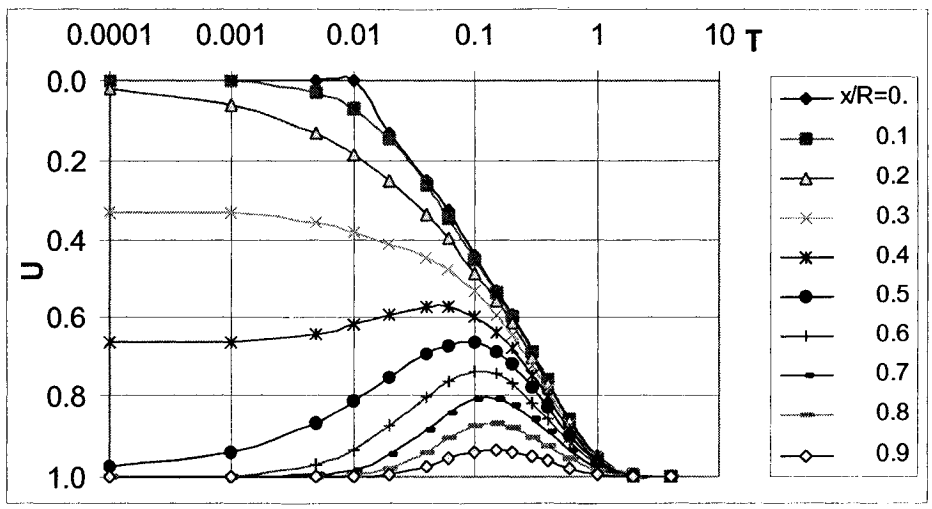

Fig. 5-12 Pore pressure-time curves at a place x/R_x and y=0 for rectangular distribution area of initial pore pressure

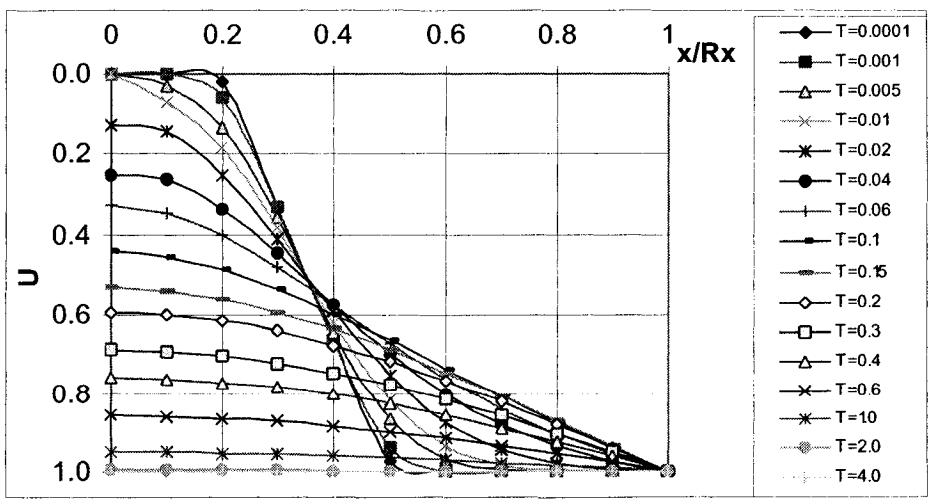

Fig. 5-13 Pore pressure contribution with time factor for rectangular distribution area of initial pore pressure

Case6: Square area problem of p.w.p horizontal dissipation, by/bx = 1.0, lx/bx = 2.5, Rx/bx = 5, η = 1.0, (bx/Rx = 0.2, lx/Rx = 0.5, by/Ry = 0.7143, ly/Ry = 0.8214, Rx/Ry = 0.3571). The calculated U-T curves and U-x/Rx curves are shown in Figs. 5-14 and 5-15

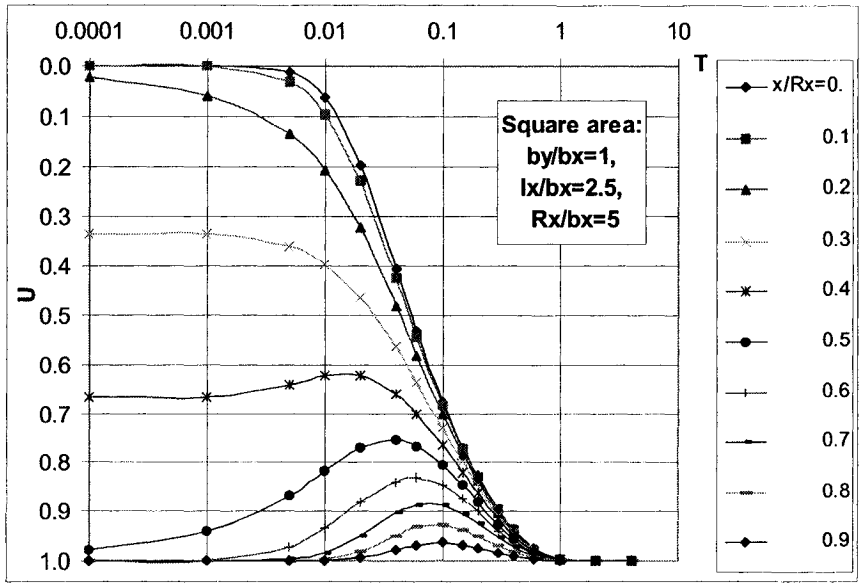

Fig. 5-14 Pore pressure-time curves at a place x/R_x and y=0

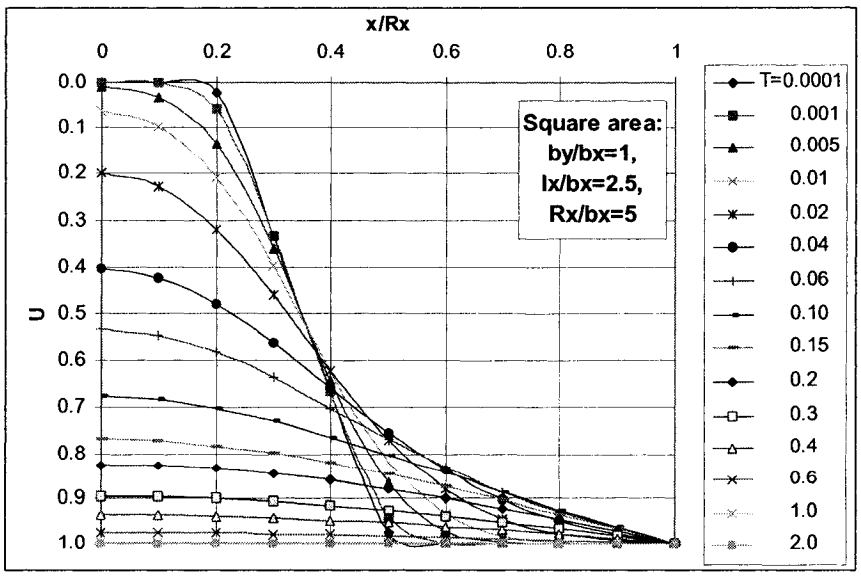

Fig. 5-15 Pore pressure contribution with time factor

5.2.4 Problem of Pore-Pressure 3-D Dissipation

(a) Rectangular Area Problem of 3-D Dissipation

One can consider the effect of vertical dissipation by simply modifying the previous rectangular area problem; p.w.p dissipation can be expressed by the following mathematical form:

$$\frac{\partial u}{\partial t} = C_h\left(\frac{\partial^2 u}{\partial x^2} + \frac{\partial^2 u}{\partial y^2}\right) + C_v \frac{\partial^2 u}{\partial z^2} \qquad (5\text{-}13)$$

$u(x,y,z,0) = \psi_3(x,y,z) = u_0(z)\cdot\psi_2(x,y)$

$$= u_0(z)\begin{cases} 1 & (A_1 : |x| \le b_x, |y| \le b_y) \\ \dfrac{l_x - x}{l_x - b_x} & (A_2 : b_x \le x \le l_x, |y| \le b_y + \eta(x - b_x)) \\ \dfrac{l_y - y}{l_y - b_y} & (A_2 : b_y \le y \le l_y, |x| \le b_x + \dfrac{1}{\eta}(y - b_y)) \\ 0 & (A_4 : l_x \le x \le R_x, l_y \le y \le R_y) \end{cases} \quad \left(\eta = \frac{l_y - b_y}{l_x - b_x}\right), \qquad (5\text{-}13a)$$

$u_0(z)$ form is shown in Fig. 5-16 or the following expression

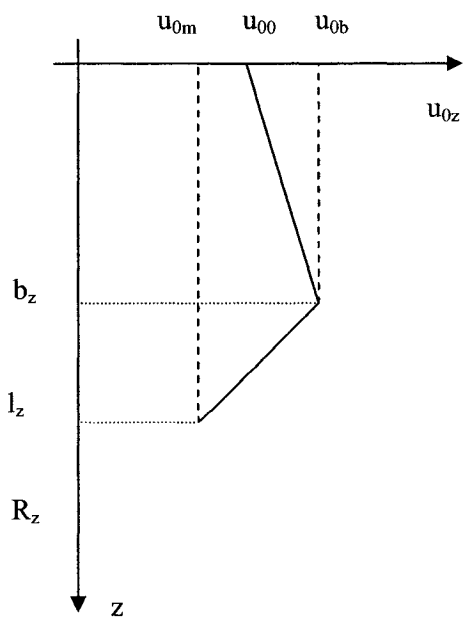

Fig. 5-16 $u_0(z)$ form

$$u_0(z) = \begin{cases} u_{00} + \dfrac{u_{0b} - u_{00}}{b_z} z & (0 \le z \le b_z) \\ u_{0l} - \dfrac{u_{0b} - u_{0m}}{l_z - b_z}(z - b_z) & (b_z \le z \le l_z) \\ 0 & (l_z \le z \le R_z) \end{cases} \quad (5\text{-}13b)$$

$$\partial u/\partial x \big|_{x=0} = 0,\ u \big|_{x=Rx} = 0 \quad (5\text{-}13c)$$

$$\partial u/\partial y \big|_{y=0} = 0,\ u \big|_{y=Ry} = 0 \quad (5\text{-}13d)$$

There are two boundary conditions on $z=R_z$:

1) Permeable boundary, $u \big|_{z=0} = 0,\ u \big|_{z=Rz} = 0$ (5-13e)

2) Impermeable boundary, $u \big|_{z=0} = 0,\ \partial u/\partial z \big|_{z=Rz} = 0$ (5-13f)

The solution to the above problem for permeable boundaries Eq. (5-13e) (**Appendix B-5**) is:

$$u(x,y,z,t) = \sum_{m=0}^{\infty}\sum_{n=0}^{\infty}\sum_{k=1}^{\infty} d_{mnk} Cos\frac{(1/2+m)\pi x}{R_x} \cdot Cos\frac{(1/2+n)\pi y}{R_y} Sin\frac{k\pi z}{R_z} \cdot \exp\left(-s_{mnk}^2 \pi^2 t\right) \quad (5\text{-}14)$$

where, $s_{mnk}^2 = C_h\left(\dfrac{(1/2+m)^2}{R_x^2} + \dfrac{(1/2+n)^2}{R_y^2}\right) + C_v \dfrac{k^2}{R_z}$ (5-14a)

$$d_{mnk} = d_k \cdot c_{mn} \quad (5\text{-}14b)$$

c_{mn} is determined by using Equations (5-10), (5-11) or (5-12);

$$d_k = \frac{2}{k\pi}\left[u_{00} - u_{0m} Cos\frac{k\pi l_z}{R_z} + \frac{u_{0l} - u_{00}}{b_z}\frac{R_z}{k\pi} Sin\frac{kb_z\pi}{R_z} + \frac{u_{0l} - u_{0m}}{l_z - b_z}\frac{R_z}{k\pi}\left(Sin\frac{k\pi b_z}{R_z} - Sin\frac{k\pi l_z}{R_z}\right)\right] \quad (5\text{-}14c)$$

Usually, for permeable condition, $l_z = R_z$, since,

$$d_k = \frac{2}{k\pi}\left[u_{00} - u_{0m} Cosk\pi + \left(\frac{u_{0l} - u_{00}}{b_z} + \frac{u_{0l} - u_{0m}}{l_z - b_z}\right)\frac{R_z}{k\pi} Sin\frac{k\pi b_z}{R_z}\right] \quad (5\text{-}14d)$$

When $b_z = l_z = R_z$, and $u_{00} = u_{0b} = u_{0m}$,

$$d_x = \frac{2}{k\pi} u_{00}(1 - Cosk\pi) \qquad (k=1, 2, 3, \ldots)$$

$$= \frac{4}{K\pi} u_{00} \qquad (K=1, 3, 5, \ldots)(5\text{-}14e)$$

Substituting equations (5-14a) ~ (5-14c) into (5-14), we get

$$u(x,y,z,t) = \sum_{m=0}^{\infty}\sum_{n=0}^{\infty}\sum_{k=1}^{\infty} d_{mn}d_k Cos(p_m x)\cdot Cos(q_n y)Sin(h_k z)\cdot Exp\left[-\left(C_h(p_m^2+q_n^2)+C_v h_k^2\right)t\right]$$

$$= \sum_{m=0}^{\infty}\sum_{n=0}^{\infty}\left\{\sum_{k=1}^{\infty} d_k Sin(h_k z)Exp\left(-C_v h_k^2 t\right)\right\} d_{mn}Cos(p_m x)\cdot Cos(q_n y)\cdot Exp\left[-C_h(p_m^2+q_n^2)t\right]$$

$$= \left\{\sum_{k=1}^{\infty} d_k Sin(h_k z)Exp\left(-C_v h_k^2 t\right)\right\}\left\{\sum_{m=0}^{\infty}\sum_{n=0}^{\infty} d_{mn}Cos(p_m x)\cdot Cos(q_n y)\cdot Exp\left[-C_h(p_m^2+q_n^2)t\right]\right\}$$

(5-15)

It can be deduced from this analysis that the Carrillo's expression of 3-D consolidation degree (Carrillo, 1942)

$$\frac{u(x,y,z,t)}{u(x,y,z,0)} = \frac{u_z(z,t)}{u_z(z,0)}\cdot\frac{u_{xy}(x,y,t)}{u_{xy}(x,y,0)} \qquad (5\text{-}16)$$

or $(1-U)=(1-U_z)\cdot(1-U_{xy})$ (5-17)

can be exact only when the initial condition u(x,y,z,0) is expressed by $\psi_1(z)\cdot\psi_2(x,y)$.

In the case where $b_z = l_z = R_z$, and $u_{00} = u_{0b} = u_{0m}$, Setting $R_z = 2H$ and using Equation (3-6):

$$\frac{u_z(z,t)}{u_z(z,0)} = \frac{1}{u_{00}}\sum_{k=1}^{\infty} d_k Sin(h_k z)\cdot Exp\left(-C_v h_k^2 t\right)$$

$$= \sum_{k=1,3,5,\ldots}^{\infty}\frac{4}{K\pi}Sin\left(\frac{K\pi}{2H}z\right)\cdot Exp\left(-C_v\frac{K^2\pi^2}{4H^2}t\right) \qquad (5\text{-}18)$$

The above form is exactly the same as the well-known Terzaghi solution for one-direction consolidation theory.

Similarly, the solution to the above problem for impermeable boundaries Eq. (5.13f) (Appendix B-5) is given by the following triple Fourier cosine-sine series,

$$u(x,y,z,t)=\sum_{m=0}^{\infty}\sum_{n=0}^{\infty}\sum_{k=1}^{\infty} d_{mnk}Cos\frac{(\frac{1}{2}+m)\pi x}{R_x}\cdot Cos\frac{(\frac{1}{2}+n)\pi y}{R_y}Sin\frac{(\frac{1}{2}+k)\pi z}{R_z}\cdot\exp\left(-s_{mnk}^2\pi^2 t\right) \tag{5-19}$$

$$\text{where, } s_{mnk}^2=C_h\left(\frac{(\frac{1}{2}+m)^2}{R_x^2}+\frac{(\frac{1}{2}+n)^2}{R_y^2}\right)+C_v\frac{(\frac{1}{2}+k)^2}{R_z^2} \tag{5-19a}$$

$$d_{mnk}=d_k\cdot c_{mn} \tag{5-19b}$$

c_{mn} is determined by using Equations (5-10), (5-11) or (512);

$$d_k=\frac{2}{k\pi}\left\{u_{00}-u_{0m}Cos\frac{(\frac{1}{2}+k)\pi l_z}{R_z}+\frac{u_{0l}-u_{00}}{b_z}\frac{R_z}{(\frac{1}{2}+k)\pi}Sin\frac{(\frac{1}{2}+k)b_z\pi}{R_z}\right.$$

$$\left.+\frac{u_{0l}-u_{0m}}{l_z-b_z}\frac{R_z}{(\frac{1}{2}+k)\pi}\left(Sin\frac{(\frac{1}{2}+k)\pi b_z}{R_z}-Sin\frac{(\frac{1}{2}+k)\pi l_z}{R_z}\right)\right\} \tag{5-19c}$$

Usually, for permeable conditions, $l_z = R_z$, since,

$$d_k=\frac{2}{k\pi}\left\{u_{00}+\frac{u_{0l}-u_{00}}{b_z}\frac{R_z}{(\frac{1}{2}+k)\pi}Sin\frac{(\frac{1}{2}+k)b_z\pi}{R_z}\right.$$

$$\left.+\frac{u_{0l}-u_{0m}}{l_z-b_z}\frac{R_z}{(\frac{1}{2}+k)\pi}\left(Sin\frac{(\frac{1}{2}+k)\pi b_z}{R_z}-(-1)^{k-1}\right)\right\} \tag{5-19d}$$

And when $b_z = l_z = R_z$, and $u_{00} = u_{0b} = u_{0m}$,

$$d_k=\frac{2}{(\frac{1}{2}+k)\pi}u_{00} \qquad (k = 1, 2, 3, \ldots) \tag{5-19e}$$

In this case,

$$\frac{u_z(z,t)}{u_z(z,0)} = \frac{1}{u_{00}} \sum_{k=1}^{\infty} d_k Sin(h_k z) \cdot Exp\left(-C_v h_k^2 t\right)$$

$$= \sum_{k=1}^{\infty} \frac{4}{(1+2k)\pi} Sin(\frac{(1+2k)\pi}{2R_z} z) \cdot Exp\left(-C_v \frac{(1+2k)^2 \pi^2}{4H^2} t\right) \qquad (5\text{-}20)$$

Setting K = 1+2k, R_z = H,

$$\frac{u_z(z,t)}{u_z(z,0)} = \sum_{k=1,3,5,\ldots}^{\infty} \frac{4}{K\pi} Sin(\frac{K\pi}{2H} z) \cdot Exp\left(-C_v \frac{K^2 \pi^2}{4H^2} t\right) \qquad (5\text{-}21)$$

Also, the above form is exactly the same as the well-known Terzaghi solution for one-direction consolidation theory. Terzaghi's solution is just a special example of this solution by equations (5-14) or (5-19).

Case7: rectangular area problem of p.w.p 3-D dissipation, b_y/b_x = 1.0, l_x/b_x = 2.5, R_x/b_x = 5, η = 1.0, (b_x/R_x = 0.2, l_x/R_x=.5, b_y/R_y = 0.2, l_y/R_y = 0.5, R_x/R_y = 1); b_z/b_x = 2, R_z/l_z = 1, C_h/C_v = 5, u_{oo}/u_{ob} = 0.6, u_{om}/u_{ob} = 0.4. The dissipation degree of pore pressure U = 1.-u(x,y,z;t)/u_{0b}. For permeable boundary ($u|_{z=0}$ = 0, $u|_{z=Rz}$ = 0), the calculated U-T-z/Rz curves are shown in Fig. 5-17.

Case 8: The same situation as for case 7 but for impermeable boundary ($u|_{z=0}$ = 0, $\partial u/\partial z|_{z=Rz}$ = 0), the calculated U-T-z/Rz curves are shown in Fig 5-18.

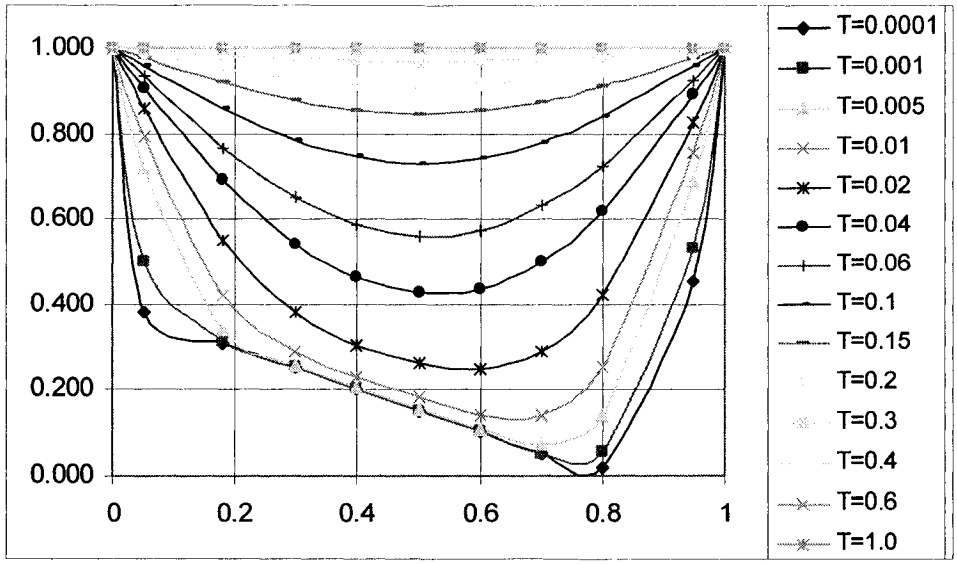

Fig. 5-17 Pore pressure contribution with time factor
for p.w.p 3-D dissipation and permeating bottom boundary

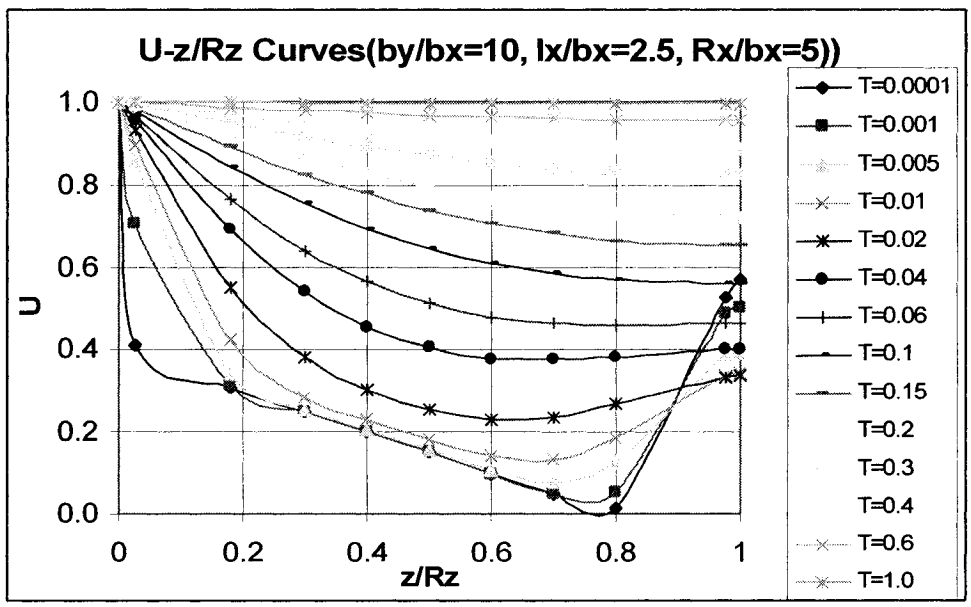

Fig. 5-18 Pore pressure contribution with time factor
for p.w.p 3-D dissipation and impermeating bottom boundary

(b) Other cases of 3-D Dissipation

It was previously proven that Carrillo's expression (Carrillo, 1942) of 3-D consolidation degree, Eq. (5-16) or (5-17), is exact only when initial condition u(x,y,z,0) can be expressed by $\psi_1(z)\cdot\psi_2(x,y)$. Therefore, we also can get similar expressions:

$$\frac{u(r,z,t)}{u(r,z,0)} = \frac{u_z(z,t)}{u_z(z,0)} \cdot \frac{u_r(r,t)}{u_r(r,0)} \qquad (5\text{-}22)$$

or $$(1-U) = (1-U_z)\cdot(1-U_r) \qquad (5\text{-}23)$$

which will be exact when initial condition u(r,z,0) can be expressed by $\psi_1(r)\cdot\psi_2(z)$.

For strip area problems of dissipation,

$$\frac{\partial u}{\partial t} = C_h \frac{\partial^2 u}{\partial x^2} + C_v \frac{\partial^2 u}{\partial z^2} \qquad (5\text{-}24)$$

$u(x,z,0)= \psi_1(x)\cdot\psi_2(z)$;

$$\psi_1(x)= \begin{cases} 1 & (0 \le |x| \le b) \\ \dfrac{l-x}{l-b} & (b \le |x| \le l) \\ 0 & (|x| \ge l) \end{cases}; \qquad (5\text{-}13b)$$

$$\psi_2(z)= u_0(z)= \begin{cases} u_{00} + \dfrac{u_{0b}-u_{00}}{b_z} z & (0 \le z \le b_z) \\ u_{0l} - \dfrac{u_{0b}-u_{0m}}{l_z-b_z}(z-b_z) & (b_z \le z \le l_z) \\ 0 & (l_z \le z \le R_z) \end{cases}$$

The horizontal boundary conditions: $\partial u/\partial x\,|_{x=0} = 0$, $u\,|_{x=Rx} = 0$

There are two types of bottom boundary conditions on $Z=R_z$:

1) Permeable boundary, $u\,|_{Z=0} = 0$, $u\,|_{Z=Rz} = 0$

2) Impermeable boundary, $u\,|_{Z=0} = 0$, $\partial u/\partial z\,|_{Z=Rz} = 0$

The solution for the bottom permeable boundary conditions is

$$u(x,z,t)=\left\{\sum_{k=1}^{\infty} d_k Sin(h_k z)Exp\left(-C_v h_k^2 t\right)\right\}\left\{\sum_{m=0}^{\infty} c_m Cos(p_m x)\cdot Exp\left(-C_h p_m^2 t\right)\right\} \qquad (5\text{-}25)$$

where $h_k = \pi k/R_z$; $p_m = \pi(m-0.5)/R_x$;

d_k is determined by (5-14c);

c_m is same with formula (5-3'), that is

$$c_m = \frac{2}{(1/2+m)^2\pi^2}\frac{R}{l-b}\left(\cos\frac{(1/2+m)\pi b}{R}-\cos\frac{(1/2+m)\pi l}{R}\right) \qquad (5\text{-}26)$$

The solution for the bottom impermeable boundary conditions is same as Equations (5-25) and (5-26), but $h_k=\pi(k-0.5)/R_z$, d_k is determined by Equation (5-19c);

For circular area problem of dissipation,

$$\frac{\partial u}{\partial t} = C_h\left(\frac{\partial^2 u}{\partial r^2}+\frac{1}{r}\frac{\partial u}{\partial r}\right)+C_v\frac{\partial^2 u}{\partial z^2} \qquad (5\text{-}27)$$

$$u(r,0)= \psi_3(r,z) = u_0(z)\cdot\psi_2(r)\,, \qquad (5\text{-}27a)$$

in which, $u_0(z)$ is the as same as in equation (5-13b),

$$\psi_2(r) = \begin{cases} 1 & (0 \le r \le b) \\ \dfrac{l^2-r^2}{l^2-b^2} & (b \le r \le l) \\ 0 & (l \le r \le R) \end{cases} \qquad (5\text{-}27b)$$

or the second kind of contribution:

$$\psi_2(r)=\begin{cases}1 & (0\le r\le b)\\ \dfrac{Ln(l/r)}{Ln(l/b)} & (b\le r\le l)\\ 0 & (l\le r\le R)\end{cases} \qquad \text{(5-27b')}$$

The horizontal boundary conditions and the bottom boundary conditions are the as same as those conditions for strip area problem of dissipation.

Thus, the solution for the bottom permeable boundary conditions and initial pore-pressure contribution (5-27b) is

$$u(r,z,t)=\left\{\sum_{k=1}^{\infty} d_k Sin(h_k z)Exp\left(-C_v h_k^2 t\right)\right\}\left\{\sum_{m=0}^{\infty} c_m J_0\left(\frac{\alpha_m}{R}r\right)\cdot Exp\left(-C_h\frac{\alpha_m^2}{R}t\right)\right\} \qquad \text{(5-28)}$$

Where

$$c_m=\frac{4\left[l^2 J_2(\frac{\alpha_m}{R}l)-b^2 J_2(\frac{\alpha_m}{R}b)\right]}{\alpha_m^2(l^2-b^2)J_1^2(\alpha_m)} \qquad \text{(5-29)}$$

h_k and d_k are determined by the bottom boundary conditions on Z = R_Z.

For the bottom permeable boundary conditions, h_k = πk/R_z , and d_k is determined by (5-14c).

For the bottom impermeable boundary conditions, h_k =π(k-0.5)/R_z , and d_k is determined by (5-19c);

The solution for the bottom permeable boundary conditions and initial pore-pressure contribution (5-27b') is of the same form as formula (5-28), except for c_m which is different:

$$c_m = \frac{2\left[J_0(\frac{\alpha_m}{R}b) - J_0(\frac{\alpha_m}{R}l)\right]}{\alpha_m^2 J_1^2(\alpha_m)\cdot Ln(l/b)} \qquad (5\text{-}30)$$

5.3 Modeling of Pore-Pressure Dissipation in Layered Soils

5.3.1 Principal Equations

- **The rectangular area problem of p.w.p 3-D dissipation for layered soils**

For layered soils, the rectangular area problem of p.w.p dissipation can be also expressed by the same form as same as Section 5.2.4:

$$C_{hk}\left(\frac{\partial^2 u}{\partial x^2}+\frac{\partial^2 u}{\partial y^2}\right)+C_{vk}\frac{\partial^2 u}{\partial z^2}=\frac{\partial u}{\partial t} \qquad (5\text{-}31)$$

$u(x,y,Z,0) = \psi_3(x,y,z) = u_0(Z)\cdot\psi_2(x,y)$

$$= u_0(Z)\times\begin{cases} 1 & (A_1: |x|\le b_x, |y|\le b_y) \\ \dfrac{l_x - x}{l_x - b_x} & (A_2: b_x \le x \le l_x, |y|\le b_y + \eta(x-b_x)) \\ \dfrac{l_y - y}{l_y - b_y} & (A_2: b_y \le y \le l_y, |x|\le b_x + \dfrac{1}{\eta}(y-b_y)) \\ 0 & (A_4: l_x \le x \le R_x, l_y \le y \le R_y) \end{cases} \quad (\eta = \frac{l_y - b_y}{l_x - b_x}), \qquad (5\text{-}31a)$$

$$u_0(Z) = \begin{cases} u_{00} + \dfrac{u_{0b} - u_{00}}{b_z} z & (0 \le Z \le b_z) \\ u_{0l} - \dfrac{u_{0b} - u_{0m}}{l_z - b_z}(z - b_z) & (b_z \le Z \le l_z) \\ 0 & (l_z \le Z \le R_z) \end{cases} \qquad (5\text{-}31b)$$

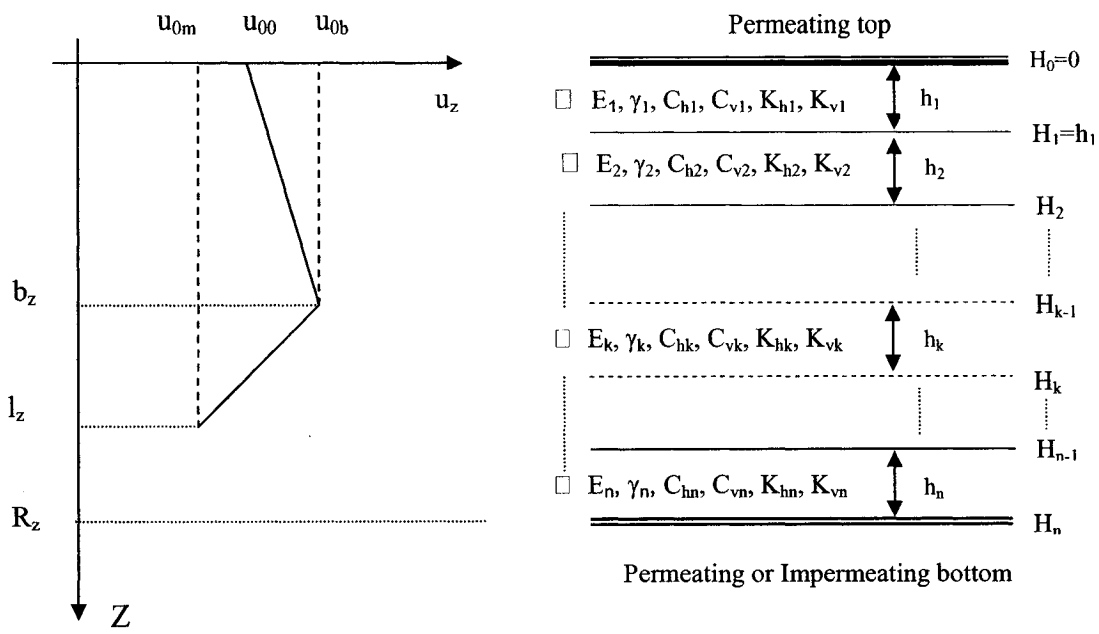

Fig. 5-19 Layered Soil and Permeability Condition

The horizontal boundary conditions:

$$\partial u/\partial x \,|_{x=0} = 0,\ u \,|_{x=Rx} = 0 \qquad (5\text{-}31c)$$

$$\partial u/\partial y \,|_{y=0} = 0,\ u \,|_{y=Ry} = 0 \qquad (5\text{-}31d)$$

Where, z is the local coordinate and Z is the global coordinate, $Z = H_k + z$, $H_k = \sum_{i=1}^{k} h_i$.

Their relationships are shown in Fig. 5-19.

There are two boundary conditions on $Z=R_z$:

1) Permeable boundary, $\quad u \,|_{Z=0} = 0,\ u \,|_{Z=Rz} = 0 \qquad (5\text{-}31e)$

or

2) Impermeable boundary, $\quad u \,|_{Z=0} = 0,\ \partial u/\partial z \,|_{Z=Rz} = 0 \qquad (5\text{-}31f)$

Because of the non-uniformity of soil, the problem can not be solved in similar means as in the above sections 5.2.1 to 5.2.4. However, in this case the finite Fourier series transform □ ( ) and Laplace transform □ ( ) have to be used in order to solve it.

Set $\tilde{\bar{F}}(p_m,q_n,z;s)=\int_{x=0}^{\infty}\int_{y=0}^{\infty}\int_{t=0}^{\infty}F(x,y,z,t)\cos(p_m x)\cos(q_n y)e^{-st}dxdydt=\square(F)$ (5-32)

$$\bar{F}(p_m,q_n,z,t)=\int_{x=0}^{\infty}\int_{y=0}^{\infty}F(x,y,z,t)\cos(p_m x)\cos(q_n y)dxdy=\square(F) \quad (5\text{-}32a)$$

$$\tilde{F}(x,y,z;s)=\int_{t=0}^{\infty}F(x,y,z,t)e^{-st}dt=\square(F) \quad (5\text{-}32b)$$

Thus: $F(x,y,z;t)=\square^{-1}(\tilde{\bar{F}})=\square^{-1}[\square^{-1}(\tilde{\bar{F}})]=\square^{-1}[\square^{-1}(\tilde{\bar{F}})]$ (5-33)

$$F(x,y,z,t)=\frac{1}{2\pi i}\sum_{m=0}^{\infty}\sum_{n=0}^{\infty}\int_{s=a-i\infty}^{a+i\infty}\tilde{\bar{F}}_{mn}(p_m,q_n,z;s)\cdot Cos(p_m x)\cdot Cos(q_n y)\,e^{ts}ds \quad (5\text{-}33a)$$

That is, $\hat{F}=\tilde{\bar{F}}=\square(F)=\square[\square(F)]$ or $\square(F)=\square[\square(F)]$; □ () is finite Fourier series transform, □ ( ) is the Laplace transform; □ ( ) is the finite Fourier Laplace transform.

Now, Equation (5-31) can be transformed by means of Eq. (5-32), e.g., using Equations (5-32a) and (5-32b), one gets

$$-C_{hk}(p^2+q^2)\tilde{\bar{u}}(p,q,z;s)+C_{vk}\frac{\partial^2\tilde{\bar{u}}(p,q,s;z)}{\partial z^2}=s\tilde{\bar{u}}(p,q,z;s)-\bar{u}(p,q,z;0) \quad (5\text{-}34')$$

or $$C_{vk}\frac{\partial^2\tilde{\bar{u}}}{\partial z^2}-\left[C_{hk}(p^2+q^2)+s\right]\cdot\tilde{\bar{u}}=-\bar{u}\big|_{t=0} \quad (5\text{-}34)$$

It is already known that $p=p_m=(^1/_2+m)\pi/R_x$, $q=q_n=(^1/_2+n)\pi/R_y$ (m=0,1,2,...; n=0,1,2, ...), and $\bar{u}\big|_{t=0}=u_0(z)\cdot c_{mn}$, in which, c_{mn} is given by Equations (5-10), (5-11) or (5-12).

Set $$\zeta^2=\frac{C_{hk}(p^2+q^2)+s}{C_{vk}} \quad (5\text{-}35)$$

Thus, Equation (5-34) becomes the subsidiary equation

$$\frac{\partial^2 \tilde{\bar{u}}}{\partial z^2} - \zeta^2 \tilde{\bar{u}} = -\bar{u}\big|_{t=0} = -u_0(z)\frac{c_{mn}}{C_{vk}} \tag{5-36}$$

Setting $$u_0(z) = \frac{u_0(h_k)-u_0(0)}{h_k} z + u_0(0) = i_k z + u_0(0) \tag{5-36a}$$

The solution of the above equation (5.36) is the subsidiary form

$$\tilde{\bar{u}}(z) = \hat{u}(z) = Ae^{\zeta z} + Be^{-\zeta z} + Cz + D \tag{5-37}$$

Substituting equation (5-37) into (5-36), one gets

$$-\zeta^2 Cz - \zeta^2 D = -\left[\frac{u_0(h_k)-u_0(0)}{h_k} z + u_0(0)\right]\frac{c_{mn}}{C_{vk}} \tag{5-37a}$$

Thus, $$C = \frac{u_0(h_k)-u_0(0)}{h_k}\frac{c_{mn}}{\zeta^2 C_{vk}}; \quad D = u_0(0)\frac{c_{mn}}{\zeta^2 C_{vk}} \tag{5-37b}$$

Substituting C and D into equation (5-37), one obtains

$$\tilde{\bar{u}}(z) = \hat{u}(z) = Ae^{\zeta z} + Be^{-\zeta z} + \{[u_0(h_k) - u_0(0)]\frac{z}{h_k} + u_0(0)\}\frac{c_{mn}}{\zeta^2 C_{vk}} \tag{5-38}$$

By the permeating law, unit permeability is defined as:

$$Q(z) = K_v \frac{\partial u}{\partial z}$$

Transforming the above by means of the finite Fourier-Laplace transform □( ), we have

$$\hat{Q}(z) = K_v \frac{\partial \hat{u}}{\partial z} \tag{5-39}$$

Substituting equation (5-38) into (5-39), one gets:

$$\hat{Q}(z) = K_{vk}\zeta A e^{\zeta z} - K_{vk}\zeta B e^{-\zeta z} + K_{vk}\frac{u_0(h_k)-u_0(0)}{h_k}\frac{c_{mn}}{\zeta^2 C_{vk}} \tag{5-40}$$

From equations (5-38) and (5-40), the following is obtained

$$\left.\begin{aligned}\hat{u}(0) &= A + B + u_0(0)\frac{c_{mn}}{\zeta^2 C_{vk}} \\ \frac{\hat{Q}(0)}{K_{vk}\zeta} &= A - B + \frac{u_0(h_k) - u_0(0)}{\zeta h_k}\frac{c_{mn}}{\zeta^2 C_{vk}}\end{aligned}\right\} \qquad (5\text{-}41)$$

Then,

$$A = \frac{1}{2}\left[\hat{u}(0) + \frac{\hat{Q}(0)}{K_{vk}\zeta} - (1 - \frac{1}{\zeta h_k})\frac{c_{mn}}{\zeta^2 C_{vk}}u_0(0) - \frac{1}{\zeta h_k}\frac{c_{mn}}{\zeta^2 C_{vk}}u_0(h_k)\right]$$

$$B = \frac{1}{2}\left[\hat{u}(0) - \frac{\hat{Q}(0)}{K_{vk}\zeta} - (1 + \frac{1}{\zeta h_k})\frac{c_{mn}}{\zeta^2 C_{vk}}u_0(0) + \frac{1}{\zeta h_k}\frac{c_{mn}}{\zeta^2 C_{vk}}u_0(h_k)\right] \qquad (5\text{-}42)$$

Substituting A and B into equations (5-38), we have

$$\hat{u}(z) = ch(\zeta z)\hat{u}(0) + \frac{sh(\zeta z)}{\zeta K_{vk}}\hat{Q}(0) + \left[\frac{sh(\zeta z)}{\zeta h_k} - ch(\zeta z) + 1 - \frac{z}{h_k}\right]\frac{c_{mn}}{\zeta^2 C_{vk}}u_0(0) + \left[\frac{z}{h_k} - \frac{sh(\zeta z)}{\zeta h_k}\right]\frac{c_{mn}}{\zeta^2 C_{vk}}u_0(h_k)$$

$$\hat{Q}(z) = sh(\zeta z)\zeta K_{vk}\hat{u}(0) + ch(\zeta z)\hat{Q}(0) + \left[\frac{ch(\zeta z) - 1}{\zeta h_k} - sh(\zeta z)\right]\frac{\zeta K_{vk} c_{mn}}{\zeta^2 C_{vk}}u_0(0) + \left[\frac{1 - ch(\zeta z)}{\zeta h_k}\right]\frac{\zeta K_{vk} c_{mn}}{\zeta^2 C_{vk}}u_0(h_k) \qquad (5\text{-}43)$$

and set $z = h_k$

$$\begin{Bmatrix}\hat{u}(h_k)\\ \hat{Q}(h_k)\end{Bmatrix} = \begin{bmatrix} ch(\zeta h_k) & \frac{sh(\zeta h_k)}{\zeta K_{vk}} \\ \zeta K_{vk} sh(\zeta h_k) & ch(\zeta h_k)\end{bmatrix}\begin{Bmatrix}\hat{u}(0)\\ \hat{Q}(0)\end{Bmatrix} + \begin{bmatrix} \frac{sh(\zeta h_k)}{\zeta h_k} - ch(\zeta h_k) & 1 - \frac{sh(\zeta h_k)}{\zeta h_k} \\ \zeta K_{vk}\left(\frac{ch(\zeta h_k) - 1}{\zeta h_k} - sh(\zeta h_k)\right) & \zeta K_{vk}\frac{1 - ch(\zeta h_k)}{\zeta h_k}\end{bmatrix}\frac{c_{mn}}{\zeta^2 C_{vk}}\begin{Bmatrix}u_0(0)\\ u_0(h_k)\end{Bmatrix} \qquad (5\text{-}44)$$

Because $\begin{Bmatrix}\hat{u}_k(h_k)\\ \hat{Q}_k(h_k)\end{Bmatrix} = \begin{Bmatrix}\hat{u}_{k+1}(0)\\ \hat{Q}_{k+1}(0)\end{Bmatrix}$ and $u_{0\,k}(h_k) = u_{0\,k+1}(0)$, we set

$$\begin{Bmatrix}\hat{u}_1\\ \hat{Q}_1\end{Bmatrix} = \begin{Bmatrix}\hat{u}_1(0)\\ \hat{Q}_1(0)\end{Bmatrix}, \qquad \begin{Bmatrix}\hat{u}_2\\ \hat{Q}_2\end{Bmatrix} = \begin{Bmatrix}\hat{u}_2(0)\\ \hat{Q}_2(0)\end{Bmatrix} = \begin{Bmatrix}\hat{u}_1(h_1)\\ \hat{Q}_1(h_1)\end{Bmatrix}, \ldots,$$

$$\begin{Bmatrix}\hat{u}_k\\ \hat{Q}_k\end{Bmatrix} = \begin{Bmatrix}\hat{u}_k(0)\\ \hat{Q}_k(0)\end{Bmatrix} = \begin{Bmatrix}\hat{u}_{k-1}(h_k)\\ \hat{Q}_{k-1}(h_k)\end{Bmatrix}, \ldots, \qquad \begin{Bmatrix}\hat{u}_{n+1}\\ \hat{Q}_{n+1}\end{Bmatrix} = \begin{Bmatrix}\hat{u}_n(h_n)\\ \hat{Q}_n(h_n)\end{Bmatrix}, \text{ and}$$

$$u_{0_1} = u_{0_1}(0), \qquad u_{0_2} = u_{0_2}(0) = u_{0_1}(h_1), \cdots,$$

$$u_{0_k} = u_{0_k}(0) = u_{0_{k-1}}(h_k), \cdots, u_{0_{n+1}} = u_{0_n}(h_n).$$

$$[A]_k = \begin{bmatrix} ch(\zeta h_k) & \dfrac{sh(\zeta h_k)}{\zeta K_{vk}} \\ \zeta K_{vk}\, sh(\zeta h_k) & ch(\zeta h_k) \end{bmatrix} \tag{5-45a}$$

$$[B]_k = \frac{c_{mn}}{\zeta^2 C_{vk}} \begin{bmatrix} \dfrac{sh(\zeta h_k)}{\zeta h_k} - ch(\zeta h_k) & 1 - \dfrac{sh(\zeta h_k)}{\zeta h_k} \\ \zeta K_{vk}\left(\dfrac{ch(\zeta h_k) - 1}{\zeta h_k} - sh(\zeta h_k) \right) & \zeta K_{vk} \dfrac{1 - ch(\zeta h_k)}{\zeta h_k} \end{bmatrix} \tag{5-45b}$$

Hence, Equation (5-44) becomes a recursive equation

$$\begin{Bmatrix} \hat{u}_{k+1} \\ \hat{Q}_{k+1} \end{Bmatrix} = [A]_k \begin{Bmatrix} \hat{u}_k \\ \hat{Q}_k \end{Bmatrix} + [B]_k \begin{Bmatrix} u_{0_k} \\ u_{0_{k+1}} \end{Bmatrix} \tag{5-46}$$

One obtains:

$$\begin{Bmatrix} \hat{u}_{n+1} \\ \hat{Q}_{n+1} \end{Bmatrix} = [A]_n \begin{Bmatrix} \hat{u}_n \\ \hat{Q}_n \end{Bmatrix} + [B]_k \begin{Bmatrix} u_{0_n} \\ u_{0_{n+1}} \end{Bmatrix} = [A]_n \left([A]_{n-1} \begin{Bmatrix} \hat{u}_{n-1} \\ \hat{Q}_{n-1} \end{Bmatrix} + [B]_{n-1} \begin{Bmatrix} u_{0_{n-1}} \\ u_{0_n} \end{Bmatrix} \right) + [B]_n \begin{Bmatrix} u_{0_n} \\ u_{0_{n+1}} \end{Bmatrix}$$

$$= [A]_n [A]_{n-1} \begin{Bmatrix} \hat{u}_{n-1} \\ \hat{Q}_{n-1} \end{Bmatrix} + [A]_n [B]_{n-1} \begin{Bmatrix} u_{0_{n-1}} \\ u_{0_n} \end{Bmatrix} + [B]_n \begin{Bmatrix} u_{0_n} \\ u_{0_{n+1}} \end{Bmatrix}$$

$$= [A]_n [A]_{n-1} \cdots [A]_k \begin{Bmatrix} \hat{u}_k \\ \hat{Q}_k \end{Bmatrix} + [A]_n [A]_{n-1} \cdots [A]_{k+1} [B]_k \begin{Bmatrix} u_{0_k} \\ u_{0_{k+1}} \end{Bmatrix}$$

$$+ \cdots + [A]_n [B]_{n-1} \begin{Bmatrix} u_{0_{n-1}} \\ u_{0_n} \end{Bmatrix} + [B]_n \begin{Bmatrix} u_{0_n} \\ u_{0_{n+1}} \end{Bmatrix}$$

$$= [A]_n [A]_{n-1} \cdots [A]_2 [A]_1 \begin{Bmatrix} \hat{u}_1 \\ \hat{Q}_1 \end{Bmatrix} + [A]_n [A]_{n-1} \cdots [A]_2 [B]_1 \begin{Bmatrix} u_{0_1} \\ u_{0_2} \end{Bmatrix} + [A]_n [A]_{n-1} \cdots [A]_3 [B]_2 \begin{Bmatrix} u_{0_2} \\ u_{0_3} \end{Bmatrix}$$

$$+ \cdots + [A]_n [A]_{n-1} \cdots [A]_{k+1} [B]_k \begin{Bmatrix} u_{0_k} \\ u_{0_{k+1}} \end{Bmatrix} + \cdots + [A]_n [B]_{n-1} \begin{Bmatrix} u_{0_{n-1}} \\ u_{0_n} \end{Bmatrix} + [B]_n \begin{Bmatrix} u_{0_n} \\ u_{0_{n+1}} \end{Bmatrix}$$

(5-47)

Letting $[\Gamma]=[\Gamma]_1=[A]_n[A]_{n-1}\cdots[A]_2[A]_1=\prod_{j=n}^{1}[A]_j$; $[\Gamma]_k=[A]_n[A]_{n-1}\cdots[A]_k=\prod_{j=n}^{k\le n}[A]_j$;

$$[\Lambda]_k=[A]_n[A]_{n-1}\cdots[A]_{k+1}[B]_k=\left(\prod_{j=n}^{k+1\le n}[A]_j\right)[B]_k=[\Gamma]_{k+1}[B]_k; \qquad (5\text{-}47a)$$

Thus equation (5-46) is changed into (5-48)

$$\begin{Bmatrix}\hat{u}_{n+1}\\ \hat{Q}_{n+1}\end{Bmatrix}=[\Gamma]\begin{Bmatrix}\hat{u}_1\\ \hat{Q}_1\end{Bmatrix}+\begin{Bmatrix}\hat{u}_o\\ \hat{q}_o\end{Bmatrix} \qquad (5\text{-}48)$$

where

$$[\Gamma]=\begin{bmatrix}\Gamma_{11} & \Gamma_{12}\\ \Gamma_{21} & \Gamma_{22}\end{bmatrix} \qquad (5\text{-}49a)$$

$$\begin{Bmatrix}\hat{u}_o\\ \hat{q}_o\end{Bmatrix}=\sum_{k=1}^{n-1}[\Lambda]_k\begin{Bmatrix}u_{0\,k}\\ u_{0\,k}\end{Bmatrix}=\sum_{k=1}^{n-1}([\Gamma]_{k+1}[B]_k)\begin{Bmatrix}u_{0\,k}\\ u_{0\,k}\end{Bmatrix}; \qquad (5\text{-}49b)$$

According to following four cases of the boundary condition, one gets $\hat{u}_1$ and $\hat{Q}_1$, or $\hat{u}_{n+1}$ and $\hat{Q}_{n+1}$ by means of equation (5-48), then can determine any $\hat{u}_k$ and $\hat{Q}_k$ by the recursive equation (5-46):

Case A: top plan is permeable but bottom is impermeable, $\hat{u}_1=0$. and $\hat{Q}_{n+1}=0$.

By equation (5-48), $\begin{Bmatrix}\hat{u}_{n+1}\\ 0\end{Bmatrix}=\begin{bmatrix}\Gamma_{11} & \Gamma_{12}\\ \Gamma_{21} & \Gamma_{22}\end{bmatrix}\begin{Bmatrix}0\\ \hat{Q}_1\end{Bmatrix}+\begin{Bmatrix}\hat{u}_o\\ \hat{q}_o\end{Bmatrix}$

Hence, $\hat{Q}_1=-\hat{q}_o/\Gamma_{22}$; $\hat{Q}_{n+1}=\Gamma_{12}\hat{Q}_1+\hat{u}_o$ (5-50a)

Case B: top plan and bottom are permeable, $\hat{u}_1=0$ and $\hat{u}_{n+1}=0$.

By equation (5-48), $\begin{Bmatrix}0\\ \hat{Q}_{n+1}\end{Bmatrix}=\begin{bmatrix}\Gamma_{11} & \Gamma_{12}\\ \Gamma_{21} & \Gamma_{22}\end{bmatrix}\begin{Bmatrix}0\\ \hat{Q}_1\end{Bmatrix}+\begin{Bmatrix}\hat{u}_o\\ \hat{q}_o\end{Bmatrix}$

Hence, $\hat{Q}_1 = -\hat{u}_o / \Gamma_{12}$; $\hat{Q}_{n+1} = \Gamma_{22}\hat{Q}_1 + \hat{q}_o$ (5-50b)

Case C: top plan is impermeable but bottom is permeable, $\hat{Q}_1 = 0$ and $\hat{u}_{n+1} = 0$.

By equation (5-48), $\begin{Bmatrix} 0 \\ \hat{Q}_{n+1} \end{Bmatrix} = \begin{bmatrix} \Gamma_{11} & \Gamma_{12} \\ \Gamma_{21} & \Gamma_{22} \end{bmatrix} \begin{Bmatrix} \hat{u}_1 \\ 0 \end{Bmatrix} + \begin{Bmatrix} \hat{u}_o \\ \hat{q}_o \end{Bmatrix}$

Hence, $\hat{u}_1 = -\hat{u}_o / \Gamma_{11}$; $\hat{Q}_{n+1} = \Gamma_{21}\hat{u}_1 + \hat{q}_o$ (5-50c)

Case D: top plan and bottom are impermeating, $\hat{Q}_1 = 0$ and $\hat{Q}_{n+1} = 0$.

By equation (5-48), $\begin{Bmatrix} \hat{u}_{n+1} \\ 0 \end{Bmatrix} = \begin{bmatrix} \Gamma_{11} & \Gamma_{12} \\ \Gamma_{21} & \Gamma_{22} \end{bmatrix} \begin{Bmatrix} \hat{u}_1 \\ 0 \end{Bmatrix} + \begin{Bmatrix} \hat{u}_o \\ \hat{q}_o \end{Bmatrix}$

Hence, $\hat{u}_1 = -\hat{q}_o / \Gamma_{21}$; $\hat{u}_{n+1} = \Gamma_{11}\hat{u}_1 + \hat{q}_o$ (5-50d)

From equations (5-35) to (5-50), it is impossible to solve analytical expressions of complex value ζ because according to (5-35),

$$\zeta = \zeta(m,n,k,j) = \sqrt{\frac{C_{hk}(p_m^2 + q_n^2) + s_j}{C_{vk}}} \qquad (5\text{-}51)$$

Where s_j is a complex variable in the inverse Laplace transform, $s_j = a\text{-}i\infty \sim a\text{+}i\infty$. Therefore, the only possible method to solve the problem is with the numerical inverse Laplace transform, $\bar{u}_{mnk}(t) = \square^{-1}[\hat{u}_{mnk}(s)]$, that is,

$$\bar{u}_{mn}(p_m, q_n, Z_k; t) = \frac{1}{2\pi i}\int_{s=a-i\infty}^{a+i\infty} \hat{u}_{mn}(p_m, q_n, Z_k; s)e^{ts}ds \qquad (5\text{-}52)$$

Then a solution for u(t) can be obtained from the finite Fourier series transform inversion, $u_k(x,y;t) = \square^{-1}[\bar{u}_{mn}(p,q,Z_k;t)]$, that is,

$$u(x, y, Z_k, t) = \sum_{m=0}^{\infty}\sum_{n=0}^{\infty} \bar{u}_{mn}(p_m, q_n, Z_k; t) \cdot Cos(p_m x) \cdot Cos(q_n y) \qquad (5\text{-}53)$$

5.3.2 Method of Numerical Laplace Transform Inversion

In equation (5-52), $s = a \pm i\omega$, thus we have

$$\bar{u}(t) = \frac{e^{at}}{2\pi i} \int_{-\omega_f}^{\omega_f} \hat{u}(a + i\omega) e^{it\omega} d\omega \qquad (5\text{-}54)$$

Where, $a > 0$ is arbitrary, but it must be chosen so that it is greater than the real parts of all the singularities of $\hat{u}(s)$. That is, there are no singularities of $\hat{u}(s)$ to the right of the origin. Moreover, the value of a must be selected such that the restrictions on the function $\bar{u}(p,q;t) < Me^{at}$ are satisfied. Therefore, if a value for a is chosen that is too small, a may not be more than the real parts of all the poles of $\hat{u}(s)$, thus $\bar{u}(p,q;t)$ may not converge to the correct value. If an unsuitable value of a is chosen, it may lead to $\bar{u}(p,q;t) \geq Me^{at}$, and thus numerical errors are introduced and divergence of the value may appear (Davies, 2002).

The upper frequency limit, ω_f, must be specified. Experience (Davies & Martin, 2002) has shown that higher values of ω_f correspond to more accurate results, but at the expense of longer computation time.

There are over 100 algorithms available for the numerical inversion of Laplace transforms. Some important comparative studies of methods have been published. In addition to these comparative studies, an enormous number of engineering application papers have been written and each investigation has the merits of a particular procedure.

Davies (2002) gave a good review of most of the algorithms. The algorithms that have passed the test of time fall into four categories according to the basic approach of the following method:

i) Fourier series expansion

Over the years, there have been about 40 algorithms developed that are based on the Fourier series method and that involve approximating the inversion integral with an infinite Fourier series. Of notable interest is that developed by Sakurai (2004); this is an effective method for handling transforms of functions with discontinuities. However, in the application of consolidation problems and pore-water pressure dissipation, this method is generally inaccurate when ω_f is not great enough, or when the amount of time is too large, and usually results in large errors.

ii) Laguerre function expansion

This is the second most popular approach to numerical inversion and it is based on the Laguerre function expansion of $f(t)$. Since 1950, about 15 algorithms have been developed based on Laguerre's approach. Abate *et al* (1996) surveyed and discussed those algorithms. Weideman (1999) developed an important contribution to the Laguerre method.

iii) Combination of Gaver function

Numerical Laplace transform inversions based on the sequence of functionals developed by Gaver (1966) are seen as a very good approach by Abate & Valkó (2004) because the method uses an acceleration scheme. Some nonlinear sequence transformations are applied to Gaver functionals, for example, the Gaver-Stehfest method utilizing Salzer summation to accelerate convergence, Wynn's rho algorithm, Levin's *u*-transformation, Lubkin's iterated *w*-transformation and Brezinski's theta algorithm. The setting $s=k\cdot log(2)/t$ makes the method ineffective when $t=0$ or t is very small or near 0 for the analysis of consolidation problems.

iv) Deforming the Bromwich Contour.

One of the best approaches to computing the inverse is to deform the standard contour in the Bromwich inversion integral

$$\bar{u}(t) = \frac{1}{2\pi i}\int_B \hat{u}(s)e^{ts}ds \qquad (5\text{-}55)$$

In (5-55) the contour B is a vertical line defined by $s=a+i\omega$, where $-\infty<\omega<\infty$. The convergence of integral (5-55) would be greatly improved if s could take on values with a large, negative, real component. Thus, we can deform the contour into any open path that wraps around the negative real axis provided no singularity of $\hat{u}_{mnk}(s)$ is crossed in the deformation of B. Therefore, by Cauchy's theorem the deformed contour is valid. The brilliant contribution due to Talbot (1979) is the carefully chosen path of the form

$$s(\theta) = a\theta(\cot\theta + i),\ -\pi<\theta<+\pi \qquad (5\text{-}56)$$

Replacing contour B in Equation (5-55) with (5-56) and noticing that $s(\theta)$ is even to θ, one finds:

$$\bar{u}(t)=\frac{a}{\pi}\int_0^{\pi}\mathrm{Re}\left[\hat{u}(s(\theta))e^{ts(\theta)}(1+i\sigma(\theta))\right]d\theta \qquad (5\text{-}57)$$

in which, $\sigma(\theta)=\theta+(\theta\cot\theta-1)\cot\theta$ (5-57')

Approximating the value of the integral in Equation (5-57) using the trapezoidal rule with step size π/M, and $\theta_k=k\pi/M$:

$$\bar{u}(t,M)=\frac{a}{M}\left\{\frac{1}{2}\hat{u}(a)e^{at}+\sum_{k=1}^{M-1}\mathrm{Re}\left[\hat{u}(s(\theta_k))e^{ts(\theta_k)}(1+i\sigma(\theta))\right]\right\} \qquad (5\text{-}58)$$

Based on numerical experiments the following is selected:

$$a=2M/(5t);\quad M=M_0+1.6t \qquad (5\text{-}59)$$

and the relative error estimate is:

$$\left|\frac{f(t)-f(t,M)}{f(t)}\right|\approx 10^{-0.6M} \qquad (5\text{-}60)$$

The above Talbot algorithm was then used to compute (5-52) by replacing t with $T=t\frac{C_k}{R_x^2}$, where C_k is the standard value of the horizontal consolidation factors of layered soils $Ts=t\frac{C_k}{R_x^2}s_k$. Thus, one should set $s=s_k\frac{C_k}{R_x^2}$, as this is the key to being successful in applying the Talbot algorithm to consolidation problems.

5.3.3 Cases analysis

Case 9: rectangular area problem of p.w.p with 3-D dissipation in uniform soils, b_y/b_x = 1.0, l_x/b_x = 2.5, R_x/b_x = 5, η = 1.0, (b_x/R_x = 0.2, l_x/R_x = 0.5, b_y/R_y = 0.2, l_y/R_y = 0.5, R_x/R_y = 1.); b_z/b_x = 2, R_z/l_z = 1, $\mathbf{C_h/C_v = 4}$, $K_h = 4K_v$, $K_v=1.0\times10^{-4}$m/day, u_{oo}/u_{ob}=0.5, u_{om}/u_{ob}=1.0. Find a solution for the dissipation degree of pore pressure U = $u(x,y,z;t)/u_{0b}$.

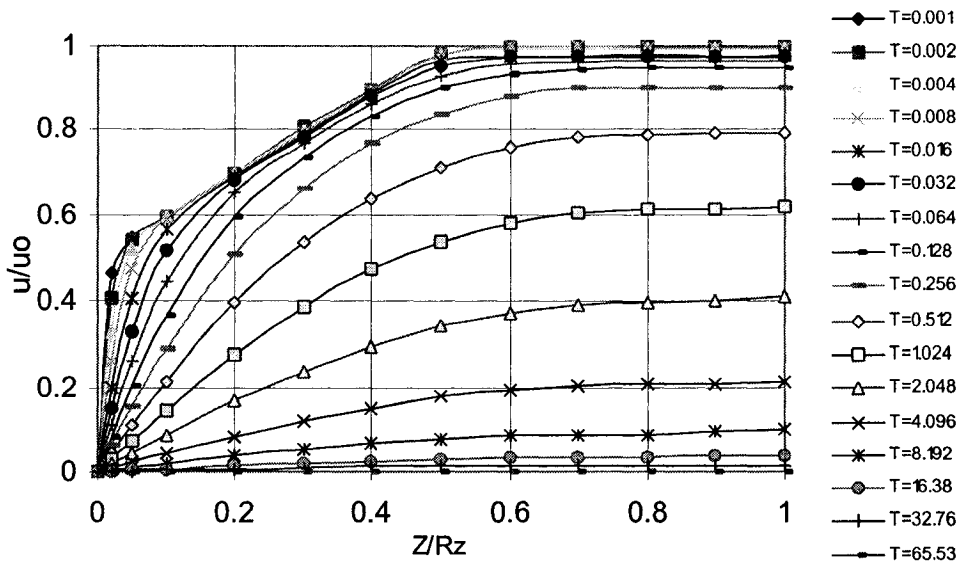

Fig. 5-20 Pore pressure contribution with time factor for p.w.p 3-D dissipation in layered soil and impermeable bottom boundary

Let the number of layers Ne = 10, h_k = 1.0m (k=1,2,...,5).

For impermeable boundary ($u|_{z=0} = 0$, $\partial u/\partial z|_{z=Rz} = 0$), the calculated U-T curves and U-z/Rz curves are shown in Figs. 5-20 and5-21.

For permeable boundary ($u|_{z=0} = 0$, $u|_{z=Rz} = 0$), the calculated U-T curves and U-x/Rx curves are shown in Figs. 5-22 and 5-23. The results are reasonable.

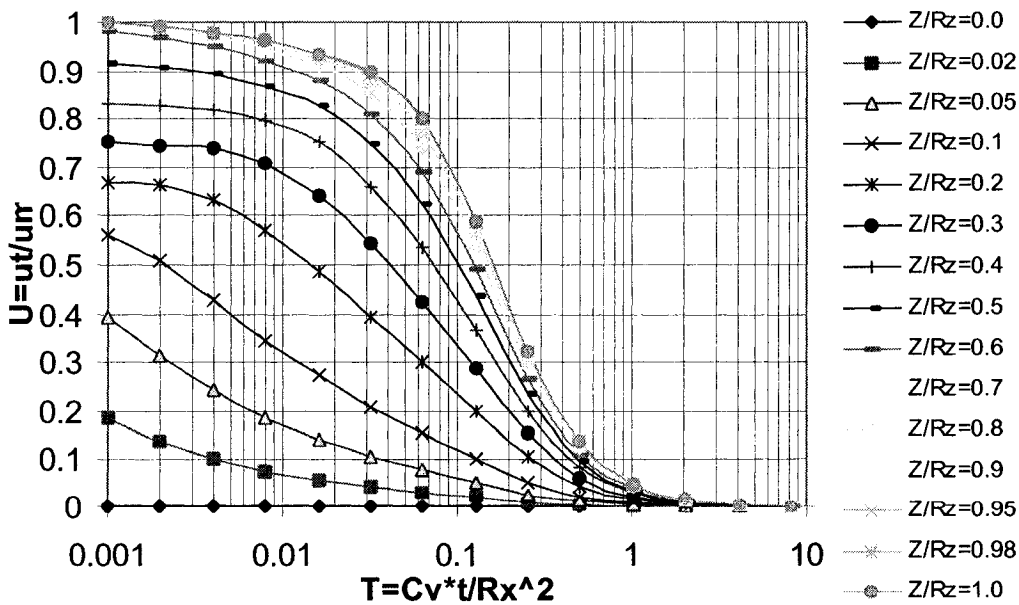

Fig. 5-21 Pore pressure dissipation degree with time factor for p.w.p 3-D dissipation in layered soil and impermeable bottom boundary

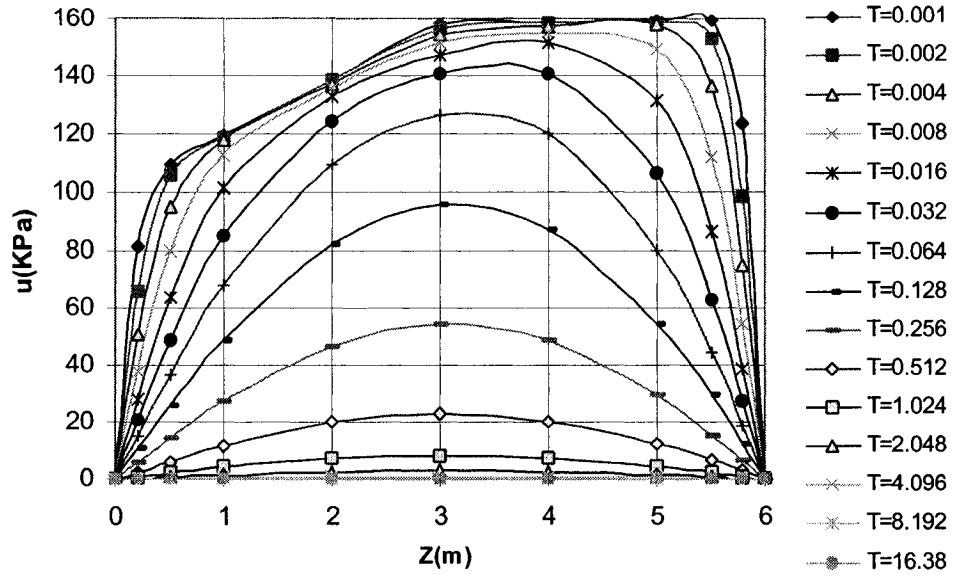

Fig. 5-22 Pore pressure contribution with time factor for p.w.p 3-D dissipation in layered soil and permeable bottom boundary

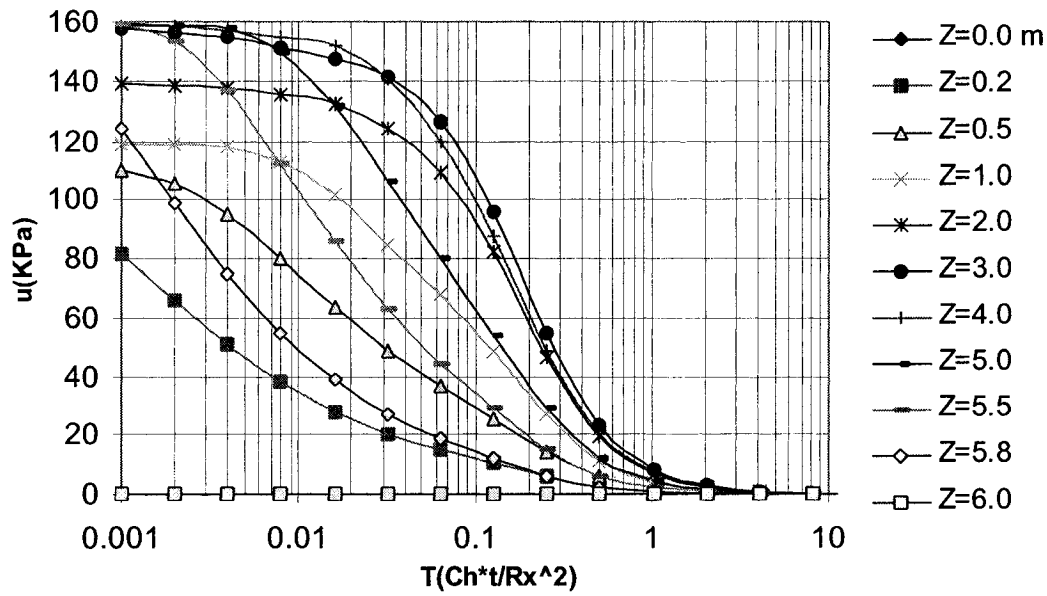

Fig. 5-23 Pore pressure dissipation with time factor for p.w.p 3-D dissipation in layered soil with permeable top and bottom boundary

Case 10: rectangular area problem of p.w.p 3-D dissipation in uniform soils, $b_y/b_x = 1.0$, $l_x/b_x = 2.5$, $R_x/b_x = 5$, $\eta = 1.0$, ($b_x/R_x = 0.2$, $l_x/R_x = 0.5$, $b_y/R_y = 0.2$, $l_y/R_y = 0.5$, $R_x/R_y = 1$), $b_z/b_x = 2$, $R_z/l_z = 1$, $u_{oo}/u_{ob} = 0.5$, $u_{om}/u_{ob} = 1.0$.

In the range of A at Z = 0~5: $C_{hA}/C_{vA} = 4$, $K_{hA} = 4K_{vA}$; $K_{vA} = 1.0\times10^{-4}$m/day;

In the range of B at Z = 5~10: $C_{hB}/C_{vB} = 4$, $K_{hB} = 4K_{vB}$; $C_{hB}/C_{hA} = 4$, $K_{hB}/K_{hA} = 2$;

Find a solution for the dissipation degree of pore pressure $U = u(x,y,z;t)/u_{0b}$.

Let the number of layers $N_e = 10$; $h_k = 1.0$m (k=1,2,...,5).

For impermeating boundary ($u|_{z=0} = 0$, $\partial u/\partial z|_{z=Rz} = 0$), the calculated U-T-z/$R_z$ curves are shown in Fig. 5-24.

For permeating boundary ($u|_{z=0} = 0$, $u|_{z=Rz} = 0$), the calculated U-T-Z/R_z curves are shown in Fig. 5-25. The results are also ideal.

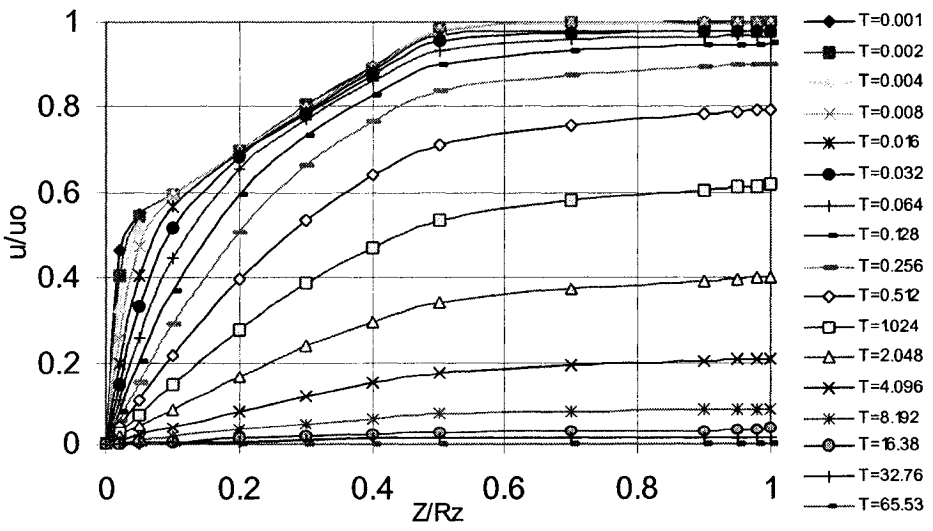

Fig. 5-24 Pore pressure contribution with time factor for p.w.p 3-D dissipation in layered soil and impermeable bottom boundary

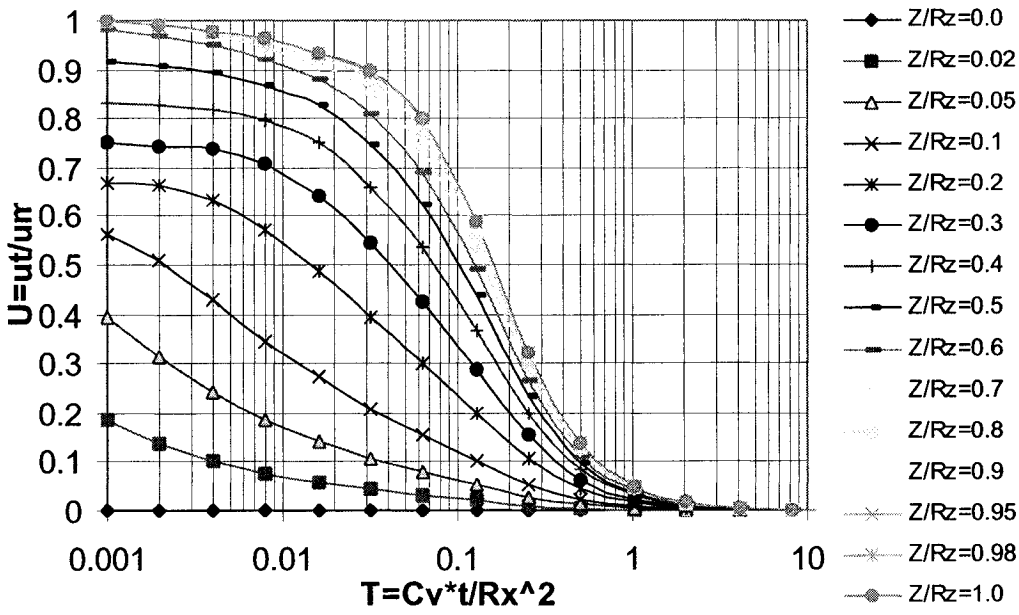

Fig. 5-25 Pore pressure dissipation degree with time factor for p.w.p 3-D dissipation in layered soil and impermeable bottom boundary

5.4 Pore-Pressure Dissipation Caused by Load Variation

The previous sections discussed the cases of pore-pressure dissipation under constant loads.

This section will now study pore-pressure dissipation under load variation, whose mathematical form is the following,

$$C_{hk}\left(\frac{\partial^2 u}{\partial x^2}+\frac{\partial^2 u}{\partial y^2}\right)+C_{vk}\frac{\partial^2 u}{\partial z^2}=\frac{\partial u}{\partial t}+f(x,y,z;t)$$

If pore pressure alteration from load variation is linearly related to time t, then

$$f(x,y,z;\,t)=\dot{g}(x,y,z)\cdot t$$

$$\dot{g}(x,y,z)=\dot{u}_0(z)\cdot\psi_2(x,y)$$

Where $\psi_2(x,y)$ is the as the same as that of equation (5.2-13)

$$\dot{u}_0(z)=\begin{cases}\dot{u}_{00}+\dfrac{\dot{u}_{0b}-\dot{u}_{00}}{b_z}z & (0\le Z\le b_z)\\ \dot{u}_{0m}-\dfrac{\dot{u}_{0b}-\dot{u}_{0m}}{l_z-b_z}(z-b_z) & (b_z\le Z\le l_z)\\ 0 & (l_z\le Z\le R_z)\end{cases}$$

Because (1-U) = $(1-U_{0z})\cdot(1-U_{0xy})$, this study only seeks to find the resolution of $u_{0z}(z;t)$, which is equal to getting the whole resolution.

5.5 Discussions

Impermeable boundary condition at $x = R_x$ does not agree with the actual situation of geotechnical engineering when time is nearing the end of consolidation. Therefore, permeable boundary condition in the horizontal direction is used.

The effect of initial pore pressure distribution on the consolidation degree is not great as time increases. In other words, although initial pore pressure distributions may be greatly different, the difference will become smaller and smaller as time increases, up to the point where it may totally disappear. However, in order to reach the same consolidation degree for different initial distributions of pore pressure different time factors are needed.

It is already known that Carrillo's expression for 3-D consolidation degree (Carrillo, 1942), $(1-U)=(1-U_{0z})\cdot(1-U_{0xy})$, is approximate. However, now it is proved that Carrillo's expression is exact only when the initial condition $u(x,y,z,0)$ can be expressed by $\psi_1(z)\cdot\psi_2(x,y)$.

When using the numerical method of Laplace transform inversion (5.3-24), numerical errors may be introduced and the divergence of the value may appear. Hence, it is necessary to choose carefully the calculation parameters and many trials to escape from the divergence of value.

CHAPTER 6

EFFECT OF PORE PRESSURE DISSIPATION ON STRESS AND UBCP IN THE INTERACTION

6.1 General

To analyze the effect of pore pressure dissipation and soil consolidation on the interaction of piles-soil-raft, related calculation series or analysis methods should first be found out, such as those described in Section 3.2. In this chapter, change of effective stress and ultimate bearing capacity of pile (UBCP) in the interaction are investigated and analyzed.

6.2 Change of Effective Stress Due to EPWP Dissipation and Loads

According to Terzaghi's effective stress theory, the initial excess pore water pressure (EPWP) in soil generated during pile driving and at the time of construction of the foundation and the structure will cause change of effective stresses in soil. The initial contribution of EPWP caused by a single pile can be estimated theoretically using Equations (2-38) to (2-50) or from measured data in the field. The contribution of EPWP in soil at the end of pile group driving may be obtained by the addition of EPWP caused by multiple piles. The maximum EPWP causes cracking of the soil as per $K_0\sigma'_{v0} + \Delta\sigma_\theta \leq 0$ or $\sigma'_v + \Delta\sigma_v \leq 0$, which is defined by equation (4-21). Based on the above, the contribution estimate of p.w.p in soil that remains until the beginning of the construction of the cap and the upper-structure is done according to the EPWP dissipation theory discussed in Chapter 5. Generally, construction stops for more than 28 days after pile driving is finished. Setting t = time length from the date of pile driving to the calculation

date, one can determine the EPWP that was caused by driving the pile, that which remains and the corresponding effective stress change.

When the pile top is loaded, the stresses in the soil will change correspondingly. This problem generated interested as early as 1960. Many researchers, such as Geddes (1966 and 1969), Mattes & Poulos (1969), Mattes (1969), as well as Butterfield & Bannerjee (1970), studied the problem and obtained many results of stresses change in soil. Slightly afterward D'Appolonia & Lambe (1970) analyzed the problem of loading a rigid pile in elastic medium with FLM and concluded that after a pile is loaded, the vertical and radial stresses in the soil surrounding the pile-soil surface have very small increases. In this study it was thought that the soil in the pile's periphery is borne by pure shear stress. Later on, Esrig et al (1977) and Kirby et al (1977) also proposed a similar view with respect to critical-state soil mechanics.

An analysis of the above yields the conclusion that after a pile is loaded axially, the soil around the pile is borne by pure shear stress under constant volume; therefore the change of EPWP in the soil caused by the load on the pile top can be neglected.

From the theory of critical void ratio of soil at ultimate strength state, shear stress caused by piles' loads do not generate additional EPWP within the soil nor does it generate additional pile lateral pressure. This is because changes of the void ratio, the EPWP of soil and the lateral pressure of a pile have all been completed during pile driving. Some data measured in the field (Tang 1990) confirmed this, as shown in Figs. 6-1 and 6-2.

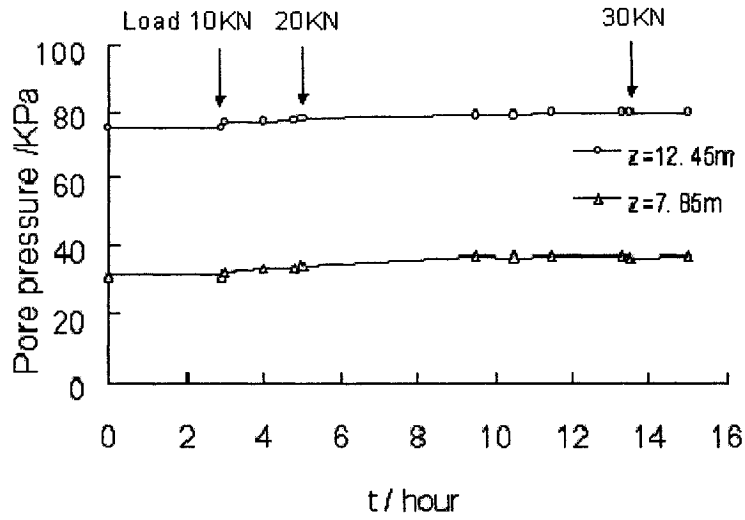

Fig. 6-1 Axial Loading Influence to Pore Pressure in Soil Around Pile (From Tang 1990)

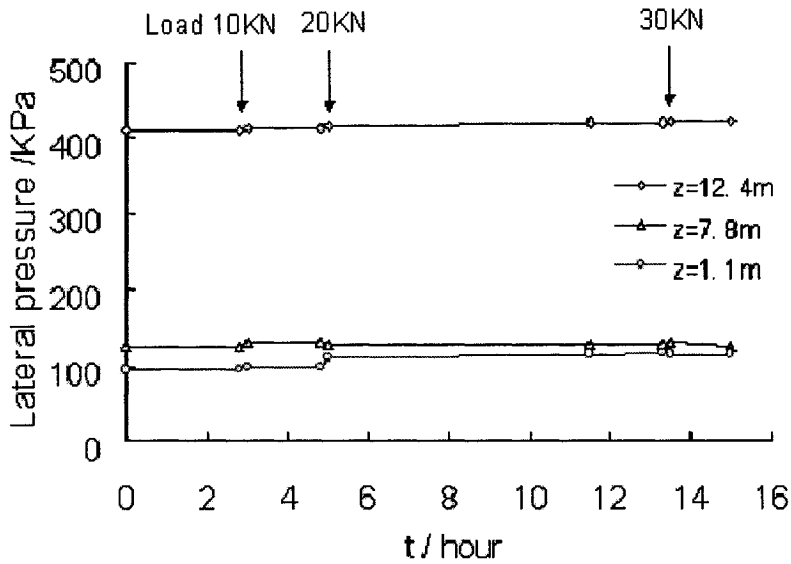

Fig. 6-2 Axial Loading Influence to Lateral Pressure at Pile (From Tang 1990)

In these figures, the pile length is 13.7m and the measured point at depth 12.4m is close to the base of the pile. This shows that the load at the pile base also does not generate additional EPWP in the soil nor does it generate additional pile lateral pressure.

So we only need to consider additional p.w.p caused by pressure of the bottom of cap.

$$\Delta u_B = \beta(\Delta\sigma_m + \alpha\Delta\tau_{oct}) \qquad (6\text{-}1)$$

in which α, β are Henkel pore pressure parameters (Henkel 1960), β=1 for complete saturated soil, α= 0.707(3A-1), A is Skempton pore pressure parameter; $\Delta\sigma_m$, $\Delta\tau_{oct}$ are octahedral body normal and shear stresses, $\Delta\sigma_m = (\Delta\sigma_x + \Delta\sigma_y + \Delta\sigma_z)/3 = (\Delta\sigma_r + \Delta\sigma_\theta + \Delta\sigma_z)/3$, $\Delta\tau_{oct} = \sqrt{\{(\Delta\sigma_1 - \Delta\sigma_2)^2 + (\Delta\sigma_2 - \Delta\sigma_3)^2 + (\Delta\sigma_3 - \Delta\sigma_1)^2\}}/3$.

According to Figs. 6-1 and 6-2 and the assumption of the critical-void-ratio state of soil, α should be taken as zero. Hence, the initial additional pore pressure from pressure of the bottom of cap is:

$$\Delta u_B(t)|_{t=0} \approx \Delta\sigma_m = (\Delta\sigma_x + \Delta\sigma_y + \Delta\sigma_z)/3$$

and the additional effective lateral pressure of the pile, $\Delta\sigma_h'$, generated by the pressure of the bottom of the cap can be determined (setting $\Delta\sigma_x = \Delta\sigma_y$),

$$\Delta\sigma_h'|_{t=0} = \Delta\sigma_x - \Delta u_B(t)|_{t=0} \approx (\Delta\sigma_x - \Delta\sigma_z)/3 <\approx 0 \qquad (6\text{-}2)$$

Equation (6-2) shows that at the beginning of the moment of loading (t = 0), the pressure at the raft's bottom and the effective lateral pressure of the pile is smaller than or close to zero and will increase with the dissipation of the EPWP. That is, the raft's increasing action on the UBC of a pile due to the increment of the effective lateral pressure of pile does not work at the beginning of the moment of loading on the raft. For a step-loading situation, the raft's increasing action goes into effect only after completing some degree

of consolidation under the former step loads.

6.3 Changing Process of Pile Bearing Capacity in the Interaction

The following analyzes present the process of sharing loads of piles and rafts, soil stresses, p.w.p and deformations from the beginning of construction to a long time after the end of construction.

This analysis can provide some results for the increasing process of the piles' ultimate bearing capacity,

$$\Delta P_u(t) = P_b \cdot \Delta\sigma_b/\sigma_b + \Sigma p \Delta\tau_f(t) \cdot \Delta z \qquad (6\text{-}3)$$

in which, p is the perimeter of the pile section, $\Delta\tau_f$ is the increment of shear strength of the soil around pile and σ_b is the initial vertical effective stress of soil at the pile tip.

Considering that the failure plane between pile and soil is actually located on the soil crust on the outside of the pile, shown in Fig. 6-3, the perimeter of pile section, p, should be calculated according to the section of soil crust outside of the pile,

$$p = 2\pi(r_0+\delta)=\pi(d+2\delta) \quad \text{(for circle pile)}$$

or $$p = 4(b+2\delta) \quad \text{(for square pile)}$$

Where, δ is the thickness of the soil crust

Tang (1990) adopted a suggestion from Gu Beizhen (1964),

$$\delta = 0.24\frac{d_e}{e} \qquad (6\text{-}4)$$

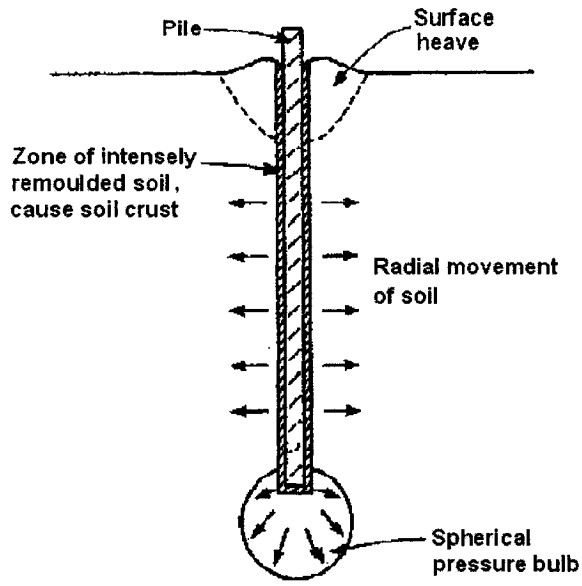

Fig. 6-3 Soil Remoulded and Soil Crust

But the value of δ given by (6-4) is usually overestimated as some references (such as the *Manual of Pile Foundation Engineering*, China Architecture and Building Press, 1995) shows that δ = 3~20mm. Here taking δ=20mm is recommended.

For stress states of the normally-consolidated soil around pile, according to Wroth et al (1979), one can use equation (4-16), e.g.,

$$\Delta\tau_f(t) = \frac{Sin\varphi'}{1+(2A_f-1)Sin\varphi'}\Delta\sigma_h'(t) \qquad (6\text{-}5)$$

and according to Randolph & Wroth (1981), or Tang (1990),

$$\Delta\tau_f(t) = \frac{Sin\varphi' Cos\varphi'}{1+Sin^2\varphi'}\Delta\sigma_h'(t) \qquad (6\text{-}6)$$

The above equation (6-6) can be derived according to Mohr-Coulomb's criterion and the stress circle analysis shown in Fig. 6-4

The difference between Equations (6-5) and (6-6) is not large when A_f= 1.0, as shown in Fig. 6-5. From this figure, it is seen that $\Delta\tau_f = \Delta\sigma_h \cdot \tan\varphi$ will overestimate the frictional stress of a pile shaft. Actually, the soil around the pile is at unload-reload state of normal stress (as shown in Fig.6-6) because of pore pressure dissipation. Thus, when using equation $\Delta\tau_f = \Delta\sigma_h \cdot \tan\varphi$, one should take $\varphi = \varphi_e$ (internal frictional angle at unload-reload state of normal stress). At φ'=30, taking $\varphi_e \approx 0.62\varphi$' and in the range φ'=15~35°, taking $\varphi_e \approx 0.35\varphi$'+9(°) is acceptable, as shown in Fig.6-5.

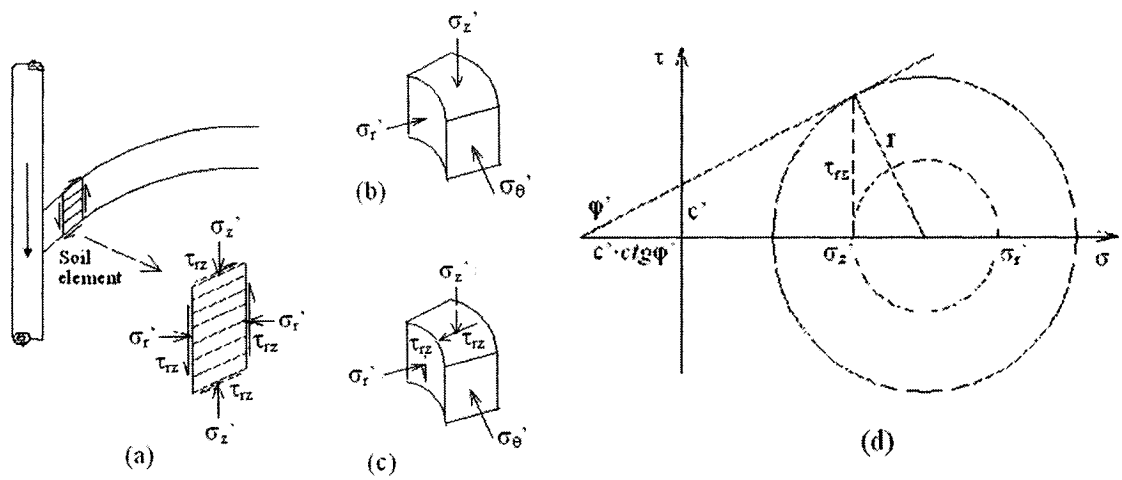

(a) Loaded pile and soil element; (b) Stresses before loading;
(c) Stresses after loading; (d) Failure at pile-soil interface

Fig 6-4 Mode of Failure at Pile-Soil Interface

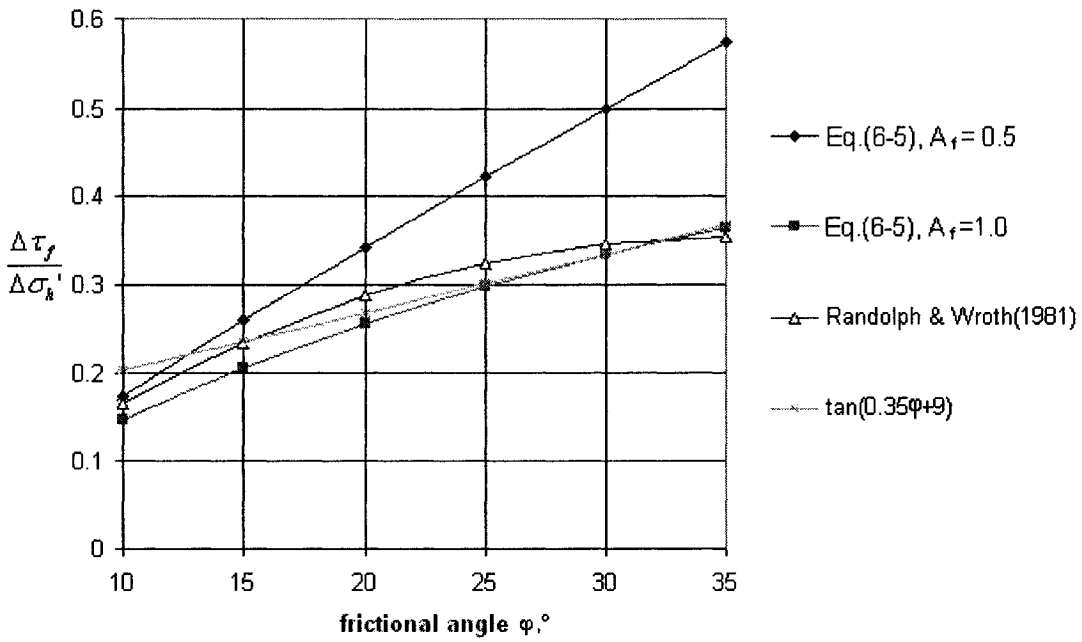

Fig. 6-5 Shear Strength of Soil around Pile

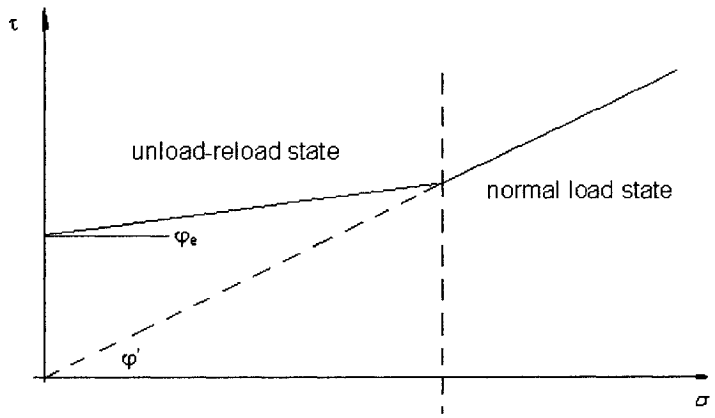

Fig. 6-6 Internal Frictional Angle in the Unload-Reload State of Normal Stress

Variations of the normal stress on the pile shaft, $\Delta\sigma_h$', should not simply be equal to the change of pore pressure Δu, because horizontal shrinking displacement of soil is occurring around the piles with EPWP dissipation.

For the case of a single pile, a relationship between $\Delta\sigma_h$' and Δu can be derived from basic physical-mechanical equations. Assuming an axial-symmetrical plane-strain problem for a single pile (set σ_r' $=\Delta\sigma_h$'), one obtains:

Equilibrium equation $$\frac{d\sigma_r^{'}}{dr}+\frac{1}{r}\left(\sigma_r^{'}-\sigma_\theta^{'}\right)+\frac{du}{dr}=0 \qquad (6\text{-}7)$$

Geometrical equation $$\varepsilon_r=\frac{du_r}{dr},\qquad \varepsilon_\theta=\frac{u_r}{r} \qquad (6\text{-}8)$$

Physical equation

$$\left.\begin{aligned}\sigma_r^{'}&=\frac{E(1-\mu)}{(1-2\mu)(1+\mu)}\left(\varepsilon_r+\frac{\mu}{1-\mu}\varepsilon_\theta\right)\\ \sigma_\theta^{'}&=\frac{E(1-\mu)}{(1-2\mu)(1+\mu)}\left(\varepsilon_\theta+\frac{\mu}{1-\mu}\varepsilon_r\right)\end{aligned}\right\} \qquad (6\text{-}9)$$

Combining equations (6-7), (6-8) and (6-9) yields:

$$\left.\begin{aligned}\sigma_r^{'}&=\Delta u-\frac{E}{1+\mu}\frac{u_r}{r}\\ \sigma_\theta^{'}&=\Delta u\frac{\mu}{1-\mu}+\frac{E}{1+\mu}\frac{u_r}{r}\end{aligned}\right\} \qquad (6\text{-}10)$$

and

$$u_r=\frac{r_0}{D}\left(\frac{\rho}{2}u_i-\frac{1}{\rho}\int\rho\,u\,d\rho\right) \qquad (6\text{-}11)$$

in which u_r is the radial deformation at a time t, $D = \frac{E(1-\mu)}{(1-2\mu)(1+\mu)}$, μ is the soil's Poisson ratio, estimated by $\mu = K_0/(1+ K_0)$, u is the excess pore pressure at time t, as discussed in chapter 5.

$\Delta u = u_i - u$, where $u_i (= u_0)$ and u are the excess pore pressures at time = 0 and = t.

$\rho = r/r_0$, where r and r_0 are respectively the radial coordinate value and the pile radius.

From the first term of equation (6-10), setting

$$\Delta\sigma_h' = \sigma_r' = \Delta u - \frac{E}{1+\mu}\frac{u_r}{r} = \Delta u - \Delta\sigma_s$$

$\Delta\sigma_s$ is the lateral stress change caused by a soil's volumetric shrinkage due to a pore pressure change.

$$\Delta\sigma_s = \frac{E}{1+\mu}\frac{u_r}{r} = \frac{E}{1+\mu}\frac{r_0}{rD}\left(\frac{\rho}{2}u_i - \frac{1}{\rho}\int \rho\, u\, d\rho\right)$$

$$= \frac{1-2\mu}{1-\mu}\left(\frac{u_i}{2} - \frac{1}{\rho^2}\int \rho\, u\, d\rho\right) \qquad \left\{set: u \approx u\big|_{r=r_0}\right\}$$

$$\approx \frac{1-2\mu}{1-\mu}\left(\frac{u_i}{2} - \frac{1}{\rho^2}\left(u\big|_{\rho=1}\right)\int \rho\, d\rho\right)$$

$$= \frac{1-2\mu}{2(1-\mu)}(u_i - u)\big|_{r=r_0} = \frac{1-2\mu}{2(1-\mu)}\Delta u\big|_{r=r_0} \qquad (6\text{-}12)$$

Substituting Equation (6-12) into the first term of (6-10) gives:

$$\Delta\sigma_h' = \sigma_r' = \Delta u - \Delta\sigma_s \approx \Delta u - \frac{1-2\mu}{2(1-\mu)}\Delta u$$

$$= \frac{1}{2(1-\mu)}\Delta u = \chi\Delta u \qquad (6\text{-}12a)$$

In which $$\chi \approx \frac{1}{2(1-\mu)} \qquad (6\text{-}12b)$$

Typically, Poisson's ratio for soft clay is $\mu = 0.42$ and $\mu=0.33$ for sand. Hence,

$$\chi \approx 0.86 \approx 0.9, \text{ or } \Delta\sigma_h' = \sigma_r' \approx 0.9\Delta u \text{ (for clay)}$$

In the case of a single pile problem (shown in Table 6-1, from Tang 1990), comparing equation (6-12) with the exact solution given by Tang (1990), one finds that equation (6-12) is not accurate enough for axial-symmetrical plane-strain problems of a single pile and that is also quite conservative.

Table 6-1 Theoretical solution of $\Delta\sigma_h'$ ~Δu relationship
($r = 1.4r_0$, from Tang 1990)

t days after driving	Δu(KPa)	$\Delta\sigma_h'$(Kpa)	$\Delta\sigma_h'/\Delta u$
14	15.9	14.2	0.8931
	27.9	24.7	0.8853
	112.7	97.7	0.8669
137	25.4	23.1	0.9094
	61.2	57.1	0.9330
	159.4	141.7	0.8890
297	27.0	24.7	0.9148
	72.0	67.0	0.9306
	161.0	143.3	0.8901
409	27.0	24.7	0.9148
	76.5	71.1	0.9294
	161.0	143.3	0.8901
Sum			10.8464
Average			0.9039

According to Tang's derivation (1990),

$$u_r = \frac{2r_0 u_{im}}{DLn(\omega)}\left\{\frac{\rho}{4}\ln\left(\frac{\omega}{\rho}\right) - \sum_{i=1}^{\infty}\frac{\omega}{\lambda_i^2 J_1^2(\lambda_i)}\left[J_1\left(\frac{\lambda_i\rho}{\omega}\right) - \frac{\omega\rho}{400\lambda_i}\right]\exp\left[-\frac{3(1-\mu)}{1+\mu}\left(\frac{\lambda_i}{\omega}\right)^2 T\right]\right\}$$

(6-13)

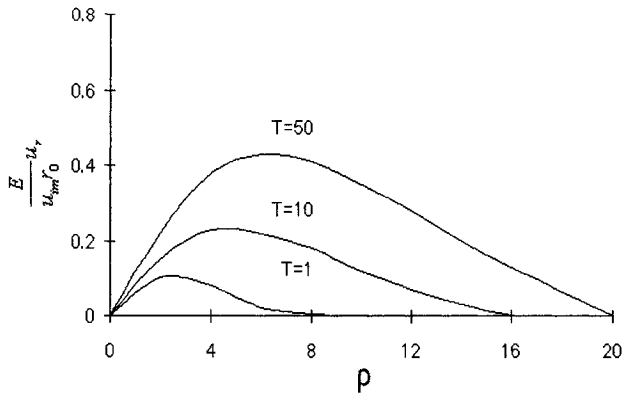

Fig. 6-7 u_r~ρ curves

The $\frac{E}{u_{im}r_0}u_r$~ρ curves given in Fig. 6-7 show that $\frac{E}{u_{im}r_0}u_r|_{Max} \approx 0.25$ at ρ = 1~1.5, μ = 0.3, T ≥ 10. Thus,

$$\Delta\sigma_s|_{\text{Max}} = \frac{E}{1+\mu}\frac{u_r|_{Max}}{r} = \frac{1}{1+\mu}\frac{Eu_r|_{Max}}{u_{im}r_0}\frac{u_{im}r_0}{r} \approx \frac{0.25}{1+\mu}\frac{u_{im}}{\rho}. \qquad (6\text{-}14)$$

When μ = 0.3, ρ = 1.4, $\Delta\sigma_s|_{\text{Max}} = 0.137u_i \approx 0.14\Delta u|_{\text{Max}}$. Then, χ = 1-0.14 = 0.86 is also proven to be acceptable.

For the case when t→∝, $\Delta u = u_i$ (= u_0), Tang (1990) derived the following:

$$\Delta\sigma_h' = \sigma_r' = \frac{u_i}{2(1-\mu)} \quad \text{(Axial-symmetrical problem)}$$

$$\sigma_r' = \frac{1+\mu}{3(1-\mu)}u_i \quad \text{(Spherical-symmetrical problem)}$$

The above equation's first term also proves that taking $\chi = \frac{1}{2(1-\mu)}$ is acceptable for 2-D axial-symmetrical problem.

For a general situation, one assumes $\chi = \chi_2$~χ_3,

$$\chi_2 = \frac{1}{2(1-\mu)} \text{ (in 2-D situation)}$$

$$\chi_3 = \frac{1+\mu}{3(1-\mu)} \text{ (in 3-D situation).}$$

Thus, taking

$$\chi = \chi_{av} = (\chi_2+\chi_3)/2 = \frac{5+2\mu}{12(1-\mu)} \qquad (6\text{-}15)$$

This considered as a reasonable choice, as shown in Fig. 6-8. χ_3 and χ_{av} can roughly be used for 3-D situation.

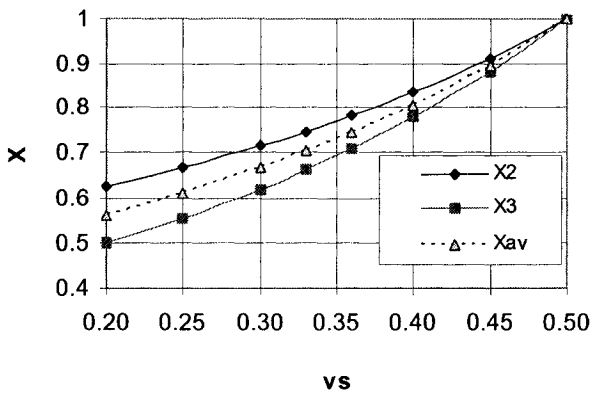

Fig. 6-8 $\chi_2(\mu)$, $\chi_3(\mu)$, $\chi(\mu)$ Function

Substituting equations (6-5) and (6-12) into (6-3), one obtains

$$\Delta P_u(t) = P_b \cdot \Delta\sigma_b(t)/\sigma_b + p\sum \frac{Sin\varphi' Cos\varphi'}{1+Sin^2\varphi'} \chi \Delta u(t) \Delta z \qquad (6\text{-}16)$$

When φ' is constant with depth z, or for $\varphi' = \overline{\varphi'}$ (φ'average in range of pile length)

$$\Delta P_u(t) = P_b \cdot \Delta\sigma_b(t)/\sigma_b + p\chi\chi_\varphi \sum \Delta u(t) \Delta z \qquad (6\text{-}17)$$

Where $$\chi_{\varphi}=\frac{Sin\varphi' Cos\varphi'}{1+Sin^2\varphi'} \tag{6-18}$$

Setting the consolidation degree of soil U

$$U(t)=\frac{\int_{z=0}^{z=l}\Delta u(t)\cdot dz}{\int_{z=0}^{z=l}u_0\cdot dz}=\frac{\sum\Delta u(t)\cdot\Delta z}{\sum u_0\Delta z} \tag{6-19}$$

Thus, $$\sum\Delta u\cdot\Delta z=U(t)\sum u_0\cdot\Delta z,$$

$$\Delta P_u(t)=P_b\cdot\Delta\sigma_b/\sigma_b+p\chi\chi_{\varphi}U(t)\sum u_0\Delta z \tag{6-20}$$

Noticing that $P_b/\sigma_b = A_p$ (A_p is the section area of pile base) and $\Delta\sigma_b = \Delta u|_{z=l}$,

$$\Delta P_u(t)=A_b\cdot\Delta\sigma_b(t)+p\chi\chi_{\varphi}U(t)\sum u_0\Delta z \tag{6-21}$$

and $$\Delta P_c=\Delta P_u(t)|_{t=\infty}=A_b\cdot u_{0b}+p\chi\chi_{\varphi}\sum u_0\Delta z \tag{6-22}$$

Now determining U(t):

$$U(t)=\frac{\int_{z=0}^{z=l}\Delta u(t)\cdot dz}{\int_{z=0}^{z=l}u_0\cdot dz}=\frac{\int_{z=0}^{z=l}(u_0-u)\cdot dz}{\int_{z=0}^{z=l}u_0\cdot dz}=\frac{A_{\Delta ut}}{A_{u0}}$$

$$=1-\frac{\int_{z=0}^{z=l}u(t)\cdot dz}{\int_{z=0}^{z=l}u_0\cdot dz}=1-\frac{A_{ut}}{A_{u0}} \tag{6-23}$$

Where u(t) is defined in chapter 5.

From Fig. 5-16 [$u_0(z)$ form], one gets

$$A_{u0}=\int_{z=0}^{z=l} u_0 \cdot dz = (u_{00}+u_{0l})b_z/2+(u_{00}+u_{0l})(l_z-b_z)/2 \qquad \text{(when } l\geq l_z,\ x\leq b_x,\ y\leq b_y\text{)} \qquad (6\text{-}24)$$

$$=(u_{00}+u_{0l})b_z/2 \qquad \text{(when } l=b_z,\ x\leq b_x,\ y\leq b_y\text{)} \qquad (6\text{-}24a)$$

According to equation (5-15)

$$A_{ut}=\int_{z=0}^{z=l} u(x,y,z;t)\cdot dz$$

$$=\int_{z=0}^{z=l}\left\{\sum_{k=1}^{\infty} d_k Sin(h_k z)Exp(-C_v h_k^2 t)\right\}\left\{\sum_{m=0}^{\infty}\sum_{n=0}^{\infty} d_{mn}Cos(p_m x)\cdot Cos(q_n y)\cdot Exp\left[-C_h(p_m^2+q_n^2)t\right]\right\}dz$$

$$=\left\{\sum_{k=1}^{\infty} d_k \int_{z=0}^{z=l} Sin(h_k z)dz\cdot Exp(-C_v h_k^2 t)\right\}\left\{\sum_{m=0}^{\infty}\sum_{n=0}^{\infty} d_{mn}Cos(p_m x)\cdot Cos(q_n y)\cdot Exp\left[-C_h(p_m^2+q_n^2)t\right]\right\}$$

$$=\left\{\sum_{k=1}^{\infty} \frac{d_k}{h_k}\left[1-Cos(h_k l)\right]Exp(-C_v h_k^2 t)\right\}\left\{\sum_{m=0}^{\infty}\sum_{n=0}^{\infty} d_{mn}Cos(p_m x)\cdot Cos(q_n y)\cdot Exp\left[-C_h(p_m^2+q_n^2)t\right]\right\}$$

$$=\left\{\sum_{k=1}^{\infty} \frac{d_k}{h_k}\left[1-Cos(h_k l)\right]Exp(-C_v h_k^2 t)\right\}\cdot\frac{u(x,y;t)}{u_0} \qquad (6\text{-}25)$$

Where $h_k = \dfrac{k\pi}{R_z}$ for a permeable bottom boundary or $\dfrac{(1+2k)\pi}{2R_z}$ for an impermeable bottom boundary.

d_k is shown in equations (5-14c to e) and (5-19c to e)

When $l = R_z$,

$$A_{ut}=\left\{\sum_{K=1,3,\cdots}^{\infty} \frac{2d_K R_z}{K\pi}\cdot Exp(-C_v h_k^2 t)\right\}\cdot\frac{u(x,y;t)}{u_0} \qquad (6\text{-}25a)$$

Similarly, for circular area problems of foundations, according to Eq. (5-28),

$$A_{ut}=\left\{\sum_{k=1}^{\infty}\frac{d_k}{h_k}\left[1-Cos(h_k l)\right]Exp\left(-C_v h_k^2 t\right)\right\}\cdot\frac{u(r;t)}{u_0} \tag{6-26}$$

or when $l = R_z$

$$A_u=\left\{\sum_{K=1,3,\cdots}^{\infty}\frac{2d_K R_z}{K\pi}\cdot Exp\left(-C_v h_k^2 t\right)\right\}\cdot\frac{u(r;t)}{u_0} \tag{6-26a}$$

In which, $u(r;t)=\left\{\sum_{m=0}^{\infty}c_m J_0\left(\frac{\alpha_m}{R}r\right)\cdot Exp\left(-C_h\frac{\alpha_m^2}{R}t\right)\right\}$; c_m is shown in Eq.(5-29).

Substituting equations (6-24) and (6-25) or (6-26) into Eq. (6-23), we have

$$U(t)=1-\frac{A_{ut}}{A_{u0}}=1-\left\{\frac{1}{A_{u0}}\sum_{k=1}^{\infty}\frac{d_k}{h_k}\left[1-Cos(h_k l)\right]Exp\left(-C_v h_k^2 t\right)\right\}\cdot\frac{u(x,y;t)}{u_0} \tag{6-27}$$

Set $$U_z=1-\frac{1}{A_{u0}}\sum_{k=1}^{\infty}\frac{d_k}{h_k}\left[1-Cos(h_k l)\right]Exp\left(-C_v h_k^2 t\right) \tag{6-28a}$$

$$U_{xy}=1-\frac{u(x,y;t)}{u_0} \tag{6-28b}$$

Thus,

$$U(t)=1-(1-U_z)\cdot(1-U_{xy}) \tag{6-29}$$

or for circular area problems,

$$U(t)=1-(1-U_z)\cdot(1-U_r) \tag{6-29a}$$

When $l = R_z$, $u_{0b} = u_{0m}$, and the bottom at the pile base is permeable, one can prove that U_z is exactly the solution of Terzaghi's 1-D consolidation theory, e.g.,

$$U_z=1-\sum_{k=1,3,5}^{\infty}\frac{8}{K^2\pi^2}Exp\left[1-C_v\left(\frac{K\pi}{2H}\right)^2 t\right] \tag{6-30}$$

in which $H = R_z/2$ for a permeable bottom or $H = R_z$ for an impermeable bottom.

For the general situation, one can use a combination of pore-pressure contribution areas in order to estimate the 1-D vertical consolidation degree U_z as per Fig. 6-9,

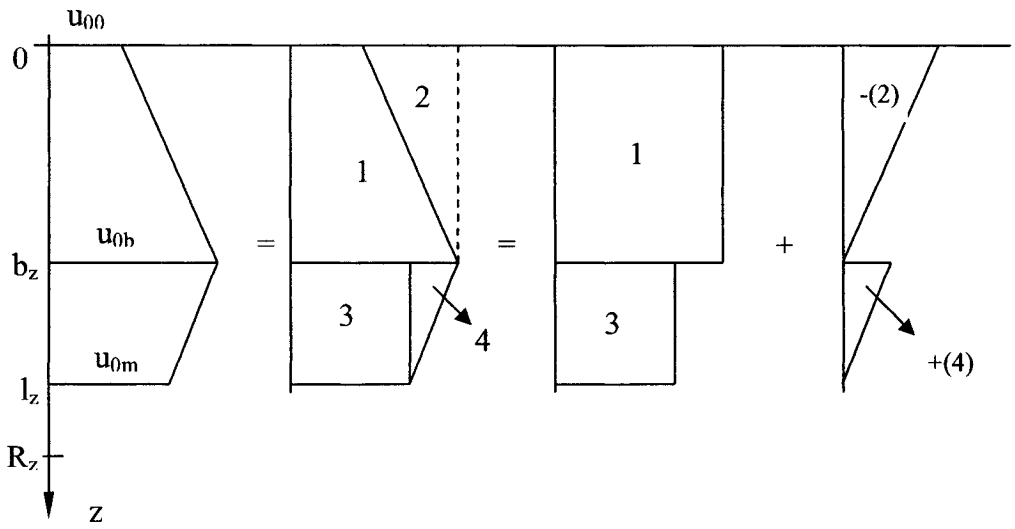

Fig. 6-9 Unit Combinations of 1-D Vertical Consolidation Degree U_z

$$U_z = \frac{A_{\Delta ut}}{A_{u0}} = \frac{A_{\Delta ut}^{(1)} - A_{\Delta ut}^{(2)} + A_{\Delta ut}^{(3)} + A_{\Delta ut}^{(4)}}{A_{u0}}$$

$$= \frac{U_z^{(1)} \cdot A_{u0}^{(1)} - U_z^{(2)} \cdot A_{u0}^{(2)} + U_z^{(3)} \cdot A_{u0}^{(3)} + U_z^{(4)} \cdot A_{u0}^{(4)}}{A_{u0}}$$

$$= U_z^{(1)} \cdot \frac{A_{u0}^{(1)}}{A_{u0}} - U_z^{(2)} \cdot \frac{A_{u0}^{(2)}}{A_{u0}} + U_z^{(3)} \cdot \frac{A_{u0}^{(3)}}{A_{u0}} + U_z^{(4)} \cdot \frac{A_{u0}^{(4)}}{A_{u0}} \qquad (6\text{-}31)$$

in which $U_z^{(i)}$ is represents the three cases depicted in Fig. 6-10. $U_z^{(1)}$ and $U_z^{(3)}$ belong to case (a) ($U_z^{(a)}$) and $U_z^{(2)}$ and $U_z^{(4)}$ belong to case (b) ($U_z^{(b)}$). Case c ($U_z^{(c)}$) can be obtained from

$$U_z^{(c)} = 2U_z^{(a)} - U_z^{(b)} \qquad (6\text{-}32)$$

The value of $U_z^{(i)}$ is given in Fig. 6-11(a1)~Fig. 6-11(b7); U_{xy} or U_r in Equation (6-27) is given in Fig. 6-12(1a)~ Fig. 6-13(g).

After determining the increasing process of ultimate bearing capacity of piles, the decreasing process of the pressure at the bottom of the cap may be correspondingly be obtained,

$$\Delta Q_F = Q - n_p \Delta P \tag{6-33}$$

and the changing process of soil, piles and raft deformations may be also obtained,

$$\Delta S = S_{cp}(t) = \Sigma[\Delta u(z,t) \cdot \Delta z / E_s] \tag{6-34}$$

which will later be described in detail in Chapter 7.

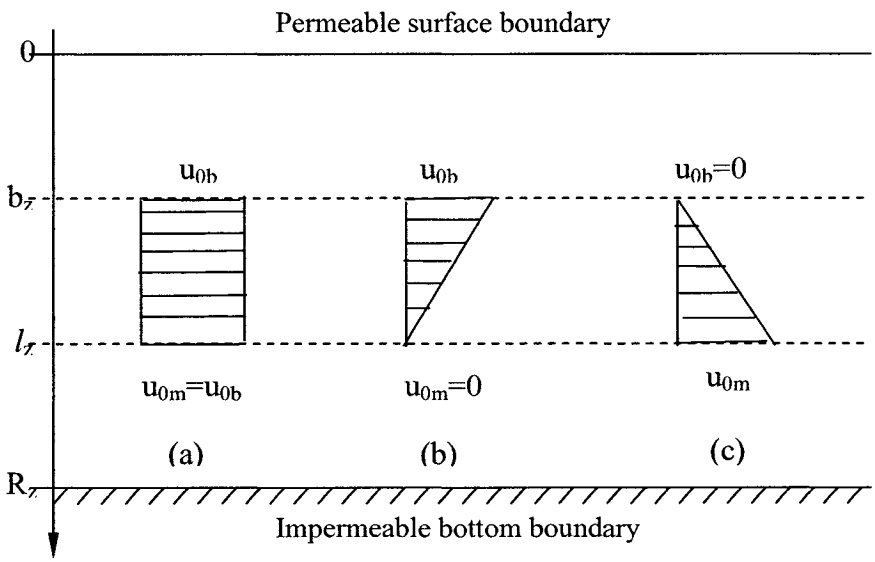

Fig. 6-10 Three typical cases of $U_z^{(i)}$

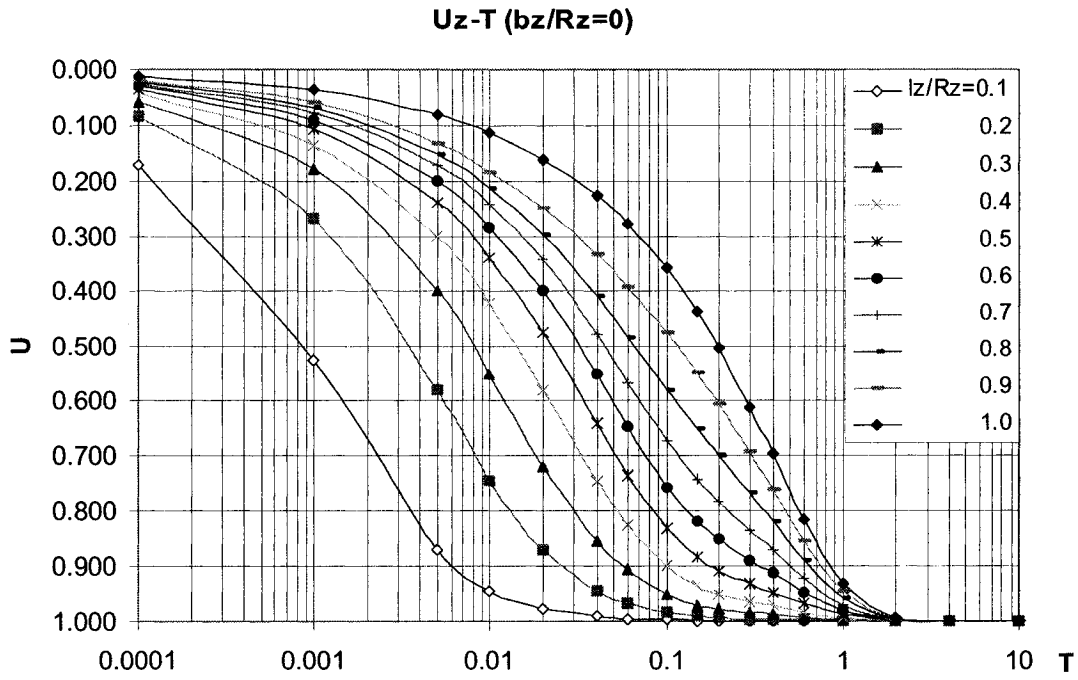

Fig.6-11(a1) 1-D Vertical Unit Consolidation Degree $U_z^{(i)}$ (Case a: $u_{0m}=u_{0b}$; $b_z/R_z=0$)

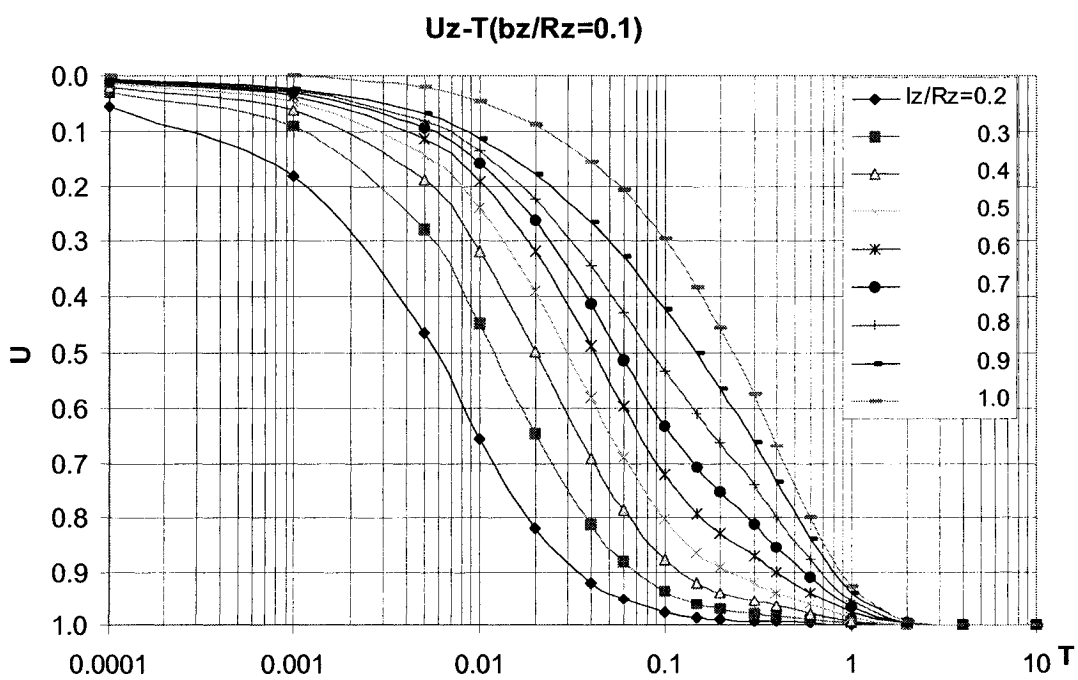

Fig.6-11(a2) Vertical Unit Consolidation Degree $U_z^{(i)}$ (Case a: $u_{0m}=u_{0b}$; $b_z/R_z=0.1$)

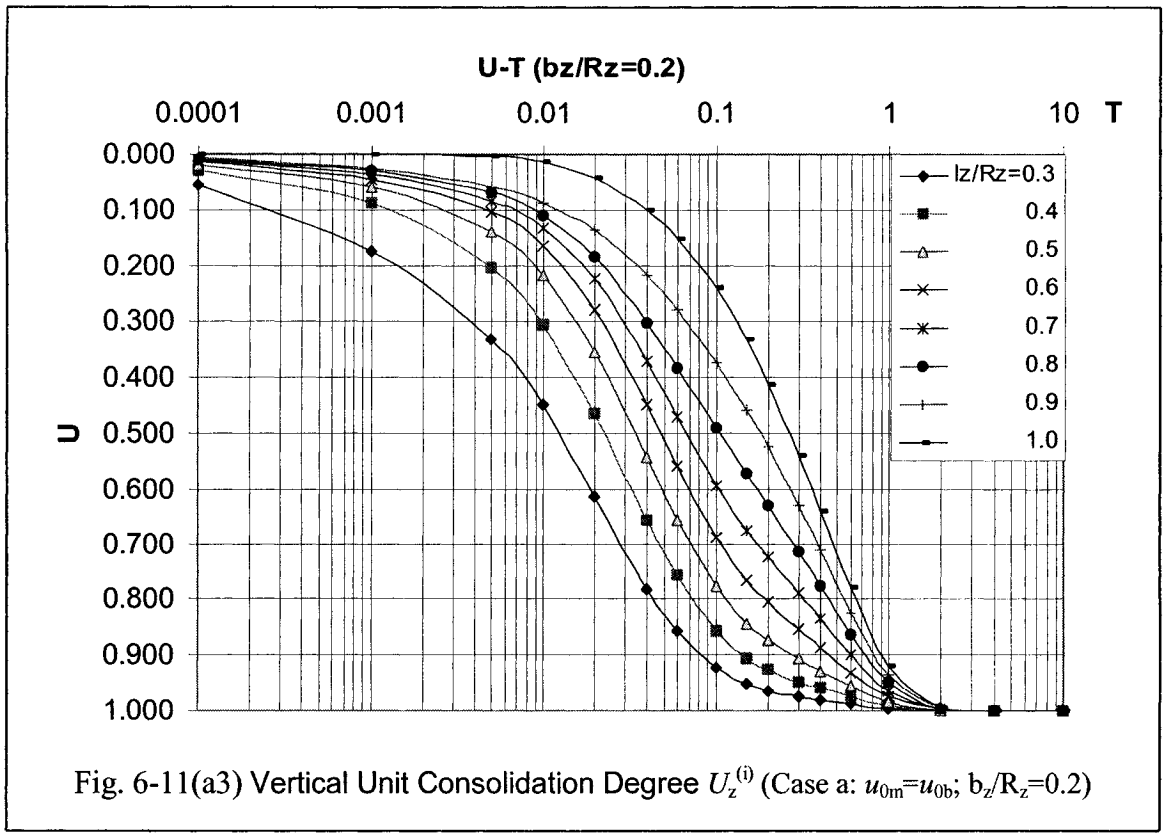

Fig. 6-11(a3) Vertical Unit Consolidation Degree $U_z^{(i)}$ (Case a: $u_{0m}=u_{0b}$; $b_z/R_z=0.2$)

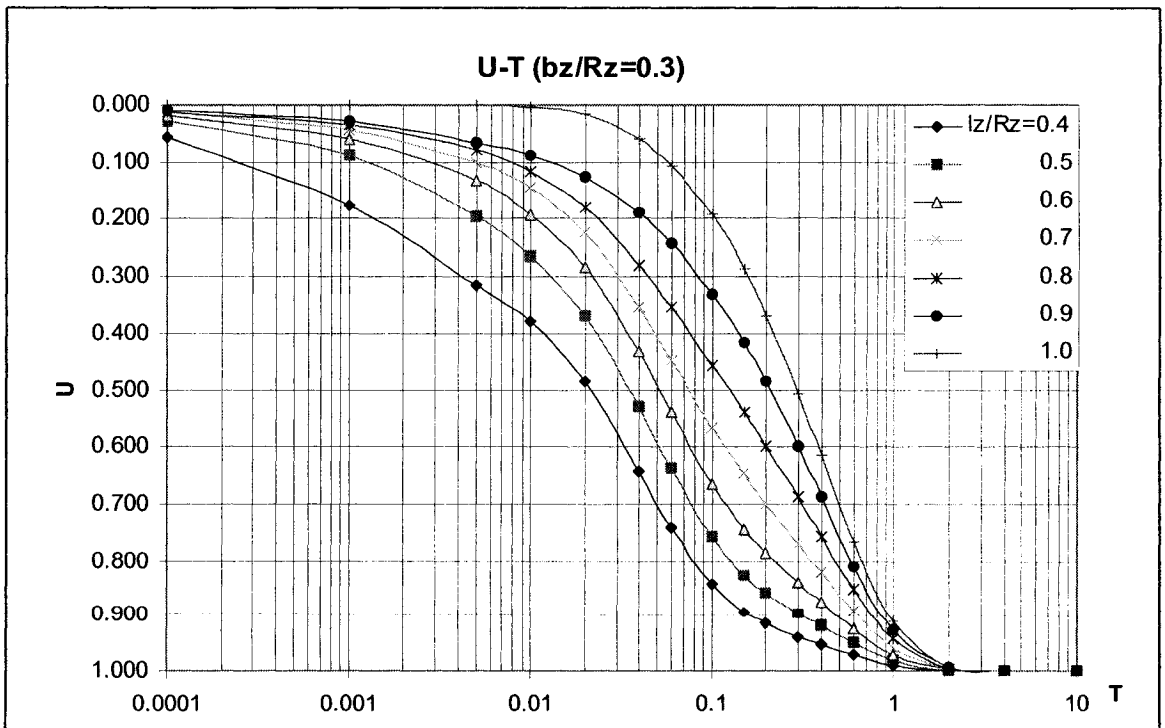

Fig. 6-11(a4) Vertical Unit Consolidation Degree $U_z^{(i)}$ (Case a: $u_{0m}=u_{0b}$; $b_z/R_z=0.3$)

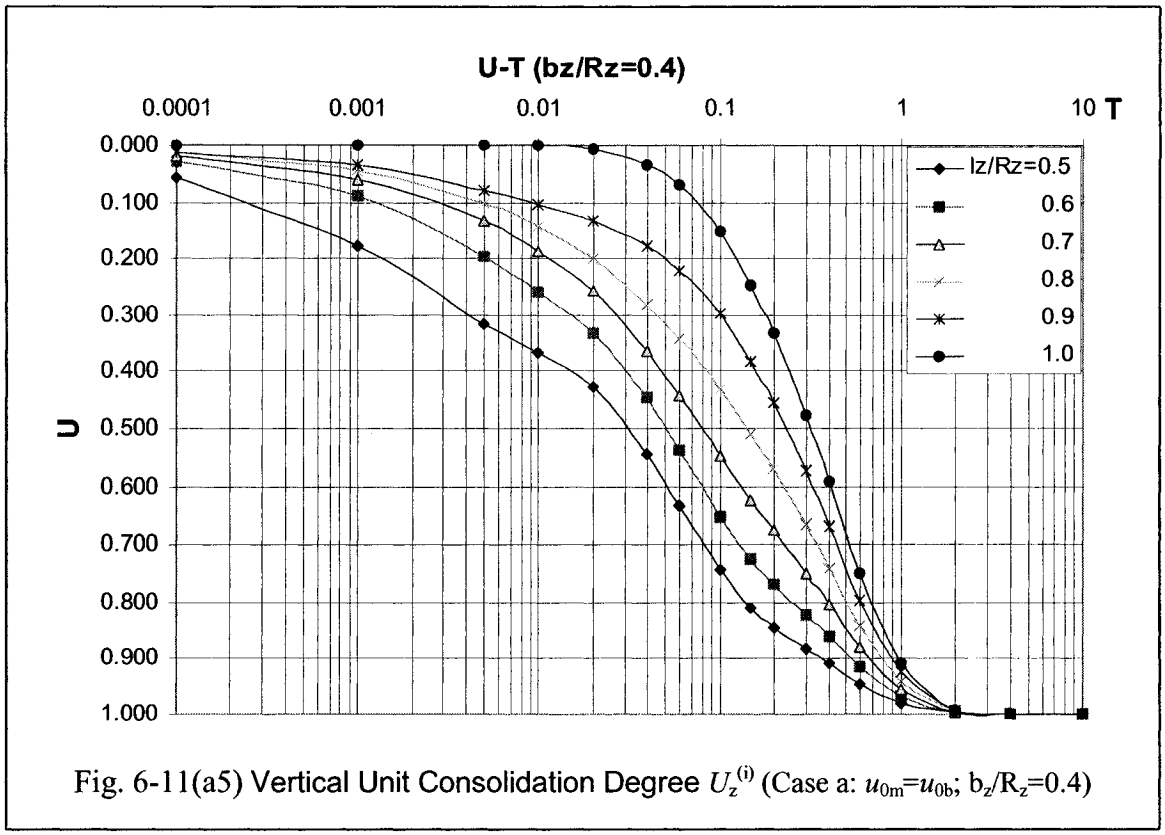

Fig. 6-11(a5) Vertical Unit Consolidation Degree $U_z^{(i)}$ (Case a: $u_{0m}=u_{0b}$; $b_z/R_z=0.4$)

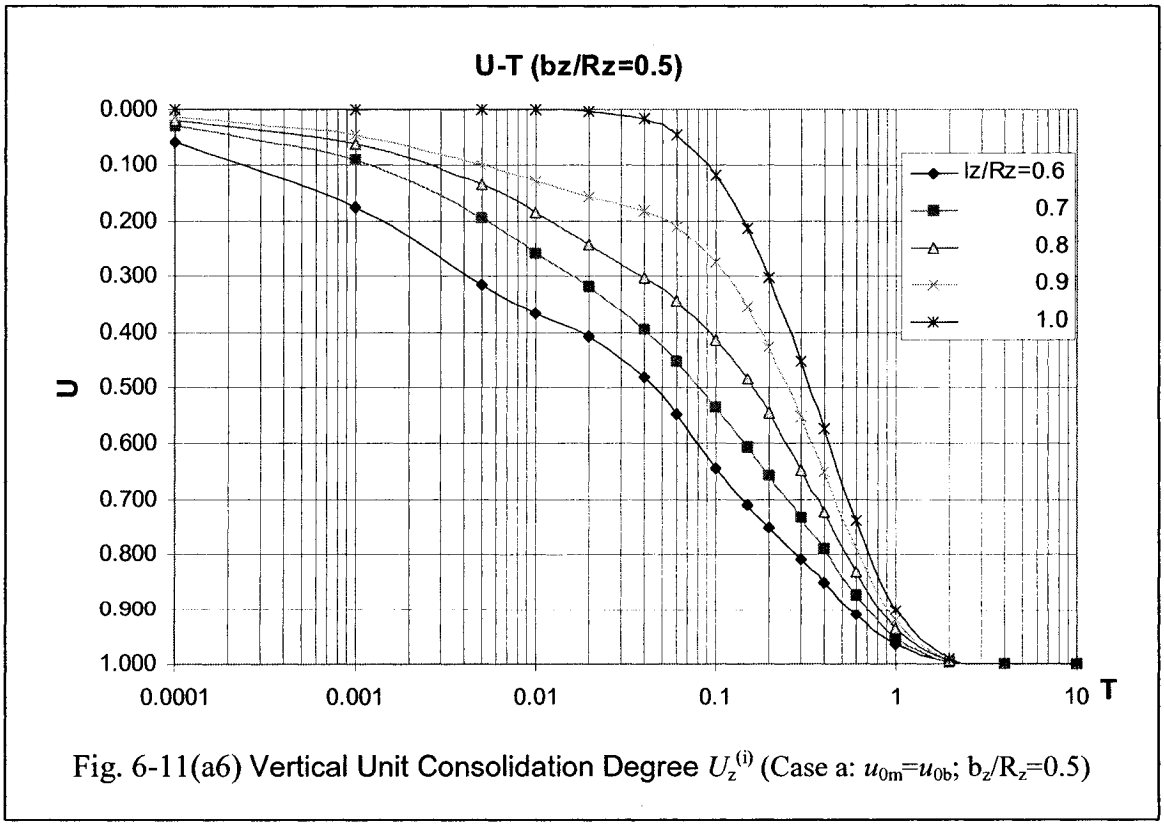

Fig. 6-11(a6) Vertical Unit Consolidation Degree $U_z^{(i)}$ (Case a: $u_{0m}=u_{0b}$; $b_z/R_z=0.5$)

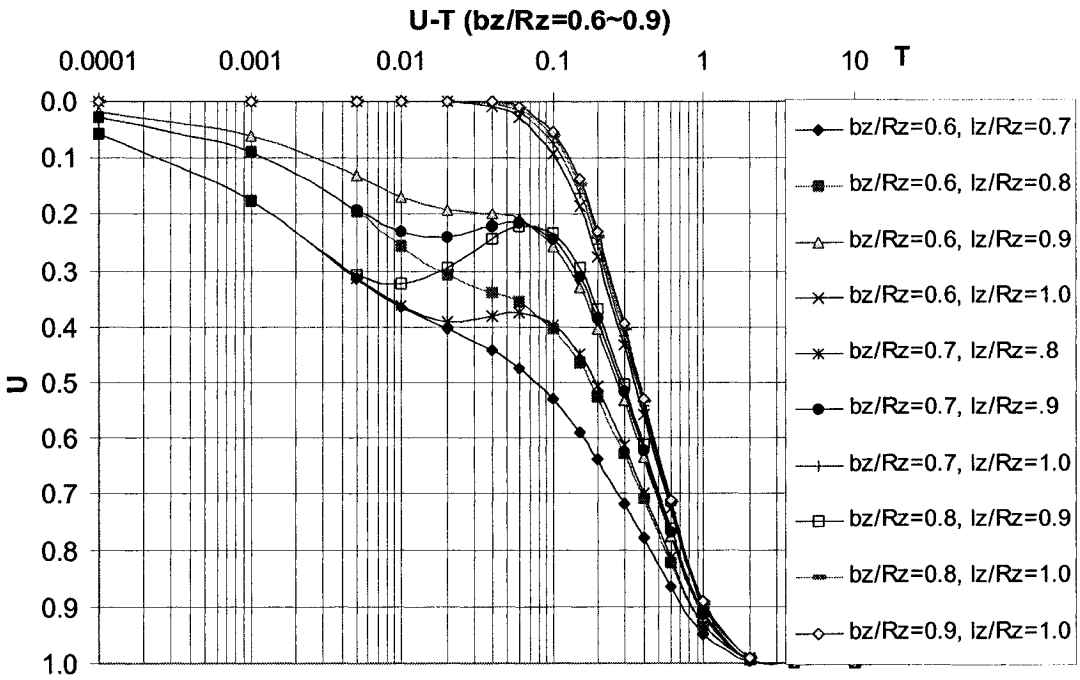

Fig. 6-11(a7) Vertical Unit Consolidation Degree $U_z^{(i)}$ (Case a: $u_{0m}=u_{0b}$; $b_z/R_z=0.6\sim0.9$)

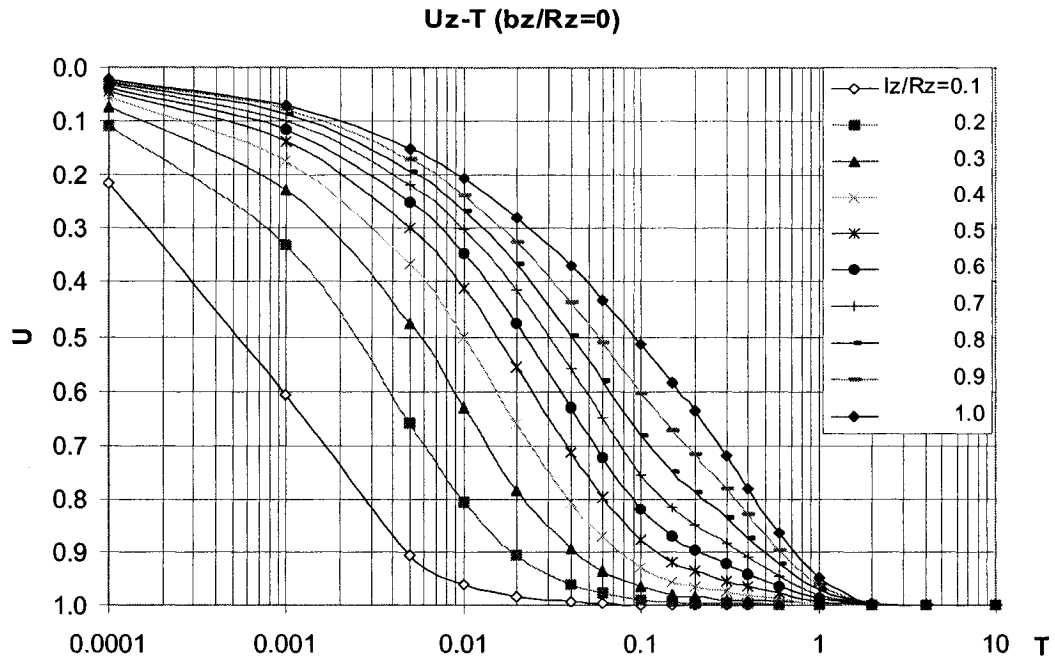

Fig. 6-11(b1) Vertical Unit Consolidation Degree $U_z^{(i)}$ (Case b: u_{0m}=0; b_z/R_z=0.0)

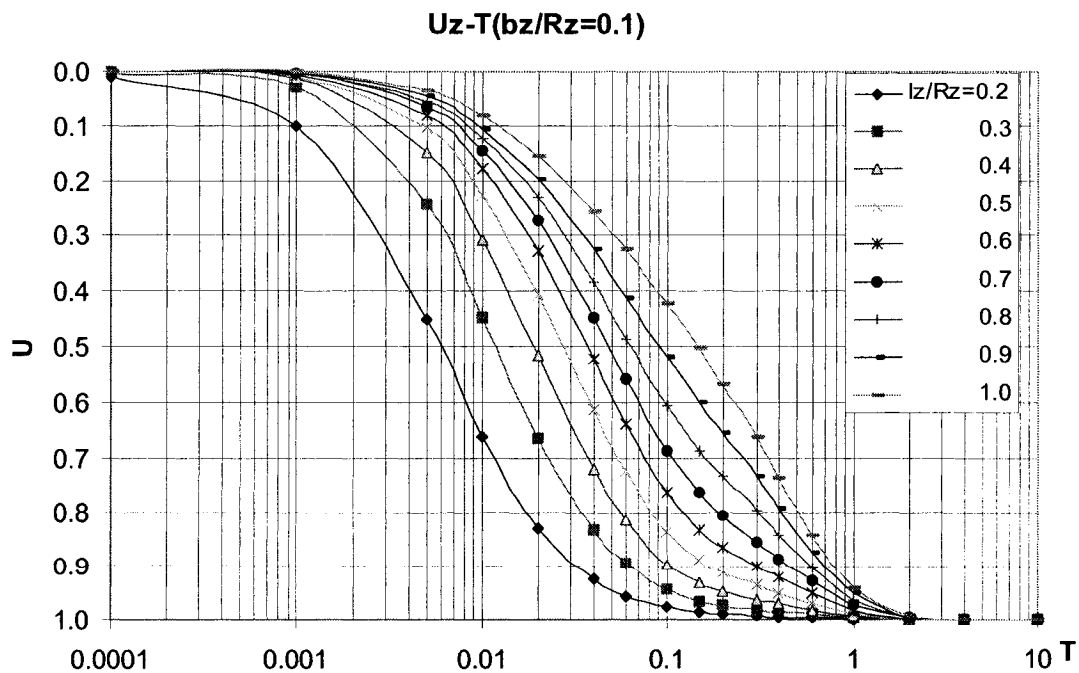

Fig. 6-11(b2) Vertical Unit Consolidation Degree $U_z^{(i)}$ (Case b: u_{0m}=0; b_z/R_z=0.1)

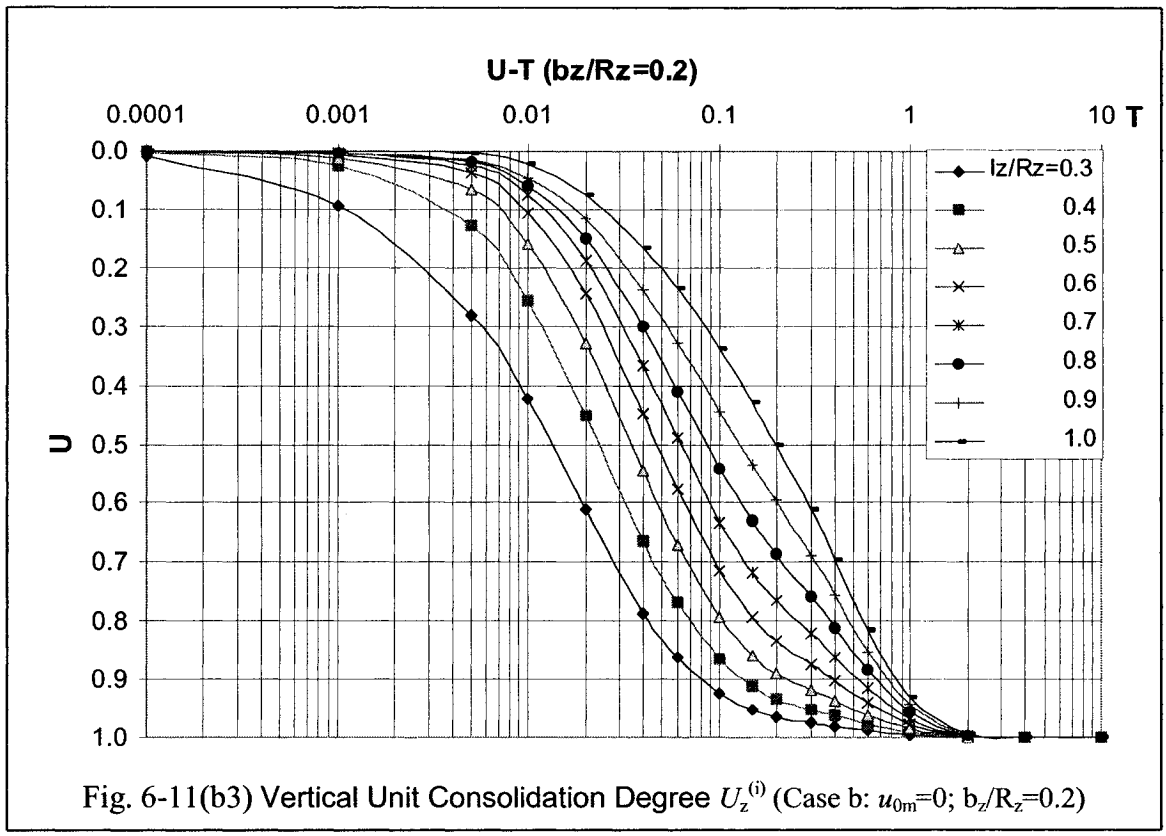

Fig. 6-11(b3) Vertical Unit Consolidation Degree $U_z^{(i)}$ (Case b: u_{0m}=0; b_z/R_z=0.2)

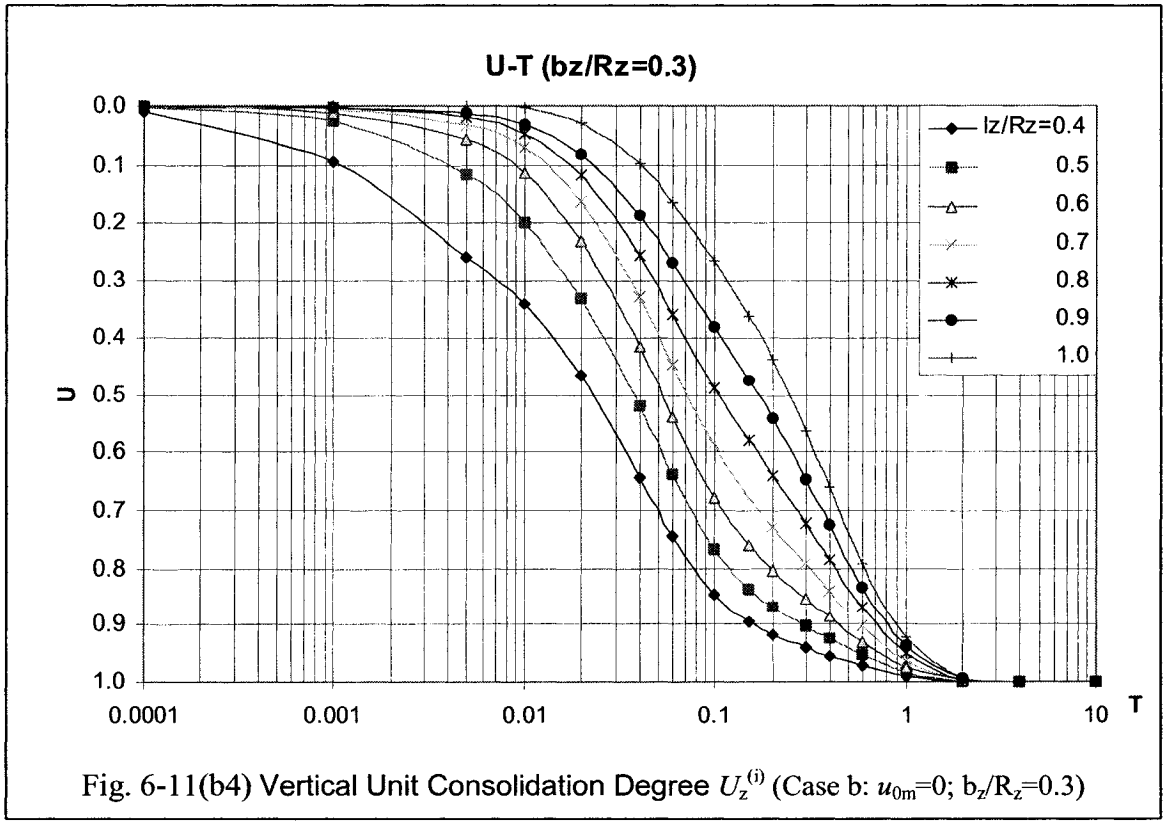

Fig. 6-11(b4) Vertical Unit Consolidation Degree $U_z^{(i)}$ (Case b: u_{0m}=0; b_z/R_z=0.3)

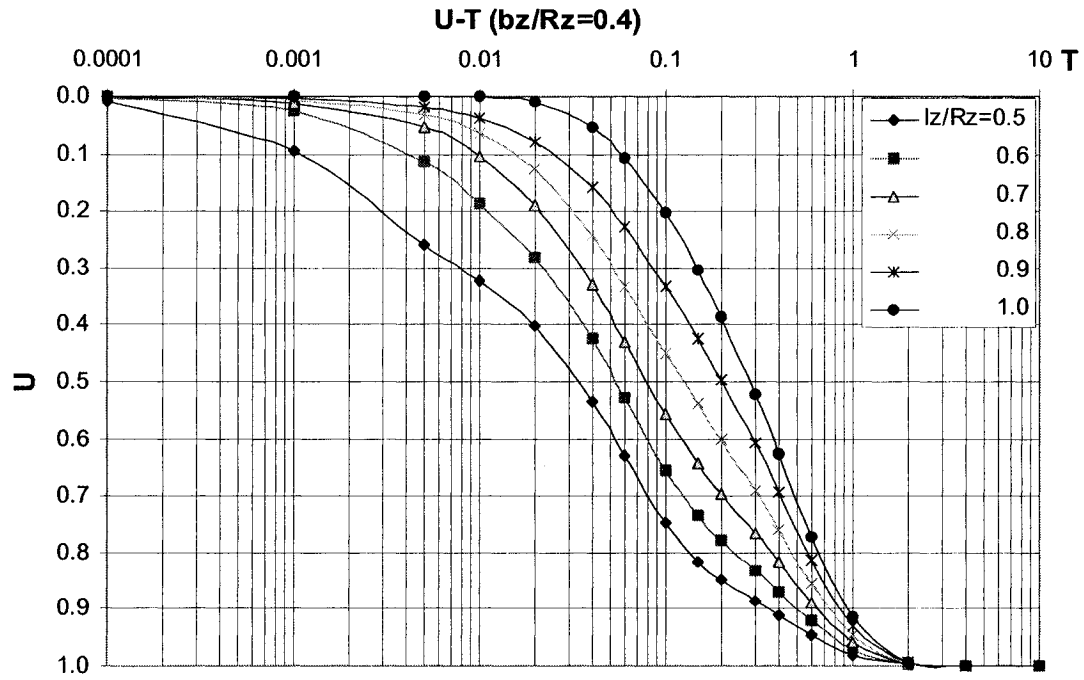

Fig. 6-11(b5) Vertical Unit Consolidation Degree $U_z^{(i)}$ (Case b: u_{0m}=0; b_z/R_z=0.4)

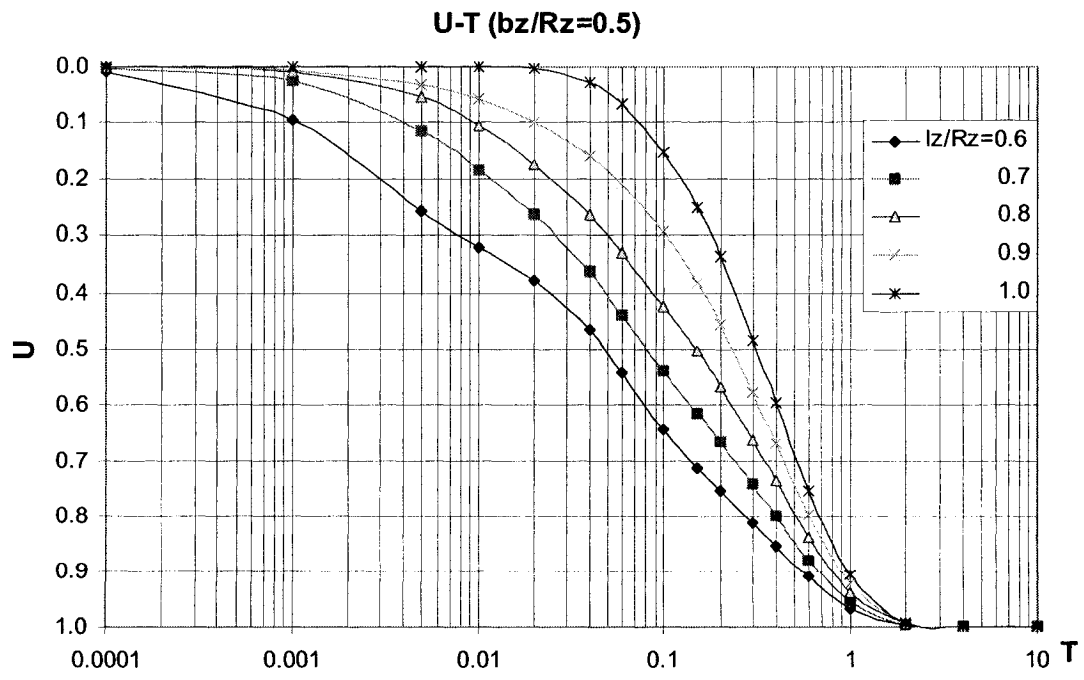

Fig. 6-11(b6) Vertical Unit Consolidation Degree $U_z^{(i)}$ (Case b: u_{0m}=0; b_z/R_z=0.5)

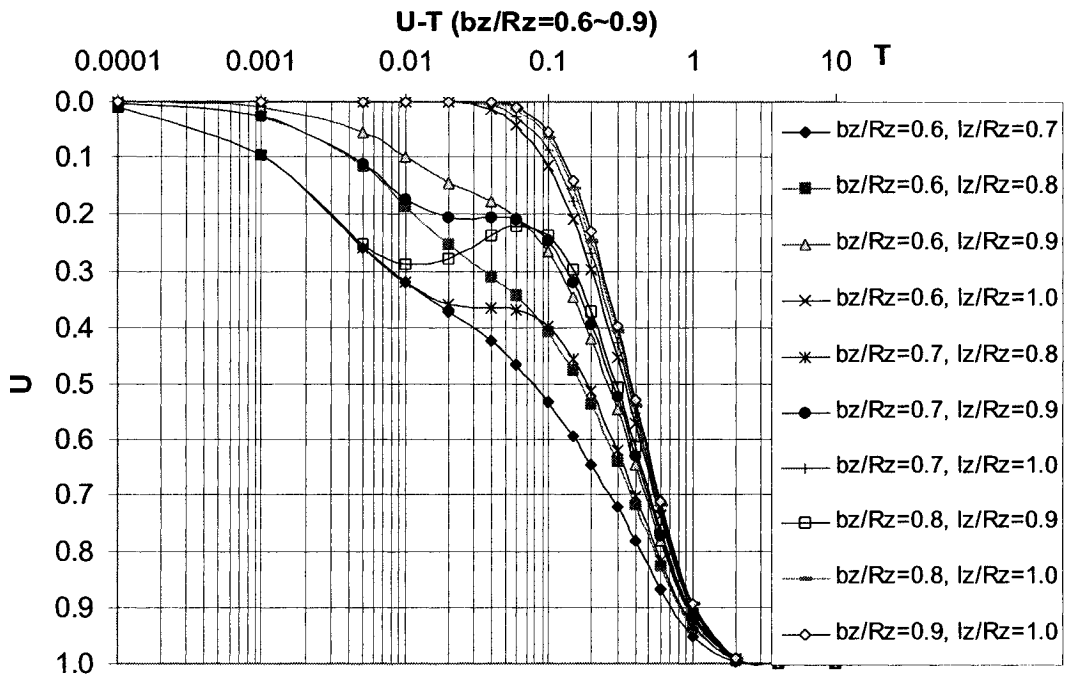

Fig. 6-11(b7) Vertical Unit Consolidation Degree $U_z^{(i)}$ (Case b: u_{0m}=0; b_z/R_z=0.6~0.9)

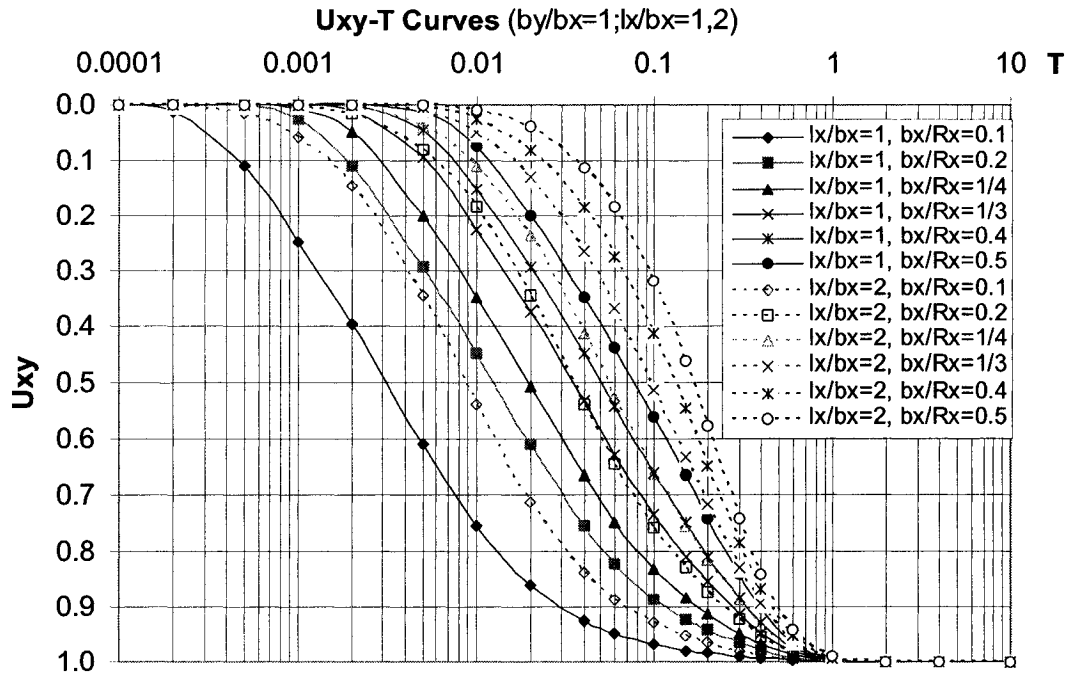

Fig.6-12(1a) Horizontal Consolidation Degree U_{xy} (Case: by/b_x=1, lx/bx=1,2)

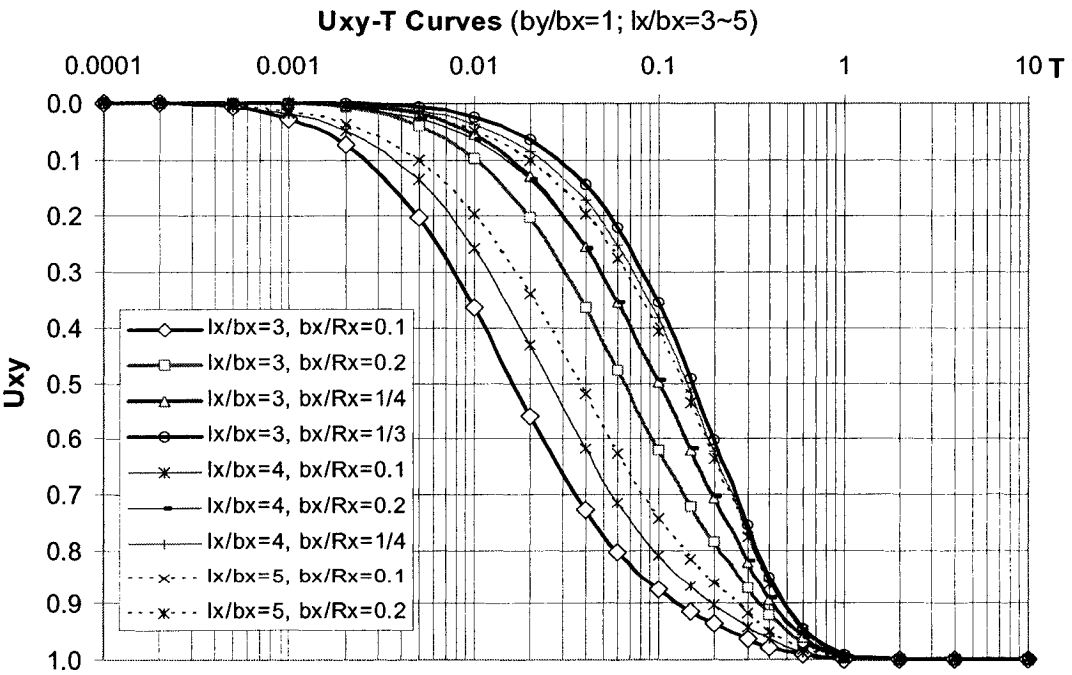

Fig. 6-12(1b) Horizontal Consolidation Degree U_{xy} (Case: by/b_x=1, l_x/b_x=3~5)

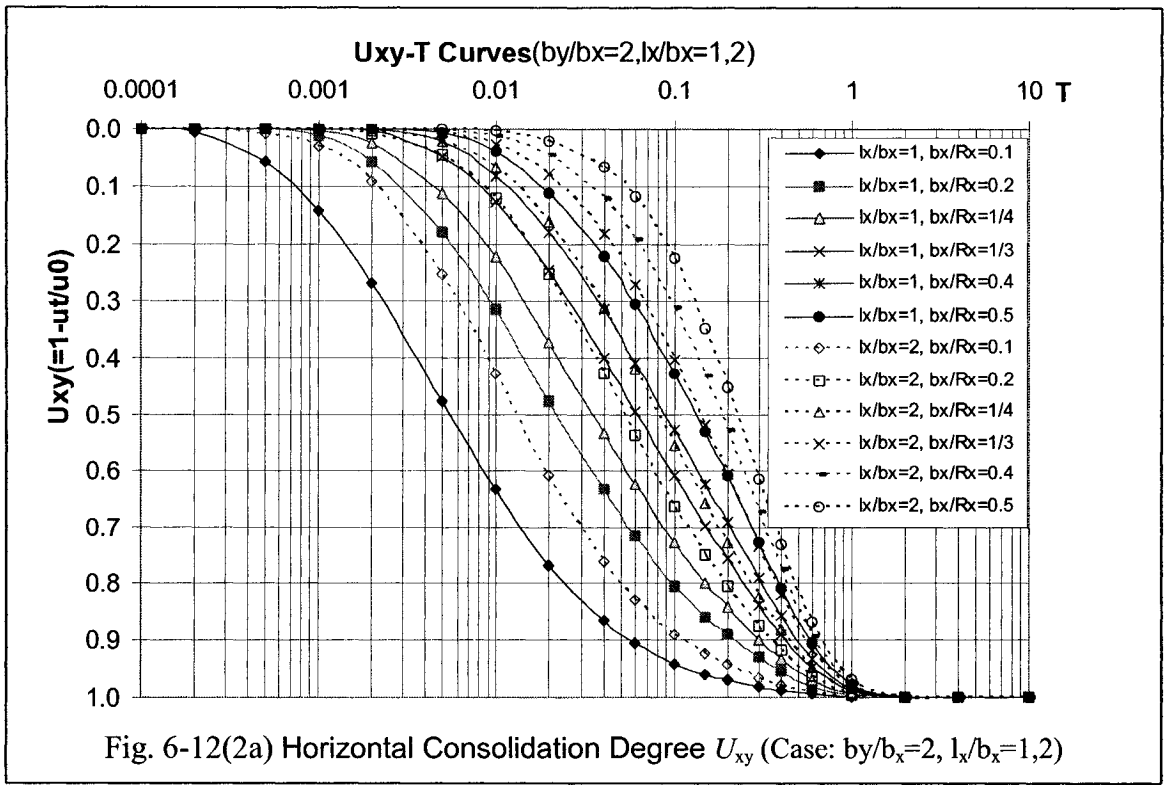

Fig. 6-12(2a) Horizontal Consolidation Degree U_{xy} (Case: by/b_x=2, l_x/b_x=1,2)

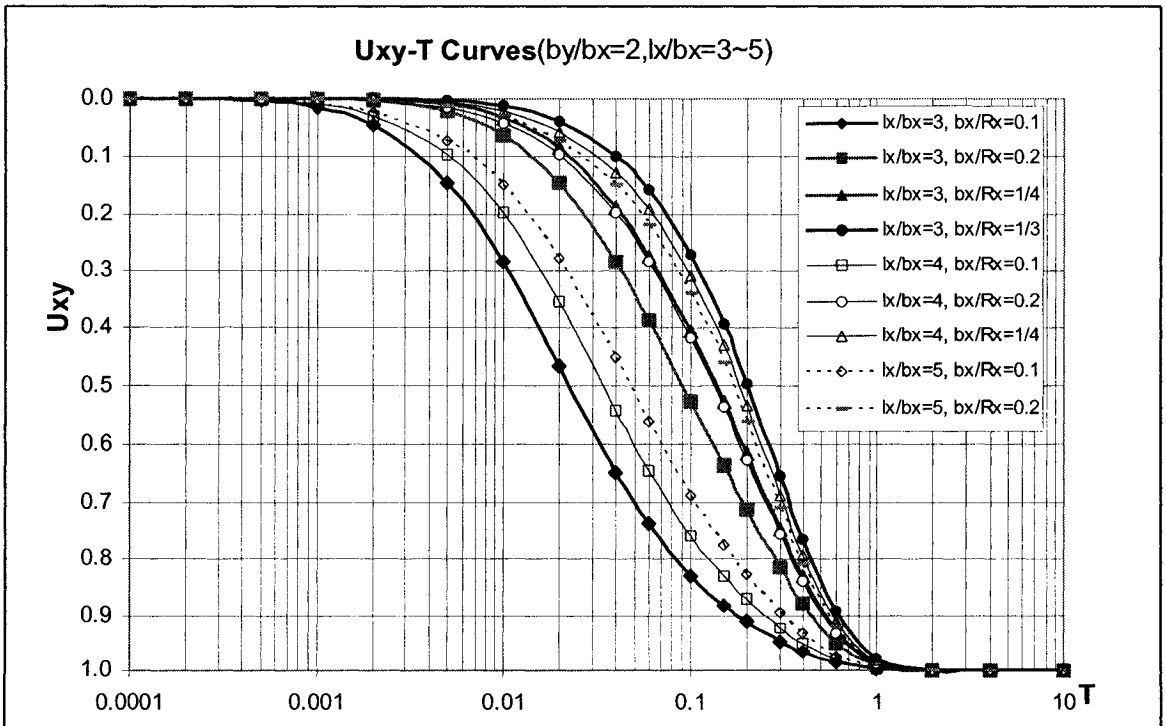

Fig. 6-12(2b) Horizontal Consolidation Degree U_{xy} (Case: : by/b_x=2, l_x/b_x=3~5)

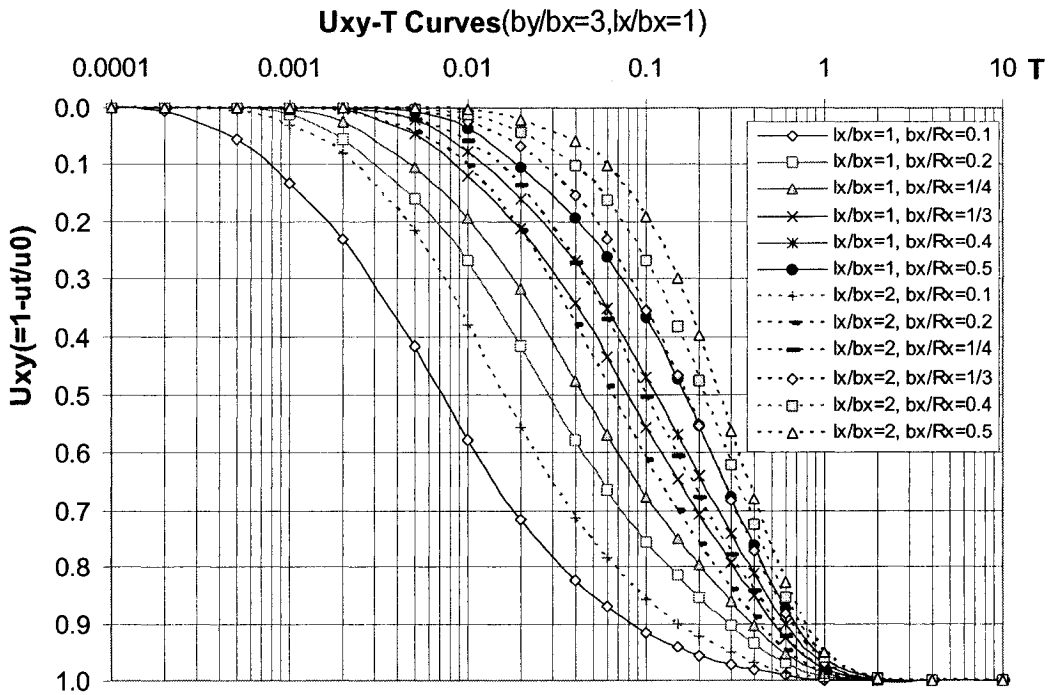

Fig. 6-12(3a) Horizontal Consolidation Degree U_{xy} (Case: by/b_x=3, l_x/b_x=1,2)

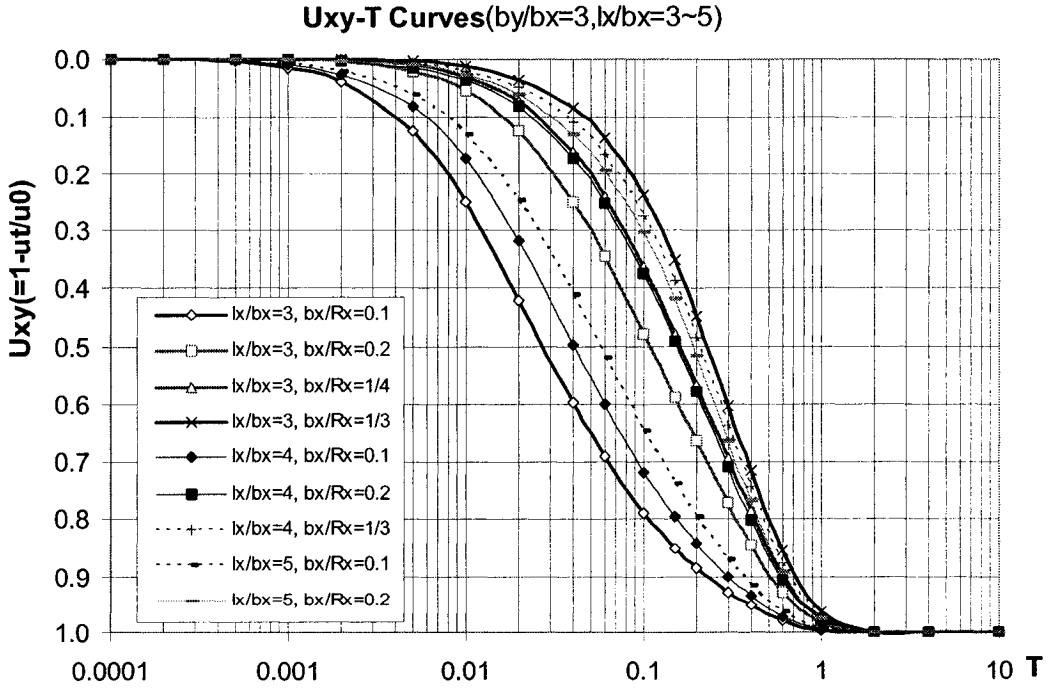

Fig. 6-12(3b) Horizontal Consolidation Degree U_{xy} (Case: by/b_x=3, l_x/b_x=3~5)

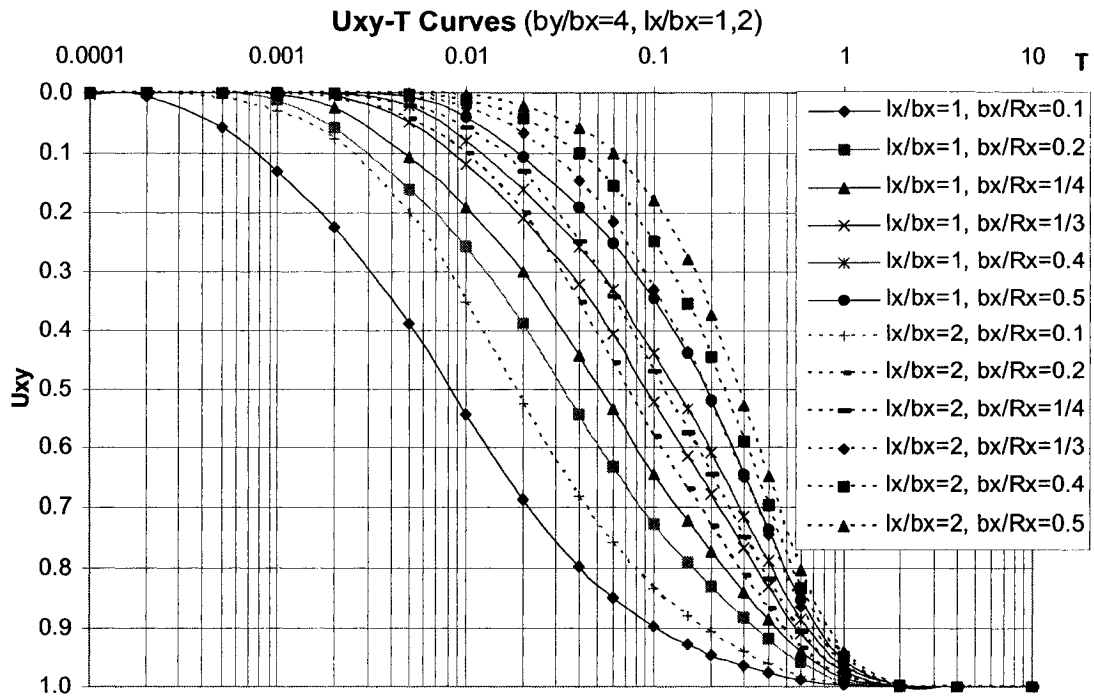

Fig. 6-12(4a) Horizontal Consolidation Degree U_{xy} (Case: by/b_x=4, l_x/b_x=1~2)

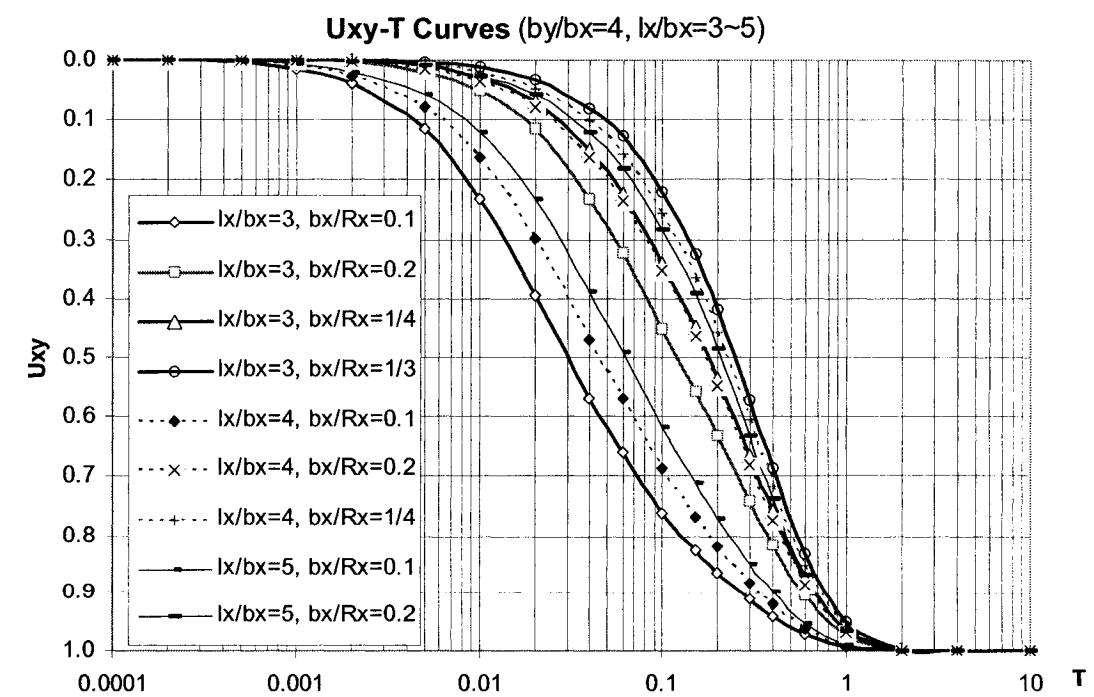

Fig. 6-12(4b) Horizontal Consolidation Degree U_{xy} (Case: by/b_x=4, l_x/b_x=3~5)

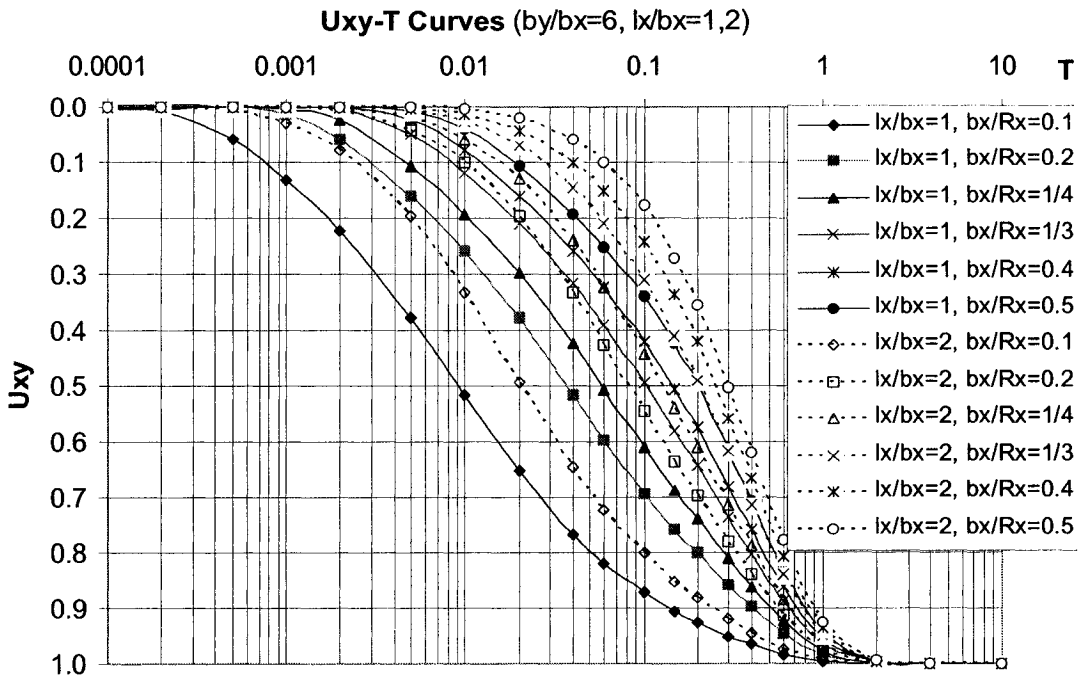

Fig. 6-12(5a) Horizontal Consolidation Degree U_{xy} (Case: b_y/b_x=6, l_x/b_x=1~2)

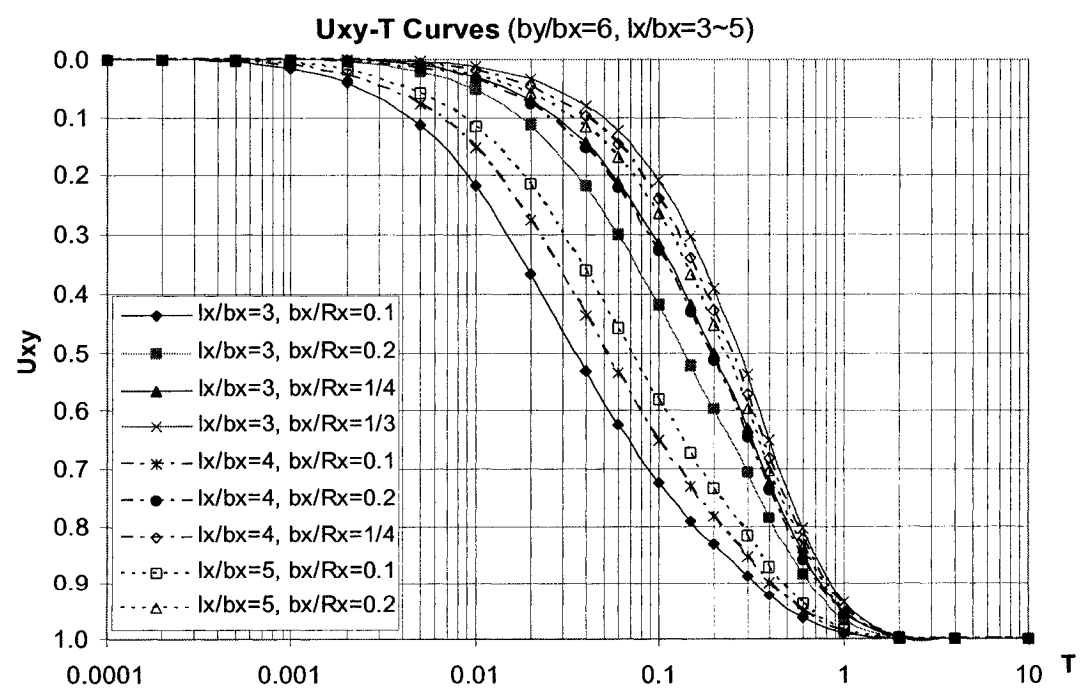

Fig. 6-12(5b) Horizontal Consolidation Degree U_{xy} (Case: b_y/b_x=6, l_x/b_x=3~5)

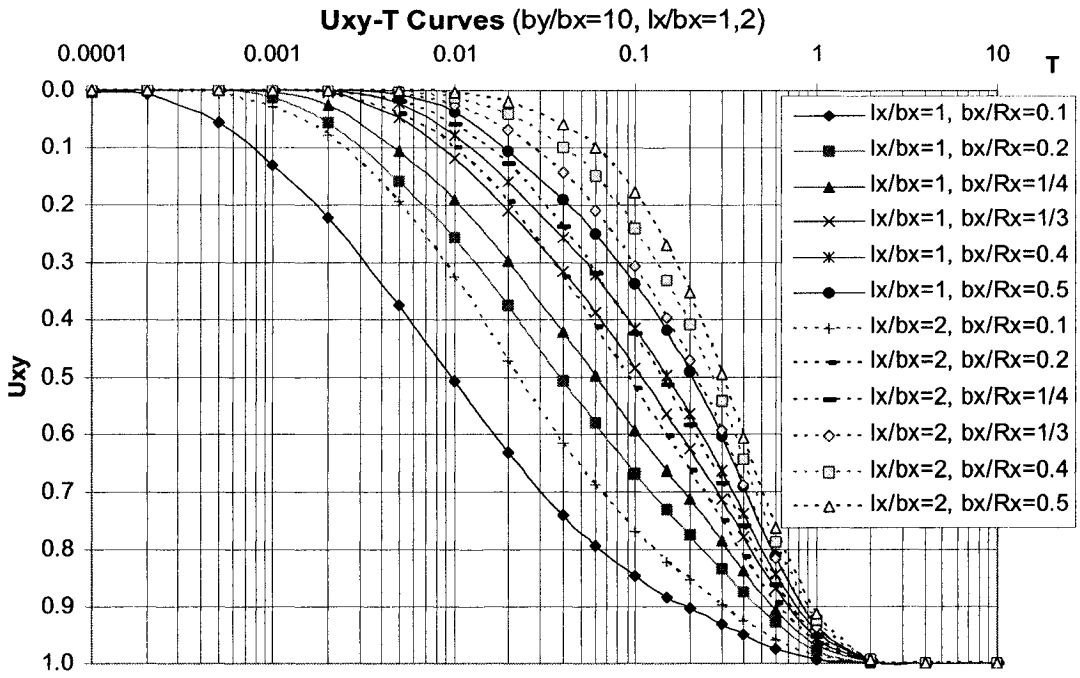

Fig. 6-12(6a) Horizontal Consolidation Degree U_{xy} (Case: b_y/b_x=10, l_x/b_x=1,2)

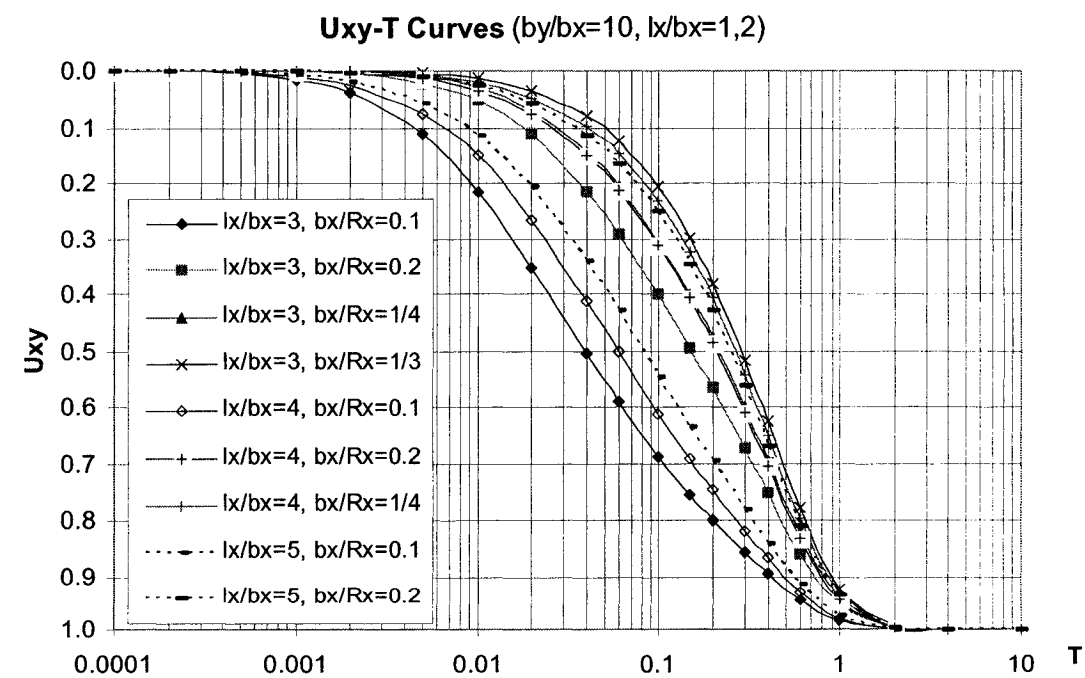

Fig. 6-12(6b) Horizontal Consolidation Degree U_{xy} (Case: b_y/b_x=10, l_x/b_x=3~5)

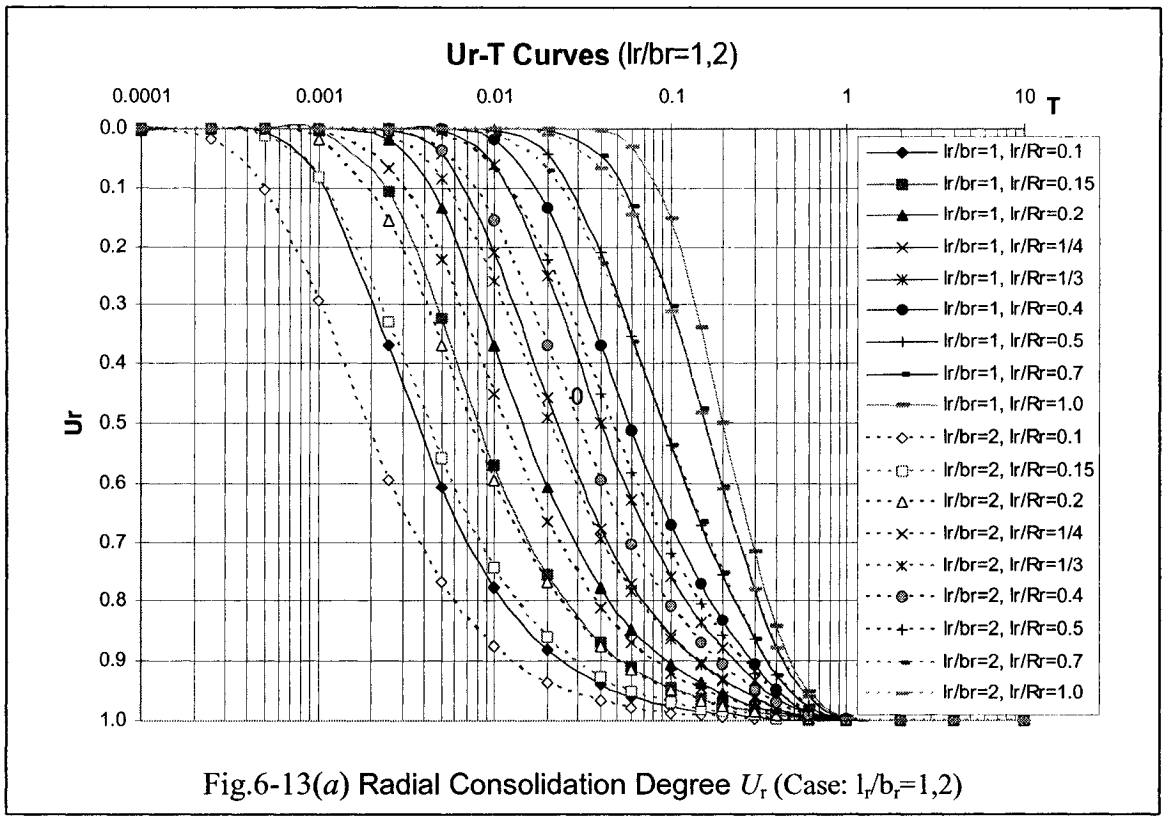

Fig.6-13(*a*) Radial Consolidation Degree U_r (Case: l_r/b_r=1,2)

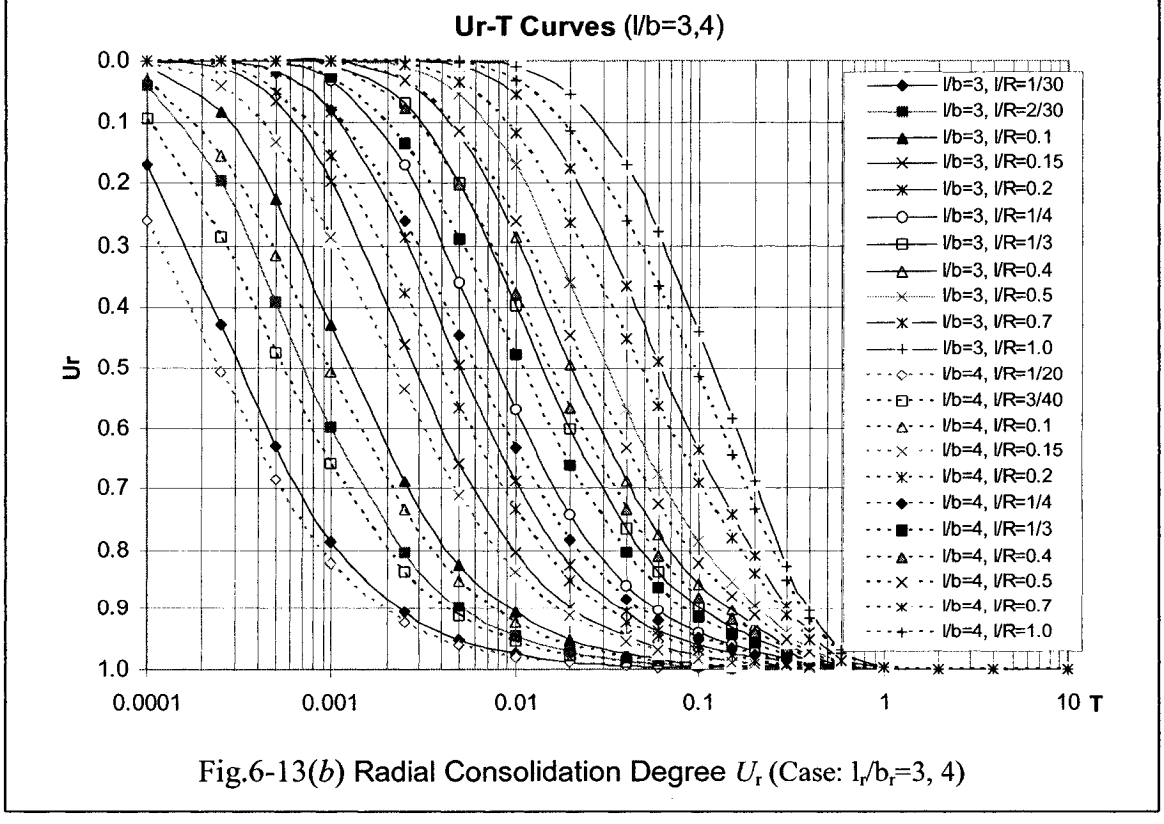

Fig.6-13(*b*) Radial Consolidation Degree U_r (Case: l_r/b_r=3, 4)

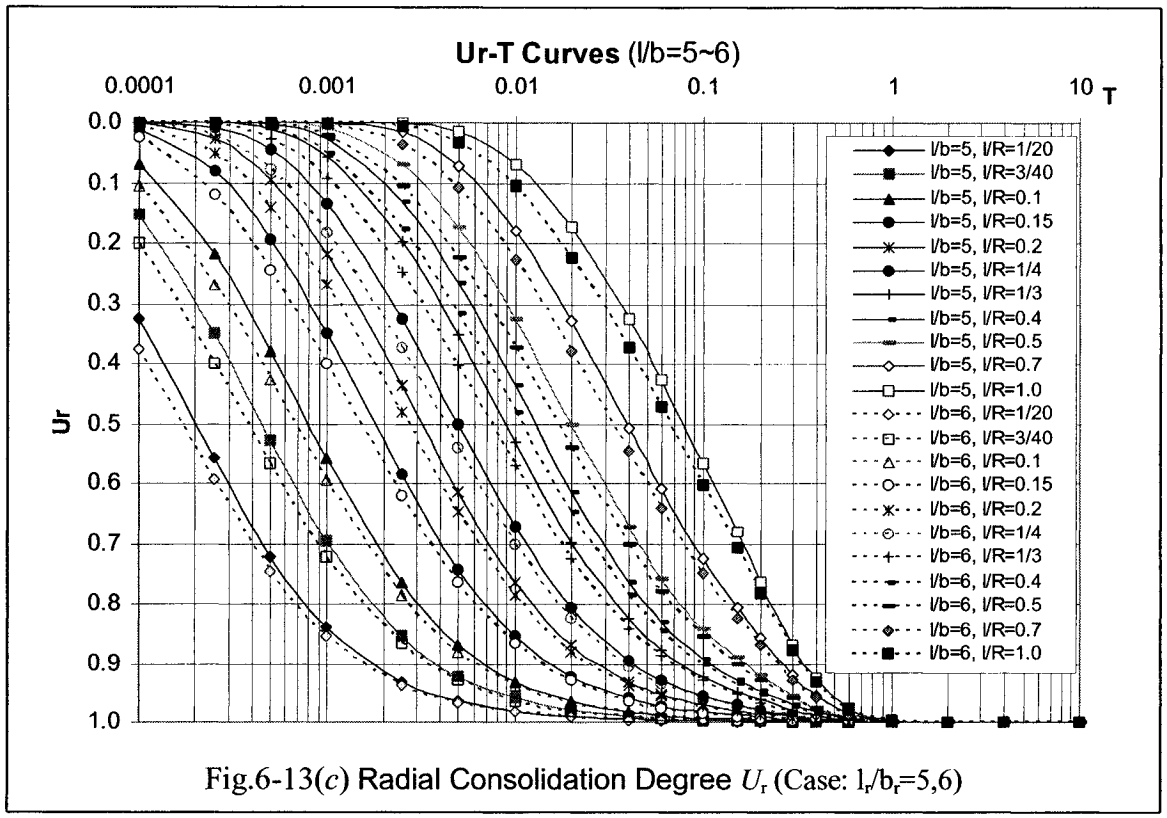

Fig.6-13(*c*) Radial Consolidation Degree U_r (Case: l_r/b_r=5,6)

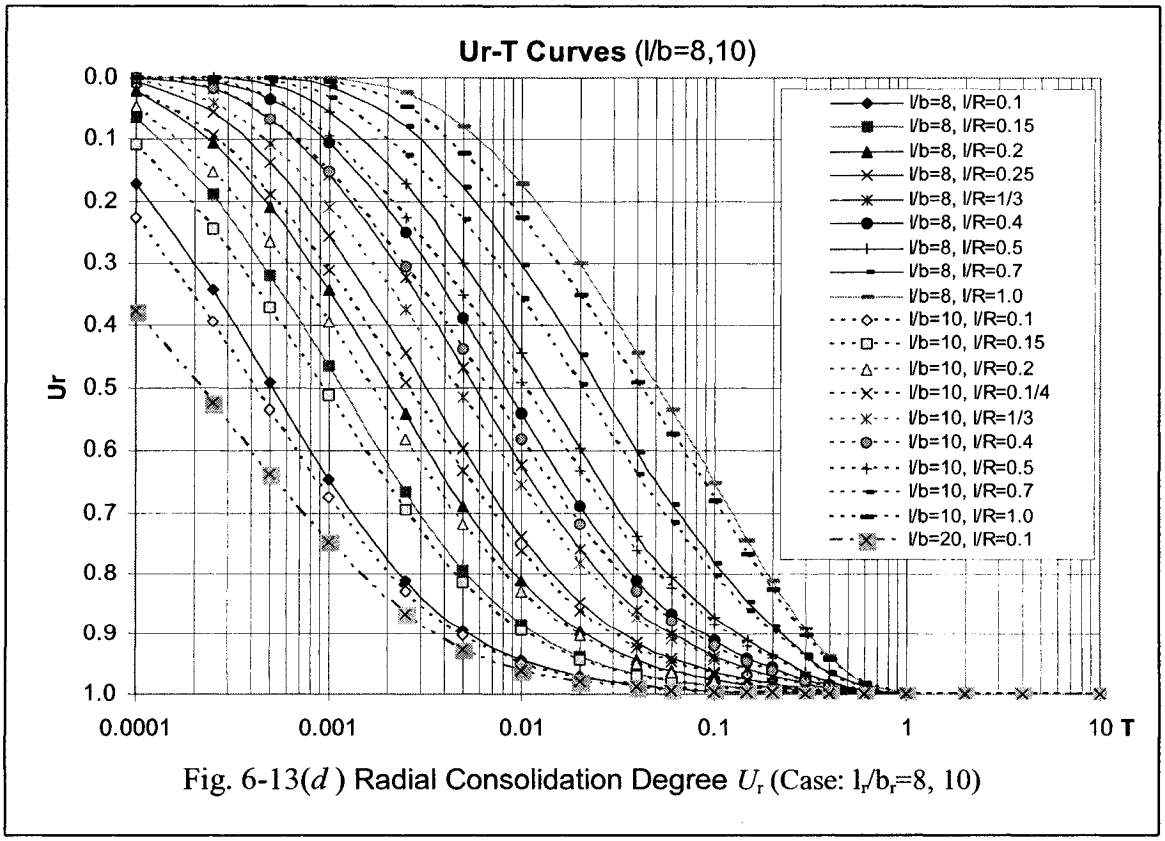

Fig. 6-13(*d*) Radial Consolidation Degree U_r (Case: l_r/b_r=8, 10)

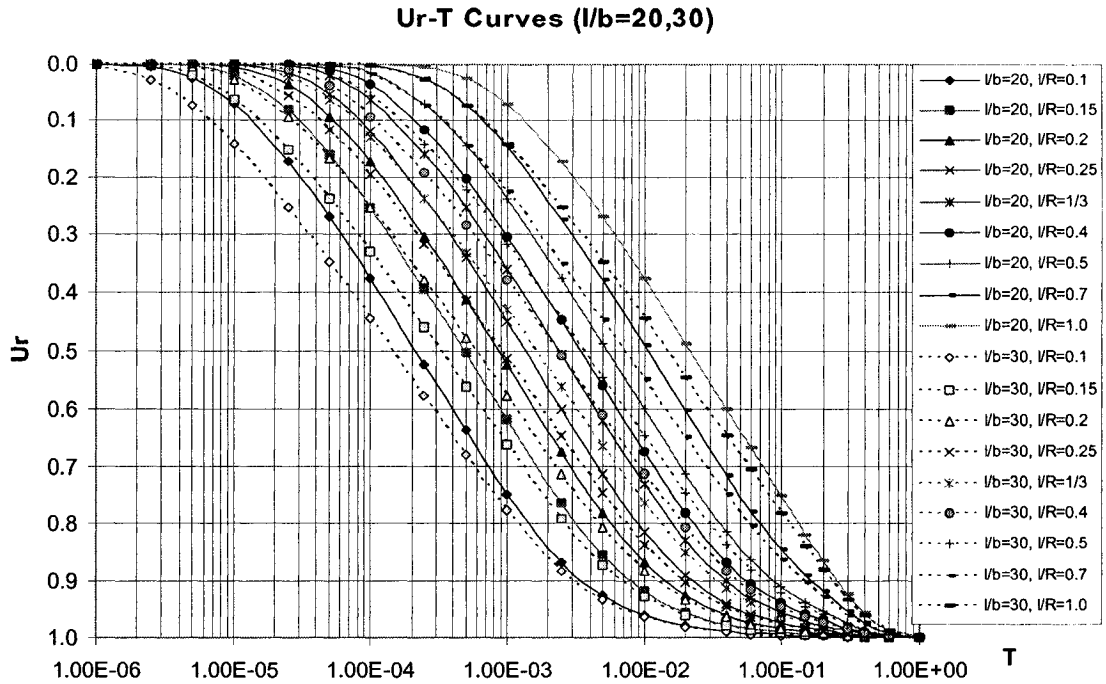

Fig.6-13(e) Radial Consolidation Degree U_r (Case: l_r/b_r=20,30)

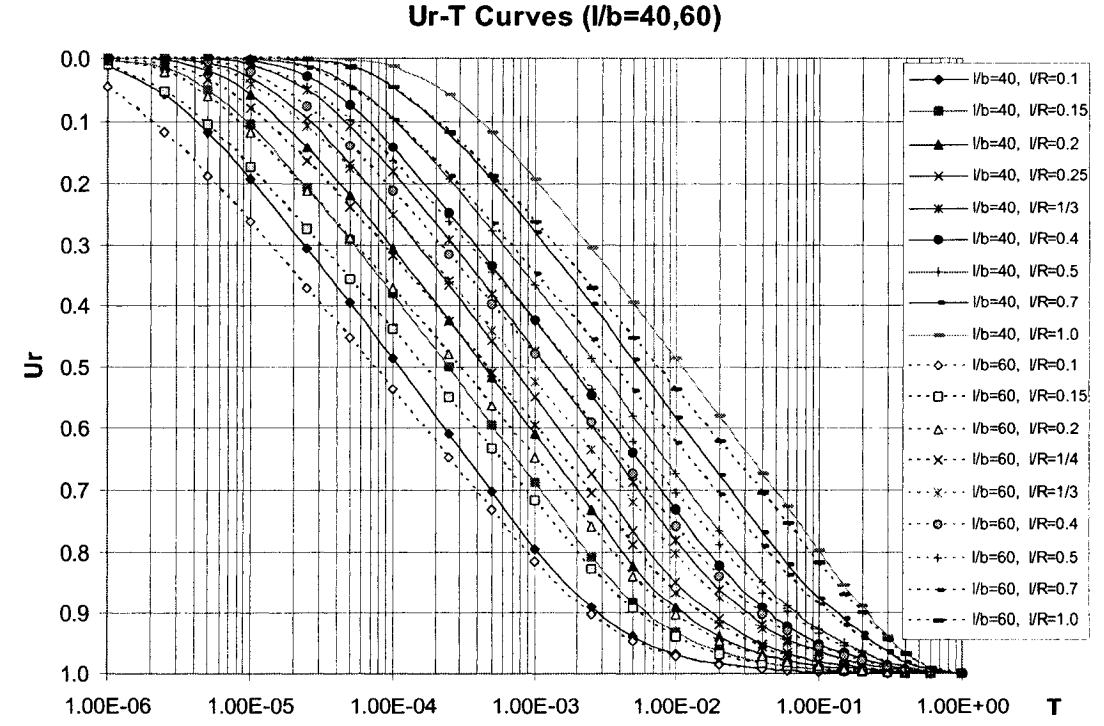

Fig. 6-13(f) Radial Consolidation Degree U_r (Case: l_r/b_r=40, 60)

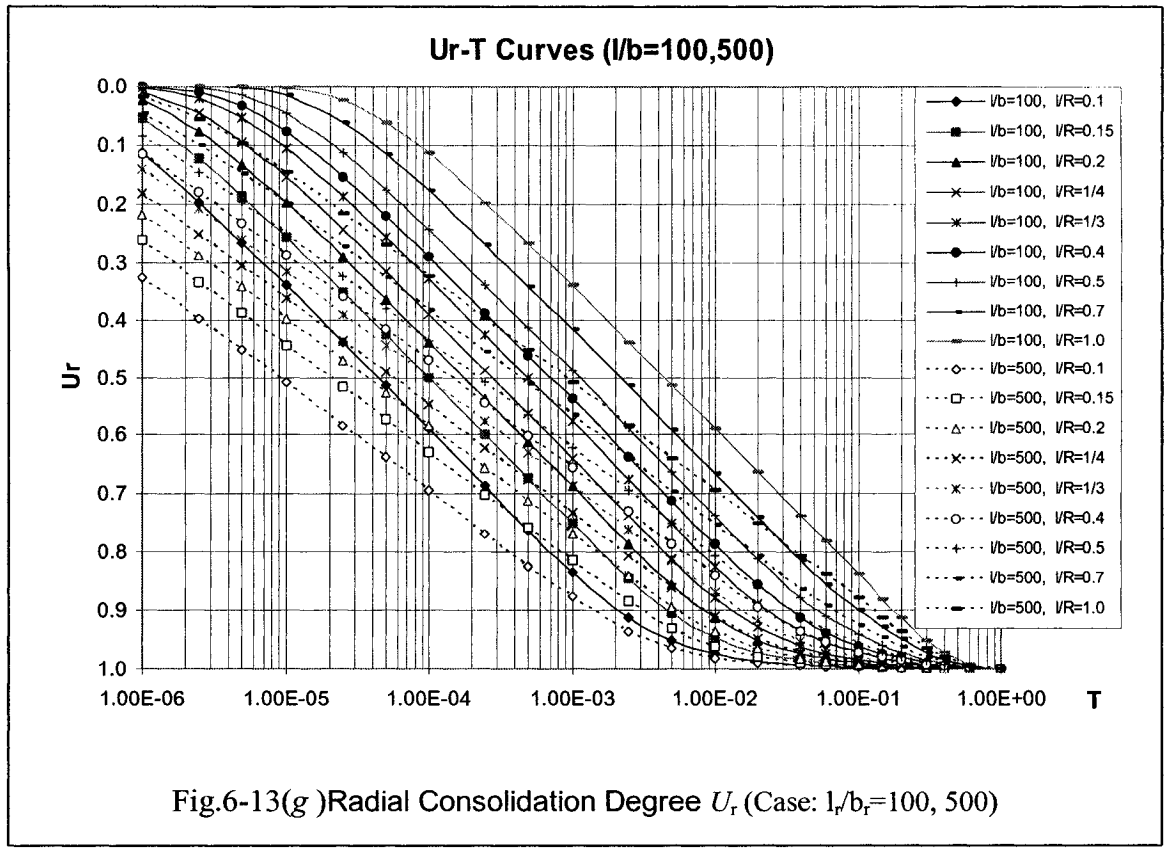

Fig.6-13(g)Radial Consolidation Degree U_r (Case: l_r/b_r=100, 500)

From Figs. 6-13(1) ~ Fig. 6-13(7), one finds that almost all of curves at the same l/b value are parallel to each other when l/b ≥ 6.

Setting $C_{30\text{-}70}$,

$$C_{30\text{-}70}=\left.\frac{\Delta U}{\Delta Log(T)}\right|_{U=30}^{70}=\frac{U_{70}-U_{30}}{Log(T_{70})-Log(T_{30})}=\frac{U_{70}-U_{30}}{Log\left(\frac{C_h t_{70}}{R^2}\right)-Log\left(\frac{C_h t_{30}}{R^2}\right)}$$

$$=\frac{U_{70}-U_{30}}{Log(t_{70})-Log(t_{30})}=\frac{\Delta U}{\Delta Log(t)} \qquad (6\text{-}35)$$

One obtains the $C_{30\text{-}70}[\Delta U/\Delta(logT)]$ ~ l/b relationship from Fig. 6-14.

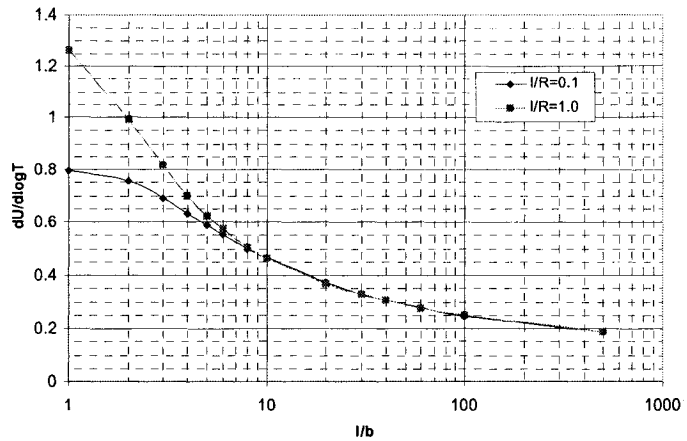

Fig. 6-14 Curves of $\Delta U/\Delta(log\mathrm{T})$ - l/b Relationship

6.4 Discussions

Shear stress caused by a piles' load does not generate additional EPWP in soil nor any additional lateral pressure of pile, because the changes of pore ratio, the EPWP of soil and the lateral pressure of the pile have all been completed during pile driving.

A raft's increasing action on the UBC of a pile due to an increment of the effective lateral pressure of pile does not work at the beginning of moment loading on a raft. For a step-loading situation, the raft's increasing action goes into effect only after completing some degree of consolidation under former step loads.

The variations of the normal stress on a pile's shaft $\Delta\sigma_h$' is not simply equal to the change of pore pressure Δu because of the horizontal shrinking displacement of soil around piles with EPWP dissipation. The relationship between $\Delta\sigma_h$' and Δu is determined approximately by equation (6-15).

A combination of pore-pressure contribution areas in the general situation can be used to estimate the 1-D vertical consolidation degree U_z as per equation (6-31,31) and according to Figs. 6-9 and 6-10.

The increasing process of piles' ultimate bearing capacity is estimated and described by Equation (6-21), which is simple and practical.

CHAPTER 7

SETTLEMENT DURING THE INTERACTION

7.1 General

The settlements in the pile-soil-raft interaction involve consolidation settlements, that are caused by the dissipation of EPWP from pile driving and from the pressure of the raft bottom, and the immediate settlements caused by raft pressure and by pile load. One of these settlement components is the consolidation settlement caused by the dissipation of EPWP from raft pressure, which interferes in the consolidation degree of raft pressure, the enhancement of the friction strength of the pile shaft and the bearing capacity of the pile base, due to the increase of effective normal stress caused by the load applied on the soil under the cap and around piles.

7.2 Changing Process of Settlements in the Interaction

Soil settlements can be divided into immediate settlements S_d and consolidation settlements S_c caused by the dissipation of EPWP

$$S = S_d + S_c \qquad (7\text{-}1)$$

Thus, settlement at a time t can be expressed by

$$S_t = S_d + S_{ct}(t) \qquad (7\text{-}2)$$

in (7-1) and (7-2), $S_{ct}(t)$ = consolidation settlement at some time, $S_c = S_{ct}(\infty)$.

(a) Immediate Settlement

Soil immediate settlement can be estimated by means of an equation for evaluating the average settlement of flexible foundation on saturated clay soils with Poisson's ratio μ_s = 0.5 under the raft-bottom pressure on the soil, in which the undrained deformation modulus E_{su} is used. Taking a symbol for the settlement of the raft-bottom pressure, S_{dr}, because shear stress caused by a pile's load does not generate additional EPWP in the soil and the load of a pile's base is a small proportion of the total load, the settlement caused by loads applied on piles tends to stabilize generally only after several hours or 1-2 days. Thus, the settlement caused by a pile's load also can be treated as immediate settlement. Another symbol is used for the settlement from load of piles, S_{dp}

$$S_d = S_{dr} + \alpha_{rp} \cdot S_{dp} \qquad (7\text{-}3)$$

(b) Consolidation Settlement

The settlement caused by a pile's load is treated as immediate settlement. Therefore, the consolidation settlements considered in the piles-soil-raft interaction are two fold: one is the settlement caused by remnant EPWP of driving, S_{cp}; the other is the settlement caused by the pressure acting on the soil under the raft bottom, S_{cr}. Thus,

$$S_c = S_{cr} + S_{cp} \qquad (7\text{-}4)$$

Moreover, one should notice that the settlement from remnant EPWP, S_{cp}, can be estimated by using swell index C_s, or unload-reload elastic modulus E_{ur}; and the settlement from raft-bottom pressure, S_{cr}, can be calculated by using compression index C_c, or E_{sc}, the deformation modulus of additional loads that is greater than a soil's in-situ effective overburden stress σ_{v0}'. According to Das (1999), the ratio of C_s/C_c is of about

1/25 to 1/3; the typical range of C_s/C_c is of about 1/10 to 1/5. Thus, one can assume that the ratio of E_{ur}/ E_{sc} is also about 5 to 10.

Substituting (7-3) and (7-4) into (7-1),

$$S = S_{dr} + \alpha_{rp} \cdot S_{dp} + S_{cr} + S_{cp}$$

$$= (S_{dr}+S_{cr}) + (\alpha_{rp} \cdot S_{dp}+ S_{cp})$$

$$= S_{rr} + S_{rp} \qquad (7\text{-}5)$$

Where $S_{rr} = S_{dr} + S_{cr}$, (7-6)

$$S_{rp} = \alpha_{rp} \cdot S_{dp}+ S_{cp} \qquad (7\text{-}7)$$

(c) Settlement at a Given Time

Similar to Equation (7-4), the consolidation settlement at some time can be expressed as

$$S_{ct}(t) = S_{crt}(t) + S_{cpt}(t)$$

$$= S_{cr}U_{cr}(t) +S_{cp}U_{cp}(t) \qquad (7\text{-}8)$$

where $S_{crt}(t)$ and $U_{cr}(t)$ are the consolidated settlement and the consolidation degree at a given time respectively, due to the dissipation of EPWP from the pressure at the bottom of the raft, and $S_{cpt}(t)$ and $U_{cp}(t)$ are respectively the consolidation settlement and the consolidation degree at a given time due to pile driving.

Thus, total settlement at some time S_t obtained from equations (7-2, 7-3 and 7-7) is

$$S_t = S_d+S_{ct}(t) = S_{dr}+\alpha_{rp} \cdot S_{dp}+ S_{cr}U_{cr}(t) +S_{cp}U_{cp}(t)$$

$$= [S_{dr} + S_{cr}U_{cr}(t)] +[\alpha_{rp} \cdot S_{dp} +S_{cp}U_{cp}(t)]$$

$$= S_{rrt}(t)+S_{rpt}\ (t) \qquad (7\text{-}9)$$

in which $S_{rrt}(t) = S_{dr}+S_{cr}U_{cr}(t)$, (7-10)

$$S_{rpt}(t)=\alpha_{rp}\cdot S_{dp}+S_{cp}U_{cp}(t) \qquad (7\text{-}11)$$

7.3 Simplified Methods of Analysis of Settlement at a Given Time

The methods to calculate settlement presented in Chapters 2 and 3 do not interfere with soil consolidation. Although Randolph's method (1994) is a very convenient approximate equation for the stiffness of a piled raft system and the load-sharing between the piles and the raft, the method is reasonable only for the elastic state of a pile-soil system but not for the plastic state. Here the development of approximate re-setup equations for the stiffness of a piled raft system considering soil consolidation and pile-soil nonlinear deformation is needed.

According to Randolph and Clancy (1993), under incremental loads of pile group and raft ΔQ_p and ΔQ_r, the settlement increment of pile group and raft ΔW_p and ΔW_r are:

$$\left.\begin{aligned}\Delta W_P &= \frac{1}{K_P}\Delta Q_P + \frac{\alpha_{pr}}{K_r}\Delta Q_r \\ \Delta W_r &= \frac{\alpha_{rp}}{K_{Pe}}\Delta Q_P + \frac{1}{K_r}\Delta Q_r\end{aligned}\right\} \qquad (7\text{-}12)$$

Where K_p is the stiffness of the pile group, K_{pe} is the elastic stiffness of the pile group, as determined by (2-4), K_r is the stiffness of the raft, as determined by (2-3), and α_{pr} and α_{rp} are the interaction factors. From the reciprocal theorem, the terms on the trailing diagonal of the flexibility matrix must be equal, so that the interaction factors are related by

$$\alpha_{pr} = \alpha_{rp}\frac{K_r}{K_{pe}} \qquad (7\text{-}13a)$$

α_{rp} can be determined by equation (2-5) for a single pile or about 0.8 times the group size's increases.

K_p and K_{pe} are related by

$$K_p = K_{pe} \cdot f(Q_p) \qquad (7\text{-}13b)$$

For example, the following load-deformation curves of pile group can be assumed:

$$W_p = \frac{Q_p}{K_{pe}\left(1 - R_f \frac{Q_p}{Q_{pu}}\right)} \qquad (7\text{-}14)$$

$$K_p = K_{pe} \cdot \left(1 - \frac{Q_p}{Q_{pu}} R_f\right)^2 \qquad (7\text{-}15)$$

or

$$K_p = \begin{cases} K_{pe} & (Q_p \le Q_{pe}) \\ K_{pe}\left(1 - \dfrac{Q_p - Q_{pe}}{Q_{pu} - Q_{pe}} R_f\right)^2 & (Q_{pe} < Q_p \le Q_{pu}) \end{cases} \qquad (7\text{-}16)$$

Where Q_{pu} is the ultimate load of the pile group, $Q_{pu} \approx 0.9 n_p P_u$; Q_{pe} is the linear-elastic limit load of the pile group, $Q_{pe} \approx (0.0\sim0.5)\, Q_{pu}$ and R_f is the failure ratio of the pile group and it should be taken as $R_f \approx 0.6$-1.0

Assuming that the average settlements of the piles and the raft are identical in a piled raft, equations (7-11) and (7-12) allow for the calculation of the overall performance of the foundation. The overall stiffness, K_{pr}, and the proportion of load carried by the raft are given by

$$\frac{\Delta Q}{\Delta W} = K_{pr} = \frac{\frac{K_{pe}}{K_p} + \frac{K_{pe}}{K_r} - 2\alpha_{rp}}{\frac{K_{pe}}{K_p} - \alpha_{rp}^2 \frac{K_r}{K_{pe}}} K_r = \frac{1 + \frac{K_p}{K_r} - 2\alpha_{rp} \frac{K_p}{K_{pe}}}{1 - \alpha_{rp}^2 \frac{K_r}{K_{pe}} \frac{K_p}{K_{pe}}} K_r \qquad (7\text{-}17)$$

$$\frac{Q}{W} = K_{pr}^{s} = \frac{\frac{K_{pe}}{K_{ps}} + \frac{K_{pe}}{K_r} - 2\alpha_{rp}}{\frac{K_{pe}}{K_{ps}} - \alpha_{rp}^2 \frac{K_r}{K_{pe}}} K_r = \frac{1 + \frac{K_{ps}}{K_r} - 2\alpha_{rp}\frac{K_{ps}}{K_{pe}}}{1 - \alpha_{rp}^2 \frac{K_r}{K_{pe}}\frac{K_{ps}}{K_{pe}}} K_r \qquad (7\text{-}17')$$

and

$$\eta_{st} = \frac{\Delta Q_r}{\Delta Q_p + \Delta Q_r} = \frac{\left(\frac{K_{pe}}{K_p} - \alpha_{rp}\right)K_r}{K_{pe} + \left(\frac{K_{pe}}{K_p} - 2\alpha_{rp}\right)K_r} = \frac{1 - \alpha_{rp}\frac{K_p}{K_{pe}}}{\frac{K_p}{K_r} + \left(1 - 2\alpha_{rp}\frac{K_p}{K_{pe}}\right)} \qquad (7\text{-}18)$$

$$\eta_s = \frac{Q_r}{Q_p + Q_r} = \frac{\left(\frac{K_{pe}}{K_{ps}} - \alpha_{rp}\right)K_r}{K_{pe} + \left(\frac{K_{pe}}{K_{ps}} - 2\alpha_{rp}\right)K_r} = \frac{1 - \alpha_{rp}\frac{K_{ps}}{K_{pe}}}{\frac{K_{ps}}{K_r} + \left(1 - 2\alpha_{rp}\frac{K_{ps}}{K_{pe}}\right)} \qquad (7\text{-}18')$$

where, $K_{ps} = K_{pe}\cdot\left(1 - \frac{Q_p}{Q_{pu}}R_f\right)$ (when $Q_p < Q_{pu}$).

When $Q_p = Q_{pu}$, $K_p = 0$, according to Equation (7-17), $\frac{\Delta Q}{\Delta W} = K_{pr} = K_r$.

A difficulty encountered in the application of equations (7-17') and (7-18') is that when $Q_p = Q_{pu}$, K_{ps} is not easily determined as it is controlled by the development of deformation W. However, Q-W curves can easily be calculated using incremental methods and equations (7-17) and (7-18).

Setting $Q_i = Q_{i-1} + \Delta Q$ and $Q_{p,I} \approx Q_i(1-\eta_{st,i-1})$, one obtains $K_{pi} = K_p\left(\frac{Q_i + Q_{i-1}}{2}\right)$, thus calculating $\eta_{st\,i}$, K_{pri} and $W_i = W_{i-1} + \Delta Q \cdot K_{pri}$ allows one to reach the data for W-Q curves, as well as η_s-Q curves.

Fig.7-1 presents the results based on Equation (7-16) where Q_{pe} = 500 kN, Q_{pu} = 1440 kN, K_{pe} = 26.74 MN/m and R_f = 0.65, in which the Q-W curve is almost identical to that of Fig. 3-9(1) from the non-linear FLM method presented in Chapter 4.

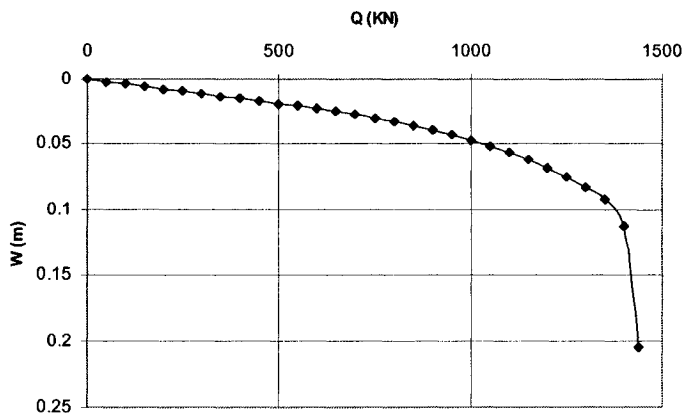

Fig. 7-1 Q-W Curve Based on Equation (7-6)

Fig.7-2 is the result based on Equation (7-17) where Q_{pe} = 500 kN, Q_{pu} = 1440 kN, K_{pe} = 26.74 MN/m, K_r = 8.32MN/m and R_f = 0.65, in which the Q-W curve is almost identical to that of Fig. 3-10(1) from the non-linear FLM method analysis of a single pile under a raft presented in Chapter 4.

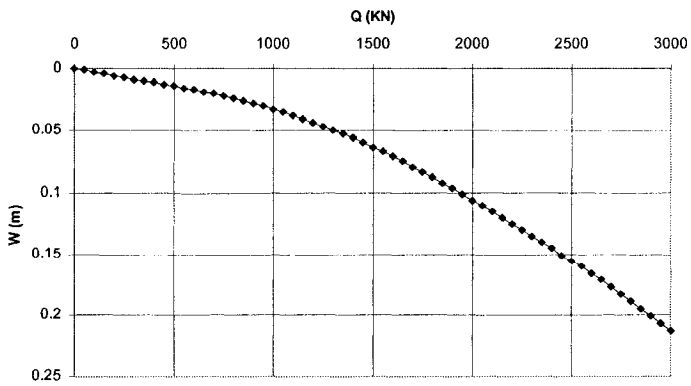

Fig. 7-2 Q-W Curve Based on Eq. (7-7)

7.4 Discussion on interaction factor α_{rp}

In the case of Case 2 presented in Chapter 4, $K_{rp} \approx 30MN/m$ when $Q_p \leq Q_{pe}$ but according to equation (7-7), inversely calculating α_{rp} obtains $\alpha_{rp} = 0.49 \leq 0.5$, greatly different with $\alpha_{rp} = 0.7211$ from Equation (2-5). This may be due to two causes: the selection of the r_m' value or formula (2-5) for a situation of the pile to raft unit that is located in the pile, which is should not be used in this situation.

Taking the r_m' value according to the elastic theoretical study of the performance of piles from Randolph (1977) and the suggestion from Randolph & Wroth (1978), $r_m = \{0.25+\xi[2.5\rho(1-\upsilon_s)-0.25]\}\, l$. However, soil is not completely elastic and cannot bear tensile stress, partly like the Winkler model, so an analysis based on the elastic solution overestimates the pile-soil interaction and its effect range r_m. The measured r_m value is far smaller than the elastic theoretical result. According to the field observed value from Cooke et al (1980), $r_m \approx 12d$, whereas API (American Petroleum Industry) recommends a value of $r_m = 8d$. Shi's pile test (1983) shows that $r_m \approx 6d$. Shen (2000) proposed $r_m = 0.5\rho(1-\upsilon_s)l$. From $r_m \approx 12d = 24r_0$, $\zeta = \ln(r_m/r_0) = 3.178$, $\alpha_{rp} = 1 - \frac{\ln(r_c/r_o)}{\zeta} = 0.5638$.

Formula (2-5), $\alpha_{rp} = S_{rp}/S_p \approx 1 - \frac{\ln(r_c/r_o)}{\zeta}$, simply represents the ratio of settlement at $r = r_c$ to that at $r = r_0$. The correct expression for α_{rp} should be the ratio of the average settlement of area $r \leq r_c$ to the settlement at $r = r_0$. Thus, $\alpha_{rp} = S_{av}/S_0$,

$$S_0 = \frac{r_o \tau_z}{G} \ln\left(\frac{r_m}{r_0}\right) \qquad (7\text{-}19)$$

$$S_{av} = \frac{1}{\pi(r_c^2 - r_0^2)} \int_{r=r_0}^{r=r_m} \frac{r_0 \tau_z}{G} Ln\left(\frac{r_m}{r}\right) 2\pi r dr = \frac{1}{(r_c^2 - r_0^2)} \frac{r_0 \tau_z}{G} \int_{r=r_0}^{r=r_m} Ln\left(\frac{r_m}{r}\right) dr^2$$

$$= \frac{1}{(r_c^2 - r_0^2)} \frac{r_0 \tau_z}{G} \left\{ Ln\left(\frac{r_m}{r}\right) \cdot r^2 \Big|_{r=r_0}^{r=r_m} - \int_{r=r_0}^{r=r_m} r^2 \left(-\frac{dr}{r}\right) \right\}$$

$$= \frac{1}{(r_c^2 - r_0^2)} \frac{r_0 \tau_z}{G} \left\{ r_c^2 Ln\left(\frac{r_m}{r_c}\right) - r_0^2 Ln\left(\frac{r_m}{r_0}\right) + \frac{1}{2}(r_c^2 - r_0^2) \right\}$$

$$= \frac{r_0 \tau_z}{G} \left\{ \left[r_c^2 Ln\left(\frac{r_m}{r_c}\right) - r_0^2 Ln\left(\frac{r_m}{r_0}\right) \right] \frac{1}{(r_c^2 - r_0^2)} + \frac{1}{2} \right\} \quad (7\text{-}20)$$

$$\alpha_{rp} = S_{av}/S_0 = \left\{ \left[r_c^2 Ln\left(\frac{r_m}{r_c}\right) - r_0^2 Ln\left(\frac{r_m}{r_0}\right) \right] \frac{1}{(r_c^2 - r_0^2)} + \frac{1}{2} \right\} \cdot \frac{1}{Ln\left(\frac{r_m}{r_0}\right)} \quad (7\text{-}21)$$

From equation (7-21) and $r_m = 24r_0$, $\alpha_{rp} = 0.4926$, which is near the 0.4927 value, the value inversely calculated from the case of Case 3 in Chapter 3. In the case, interaction factor just is not modified by the means of equation (3-2).

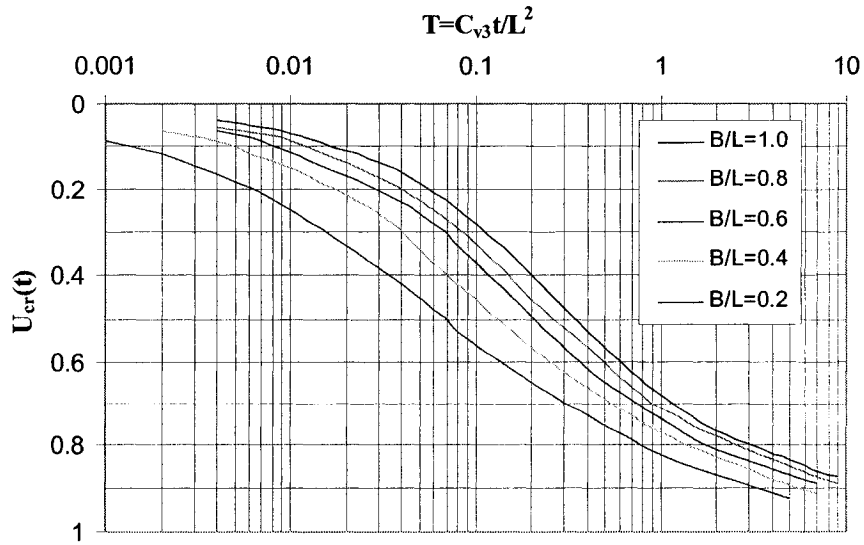

Fig. 7-3 Consolidation Degree of Settlement below the Corner of a Rectangular Area of Uniform Pressure of a Raft (from Gibson & Mc Namee 1957)

7.5 Consolidation and Time Factors in the Simplified Methods

The settlement caused by the pressure of a raft is divided into two parts: immediate settlement and consolidation settlement. Thus,

$$\frac{1}{K_r} = \frac{1}{K_{dr}} + \frac{U_{cr}(t)}{K_{cr}} \qquad (7\text{-}22)$$

in which K_{dr} is the soil stiffness of immediate deformation, calculated according to μ_s=0.5, $K_{dr} \approx 1.3467 E_{su} B$ for a square raft, K_{cr} is the soil stiffness of consolidation deformation, U_{cr} is the consolidation degree of settlement under the corner of a rectangular area of uniform pressure of a raft, shown in Fig. 7-3, which is the solution proposed by Gibson & Mc Namee (1957).

In the figure,

T is the time factor, $T = C_{v3}\, t/L^2$,

C_{v3} is the consolidation coefficient, $C_{v3} = \dfrac{2kG(1-\mu)}{\gamma_w(1-2\mu)} = \dfrac{kE(1-\mu)}{\gamma_w(1+\mu)(1-2\mu)} = \dfrac{k(1+e)}{\gamma_w a}$,

E, G, μ are the deformation modulus, the shear modulus, and Poisson's ratio of soilrespectively;

k, a, e are respectively permeability coefficient, 1-D compressibility coefficient, and void ratio of soil,

and γ_w is the unit weight of water.

For a square or circular raft on homogenous soil,

$$K_{dr} \approx 1.35 E_{su} B/\alpha_r \text{ , or } K_{dr} \approx 5.5 G_u B/\alpha_r \qquad (7\text{-}23)$$

$$K_r \approx 1.01 E_{sc} B/[\alpha_r(1-\mu_s^2)] \qquad (7\text{-}24)$$

in which, E_{su} is undrained elastic (immediate) deformation modulus; E_{sc} is drained deformation modulus; the value of α_r is for various length-to-width ratios (L/B), and can be obtained from the page 241~243 of Das (1999), α_r=0.88 for circular and square raft.

Thus, $S_{rrt}(t) = S_{dr}+S_{cr}U_{cr}(t)$ (7-10)

$= S_{dr}+(S_{rr}-S_{dr})U_{cr}(t)$ (7-25)

$S_{dr} = Q_r/ K_{dr}$ (7-25a)

$S_{cr} = Q_r(1/ K_r-1/ K_{dr})=Q_r/K_{cr}$ (7-25b)

$S_{rr} = Q_r/ K_r$ (7-25c)

$S_{dp} = Q_p/ K_p$ (7-25d)

Theoretically, $S_{rr}/S_{dr} = K_{dr}/K_r=2(1-\mu) = 1.34\sim1.0$ for $\mu = 0.33\sim0.5$.

Equation (7-25) can be also be used in the incremental method for non-linear curves.

The settlement caused by the dissipation of remnant EPWP of driving can be estimated by the following formula

$$S_{cpt}(t) = S_{cp}\cdot U_{cp}(t) \qquad (7\text{-}26)$$

S_{cp} is caused only by the dissipation of remnant EPWP and by no other surface load. In the *center area of the cap*, soil settlement can be considered as 1-D consolidation,

$$S_{cp}= \int_{z=0}^{R_z} m_v u_0 dz = \int_{z=0}^{R_z} \frac{(1+\mu)(1-2\mu)}{(1-\mu)} \frac{u_0}{E_{ur}} dz \qquad (7\text{-}27a)$$

For homogenous soil,

$$S_{cp} = \frac{(1+\mu)(1-2\mu)}{(1-\mu)E_{ur}} \int_{z=0}^{R_z} u_0 dz = m_v A_{u0} = \frac{(1+\mu)(1-2\mu)}{(1-\mu)E_{ur}} A_{u0} \quad (7\text{-}28a)$$

In the *edge or corner area of cap*, soil deformation should be 3-D, so

$$S_{cp} = \int_{z=0}^{R_z} \frac{\left[\Delta\sigma'_z - \mu(\Delta\sigma'_x + \Delta\sigma'_y)\right]_{t=\infty}}{E_{ur}} dz$$

$\Delta\sigma_z \approx 0$ during t=0~∝, $\Delta u|_{t=\infty} = 0$, $\Delta\sigma'_z = \Delta\sigma_z - \Delta u = \Delta\sigma_z - (\Delta u|_{t=\infty} - \Delta u|_{t=0}) = u_0 = u_i$. And $\Delta\sigma'_h \approx$ $\chi_{av} u_i$, from Fig. 7.4-6, $[\Delta\sigma'_z - \mu(\Delta\sigma'_x + \Delta\sigma'_y)]_{t=\infty} \approx u_i(1-2\mu\chi_{av}) = \frac{(6+\mu)(1-2\mu)}{6(1-\mu)} u_0$

Then, $$S_{cp} \approx \int_{z=0}^{R_z} \frac{(6+\mu)(1-2\mu)}{6(1-\mu)E_{ur}} u_0 dz \quad (7\text{-}27b)$$

For homogenous soil,

$$S_{cp} \approx \frac{(6+\mu)(1-2\mu)}{6(1-\mu)E_{ur}} \int_{z=0}^{R_z} u_0 dz = \frac{(6+\mu)(1-2\mu)}{6(1-\mu)E_{ur}} A_{u0} = m_{vb} A_{u0} \quad (7\text{-}28b)$$

Where, $m_{vb} = \frac{(6+\mu)(1-2\mu)}{6(1-\mu)E_{ur}}$

For soils having μ = 0.33~0.42, $S_{cp} = (0.54\sim0.30) A_{u0}/E_{ur}$.

For stepping load situations, one can use the approximate method to estimate settlement caused by raft-bottom pressure, as shown in Fig. 7-4

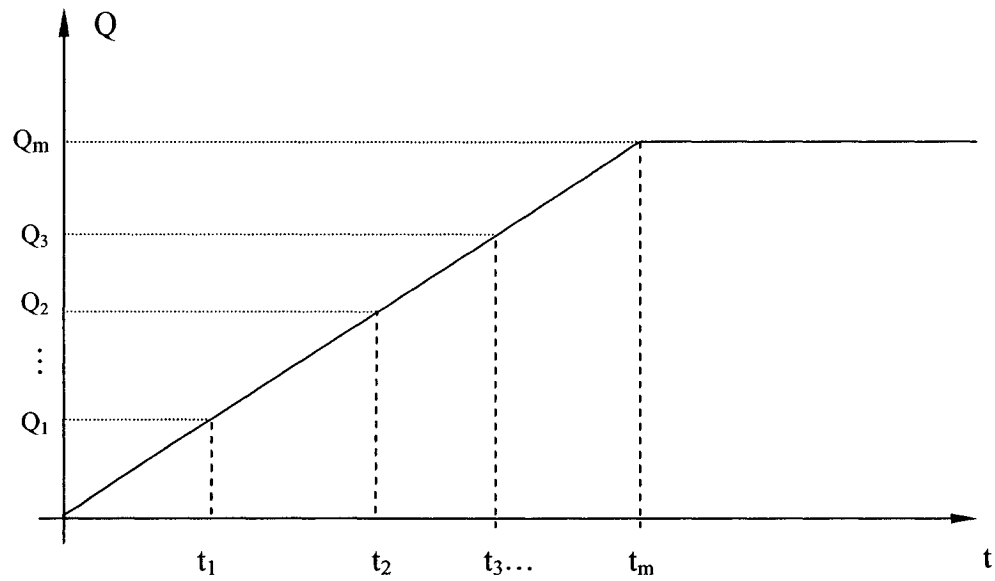

Fig. 7-4 Step Load-Time Relationship

$S_{rr1} \approx S_{dr1} + \Delta S_{cr1} U_{cr}(\Delta t_1/2)$;

$S_{rr2} \approx S_{rr1} + \Delta S_{dr2} + \Delta S_{cr1}[U_{cr}(\Delta t_1/2+\Delta t_2) - U_{cr}(\Delta t_1/2)] + \Delta S_{cr2} U_{cr}(\Delta t_2/2)$

$= S_{dr2} + \Delta S_{cr1} U_{cr}(\Delta t_1/2+\Delta t_2) + \Delta S_{cr2} U_{cr}(\Delta t_2/2)$;

$S_{rr3} \approx S_{dr3} + \Delta S_{cr1} U_{cr}(\Delta t_1/2+\Delta t_2+\Delta t_3) + \Delta S_{cr2} U_{cr}(\Delta t_2/2+\Delta t_3) + \Delta S_{cr3} U_{cr}(\Delta t_3/2)$;

$\vdots$

$$S_{rrt}(t_k) = S_{rrk} \approx S_{drk} + \sum_{i=1}^{k-1} \Delta S_{cri} U_{cr}\left(\frac{\Delta t_i}{2} + \sum_{j=i+1}^{k} \Delta t_j\right) + \Delta S_{crk} U_{cr}\left(\frac{\Delta t_k}{2}\right) \quad (k \le m)$$

$$= S_{drk} + S_{crt}(t_k) \qquad (7\text{-}29)$$

in which, $S_{crt}(t) = \sum_{i=1}^{k-1} \Delta S_{cri} U_{cr}\left(\frac{\Delta t_i}{2} + \sum_{j=i+1}^{k} \Delta t_j\right) + \Delta S_{crk} U_{cr}\left(\frac{\Delta t_k}{2}\right)$, and $S_{drk} = \frac{Q_{rk}}{K_{dr}}$.

$$\Delta S_{crk} = \left(\frac{1}{K_r} - \frac{1}{K_{dr}}\right)\Delta Q_{rk}; \quad S_{crk} = \left(\frac{1}{K_r} - \frac{1}{K_{dr}}\right) Q_{rk};$$

$$S_{crt}(t_k) = \left(\frac{1}{K_r} - \frac{1}{K_{dr}}\right)\left[\sum_{i=1}^{k-1} \Delta Q_{ri} U_{cr}\left(\frac{\Delta t_i}{2} + \sum_{j=i+1}^{k} \Delta t_j\right) + \Delta Q_{rk} U_{cr}\left(\frac{\Delta t_k}{2}\right)\right]$$

$$= S_{crk}U_{crl}(t_k) \tag{7-30}$$

Where

$$U_{crl}(t_k) = \frac{1}{Q_{rk}}\left[\sum_{i=1}^{k-1}\Delta Q_{ri}U_{cr}\left(\frac{\Delta t_i}{2}+\sum_{j=i+1}^{k}\Delta t_j\right)+\Delta Q_{rk}U_{cr}\left(\frac{\Delta t_k}{2}\right)\right] \quad (k\leq m) \tag{7-31}$$

Thus,

$$S_{rrt}(t_k) = S_{rrk} \approx S_{drk} + S_{crk}U_{crl}(t_k) \tag{7-32}$$

After t_m (k>m),

$$S_{rrt}(t_k) = S_{rrk} \approx S_{drm} + \sum_{i=1}^{m}\Delta S_{cri}U_{cr}\left(\frac{\Delta t_i}{2}+\sum_{j=i+1}^{k}\Delta t_j\right) \quad (k>m)$$

$$= S_{drm} + S_{crk}U_{crl}(t_k) \tag{7-33}$$

$$U_{crl}(t_k) = \sum_{i=1}^{m}\frac{\Delta Q_{ri}}{Q_{rm}}U_{cr}\left(\frac{\Delta t_i}{2}+\sum_{j=i+1}^{k}\Delta t_j\right) \quad (k>m) \tag{7-34}$$

If $t_k >> t_m$,

$$S_{rrt}(t_k) = S_{rrk} \approx S_{drm} + S_{cr}\cdot U_{cr}\left(\frac{t_m}{2}+(t_k - t_m)\right) \quad (k>m) \tag{7-35}$$

In the process of piles-soil-raft interaction, when the total load Q is stable, the raft's sharing load Q_r may decrease with an increase of the piles' sharing load, that is, $\Delta Q_{rm+j} < 0$ $_{(j=1,2,\ldots)}$, as shown in Fig. 7-5. In the special situation where $\Delta Q_r < 0$, when $t_k \leq t_m$, equations (7-30) and (7-31) is still right and when $t_k > t_m$, the calculation formula should be modified as follows:

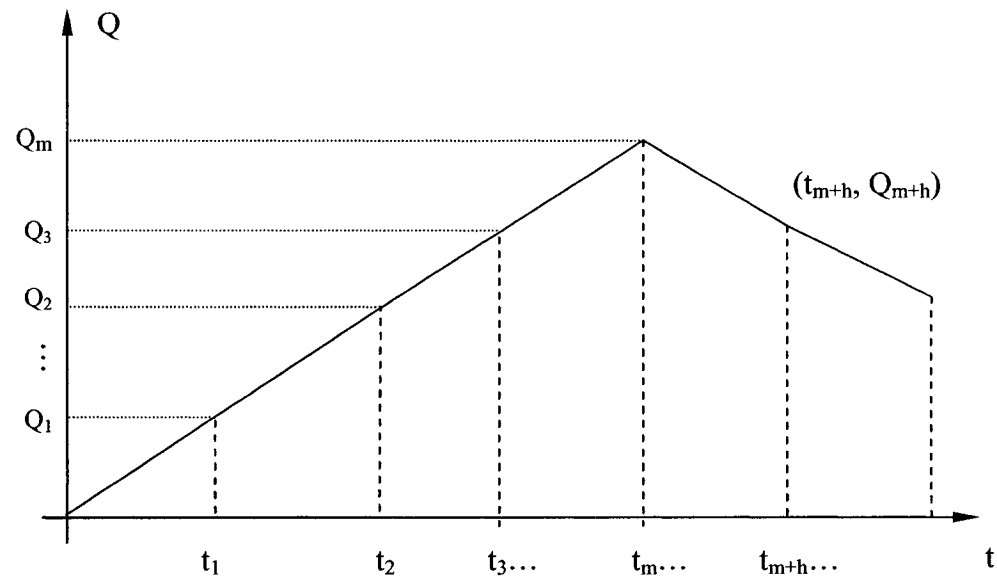

Fig. 7-5 Step Load-Time Relationship with Case of $\Delta Q_{rm+i}<0$

If $Q_{rm+h} \geq Q_{rm-1}$ (that is, $\Delta Q_{rm} \geq \sum_{j=1}^{h} \Delta Q_{r,m+j}$),

$$U_{crl}(t_{m+h}) = \frac{1}{Q_{rk}} \left\{ \sum_{i=1}^{m-1} \Delta Q_{ri} U_{cr} \left(\Delta t_i/2 + \sum_{j=i+1}^{m+h} \Delta t_j \right) + \sum_{i=m+1}^{m+h} \Delta Q_{ri} U_{cr} \left(\frac{\Delta t_m}{2} + \frac{\Delta t_i}{2} + \sum_{j=m+1}^{i-1} \Delta t_j \right) \right\} \tag{7-36}$$

If $Q_{rm-2} \leq Q_{rm+h} < Q_{rm-1}$ (that is, $\sum_{j=1}^{h-1} \Delta Q_{r,m+j} \leq \Delta Q_{rm} < \sum_{j=1}^{h} \Delta Q_{r,m+j}$),

$$\begin{aligned} U_{crl}(t_{m+h}) = \frac{1}{Q_{rk}} \Bigg\{ & \sum_{i=1}^{m-2} \Delta Q_{ri} U_{cr} \left(\Delta t_i/2 + \sum_{j=i+1}^{m+h} \Delta t_j \right) \\ & + (Q_{r,m+h} - Q_{r,m-2}) U_{cr} \left(\frac{\Delta t_{m-1}}{2} + \sum_{j=m}^{m+h} \Delta t_j \right) \\ & + (Q_{r,m-1} - Q_{r,m+h}) U_{cr} \left(\frac{\Delta t_{m-1}}{2} + \frac{\Delta t_{m+h}}{2} + \sum_{j=m}^{m+h-1} \Delta t_j \right) \\ & + \sum_{i=m+1}^{m+h} \Delta Q_{ri} U_{cr} \left(\frac{\Delta t_m}{2} + \frac{\Delta t_i}{2} + \sum_{j=m+1}^{i-1} \Delta t_j \right) \Bigg\} \end{aligned} \tag{7-37}$$

From equation (7-37), it is possible that $U_{crl}(t_{m+h}) > 1.0$, where $U_{crl}(t_{m+h})$ is taken to be 1.0 when $U_{crl}(t_{m+h})$ is used to estimate the cap's increasing action on the UBC of piles.

For the case of $Q_{rm-k-1} \leq Q_{rm+h} < Q_{rm-k}$, one can use a similar principle to the above in order to estimate the consolidation degree $U_{crl}(t_{m+h})$.

7.6 Effect of Raft's Interaction on UBC of Piles

According to equations (7-31) and (7-34), the $U_{crl}(t)$, consolidation degree at a given time from the raft-bottom pressure increases linearly with time, which may cause the UBC of a pile to increase. The UBC increment of pile from raft-bottom pressure, $\Delta P_{ur}(t)$ is

$$\Delta P_{ur}(t) = A_b \cdot \Delta\sigma_b(t) + p\sum \Delta\tau_f(t) \cdot \Delta z$$

The above equation is the same as (6-3) except that the mode of failure at pile-soil interface before the load action of raft on soil (and after pile driving) is different than that following the load action of the raft, where σ_z' may be larger than σ_h' in Fig. 6-4(d). If $\sigma_z' \leq \sigma_h'$, $\Delta\tau_f(t) = \sigma_z'(t) \cdot tg\varphi$ or if equation (6-6) is derived from Fig. 6-4(d), then $\sigma_z' > \sigma_h'$, $\Delta\tau_f(t) = \sigma_h'(t) \cdot tg\varphi$. This is not a good model. The suggestion from the assumption of the 1-D consolidation for piles near the center of the raft was adopted.

$$\Delta\tau_f(t) = \sigma_h'(t) \cdot tg\varphi \approx \sigma_z'(t) K_0 \cdot tg\varphi' \approx \sigma_z'(t)(1 - Sin\varphi') \cdot tg\varphi' \qquad (7\text{-}38)$$

Thus,

$$\Delta P_{ur}(t) = A_b \cdot \Delta\sigma_b(t) + p\sum \Delta\sigma_z'(t) K_0 tg\varphi' \cdot \Delta z \qquad (7\text{-}39)$$

For uniform soils,

$$\Delta P_{ur}(t) = A_b \cdot \Delta\sigma_b(t) + pK_0 tg\varphi' \cdot \sum \Delta\sigma'_z \, \Delta z \qquad (7\text{-}40)$$

Noting that

$$\sum \Delta\sigma'_z \, \Delta z = U_{crl}(t_k) \sum \Delta\sigma_z\big|_{t=0} \Delta z = U_{crl}(t_k) \sum \Delta u\big|_{t=0} \Delta z = U_{crl}(t_k) A_{u0r} \qquad (7\text{-}41)$$

Hence,

$$\Delta P_{ur}(t) = A_b \cdot \Delta\sigma_b(t) + pK_0 \cdot tg\varphi' U_{crl}(t_k) \, A_{u0r} \qquad (7\text{-}42)$$

and,
$$A_{u0r} = \sum \Delta u\big|_{t=0} \Delta z \approx \sum \Delta\sigma_z\big|_{t=0} \Delta z = p_r[H_2 I_{a(\mathrm{H2})} - H_1 I_{a(\mathrm{H1})}] \qquad (7\text{-}43)$$

$$\Delta\sigma_b(t) = \Delta\sigma'_z(t)\big|_{z=1} = p_r I \qquad (7\text{-}44)$$

where, $I = 4I_c$, where I_c is the influence factor of vertical stress below the corner of a rectangular area which can be obtained from pages 223~225 of Das (1999), $I_{a(\mathrm{H1})}$ and $I_{a(\mathrm{H2})}$ are the average stress influence factors below the corners of a uniformly loaded rectangular area with limits of depth z = 0 to z = H_1 and z = 0 to z = H_2 respectively, as proposed by Griffiths (1984) and that can be determined from page 231 of Das (1999).

7.7 Discussions

In this Chapter, the method analyzing non-linear settlement of a raft considering the pile-soil-raft interaction, consolidation and time factors was set up. Randolph and Clancy's (1993) method for the elastic response under a load on the system of pile-soil-raft interaction is generalized by the incremental method for the nonlinear response of the interaction. Meanwhile the method to estimate the UBC increment of pile from raft-bottom pressure, $\Delta P_{ur}(t)$, is derived out.

CHAPTER 8

CASE ANALYSES AND COMPARISON

8.1 General

This chapter presents two case analyses. One is to estimate the increment of the UBC of a single pile due to the dissipation of EPWP from pile driving, which uses the method discussed in Chapter 6. Another is to analyze the whole process change of the load shares of piles and raft and the settlement in the pile-soil-raft interaction from the end of pile group driving to a long time after the end of the superstructure's construction, which uses the method discussed in Chapter 6 and 7. These cases are according to practical situations in civil or building engineering. From analysis and calculation of these cases, some important general conclusions are obtained.

8.2 Case 1: Analysis of UBC Change of a Single Pile

The case data is that of Tang (1990); a test pile b × b × L = 0.5 × 0.5 × 24.5 m^3, pile weight 125 kN. The test field is in the Zhang Hua-bing area of Shanghai, China. The soil layers' field data for pile load tests is shown in Table 8-1. The pile load tests were carried out 14, 137, 297, and 409 days after driving. The test results of the ultimate bearing capacity of pile (UBCP) are shown in Table 8-2 and Fig. 8-1.

The maximum EPWP is estimated according to Lo & Stermac's (1965) Equation (2.5-1), shown in Table 8-3 and Fig. 8-2

Table 8-1 Geotechnical Data of Pile Load Test Field

soil Layer	soil type	thickness (m)	unit weigth γ(KN/m^3)	water content w(%)	plasticity	void ratio e	consolidation coefficient C_h(cm^2/s)	effective friction angle φ' (°)	Cone panetration resistance p_s(MPa)
1	Mucky loam	7	18	40-49	Low	1.15	6.75×10^{-3}	30	0.4~1.0
2	Clay	10	17.2	42-55	Higher	1.38	1.32×10^{-3}	26	0.4~.08
3	Loam	14 (7.5)	18	35-40	Lower	1.12	12.45×10^{-3}	32	0.6~1.0
Average in depth 24.5m			17.7			1.23	5.5×10^{-3}	29	

Value in brackets ( ) is the thickness occupied by pile; Poisson ratio μ=0.30~0.42, average μ=.38

Table 8-2 Result of Pile Load Test

t /days after driving	0	14	137	297	409	2000
P_t/KN	(300)	1400	1760	1860	1930	2110

Value in brackets ( ) is estimated by the formula for penetration resistance during driving

Table 8-3 Maximum EPWP

z (m)	σ'_{ov}(kPa)	u_{im}(kPa)
0	0	0
3.50	28.0	27.0
12.00	92.0	90.0
20.75	158.0	161.0
24.50	188.0	230.0

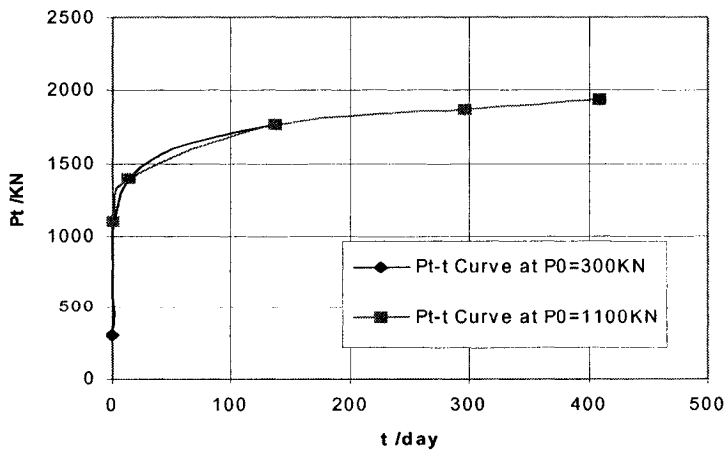

Fig. 8-1 Measured P_t-t Curves

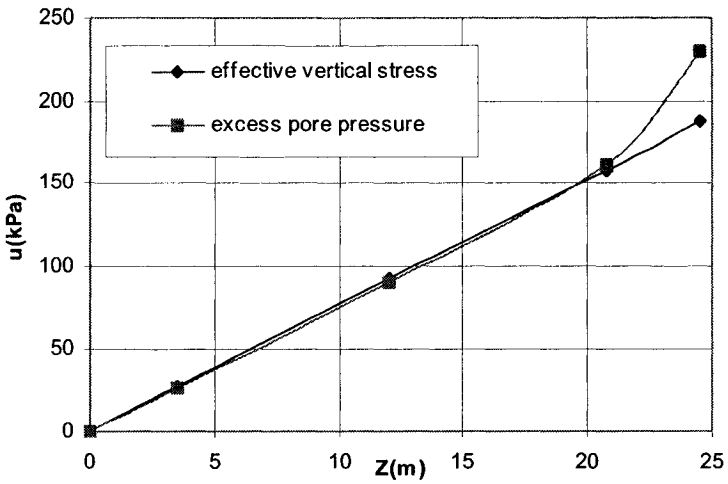

Fig. 8-2 Estimated Maximum EPWP

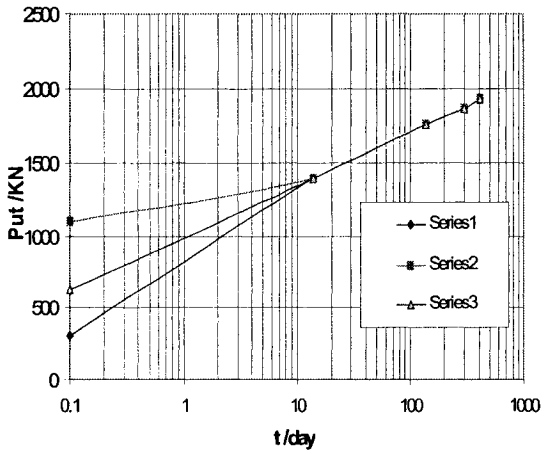

Fig. 8-3(a) P_{ut}-*log*(t) curves

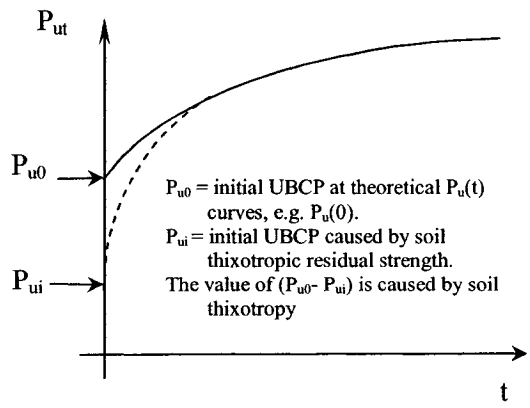

Fig. 8-3(b) Relationship of P_{u0} and P_{ui}

The initial UBCP, P_{ui}, was set at 300 kN in Table 8-2, which is actually an estimated value of dynamic penetration resistance (due to thixotropic residual strength) during pile driving, and is not P_{u0}, a static UBCP at the exact time that driving ends on P_{ut} curve. The value of (P_{u0}- P_{ui}) is caused by soil thixotropy, shown in Fig. 8-3(b).

From Fig. 8-1, P_{u0} can be 300~1100 kN. Converting Fig. 8-1 into Fig. 8-3(a), one finds that P_t-*log*(t) curve at P_{u0} = 300~630 kN when t ≈ 0.1day ≈ 2.4*hr* is not reasonable theoretically, as it is does not agree with the initial tendency of the consolidation curve.

Hence, only P_{u0} = 630~1100 kN is possible. But the P_t-lot(t) curve at P_{u0} = 300~630 kN may appear in the practice of engineering, due to the soil thixotropy and the cohesion's (c) recovery with time, not being caused by the consolidation of EPWP. Assume that the soil cohesion c has recovered in 2.4hr ~1day. The real theoretical meaning of P_{u0} is the initial UBCP when soil cohesion c has recovered from soil thixotropy in a condition where EPWP is constant or the consolidation degree remains zero.

On the other hand, one can choose a different P_{u0} (initial ultimate bearing capacity of pile) consolidation degree curve U(t), as shown in Fig. 8-4. According to the relation of equation (6-35), U(t) curves should be parallel to U(T) curves. Fig.6-14 shows curves of $\Delta U/\Delta(log T)$ - l/b relationship. From Fig. 8-4, $\Delta U/\Delta(log T) \approx 0.2$ when P_{u0} = 300 kN, the corresponding situation is l_r/b_r=300, shown in Fig. 8-5. Usually l/b ≤ R/b ≤ R/r_0 = 30~60 according to Fig. 2-7 (from Poulos & Davis, 1980). Thus, the situation where P_{u0} = 300 kN and the corresponding l/b = 300 is not reasonable.

Comparatively, $\Delta U/\Delta(log T) \approx 0.36$ at P_{u0} = 1100 kN in Fig. 8-4, the corresponding situation of l/b = 21 in Fig. 8-5, is possible.

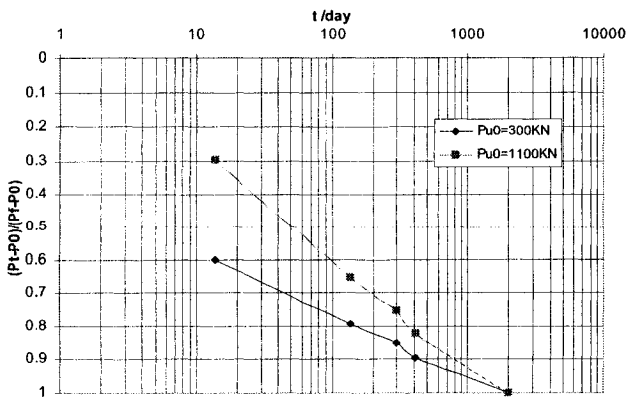

Fig. 8-4 Effect of Choosing P_{u0} on Measured U(t) Curves

Equivalent radius of pile $r_e = \sqrt{\frac{1}{\pi}}b = \sqrt{\frac{1}{\pi}}0.5 = 0.282m$

Thickness of soil crust $\delta = 20mm$

Failure plane radius $r_0 = r_e + \delta = 0.28 + 0.02 = 0.30m$

Radius of maximum EPWP $b_r = 2r_e = 0.60m$

Radius of zero EPWP $l_r = 21b_r = 12.6`m$

Radius of permeable boundary $R_r = l_r = 12.6m$ ($\omega = R_r/r_e = 45$, $\in 30\sim60$)

Depth of vertical permeable boundary $R_z = l_z = 30$m (assumed)

By (6-22), the increment of UBC, ΔP_c, is:

$$\Delta P_c = \Delta P|_{t=\infty} = \Delta P_{cb} + \Delta P_{cs} = A_b \cdot u_{0b} + p\chi_\sigma\chi_\varphi\sum u_0\Delta z$$

Now, $A_b = 0.25\text{m}^2$, $u_{0b} = 230$ kPa, $p = 4 \times \text{b} = 2$ m, $\chi_\sigma = \chi_{av} = 0.7742$, $\chi_\varphi = 0.3433$, $A_{u0} = \sum u_0\Delta z = 188 \times 24.5/2 = 2303$ kPa·m. Hence, $\Delta P_{cb} = 57.5$KN, $\Delta P_{cs} = 1224.2$ kN; $\Delta P_c = \Delta P|_{t=\infty} = \Delta P_{cb} + \Delta P_{cs} = 1282$ kN. Let $P_{u0} = 1000$ kN

The calculation of $U(t)$ and $P_{ut}(t)$ is shown in Table 8-4. A comparison of the measured and calculated values is shown in Fig. 8-5.

The above results give the following conclusions.

(1) The effect of vertical consolidation can be ignored under conditions where the consolidation coefficient $C_v \leq C_h/4$ and the horizontal radius of zero EPWP $l_r \leq l_z/2$.

(2) The result obtained by considering the real meaning of P_{uo} presented in this thesis is better than that proposed by Tang (1990).

Table 8-4 Calculation and Comparison of UBCP

$Rr=$	12.5	$Rz=$	30			
$Ch=$	0.0543	$Cv=$	0.0136			
t	0	14	137	297	409	2000
$Pt(KN)$ (the measured)	(300)	1400	1760	1860	1930	2110
T_r		0.0019	0.01858	0.04029	0.05548	0.2713
U_r (l_r/b_r=20)		0.31	0.64	0.77	0.83	0.995
T_v		0.00021	0.00206	0.00448	0.00616	0.0301
U_{v1}		0.03	0.12	0.17	0.21	0.44
U_{v3}		0.001	0.015	0.05	0.08	0.275
$U_v=2U_{v1}-U_{v3}$		0.059	0.225	0.29	0.34	0.605
$U_t=1-(1-U_r)(1-U_z)$		**0.35071**	**0.721**	**0.8367**	**0.8878**	**0.998**
$\Delta\sigma'_b(t)$		71	147	177	190	230
$\Delta P_{cb}=A_b\cdot\Delta\sigma'_b(t)$		17.75	36.75	44.25	47.5	57.5
$\Delta P_{us}=P_{cs}\cdot U_t$		369.12	758.85	880.63	934.41	1050
$P_{ut}=P_{u0}+\Delta P_{cb}+\Delta P_{us}$	1000	1386.9	1795.6	1924.9	1981.9	2108
The calculated by Tang(1990)	300	1300.7	1936	2038	2073	2139

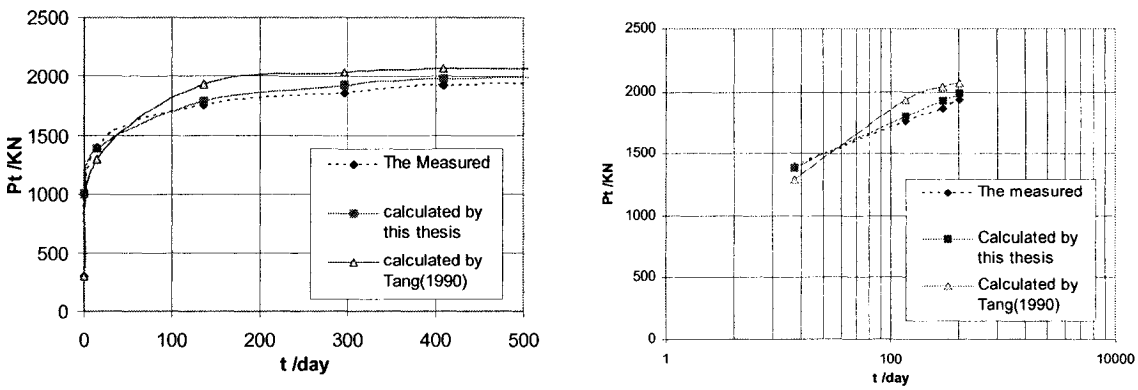

(a) P_t-t Curves (b) P_t-log(t) Curves

Fig. 8-5 Comparison of the Measured and the Calculated UBCP

8.3 Case 2: Change of Load Share and Settlement of a Raft with 9-Pile

This is a low raft (i.e. the bottom of the raft comes into contact with the soil) with 9 piles. The raft is the as same as that in Case 5 of Chapter 3. The piles and soil conditions are the same as those of Tests 7 and 8, i.e., raft B × B = 7.6 m × 7.6 m, reinforced concrete pile, L × b × b = 20 m × 0.4 m × 0.4 m, its elastic modulus E_p = 22 GPa, pile spacing s = 2.4 m, s/d = 2.4/0.4514 ≈ 5.32. The depth of the burden foundation bottom D_f = 1m and the depth of the underground water level d_w = 1.0m

Soil conditions:

The soil at depth 0.0 ~ 21.0 m is a soft silt clay: unit weight γ = 18 kN/m^3, E_s = 10 MPa, Poisson ratio μ = 0.4, G_{vl} = 3.57MPa; soil shear strength τ_f = 40 kPa, (estimated when driving has ended after 28 days); coefficient of consolidation in the vertical direction C_v = 3.0×10^{-2} m^2/day; horizontal coefficient of consolidation $C_h \approx 2C_v = 6.0\times10^{-2}$ m^2/day, soil effective internal frictional angle φ' = 28°.

The soil at depth 21.0 ~ 50.0 m is a better quality silt sand (permeable soil), E_s = 20 MPa, Poisson ratio μ = 0.4, G_{vl} = 7.14MPa; pile base ultimate bear capacity σ_{bf} = 1000 kPa, the linear-elastic critical pile-base stress σ_{be} = 450 kPa.

The total ultimate bearing capacity of a pile P_{uk} = 1440 kN (estimated when driving has ended for 28 days).

The modeling relationship between the shaft shear stress and plastic displacement is adopted from the model of Yang & Zai (1994).

Construction procedure: at t_1 = 45 days after driving, the construction of foundation and superstructure takes 200 days.

8.3.1Checking Safety without Considering the Effect of EPWP

When one does not consider the effect of EPWP, one can solve the problem and get that at total load Q = 20 MN, settlement S = 0.1 m = 10cm, the load shared by raft Q_s = 8.5MN, $\eta_s = Q_s/Q$ = 42.5%; the load shared by nine piles Q_P = 11.5 MN, the average top force of a single pile $\overline{P_0}$ = 11.5/9 = 1.28 MN = 1278 kN ≈ 0.9P_{uk} = 1296 kN.

Considering a certain degree of consolidation during the 200-day time length of construction, an estimate can be made for $U_{crl}(t_m)$ = 0.3 that assumes the following soil strength parameters: total stress cohesion c = 40 kPa; total stress internal frictional angle $\varphi = tan^{-1}[U_{crl}(t_m)tan\varphi'] = arctan\ (0.3\times tan28°) = 9.06°$, conservatively taking φ=7°.

Using Vesic's (1973) ultimate bearing capacity formula, bearing capacity factors N_c = 7.16, N_q = 1.72, N_r = 0.71; shape factors F_{cs} = 1.26, F_{qs} = 1.12, F_{rs} = 0.6; depth factors F_{cd} = 1.053, F_{qd} = 1.025, F_{rd} = 1.0; rigidity index I_r > critical rigidity index $I_{r(cr)}$, then compressibility factors $F_{cc} = F_{qc} = F_{rc}$ = 1.0; Hence, the soil ultimate bearing capacity q_u = $cN_cF_{cs}F_{cd}F_{cc} + \gamma_qDN_qF_{qs}F_{qd}F_{qc} + \frac{1}{2}\gamma BN_rF_{rs}F_{rd}F_{rc} = 380.0 + 35.5 + 13.0 = 428\ kPa$. The increment factor of soil bearing capacity $\eta_r = 1+\Delta q_{ur}/q_{ur} = 1+117/428 = 1.27$.

Thus, the total ultimate load $Q_{ult} = \eta_r q_u A + \eta_g \xi_{\supset p} n P_u = 1.27 \times 428 \times 7.6^2 + 1.0 \times 0.94 \times 9 \times 1440 = 31396 + 12182 = 43578$ kN = 43.58 MN. The total safety factor $F_t = Q_{ult}/Q$ = 2.18. Surficially, the total safety factor is adequate but not great enough. Indeed, a pile's UBC P_u will greatly increase with the dissipation of EPWP during the intermission time 28

days after the end of driving, before construction and during the 200 days construction period. This F_t is temporary at the moment when both the total load and the raft load reach their respective maximum values, afterward, the total load will be constant but the raft's load will fall to a lower value. The long-term total safety factor should be great enough.

8.3.2Checking Total Safety Factor Increasing With Consolidation

Considering the effect of EPWP, the following new results are obtained:

a) Calculation of Parameters:

Equivalent radius of pile $r_e = \sqrt{\frac{1}{\pi}}b = \sqrt{\frac{1}{\pi}}\ 0.4$=0.2257m, d=$2r_e$≈0.45m

Equivalent diameter of group piles $D_e = \sqrt{\frac{4}{\pi}n_p A_p} = \sqrt{\frac{4}{\pi}\times 9\times 0.4^2}$ =1.3541m

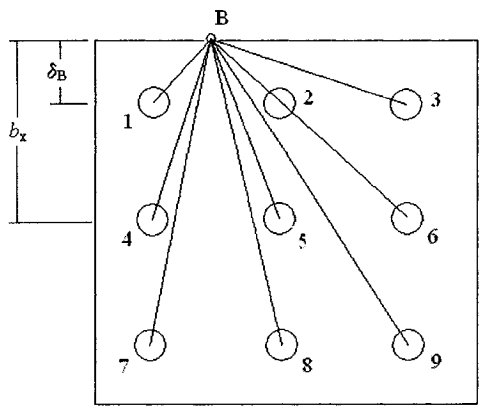

Fig. 8-6 Schematic Diagram of Piles and Raft

Half breadth of maximum EPWP $b_x = S+\delta_B$ (Shown in Fig. 8-6)

Set $\delta_B = \eta d$

According to (6.2-3),

$$u_B = \frac{\Delta u_m}{Ln\omega}\left[nLn(\omega r_0) - \sum_i^n Ln(r_i)\right] = \frac{\Delta u_m}{Ln\omega}\left[9Ln\left(\omega\frac{d}{2}\right) - \sum_{i=1}^{9} Ln(r_i)\right] \le \Delta u_m$$

$$\therefore f(\eta) = 9Ln(\tfrac{1}{2}\omega) - Ln\omega - Ln\{(9+\eta^2)[9+(6+\eta)^2][9+(12+\eta)^2]\}$$

$$- 0.5\,Ln\{(81+\eta^2)[81+(6+\eta)^2][81+(12+\eta)^2]\} = 0$$

When $\omega = 25$, $\eta = 1.762$, $f(\eta) = 8.8\times10^{-5} \approx 0$

Thus, $\delta_B = \eta d = 1.762 * 0.45 = 0.793 \approx 0.8$ m

According to (6.2-2), similarly,

$$u_B = \Delta u_m R^2 \sum_{i=1}^{n} \frac{1}{r_i^2} = \Delta u_m (0.5a \cdot d)^2 \sum_{i=1}^{n} \frac{1}{r_i^2} \le \Delta u_m$$

$$\therefore f(\eta) = (0.5a)^2\left(\frac{2}{9+\eta^2} + \frac{2}{9+(6+\eta)^2} + \frac{2}{9+(12+\eta)^2}\right.$$

$$\left. + \frac{1}{81+\eta^2} + \frac{1}{81+(6+\eta)^2} + \frac{1}{81+(12+\eta)^2}\right) = 1$$

When $a = 4$, $\eta = 1.3614$, $f(\eta) = 0.99964 \approx 1$

Thus, $\eta = 1.3614$~1.762; taking $\eta = 1.56$

Take $\delta_B = 0.7$ m

Hence, $b_x = b_y = (S/d+\eta)d = (6+1.56)d = 7.56 \times 0.45 = 3.4$ m

The radius of zero EPWP, according to experimental results (Tang 1990),

(1) $l_r = 1.5L = 1.5 \times 20\ m = 30$ m ($\omega = l_r/b_x = 30/3.4 = 8.82$)

or (2) $l_r = 4(B/2) \approx 2 \times 8.1 = 16.2\ m$

(3) $l_r = 12D_e = 12 \times 1.354 = 16.25$ m

From the above (1)~(3), taking $l_x = 17$ m ($\omega = l_x/b_x = 17/3.4 = 5$) is better.

Radius of permeable boundary

$R_x = l_x = 17m$ ($b_x/R_x = 3.4/17 = 0.2$, $U_{xy}(T)$ curve in Fig. (7.4-10-1b)

Depth of vertical permeable boundary

$R_z = l_z = 10$ m (permeable bottom boundary)

Contribution of initial EPWP: $\Delta u_m(z)=\sigma'_{vo}(z)=\gamma d_w+\gamma'(D-d_w)+\gamma' z = 18+8z$ (Kpa)

b) Increment of UBCP (ultimate bearing capacity of pile)

by (7.4-15a),

$$\Delta P_c=\Delta P|_{t=\infty} = \Delta P_{cb}+\Delta P_{cs} = A_b \cdot u_{0b} + p\chi_\sigma\chi_\varphi \sum u_0 \Delta z$$

Now, $A_b = 0.16\text{m}^2$, $u_{0b}=18+8\times20=178$ kPa, $p = 4\times b = 1.6$m, $\chi_\sigma = \chi_{av} = \dfrac{5+2\mu}{12(1-\mu)} = 0.8056$,

$\chi_\varphi = \dfrac{Sin\varphi' Cos\varphi'}{1+Sin^2\varphi'} = 0.3659$, $A_{u0} = \sum u_0 \Delta z = (18+160) \times 20/2 = 1780$ kPa·m.

Hence, $\Delta P_{cb} = 28.5$ kN, $\Delta P_{cs} = 839.5$ kN, $\Delta P_c = \Delta P|_{t=\infty} = 28.5+839.5 = 868$ kN.

Because, $P_{uk}=1440=P_{ut}|_{t=28day} = P_{u0}+\Delta P|_{t=28day}$

$\Delta P|_{t=28day} = 122.8$ kN (determined by Table7.4-5)

$\therefore$ $P_{u0} = P_{uk} - \Delta P|_{t=28day} = 1440-122.8 = 1317.2$ kN

Calculation of $U(t)$ and $P_{ut}(t)$ is shown in Table 8-5.

Considering a raft's effect on the UBC of piles according to Eqs (7-40) and (7-41):

Because of the permeable bottom boundary, $\Delta\sigma_b(t) \equiv \Delta\sigma_b = Ip_r = IQ_r/A = 0.064Q_r/A$, regardless of whether this is for a center pile, edge piles or corner piles, because of Saint Venant's principle in elastic mechanics .

Selecting H_1=0, H_2=20. Griffith's influence factor, $I_{a(H2)} = 4 \times 0.09 = 0.36$ for a center pile, $I_{a(H2)} = 2 \times (0.11+0.055) = 0.33$ for edge piles, $I_{a(H2)} = 0.13 + 2 \times 0.06 + 0.035 = 0.285$ for corner pile; average $I_{a(H2)} = (0.36 + 4 \times 0.33 + 4 \times 0.285)/9 = 0.313$

□ $A_{u0r} = 0.313H_2 \cdot p_r = 6.26p_r = 6.26Q_r/A$;

$pK_0 tg\bar{\varphi}' \approx p(1-sin\bar{\varphi}')tg\bar{\varphi}' = 1.6\times(1-sin28°)tan28° = 0.4513$m

$\Delta P_{ur}(t) = A_b \cdot \Delta\sigma_b(t) + pK_0 \cdot tg\varphi' U_{crl}(t)\, A_{u0r} = 0.16\times0.064Q_r/A + 0.4513\times6.26U_{crl}(t)\, Q_r/A$

$= [0.0102+2.825U_{crl}(t)]\, Q_r/A$

The consolidation coefficient in 3-D is taken as $C_{v3}=(2C_h+C_v)/3=5\times10^{-2}$ m^2/day

The raft's effect on the UBC of piles and a comparison among values calculated according to different considerations is shown in Table 8-5 and Fig. 8-7.

c) Total Safety Factor Increasing With Consolidation

Taking into account the dissipation of EPWP from driving and from raft-bottom pressure, at the moment t_m, when total load reaches its maximum and remains stable and the raft's bearing load reaches its summit, $Q_{ult} = \eta_r q_u A + \eta_g \xi_p n P_u = 1.27\times428\times7.6^2 + 1.0\times 0.90\times9\times1883 = 31396 + 15252 = 46648$ kN, Total Safety Factor $F_t = Q_{ult}/Q = 2.33$.

At the final stage, taking c = 10 kPa, φ = 28°; $N_c = 25.80$, $N_q = 14.72$, $N_r = 16.72$; $F_{cs} = 1.57$, $F_{qs} = 1.53$, $F_{rs} = 0.6$; $F_{cd} = 1.053$, $F_{qd} = 1.039$, $F_{rd} = 1.0$; $q_u = 1152.7$ kPa; without considering the raft's increasing effect, $Q_{ult} = \eta_r q_u A + \eta_g \xi_p n P_u = 1.1\times1152.7\times7.6^2 +$

$1.0\times0.90\times9\times2163.5 = 73238 + 17524 = 90762$ kN, $F_t = Q_{ult}/Q = 4.54$.

Considering a raft's increasing effect, $Q_{ult} = \eta_r q_u A + \eta_g \xi_p n P_u = 73238 + 1.0\times0.90\times9 \times2250.4 = 73238 + 18228 = 91466$ kN, $F_t = Q_{ult}/Q = 4.57$.

A comparison of the results from different analysis methods with or without EPWP effect due to driving and to raft-bottom pressure is shown Table 8-8.

Table 8-5 Calculation and Comparison of UBCP

R_r=	17	m,	R_z=	10	m,	P_{cs}=	839.5	KN,			
C_h=	0.06	m^2/d,	C_v=	0.03	m^2/d,	P_{cb}=	28.5	KN			
t (day)	0	10	**28**	45	100	150	250	345	500	1000	2000
T_{xy}	0	0.00384	0.00581	0.00934	0.02076	0.03114	0.05190	0.07163	0.10381	0.20761	0.41523
U_{xy} (l_x/b_x=5)	0	0	0.01	0.03	0.075	0.14	0.215	0.29	0.38	0.62	0.86
T_v		0.003000	0.0084	0.01350	0.03000	0.0450	0.0750	0.1035	0.150	0.30	0.60
U_v		0.062	0.103	0.131	0.195	0.239	0.326	0.372	0.440	0.613	0.816
U_t=1-(1-U_r)(1-U_z)	0	0.062	0.112	0.157	0.256	0.346	0.471	0.554	0.653	0.853	0.974
$\Delta\sigma'_b(t)$	178	178	178	178	178	178	178	178	178	178	178
$\Delta P_{cb}(t)=A_b\cdot\Delta\sigma'_b(t)$	28.48	28.48	28.48	28.48	28.48	28.48	28.48	28.48	28.48	28.48	28.48
$\Delta P_{us}(t)=P_{cs}\cdot U_t$	0	51.88	94.35	131.95	214.73	290.34	395.57	465.25	548.12	716.16	817.82
$\Delta P_{ut}=\Delta P_{cb}(t)+\Delta P_{us}(t)$	0	80.36	**122.8**	160.43	243.21	318.82	424.05	493.73	576.60	744.64	846.30
$P_{up}(t)=P_{u0}+\Delta P_{cb}+\Delta P_{us}$	1317.2	1397.5	1440	1477.6	1560.4	1636.0	1741.2	1810.9	1893.8	2061.8	2163.5
$Qt(MN)$	0	0	0	0	3.67	7	13.67	20	20	20	20
$Q_r=Q_t-\xi_p\times n_p\times P_{up}$ (KN)					(623.9)*	(1400)*	(3400)*	5332	4660	3299	2476
Δt_k				0	55	50	100	95	155	500	1000
$T_k=C_{v3}t_k/B^2$					.0476	0.091	0.177	0.26	0.394	0.827	1.69
$U_{cr}(\Delta t_k/2)$					0.125	0.12	0.175	0.17	0.22	0.54	0.65
$U_t(t_k)$ by (7.5-31,or 36, 37)					0.125	0.165	0.232	0.308	0.528	1.0(1.07)	1.0
$\Delta P_{ur}(t)=[0.0102+2.825U_{cr}(t)]\ Q_r/A$	0	0	0	0	3.9	11.5	39.2	72.2	100.0	115.9	86.9
$P_u=P_{up}+\Delta P_{ur}$	1317.2	1397.5	1440	1477.6	1564.3	1647.5	1780.4	1883.1	1993.8	2177.7	2250.4
Modified $Q_t-\xi_p\times n_p\times P_u(t)$ (KN)					623.9	1400	3400	4748	3850	2361	1772

Value in brackets ( ) is estimated by the theoretical formula (7.5-18) when pile load < UBCP

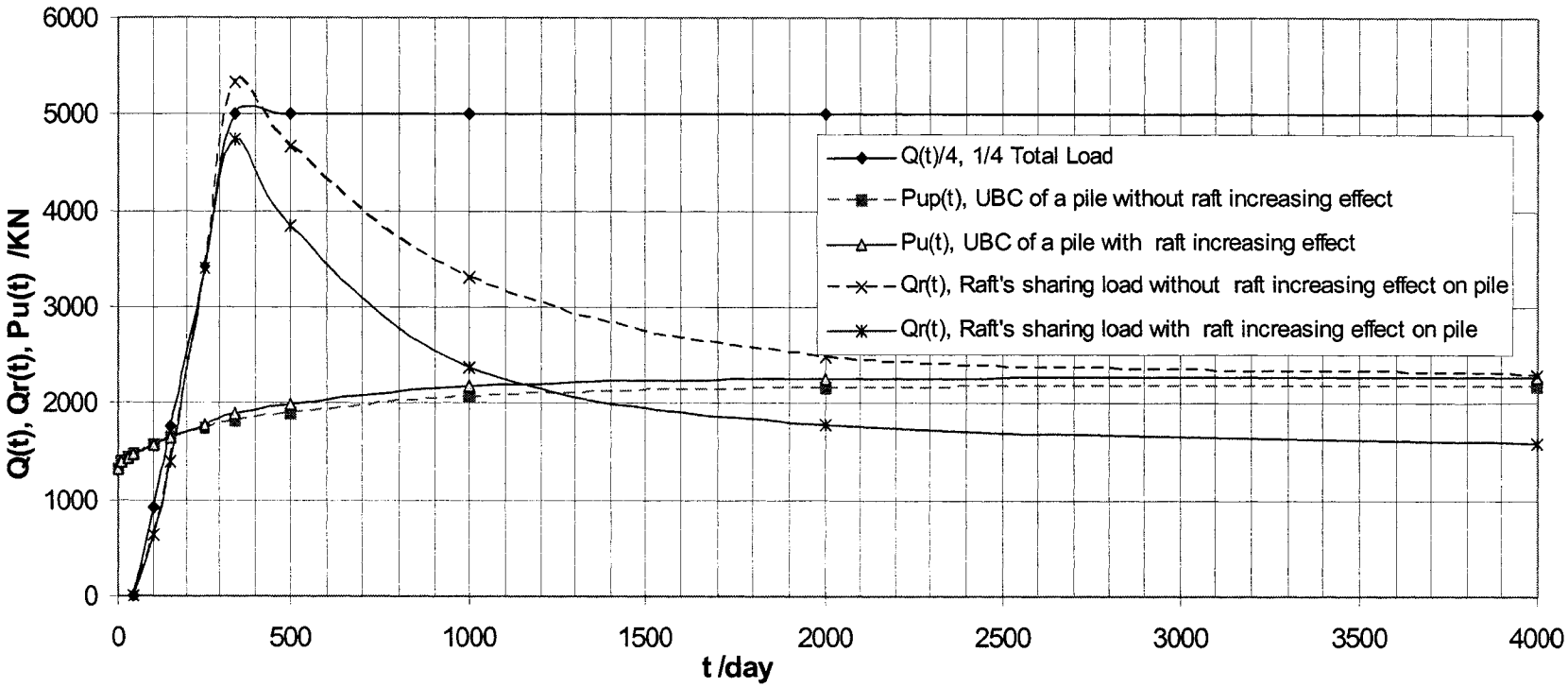

Fig. 8-7 Shared Loads-Time Curves

8.3.3 Estimation of Settlement

Computation of k_1: Method 1, by Randolph & Wroth (1978):

$$k_{e1} = \frac{P_{top}}{W_{top}} = \frac{\dfrac{4\eta}{(1-\mu_s)\xi} + \rho\dfrac{2\pi}{\varsigma}\dfrac{\tanh\mu l}{\mu l}\dfrac{l}{r_0}}{1+\dfrac{1}{\pi\lambda}\dfrac{4\eta}{(1-\mu_s)\xi}\dfrac{\tanh\mu l}{\mu l}\dfrac{l}{r_0}} G_l r_0 = \frac{13.33+556.69\frac{\tanh\mu\ell}{\mu\ell}/\zeta}{1+0.02564\frac{\tanh\mu\ell}{\mu\ell}} \qquad (8\text{-}1)$$

in which the meanings of the above are the same as in equation (3.1-8): $l/r_o = 20/0.2257 = 88.6$, $\eta = r_b/r_o = 1$, $\xi = G_l/G_b = 0.5$, $\rho = G_{av}/G_l = 1$, $\lambda = E_p/G_l = 22\text{GPa}/3.6\text{ MPa} = 6111$, $\zeta = \ln(r_m/r_o) = \ln\{\langle 0.25+\xi[2.5\rho(1-\upsilon_s)-0.25]\rangle l/r_o\} = \ln(0.875\, l/r_o) = \ln(77.525) = 4.97$, $\mu l = (l/r_o)\sqrt{(2/\zeta\lambda)} = 0.4641$. Hence, $k_{e1} = 115.18 G_l r_o = 93.6$MN/m. This is an under-estimate of k_{e1} but taking $\zeta = \ln(r_m/r_o) = \ln(40) = 3.69$, $k_{e1} = 150.62 G_l r_o = 122.4$ MN/m.

Method 2, by Poulos & Davis (1980),

$$k_{e1} = \frac{P_{top}}{W_{top}} = \frac{E_s d}{I} = \frac{E_s d}{I_0 R_K R_H R_b R_v} \qquad (8\text{-}2)$$

According to pages 87~89 of Poulos & Davis (1980), for $l/d = 20/0.45 = 44$, $I_0 = 0.046$, $R_K = 1.0$, $R_H = 0.85$, $R_b = 0.97$, $R_v = 0.96$ when Poisson's ratio $\mu = 0.40$. Hence, $k_{e1} = 27.4650\, E_s d = 124.0$MN/m.

Hence, k_{e1}=123MN/m.

Computation of K_{pe}:

Method 1, according to (2-4),

$$K_{pe} \approx k_{e1} \cdot n^{1-e} \qquad (2\text{-}4)$$

Where e = 0.55×1.1×0.83×1.05×0.97 = 0.5114 from page 192 of Fleming et al (1992). Hence, $K_{pe} \approx 123 \times 9^{1-0.5114} = 360$MN/m.

Method 2, using conception of settlement ratio,

$$K_{pe} \approx k_{e1} \cdot n/R_s \qquad (8\text{-}3)$$

Where $R_s = R_{s0}\xi_h\xi_b\xi_v$. According to pages 118~125 of Poulos & Davis (1980), $R_{s0} = 3.6$, ξ_h=0.92, ξ_b=0.95, ξ_v=1.025 when Poisson's ratio μ=0.40, R_s=3.26. Hence, $K_{pe} \approx k_{e1} \cdot n/R_s$ =123×9/3.26=340MN/m

Method 3, using conception of pile-pile interaction factor, shown in Table 8-6.

Table 8-6 Factor of pile-pile interaction

r	0	S	S√2	2S	S√5	S2√2
r/d	0	6.0	8.485	12.0	13.416	16.968
α_{ij}	1.0	0.244	0.191	0.139	0.122	0.086

Notice P_1=P_3=P_7=P_9, P_2=P_4=P_6=P_8, we have

$$\left.\begin{aligned} S_5 &= \frac{P_5}{k_1} + 4\alpha_{pp}(S)\frac{P_2}{k_1} + 4\alpha_{pp}(S\sqrt{2})\frac{P_1}{k_1} \\ S_2 &= \alpha_{pp}(S)\frac{P_5}{k_1} + [1 + 2\alpha_{pp}(S\sqrt{2}) + \alpha_{pp}(2S)]\frac{P_2}{k_1} + 2[\alpha_{pp}(S) + \alpha_{pp}(S\sqrt{3})]\frac{P_1}{k_1} \\ S_1 &= \alpha_{pp}(S\sqrt{2})\frac{P_5}{k_1} + 2[\alpha_{pp}(S) + \alpha_{pp}(S\sqrt{3})]\frac{P_2}{k_1} + [1 + 2\alpha_{pp}(2S) + \alpha_{pp}(S2\sqrt{2})]\frac{P_1}{k_1} \end{aligned}\right\} \qquad (8\text{-}4)$$

Set C=k_1S_5= k_1S_2 =k_1S_1=k_1S, (7.6-4) become

$$\left.\begin{aligned} C &= 1.000P_5 + 0.976P_2 + 0.764P_1 \\ C &= 0.244P_5 + 1.5218P_2 + 0.732P_1 \\ C &= 0.191P_5 + 0.732P_2 + 1.364P_1 \end{aligned}\right\} \qquad (8\text{-}5)$$

Solving (8-5) obtains, P_1=0.4944C, P_2=0.3791C, P_5=0.2523C

$$Q=4P_1+4P_2+P_5$$

$$=3.7461C$$

$$=3.7461\ k_1S \qquad (8\text{-}6)$$

Hence, $K_{pe}=Q/S=3.7461k_1=460.8$ MN/m

Method 4, the results from FLM (δ_{ij} values are corrected by modified factor) in Test 9, Chapter 4, $K_{pe} = Q/S \approx 417$MN/m.

Discussion: The values of K_{pe} from equations (2-4) and (8-3) are based on solutions of complete elastic theory and they are not corrected by modification factors. The values of K_{pe} from Methods 3 and 4 are corrected by the modification factors, and so may agree more with the actual situation.

For a comparison of the simplified and numerical methods, we take K_{pe} = 360MN/m.

Computation of K_r:

According to (2-3) (from Poulos & Davis 1974),

$$K_r \approx 2.25G_sB/(1-\nu_s) = 108.44 \text{ MN/m},\ K_r \approx 1.01E_sB/(1-\nu_s^2) = 97.4 \text{ MN/m}$$

Take K_r = 100 MN/m

Computation of K_{pr}:

According to Equation (2-5) (from Randoph & Clancy, 1993), an equivalent interactive factor value can be taken

$$\alpha_{rp} \approx 1-\frac{Ln(r_c/r_0)}{\zeta} = 0.5161,\ 0.3483 \text{ or } 0.1972 \text{ (when } \zeta = 4.97,\ 3.69 \text{ or } 2.996)$$

Hence, in the elastic state

$$K_p = K_{pe} = K_{ps} = 360\text{MN/m},\ K_{pe}/K_r = 360/100 = 3.6$$

$$K_{pr} = \frac{1+\frac{K_p}{K_r}-2\alpha_{rp}\frac{K_p}{K_{pe}}}{1-\alpha_{rp}^2\frac{K_r}{K_{pe}}\frac{K_p}{K_{pe}}}K_r = \frac{1+3.6-2\times\alpha_{rp}}{1-\alpha_{rp}{}^2/3.6}\times 100 = \begin{pmatrix}3.85\\4.04\\4.25\end{pmatrix}\times 100 = \begin{pmatrix}385\\404\\425\end{pmatrix}\text{MN/m}$$

$$\eta_s = \frac{Q_r}{Q_p+Q_r} = \frac{1-\alpha_{rp}\frac{K_{ps}}{K_{pe}}}{\frac{K_{ps}}{K_r}+\left(1-2\alpha_{rp}\frac{K_{ps}}{K_{pe}}\right)} = \frac{1-\alpha_{rp}}{3.6+1-2\times\alpha_{rp}} = \begin{cases}13.87\% & (\zeta = 4.97)\\17.05\% & (\zeta = 3.69)\\19.44\% & (\zeta = 3.00)\end{cases}$$

From FLM result (Modified elastic theory method), Fig. 3-12(3), η_s=17.23%, approximates the value when ζ=3.69. Hence, take α_{rp}=0.348.

In non-linear state, set $Q_{pu}=0.9nP_u$=11.66MN.

Load-Settlement Curve without Consolidation Factor

Similar to the method of Fig.7-2, setting $\Delta Q = 0.5\ MN$, $Q_i = Q_{i-1} + \Delta Q$, $Q_{pi} \approx Q_i(1-\eta_{st\ i-1})$, $K_{pi} = K_p[(Q_i + Q_{i-1})/2]$ (i=1,2,3,...); thus calculating $\eta_{st\ i}$, K_{pri} and $W_i = W_{i-1}+\Delta Q \cdot K_{pri}$ reaching the data of Q-W curves in Fig. 8-8, in which consolidation and time factors are not considered. The Q-W curve from Equation (7-7) in Fig. 8-8 is very close to that obtained from the numerical result in Fig. 3-12(1).

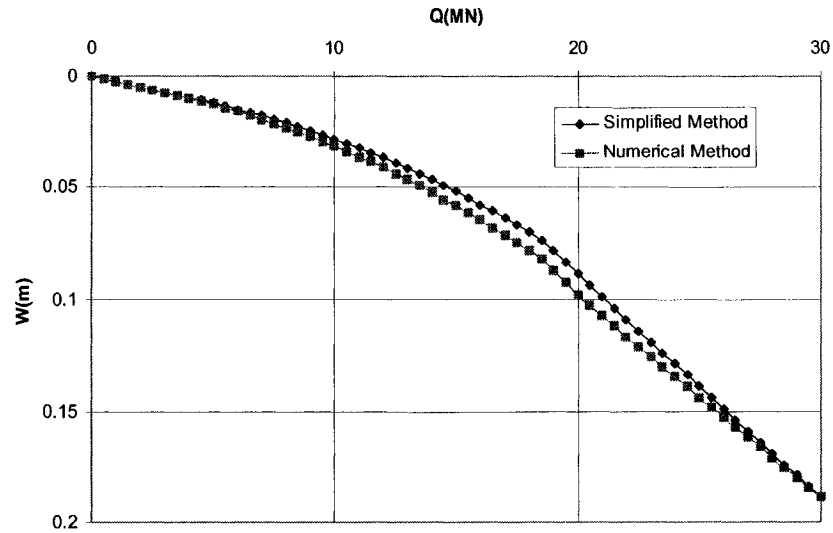

Fig. 8-8 Q-W Curves from Simplified and Numerical Methods

Settlement-Time Curve with Consolidation Factor

Setting soil drained formation modulus $E_{sc}=E_s=10MPa$, the shear modulus $G_s=\frac{E_s}{2(1+\mu_s)}=3.57$ MPa. Thus, soil undrained formation modulus $E_{su}=3G_s=10.71MPa$.

On the other hand, according to empirical formulae, $E_{su}=(250\sim500)c_u=(250\sim500)\times40=10\sim20$ MPa. Thus, taking $E_{su}=15$ MPa is more reasonable.

The soil unload-reload deformation modulus is taken as $E_{ur}=2.5E_{sc}=25\ MPa$. Hence,

$K_{dr}\approx 1.35E_{su}B/\alpha_r=174.9$ MN/m; $K_{pe}=360$ MN/m;

$K_r\approx 1.01E_{sc}B/[\alpha_r(1-\mu_s^2)]=91.4$ MN/m; $K_{cd}=1/(1/K_r-1/K_{dr})=191.5$ MN/m

$$m_v=\frac{(1+\mu)(1-2\mu)}{(1-\mu)E_{ur}}=0.47/E_{ur}$$

Near the center, $S_{cp}=m_v A_{u0}=0.47\times1780/25000=0.0335$ m (=3.35 cm);

Near an edge or a corner, $m_{vb}=\frac{(6+\mu)(1-2\mu)}{6(1-\mu)E_{ur}}=0.36/E_{ur}$, $S_{cp}=m_{vb}A_{u0}=0.0257$ m =

2.57 cm.

The average $S_{cp} = (2.57+2\times3.35)/3 = 3.09$cm.

According to (7-15a~c), (7-16), one can estimate S_{dr}, S_{dp}, S_{cr}, and $S_{cp}(t)$, shown in Table 8-7. The final total settlement–time curves are estimated according to equations (7-18~20), shown in Fig. 8-9. A comparison of different settlement-time curves with or without raft's increasing effect on UBC of pile is shown in Fig. 8-10.

Table 8-7 Calculation of Settlement for Interactive Piled Raft

R_r=	12.5	R_z=	10		K_{dr}=	174.9 MN/m		K_r=	91.4 MN/m		S_{cp}=	0.0309
C_h=	0.06	C_v=	0.03 day		K_{pe}=	360 MN/m		K_{cr}=	191.5 MN/m		α_{rp}=	0.348
t (day)	0	10	28	45	100	150	250	345	500	1000	2000	4000
$U_{cp}(t)$	0	0.062	0.112	0.157	0.256	0.346	0.471	0.554	0.653	0.853	0.974	0.999
$S_{cpt}(t)=S_{cp}U_{cp}(t)$	0	0.0019	0.0035	0.0049	0.0079	0.0107	0.0146	0.0171	0.0202	0.0264	0.0301	0.0309
t_k (day)				0	55	105	205	300	455	955	1955	3955
$\Delta\tau_k$				0	55	50	100	955	155	500	1000	2000
$T_k=C_{v3}t_k/B^2$				0	0.0476	0.091	0.177	0.26	0.394	0.827	1.692	3.42
$U_{cr}(t_k)$				0	0.18	0.28	0.37	0.5	0.53	0.65	0.72	0.8
$U_{crl}(t_k)$				0	0.125	0.165	0.232	0.308	0.528	1(1.07)	1(1.18)	1(1.26)
Q_t(MN)				0	3.67	7	13.67	20	20	20	20	20
ΔQ_t				0	3.67	3.33	5.332	6.33	0	0	0	0
Q_r				0	0.6239	1.400	3.400	4.748	3.850	2.361	1.772	1.590
ΔQ_r				0	0.6239	0.776	2.000	1.348	-0.898	-1.489	-0.589	-0.182
Q_p				0	3.046	5.600	10.270	15.252	16.150	17.639	18.228	18.410
ΔQ_p				0	3.0461	2.5539	4.6700	4.9820	0.8980	1.4890	0.5890	0.1820
$\Delta S_{drk}=\Delta Q_r/K_{dr}$				0	0.0036	0.0044	0.0114	0.0077	-0.001	-0.0017	-0.0007	-0.0002
$S_{drk}=Q_r/K_{dr}$				0	0.0036	0.0080	0.0194	0.0271	0.0261	0.0244	0.0237	0.0235
$\Delta S_{dpk}=\Delta Q_p/K_p$				0	0.0085	0.0071	0.0130	0.0138	0.0025	0.0041	0.0016	0.0005
$S_{dpk}=Q_p/K_p$				0	0.0085	0.0156	0.0285	0.0424	0.0459	0.0490	0.0506	0.0511
$S_d=S_{drk}+\alpha_{rp}*S_{dpk}$				0	0.0065	0.0134	0.0294	0.0419	0.0421	0.0415	0.0414	0.0413
$\Delta S_{crk}=\Delta Q_r/K_{cr}$				0	0.0033	0.0041	0.0104	0.0070	-0.0009	-0.0016	-0.0006	-0.0002
$S_{crk}=Q_r/K_{cr}$				0	0.0033	0.0073	0.0178	0.0248	0.0239	0.0223	0.0217	0.0215
$S_{crt}(t)=S_{crk}*U_{crl}(t_k)$				0	0.0004	0.0012	0.0041	0.0076	0.0126	0.0223	0.0217	0.0215
$S_{ct}(t)=S_{crt}(t)+S_{cpt}(t)$	0	0.0019	0.0035	0.0049	0.0083	0.0119	0.0187	0.0247	0.0338	0.0487	0.0518	0.0524
$S_{rrt}(t)=S_{dr}+S_{crt}(t)$				0	0.0040	0.0092	0.0236	0.0348	0.0397	0.0467	0.0454	0.0450
$S_{rpt}(t)=\alpha_{rp}*S_{dpk}+S_{crt}(t)$				0	0.0034	0.0066	0.0140	0.0224	0.0292	0.0394	0.0393	0.0393
$S(t)=S_d+S_{ct}(t)$	0	0.0019	0.0035	0.0049	0.0148	0.0253	0.0481	0.0666	0.0759	0.0902	0.0931	0.0937

1). Value in brackets ( ) is the value calculated by the theoretical formula (7-36, 37). Because they >1, take them as 1.

2). When $\Delta Q_r<0$, calculating ΔS_{drk} and ΔS_{crk} using unload modulus E_{ud} or E_{uc} is 5 times of loading modulus.

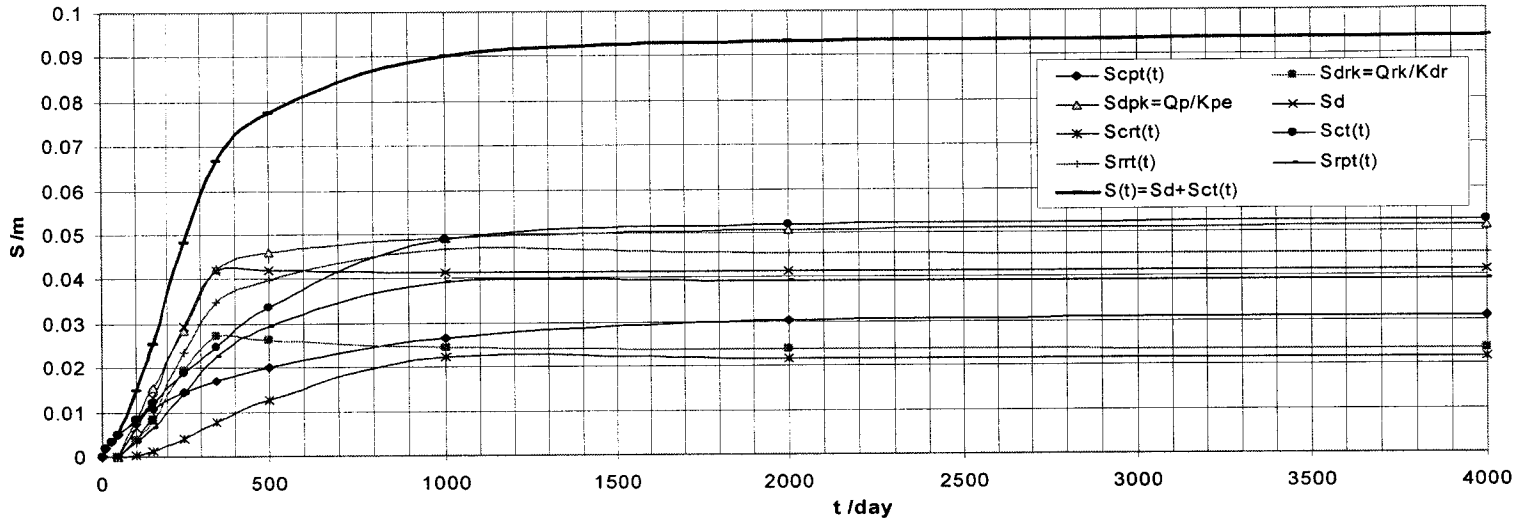

(a) S(t) curves

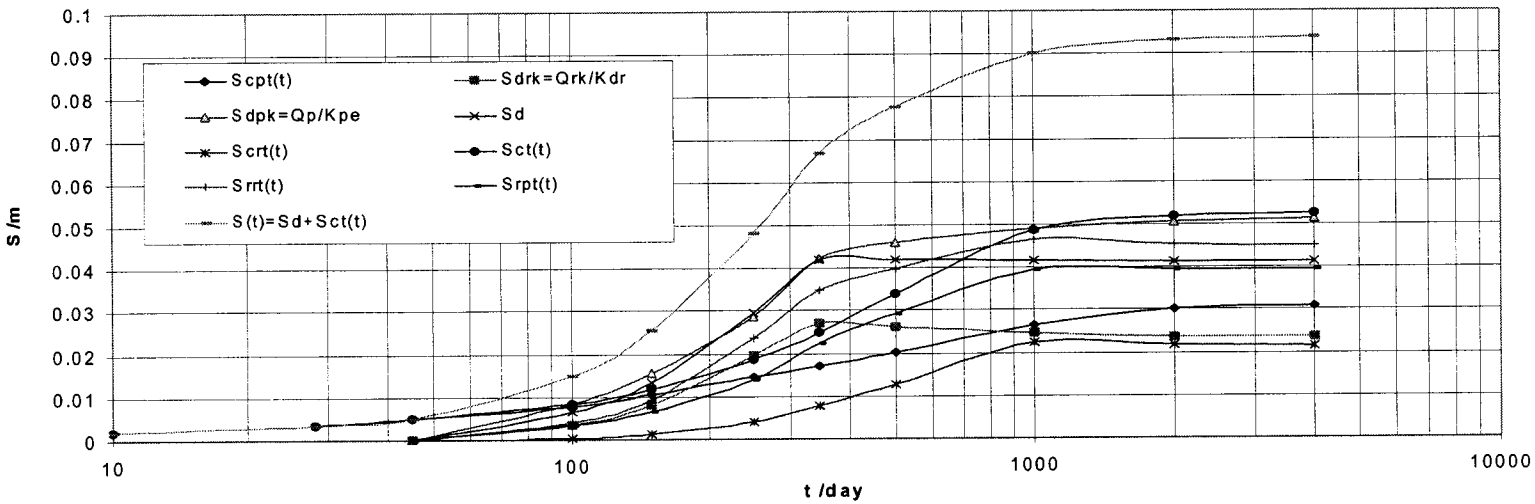

(b) S-$\log_e$(t) curves

Fig. 8-9 Estimated Settlement-Time Curves with Raft's Increasing Effect on UCB of Piles

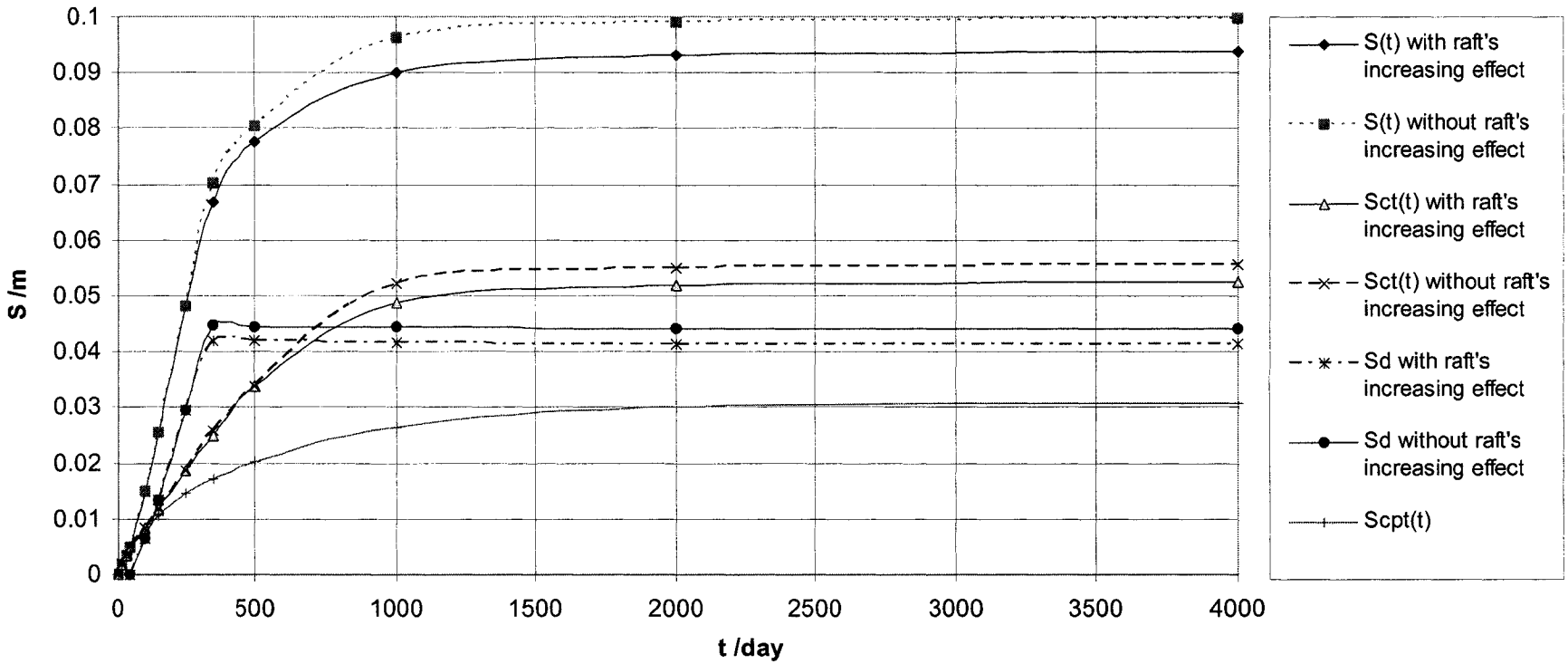

Fig. 8-10 Comparison of different Settlement-Time Curves due to Raft's Increasing Effect on UCB of Piles

8.3.4 Analysis Method Comparison

Table 8-8 presents a comparison of the results from different analysis methods with or without EPWP effects due to driving and to raft-bottom pressure. From the comparison, it is known that the total stress analysis method without EPWP effect is a conservative and safe method, one need not fear for the settlement problem from EPWP effect due to driving and to raft-bottom pressure, so long as the in-design pressure of the raft bottom is controlled under enough safety factor, e.g. $F_t > 2$ in the case of the maximum load of the superstructure, because an increase of the piles' UBC from EPWT dissipation and soil consolidation will greatly decrease the raft-bottom's pressure and consequently reduce the settlement.

The analysis methods with the EPWP effect due to driving and to raft-bottom pressure give us a more detailed and accurate way to estimate shared loads, settlement and safety factor, or stability degree, of the pile-soil-raft interaction during construction and at the final stage.

Table 8-8 Comparison of Analysis Methods

Analysis Methods	**State at Peak Load ($t=t_m$)**	**State at the final ($t=\infty$)**
(A) Total stress analysis without EPWP effect	P_{uA}=1.440MN; Q_{pA}=11.5MN; Q_{sA}=8.5MN; η_{sA}=42.5%; F_{tA}=2.12 ; $S_A(t_m)$=10.0cm	No time factor in analysis, so P_{uA}=1.440MN; Q_{pA}=11.5MN; Q_{sA}=8.5MN; η_{sA}=42.5%; But, F_{tA}=4.27; $S_A(\infty)$=10.0cm;
(B) with EPWP effect but without raft effect	P_{uB}=1.810MN; Q_{pB}=14.66 MN; Q_{sB}=5.330MN; η_{sB}=26.7%; F_{tB}=2.30 ; $S_B(t_m)$=7.03cm	P_{uB}=2.163MN; Q_{pB}=17.524MN; Q_{sB}=2.476 MN; η_{sB}=12.4 %; F_{tB}=4.54 ; $S_B(\infty)$=9.97cm
(C) with EPWP effect and raft effect on piles	P_{uC}=1.883 MN; Q_{pC}=15.25MN; Q_{sC}=4.748 MN; η_{sC}=23.7%; F_{tC}=2.33 ; $S_C(t_m)$=6.66cm	P_{uC}=2.225MN; Q_{pC}=18.02 MN; Q_{sC}=1.98 MN; η_{sC}=9.9%; F_{tC}= 4.57 ; $S_C(\infty)$=9.37cm
Comparison of the results	P_{uB}/P_{uA}=1.257; P_{uC}/P_{uA}=1.308; Q_{sB}/Q_{sA}=0.627; Q_{sC}/Q_{sA}=0.559; F_{tB}/F_{tA}=1.085; F_{tC}/F_{tA}=1.099; S_B/S_A=0.703; S_C/S_A=0.666.	P_{uB}/P_{uA}=1.502; P_{uC}/P_{uA}=1.545; Q_{sB}/Q_{sA}=0.291; Q_{sC}/Q_{sA}=0.233; F_{tB}/F_{tA}=1.063; F_{tC}/F_{tA}=1.070; S_B/S_A=0.997; S_C/S_A=0.937.

P_u=Average UBCP; Q_p=Load born by all piles; Q_s=Load born by raft; $\eta_s=Q_s/(Q_s+Q_p)$; F_t=total safty factor; S=Settlement; Subcripts A, B and C are respectively reponsed to Analysis Methods (A), (B) and (C).

8.4 Discussions

From the above analysis and case calculations, some interesting conclusions are obtained:

1) Theoretical studies and field measured data both point out that after a pile is loaded axially, the soil around the pile is borne by pure shear stress under constant volume; therefore the change of EPWP in the soil around the pile shaft caused by the load on the pile top can be neglected in calculations of UBCP variation with time.
2) The method to calculate the UBCP's change with time based on Equation (6-21) is practical and convenient. By the means of this method, one can estimate the change of the UBCP with the time factor and the soil consolidation not only for a single pile but also for piles in groups.
3) The value of the dynamic penetration resistance during pile driving is not the initial UBCP, when soil cohesion c has recovered in the condition in which EPWP is constant or the consolidation degree remains zero. Hence, the value cannot be used in calculations of the UBCP's change with time.
4) The simplified and convenient method to calculate non-linear load-settlement curves based on equations (7-7) and (7-8), established in this thesis, reaches desirable results when compared to that of numerical analysis. In this method, the interactive factor of pile to raft, α_{rp}, is reset, and the method can estimate whole load-settlement curves of pile-soil-raft nonlinear interactions and the variations of load sharing proportions.
5) Because the effective additional vertical stress from change in the EPWP that remains during pile driving is unload-reload stress, the settlement from consolidation of the EPWP can be estimated by using the swell index C_s, or the unload-reload elastic

modulus E_{ur} and so long as the settlement proportion in the total settlement is not large.

6) When total load Q reaches its maximum, e.g., usually end of superstructure construction and end of all other loads, the load shared by raft Q_s reaches up to a maximum (point $t \rightarrow t_m$ = 345 days in Fig. 8-7). Afterward, Q_s will decrease because the load shared by piles Q_p increases with the dissipation of EPWP and the consolidation of soil. One also can see that before the time ($t \leq \approx t_m$), settlement velocity reaches a maximum; while after time ($t > t_m$), the settlement velocity tends to get smaller and smaller, down to zero, and the settlement of the point is of about 0.8 times that of the total settlement. Therefore, loads and settlement of the point are selected as design check points.

7) In case 2 with linear loading with time, when $t_1 = t_m = 345$ days for $S_{cpt}(t)$, $t_2 = t_m = 300$ days for $S_{crt}(t)$, the consolidation degree from the pressure of raft bottom according to (7-33,34), $U_{cri}(t) = \frac{1}{S_{cr}} \sum_{i=1}^{n} \Delta S_{cri} U_{cr} \left(\frac{\Delta t_i}{2} + \sum_{j=i+1}^{n} \Delta t_j \right) \approx U_{cr}(t_n/2) = 0.3$, which may cause the UBC of pile to increase. It is noticed that the consolidation from the pressure of raft bottom always delay the shear stress action on the pile shaft. Hence, the increasing effect of a cap on the UBC of a pile may not be as great as that of the situation where the pressure on the raft bottom develops in the meantime with shear stress action on the pile shaft, which is similar to the results from Katzenbach (1998).

CHAPTER 9

CONCLUSIONS AND RECOMMENDATIONS

9.1 General

The nonlinear interaction of piles in pile-soil-cap was analysed during the pore water pressure dissipation. Accordingly, the bearing capacity and the settlement of the system were evaluated. Due to the immaturity of FEM in modeling volumetric locking problem and further due to the complexity of the interactions among these elements, this research work was divided into a series of steps including:

1) The development of Hybrid method, combining FLM with GSDT analyzes behaviours of pile-soil-cap nonlinear interaction without pore pressure factor;
2) Estimating the initial distribution of the excess pore water pressure after driving the pile group;
3) The development of analytical solutions to predict the pore pressure dissipation during the consolidation process;
4) Evaluation of the changing process of the ultimate bearing capacity of the pile group as a result of the system interaction;
5) The development of a simplified method to predict settlements and load ratios of the pile, soil and cap system as time dependants;
6) Cases analyses where several important conclusions for pile-soil-cap interaction can be drawn.

9. 2 Summary and Conclusions

Based on the results of the present investigation, the following findings and conclusions can be drawn:

1) The interactive effects on pile groups and piled-raft are meaningful only if the applied loads on the piles are near the ultimate bearing load.

2) Although the mechanism of the non-linear interaction of piles-soil-cap-raft (or box) is very complex, a relatively simplified and practical analysis method of the interaction has been developed and presented in this thesis. The method does not involve only the physical and the mechanical properties of the material making the system but also the on-going processes of the pore water pressure dissipation, soil consolidation, and deformations of soil and piles.

3) The FLM method was established on the basis of Fourier series to calculate the interaction between the raft and soil. However, in case of a longer range (Lg), the settlement coefficients in FLM analysis was fluctuating along the considered distance. To avoid such fluctuation, an appropriate maximum number of the finite Fourier series (Nr) was selected. Nevertheless, by increasing Nr values calculation volume will increase. Accordingly, a trial and error procedure was adopted to determine the appropriate Lg and the corresponding Nr.

4) The results of analysis using FLM-GSDT hybrid method showed that the ratio of pile-base load over pile–head load vary according to load location and level on the raft, even during the elastic phase. Hence taking the ratio as a constant as stated in the

literature is not reasonable. However, when the applied load on piles is near to the plastic or ultimate state, these ratios tend to stabilized.

5) The raft-decreasing-effect factor of a pile (ξ_p) was formularized in equations (3-21) and (3-22), and (3-23) for uniform soil. This provides better treatment as compared to the recommended value (0.9) by Zai (1992) and Burland (1995). In fact, equation (3-23) states that ξ_p is a function of the ratio of cap width over pile length (B/L), which provides a simple and convenient control of using bearing capacity of piles.

6) The results of the present numerical model of a single pile showed that the pore pressure generated during driving is not only due to cavity expansion but also due to an increase in the mean total stress caused by the skin friction along the pile and the point load at the pile's tip (Chapter 4). The effect on the pore pressure caused by residual forces is quite small and can be neglected.

7) The analysis of strength-stress relationships and field measurements showed that the excess pore pressure generated during pile driving increases almost linearly with depth. Fractures in soil and water during pile driving make the excess pore pressure fall into a stable level, in the order of the effective overburden pressure σ'_v. This becomes a major factor in predicting the excess pore pressure in the vicinity of a pile group.

Based on case calculation and field data, the variation of EPWP in a pile group with the horizontal distance is found to be linear.

8) Analytical solutions of pore pressure dissipation and consolidation were derived. These solutions are applicable for homogeneous soils under plane-strain, axi-symmetrical and three dimensional loading conditions.

9) It was proved that the well-known Carrillo's expression for 3-D consolidation degree, $(1-U)=(1-U_z)\cdot(1-U_{xy})$, is accurate when the initial condition u(x,y,z,0) can be expressed by the form of $\psi_1(z)\cdot\psi_2(x,y)$.

10) The value of the initial pore-pressure has little or no effect on the distribution of the pore water pressure after driving and with time. In fact, the PWP distributions were found to be small and become even smaller with time up to the point where these differences will disappear. Therefore, rough estimation of initial pore-pressure distribution may not produce large error on calculation of pore-pressure dissipation.

11) The effect of vertical consolidation can be neglected for cases where the ratio of the vertical consolidation coefficient over horizontal consolidation coefficient, C_v/C_h, is smaller than 0.25 and the ratio of vertical dissipation distance over horizontal dissipation distance, l_z/l_r, is larger than 2.

12) When using the numerical inversion of Laplace transform to solve the case of pore-pressure dissipation in layered soil, errors were introduced and divergences in the obtained values were appeared. Accordingly, it was necessary to carefully choose the calculation parameters and the number of trials to avoid such divergence of values.

13) The present analytical models and field measurements indicated that shortly after a pile is axially loaded, the soil around the pile will act in pure shear stress under constant volume; therefore the change of EPWP in the soil around the pile shaft, due to pile loading, can be neglected in the calculation of UBCP with time.

14) The variation of the normal stress on a pile's shaft $\Delta\sigma_h$' is not simply equal to the change of pore pressure Δu, due to mainly the horizontal displacement, which takes place as a results of the shrinkage of soil around piles during EPWP dissipation. The relationship between $\Delta\sigma_h$' and Δu was given by Equation (6-15).

15) A design theory is presented to evaluate the UBCP of a pile-soil-raft system during the consolidation process (Eq. 6-21). The proposed theory is practical and convenient to use. Furthermore, design charts are presented to provide the consolidation degree for soil in a given pile arrangement in a group (Figs. 6-9 and 6-10).

16) The deduced value of the dynamic penetration resistance during pile driving should not be taken as the initial UBCP, in cases of soil cohesion c has recovered, EPWP is constant or the consolidation degree remains zero. Hence, these values should not be used in the calculation of UBCP with time.

17) A simplified and convenient interaction analysis method to estimate the load-settlement curves of pile-soil-raft nonlinear interactions and the variations of load sharing proportions is established. The theory developed was validated by the results obtained by sophisticated numerical models and can be used to evaluate the

interactions of pile-soil-raft system. In the proposed method, the interactive factor of pile to raft, α_{rp}, was presented by Equation (7-21).

18) The change process of effective vertical stresses due to EPWP generation during piles drives and dissipation after the driving is an unload-reload cycling. Hence, the settlement produced as a result of the consolidation can be estimated by using the swelling index C_s, or the unload-reload elastic modulus E_{ur}. The settlement proportion in total settlement of the interaction was not found to be large.

19) For a step-loading situation, the raft's increasing action on the UBC of piles, due to an increment of the effective lateral pressure of the piles, goes into effect only after the completion of the consolidation under the previous step loads, but does not work at the beginning moment of loading, because the consolidation need a time.

20) Total load shared by the raft, Q_s, reaches a maximum value at the end of the construction. Afterward, Q_s decreases due to the load shared by piles, Q_p, increasing during the dissipation of EPWP and the consolidation of soil. Furthermore, it can be noted that at the end of construction, settlement velocity reaches a maximum; then tend to become smaller and smaller, until it reach a zero value. Case analyses show that the settlement at the time is main part (approximate 0.7 time) of the total settlement. Therefore, the loads and settlement of the time should be seen as critical key checking point of design.

21) The total safety factor of piles-soil systems is given by Eq. (2-11), in which the raft-decreasing-effect factor of the pile ξ_p can be estimated using Eqs. (3-21) and (3-22),

or (3-23). After selecting the total safety factor, the ratio of soil bearing capacity is determined using Eq. (2-11), and the number of piles (n_p) is then determined by Eq. (2-13). This design will allow the pile load to reach a state close to the ultimate bearing load, P_u, which should be added by the part increased due to consolidation according to Eq. (6-21), when the load shared by the raft, Q_s, also reaches its maximum.

22) The settlement due to the EPWP produced during piles driving is relatively small, because the part of settlement can be seen as due to unload-reload stress. The settlement due to the pressure of raft bottom is dominant. Therefore, besides controlling the total factor of safety, designer should also control the total settlements smaller than the allowed settlement. The settlement-load relationship for pile-soil—raft system is nonlinear and can be depicted from by Eqs. (7-7) and (7-8).

23) Under sufficient total safety factor, the settlements due to in-design pressures of a raft's bottom in the interactive foundation is deferent from that in un-piled foundation. Because after the superstructure's maximum load, an increase of piles' UBC due to EPWT dissipation and soil consolidation will greatly decrease the raft-bottom's pressure and accordingly greatly reduce the final settlement.

9.3 Recommendation for Future Research

In order to enhance the knowledge of foundation of the pile-soil-raft system and understanding further the interaction concepts and in order to encourage their applications in practice, future research should be directed toward the following:

1. Conduct field tests in order to further examine the theoretical models developed in the present investigation, as well as conclusions drawn from theoretical or numerical analysis given in the literature.
2. Develop theoretical models or empirical formulas to determine relationships between EPWP contribution to the UBC for piles during and after driving.
3. Investigate the effect of the parameters affecting the UBC and the settlement of piled foundations when superstructure loads reach their maximum.
4. Examine the performance of interactive piled foundations at resisting lateral forces and overturning moments due to wind or earthquakes.
5. Develop construction techniques to clarify the present research results of interactive piled foundation in order to economize on the construction costs.

REFERENCES

1. Abate, J. and Valkó, P. P. (2004), Multi-precision Laplace transform inversion, *Int. J. Numer. Meth. Engng.* 60: 979-993

2. Alawneh, A. S., Nusier, O., Malkawi, A. I. H. & Al-Kateeb, Mustafa (2001), Axial compressive capacity of driven piles in sand: a method including post-driving residual stresses, *Can. Geotech. J.* 38: 364-377.

3. Anagnostopoulos, C. & Georgiadis, M. (1998), A Simple Analysis of Piled Raft Foundations, *Geotechnical Engineering* 29(1): 71-83.

4. Armaleh, S. & Desai, C. S. (1987), Load-Deformation Response of Axially Loaded Piles, *ASCE* 113(GT12): 1483-1500.

5. Azzouz, A.S. & Morrison, M. J. (1988), Field Measurements on Pile in Tow Clay Deposits, J. Geot. Engrg., ASCE, 114(1):104-121.

6. Badoni, D. & Makris, N. (1997), Pile-to-pile interaction in the time domain—nonliear axial group response under harmonic loading, *Geotechnique* 47(2): 299-317.

7. Baguelin, F. & Frank, R., (1983), Discussion: Theoretical t-z curves. *J. of G.E. Div., ASCE*, 109(GT10):1349-1353.

8. Balakrishnan, E. G., Balasubramaniam, A. S. & Noppadol, P. (1999), Load Deformation analysis of bored piles in residual weathered formation, *J. of Geotech. & Geoenvon. Eng., ASCE* 125(2): 122-131.

9. Banerjee, P.K. and Davies, T.G. (1977), Analysis of pile groups embedded in Gibson soil. *In Proc. Of the 9th Int. Conf. on Soil Mechnics and Foundation Engineering,* Tokyo, Japan, Vol. 1:381-386

10. Banerjee, P.K.(1978), Analysis of axially and laterally loaded pile groups. *In* Developments in Soil Mechanics. Edited by C.R. Scott. Applied Science Publishers, U.K.

11. Basile, F. (1999), Non-linear analysis of pile groups, Proc. *Instn Civ. Engrs, Geotech. Engng.* 137: 105-115.

12. Bjerrum, L. & Andersen, K.H. (1972), In Situ Measurements of Lateral Pressures in Clay, *Proc. 5th European Conf. on S.M. and F.E.*, Madrid, Vol 1: 11-20

13. Bjerrum, L., Brinch Hansen, J., & Sevaldson, R. (1958), Geotechnical Investigations for a Quay Structure in Horten, *N.G.I.*, pub. No.28:1-17

14. Bjerrum, L. & Johannessen, I. J. (1960), Pore Pressure Resulting from Driving Piles in Soft Clay, *Conf. on Pore Pressure and Suction in Soil*: 14~17

15. Bolin, H.W. (1941), The Pile Efficiency formula of the Uniform Building Code, *Building Standard Monthly*, 1:4-5

16. Braja M. Das (1999), Principles of Foundation Engineering (4th Edition), An International Thomson Publishing Co. :229~232, 241~243

17. Brown, P. T. & Wiesner, T. J. (1975), The Behaviour of Uniformly Loaded Piled Strip Footings. *Soils & Foundations, Japanese Societ of SMFE* 15(4): 13~21

18. Bullen, F.R. (1958), Phenomena Connected with the settlement of driven piles, *Geotechniqu* 8: 121-133.

19. Butterfield, R., and Banerjee, P.K. (1968), Application of electro-osmosisto soil, part 2, *Civil Engineering Research Report*, No. 31, Dept. of Civ. Engrg., Southamptom Univ., U.K.

20. Butterfield, R., and Banerjee, P.K. (1970), The effects of Pore Water Pressure on Ultimate Bearing Capacity of Driven Piles., *Proc. 2nd South-East Asian Regional Conf. on S.M.F.E.*, Singapore:385-394

21. Butterfield, R., and Banerjee, P.K. (1971a), The Problem of Pile Group—Pile Cap Interaction, *Geotechnique*, 21(1): 135-142.

22. Butterfield, R., and Banerjee, P.K. (1971b), The elastic analysis of compressible piles and pile groups. *Geotechnique,* 21(2): 43-60.

23. Carter, J.P., Randolph, M.F. & Wroth, C.P. (1979), Stress and pore pressure changes in clay during and after the expansion of a cylindrical cavity, *Int. Jour. Num. and Analy. Methods in Geotech.*, 3:217~229.

24. Castelli, F. & Maugeri, M. (2002), Simplified Nonlinear Analysis for Settlement Prediction of Pile Groups, *J. of G. & G. E., ASCE* 128(1): 76-84.

25. Chattopadhyay, B. C. (1994), Uplift capacity of pile groups, *Proc. 13th Conf. ICSMFE*, 539-542.

26. Cheung, Y. K., Tham, L. G. & Guo, D. J. (1988), Analysis of pile group by infinite layer method, *Geotechnique* 38(3): 415-431.

27. Cheung, Y. K., Lee, P. K., & Zhao, W. B. (1991), Elastoplastic Analysis of Soil-Pile Interaction, *Computers and Geotechnics* 12: 115-132.

28. Chen, W. (1999), Pile Jacked in Saturated Clay – Mechanism of Penetration and Soil Compaction Effect, for the Degree of Master, Institute of Geotechnical Engineering, Hohai University, Nanjing, China.

29. Chen, Zhuchang & Song, Rong (1991), A Study on Compression of Shaft of Individual Pile, *Piling and Deep Foundations, 4th international DFI Conference*, Balkema, Rotterdam. ISBN9061911850, Vol. 1: 401-408.

30. Chin, J.T. & Poulos, H.G. (1990), Numerical Analysis of Axially Loaded vertical Piles and Pile Groups, *Computers and Geotechnics,* 9: 273-290.

31. Chow, Y.K.(1986), Analysis of vertically loaded pile groups. *Int. J. of Num. & Anal. Meth. In Geomechanics,* 10(1): 59-72.

32. Chow, Y.K. (1987), Axial and Lateral Response of Pile Groups Embedded in Non-homogeneous Soils, *Int. J. for Num. & Anal. Meth. in Geomechanics* 11: 621-638.

33. Chow, Y.K & Thevendran, V. (1987), Optimization of pile groups, *Computers and Geotechnics* 4: 43-58.

34. Chow, Y.K. (1989), Axially loaded Piles and pile groups embedded in a cross-anisotropic soil, *Geotechnique* 39(2): 203-211.

35. Chow, Y. K., & Chin, J.T. (1991), Downdrag faces in piles and pile groups, *Computer methods and Advances in Geomechanics,* Balkema, Rotterdam. ISBN9061911893: 127-132.

36. Chow, Y. K. & The, C. I. (1991), Pile-Cap—Pile-Group Interaction in Nonhomogeous Soil, *ASCE* 117(GT11): 1655-1668.

37. Clancy, P. & Randolph, M. F. (1993), An Approximate Analysis Procedure for Piled Raft Foundations, *Int. J. for Num. & Anal. Meth. in Geomechanics* 17: 849-869.

38. Clancy, P. & Randolph, M. F. (1996), Simple design tools for piled raft foundations, *Geotechnique* 46(2): 313-328.

39. Clark, J.I. & Meyerhof, G.G. (1972), The behavior of piles Driven in clay: I. An investigation of soil stress and pore water pressure as related to soil properties, *Canadian Geotechnical Journal* 9: 351-373.

40. Cooke, R. W. & Whitaker, T. (1961), Experiments on model pilesmwith Enlarged bases, *Geotechniqu* 11(1): 1-13.

41. Cooke, R. W. (1986), Piled raft foundations on stiff clays—a contribution to design philosophy, *Geotechnique* 36(2): 169-203.

42. Cooke, R.W. (1974), The settlement of friction pile foundations. *Proc. Conf. on Tall Buildings, Kuala Lumpur,* 7-19.

43. Cooke, R.W. (1979), The influence of residual installation forces on the stress transfer and settlement under working loads of jacked and bored piles in cohesive soils. *ASTM Symp. on behaviour of deep foundations, ASTM STP* 670, 231-249.

44. Cooke, R.W., Price, G. & Tarr, K.(1979), Jacked piles in London Clay: a study of load transfer and settlement under working conditions. *Geotechnique* 29(4): 461-468.

45. Cooke, R.W., Price, G. & Tarr, K.(1980), Jacked piles in London Clay: interaction and group behavior under working conditions. *Geotechnique* 30(2): 97-136.

46. Coyle, H.M., and Reese, L.C. (1966), Load transfer for axially loaded piles in clay. *J. of SMFE Div., ASCE,* **97**(SM12): 1657-1673.

47. D'Amore, L., Lacetti, G. and Murli, A. (1999), An implementation of a Fourier-series method for the numerical inversion of the Laplace transform. *ACM Transactions on mathematical Software* **25**: 279-305

48. D'Appolonia, D.J. & Lambe, T.W. (1971), Performance of Four Foundations on End-Bearing Piles, *J. of SMFE Div., ASCE,* **97**(SM1): 77-93.

49. Das, Braja M. (1999), *Principles of Foundation Engineering (4th Ed.)*, PWS Publishing, ISBN 0-534-95403-0

50. Davies, B. & Martin, B. (2002), Numerical inversion of the Laolace transform: a survey and comparison of methods, *Journal of Computational Physics*, 33:1-32

51. Desai, C. S. (1974), Numerical design-analysis for piles in sand. *Journal of Geot. Eng. Div., ASCE* **100**(6): 613-635.

52. Desai, C.S. (1987) from Zhang, J.R., & Zhu, X.R. (1997).

53. Dubner, H. & Abate, J. (1968), Numerical Inversion of Laplace Transforms by Relating Them to the Finite Fourier Cosine Transform. *J. of the Association for Computing Machinery*, 15(1): 115-123.

54. Durbin, F. (1974), Numerical Inversion of Laplace Transforms: an efficient improvement to Dubner and Abate's method. *JACM*, 17(4):371-376.

55. Esrig, M.F., Kirby, R.C. & Bea, R.G. (1977), Initial Development of a General Effective Stress Method for the prediction of Axial Capacity for driven piles in Clay, Proc. 9th OTC 2943, pp.496-506.

56. Esrig, M.F. & Kirby, R.C. (1979), Advances in General Effective Stress Method for the prediction of Axial Capacity for driven piles in Clay, Proc. 11th OTC 3406, pp.437-448.

57. Faruque, M. O., Mahmood, A. & Zaman, M. M. (1991), Analysis of unrestrained thin and moderately thick circular plates on elastic, *Computer Methods and Advances in Geomechanics,* Balkema, Rotterdam. ISBN9061911893: 1147-1152.

58. Feld, J. (1943), Discussion on friction pile foundation, Trans. Amer. Civ. Engrs, 108:143-144

59. Fleming, K.G.W. et al (1992), Piling Engineering, 2nd edit. Glasgow & London. 351-358, 371-373.

60. Fleming, K.G.W. (1992), A New Method for Single Pile Settlement Prediction and Analysis, *Geotechniqe* 42 (3), 411-425.

61. Fraser, R.A. & Wardle, L.J. (1976), Numerical Analysis of Rectangular Rafts on Layered Foundations, Geotechnique, 26(4), 613-627.

62. Geddes, J.D. (1966), Strsses in Foundation Soils Due to Vertical Sbsurface Loading, J. Geotechnique, 16(3):231~255

63. Gibson, R. E. & Lumb, P. (1953), Numerical Solution of Some Problems in the Consolidation of Clay, *Proc. Inst. Civ. Engrs.*, London:182

64. Gibson, R. E. & Mc Namee (1957), The Consolidation Settlement of A Load Uniformly Distributed over Rectangular Area, *Proc. of 4th ICSMFE*, Vol. 1: 259

65. Griffiths, D. V., Clancy, P. & Randolph, M. F. (1991), Piled raft foundation analysis by finite elements, *Computer Methods and Advances in Geomechanics,* Balkema, Rotterdam. ISBN9061911893: 1153-1157.

66. Gu, B. (1964), Bearing Capacity of Frictional Piles in Soft Clay During Different Time,

67. Guo, D. J. & Cheung, Y. K. (1987), Infinite Layer for the Analysis of A Single Pile, *Computers and Geotechnics* 3: 229-249.

68. Guo, W. D. & Randolph, M. F. (1997), Vertically Loaded Piles in Non-Homogeneous Media, *Int. J. for Num. & Anal. Meth. in Geomechanics* 21: 507-532.

69. Guo, W.D., and Randolph, M.F. (1999), An efficient approach for settlement prediction of pile groups. *Geotechnique* 49(2), 161-179.

70. Gwizdztz, K. & Tejchman, A. (1996), Numerical Modeling of pile-subsoil interaction, Soil & Foundation, 27: 673-676

71. Ha, HoBoo & O'neill, Michael W., (1983), Discussion: Theoretical t-z curves. *J. of G.E. Div., ASCE*, 109(GT10):1353-1355.

72. Hain, S. J. & Lee, I. K. (1978), The analysis of flexible raft-pile systems, *Geotechnique* 28(1): 65-83.

73. Hamza, M.M. (1991), Short and long term shaft resistance of driven instrumented pile in soft clay, *Piling and Deep Foundations, 4th international DFI Conference*, Vol. 1: 579-585.

74. Hanna, T. H. (1963), Model studies of foundation groups in sand, *Geotechniqu* 13: 334-351.

75. Hanna, T. H. (1967), The Measurement of Pore Water Pressure Adjacent to a Driven Pile, *Can. Geot. Jnl.*, 4(3): 313

76. He, X. & Chen, Z.C. (1991) The prediction of load-displacement characteristics for axially loaded piles, *Piling and Deep Foundations, 4th international DFI Conference*, Vol. 1: 673-678.

77. Hirayama, H. (1991), Pile-group settlement interaction considering soil non-linearity, *Computer methods and Advances in Geomechanics,* Balkema, Rotterdam. ISBN9061911893: 130-144.

78. Hongladaromp, T., Chen, N.J. & Lee, S.L. (1973), Load Distributions in Rectangular Footings on Piles, *Geotechnical Engineering,* 4(2):77-90

79. Horikoshi, K. & Randolph, M.F. (1996), Centrifuge modeling of piled raft foundations on clay, *Geotechnique* 46(4): 741-752.

80. Huntsman, S.R. & Mitchell, J.K. (1986), Lateral stress measurement during cone penetration, *Use of in situ Tests in Geotech. Engrg.,* Clemence, S.P., eds., A.S.C.E., New York: 617-634.

81. Jardine, R. J., Potts, D. M., Fourie, A. B. & Burland, J. B. (1986), Studies of the influence of non-linear stress-strain characteristics in soil-structure interaction, *Geotechnique* 36(2): 377-396.

82. Kalsrud, K. & Haugen, T. (1985), Axial static capacity of steel model piles in overconsolidated clay, *XI Int. Conf. SMFE*, S. Francisco, Vol. 2: 1401-1406

83. Katzenbach, R., Arslan, U., Moormann, C. & Reul, O. (1998), Piled Raft Foundation – Interaction Between Piles and Raft, Darmstadt Geotechnics, Darmstadt University of Technology, 4:279-296

84. Kezdi, A. (1957), The bearing capacity of piles and pile groups, *Proc. 4th Int. Conf. Soil Mech.*, 2: 46~51

85. Kezdi. A. (1975), Pile foundations. In foundation engineering handbook. Edited by H.F.winterkorn and H.Y.Fang. Van Nostrand Reinhold Company, New York, Chap. 19.

86. Kiousis, P. D. & Elansary, A. S. (1987), Load Settlement Relation for Axially Loaded Piles, *ASCE* 113(GT6): 655-661.

87. Koizumi, Y. & Ito, K. (1967), Field Tests with Regard to Pile Driving and Bearing Capacity of Piled Foundations, *Soils and Fndns.*, 3:30

88. Koyasu, W. (1956), Bearing-Capacity Mechanism of foundational Pile (in Japanese, 基礎杭の 支持の力學機構), *Geotechnique (土工の技術)*, Vol.20 No.1~No.5.

89. Kraft, L.M., Ray, R.P. and Kagawa, T. (1981), Theoretical t-z curves. *J. of G.E. Div., ASCE*, 107(9):1449-1461.

90. Kurkur, M.M. (1991), Prediction of load-settlement curve of pile groups in Egyptian soils, *Piling and Deep Foundations, 4th international DFI Conference*, Vol. 1: 401-408.

91. Kuwabara, Fumio (1989), An Elastic Analysis for Piled Raft Foundations in a Homogeneous Soil, *Soils & Foundations, Japanese Societ of SMFE*, V.29(1): 82-92.

92. Lai, J.Y., and Booker, J.R. (1989), Application of discrete Fourier series to the finite element stress analysis of axisymmetric solids. Res. Report 605, University of Sydney, Australia.

93. Lambe, T.W. & Horn, H.M. (1965), The influence on an Adjacent Building of Pile Driving for the M.I.T. Materials Center, *Proc. 6th Int. Conf. S.M. & F.E.*, Vol. 2: 280

94. Lee, C. Y. & Poulos, H.G. (1990), Axial Response Analysis of Piles in Vertically and Horizontally Non-homogeneous Soils, *Computers and Geotechnics*, 9(3), 133-148

95. Lee, C.Y. (1991) Axial response of axially loaded piles and pile groups. *Computers Geotech.* 11(4), 295-313.

96. Lee, C.Y. (1991), Discrete Layer Analysis of Axially Loaded Piles and Pile Group, *Computers and Geotechnics* 11: 295-313

97. Lee, C.Y., and Small, J.C. (1991), Finite-layer analysis of axially loaded piles. *J. of G.E., ASCE,* Vol. 117(11): 1706-1722.

98. Lee, C.Y. (1993), Settlement of pile groups—Practical approach. *J. G.E., ASCE*, 119(9):1449-1461.

99. Lee, C.Y. (1993), Pile Group Settlement Analysis by Hybrid Layer Approach, *J. G.E., ASCE*, 119(6):984-997

100. Lee, K.M., & Xiao, Z.R. (2001), A simplified nonlinear approach for pile group settlement analysis in multi-layered soils. *Can. Geotech. J.* 38:1063-1080.

101. Lee, C.J., Bolton, M.D. & Al-Tabbaa, A.(2002), Numerical modeling of group effects on the distribution of dragloads in pile foundations. *Geotechnique* 52(5): 325-335.

102. Lee, C.Y. & Small, J. C. (1991), Finite-Layer Analysis of Axially Loadd Piles *J. of G.E., ASCE,* Vol. 117(11): 1706-1722.

103. Leroueil, S., Tavenas, F., Brucy, F., La Rochelle, P., & Roy, M. (1979), Behaviour of destructured natural Clays, *ASCE J. of Geot. Engeg. Div.*, 105(GT6):759-778.

104. Lin, Bai, Zhu, X. & Lou, W. (1989), Application of Dualistic Simultaneous Equations in Solving the Settlement of Sparse Piled Foundation, *Building Science of China, Vol. 23, No.6*: 49-53.

105. Liu, J. L., Huang, Q., Li, H., L., X. & Hu, W. (1994), Experimental research on bearing behaxiour of pile groups in soft soil, *Proc. 13th Conf. ICSMFE*, 535-538.

106. Liu, Q. F. & Meyerhof, G. G. (1987), New Method for Non-linear Analysis of Gigid Piles in Clay, *Computers and Geotechnics* 3: 185-212.

107. Lo, K.Y. & Stermac, A. G. (1965), Induced Pore Pressures During Pile Driving Operations, Proc. 6th Int. Conf. S.M. & F.E., Vol. 2: 285~289.

108. Lunne, T., Eidsmoen, T., Gillespie, D. & Howland, J.D. (1986), Laboratory and field evaluation of cone penetrometers, *Use of in situ Tests in Geotech. Engrg., Clemence, S.P., eds., A.S.C.E.*, New York: 714-729

109. Luo, X.H. (1997), Estimation of Pore Water Pressures Due to Driving Pile and Extruding Soil, *J. of Wuhan City Construction Inst.* No. 3.

110. Lyndon, A., Wei, M.J., & Turner, J. G. (1991), Centrifugal modelling of stress-reducing piled foundations on sand, *Piling and Deep Foundations, 4th international DFI Conference*, Vol. 1: 611-616.

111. Mandolini, A., and Viggiani, C. (1997), Settlement of piled foundations *Geotechnique,* 47(4):791-816.

112. Masood, T. & Mitchell, J.K. (1993), Estimation of in situ lateral stresses in soils by cone-penetration test, *J. Geotech. Engrg., ASCE*, 119(10):1624-1639.

113. Massarsch, K.R. and Broms, B.B. (1977), Fracturing of Soil Caused by Pile Driving in Clay, *9th ICSMFE*, Tokyo, Japan: 197-200

114. Maugeri, M., Amenta, G., Castelli, F. & Motta, E. (1997), Settlements of a piled foundation duo to negative skin friction: Acase history, *Soils & Foundation*: 1111-1114.

115. Mayne, P. W. & Poulos, H. G. (1999), Approximate Displacement Influence Factors for Elastic Shallow Foundations, *J. of Geotech. & Geoenviron. Engrg., ASCE*, 125(6): 453-460.

116. Meng, F. Basile (1999), Non-linear Analysis of Pile Groups, *Proc. Insrn. Civ. Engng*, 137, April: 105-115

117. Mendoza, M. J. & Romo, M.P. (1996), Behaviour of a friction pile-box foundation in Mexico City during construction, *Soil & Foundation* , 843-846.

118. Meyerhof, G.G. (1959). Compaction of Sands and Bearing Capacity of Piles. *ASCE 85*(SM6):1-29.

119. Milligan, V., Soderman, L. & Rutka, A. (1962), Experience with Canadian Varved Clays, J.S.M.F., ASCE, 88(SM4): 32-67.

120. Mylonakis, G. (2001), Winkler modulus for Axially Loaded Piles, *Geotechnique* 51(5): 455-461.

121. Naggar, M.H. & Novak, M. (1994), Non-linear model for dynamic axial pile response. *J. Geo. Engrg. Div., ASCE* 120(2): 308-329.

122. Ni, X.H. (1991), Numerical Analysis of Raft—Piles—Soil Interaction, *Ph.D. Thesis, Tongji University*, Shanghai.

123. Nogami, T., & Paulson, S. K. (1985), Transfer matrix approach for nonlinear pile group response analysis, *Int. J. for Num. & Ana. Meth. in Geomech., Vol.* 9: 299-316

124. Nan, Y. H.(1991), Project Case of considering pile-soil-raft interaction in design of piled raft, *Conf. Proc. of New Development of pile foundation Technology,* Nengbu.

125. Ottaviani, M. (1975), Three-dimensional finite element analysis of vertically loaded pile groups. *Geotechnique*, 25(2): 159-174.

126. Orrje, O. & Broms, B.B. (1967), Effects of Pile Driving on Soil Properties, *J.S.M.F.D., ASCE*, 93(SM5): 59-73

127. Poorooshasb, H. B. & Noorzad, Ali (1995), Analysis of pile-raft foundation, Numerical Mothods in Geomechanics-NUMOG V, Balkema, Rotterdam, ISBN9054105682: 565-571.

128. Poulos, H.G. (1968), Analysis of the settlement of Pile Groups, Geotechnique 18: 449-471.

129. Poulos, H. G. & Davis, E. H. (1968), The settlement behaiour of single axially loaded incompressible piles and piers, *Geotechnique* 18:351-371.

130. Poulos, H.G. (1979), Group factors for pile-deflection estimation., J. of G. E. D., ASCE 105(GT12): 1489-1509.

131. Poulos, H.G. and Davis, E.H. (1980), Pile Foundation Analysis and Design. John wiley and sons, New York.

132. Poulos, H. G. (1989), Pile Behaiour—Theory and Application, *Geotechnique* 39(3):365-415.

133. Poulos, H.G. (1991), Analysis of Piled Strip Foundations, *Computer Methods and Advances in Geomechanics,* Balkema, Rotterdam. ISBN9061911893: 183-191.

134. Poulos, H. G. (1993), Settlement prediction for bored pile groups, *Deep Foundation on bored and auger piles, Van Impe(ed.), Balkema, Rotterdam,* ISBN 9054103132: 103-130

135. Poulos, H. G. (1994), An Approximate Analysis of Pile—Raft Interaction, *Int. J. for Num. & Anal. Meth. in Geomechanics* 18: 73-92.

136. Poulos, H. G. (2000), Pile-Raft Interaction — Alternative Methods of Analysis, *Developments in Theor. Geomechanics*, Ed. D.W. Smith, & J.P. Carter, Balkma, Rotterdam: 445-468.

137. Poulos, H. G. (2001), Methods of Analysis of Piled Raft Foundation, *A report prepared on Behalf of Technical Committee TC18 on Piled Foundations, Int. Society of SMGE.*

138. Poulos, H. G. (2001), Piled Raft Foundations — Design and Applications, *Geotechnique* 50(2): 95-113.

139. Prakoso, W. A. & Kulhawy, F. H. (2001), Contribution to Piled Raft Foundation Design, *J. of Geotech. & Geoenviron. Engrg., ASCE*, 127(1): 17-24.

140. Press, H. (1933), The bearing capacity of pile groups in relation to that a single pile, Bautechnik, 2:625~627

141. Pressley, J.S. & Poulos, H.G. (1986), Finite element analysis of mechanisms of pile group behaviour, *Int. J. for Num. & Anal. Meth. in Geomechanics,* 10(1): 213-221.

142. Radugin, A.E. (1969), Increase of Bearing Capacity of Short Piles With Time, Soil Mechanics and Foundation Engineering, March-April:103-107

143. Randolph, M.F. (1977), A Theoretical Study of the performance of Plies, Ph.D. Thesis, Cambridge Univ., U.K.

144. Randolph, M.F., and Wroth, C.P. (1978), Analysis of Deformation of Vertically Loaded Piles. *J. of G.E. Div., ASCE,* 104(GT12):1465-1488.

145. Randolph, M.F., and Wroth, C.P. (1979), An Analysis of Deformation of Pile Groups. *Geotechnique*, 29, 423-439.

146. Randolph, M.F. (1983), Settlement Considerations in the Design of Axially Loaded Piles, *Ground Engineering* 16(4): 28-32.

147. Randolph, M.F. (1983), Design of Piled Raft Foundations, *Recent Developments in Laboratory and Field Tests and Analysis of Geotechnical Problems , Bangkok*: 525-537

148. Randolph, M.F., Carter, J.P. & Wroth, C.P. (1979), Driven Piles in Clay – the Effects of Installation and Sudsequent Consolidation, *Geotechnique*, 29(4): 361-393

149. Randolph, M.F. & Clancy, P. (1993), Efficient design of piled raft, *Deep Foundation on bored and auger piles, Van Impe(ed.), Balkema, Rotterdam,* ISBN 9054103132: 119-130

150. Randolph, M. F. (1994), Design Methods for Pile Group and Piled Rafts, *Proc. 13th Conf. ICSMFE*, New Delhi: 61-82.

151. Richwien, W., and Wang, Z. (1999), Displacement of a pile under axial load. *Geotechnique* 49(4): 537-541.

152. Romanel, C., Filho, P. R. & Cangussu, M.A. (1994), Settlement Analysis of Axially Loaded Piles in A Layered Soil, *Proc. 13th Conf. ICSMFE*, 497-500.

153. Roy, M., Blanchet, R., Tavenas, F. & La Rochelle, P. (1981), Behaviour of a Sensitive Clay during Pile Driving, *Can. Geotech. J.*, 18: 67-85

154. Roy, M., Tremblay, M., Tavenas, F. & La Rochelle, P. (1982), Development of pore pressure in quasi-static penetration tests in sentive clay, *Can. Geotech. J.*, 19: 124-138

155. Russo, G. (1998), Numerical Analysis of Piled Rafts, *Int. J. for Num. & Anal. Meth. in Geomechanics* 22: 477-493.

156. Seiler, J.F. & Keeney, W. D. (1944), The efficiency of piles in groups, Wood-preserving News, N.Y., 22: 109~118.

157. Shen, W.Y., Chow, Y.K., & Yong, K.Y. (1997), A variational approach for vertical deformation analysis of pile groups. *Int. J. Numer. Analyt. Meth. Geomech.*, 21(11): 741-752.

158. Shen, W.Y., Chow, Y.K., & Yong, K.Y. (1999), A variational solution for vertically loaded pile groups in an elastic half space. Geotechnique 49(2): 199-213.

159. Shen, W.Y., Chow, Y.K., & Yong, K.Y. (2000), Practical method for settlement analysis of pile groups. *J. Geotech. Geoenviron. Eng., ASCE*, 126(10): 890-897.

160. Shen, W.Y., & The, C.I. (2002), Practical solution for group stiffness analysis of piles. J. *of Geotech. & Geoenviron. Engrg., ASCE*, 128(8): 692-697.

161. Shen, Z.J. (1992), Piles' resistance from soil sliding and limit design of resisting-sliding piles, Chinese Journal of Geotechnical Engineering, (1): 51~56

162. Shen, Z. J. (2000), Theoretical Soil Mechanics, Beijing: Water Resources and Hydropower Press of China, ISBN 7-5084-0299-5: 224~225.

163. Skempton, A.W., Yassin, A.A. & Gibson, R.E. (1953), The Theory of the bearing capacity of piles in sand, Ann. Inst. Batim., Nos 63-64:285

164. Skempton, A.W. (1953), Discussion: Piles and pile foundations, settlement of pile foundation, *Proc. 3rd Int. Conf. Soil Mechanics*, 3:172

165. Skempton, A.W. (1957), The Planning and Design of New Hong Kong Airport, *Preceedings, the Institute of Civil Engineers*, London, Vol.7:305-307

166. Small, J.C., and Booker, J.R. (1984), Finite layer analysis of layered elastic materials using a flexibility approach. Part 1——**strip loadings**. *Int. J. Num. Meth. In Engrg.*, 20, 1025-1037.

167. Small, J.C., and Booker, J.R. (1986), Finite layer analysis of layered elastic materials using a flexibility approach. Part 2——**circular and rectangular loadings**. *Int. J. Num. Meth. In Engrg.*, 23(5): 959-978.

168. Smith & Griffith (1988). *Programming the finite element method*, 2nd Ed., John Wiley and Sons, New York, N.Y.

169. Smith, I. M. & Wang, A. (1998), Analysis of Piled Rafts, *Int. J. for Num. & Anal. Meth. in Geomech.* 22: 777-790.

170. Soderberg, L. (1962), Consolidation Theory Applied to Foundation Pile Time Effects, Geotechnique, Vol. 12: 217.

171. Sooysmith, C. (1896), Concerning foundations for heavy buildings in New York City, Trans. Amer Soc. Civ. Engrs, 35: 464-465.

172. Sommer, H. (1993), Development of locked stresses and negative shaft resistance at the piled raft foundation —— Messeturm Frankfurt/Main, *Deep Foundation on bored and auger piles, Van Impe(ed.), Balkema, Rotterdam,* ISBN 9054103132: 347-349

173. Stuckrath, L. and Descoeudres, F. (1991), Model pile tests to determine the effects of installation method and form on load transfer under static load, *Piling and Deep Foundations, 4th international DFI Conference*, Vol. 1: 647-654.

174. Ta, L.D. & Small, J.C. (1995), Finte layer analysis of pile groups in layered soils, *Numerical Models in Geomechanics – NUMOG* V, Balkema, Rotterdam, ISBN9054105682: 577-582.

175. Ta, L. D. & Small, J. C. (1996), Analysis of Piled Raft systems in Layered Soils, *Int. J. for Num. & Anal. Meth. in Geomechanics* 20:57-72.

176. Ta, L. D. & Small, J. C. (1997), An Approximate for Analysis of Raft and Piled Raft Foundations, *Computers and Geotechnics* 20(2): 105-123.

177. Talbot, A. (1979), The accurate numerical inversion of Laplace transforms, *Journal of the Institute of Methematics and Its Applications*, 23:97-120

178. Tang, S. D. (1985), Pore-Pressure CPT: Instrument, Test-Data Interpretation and Application. Thesis for Master Degree, Department of Geotechnical Engineering, Tongji University, China.

179. Tang, S. D. (1990), Analysis of the Variation of Pile Capacity by Principle of Effective Stress. Thesis for Doctoral Degree, Department of Geotechnical Engineering, Tongji University, China.

180. Terzaghi, K., Peck, R.B., & Mesri, G. (1996), Soil Mechanics in Engineering Practice (3rd Edition), John Wiley & Sons Inc.

181. Tong, J.G. & Zhao, X.H. (1989), Simple Method Calculating Settlement of Piled Raft (Box) Foundation of High-Rise Building, *Design Theory of Piled Raft and Piled Box Foundation of Shanghai High-Rise Building*, Shanghai: Tongji University Press: 179-194

182. Tong, J.G., Zhao, X.H., Shi, A.K., Liang, J.Q. & Qin, J.F. (1989), Field Measurement of Piled Box Foundation of A Shear-Well Structure Building in Shanghai, *Design Theory of Piled Raft and Piled Box Foundation of Shanghai High-Rise Building*, Shanghai: Tongji University Press: 55-69

183. Tong, J. G. & Zhao, Xihong (1997), Theory and Practice of Soil-Foundation Interaction of High-rise Building, Shanghai: Tongji University Press

184. Trochanis, A.M., Bielak, J., and Christiano, P. (1991), Three-dimensional nonlinear study of piles, *J. of GM, ASCE*, 117(3): 429-447.

185. Valkó, P. P. and Abate, J. (2004), Comparison of Sequence Accelerators for the Gaver Method of Numerical Laplace Transform Inversion, *Computers and Mathematics with Application* 48: 629-636

186. Vaziri, H. H. & Xie, J. (1990), A Method for Analysis of Axially Loaded Piles in Nonlinear Soils, *Computers and Geotechnics* 10: 149-159.

187. Vesic, A.S. (1972), Expansion of Cavity in infinite Soil Mass, *Jour. SMF Div., ASCE*, 98(3): 265-289

188. Viiggiani, C. (1998), Pile Groups and Piled Rafts Behaviour, *Deep Foundation on Bored and Auger Piles*, BapIII, van Impe and Haegman (eds), Balkema, Rotterdam, 77-90

189. Vijayvergiya, V.N. (1977), Load-movement characteristics of piles. *4th Syposium of waterway, port, coastal and ocean division,* ASCE, Long Beach, Calif., Vol. 2: 269-284.

190. Vogrincic, G. (1992), Analyses of stress and strain states in the soil surrounding the axially loaded pile, Soil and foundation 25: 743-746

191. Whitaker, T. (1957), Experiments with model piles in groups, *Geotechniqu* 7: 147-160.

192. Wroth, C.P., Carter, J.P. & Randolph, M.F. (1979), Stress Changes Around a Pile Driven into Cohesive Soil, *Conf. on Recent Devel. in the Design and Constrn. of Piles*, Inst. Civ. Engrs., London

193. Yamashita, K. & Kakurai, M. (1991), Settlement behavior of the raft foundation with friction piles, *Piling and Deep Foundations, 4th international DFI Conference*, Vol. 1: 461-466.

194. Yamashita, K., Kakurai, M. & Yamada, T. (1994), Investigation of a pile raft foundation on stiff clay, *Proc. 13th Conf. ICSMFE*, 543-546.

195. Yang, J., Song, E., & Chen, Z. (2000), Volumetric locking analysis and element choice in 3D elasoplastic analysis of soil, *Engineering Mechanics* (in Chinese), 17 (6):6-13.

196. Yang, R. & Zai, J. (1994), The mechanics of the pile-soil-cap interaction, . *J. of Nanjing Arch. & Civ. Engrg. Inst.* 28(1):1-7.

197. Yang, R. & Zai, J. (1994), The Principle of the generalized shear-displacement method for analyzing the nonlinear interaction of piles-soil-pilecap. *Chinese Journal of Geotechnical Engineering* 16(6):105-116.

198. Yang, R. & Zai, J. (1995), The theory of the ultimate bearing capacity increment of soil under a **strip** cap with sparse piles —— The resist and strengthening action of piles in pile-soil-cap interaction, . *J. of Nanjing Arch. & Civ. Engrg. Inst.* 33(2):1-11.

199. Yang, R. & Zai, J. (1996), The theory of the ultimate bearing capacity increment of soil under a **circular** cap with sparse piles —The resist and strengthening action of piles in pile-soil-cap interaction, . *J. of Nanjing Arch. & Civ. Engrg. Inst.* 38(3):1-10.

200. Yao, X.Q. & Wu, Z.X. (1997), Estimation of Pore Water Pressure Caused by Pile Driving in Saturated Soft Soil, *Rock and Soil Mechanics* (Chinese), 18(4).

201. Zai, J. (1989), The Finite layer model of soil for tall building—supporting soil interactive analysis, *Proc. Of Int. Conf. on High-rise Buildings,* Vol. 2, 25-27 March, Nanjing, 1989.

202. Zai, J. (1992), Sparse-Pile Foundation Designed by Ultimate Bearing Capacity of Singer Pile, *J. of Nanjing Arch. & Civ. Engrg. Inst.* 23(4):1-16.

203. Zai, J. & Yang, R. (1993a) The generalized Shear Displacement Method for analysis of nonlinear deformation in soil around the piles. *J. of Nanjing Arch. & Civ. Engrg. Inst.* 24(1):1-16.

204. Zai, J. & Yang, R. (1993b), Non-linear interactive analysis of pile group—soil—pile cap. *J. of Nanjing Arch. & Civ. Engrg. Inst.* 24(2):1-14.

205. Zai, Jinmin and Zai, Jinzhang (1993). *Analsis and Design for Foundation of Tall Building —— The Theory and Application of Soil-Structure Interaction (Chinese).* China Architectural Industry Press, Bejing: 1-3, 22-25.

206. Zeevaert, L. (1956), Compensated Friction-pile Foundation to Reduce the Settlement of Buildings on the Highly Compressible Volcanic Clay of Mexico City, *Proc.ICE.*Vol. 3: 81-86.

207. Zeevaert, L. (1957), Foundation design and behaviour of tower Latino Americana in Mexico City, *Geotechnique* 7:115-133.

208. Zhang, B. & Small, J. C. (1991), Analysis of raft on foundations of variable stiffness, *Computer Methods and Advances in Geomechanics,* Balkema, Rotterdam. ISBN9061911893: 1103-1108.

209. Zhang, J.R., & Zhu, X.R. (1997), Concise Calculating and Design handbook of Building Foundation (Chinese), Chinese Architectural Industry Press, Bejing, Chap.6: 205-234.

210. Zhang, H. H. & Small, J. C. (2000), Analysis of capped pile groups subjected to horizontal and vertical loads, *Computers and Geotechnics* 26(1): 1-21.

211. Zhang, W.Q., Zhao, X.H., and Zai, J.(1981), Finite layer method for analyaing layered and elastic half-space under arbitrary force system, *Chinese J. of Geotech. Engrg.,* 1981(2), 12-25.

212. Zhang, W.Q., Zhao, X.H., and Zai, J.(1982), Finite layer analysis of layered and elastic half-space under arbitrary force system, Proc. Of int. Conf. on FEM, Shanghai, 1982.

213. Zhu, H. & Chang, M. F. (2002), Load Transfer Curves along Bored Piles Considering Modulus Degradation, *J. of Geot. & Geoenviron. Engrg., ASCE* 128(9): 764-774.

214. Zhu, B. L. & Shen, Z. J. (1990), Numerical Soil Mechanics, Shanghai: Shanghai Scientific Technology Press: 160~170

215. Zhu, X. L. & Tang, S. D. (1986), Theoretical Analysis of Estimation of Consolidation Coefficient of Soft Clay by Pore-Pressure CPT, Geotechnical Investigation of China, No. 6.

216. Gardner, (1975) from Zhang, J.R., & Zhu, X.R. (1997).

217. Desai, C.S.(1987) from Zhang, J.R., & Zhu, X.R. (1997).

APPENDIX A

Formulae of Gedds (1961) Stresses Solution
Due to Vertical Subsurface Loading

Appendix A

Formulae of Gedds (1961) Stresses Solution
Due to Vertical Subsurface Loading

Additional Stress coefficients Due to Vertical Subsurface Loading (From Geddes, 1961)

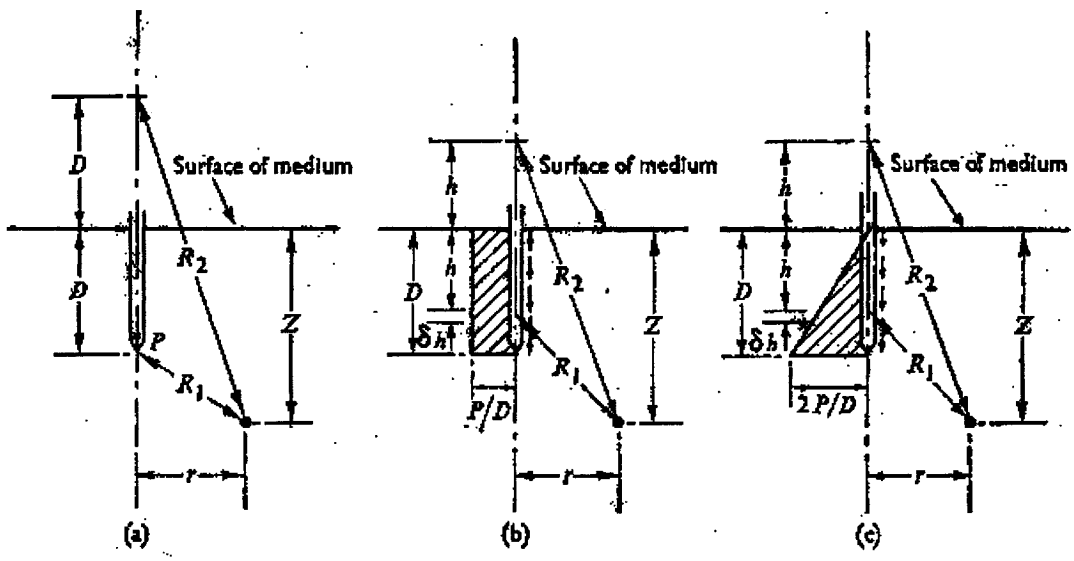

Fig. A-1 Loading conditions

$$\left.\begin{aligned}
\Delta\sigma_z &= (I_{z\text{-}b}\,P_b + I_{z\text{-}u}\,P_u + I_{z\text{-}t}\,P_t)/D^2 \\
\Delta\sigma_r &= (I_{r\text{-}b}\,P_b + I_{r\text{-}u}P_u + I_{r\text{-}t}\,P_t)/D^2 \\
\Delta\sigma_\theta &= (I_{\theta\text{-}b}\,P_b + I_{\theta\text{-}u}\,P_u + I_{\theta\text{-}t}\,P_t)/D^2 \\
\Delta\tau_{rz} &= (I_{\tau\text{-}b}\,P_b + I_{\tau\text{-}u}\,P_u + I_{\tau\text{-}t}\,P_t)/D^2
\end{aligned}\right\} \qquad (3.3\text{-}2)$$

Set $n = \dfrac{r}{D}, \qquad m = \dfrac{z}{D},$

and $A^2 = n^2 + (m-1)^2, \quad B^2 = n^2 + (m+1)^2, \quad F^2 = n^2 + m^2$

Thus, for point Load P_b,

$$I_{z\text{-}b} = \frac{1}{8\pi(1-\mu)}\left[-\frac{(1-2\mu)(m-1)}{A^3} + \frac{(1-2\mu)(m-1)}{B^3} - \frac{3(m-1)^3}{A^5} - \frac{3(3-4\mu)m(m+1)^2 - 3(m+1)(5m-1)}{B^5} - \frac{30m(m+1)^3}{B^7}\right] \qquad (AI\text{-}1)$$

$$I_{r\text{-}b} = \frac{1}{8\pi(1-\mu)}\left[\frac{(1-2\mu)(m-1)}{A^3} - \frac{(1-2\mu)(m+7)}{B^3} + \frac{4(1-\mu)(1-2\mu)}{B(B+m+1)} - \frac{3n^2(m-1)}{A^5} + \frac{6(1-2\mu)(m+1)^2 - 6(m+1) - 3(3-4\mu)n^2(m-1)}{B^5} - \frac{30n^2m(m+1)}{B^7}\right] \quad \text{(AI-2)}$$

$$I_{\theta\text{-}b} = \frac{1}{8\pi(1-\mu)}\left[\frac{(1-2\mu)(m-1)}{A^3} + \frac{(1-2\mu)(3-4\mu)(m+1) - 6(1-2\mu)}{B^3} - \frac{4(1-\mu)(1-2\mu)}{B(B+m+1)} + \frac{6(1-2\mu)(m+1)^2 - 6(m+1)}{B^5}\right] \quad \text{(AI-3)}$$

and,

$$I_{\tau\text{-}b} = \frac{n}{8\pi(1-\mu)}\left[-\frac{(1-2\mu)}{A^3} + \frac{(1-2\mu)}{B^3} - \frac{3(m-1)^2}{A^5} - \frac{3(3-4\mu)m(m+1) - 3(3m+1)}{B^5} - \frac{30m(m+1)^2}{B^7}\right] \quad \text{(AI-4)}$$

For uniform skin friction P_u,

$$I_{z\text{-}u} = \frac{1}{8\pi(1-\mu)}\left[-\frac{2(1-2\mu)}{A} + \frac{2(2-\mu) + 2(1-2\mu)m(m+1)/n^2}{B} - \frac{2(1-2\mu)(m/n)^2}{F} + \frac{n^2}{A^3} + \frac{4m(1+\mu)(m+1)^3/n^2 - (4m^2+n^2)}{B^3} + \frac{4m^2[1-(1+\mu)(m/n)^2]}{F^3} + \frac{6m^2(m^4-n^4)/n^2}{F^5} + \frac{6m[mn^2 - (m+1)^5/n^2]}{B^5}\right] \quad \text{(AI-5)}$$

$$I_{r\text{-}u} = \frac{1}{8\pi(1-\mu)}\left[\frac{(1-2\mu)}{A} + \frac{(7-2\mu) - 12(1-\mu)m(m+1)/n^2}{B} - \frac{4(2-\mu) - 12(1-\mu)(m/n)^2}{F} - \frac{n^2}{A^3} - \frac{2(1+2\mu)m(m+1)^3/n^2 - 2m^2 + 3n^2}{B^3} + \frac{4n^2 - 2m^2 + 2(1+2\mu)m^2(m/n)^2}{F^3} + \frac{6m^2(n^4 - m^4/n^2)}{F^5} - \frac{6m[mn^2 - (m+1)^5/n^2]}{B^5}\right] \quad \text{(AI-6)}$$

$$I_{\theta\text{-}u} = \frac{1}{8\pi(1-\mu)}\left[\frac{(1-2\mu)}{A} + \frac{6 - (1-2\mu)(3-4\mu) + 6(1-2\mu)m(m+1)/n^2}{B} + \frac{2(1-2\mu)^2 - 6(1-2\mu)(m/n)^2 - 6}{F} + \frac{2(1+2\mu)m(m+1)^3/n^2 + 2m^2 - 4\mu n^2)}{B^3}\right]$$

$$+\frac{4\mu n^2-2m^2-2(1+2\mu)m^2(m/n)^2}{F^3}-4(1-\mu)(1-2\mu)\left(\frac{1}{F+m}-\frac{1}{B+m+1}\right)\Bigg] \tag{AI-7}$$

and,

$$I_{\tau\text{-}u}=\frac{n}{8\pi(1-\mu)}\Bigg[\frac{(1-2\mu)(m-1)/n^2}{A}+\frac{(m-1)^3/n^2}{A^3}+\frac{[(1-2\mu)-6(m/n)^2](m+1)/n^2}{B}$$
$$+\frac{(m+1)^3(1+12m^2/n^2)/n^2+12m-4\mu n)}{B^3}-\frac{6m[n^2-m(m+1)^5/n^4]}{B^5}$$
$$+\frac{6m[m^2-2(1-2\mu)]/n^2}{F}+\frac{4(\mu-3)m-2m^3[1+6(m/n)^2]/n^2}{F^3}+\frac{6m(n^2+m^6/n^4)}{F^5}\Bigg] \tag{AI-8}$$

For linear variation of skin friction, Pt

$$I_{z\text{-}t}=\frac{1}{4\pi(1-\mu)}\Bigg[-\frac{2(1-2\mu)}{A}+\frac{mn^2+(m-1)^3}{A^3}+\frac{2(2-\mu)(4m+1)-2(1-2\mu)(m+1)m^2/n^2}{B}$$
$$+\frac{2(1-2\mu)m^3/n^2-8(2-\mu)m}{F}+\frac{m[(4\mu-15)n^2+4m^2]+(m+1)^3[1-2(5+2\mu)m^2/n^2]}{B^3}$$
$$+2m\frac{(7-2\mu)n^2-6m^2+2(5+2\mu)m^2(m/n)^2]}{F^3}+\frac{6m[n^2(n^2-m^2)-2(m+1)^5m/n^2]}{B^5}$$
$$+6m\frac{12m^6/n^2+n^2(n^2-m^2)}{F^5}-2(2-\mu)\log_e\left(\frac{(A+m-1)(B+m+1)}{(F+m)^2}\right)\Bigg] \tag{AI-9}$$

$$I_{r\text{-}t}=\frac{1}{4\pi(1-\mu)}\Bigg[\frac{(1-2\mu)}{A}+\frac{(7-2\mu)-12m+12(1-\mu)(m+1)m^2/n^2}{B}+12m\frac{1-(1-\mu)(m/n)^2}{F}$$
$$-\frac{(m-1)^3+mn^2}{A^3}+\frac{(m+1)^3[3+2(5+2\mu)m^2/n^2]+m[(21-4\mu)n^2-2m^2]}{B^3}$$
$$-2m\frac{(5+2\mu)m^2(m/n)^2+2(5-\mu)n^2}{F^3}+\frac{6m[n^2(m^2-n^2)-2(m+1)^5m/n^2]}{B^5}$$
$$-\frac{6m[n^2(m^2-n^2)-2m^6/n^2]}{F^5}+(1-2\mu)\log_e\left(\frac{A+m-1}{F+m}\right)$$
$$+[(1-2\mu)^2-6]\log_e\left(\frac{B+m+1}{F+m}\right)+2(1-\mu)(1-2\mu)\left(\frac{m-1}{B+m+1}-\frac{m}{F+m}\right)\Bigg] \tag{AI-10}$$

$$I_{\theta\text{-}t}=\frac{1}{4\pi(1-\mu)}\Bigg[\frac{(1-2\mu)}{A}+\frac{(1-2\mu)[(3-4\mu)+6(m+1)m^2/n^2]+6(2m-1)}{B}$$
$$+\frac{6m[(1-2\mu)(m/n)^2-2]}{F}-(1-2\mu)\frac{2(m+1)^3(1-m^2/n^2)+2mn^2)}{B^3}$$

$$+\frac{2(m+1)^3(1-6m^2/n^2)+2m(3n^2-m^2)}{B^3}+\frac{2(1-2\mu)m(m^2+2n^2-m^4/n^2)-6m(n^2-m^4/n^2)}{F^3}$$

$$+$$

$$+(1-2\mu)\log_e\left(\frac{A+m-1}{F+m}\right)+[(1-2\mu)^2-6]\log_e\left(\frac{B+m+1}{F+m}\right)$$
$$+2(1-\mu)(1-2\mu)\left(\frac{m-1}{B+m+1}-\frac{m}{F+m}\right)\ \Bigg] \qquad \text{(AI-11)}$$

and,

$$I_{\tau\text{-}t}=\frac{n}{4\pi(1-\mu)}\Bigg[\frac{2(2-\mu)+(1-2\mu)(m-1)m/n^2}{A}-\frac{6(m/n)^4}{F}+\frac{(m-1)^3m/n^2-n^2}{A^3}$$
$$-\frac{2(2-\mu)+[(1-2\mu)-6(m/n)^2](m+1)m/n^2}{B}-6\frac{(m^2/n^2-1)m(m+1)^5/n^2+2m^2n^2}{B^5}$$
$$-\frac{(3-4\mu+12m^2/n^2)(m+1)^3m/n^2+4m^2(5-\mu)-n^2}{B^3}-6m^2\frac{(m^2/n^2-1)m^4/n^2+2n^2}{F^5}$$
$$+2m^2\frac{(1-2\mu)m^2/n^2+6m^4/n^4+2(5-\mu)}{F^3} \qquad \text{(AI-12)}$$

APPENDIX B

Derivation of Solutions of Pore Pressure Dissipation

Appendix B-1

The solution of equations (5.2-1) and (5.2-1a,b)

$$\frac{\partial u}{\partial t} = C_h \frac{\partial^2 u}{\partial x^2} \qquad (5.2\text{-}1)$$

$$u(x,0) = \psi(x) = \begin{cases} u_0 & (0 \le x \le b) \\ u_0 \dfrac{l-x}{l-b} & (b \le x \le l) \\ 0 & (x \ge l) \end{cases} \qquad (5.2\text{-}1a)$$

$$\partial u/\partial x \,|_{x=0} = 0, \; \partial u/\partial x \,|_{x=R} = 0 \qquad (5.2\text{-}1b)$$

Set $u(x,t) = X(x)T(t)$ (B-1)

By substituting this into the (5.2-1), gives $XT' = C_h X'' T$ with $T' = dT/dt$ and $X'' = d^2X/dx^2$. To separate the variables, we divide by $C_h \cdot X \cdot T$, obtaining

$$\frac{T'}{C_h T} = \frac{X''}{X} \qquad (B\text{-}2)$$

The left side depends only on t and the right side only on x, so that both side must be equal to a constant k. But we may show that for $k > 0$ the only solution is infinite when $t \to \infty$;{for $k = 0$ the only solution is not zero when $t \to \infty$ or $u \equiv 0$ from $X'(R)=0$. Hence we left with the possibility of choosing k negative, $k = -p^2$. Thus,

$$\frac{T'}{C_h T} = \frac{X''}{X} = -p^2 \qquad (B\text{-}3)$$

This yields immediately tow ordinary linear differential equations, namely

$$T' + C_h p^2 T = 0 \qquad (B\text{-}4)$$

And $$X'' + p^2 X = 0 \qquad (B\text{-}5)$$

The general solution of (B-5) is

$$X(x) = A \cos px + B \sin px$$

$$X'(x) = -A \sin px + Bp \cos px$$

From this and (5.2-1b) we have

$$X'(0) = Bp = 0$$

and $$X'(R) = -Ap \sin pR = 0$$

we must take $A \neq 0$ since otherwise $X \equiv 0$. Hence $\sin pR = 0$, thus

$$pR = n\pi, \quad \text{so that } p = p_n = n\pi/R \qquad (n=1,2,3\ldots.)$$

Setting A=1, we obtain the following solutions of (B-5) satisfying (5.2-1b):

$$X_n = \cos(n\pi x/R)$$

The general solution of (B-4) corresronding eigenvalues $\lambda_n^2 = C_h p_n^2$ is

$$T_n = \exp\left(-C_h p^2 t\right)$$

$$= \exp\left(-C_h \frac{n^2\pi^2}{R^2} t\right) \qquad (n=1,2,3,\ldots)$$

Thus, solution of (5.2-1)satisfying satisfying (5.2-1b) are $u_n = X_n T_n$, written out

$$u_n(x,t) = a_n \cos\left(\frac{n\pi x}{R}\right)\exp\left(-C_h \frac{n^2\pi^2}{R^2} t\right) \qquad (n=1,2,3,\ldots)$$

To obtain a solution also satisfying the initial condition (5.2-1a), we consider a series of the these eigenfunction corresponding to the eigenvalues $p_n = n\pi/R$ and $\lambda_n = \sqrt{C_h}\, p_n$,

$$u(x,t) = \sum_{n=1}^{\infty} u_n(x,t) = \sum_{n=1}^{\infty} a_n \cos\left(\frac{n\pi x}{R}\right)\exp\left(-C_h \frac{n^2\pi^2}{R^2} t\right) \qquad \text{(B-6)}$$

From this and (5.2-1a) we have

$$u(x,0) = \sum_{n=1}^{\infty} a_n \cos\left(\frac{n\pi x}{R}\right) = \psi(x) \qquad \text{(B1-7)}$$

Hence for (B-6) to satisfy (4-1'), the a_n's must be the coefficients of the Fourier cosine series,

$$\{a_0 = \frac{1}{R}\int_0^R \psi(x)dx = \frac{1}{R}\int_0^b u_0 dx + \frac{1}{R}\int_b^l \frac{u_0}{l-b}(l-x)dx + \frac{1}{R}\int_l^R 0dx$$

$$= u_0\frac{b}{R} + u_0\frac{l}{R}\frac{x}{l-b}\Big|_{x=b}^{x=l} - u_0\frac{1}{R(l-b)}\frac{x^2}{2}\Big|_{x=b}^{x=l} + 0$$

$$= u_0\frac{b}{R} + u_0\frac{l}{R} - u_0\frac{1}{R(l-b)}\frac{(l^2-b^2)}{2} = u_0\frac{b+l}{R} - u_0\frac{l+b}{2R}$$

$$= u_0\frac{l+b}{2R}\}$$

$$a_n = \frac{2}{R}\int_0^R \psi(x)\cos\frac{n\pi x}{R}dx$$

$$= \frac{2}{R}\int_0^b u_0\cos\frac{n\pi x}{R}dx + \frac{2}{R}\int_b^l u_0\frac{l-x}{l-b}\cos\frac{n\pi x}{R}dx + \frac{2}{R}\int_l^R 0dx$$

$$= 2u_0 \frac{1}{n\pi} \sin \frac{n\pi x}{R}\Big|_{x=0}^{x=b} + \frac{2u_0 l}{l-b} \frac{1}{n\pi} \sin \frac{n\pi x}{R}\Big|_{x=b}^{x=l} - \frac{2u_0}{l-b} \frac{1}{n\pi} \int_b^l x d\left(\sin \frac{n\pi x}{R} \right)$$

$$= \frac{2u_0}{n\pi} \sin \frac{n\pi b}{R} + \frac{2u_0}{n\pi} \frac{l}{l-b} \left(\sin \frac{n\pi l}{R} - \sin \frac{n\pi b}{R} \right) - \frac{2u_0}{n\pi} \frac{x}{l-b} \sin \frac{n\pi x}{R}\Big|_{x=b}^{l}$$
$$+ \frac{2u_0}{n\pi} \frac{1}{l-b} \int_b^l \sin \frac{n\pi x}{R} dx$$

$$= \frac{2u_0}{n\pi} \sin \frac{n\pi b}{R} + \frac{2u_0}{n\pi} \frac{l}{l-b} \left(\sin \frac{n\pi l}{R} - \sin \frac{n\pi b}{R} \right) - \frac{2u_0}{n\pi} \frac{1}{l-b} \left(l \sin \frac{n\pi l}{R} - b \sin \frac{n\pi b}{R} \right)$$
$$- \frac{2u_0}{n\pi} \frac{1}{l-b} \frac{R}{n\pi} \cos \frac{n\pi x}{R}\Big|_{x=b}^{x=l}$$

$$= \frac{2u_0}{(n\pi)^2} \frac{R}{l-b} \left(\cos \frac{n\pi b}{R} - \cos \frac{n\pi l}{R} \right) \qquad \text{(B1-8)}$$

Thus,

$$u(x,t) = u_0 \frac{l+b}{2R} + u_0 \sum_{n=1}^{\infty} \frac{2}{(n\pi)^2} \frac{R}{l-b} \left(\cos \frac{n\pi b}{R} - \cos \frac{n\pi l}{R} \right) \cos \left(\frac{n\pi x}{R} \right) \exp \left(-C_h \frac{n^2 \pi^2}{R^2} t \right)$$

(B1-9)

When $R=l$, $a_n = \frac{2u_0}{(n\pi)^2} \frac{l}{l-b} \left(\cos \frac{n\pi b}{l} - \cos n\pi \right)$

$$\text{u(x,t)} = u_0 \frac{1}{2} \left(1 + \frac{b}{l} \right) + u_0 \sum_{n=1}^{\infty} \frac{2l}{n^2 \pi^2 (l-b)} \left(\cos \frac{n\pi b}{l} - \cos n\pi \right) \cos \left(\frac{n\pi x}{l} \right) e^{-C_h \frac{n^2 \pi^2}{l^2} t}$$

(B1-9')

when b=l, $a_n = \frac{2u_0}{n\pi} \sin \frac{n\pi b}{R}$

$$\text{u(x,t)} = u_0 \frac{1}{2} \left(1 + \frac{b}{l} \right) + u_0 \sum_{n=1}^{\infty} \frac{2u_0}{n\pi} \sin \frac{n\pi b}{R} \cdot \cos \left(\frac{n\pi x}{l} \right) e^{-C_h \frac{n^2 \pi^2}{l^2} t} \qquad \text{(B1-9'')}$$

Appendix B-2 the solution of equations (5.2-1) and (5.2-1a,c)

$$\frac{\partial u}{\partial t} = C_h \frac{\partial^2 u}{\partial x^2} \qquad (5.2\text{-}1)$$

$$u(x,0) = \psi(x) = \begin{cases} u_0 & (0 \le x \le b) \\ u_0 \dfrac{l-x}{l-b} & (b \le x \le l) \\ 0 & (x \ge l) \end{cases} \qquad (5.2\text{-}1a)$$

$$\partial u/\partial x \,|_{x=0} = 0,\ u \,|_{x=R} = 0 \qquad (5.2\text{-}1c)$$

Set $u(x,t) = X(x)T(t)$ (B2-1)

By substituting this into the (5.2-1), gives $XT' = C_h X'' T$ with $T' = dT/dt$ and $X'' = d^2X/dt^2$. To separate the variables, we divide by Ch·X·T, obtaining

$$\frac{T'}{C_h T} = \frac{X''}{X} \qquad (B2\text{-}2)$$

The left side depends only on t and the right side only on x, so that both side must be equal to a constant k. But we may show that for $k > 0$ the only solution is infinite when $t \to \infty$; for $k = 0$ the only solution is not zero when $t \to \infty$ or $u \equiv 0$. Hence we left with the possibility of choosing k negative, $k = -p^2$. Thus,

$$\frac{T'}{C_h T} = \frac{X''}{X} = -p^2 \qquad (B2\text{-}3)$$

This yields immediately tow ordinary linear differential equations, namely

$$T' + C_h p^2 T = 0 \qquad (B2\text{-}4)$$

And $X'' + p^2 X = 0$ (B2-5)

The general solution of (B-5) is

$$X(x) = A \cos px + B \sin px$$

From this and (4-1'') we have

$$X'(0) = Bp = 0$$

and $X(R) = A \cos pR = 0$

we must take $A \neq 0$ since otherwise $X \equiv 0$. Hence $\cos pR = 0$, thus

$$pR = (1/2+n)\pi, \qquad \text{so that } p = p_n = \frac{(1/2+n)\pi}{R} \qquad (n=1,2,3\ldots.)$$

Setting A=1, we obtain the following solutions of (B-5) satisfying (4-1''):

$$X_n = \cos\left[\left(\tfrac{1}{2}+n\right)\frac{\pi x}{R}\right]$$

The general solution of (B-4) corresronding eigenvalues $\lambda_n^2 = C_h p_n^2$ is

$$T_n = \exp(-C_h\, p_n^2 t)$$

$$= \exp\left[-C_h(1/2+n)^2 \frac{\pi^2}{R^2} t\right] \qquad (n=1,2,3,\ldots)$$

Thus, solution of (4-1) satisfying (4-1'') are $u_n = X_n T_n$, written out

To obtain a solution also satisfying the initial condition (4-1'), we consider a series of the these eigenfunction corresponding to the eigenvalues $p_n = \frac{(1/2+n)\pi}{R}$ and $\lambda_n = \sqrt{C_h} p_n$,

$$u(x,t) = \sum_{n=1}^{\infty} u_n(x,t) = \sum_{n=1}^{\infty} a_n \cos\left[(1/2+n)\frac{\pi x}{R}\right] \exp\left[-C_h(1/2+n)^2 \frac{\pi^2}{R^2} t\right] \qquad \text{(B2-6)}$$

From this and (4-1') we have

$$u(x,0) = \sum_{n=1}^{\infty} a_n \cos\frac{(1/2+n)\pi x}{R} = \psi(x) \qquad \text{(B2-7)}$$

Hence for (B-6) to satisfy (4-1'), the a_n's must be the coefficients of the Fourier cosine series,

$$a_n = \frac{2}{R}\int_0^R \psi(x)\cos\left[(1/2+n)\frac{\pi x}{R}\right]dx$$

$$= \frac{2}{R}\int_0^b u_0 \cos\frac{(1/2+n)\pi x}{R}dx + \frac{2}{R}\int_b^l u_0 \frac{l-x}{l-b}\cos\frac{(1/2+n)\pi x}{R}dx + \frac{2}{R}\int_l^R 0\,dx$$

$$= 2u_0 \frac{1}{(1/2+n)\pi}\sin\frac{(1/2+n)\pi x}{R}\Bigg|_{x=0}^{x=b} + \frac{2u_0 l}{l-b}\frac{1}{(1/2+n)\pi}\sin\frac{(1/2+n)\pi x}{R}\Bigg|_{x=b}^{x=l}$$

$$-\frac{2u_0}{l-b}\frac{1}{(1/2+n)\pi}\int_b^l x\,d\left(\sin\frac{(1/2+n)\pi x}{R}\right)$$

$$= \frac{2u_0}{(1/2+n)\pi}\sin\frac{(1/2+n)\pi b}{R} + \frac{2u_0}{(1/2+n)\pi}\frac{l}{l-b}\left(\sin\frac{(1/2+n)\pi l}{R} - \sin\frac{(1/2+n)\pi b}{R}\right)$$

$$-\frac{2u_0}{(1/2+n)\pi}\frac{x}{l-b}\sin\frac{(1/2+n)\pi x}{R}\Bigg|_{x=b}^{l} + \frac{2u_0}{(1/2+n)\pi}\frac{1}{l-b}\int_b^l \sin\frac{(1/2+n)\pi x}{R}dx$$

$$= \frac{2u_0}{(1/2+n)\pi}\sin\frac{(1/2+n)\pi b}{R} + \frac{2u_0}{(1/2+n)\pi}\frac{l}{l-b}\left(\sin\frac{(1/2+n)\pi l}{R} - \sin\frac{(1/2+n)\pi b}{R}\right)$$

$$-\frac{2u_0}{(1/2+n)\pi}\frac{1}{l-b}\left(l\sin\frac{(1/2+n)\pi l}{R} - b\sin\frac{(1/2+n)\pi b}{R}\right)$$

$$-\frac{2u_0}{(1/2+n)\pi}\frac{1}{l-b}\frac{R}{(1/2+n)\pi}\cos\frac{(1/2+n)\pi x}{R}\Bigg|_{x=b}^{x=l}$$

$$= \frac{2u_0}{(\frac{1}{2}+n)^2\pi^2}\frac{R}{l-b}\left(\cos\frac{(\frac{1}{2}+n)\pi b}{R} - \cos\frac{(\frac{1}{2}+n)\pi l}{R}\right) \qquad \text{(B2-8)}$$

Thus,

$$u(x,t) = u_0\sum_{n=1}^{\infty}\frac{2}{(\frac{1}{2}+n)^2\pi^2}\frac{R}{l-b}\left(\cos\frac{(\frac{1}{2}+n)\pi b}{R} - \cos\frac{(\frac{1}{2}+n)\pi l}{R}\right)\cos\left(\frac{(\frac{1}{2}+n)\pi x}{R}\right)$$
$$\exp\left(-C_h\frac{(\frac{1}{2}+n)^2\pi^2}{R^2}t\right) \qquad \text{(B2-9)}$$

If 1 = b, $\quad a_n = \frac{2u_0}{(\frac{1}{2}+n)\pi}\sin\frac{(\frac{1}{2}+n)\pi b}{R}$

$$u(x,t) = u_0\sum_{n=1}^{\infty}\frac{2}{(\frac{1}{2}+n)\pi}Sin\frac{(\frac{1}{2}+n)\pi b}{R}Cos\left(\frac{(\frac{1}{2}+n)\pi x}{R}\right)Exp\left(-C_h\frac{(\frac{1}{2}+n)^2\pi^2}{R^2}t\right) \qquad \text{(B2-9')}$$

Appendix B-3 the solution of equations (5-4) and (5-4a), (5-4b)

$$\frac{\partial u}{\partial t} = C_h\left(\frac{\partial^2 u}{\partial r^2} + \frac{1}{r}\frac{\partial u}{\partial r}\right) \tag{5-4}$$

$$u(x,0)= \omega(r) = \begin{cases} u_0 & (0 \le r \le b) \\ u_0 \dfrac{l^2 - r^2}{l^2 - b^2} & (b \le r \le l) \\ 0 & (l \le r \le R) \end{cases} \tag{5-4a}$$

$$\partial u/\partial r\,|_{r=0} = 0,\ u\,|_{r=R} = 0 \tag{5-4b}$$

$$\text{or } \partial u/\partial r\,|_{r=0} = 0,\ \partial u/\partial r\,|_{r=R} = 0 \tag{5-4b'}$$

Set $u(x,t) = \Phi(r)T(t)$ (B3-1)

By substituting this into the Eq. (5-4), gives $\Phi T' = C_h(\Phi'' + \Phi' T/r)$ with $T' = dT/dt$ and $\Phi'' = d^2\Phi/dr^2$. To separate the variables, we divide by $C_h \cdot X \cdot T$, obtaining

$$\frac{T'}{C_h T} = \frac{\Phi'' + \Phi'/r}{\Phi} \tag{B3-2}$$

The left side depends only on t and the right side only on r, so that both sides must be equal to a constant k. But we may show that for $k > 0$ the only solution is infinite when $t \to \infty$; for $k = 0$ the only solution is not zero when $t \to \infty$ or $u \equiv 0$ from $\Phi'(R)=0$. Hence we left with the possibility of choosing k negative, $k = -p^2$. Thus,

$$\frac{T'}{C_h T} = \frac{\Phi'' + \Phi'/r}{\Phi} = -k^2 \tag{B3-3}$$

This yields immediately two ordinary linear differential equations, namely

$$T' + C_h k^2 T = 0 \tag{B3-4}$$

And $$\Phi'' + \Phi'/r + k^2\Phi = 0 \tag{B3-5}$$

The general solutions of Eq. (B3-5) are the Bessel functions $J_0(kr)$ and $Y_0(kr)$ of the first and second kind (See sec.4.5, 4.6 of Advanced Engineering Mathematics, Erwin Kreyszig,1999). Now $Y_0(kr)$ becomes infinite at r=0, so that we cannot use it because u must always remain finite. This leaves us with

$$\Phi(r) = J_0(kr) \tag{B3-6}$$

On the boundary r=R, By Eq.(5-4b) we get $\Phi(R) = J_0(kR) = 0$, we can satisfy this condition because $J_0(kR)$ has infinitely many positive zeroes, $kR = \alpha_1, \alpha_2, \alpha_3, \ldots\ldots$with numerical values α_1=2.40483, α_2=5.52008, α_3=8.65373, α_4=11.79153, α_5=14.93092, α_6=18.07106, α_7=21.21164,

α_8=24.35247, α_9=27.49348, α_{10}=30.63461, α_{11}=33.7758, α_{12}=36.9171, α_{13}=40.0584, α_{14}=43.1998, α_{15}=46.3412, α_{16}=49.4826, ...

$kR=\alpha_m$, thus $k=k_m=\alpha_m/R$, m=1,2,3,.....(B3-7)

Hence, the functions

$$\Phi_m(r)= J_0(k_m r) = J_0(\frac{\alpha_m}{R} r) \qquad m=1,2,3,.....(B3\text{-}8)$$

are solutions of Eq.(B3-5) that vanish at r=R.

For $\Phi_m(r)$ in Eq.(B3-8), a corresponding general solution of Eq.(B3-4) with $\lambda = C_h k^2 = C_h k_m^2 = C_h(\alpha_m/R)^2$ is

$$T_m= \exp\left(-C_h \frac{\alpha_m^2}{R^2} t\right) \qquad m=1,2,3,.....(B3\text{-}9)$$

Thus,

$$u_m(r,t) = b_m\Phi_m(r)\, T_m(t) = b_m J_0(\frac{\alpha_m}{R} r)\, \exp\left(-C_h \frac{\alpha_m^2}{R^2} t\right)$$

$$u(r,t) = \sum_{m=1}^{\infty} b_m J_0\left(\frac{\alpha_m}{R} r\right)\exp\left(-C_h \frac{\alpha_m^2}{R^2} t\right) \qquad (B3\text{-}10)$$

Setting t=0,

$$u(r,0) = \sum_{m=1}^{\infty} b_m J_0\left(\frac{\alpha_m}{R} r\right) = \omega(r)$$

$$b_m= \frac{2}{R^2 J_1^2(\alpha_m)} \int_0^R r\omega(r) J_0\left(\frac{\alpha_m}{R} r\right) dr \quad \text{(For the 1st kind boundary condition)}$$

$$= \frac{2}{R^2 J_1^2(\alpha_m)}\left[\int_0^b u_0 r J_0\left(\frac{\alpha_m}{R} r\right)dr + \int_b^l u_0 \frac{l^2-r^2}{l^2-b^2} r J_0\left(\frac{\alpha_m}{R} r\right)dr + \int_l^R 0\, dr\right]$$

$$= \frac{2u_0}{R^2 J_1^2(\alpha_m)}\left\{\frac{R}{\alpha_m} r J_1\left(\frac{\alpha_m}{R} r\right)\Big|_{r=0}^{r=b} + \frac{R}{\alpha_m}\int_b^l \frac{l^2-r^2}{l^2-b^2} d\left[r J_1\left(\frac{\alpha_m}{R} r\right)\right]\right\}$$

$$= \frac{2u_0}{R J_1^2(\alpha_m)}\frac{1}{\alpha_m}\left\{b J_1\left(\frac{\alpha_m}{R} b\right) + \frac{1}{l^2-b^2}\left[(l^2-r^2) r J_1\left(\frac{\alpha_m}{R} r\right)\Big|_{r=b}^{r=l} + 2\int_b^l r^2 J_1\left(\frac{\alpha_m}{R} r\right)dr\right]\right\}$$

$$= \frac{2u_0}{R J_1^2(\alpha_m)}\frac{1}{\alpha_m}\left\{b J_1\left(\frac{\alpha_m}{R} b\right) - b J_1\left(\frac{\alpha_m}{R} b\right) + \frac{2}{l^2-b^2}\frac{R}{\alpha_m} r^2 J_2\left(\frac{\alpha_m}{R} r\right)\Big|_{r=b}^{r=l}\right\}$$

$$= \frac{4u_0}{\alpha_m^2 J_1^2(\alpha_m)} \frac{1}{l^2 - b^2} \left[l^2 J_2\left(\frac{\alpha_m}{R} l\right) - b^2 J_2\left(\frac{\alpha_m}{R} b\right) \right] \qquad \text{(B3-11)}$$

where, $J_2(x) = \frac{2J_1(x)}{x} - J_0(x)$

By substituting b_m into the (B3-10), gives

$$u(r,t) = \sum_{m=1}^{\infty} \frac{4u_0 \left[l^2 J_2(\frac{\alpha_m}{R} l) - b^2 J_2(\frac{\alpha_m}{R} b) \right]}{\alpha_m^2 (l^2 - b^2) J_1^2(\alpha_m)} J_0\left(\frac{\alpha_m}{R} r\right) \exp\left(-C_h \frac{\alpha_m^2}{R^2} t\right) \qquad \text{(B3-12)}$$

When l = R, $J_2(\alpha_m) = \frac{2J_1(\alpha_m)}{\alpha_m} - J_0(\alpha_m) = \frac{2J_1(\alpha_m)}{\alpha_m}$

When l = b, $b_m = \frac{2u_0}{\alpha_m J_1^2(\alpha_m)} \frac{b}{R} J_1\left(\frac{\alpha_m}{R} b\right)$

$$u(r,t) = \sum_{m=1}^{\infty} \frac{2u_0}{\alpha_m J_1^2(\alpha_m)} \frac{b}{R} J_1\left(\frac{\alpha_m}{R} b\right) J_0\left(\frac{\alpha_m}{R} r\right) \exp\left(-C_h \frac{\alpha_m^2}{R^2} t\right) \qquad \text{(B3-12')}$$

********** *

On the boundary r=R, By Eq.(5-4b'), we get $\Phi'(r) \mid_{r=R} = - krJ_1(kr) \mid_{r=R} = kRJ_1(kR)=0$, we can satisfy this condition because $J_1(kR)$ has infinitely many positive zeroes, $kR=\beta_1, \beta_2, \beta_3, \ldots\ldots$ with numerical values $\beta_0=0$, $\beta_1=3.8317$, $\beta_2=7.0156$, $\beta_3=10.1735$, $\beta_4=13.3237$, $\beta_5=16.4706$, $\beta_6=19.6159$, $\beta_7=22.7601$, $\beta_8=25.9037$, $\beta_9=29.0468$, $\beta_{10}=32.1897$, $\beta_{11}=35.3323$, $\beta_{12}=38.4748$, $\beta_{13}=41.6171$, $\beta_{14}=44.7593$, $\beta_{15}=47.9015$, $\beta_{16}=51.0455$, ……

$$kR=\beta_m, \text{ thus } k=k_m=\beta_m/R, \quad (m=1,2,3,\ldots\ldots) \qquad \text{(B2-13)}$$

Hence, the functions

$$\Phi_m(r) = J_0(k_m r) = J_0\left(\frac{\beta_m}{R} r\right) \quad (m=1,2,3,\ldots\ldots) \qquad \text{B2-14)}$$

are solutions of Eq. (B3-2) that vanish at r=R.

For $\Phi_m(r)$ in Eq. (B3-8), a corresponding general solution of Eq.(B3-4) with $\lambda = C_h k^2 = C_h k_m^2 = C_h(\beta_m/R)^2$ is

$$T_m = \exp\left(-C_h \frac{\beta_m^2}{R^2} t\right) \qquad (m=1,2,3,\ldots\ldots) \qquad \text{(B3-15)}$$

Thus,

$$u_m(r,t) = b_m \Phi_m(r)\, T_m(t) = b_m J_0\left(\frac{\beta_m}{R} r\right) \exp\left(-C_h \frac{\beta_m^2}{R^2} t\right)$$

$$u(r,t) = \sum_{m=1}^{\infty} b_m J_0\left(\frac{\beta_m}{R} r\right) \exp\left(-C_h \frac{\beta_m^2}{R^2} t\right) \qquad \text{(B3-16)}$$

Setting t=0,

$$u(r,0) = \sum_{m=1}^{\infty} b_m J_0\left(\frac{\beta_m}{R} r\right) = \omega(r)$$

$$b_m = \frac{2}{R^2 J_0^2(\beta_m)} \int_0^R r\omega(r) J_0\left(\frac{\beta_m}{R} r\right) dr \qquad \text{(For the 2nd kind boundary condition)}$$

$$= \frac{4u_0}{\beta_m^2 J_0^2(\beta_m)} \frac{1}{l^2 - b^2} \left[l^2 J_2\left(\frac{\beta_m}{R} l\right) - b^2 J_2\left(\frac{\beta_m}{R} b\right) \right] \qquad \text{(B3-17)}$$

Where, $J_2(x) = \frac{2J_1(x)}{x} - J_0(x)$.

By substituting b_m into the (B3-16), gives

$$u(r,t) = \sum_{m=1}^{\infty} \frac{4u_0 \left[l^2 J_2(\frac{\beta_m}{R} l) - b^2 J_2(\frac{\beta_m}{R} b) \right]}{\beta_m^2 (l^2 - b^2) J_0^2(\beta_m)} J_0\left(\frac{\beta_m}{R} r\right) \exp\left(-C_h \frac{\beta_m^2}{R^2} t\right) \qquad \text{(B3-18)}$$

When R = l, $J_2(\beta_m) = \frac{2J_1(\beta_m)}{\beta_m} - J_0(\beta_m) = -J_0(\beta_m)$

When l = b, $b_m = \frac{2u_0}{\beta_m J_0^2(\beta_m)} \frac{b}{R} J_1\left(\frac{\beta_m}{R} b\right)$

$$u(r,t) = \sum_{m=1}^{\infty} \frac{2u_0}{\beta_m J_0^2(\beta_m)} \frac{b}{R} J_1\left(\frac{\beta_m}{R} b\right) J_0\left(\frac{\beta_m}{R} r\right) \exp\left(-C_h \frac{\beta_m^2}{R^2} t\right) \qquad \text{(B3-18')}$$

Appendix B- 4 the solution of equations (5-7) and (5-7a,b)

$$\frac{\partial u}{\partial t} = C_h\left(\frac{\partial^2 u}{\partial x^2} + \frac{\partial^2 u}{\partial y^2}\right) \qquad (5.2\text{-}7)$$

$$u(x,y,0)=\chi(x,y) = \begin{cases} u_0 & (A_1 : |x| \le b_x, |y| \le b_y) \\ u_0 \dfrac{l_x - x}{l_x - b_x} & (A_2 : b_x \le x \le l_x, |y| \le b_y + \dfrac{l_y - b_y}{l_x - b_x}(x - b_x) \\ u_0 \dfrac{l_y - y}{l_y - b_y} & (A_2 : b_y \le y \le l_y, |x| \le b_x + \dfrac{l_x - b_x}{l_y - b_y}(y - b_y) \\ 0 & (A_4 : l_x \le x \le R_x, l_y \le y \le R_y) \end{cases} \qquad (5.2\text{-}7')$$

$$\partial u/\partial x\,|_{x=0} = 0,\ u\,|_{x=Rx} = 0 \qquad (5.2\text{-}7'')$$

$$\partial u/\partial y\,|_{y=0} = 0,\ u\,|_{y=Ry} = 0 \qquad (5.2\text{-}7''')$$

where, $\eta = \dfrac{l_y - b_y}{l_x - b_x}$

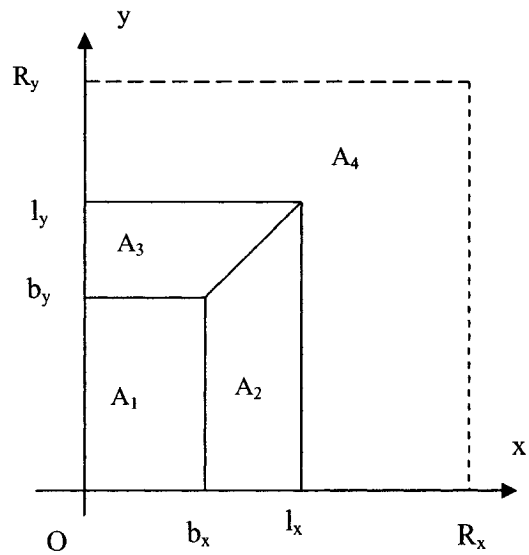

Fig.4-3 rectangle area of initial pore pressure contribution

Solution:

Set

$$u(x,y,t) = X(x)\cdot Y(y)\cdot T(t) \qquad (B4\text{-}1)$$

By substituting this into the (4-7), gives $XYT'=C_h(X''YT+XY''T)$ with $T'=dT/dt$, $X''=d^2X/dx^2$ and $Y''=d^2Y/dy^2$. To separate the variables, we divide by $Ch\cdot X\cdot Y\cdot T$, obtaining

$$\frac{T'}{C_h T} = \frac{X''}{X} + \frac{Y''}{Y} \qquad (B4\text{-}2)$$

The left side of the above depends only on time t and the right side only on x and y, so that both side must be equal to a constant k. But we may show that for k>0 the only solution is infinite when $t\to\infty$; for k=0 the only solution is not zero when $t\to\infty$. Hence we left with the possibility of choosing k negative, let $k= - h^2$. Thus,

$$\frac{T'}{C_h T} = \frac{X''}{X} + \frac{Y''}{Y} = - h^2 \qquad (B4\text{-}3)$$

This yields immediately tow ordinary linear differential equations, namely

$$T'+C_h h^2 T=0 \qquad (B4\text{-}5)$$

And

$$\frac{X''}{X} = -\frac{Y''}{Y} - h^2 \qquad (B4\text{-}6)$$

The left side of the (B4-6) depends only on x and the right side only on y, so that both side must be equal to a constant k'. But we may show similarly that only for k'<0 the solution will be reasonable. Thus, we left with the possibility of choosing k' negative, let $k' = -p^2$. Hence,

$$\frac{X''}{X} = -\frac{Y''}{Y} - h^2 = -p^2 \qquad \text{(B4-7)}$$

(B4-7) also yields immediately tow ordinary linear differential equations, that is

$$X'' + p^2X = 0 \qquad \text{(B4-8)}$$

And $$Y'' + q^2Y = 0 \qquad \text{(B4-9)}$$

Where $q^2 = h^2 - p^2$, that is,

$$h^2 = p^2 + q^2 \qquad \text{(B4-10)}$$

The general solution of (B4-8) is

$$X(x) = A\cdot Cospx + B\cdot Sinpx$$

From this and (4-1") we have

$$X'(0) = Bp = 0, \quad \therefore B=0$$

And $$X(R_x) = A\cdot Cos(pR_x) = 0$$

We must take $A \neq 0$ since otherwise $X \equiv 0$. Hence $\cos(pR_x) = 0$, thus

$$pR_x = (\tfrac{1}{2}+m)\pi,$$

so that $p = p_m = (\tfrac{1}{2}+m)\pi/R_x \qquad (m=0,1,2,3,\ldots)$

Setting A=1, we obtain the following solutions of (B4-8) satisfying (4-7"):

$$X_m = Cos[(\tfrac{1}{2}+m)\pi x/R_x] \qquad \text{(B4-11)}$$

Similarly, we obtain the solutions of (B4-9) satisfying (4-7"):

$$q = q_m = (\tfrac{1}{2}+n)\pi/R_y \qquad (n=0,1,2,3,\ldots)$$

$$Y_n = Cos[(\tfrac{1}{2}+n)\pi y/R_y] \qquad \text{(B4-12)}$$

By (B4-11) and (B4-12), to obtain the general solution of (B4-5) corresronding to the eigenvalues $\lambda_{mn}^2 = Ch\cdot h_{mn}^2 = C_h(p_m^2 + q_n^2)$, $\lambda_{mn}^2 = \sqrt{C_h}h_{mn}$, is

$$T_{m,n} = Exp[-C_h(p_m^2+q_n^2)t\,]$$

$$= Exp\left[-\left(\left(\tfrac{1}{2}+m\right)^2 + \left(\tfrac{1}{2}+n\right)^2\left(R_x/R_y\right)^2\right)\pi^2\frac{C_h}{R_x^2}t\right] \qquad \text{(B4-13)}$$

Set $$\mu_{mn} = \left(\tfrac{1}{2}+m\right)^2 + \left(\tfrac{1}{2}+n\right)^2\left(R_x/R_y\right)^2$$

$$T_{m,n} = Exp[-\mu_{mn}\pi^2C_ht/R_x^2\,] \qquad (m=0,1,2,3,\ldots,\ n=0,1,2,3,\ldots)$$

(B4-13')

Thus, a solution of (4-7) satisfying (4-7'') are $u_n = X_m Y_n T_n$, written out

$$u_{m,n}(x,y,t) = c_{mn} Cos\left(\frac{(1/2+m)\pi x}{R_x}\right) Cos\left(\frac{(1/2+n)\pi y}{R_y}\right) Exp\left(-\mu_{mn}\pi^2 \frac{C_h}{R_x^2} t\right)$$

(m=0,1,2,3,..., n=0,1,2,3,...) (B4-14)

To obtain a solution also satisfying the initial condition (4-7'), we consider a double series of the these eigenfunctions corresponding to the eigenvalues $p_m = (1/2+m)\pi/R_x$, $q_n = (1/2+n)\pi/R_y$ and $\lambda_n = \sqrt{C_h} h_{mn}$,

$$u(x,y,t) = \sum_{m=1}^{\infty}\sum_{n=1}^{\infty} u_{m,n}(x,y,t)$$

$$= \sum_{m=1}^{\infty}\sum_{n=1}^{\infty} c_{mn} Cos\frac{(1/2+m)\pi x}{R_x} \cdot Cos\frac{(1/2+n)\pi y}{R_y} \cdot \exp\left(-\mu_{mn}\pi^2 \frac{C_h}{R_x^2} t\right)$$

(B4-15)

From this and (B4-7'), we have

$$u(x,y,0) = \sum_{m=1}^{\infty}\sum_{n=1}^{\infty} c_{mn} Cos\frac{(1/2+m)\pi x}{R_x} \cdot Cos\frac{(1/2+n)\pi y}{R_y} = \chi(x,y)$$

Hence for (B4-15) to satisfy (4-7'), the c_{mn}'s must be the coefficients of the double Fourier cosine series,

$$c_{mn} = \frac{4}{R_x R_y}\int_{x=0}^{R_x}\int_{y=0}^{R_y} \chi(x,y) \cdot Cos\frac{(1/2+m)\pi x}{R_x} \cdot Cos\frac{(1/2+n)\pi y}{R_y} dxdy$$

$$= \frac{4u_0}{R_x R_y}\left\{\iint_{A_1} Cos\frac{(1/2+m)\pi x}{R_x} \cdot Cos\frac{(1/2+n)\pi y}{R_y} dxdy\right.$$

$$+ \iint_{A_2} \frac{l_x - x}{l_x - b_x} Cos\frac{(1/2+m)\pi x}{R_x} \cdot Cos\frac{(1/2+n)\pi y}{R_y} dxdy$$

$$\left. + \iint_{A_3} \frac{l_y - y}{l_y - b_y} Cos\frac{(1/2+m)\pi x}{R_x} \cdot Cos\frac{(1/2+n)\pi y}{R_y} dxdy + \iint_{A_4} 0 dxdy\right\}$$

$$= \frac{4u_0}{R_x R_y}\left\{ \iint_{A_1} + \iint_{A_2} + \iint_{A_3} \right\} \tag{B4-16}$$

in which,

$$\iint_{A_1} = \int_0^{b_x} Cos\frac{(1/2+m)\pi x}{R_x}dx \cdot \int_0^{b_y} \cdot Cos\frac{(1/2+n)\pi y}{R_y}dy$$

$$= \frac{R_x}{(1/2+m)\pi} Sin\frac{(1/2+m)\pi x}{R_x}\Bigg|_{x=0}^{x=b_x} \cdot \frac{R_x}{(1/2+m)\pi} Sin\frac{(1/2+n)\pi y}{R_y}\Bigg|_{y=0}^{y=b_y}$$

$$= \frac{R_x R_x}{(1/2+m)(1/2+m)\pi^2} Sin\frac{(1/2+m)\pi b_x}{R_x} \cdot Sin\frac{(1/2+n)\pi b_y}{R_y} \tag{B4-17}$$

$$\iint_{A_2} = \int_{x=b_x}^{l_x} \frac{l_x - x}{l_x - b_x} Cos\frac{(1/2+m)\pi x}{R_x} \cdot \left\{ \int_0^{b_y + \frac{l_y - b_y}{l_x - b_x}(x-b_x)} Cos\frac{(1/2+n)\pi y}{R_y}dy \right\} dx$$

$$= \int_{x=b_x}^{l_x} \frac{l_x - x}{l_x - b_x} Cos\frac{(1/2+m)\pi x}{R_x} \cdot \left\{ \frac{R_y}{(1/2+n)\pi} Sin\frac{(1/2+n)\pi y}{R_y}\Bigg|_{y=0}^{y=b_y + \frac{l_y - b_y}{l_x - b_x}(x-b_x)} \right\} dx$$

$$= \frac{R_y}{(1/2+n)\pi} \int_{x=b_x}^{l_x} \frac{l_x - x}{l_x - b_x} \cdot \underbrace{Cos\frac{(1/2+m)\pi x}{R_x} \cdot Sin\left[\frac{(1/2+n)\pi}{R_y}\left(b_y + \frac{l_y - b_y}{l_x - b_x}(x-b_x) \right) \right]}_{I} dx$$

According to $Cos\mathrm{B}\cdot Sin\mathrm{A} = \frac{1}{2}[Sin(\mathrm{A+B}) + Sin(\mathrm{A-B})]$,

$$I = \frac{1}{2}\left\{ Sin\left[\frac{(1/2+n)\pi}{R_y}\left(b_y + \frac{l_y - b_y}{l_x - b_x}(x-b_x) \right) + \frac{(1/2+m)\pi}{R_x}x \right] \right.$$

$$\left. + Sin\left[\frac{(1/2+n)\pi}{R_y}\left(b_y + \frac{l_y - b_y}{l_x - b_x}(x-b_x) \right) - \frac{(1/2+m)\pi}{R_x}x \right] \right\}$$

$$= \frac{1}{2}\left\{ Sin\left[\underbrace{\frac{(1/2+n)\pi}{R_y}\left(b_y - \frac{l_y - b_y}{l_x - b_x}b_x \right)}_{\alpha} + \underbrace{\left(\frac{(1/2+n)\pi}{R_y}\frac{l_y - b_y}{l_x - b_x} + \frac{(1/2+m)\pi}{R_x} \right)}_{\beta} x \right] \right.$$

$$+Sin\left\{\underbrace{\frac{(1/2+n)\pi}{R_y}\left(b_y-\frac{l_y-b_y}{l_x-b_x}b_x\right)}_{\alpha}+\underbrace{\left(\frac{(1/2+n)\pi}{R_y}\frac{l_y-b_y}{l_x-b_x}-\frac{(1/2+m)\pi}{R_x}\right)}_{\gamma}x\right\}$$

$$=\frac{1}{2}\left[Sin(\alpha+\beta x)+Sin(\alpha+\gamma x)\right] \qquad \text{(B4-19)}$$

where,

$$\alpha=\frac{(1/2+n)\pi}{R_y}\left(b_y-\frac{l_y-b_y}{l_x-b_x}b_x\right)$$

$$\beta=\frac{(1/2+n)\pi}{R_y}\frac{l_y-b_y}{l_x-b_x}+\frac{(1/2+m)\pi}{R_x}$$

$$\gamma=\frac{(1/2+n)\pi}{R_y}\frac{l_y-b_y}{l_x-b_x}-\frac{(1/2+m)\pi}{R_x} \qquad \text{(B4-20)}$$

If $\gamma \neq 0$, Substitute I into $\iint_{A_2}$, we get

$$\iint_{A_2}=\frac{R_y}{(1/2+n)\pi}\int_{x=b_x}^{l_x}\frac{l_x-x}{l_x-b_x}\cdot\frac{1}{2}\left[Sin(\alpha+\beta x)+Sin(\alpha+\gamma x)\right]dx \qquad \text{(B4-21)}$$

$$=\frac{1}{2}\frac{R_y}{(1/2+n)\pi}\left\{-\frac{l_x-x}{l_x-b_x}\left[\frac{1}{\beta}Cos(\alpha+\beta x)+\frac{1}{\gamma}Cos(\alpha+\gamma x)\right]\Bigg|_{x=b_x}^{l_x}\right.$$

$$\left.-\int_{x=b_x}^{l_x}\frac{1}{l_x-b_x}\left[\frac{1}{\beta}Cos(\alpha+\beta x)+\frac{1}{\gamma}Cos(\alpha+\gamma x)\right]dx\right.$$

$$=\frac{1}{2}\frac{R_y}{(1/2+n)\pi}\left\{\frac{1}{\beta}Cos(\alpha+\beta b_x)+\frac{1}{\gamma}Cos(\alpha+\gamma b_x)\right.$$

$$\left.-\frac{1}{l_x-b_x}\left[\frac{1}{\beta^2}Sin(\alpha+\beta x)+\frac{1}{\gamma^2}Sin(\alpha+\gamma x)\right]_{x=b_x}^{x=l_x}\right\}$$

$$=\frac{1}{2}\frac{R_y}{(1/2+n)\pi}\left\{\frac{1}{\beta}Cos(\alpha+\beta b_x)+\frac{1}{\gamma}Cos(\alpha+\gamma b_x)\right.$$

$$-\frac{1}{l_x-b_x}\left[\frac{1}{\beta^2}[Sin(\alpha+\beta l_x)-Sin(\alpha+\beta b_x)]+\frac{1}{\gamma^2}[Sin(\alpha+\gamma l_x)-Sin(\alpha+\gamma l_x)]\right]\Bigg\}$$

(B4-21')

$$\alpha+\beta b_x=\frac{(1/2+n)\pi}{R_y}\left(b_y-\frac{l_y-b_y}{l_x-b_x}b_x\right)+\left(\frac{(1/2+n)\pi}{R_y}\frac{l_y-b_y}{l_x-b_x}+\frac{(1/2+m)\pi}{R_x}\right)b_x$$

$$=\frac{(1/2+n)\pi}{R_y}b_y+\frac{(1/2+m)\pi}{R_x}b_x=\mathrm{B_y}+\mathrm{B_x};$$

$$\alpha+\gamma b_x=\frac{(1/2+n)\pi}{R_y}\left(b_y-\frac{l_y-b_y}{l_x-b_x}b_x\right)+\left(\frac{(1/2+n)\pi}{R_y}\frac{l_y-b_y}{l_x-b_x}-\frac{(1/2+m)\pi}{R_x}\right)b_x$$

$$=\frac{(1/2+n)\pi}{R_y}b_y-\frac{(1/2+m)\pi}{R_x}b_x=\mathrm{B_y}-\mathrm{B_x};$$

$$\alpha+\beta l_x=\frac{(1/2+n)\pi}{R_y}\left(b_y-\frac{l_y-b_y}{l_x-b_x}b_x\right)+\left(\frac{(1/2+n)\pi}{R_y}\frac{l_y-b_y}{l_x-b_x}+\frac{(1/2+m)\pi}{R_x}\right)l_x$$

$$=\frac{(1/2+n)\pi}{R_y}l_y+\frac{(1/2+m)\pi}{R_x}l_x=\mathrm{L_y}+\mathrm{L_x};$$

$$\alpha+\gamma l_x=\frac{(1/2+n)\pi}{R_y}\left(b_y-\frac{l_y-b_y}{l_x-b_x}b_x\right)+\left(\frac{(1/2+n)\pi}{R_y}\frac{l_y-b_y}{l_x-b_x}-\frac{(1/2+m)\pi}{R_x}\right)l_x$$

$$=\frac{(1/2+n)\pi}{R_y}l_y-\frac{(1/2+m)\pi}{R_x}l_x=\mathrm{L_y}-\mathrm{L_x};$$

(B4-22)

That is,

$$\mathrm{L_x}=\frac{(1/2+m)\pi}{R_x}l_x;\qquad \mathrm{L_y}=\frac{(1/2+n)\pi}{R_y}l_y;$$

$$\mathrm{B_x}=\frac{(1/2+m)\pi}{R_x}b_x;\qquad \mathrm{B_y}=\frac{(1/2+n)\pi}{R_y}b_y;$$

$$\mathrm{D_x}=\mathrm{L_x}-\mathrm{B_x}=\frac{(1/2+m)\pi}{R_x}(l_x-b_x);$$

$$D_y = L_y - B_y = \frac{(1/2 + n)\pi}{R_y}(l_y - b_y)$$

(B4-23)

Then, $\alpha = D_y\left(\frac{b_y}{l_y - b_y} - \frac{b_x}{l_x - b_x}\right)$;

$$\beta = \frac{D_y + D_x}{l_x - b_x}; \qquad \gamma = \frac{D_y - D_x}{l_x - b_x};$$

(B4-24)

Substitute the above into (B4-21'), thus

$$\iint_{A_2} = \frac{1}{2}\frac{R_y}{(1/2 + n)\pi}\left\{(l_x - b_x)\left[\frac{Cos(B_y + B_x)}{D_y + D_x} + \frac{Cos(B_y - B_x)}{D_y - D_x}\right]\right.$$

$$\left. -(l_x - b_x)\left[\frac{Sin(L_y + L_x) - Sin(B_y + B_x)}{(D_y + D_x)^2} + \frac{Sin(L_y + L_x) - Sin(B_y + B_x)}{(D_y - D_x)^2}\right]\right\}$$

$$= \frac{1}{2}\frac{R_x R_y}{(1/2 + m)(1/2 + n)\pi^2}\left\{D_x\left[\frac{Cos(B_y + B_x)}{D_y + D_x} + \frac{Cos(B_y - B_x)}{D_y - D_x}\right]\right.$$

$$\left. - D_x\left[\frac{Sin(L_y + L_x) - Sin(B_y + B_x)}{(D_y + D_x)^2} + \frac{Sin(L_y - L_x) - Sin(B_y - B_x)}{(D_y - D_x)^2}\right]\right\}$$

(B4-25)

Similarly,

$$\iint_{A_3} = \frac{1}{2}\frac{R_x R_y}{(1/2 + m)(1/2 + n)\pi^2}\left\{D_y\left[\frac{Cos(B_y + B_x)}{D_y + D_x} - \frac{Cos(B_y - B_x)}{D_y - D_x}\right]\right.$$

$$\left. - D_y\left[\frac{Sin(L_y + L_x) - Sin(B_y + B_x)}{(D_y + D_x)^2} - \frac{Sin(L_y - L_x) - Sin(B_y - B_x)}{(D_y - D_x)^2}\right]\right\}$$

(B4-26)

Then, Eq.(B4-25) + Eq.(B4-26),

$$\iint_{A_2} + \iint_{A_3} = \frac{1}{2}\frac{R_x R_y}{(1/2 + m)(1/2 + n)\pi^2}\left\{(D_x + D_y)\frac{Cos(B_y + B_x)}{D_y + D_x} + (Dx - Dy)\frac{Cos(B_y - B_x)}{D_y - D_x}\right.$$

$$-(D_x+D_y)\frac{Sin(L_y+L_x)-Sin(B_y+B_x)}{(D_y+D_x)^2}-(D_x-D_y)\frac{Sin(L_y-L_x)-Sin(B_y-B_x)}{(D_y-D_x)^2}\Bigg\}$$

$$=\frac{1}{2}\frac{R_xR_y}{(1/2+m)(1/2+n)\pi^2}\Big\{Cos(B_y+B_x)-Cos(B_y-B_x)$$

$$-\frac{Sin(L_y+L_x)-Sin(B_y+B_x)}{(D_y+D_x)}+\frac{Sin(L_y-L_x)-Sin(B_y-B_x)}{(D_y-D_x)}\Bigg\}$$

$$=\frac{1}{2}\frac{R_xR_y}{(1/2+m)(1/2+n)\pi^2}\Big\{-2\cdot SinB_x\cdot SinB_y$$

$$-\frac{Sin(L_y+L_x)-Sin(B_y+B_x)}{(D_y+D_x)}+\frac{Sin(L_y-L_x)-Sin(B_y-B_x)}{(D_y-D_x)}\Bigg\}$$

(B4-27)

$$c_{mn}=\frac{4u_0}{R_xR_y}\left\{\iint_{A_1}+\iint_{A_2}+\iint_{A_3}\right\}$$

$$=\frac{2u_0}{(1/2+m)(1/2+n)\pi^2}\left[\frac{Sin(B_y+B_x)-Sin(L_y+L_x)}{(D_y+D_x)}-\frac{Sin(B_y-B_x)-Sin(L_y-L_x)}{(D_y-D_x)}\right]$$

(B4-28)

Some special cases:

1) If $l_x=b_x$ and $l_y=b_y$, then $\iint_{A_2}=\iint_{A_3}=0$; thus,

$$c_{mn}=\frac{4u_0}{(1/2+m)(1/2+m)\pi^2}SinB_x\cdot SinB_y \qquad \text{(B4-29)}$$

2) If $\gamma=0$, that is, $D_y=D_x$, $\alpha=B_y-B_x=L_y-L_x$; thus, from Eq.(B4-21),

$$\iint_{A_2}=\frac{R_y}{(1/2+n)\pi}\int_{x=b_x}^{l_x}\frac{l_x-x}{l_x-b_x}\cdot\frac{1}{2}[Sin(\alpha+\beta x)+Sin\alpha]dx$$

$$= \frac{R_y}{2(\frac{1}{2}+n)\pi}\left\{\frac{Sin\alpha}{l_x-b_x}\left(l_x x-\frac{1}{2}x^2\right)\Big|_{x=b_x}^{x=l_x} - \frac{l_x-x}{l_x-b_x}\frac{1}{\beta}Cos(\alpha+\beta x)\Big|_{x=b_x}^{x=l_x} - \int_{x=b_x}^{l_x}\frac{1}{l_x-b_x}\cdot\frac{1}{\beta}Cos(\alpha+\beta x)dx\right\}$$

$$= \frac{R_y}{2(\frac{1}{2}+n)\pi}\left\{\frac{1}{2}(l_x-b_x)Sin\alpha + \frac{1}{\beta}Cos(\alpha+\beta b_x) - \frac{1}{l_x-b_x}\frac{1}{\beta^2}Sin(\alpha+\beta x)\Big|_{x=b_x}^{x=l_x}\right\}$$

$$= \frac{R_y}{2(\frac{1}{2}+n)\pi}\left\{\frac{1}{2}(l_x-b_x)Sin(B_y-B_x) + \frac{l_x-b_x}{D_y+D_x}Cos(B_y+B_x) - (l_x-b_x)\frac{Sin(L_y+L_x)-Sin(B_y+B_x)}{(D_y+D_x)^2}\right\}$$

$$= \frac{R_x R_y}{2(\frac{1}{2}+m)(\frac{1}{2}+n)\pi^2}\left\{\frac{1}{2}D_x Sin(B_y-B_x) + \frac{D_x}{D_y+D_x}Cos(B_y+B_x) - D_x\frac{Sin(L_y+L_x)-Sin(B_y+B_x)}{(D_y+D_x)^2}\right\}$$

(B4-30)

Similarly,

$$\iint_{A_3} = \frac{R_x R_y}{2(\frac{1}{2}+m)(\frac{1}{2}+n)\pi^2}\left\{\frac{1}{2}D_y Sin(B_x-B_y) + \frac{D_y}{D_y+D_x}Cos(B_x+B_y) - D_y\frac{Sin(L_y+L_x)-Sin(B_y+B_x)}{(D_y+D_x)^2}\right\}$$

(B4-31)

Then, Eq.(B4-25) +Eq.(B4-26),

$$\iint_{A_2} + \iint_{A_3} = \frac{R_x R_y}{2(\frac{1}{2}+m)(\frac{1}{2}+n)\pi^2}\left\{\frac{1}{2}(D_x-D_y)Sin(B_y-B_x) + \frac{D_x+D_y}{D_y+D_x}Cos(B_y+B_x) - (D_x+D_y)\frac{Sin(L_y+L_x)-Sin(B_y+B_x)}{(D_y+D_x)^2}\right\}$$

$$= \frac{R_x R_y}{2(\frac{1}{2}+m)(\frac{1}{2}+n)\pi^2}\left[Cos(B_y+B_x) - \frac{Sin(L_y+L_x)-Sin(B_y+B_x)}{D_y+D_x}\right]$$

(B4-32)

$$c_{mn} = \frac{4u_0}{R_x R_y}\left\{\iint_{A_1} + \iint_{A_2} + \iint_{A_3}\right\} =$$

$$\frac{2u_0}{2(\frac{1}{2}+m)(\frac{1}{2}+m)\pi^2}\left[2SinB_xSinB_y + Cos(B_y+B_x) - \frac{Sin(L_y+L_x)-Sin(B_y+B_x)}{D_y+D_x}\right]$$

$$= \frac{2u_0}{2(\frac{1}{2}+m)(\frac{1}{2}+m)\pi^2}\left[Cos(B_y-B_x) - \frac{Sin(L_y+L_x)-Sin(B_y+B_x)}{D_y+D_x}\right]$$

(B4-33)

Appendix B-5: the solution of equation (5.2-13)

$$\frac{\partial u}{\partial t} = C_h\left(\frac{\partial^2 u}{\partial x^2} + \frac{\partial^2 u}{\partial y^2}\right) + C_v \frac{\partial^2 u}{\partial z^2} \qquad (5.2\text{-}13)$$

$u(x,y,z,0)=\psi_3(x,y,z)= = u_0(z)\cdot\psi_2(x,y)$

$$= \begin{cases} u_0(z) & (A_1 : |x| \le b_x, |y| \le b_y) \\ u_0(z)\dfrac{l_x - x}{l_x - b_x} & (A_2 : b_x \le x \le l_x, |y| \le b_y + \eta(x - b_x)) \\ u_0(z)\dfrac{l_y - y}{l_y - b_y} & (A_2 : b_y \le y \le l_y, |x| \le b_x + \dfrac{1}{\eta}(y - b_y)) \\ 0 & (A_4 : l_x \le x \le R_x, l_y \le y \le R_y) \end{cases} \quad (\eta = \frac{l_y - b_y}{l_x - b_x}), \qquad (5\text{-}13a)$$

$$u_0(z) = \begin{cases} u_{00} + \dfrac{u_{0b} - u_{00}}{b_z} z & (0 \le z \le b_z) \\ u_{0l} - \dfrac{u_{0b} - u_{0m}}{l_z - b_z}(z - b_z) & (b_z \le z \le l_z) \\ 0 & (l_z \le z \le R_z) \end{cases} \qquad (5.2\text{-}13b)$$

in which, b_z can be the length of pile.

$\partial u/\partial x \,|_{x=0} = 0$, $u \,|_{x=Rx} = 0$ (5.2-13c)

$\partial u/\partial y \,|_{y=0} = 0$, $u \,|_{y=Ry} = 0$ (5.2-13d)

There are two boundary conditions on $z=R_z$:

1) Permeating boundary, $u \,|_{z=0} = 0$, $u \,|_{z=Rz} = 0$ (5.2-13e)

2) Impermeating boundary, $u \,|_{z=0} = 0$, $\partial u/\partial z \,|_{z=Rz} = 0$ (5.2-13f)

Solution:

Set

$$u(x,y,z,t) = X(x)\cdot Y(y)\cdot Z(z)\cdot T(t) \qquad (B5\text{-}1)$$

By substituting this into the (5.2-13), gives $XYZT'=C_h(X"YZT+XY"ZT)+C_vXYZ"T$ with $T'=dT/dt$, $X"=d^2X/dx^2$, $Y"=d^2Y/dy^2$ and $Z"= d^2Z/dz^2$. To separate the variables, we divide by $X\cdot Y\cdot Z\cdot T$, obtaining

$$\frac{T'}{C_h T} = C_h\left(\frac{X''}{X} + \frac{Y''}{Y}\right) + C_v \frac{Z''}{Z} \qquad (B5\text{-}2)$$

The left side of the above depends only on time t and the right side only on x, y and z, so that both side must be equal to a constant k. But we may show that for k>0 the only solution is infinite when t→∝; for k=0 the only solution is not zero when t→∝. Hence we left with the possibility of choosing k negative, let k= - s^2. Thus,

$$\frac{T'}{T} = C_h\left(\frac{X''}{X} + \frac{Y''}{Y}\right) + C_v\frac{Z''}{Z} = -s^2 \qquad \text{(B5-3)}$$

This yields immediately tow ordinary linear differential equations, namely

$$T' + s^2T = 0 \qquad \text{(B5-4)}$$

And

$$C_h\left(\frac{X''}{X} + \frac{Y''}{Y}\right) = -C_v\frac{Z''}{Z} - s^2 \qquad \text{(B5-5)}$$

Similarly, the left side of the Eq.(B5-5) depends only on x,y and the right side only on z, so that both side must be equal to a constant k'. But we may show similarly that only for k'<0 the solution will be reasonable. Thus, we left with the possibility of choosing k' negative, let k' = - g^2. Hence,

$$C_h\left(\frac{X''}{X} + \frac{Y''}{Y}\right) = -C_v\frac{Z''}{Z} - s^2 = -g^2 \qquad \text{(B5-6)}$$

This also yields tow ordinary linear differential equations, namely

$$\frac{Z''}{Z} = -h^2 = -\frac{s^2 - g^2}{C_v} \qquad \text{(B5-7)}$$

$$C_h\left(\frac{X''}{X} + \frac{Y''}{Y}\right) = -g^2 \qquad \text{(B5-8)}$$

From Eq.(B5-7)

$$s^2 = g^2 + C_v h^2 \qquad \text{(B5-9)}$$

$$Z'' + h^2Z = 0 \qquad \text{(B5-10)}$$

And from Eq.(B5-8)

$$\frac{X''}{X} = -\frac{Y''}{Y} - \frac{g^2}{C_h} \qquad \text{(B5-11)}$$

Like the case of Appendix I-4, from Eq.(B5-11)

$$\frac{X''}{X} = -\frac{Y''}{Y} - \frac{g^2}{C_h} = -p^2 \qquad \text{(B5-12)}$$

Eq.(B5-12) also yields immediately tow ordinary linear differential equations, that is

$$X'' + p^2X = 0 \qquad \text{(B5-13)}$$

And

$$Y'' + q^2Y = 0 \qquad \text{(B5-14)}$$

Where $q^2 = g^2/C_h - p^2$, that is,

$$g^2 = C_h(p^2 + q^2) \qquad \text{(B5-15)}$$

By Eq.(B5-9) $$s^2 = C_h(p^2 + q^2) + C_v h^2 \qquad \text{(B5-16)}$$

From Appendix B-4, the solution of Eq.(B5-13) satisfying Eq.(5.2-13c) is

$$p = p_m = (½+m)\pi/R_x \qquad (m=0,1,2,3,\ldots) \qquad \text{(B5-17)}$$

$$X_m = \text{Cos}[(½+m)\pi x/R_x] \qquad \text{(B5-18)}$$

And the the solution of (B5-14) satisfying (5.2-13d) is

$$q = q_n = (½+n)\pi/R_y \qquad (n=0,1,2,3,\ldots) \qquad \text{(B5-19)}$$

$$Y_n = \text{Cos}[(½+n)\pi y/R_y] \qquad \text{(B5-20)}$$

For Eq.(B5-10), according to condition of permeating boundary (5.2-13e),

$$h = h_k = k\pi/R_z \ (k=0,1,2,3,\ldots) \qquad \text{(B5-19)}$$

$$Z_k = \text{Sin}(k\pi z/R_z] \qquad \text{(B5-20)}$$

According to condition of impermeating boundary (5.2-13f),

$$h = h_k = (½+k)\pi/R_z \qquad (k=0,1,2,3,\ldots) \qquad \text{(B5-19)}$$

$$Z_k = \text{Sin}[(½+k)\pi z/R_z] \qquad \text{(B5-20)}$$

By (B5-4) and (B5-16), to obtain the general solution of (B5-4) corresronding to the eigenvalues $s_{mnk}^2 = C_v \cdot h_k^2 + C_h \cdot (p_m^2 + q_n^2)$ is

$$T_{m,n,k} = \text{Exp}[-s_{mnk}^2 t\,]$$

$$= Exp\left[-\left(\left(\tfrac{1}{2}+m\right)^2 + \left(\tfrac{1}{2}+n\right)^2\left(R_x/R_y\right)^2 + \frac{C_v}{C_h}k^2\left(R_x/R_z\right)^2\right)\pi^2\frac{C_h}{R_x^2}t\right] \qquad \text{(B5-21)}$$

(m=0,1,2,3,..., n=0,1,2,3,..., k=1,2,3,...,)

$$s_{mnk}^2 = \left(\left(\tfrac{1}{2}+m\right)^2 + \left(\tfrac{1}{2}+n\right)^2\left(R_x/R_y\right)^2 + \frac{C_v}{C_h}k^2\left(R_x/R_z\right)^2\right)\pi^2\frac{C_h}{R_x^2}$$

$$= \left[C_h\left(\frac{\left(\tfrac{1}{2}+m\right)^2}{R_x^2} + \frac{\left(\tfrac{1}{2}+n\right)^2}{R_y^2}\right) + C_v\frac{k^2}{R_z^2}\right]\pi^2 \qquad \text{(B5-21')}$$

Thus, a solution of (B5-6) satisfying boundary condition (5.2-13c,d) and (5.2-13e) are $u_{mnk} = X_m Y_n Z_k T_{mnk}$, written out

$$u_{m,n,k}(x,y,z,t) = d_{mnk} Cos\left(\frac{(\frac{1}{2}+m)\pi x}{R_x}\right) Cos\left(\frac{(\frac{1}{2}+n)\pi y}{R_y}\right) Sin\frac{k\pi z}{R_z} Exp\left(-s_{mnk}^2 t\right)$$

(m=0,1,2,3,..., n=0,1,2,3,..., k=1,2,3,...) (B5-22)

$s_{mnk}^2 = C_v \cdot h_k^2 + C_h \cdot (p_m^2 + q_n^2)$

And, a solution of (B5-6) satisfying (5.2-13c,d) and (5.2-13f) are

$$u_{m,n,k}(x,y,z,t) = d_{mnk} Cos\left(\frac{(\frac{1}{2}+m)\pi x}{R_x}\right) Cos\left(\frac{(\frac{1}{2}+n)\pi y}{R_y}\right) Sin\frac{(\frac{1}{2}+k)\pi z}{R_z} Exp\left(-s_{mnk}^2 t\right)$$

(m=0,1,2,3,..., n=0,1,2,3,..., k=1,2,3,...) (B5-22')

To obtain a solution also satisfying the initial condition (5.2-13a) and (5.2-13b), we consider a triple series of the these eigenfunctions corresponding to the eigenvalues $p_m = (½+m)\pi/R_x$, $q_n = (½+n)\pi/R_y$, and $h_k = (½+k)\pi/R_z$,

$$u(x,y,z,t) = \sum_{m=0}^{\infty}\sum_{n=0}^{\infty}\sum_{k=1}^{\infty} u_{m,n,k}(x,y,z,t)$$

$$= \sum_{m=0}^{\infty}\sum_{n=0}^{\infty}\sum_{k=1}^{\infty} d_{mnk} Cos\left(\frac{(\frac{1}{2}+m)\pi x}{R_x}\right) Cos\left(\frac{(\frac{1}{2}+n)\pi y}{R_y}\right) Sin\frac{k\pi z}{R_z} Exp\left(-s_{mnk}^2 t\right)$$

(B5-23)

From this and (5.2-13a) and (5.2-13b), we have

$$u(x,y,z,0) = \sum_{m=0}^{\infty}\sum_{n=0}^{\infty}\sum_{k=1}^{\infty} d_{mnk} Cos\left(\frac{(\frac{1}{2}+m)\pi x}{R_x}\right) Cos\left(\frac{(\frac{1}{2}+n)\pi y}{R_y}\right) Sin\frac{k\pi z}{R_z} = \psi_3(x,y,z)$$

Hence, for (B5-22) to satisfy (5.2-13a,b), the d_{mnk}'s value must the coeffients of the triple Fourier cosine series,

$$d_{mnk} = \frac{8}{R_x R_y R_z}\int_{z=0}^{R_z}\int_{x=0}^{R_x}\int_{y=0}^{R_y} \psi_3(x,y,z) Cos\left(\frac{(\frac{1}{2}+m)\pi x}{R_x}\right) Cos\left(\frac{(\frac{1}{2}+n)\pi y}{R_y}\right) Sin\frac{k\pi z}{R_z} dxdydz$$

$$= \frac{2}{R_z}\int_{z=0}^{R_z} u_0(z)\cdot Sin\frac{k\pi z}{R_z} dz \cdot \frac{4}{R_x R_y}\int_{x=0}^{R_x}\int_{y=0}^{R_y} \psi_2(x,y) Cos\left(\frac{(\frac{1}{2}+m)\pi x}{R_x}\right) Cos\left(\frac{(\frac{1}{2}+n)\pi y}{R_y}\right) dxdy$$

$$= \frac{2}{R_z}\int_{z=0}^{R_z} u_0(z)\cdot Sin\frac{k\pi z}{R_z} dz \cdot \frac{c_{mn}}{u_0}$$

$$= d_k \cdot d_{mn} \quad \text{(B5-24)}$$

where,

$$d_{mn}=\frac{c_{mn}}{u_0}, \qquad \text{(B5-25)}$$

c_{mn}'s values are determined by (B4-28), or (B4-29), or A4-33).

$$d_k=\frac{2}{R_z}\int_{z=0}^{R_z} u_0(z)\cdot Sin\frac{k\pi z}{R_z}dz$$

$$=\frac{2}{R_z}\left\{\int_{z=0}^{b_z}\left(u_{00}+\frac{u_{0l}-u_{00}}{b_z}z\right)\cdot Sin\frac{k\pi z}{R_z}dz+\int_{z=b_z}^{l_z}\left(u_{0l}-\frac{u_{0l}-u_{0m}}{l_z-b_z}(z-b_z)\right)\cdot Sin\frac{k\pi z}{R_z}dz+\int_{z=l_z}^{R_z}0dz\right\}$$

$$=\frac{2}{R_z}\left\{\frac{-R_z}{k\pi}\left(u_{00}+\frac{u_{0l}-u_{00}}{b_z}z\right)Cos\frac{k\pi z}{R_z}\Big|_{z=0}^{z=b_z}+\frac{R_z}{k\pi}\int_{z=0}^{b_z}\frac{u_{0l}-u_{00}}{b_z}Cos\frac{k\pi z}{R_z}dz\right.$$

$$\left.+\frac{-R_z}{k\pi}\left(u_{0l}-\frac{u_{0l}-u_{0m}}{l_z-b_z}(z-b_z)\right)Cos\frac{k\pi z}{R_z}\Big|_{z=b_z}^{z=l_z}-\frac{R_z}{k\pi}\int_{z=b_z}^{l_z}\frac{u_{0l}-u_{0m}}{l_z-b_z}Cos\frac{k\pi z}{R_z}dz\right\}$$

$$=\frac{2}{k\pi}\left\{u_{00}-u_{0l}Cos\frac{k\pi b_z}{R_z}+\frac{R_z}{k\pi}\frac{u_{0l}-u_{00}}{b_z}Sin\frac{k\pi z}{R_z}\Big|_{z=0}^{z=b_z}\right.$$

$$\left.+u_{0l}Cos\frac{k\pi b_z}{R_z}-u_{0m}Cos\frac{k\pi l_z}{R_z}-\frac{R_z}{k\pi}\frac{u_{0l}-u_{0m}}{l_z-b_z}Sin\frac{k\pi z}{R_z}\Big|_{z=b_z}^{z=l_z}\right\}$$

$$=\frac{2}{k\pi}\left\{u_{00}+\frac{R_z}{k\pi}\frac{u_{0l}-u_{00}}{b_z}Sin\frac{k\pi b_z}{R_z}-u_{0m}Cos\frac{k\pi l_z}{R_z}-\frac{R_z}{k\pi}\frac{u_{0l}-u_{0m}}{l_z-b_z}\left(Sin\frac{k\pi b_z}{R_z}-Sin\frac{k\pi l_z}{R_z}\right)\right\}$$

(B5-26)

when $l_z=b_z(u_{0l}=u_{0m})$,

$$d_k=\frac{2}{k\pi}\left\{u_{00}+\frac{R_z}{k\pi}\frac{u_{0l}-u_{00}}{b_z}Sin\frac{k\pi b_z}{R_z}-u_{0l}Cos\frac{k\pi b_z}{R_z}\right\} \qquad \text{(B5-26')}$$

usually, for permeating condition, $l_z=R_z$, since,

$$d_k=\frac{2}{k\pi}\left\{u_{00}-u_{0m}Cosk\pi+\frac{R_z}{k\pi}\left(\frac{u_{0l}-u_{00}}{b_z}+\frac{u_{0l}-u_{0m}}{l_z-b_z}\right)Sin\frac{k\pi b_z}{R_z}\right\} \qquad \text{(B5-26")}$$

when $b_z=l_z=R_z(u_{0l}=u_{0m})$,

$$d_k=\frac{2}{k\pi}(u_{00}-u_{0l}Cosk\pi) \qquad \text{(B5-26"')}$$

And when $b_z=l_z=R_z$ and $u_{00}=u_{0l}=u_{0m}$

$$d_k=\frac{2}{k\pi}u_{00}(1-Cosk\pi) \qquad (k=1,2,3,\ldots,)$$

$$=\frac{4}{K\pi}u_{00} \qquad (K=1,3,5,\ldots) \qquad \text{(B5-27)}$$

By (B5-23,24,25,26,or,27)

$$u(x,y,z,t)=\sum_{m=0}^{\infty}\sum_{n=0}^{\infty}\sum_{k=1}^{\infty} d_{mnk}Cos\left(\frac{(1/2+m)\pi x}{R_x}\right)Cos\left(\frac{(1/2+n)\pi y}{R_y}\right)Sin\frac{k\pi z}{R_z}Exp\left(-s_{mnk}^2 t\right)$$

$$=\sum_{m=0}^{\infty}\sum_{n=0}^{\infty}\sum_{k=1}^{\infty} d_{mn}d_k Cos(p_m x)\cdot Cos(q_n y)\cdot Sin(h_k z)\cdot Exp\left[-\left(C_h(p_m^2+q_n^2)+C_v h_k^2\right)t\right]$$

$$=\sum_{m=0}^{\infty}\sum_{n=0}^{\infty}\left\{\sum_{k=1}^{\infty} d_k Sin(h_k z)Exp\left(-C_v h_k^2 t\right)\right\}d_{mn}Cos(p_m x)\cdot Cos(q_n y)\cdot Exp\left[-C_h(p_m^2+q_n^2)t\right]$$

$$=\left\{\sum_{k=1}^{\infty} d_k Sin(h_k z)Exp\left(-C_v h_k^2 t\right)\right\}\left\{\sum_{m=0}^{\infty}\sum_{n=0}^{\infty} d_{mn}Cos(p_m x)\cdot Cos(q_n y)\cdot Exp\left[-C_h(p_m^2+q_n^2)t\right]\right\} \quad \text{(B5-28)}$$

From this, we prove that Carrillo's expression of 3-D consolidation degree (Carrillo, 1942)

$$\frac{u(x,y,z,t)}{u(x,y,z,0)}=\frac{u_{0z}(z,t)}{u_{0z}(z,0)}\cdot\frac{u_{0xy}(x,y,t)}{u_{0xy}(x,y,0)} \quad \text{(B5-29)}$$

or $(1-U)=(1-U_{0z})\cdot(1-U_{0xy})$ (B5-29')

can be exact only when initial condition u(x,y,z,0) can be expressed by $\psi_1(z)((2(x,y)$.

In the case when $b_z=l_z=R_z$ and $u_{00}=u_{0l}=u_{0m}$, set $R_z=2H$ and using (B5-27)

$$\frac{u_{0z}(z,t)}{u_{0z}(z,0)}=\frac{1}{u_{00}}\sum_{k=1}^{\infty} d_k Sin(h_k z)\cdot Exp\left(-C_v h_k^2 t\right)$$

$$=\sum_{k=1,3,5}^{\infty}\frac{4}{K\pi}Sin\left(\frac{K\pi}{2H}z\right)Exp\left(-C_v\frac{K^2\pi^2}{4H^2}t\right) \quad \text{(B5-30)}$$

The above form is exactly as same as well-known Terzaghi's solution of one-directional consolidation theory.

Similarly, for (B5-22') to satisfy (5.2-13a), the d_{mnk}'s value must the confidents of the triple Fourier cosine series,

$$u(x,y,z,t)=\sum_{m=0}^{\infty}\sum_{n=0}^{\infty}\sum_{k=0}^{\infty} d_{mnk}Cos\left(\frac{(1/2+m)\pi x}{R_x}\right)Cos\left(\frac{(1/2+n)\pi y}{R_y}\right)Sin\frac{(1/2+k)\pi z}{R_z}Exp\left(-s_{mnk}^2 t\right) \quad \text{(B5-31)}$$

in which,

$$s_{mnk}^2=\left[C_h\left(\frac{(1/2+m)^2}{R_x^2}+\frac{(1/2+n)^2}{R_y^2}\right)+C_v\frac{(1/2+k)^2}{R_z^2}\right]\pi^2 \quad \text{(B5-31')}$$

$$d_{mnk}=\frac{8}{R_xR_yR_z}\int_{z=0}^{R_z}\int_{x=0}^{R_x}\int_{y=0}^{R_y}\psi_3(x,y,z)Cos\left(\frac{(\frac{1}{2}+m)\pi x}{R_x}\right)Cos\left(\frac{(\frac{1}{2}+n)\pi y}{R_y}\right)Sin\frac{(\frac{1}{2}+k)\pi z}{R_z}dxdydz$$

$$=\frac{2}{R_z}\int_{z=0}^{R_z}u_0(z)\cdot Sin\frac{(\frac{1}{2}+k)\pi z}{R_z}dz\cdot\frac{4}{R_xR_y}\int_{x=0}^{R_x}\int_{y=0}^{R_y}\psi_2(x,y)Cos\left(\frac{(\frac{1}{2}+m)\pi x}{R_x}\right)Cos\left(\frac{(\frac{1}{2}+n)\pi y}{R_y}\right)dxdy$$

$$=\frac{2}{R_z}\int_{z=0}^{R_z}u_0(z)\cdot Sin\frac{(\frac{1}{2}+k)\pi z}{R_z}dz\cdot\frac{c_{mn}}{u_0}$$

$$=d_k\cdot d_{mn} \qquad \text{(B5-32)}$$

$$d_k=\frac{2}{(\frac{1}{2}+k)\pi}\left\{u_{00}+\frac{R_z}{(\frac{1}{2}+k)\pi}\frac{u_{0l}-u_{00}}{b_z}Sin\frac{(\frac{1}{2}+k)\pi b_z}{R_z}-u_{0m}Cos\frac{(\frac{1}{2}+k)\pi l_z}{R_z}\right.$$

$$\left.-\frac{R_z}{(\frac{1}{2}+k)\pi}\frac{u_{0l}-u_{0m}}{l_z-b_z}\left(Sin\frac{(\frac{1}{2}+k)\pi b_z}{R_z}-Sin\frac{(\frac{1}{2}+k)\pi l_z}{R_z}\right)\right\} \qquad \text{(B5-33)}$$

when $l_z=b_z(u_{0l}=u_{0m})$,

$$d_k=\frac{2}{(\frac{1}{2}+k)\pi}\left\{u_{00}+\frac{R_z}{(\frac{1}{2}+k)\pi}\frac{u_{0l}-u_{00}}{b_z}Sin\frac{(\frac{1}{2}+k)\pi b_z}{R_z}-u_{0l}Cos\frac{(\frac{1}{2}+k)\pi b_z}{R_z}\right\} \qquad \text{(B5-33')}$$

usually, for permeating condition, $l_z=R_z$, since,

$$d_k=\frac{2}{(\frac{1}{2}+k)\pi}\left\{u_{00}+\frac{R_z}{(\frac{1}{2}+k)\pi}\frac{u_{0l}-u_{00}}{b_z}Sin\frac{(\frac{1}{2}+k)\pi b_z}{R_z}\right.$$

$$\left.-\frac{R_z}{(\frac{1}{2}+k)\pi}\frac{u_{0l}-u_{0m}}{l_z-b_z}\left(Sin\frac{(\frac{1}{2}+k)\pi b_z}{R_z}-(-1)^{k+1}\right)\right\} \qquad \text{(B5-33")}$$

when $b_z=l_z=R_z(u_{0l}=u_{0m})$,

$$d_k=\frac{2}{(\frac{1}{2}+k)\pi}\left\{u_{00}+\frac{u_{0l}-u_{00}}{(\frac{1}{2}+k)\pi}(-1)^{K+1}\right\} \qquad \text{(B5-33"')}$$

And when $b_z=l_z=R_z$ and $u_{00}=u_{0l}=u_{0m}$

$$d_k=\frac{2}{(\frac{1}{2}+k)\pi}u_{00}$$

$$=\frac{4}{(1+2k)\pi}u_{00} \qquad (k=0,1,2,3,\ldots,)$$

$$=\frac{4}{K\pi}u_{00} \qquad (K=1,3,5,\ldots) \qquad \text{(B5-34)}$$

In this case,

$$\frac{u_{0z}(z,t)}{u_{0z}(z,0)} = \frac{1}{u_{00}} \sum_{k=1}^{\infty} d_k Sin(h_k z) \cdot Exp\left(-C_v h_k^2 t\right)$$

$$= \sum_{k=1}^{\infty} \frac{2}{(\frac{1}{2}+k)\pi} Sin\left(\frac{(\frac{1}{2}+k)\pi}{R_z} z\right) \cdot Exp\left(-C_v \frac{(\frac{1}{2}+k)^2 \pi^2}{R_z^2} t\right)$$

$$= \sum_{k=1}^{\infty} \frac{4}{(1+2k)\pi} Sin\left(\frac{(1+2k)\pi}{2R_z} z\right) \cdot Exp\left(-C_v \frac{(1+2k)^2 \pi^2}{4R_z^2} t\right)$$

Set K=1+2k, Rz=H,

$$\frac{u_{0z}(z,t)}{u_{0z}(z,0)} = \sum_{k=1,3,5}^{\infty} \frac{4}{K\pi} Sin\left(\frac{K\pi}{2H} z\right) Exp\left(-C_v \frac{K^2 \pi^2}{4H^2} t\right) \qquad \text{(B5-35)}$$

Also, the above form is exactly as same as Terzaghi's solution of One-Dimensional consolidation theory. And Terzaghi's solution just is a special example of the solution (B5-26) or (B5-33).

APPENDIX C

Computer Program Code

Appendix C-1: Fortran 90 Code of FLM +GSDT Program

```
C
C          ######################################
C          #                                    #
C          #         PROGRAM FLMGSDT            #
C          #      ---------------------------   #
C          #         RONGCHANG   YANG           #
C          #       CONCORDIA  UNIVERSITY        #
C          #  CIVIL ENGINEERING DEPARTMENT      #
C          #                2005                #
C          ######################################
C
C        PROGRAME ANALYSING Pile-Soil-Raft Non-linear Interaction:
C        RAFT is rigid;   PILES are Elastic;
C        Relations between Pile and Soil are Non-linear, and Established
C        by General Shear-Displacement Mathod;
C        Relation between Soil and Soil is Elastic, and edstablished
C        by Finite Layer Method
$DEBUG
$LARGE: MD,W,WP
        DIMENSION  A(291),DA(61),B(0:60,20),F(2646),MD(209,209),MF(20),
     2  CE(20),EN(20),EE2(20),EM1(20),EM2(20),EG2(20),MW(2646),
     3  CC(2646),XY1(2646,6),
     4  X(81),Y(81),LQA(81),LQB(81),LP(81),LX(81),LCO(10), W(212,212),
     5  C(212),CX(209),BE(209),BE1(209),P(209),FG(209),KO(20),KOP(10),
     6  KT(20),RP(20),RT(20),KP(11,4),PX(11,4),LCP(10),lxp(20),Z(11),
     7  LS(20,11),PE(20,11),FTE(20,11),PZ(20,11),FTZ(20,11),FZ(20,11),
     8  FE(20,11),alfa(20),EP(20),AP(20),WP(128,128),MPR(10),sz(20,11)
        INTEGER    P1,P10,FHS,SYS,MSYB(4),MSYP(4)
        INTEGER*2  R,R1,P2,DA,MW,MD,MF
        REAL     L,LQA,LQB,LOAD,MX,MY,LP,KT,KP,LOAD1
        EQUIVALENCE    (W(1,1),XY1(1,1))
           COMMON /COM1/A,DA/COM2/B/COM4/W/COM5/C/COMP/LCO,KOP/CEPM/CE,EP,AP
     *  /CONTR/P1,NP1,IP,IPL,MP,FHS,MTT,LT1,LPT1/ABP/LQA,LQB,LP,KO
     *  /COEN/EN,EE2,EM1,EM2,EG2/COXYZ/X,Y,Z
     *  /COFC/F,CC/COMD/MW,MF,MD/COP/WP/SYS/MSYB,MSYP
     *   /CFLM/L,NE,NR1,NR,INF
        CALL WR1
        OPEN(5,FILE='INA0.DAT')
        READ(5,*) L,NE,NR1,NR,INF,P1,NB
        READ(5,*) (CE(I),EN(I),EE2(I),EM1(I),EM2(I),EG2(I),I=1,NE)
        READ(5,*) (X(I),Y(I),LQA(I),LQB(I),LP(I),LX(I),I=1,P1)
        READ(5,*) LT,(LCO(I),I=1,LT)
        READ(5,*) LOAD,XX,YY,MX,MY
        READ(5,*) NP,AMAX,IJ
        READ(5,*) IP,IPL,LS3,mpt,FHS,SYS
        READ(5,*) (MSYB(I),I=1,4),(MSYP(I),I=1,4)
        READ(5,*)F0,F01,F02
        IF(IP.EQ.0) GO TO 37
        READ(5,*) (KO(I),I=1,IP)
        READ(5,*) NPR,(MPR(I),I=1,NPR)
        READ(5,*)MP
        IF(MP.LE.1)THEN
        READ(5,*)EEP
        IF(MP.EQ.0) GOTO 17
```

```
      DO 15 I=1,IP
15    EP(I)=EEP
      ELSE
      READ(5,*)(RP(I),I=1,MP),(MF(I),I=1,IP)
      DO 16 I=1,IP
16    EP(I)=RP(MF(I))
      ENDIF
17    IF(LS3.LE.0) GOTO 37
      READ(5,*)MNL,DF,((PX(I,J),J=1,LS3),
     *(KP(I,J),J=1,LS3),I=1,IPL+1)
      DO 20 I=1,IPL+1
      PX(I,LS3+1)=PX(I,LS3)
      KP(I,1)=1.E+20
      IF(MNL.EQ.3.OR. I.EQ.IPL+1) GOTO 20
      IF(MNL.EQ.2) THEN
      IF(I.EQ.1)THEN
      CH=.5*CE(1)
      ELSE IF(I.LT.IPL) THEN
      CH=.5*(CE(I-1)+CE(I))
      ELSE
      CH=.5*CE(IPL-1)+CE(IPL)
      ENDIF
      DO 21 J=1,LS3+1
      PZ(I,J)=CH*PX(I,J)
21    PE(I,J)=CH*KP(I,J)
      GOTO 20
      ENDIF
      DO 23 J=1,LS3+1
      PX(I,J)=.5*PX(I,J)*CE(I)
23    KP(I,J)=.5*KP(I,J)*CE(I)
20    continue
      IF(MNL.EQ.3) GOTO 37
      DO 30 J=1,LS3+1
      PZ(IPL+1,J)=PX(IPL+1,J)
      PE(IPL+1,J)=KP(IPL+1,J)
      IF(MNL.EQ.2) GOTO 30
      PZ(1,J)=PX(1,J)
      PE(1,J)=KP(1,J)
      DO 25 I=2,IPL-1
      PZ(I,J)=PX(I-1,J)+PX(I,J)
25    PE(I,J)=KP(I-1,J)+KP(I,J)
      PZ(IPL,J)=PX(IPL-1,J)+2*PX(IPL,J)
      PE(IPL,J)=KP(IPL-1,J)+2*KP(IPL,J)
30    CONTINUE
36    DO 35 I=1,IPL+1
      DO 35 J=1,LS3+1
      PX(I,J)=PZ(I,J)
      KP(I,J)=PE(I,J)
      IF(KP(I,j).LT..1E-20) KP(I,j)=.1E-20
35    CONTINUE
37    LPT=0
      DO 40 I=1,IP
      K=KO(I)
      Ap(i)=lp(k)**2
      DO 40 J=1,LT
      IF(K.EQ.LCO(J)) THEN
      LPT=LPT+1
      LXP(I)=LPT
```

```
      LCP(LPT)=I
      KOP(LPT)=K
      ENDIF
40    CONTINUE
      Z(1)=0.
      IF(IP.LE.0) GOTO 60
      DO 50 I=1,IPL
50    Z(I+1)=Z(I)+CE(I)
60    LTT=LT+LPT*(IPL+1)
      NP1=P1+IP*(IPL+1)
      IF(NE.GT.20) WRITE(*,801)
      IF(P1.GT.81) WRITE(*,802)
      IF(LTT.GT.20) WRITE(*,803)
      IF(IP.GT.20) WRITE(*,804)
      IF(LTT*NP1.GT.2646) WRITE(*,805)
801   FORMAT(10X,'** ERROR  1 : NE.GT.20  **')
802   FORMAT(10X,'** ERROR  2 : P1.GT.64  **')
803   FORMAT(10X,'** ERROR  3 : LTT.GT.60 **')
804   FORMAT(10X,'** ERROR  4 : IP.GT.20  **')
805   FORMAT(10X,'** WARNING  5 : NM.GT.2646 **')
      CLOSE(5)
      OPEN(11,FILE='FYO.DAT')
      WRITE(11,1) L,NE,NR1,NR,INF,P1,IP,NP1,NB
1     FORMAT(/30X,'CONTROL PARAMATER',/4X,'L',8X,'NE',7X,'NR1',6X,'NR',
     *  7X,'INF',6X,'P1',7X,'IP',6X,'NP1',7X,'NB',/1X,F5.2,8I9)
      WRITE(11,2)(CE(I),EN(I),EE2(I),EM1(I),EM2(I),EG2(I),I=1,NE)
2     FORMAT(/25X,'MATERIAL IN EVERY LATRY',/7X,'CE',11X,'EN',
     *  10X,'EE2',10X,'EM1',10X,'EM2',10X,'EG2',/(1X,F8.2,5F13.2))
      WRITE(11,3) (I,X(I),Y(I),LQA(I),LQB(I),LP(I),LX(I),I=1,P1)
3     FORMAT(/29X,'CALCULATRE POINT',/10X,'POINT  X-COOD   Y-COOD
     *  LQA     LQB      LP  TYPE'/(5X,I8,5F10.2,I6))
      WRITE(11,4) (I,LCO(I),I=1,LT)
4     FORMAT(/15X,'THE TYPE OF RAFT ELEMENT SHAPE'/
     *  15X,'NO.',2X,'THE CORD OF POINT'/(15X,I2,8X,I4))
      WRITE(11,5) NP,AMAX,IJ
5     FORMAT(15X,'CONTROL OF PRINTING =',I3
     #  /15X,'MAXIUM LOAD =',E10.4
     #  /15X,'FLEXIBLE MATRIX IN DISK( 0/NO,1/YES) =',I2)
      WRITE(11,6) IP,IPL,LS3
6     FORMAT(/10X,'TOTAL NUMBER OF PILE :IP*IPL=',I3,'*',I3,',LS3=',
     &  I3)
      IF(IP.EQ.0) GO TO 73
      WRITE(11,7)
7     FORMAT(15X,'THE NODE OF PILE:  KO,  LXP ')
      WRITE(11,8) (KO(I),LXP(I),I=1,IP)
8     FORMAT(31X,2I5)
      WRITE(11,9) (LCP(I),I=1,LPT)
9     FORMAT(15X,'THE TYPE OF PILE: LCP'/(31X,5I4))
      IF(MP.GT.0) WRITE(11,*)'       Pile is compressible,',
     *  'modus of pile is ',(Ep(i),I=1,IP)
      IF(LS3.EQ.0) GOTO 73
      WRITE(11,10)
      WRITE(11,11) (J,Z(J),(PX(J,I),KP(J,I),I=1,3),J=1,IPL+1)
10    FORMAT(15X,'PARAMEER OF PILE'/3X,' NO:   Z     PX1',
     *  '    KP1     PX2     KP2     PX3     KP3  ')
11    FORMAT(2X,I3,7E10.4)

73    LT1=LT
```

```
      LPT1=LPT
      MTT=LTT
      if(FHS.eq.0) then
      LT1=0
      MTT=MTT-LT
      NP1=NP1-P1
      P1=0
      DO 77 K=1,4
77    MSYB(K)=0
      WRITE(*,13)
      WRITE(11,13)
13    FORMAT(/20X,'The foundation is high raft'//)
      endif
      WRITE(*,12)MTT,NP1
      WRITE(11,12)MTT,NP1
12    FORMAT(10X,'LTT=',I3,'  NP1=',I6/)

C     ##################################################
      NB1=NP1
      IF(IJ.EQ.0) GOTO 800
      IF(IJ.EQ.3) THEN
      IF(SYS.GT.0) NP1=MSYB(3)+MSYP(3)*(IPL+1)
      GOTO 799
      ENDIF
      OPEN(6,FILE='\FLM\MD.DAT')
      READ(6,*) NN,((MD(I,J),I=1,NP1),J=1,NP1)
      CLOSE(6)
      IF(IJ.EQ.2) GOTO 699

800   CALL MDD(IJ,NN)
      IF(IJ.EQ.1) GOTO 599
      IF(NN.GT.2646) GOTO 2001
      CALL FLM(NN,MPT)
      IF(IJ.NE.1) GOTO 595
599   OPEN(6,FILE='\FLM\FO.DAT')
      READ(6,*) (F(I),I=1,NN)
      CLOSE(6)

595   IF(ABS(F0-1)+ABS(F01-1)+ABS(F02-1).LT.0.001) GOTO 695
      DO 187 M=1,MTT
      IF(M.LE.LT1) FM0=F01
      IF(M.GT.LT1) FM0=F02
      IF(ABS(FM0-1).LT.0.0001) GOTO 187
      DO 188 K=MF(M)+1,MF(M+1)
      DST=XY1(K,3)
      DZ=ABS(XY1(K,4)-XY1(K,5))
      IF(DST.LT.0.01) THEN
      IF(DZ.LT.0.01.AND.ABS(F0-1).GT.0.001) THEN
      F(K)=F0*F(K)
      ELSE
      F(K)=F(K)*FM0**(-DZ/SQRT(XY1(K,6)))
      ENDIF
      ELSE
      F(K)=F(K)*FM0**(-DST/SQRT(XY1(K,6)))
      ENDIF
188   CONTINUE
187   CONTINUE
      OPEN(6,FILE='\FLM\F1.DAT')
```

```
      WRITE(6,600) (F(I),I=1,NN)
      CLOSE(6)

      IF(IJ.NE.2) GOTO 695
699   READ(22,*) (F(I),I=1,NN)

695   IF(SYS.GT.0) NP1=MSYB(3)+MSYP(3)*(IPL+1)
      DO 180 I=1,NP1+3
      DO 180 J=1,NP1+3
180   W(J,I)=0.
      IF(SYS.LE.0) THEN
      DO 320 I=1,NP1
      W(I,I)=F(MD(I,I))
      DO 320 J=I+1,NP1
      W(I,J)=.5*(F(MD(I,J))+F(MD(J,I)))
      W(J,I)=W(I,J)
320   CONTINUE
      ELSE
      CALL SYSW
      ENDIF
      OPEN(6,FILE='\FLM\OUT1.DAT')
      WRITE(6,600) ((W(I,K),I=1,NP1+1),K=1,NP1+1)
      CLOSE(6)
600   FORMAT(2X,5E15.8)
      P10=P1
      IP0=IP
      IF(SYS.GT.0) THEN
      P1=MSYB(3)
      IP=MSYP(3)
      ENDIF
      IF(IJ.NE.3) GO TO 795
799    OPEN(7,FILE='\FLM\OUT1.DAT')
      READ(7,*) ((W(I,J),I=1,NP1+1),J=1,NP1+1)
      CLOSE(7)

C   ####################
795   IF(MP.GT.0.AND.IP.GT.0) CALL STIFP
      DO 350 I=1,NP1
      CX(I)=0.
350   BE1(I)=0.
      DO 360 I=1,IP
      RP(I)=0.
360   RT(I)=0.
      DO 370 I=1,IP
      DO 370 J=1,IPL+1
370   LS(I,J)=1
      LOAD1=0.
      SETTLE=0.
      NF=0
      MQ=0
377   write(*,369)
369   format(10X,'*****     MATIVT is running    *****')
      CALL MATIVT(NP1)
      WRITE(*,368)
368   FORMAT(10X,'$$$$$    MATIVT run finished   $$$$$')
      DO 380 I=1,NP1
      P(I)=1.
380   FG(I)=0.
```

```
      DO 391 I=1,NP1
      DO 390 J=1,NP1
390   FG(I)=FG(I)+W(I,J)*P(J)
      IF(I.LE.P1.AND.FG(I).LT.0) FG(I)=-0.1E-06
391   CONTINUE
      WRITE(11,301) (FG(I),I=1,P1)
301   FORMAT(/20X,'A FORCE OF THE UNITE SETTLEMENT',/(2X,7E10.4))
      WRITE(11,3011) (FG(I),I=P1+1,NP1)
3011  FORMAT(/(2X,6E12.4))
      DO 400 I=1,IP
400   KT(I)=FG(KO(I))
      NLOAD=0
      OPEN(15,FILE='\DAG\GRAM.DAG')
      OPEN(20,FILE='\DAG\S-Q.DAG')
      IF(FHS.GT.0) THEN
      OPEN(21,FILE='\DAG\Qs%-Q.DAG')
      OPEN(22,FILE='\DAG\Qs-Q.DAG')
      OPEN(23,FILE='\DAG\Qp-Q.DAG')
      ENDIF
      IF(IP.LE.0) GOTO 404
      OPEN(24,FILE='\DAG\P1-Q.DAG')
      OPEN(25,FILE='\DAG\Afa-Q.DAG')
      OPEN(26,FILE='\DAG\P1-S.DAG')
C     OPEN(27,FILE='\DAG\P3-S.DAG')
      OPEN(28,FILE='\DAG\Pp-Q.DAG')
      OPEN(29,FILE='\DAG\Sp-Pp.DAG')
      OPEN(30,FILE='\DAG\Sp-S.DAG')
      open(40,file='\DAG\F-S.DAG')
      open(41,file='\DAG\Pz-Po.DAG')
404   WRITE(20,401)
      IF(FHS.GT.0) WRITE(22,401)
      IF(FHS.GT.0) WRITE(23,401)
      IF(IP.LE.0) GOTO 2000
      WRITE(24,401)
      WRITE(25,401)
      WRITE(26,401)
C     WRITE(27,401)
      WRITE(28,401)
      WRITE(29,401)
      WRITE(30,401)
      write(40,*) ipl
      write(41,*) ipl+1
401   FORMAT(3X,'0.',5X,'0.')
2000  LZ=0
      OPEN(7,FILE='\FLM\OUT1.DAT')
      READ(7,*) ((W(I,J),J=1,NP1+1),I=1,NP1+1)

      CLOSE(7)
      MQ=0
      DO 409 I=1,P1
      IF(FG(I).GT.0) GOTO 409
      MQ=MQ+1
      W(I,I)=5.*W(I,I)
409    CONTINUE
      IF(IP.EQ.0) GO TO 575
C     WRITE(11,522)
      IF(LS3.EQ.0.OR.NLOAD.EQ.0) GOTO  575
      WRITE(11,525)((I,J,LS(I,J),4.*LP(KO(I))*PX(J,LS(I,J)),
```

```
   *      KP(J,LS(I,J)),J=1,IPL+1),I=1,IP)
522       FORMAT(/15X,'*******************************************')
525       FORMAT(/1X,2('PNO DNO LS     PX      KP',6X),
   *      /2(I2,I4,I4,F10.4,f10.4,6X))
          IF(LS3.EQ.0) GOTO 575
          MWW=0
C         WRITE(*,666)
666       FORMAT(1X,'00000000000000000000000000')
          DO 410 I=P1+1,NP1
          II=MOD(I-P1-1,IP)+1
          JJ=1+(I-P1-1)/IP
          LSS=LS(II,JJ)
          IF(LSS.LE.1) GOTO 410
C         Dr=FTZ(II,JJ)/( 4.*LP(KO(II))*PX(JJ,LSS-1) )
          IF(LSS.GE.LS3+1)THEN
          W(I,I)=.1E21
          ELSE
          IF(JJ.LT.IPL+1) THEN
           IF(MNL.EQ.3) Dr=1.
          IF(MNL.EQ.1)Dr=.5*LP(KO(II))*
   *      (FTZ(II,JJ)/LP(KO(II))/4.-PX(JJ,LSS-1))/PX(JJ,LSS-1)
          IF(MNL.EQ.0.OR.MNL.EQ.2)THEN
          Dr=LOG( FTZ(II,JJ)/(4.*LP(KO(II))*PX(JJ,LSS-1)) )/6.2831853
          ENDIF
          ELSE
          Dr=LP(KO(II))**2
          ENDIF
          W(I,I)=W(I,I)+Dr/KP(JJ,LSS)
          ENDIF
          IF(W(I,I).GE..1E20) THEN
          W(I,I)=.1E20
          MWW=MWW+1
          ENDIF
410       CONTINUE
C         WRITE(*,666)
C         goto 575
          IF(MWW.EQ.NP1) THEN
          DO 412 K=1,NP1
          C(K)=0.
412       BE(K)=BE(K)*4.
          SE=SE*4.
          C(NP1+1)=C(NP1+1)*4.
          C(NP1+2)=C(NP1+2)*4.
          C(NP1+3)=C(NP1+3)*4.
          GOTO 1500
          ENDIF

575       OPEN(8,FILE='\FLM\OUT2.DAT')
          WRITE(8,600) ((W(I,K),K=1,NP1+1),I=1,NP1+1)
          CLOSE(8)

C         WRITE(*,461)
C461      FORMAT('    ******  MATIVT is running secondly   ******')
C         CALL MATIVT(NP1)
C         WRITE(*,462)
C462      FORMAT('    ######  MATIVT second run finished   ######')
C         OPEN(9,FILE='OUT3.DAT')
C         WRITE(9,600) ((W(I,K),K=1,NP1+3),I=1,NP1+3)
```

```
C       CLOSE(9)
C       OPEN(8,FILE='OUT2.DAT')
C       READ(8,*) ((W(I,K),K=1,NP1+3),I=1,NP1+3)
C       CLOSE(8)
        IF(MP.GT.0) THEN
        DO 420 I=1,IP*(IPL+1)
        II=P1+I
        DO 420 J=1,IP*(IPL+1)
        JJ=P1+J
        W(II,JJ)=W(II,JJ)+WP(I,J)
420     CONTINUE
        ENDIF
        DO 430 J=1,NP1
        IF(J.LE.P1)THEN
        JJ=J
        ELSE
        JXP=MOD(J-P1-1,IP)+1
        JZ=(J-P1-1)/IP+1
        J0=P10+(JZ-1)*IP0+JXP
        JJ=KO(JXP)
        ENDIF
        XXM=X(JJ)
        YYM=Y(JJ)
        MMG=1
        IF(SYS.GT.0) THEN
        IF(JJ.LE.MSYB(1)) THEN
        ELSE IF(JJ.LE.MSYB(2) )THEN
        MMG=2
        IF(J.LE.P1) KK=JJ+MSYB(4)-MSYB(1)
        IF(J.GT.P1) KK=KO(JXP+MSYP(4)-MSYP(1))
        XXM=XXM+X(KK)
        YYM=YYM+Y(KK)
        ELSE
        MMG=4
        MMK=MSYB(3)-MSYB(2)
        IF(J.GT.P1) MMK=MSYP(3)-MSYP(2)
        DO 431 K=1,3
        IF(J.LE.P1) KK=JJ+MMK*K
        IF(J.GT.P1) KK=KO(JXP+MMK*K)
        XXM=XXM+X(KK)
431     YYM=YYM+Y(KK)
        ENDIF
        ENDIF
        W(NP1+1,J)=MMG
        W(J,NP1+1)=-1
        W(NP1+2,J)=XXM
        W(J,NP1+2)=-X(JJ)
        if(FHS.EQ.0.AND.IP.EQ.1) GOTO 430
        W(NP1+3,J)=YYM
        W(J,NP1+3)=-Y(JJ)
430     CONTINUE
        DO 440 I=1,NP1+3
440     C(I)=0
        C(NP1+1)=LOAD
        C(NP1+2)=MX+LOAD*XX
        IF(FHS.EQ.0.AND.IP.EQ.1)THEN
        NP3=NP1+2
        ELSE
```

```
      C(NP1+3)=MY+LOAD*YY
      NP3=NP1+3
      ENDIF
      WRITE(*,453)NLOAD
453   FORMAT('     ***** SLNPD(No:',I2,') is running    *****')
      CALL SLNPD(D,NP3)
      WRITE(*,454)
454   FORMAT('     #####   SLNPD run finished   #####')

      OPEN(8,FILE='\FLM\OUT2.DAT')
      READ(8,*) ((W(I,K),K=1,NP1+1),I=1,NP1+1)
      CLOSE(8)
      SE=0.
      DO 470 I=1,NP1
      BE(I)=0.
      DO 460 J=1,NP1
      BE(I)=BE(I)+W(I,J)*C(J)
460   CONTINUE
470   CONTINUE
      IF(FHS.EQ.0.AND.IP.GT.0)THEN
      DO 472 I=1,IP
472   SE=SE+BE(P1+I)
      SE=SE/IP
      ELSE
      DO 474 I=1,P1
474   SE=SE+BE(I)
      SE=SE/P1
      ENDIF
1500  IF(MWW.LT.NP1) LOAD1=LOAD1+LOAD
      NF=NF+1
      DO 450 I=1,NP1
450   CX(I)=CX(I)+C(I)
      DO 480 I=1,NP1
480   BE1(I)=BE1(I)+BE(I)
      SETTLE=SETTLE+SE
      FORCE=0.
      DO 490 I=1,NP1
      MQ=1
      IF(SYS.LE.0) GOTO 490
      IF(I.LE.MSYB(1)) THEN
      ELSE IF(I.LE.MSYB(2)) THEN
      MQ=2
      ELSE IF(I.LE.MSYB(3)) THEN
      MQ=4
      ELSE
      IF(IP.GT.0)THEN
      II=MOD(I-MSYB(3)-1,MSYP(3))+1
       IF(II.LE.MSYP(1))THEN
      MQ=1
      ELSE IF(II.LE.MSYP(2)) THEN
      MQ=2
      ELSE
      MQ=4
      ENDIF
      ENDIF
      ENDIF
490   FORCE=FORCE+MQ*CX(I)
      DLOAD=ABS(LOAD1-FORCE)
```

```
      IF(DLOAD.GT.0.01) FORCE=FORCE+DLOAD*.5
C
      DO 500 I=P1+1,NP1
      II=MOD(I-P1-1,IP)+1
      JJ=1+(I-P1-1)/IP
      IF(FHS.EQ.1) RT(II)=CX(KO(II))
      SZ(II,JJ)=BE1(I)
500   FTZ(II,JJ)=CX(I)
      IF(MWW.EQ.NP1) GOTO 2500
      QP=0.
      DO 520 I=1,IP
      MPP=1
      IF(SYS.GT.0) THEN
      IF(I.LE.MSYP(1)) THEN
      ELSE IF(I.LE.MSYP(2))THEN
      MPP=2
      ELSE
       MPP=4
      ENDIF
      ENDIF
      BP=LP(KO(I))
      UP=4.*BP
      AAP=BP*BP
      FTE(I,1)=FTZ(I,1)+FTZ(I,2)*CE(1)/(CE(1)+CE(2))
      FE(I,1)=FTE(I,1)/CE(1)/UP
      FZ(I,1)=2.*FTZ(I,1)/CE(1)/UP
      FZ(I,2)=FTZ(I,2)*2./(CE(1)+CE(2))/UP
      FTE(I,2)=FTZ(I,2)*CE(2)/(CE(2)+CE(1))
       +FTZ(I,3)*CE(2)/(CE(2)+CE(3))
      FE(I,2)=FTE(I,2)/CE(2)/UP
C
      FTE(I,IPL+1)=FTZ(I,IPL+1)
      FTE(I,IPL)=FTZ(I,IPL)*CE(IPL)/(CE(IPL)+.5*CE(IPL-1))
      FTE(I,IPL-1)=FTZ(I,IPL)*.5*CE(IPL-1)/(CE(IPL)+.5*CE(IPL-1))
   *       +FTZ(I,IPL-1)*CE(IPL-1)/(CE(IPL-1)+CE(IPL-2))
      PE(I,IPL+1)=FTZ(I,IPL+1)
      FE(I,IPL+1)=FTZ(I,IPL+1)/AAP
C     PE(I,IPL)=PE(I,IPL+1)+FTE(I,IPL)
      FE(I,IPL)=FTE(I,IPL)/CE(IPL)/UP
      PZ(I,IPL+1)=FTZ(I,IPL+1)
      FZ(I,IPL+1)=FTZ(I,IPL+1)/AAP
C     PZ(I,IPL)=PZ(I,IPL+1)+FTZ(I,IPL)
      FZ(I,IPL)=FTZ(I,IPL)/(.5*CE(IPL-1)+CE(IPL))/UP
      DO 510 J=IPL,1,-1
      IF(J.EQ.IPL-1) GOTO 512
      IF(J.GT.IPL-1.OR.J.LE.2) GOTO 511
      FTE(I,J)=FTZ(I,J)*CE(J)/(CE(J-1)+CE(J))
   *    +FTZ(I,J+1)*CE(J)/(CE(J+1)+CE(J))
512   FE(I,J)=FTE(I,J)/CE(J)/UP
      FZ(I,J)=FTZ(I,J)*2./(CE(J-1)+CE(J))/UP
511   PZ(I,J)=PZ(I,J+1)+FTZ(I,J)
      PE(I,J)=PE(I,J+1)+FTE(I,J)
510   CONTINUE
C     PZ(I,2)=PZ(I,3)+FTZ(I,2)
C     PE(I,2)=PE(I,3)+FTE(I,2)
C     PZ(I,1)=PZ(I,2)+FTE(I,1)
C     PE(I,1)=PE(I,2)+FTE(I,1)
      IF(ABS(PZ(I,1)-PE(I,1)).GE. .01)
```

```
   *     WRITE(*,700) I,PZ(I,1),PE(I,1)
         RP(I)=PZ(I,1)
         ALFA(I)=PZ(I,IPL+1)/PZ(I,1)
         QP=QP+MPP*RP(I)
520      CONTINUE
         QS=FORCE-QP
700      FORMAT(10X,'******** ERROR  8  ********'/(10X,
   *     'I=',I3,'  PZ1=',E12.6,'  PE1=',E12.6))
          IF(LS3.EQ.0) GOTO 540
         DO 530 I=1,IP
         DO 530 J=1,IPL+1
         LSS=LS(I,J)
         FPU=4.*LP(KO(I))
         IF(J.EQ.IPL+1) FPU=ap(i)
         FPU=FPU*PX(J,LSS)
         IF(FTZ(I,J).GE.FPU*DF)THEN
         LS(I,J)=LSS+1
         IF(LS(I,J).GT.LS3+1) LS(I,J)=LS3+1
         LZ=LZ+1
         ENDIF
530      CONTINUE
C
540      IF(NF.EQ.NP) NF=0
         IF(NF.EQ.0) GO TO 2500
         IF(LZ.EQ.0) GO TO 3000
2500     NLOAD=NLOAD+1
         WRITE(11,601) LOAD1,XX,YY,MX,MY,FORCE
601      FORMAT(/15X,'LOAD=',E9.3,2X,'XX=',E8.2,2X,'YY=',E8.2
   *    /15X,'MX=',E8.2,4X,'MY=',E8.2,2X,'FORCE=',E9.3)
         WRITE(11,602) (CX(I)/(LQA(I)*LQB(I)-LP(I)*LP(I)),I=1,P1)
602      FORMAT(/20X,'THE DISTRIBUTION OF RAFT LOAD',/(2X,7E10.4))
         WRITE(11,6021) (CX(I),I=P1+1,NP1)
6021     FORMAT(20X,'THE RESULT OF PILES LOAD',/(2X,6E12.4))
         WRITE(11,603) (C(I),I=NP1+1,NP1+3)
603      FORMAT(/15X,'W0=',E12.4,' @x=',E12.4,' @y=',E12.4)
         WRITE(11,604) (BE1(I),I=1,P1)
604      FORMAT(/20X,'THE RESULT OF RAFT DISPLACEMENT',/(2X,7E10.4))
         WRITE(11,6041) (BE1(I),I=P1+1,NP1)
6041     FORMAT(/20X,'THE RESULT OF PILES DISPLACEMENT',/(2X,6E12.4))
         IF(IP.EQ.0) GO TO 476
         WRITE(11,605)
         WRITE(11,606) (KO(I),RT(I)/(LQA(KO(I))*LQB(KO(I))-LP(KO(I))**2)
   *     ,RP(I),I=1,MPR(NPR))
605      FORMAT(/15X,'NO.',2X,'A FORCE OF SOIL',2X,'A FORCE OF PILE')
606      FORMAT(15X,I2,4X,E10.4,7X,E10.4)
         DO 1111 I=1,MPR(NPR)
         WRITE(11,607)(I,J,PZ(I,J),FTZ(I,J),FZ(I,J),
   *     PE(I,J),FTE(I,J),FE(I,J),J=1,IPL+1)
607       FORMAT(1X,'PNO DNO      Pz       Fz       fz       Pe',
   *     '      Fe       fe'/(1X,2I3,1X,E10.4 ,1X,E10.4,1X,E10.4,
   *     1X,E10.4,1X,E10.4 ,1X,E10.4 ))
          WRITE(11,677) ALFA(I)
677      FORMAT(25X,'ALFA=',F8.4)
1111     CONTINUE
C
476      IF(FHS.EQ.1) QF=QS/((ABS(X(P1)-X(1))+(LQA(P1)+LQA(1))/2.)
   #           *(ABS(Y(P1)-Y(1))+(LQB(P1)+LQB(1))/2.))
         BF=QS/LOAD1*100
```

```
      WRITE(11,608) LOAD1,QS,QP,BF,QF
608   FORMAT(/25X,'Q=',F12.2,'(T)',
     #  /15X,'Qs=',F8.2,'(T)',2X,',   Pp=',F8.2,'(T)',
     #  /15X,'Qs/Q=',F6.2,'%',4X,',   qf=',F8.2,'(T/M**2)')
      WRITE(11,609)
609   FORMAT(/12X,'************************************************')
      WRITE(20,402) FORCE,SETTLE
      IF(FHS.GT.0) THEN
      WRITE(21,402) FORCE,QS
      WRITE(22,402) FORCE,BF
      WRITE(23,402) FORCE,QP
      ENDIF
      IF(IP.LE.0) GOTO 3000
      WRITE(24,402) FORCE,PZ(MPR(1),1)
      WRITE(25,402) FORCE,ALFA(MPR(1))
      WRITE(26,402) SETTLE,PZ(MPR(1),1)
C     WRITE(27,402) SETTLE,PZ(MPR(2),1)
      WRITE(28,402) FORCE,PZ(MPR(1),IPL+1)
      WRITE(29,402) PZ(MPR(1),IPL+1),SZ(MPR(1),IPL+1-FHS)
      WRITE(30,402) SETTLE,SZ(MPR(1),IPL+1-FHS)
402   FORMAT(1X,2E14.6)
      write(40,714) nload
      write(41,714) nload
       write(40,712) (SZ(MPR(1),J),FZ(MPR(1),J),J=1,IPL)
      write(41,712) (pz(mpr(1),1),pz(mpr(1),j),j=1,ipl+1)
      IF(NLOAD.EQ.1) THEN
      WRITE(15,711) MPR(NPR),IPL+1,BP,Z(IPL+1)
      WRITE(15,712) Z(1),(Z(I)+.5*CE(I),I=1,IPL-1),Z(IPL+1)
      WRITE(15,712) (Z(I),I=1,IPL+1)
      WRITE(15,712) (Z(I),I=1,IPL+1)
      WRITE(15,712) (Z(I)+.5*CE(I),I=1,IPL),Z(IPL+1)
      ENDIF
      WRITE(15,714) NLOAD
      DO 555 I=1,MPR(NPR)
      WRITE(15,712) (PZ(I,J),fz(i,j),PE(I,J),Fe(I,J),J=1,IPL+1)
c     WRITE(15,712) (fz(i,j),J=1,IPL+1)
c     WRITE(15,712) (PE(I,J),J=1,IPL+1)
c     WRITE(15,712) (FE(I,J),J=1,IPL+1)
555   CONTINUE
711   FORMAT(1X,2I4,2E10.4)
712   FORMAT(1X,6E13.6)
714   FORMAT(1X,I4)
716   FORMAT(4X,'0')
3000  IF(LOAD1.GE.AMAX.or.nload.ge.25.OR.MWW.EQ.NP1) GO TO 2001
      IF(LZ.NE.0) GO TO 2000
      IF(LZ.EQ.0) GO  TO 1500
2001  WRITE(15,716)
      WRITE(20,403)
      IF(FHS.GT.0) THEN
      WRITE(21,403)
      WRITE(22,403)
      WRITE(23,403)
      ENDIF
      IF(IP.LE.0) GOTO 7777
      WRITE(24,403)
      WRITE(25,403)
      WRITE(26,403)
C     WRITE(27,403)
```

```
      WRITE(28,403)
      WRITE(29,403)
      WRITE(30,403)
      write(40,716)
      write(41,716)
403   FORMAT(4X,'-.100000E+20, -.100000E+20')
      CLOSE(11)
      CLOSE(15)
7777  STOP
      END


C     ##########################
      SUBROUTINE WR1
      WRITE(*,717)
717   FORMAT(/18X,'  ##################################',/
     *   18X,'  #                              #',/
     *   18X,'  #     PROGRAM FLMGSDT          #',/
     *   18X,'  #     ---------------          #',/
     *   18X,'  #       RONGCHANG YANG         #
     *   18X,'  #      CONCORDIA UNIVERSITY      #',/
     *   18X,'  # CIVIL ENGINEERING DEPARTMENT  #',/
     *   18X,'  #          2005                #',/
     *   18X,'  #                              #',/
     *   18X,'  ##################################',//
     *   12X,'PROGRAME ANALYSING Pile-Soil-Raft Non-linear Interaction:'
     *   ,/12x,'     RAFT is rigid;    PILES are Elastic;',/12x,
     *   'Relations between Pile and Soil are Non-linear, and Established'
     *   ,/12x,'by General Shear-Displacement Mathod;',/12x,
     *   'Relation between Soil and Soil is Elastic, and edstablished',
     *   /12x,'by Finite Layer Method')
      RETURN
      END

C#############################
$DEBUG
$LARGE:MD,W
      SUBROUTINE MDD(IJ,NN)
      DIMENSION XY1(2646,6)
      INTEGER*2  MD,MW,MF
      INTEGER   P1,FHS
C     REAL DIST,RA,DSA
    COMMON /COM4/W(212,212)/CONTR/P1,NP1,IP,IPL,MP,FHS,MTT,LT1,LPT1
      COMMON /ABP/LQA(81),LQB(81),LP(81),KO(20)/COMP/LCO(10),KOP(10)
   *  /CEPM/CE(20),EP(20),AP(20)
    *  /COXYZ/X(81),Y(81),Z(11)/COFC/F(2646),CC(2646)
      COMMON /COMD/MW(2646),MF(20),MD(209,209)
      EQUIVALENCE (W(1,1),XY1(1,1))

800   MN=0
      MK=0
      MF(1)=0
      DO 90 M=1,MTT
      CALL IJZ(M,MI,MZ,ARM,LT1,LPT1,2)
      ZI=Z(MZ)
      IF(M.LE.LT1)THEN
      XA=LQA(MI)
      XB=LQB(MI)
```

```
        ABM=XA/XB
        ENDIF
        RA=SQRT(ARM)
        DO 80 I=1,NP1
        CALL IJZ(I,II,IZ,ARE,P1,IP,1)
        X1=ABS(X(II)-X(MI))
        Y1=ABS(Y(II)-Y(MI))
        DIST=SQRT(X1**2+Y1**2)
C       DSA=DIST/RA
        ZJ=Z(IZ)
        IF(MN.LT.NB) GOTO 88
        DO 75 K=1,MN
        IF( ABS(XY1(K,3)-DIST).LE.0.001 .AND.
     *  (ABS(XY1(K,4)-ZI)+ABS(XY1(K,5)-ZJ).LE.0.001 .OR.
     *  ABS(XY1(K,4)-ZJ)+ABS(XY1(K,5)-ZI).LE.0.001) )THEN
        IF(DIST/RA.GT.1.5.OR.ZI/RA.GT.1.5.OR.ZJ/RA.GT.1.5  .OR.
     *  (ZI.GT.0.001.AND.ZJ.GT.0.001) )THEN
        GOTO 80
        ELSE IF(ABS(XY1(K,6)-ARM).LE.0.001)THEN
        IF(X1+Y1.LE.0.001) GOTO 80
         IF(ABM.GE.0.75.AND.ABM.LE.1.33)THEN
          IF(ABS(XY1(K,1)-X1).LE.0.001 .OR.
     *     ABS(XY1(K,1)-Y1).LE.0.001)  GOTO 80
         ELSE
          IF(XA.EQ.F(K) .AND.ABS(XY1(K,1)-X1).LE.0.001) GOTO 80
          IF(XA.EQ.CC(K).AND.ABS(XY1(K,2)-X1).LE.0.001) GOTO 80
         ENDIF
        ENDIF
        ENDIF
75      CONTINUE
88      MN=MN+1
        XY1(MN,1)=X1
        XY1(MN,2)=Y1
         XY1(MN,3)=DIST
        XY1(MN,4)=ZI
        XY1(MN,5)=ZJ
        XY1(MN,6)=ARM
        F(MN)=XA
        CC(MN)=XB
        MW(MN)=IZ
89      FORMAT(3X,' MI  I  MN    X1       Y1      DIST      ZI',
     *  '      ZJ       ARE '/(2X,2I3,I5,6E10.4))
776     FORMAT(15X,'MN=',I6,'I=',I6,'MK=',I6)
C       WRITE(*,776) MN,I,MK
80      CONTINUE
C       IF(M-LT1.GE.1) WRITE(*,89) M-LT1,I,MN,(XY1(MN,K),K=1,6)
        MF(M+1)=MN
90      CONTINUE
        NN=MN
        WRITE(*,132) (I,MF(I),I=1,MTT+1)
132     FORMAT(15X,'M',15X,'MF(M)'/(12X,I4,12X,I6))
        WRITE(*,887) NN
887     FORMAT(15X,'NN=',I3)
        IF(IJ.EQ.1) GOTO 599

C       WRITE(*,127) (I,MW(I),I=1,NN)
127     FORMAT(15X,'NI=',I3,',   MW(NI)=',I4)
        DO 160 I=1,NP1
```

```
      CALL IJZ(I,II,IZ,AREI,P1,IP,1)
      ZSI=Z(IZ)
      IF(I.LE.P1) THEN
      XA=LQA(II)
      XB=LQB(II)
      ABM=XA/XB
      ENDIF
      SA=SQRT(AREI)
      DO 150 J=1,NP1
      CALL IJZ(J,JJ,JZ,AREJ,P1,IP,1)
      MD(J,I)=0
      X1=ABS(X(II)-X(JJ))
      Y1=ABS(Y(II)-Y(JJ))
      AS=SQRT(X1**2+Y1**2)
      DSA=AS/SA
      ZSJ=Z(JZ)
      DO 140 K=1,NN
      IF(ABS(AS-XY1(K,3)).LE.0.001   .AND.
     * (ABS(ZSI-XY1(K,4))+ABS(ZSJ-XY1(K,5)).LE. 0.001 .OR.
     * ABS(ZSI-XY1(K,5))+ABS(ZSJ-XY1(K,4)).LE. 0.001) )THEN
      IF(DSA.GT.1.5 .OR. ZSI/SA.GT.1.5 .OR. ZSJ/SA.GT.1.5 .OR.
     * (ZSI.GT.0.001 .AND. ZSJ.GT.0.001)) THEN
C     MD(I,J)=K
      MD(J,I)=K
C     WRITE(*,153)I,J,K
153   FORMAT(11X,'I=',I4,', J=',I4,', MD=',I6,'** Case 1 **')
      GO TO 150
      ELSE IF(ABS(XY1(K,6)-AREI).LE.0.001) THEN
      IF(DIST.LE.0.001)THEN
      MD(J,I)=K
C     WRITE(*,154)I,J,K
154   FORMAT(11X,'I=',I4,', J=',I4,', MD=',I6,'** Case 2 **')
      GOTO 150
      ENDIF
      IF(ABM.GE.0.75.AND.ABM.LE.1.33) THEN
      IF(ABS(X1-XY1(K,1)).LE.0.001.OR.ABS(Y1-XY1(K,1)).LE.0.001)THEN
      MD(J,I)=K
C     MD(I,J)=K
C     WRITE(*,155)I,J,K
155   FORMAT(11X,'I=',I4,', J=',I4,', MD=',I6,'** Case 2 **')
      GO TO 150
       ENDIF
      ELSE
      IF(XA.EQ.F(K).AND.ABS(X1-XY1(K,1)).LE.0.001)THEN
      MD(J,I)=K
C     MD(I,J)=K
C     WRITE(*,156)I,J,K
156   FORMAT(11X,'I=',I4,', J=',I4,', MD=',I6,'** Case 3 **')
      GO TO 150
      ENDIF
       IF(XA.EQ.CC(K).AND.ABS(X1-XY1(K,2)).LE.0.001) THEN
      MD(J,I)=K
C     MD(I,J)=K
C     WRITE(*,157)I,J,K
157   FORMAT(11X,'I=',I4,', J=',I4,', MD=',I6,'** Case 4 **')
      GOTO 150
      ENDIF
      ENDIF
```

```
        ENDIF
        ENDIF
140     CONTINUE
        IF (MD(J,I).EQ.0) THEN
        WRITE(*,151)I,J,MD(I,J),ZSI,ZSJ,AREJ
151     FORMAT(2X,'I=',I4,',J=',I4,',MD=',I5,',ZI=',F8.4,',ZJ=',
     * F8.4,',AREJ=',F10.6)
        PAUSE'MD=0'
        ENDIF
150     CONTINUE
160     CONTINUE
        DO 170 I=1,NP1
        DO 170 J=1,NP1
        IF(MD(J,I).EQ.0) THEN
        DO 171 M=1,MTT
        K=LCO(M)
        IF(I.EQ.K .OR. J.EQ.K)THEN
        WRITE(*,*)'I=',I,',J=',J
        STOP'  ERROR IN MD(I,J)=0'
        ENDIF
171     CONTINUE
C       LT1=LT1+LT1
C       IF(I.LE.P1) THEN
C       LCO(LT1)=J
C       MTT=MTT+1
C       ELSE
C       II=MOD(I-P1-1,IP)+1
C       LPT1=LPT1+1
C       LCO(LT1)=KO(II)
C       LXP(II)=LPT1
C       LCP(LPT1)=II
C       KOP(LPT1)=KO(II)
C       MTT=LT1+LPT1*(IPL+1)
C       ENDIF
C       WRITE(*,810) MTT,I,LT1,LPT1,I,J
C       IF(MMT.GT.60) WRITE(*,803)
        IF(MTT*P1.GT.2646) WRITE(*,805)
        PAUSE'                MD=0'
        GO TO 800
        END IF
170     CONTINUE
805     FORMAT(10X,'**  ERROR  5 : NM.GT.2646 **')
810     FORMAT(10X,' MTT =',I3,'    CORD OF ADD PIONT =',I3,
     *  /10X,'LT1=',I3,', LPT1=',I3,/20X,'I=',I3,',J=',I3)
        WRITE(*,811) NN
811     FORMAT(15X,'NN=',I7)

599     RETURN
        END
C#########################

    SUBROUTINE IJZ(I,II,IZ,ARE,N,IP,IT)
        DIMENSION A(81),B(81),BP(81),KO(20),LCO(10),KOP(10)
        COMMON /ABP/A,B,BP,KO/COMP/LCO,KOP
C     *    /CONTR/N1,NP1,NIP,IPL,MP,MFH,MTT,LT1,LTP1
        IF(I.LE.N) THEN
        II=I
        IF(IT.EQ.2) II=LCO(II)
```

```
      IZ=1
      ARE=A(II)*B(II)-BP(II)*BP(II)
      ELSE
      II=MOD(I-N-1,IP)+1
      IZ=1+(I-N-1)/IP
      IF(IT.EQ.1) II=KO(II)
      IF(IT.EQ.2) II=KOP(II)
      ARE=BP(II)*BP(II)
      ENDIF
      RETURN
      END

C################################
$LARGE:MD,W
      SUBROUTINE FLM(NN,MPT)
      REAL L,LP(81),LQA(81),LQB(81)
      REAL B1,B2,CBM,CBN,SBM,SBN,BP
      INTEGER*2 MD(209,209),MW(2646),MF(20),DA(0:61),R,R1,P2
      DIMENSION S(21),D1(20),D2(20),D3(20),D4(20),D5(20),D6(20),
     *    W(212,212),XY1(2646,6),A(291),KO(20)
      EQUIVALENCE (W(1,1),XY1(1,1))
      COMMON /COEN/EN(20),EE2(20),EM1(20),EM2(20),EG2(20)/COM4/W
     * /CEPM/CE(20),EP(20),AP(20)  /COFC/F(2646),CC(2646)
     * /CONTR/KP1,NP1,IP,IPL,MP,MFH,MTT,LT1,LPT1/COMP/LCO(10),KOP(10)
     * /COMD/MW,MF,MD/ABP/LQA,LQB,LP,KO
     *  /COM1/A,DA/COM2/B(60,20)/CFLM/L,NE,NR1,NR,INF
      DO 210 I=1,NE
      FK=EE2(I)/(1.0+EM1(I))/(1.0-EM1(I)-2.0*EN(I)*EM2(I)*EM2(I))
      D1(I)=FK*EN(I)*(1.0-EN(I)*EM2(I)*EM2(I))
      D2(I)=FK*EN(I)*(EM1(I)+EN(I)*EM2(I)*EM2(I))
      D3(I)=FK*EN(I)*EM2(I)*(1.0+EM1(I))
      D4(I)=FK*(1.0-EM1(I)*EM1(I))
      D5(I)=EN(I)*EE2(I)/(1.0+EM1(I))/2.0
210   D6(I)=EG2(I)
      DO 190 I=1,NN
190   F(I)=0.
      P2=21
      DA(0)=0
      DA(1)=1
      DA(2)=3
      DA(3)=6
      DO 200 I=2,NE
      DA(3*I)=15*I-9
      DA(3*I-1)=DA(3*I)-6
200   DA(3*I-2)=DA(3*I)-11
      DO 444 MR=NR1,NR
      R1=2*MR-1
      DO 333 R=1,R1
      IF(R.LE.MR) THEN
      IF(INF.EQ.1) THEN
      M=2*R
      N=2*MR
      ELSE
      M=2*R-1
      N=2*MR-1
      ENDIF
      ELSE
      IF(INF.EQ.1) THEN
```

```
      M=2*MR
      N=2*(R-MR)
      ELSE
      M=2*MR-1
      N=2*(R-MR)-1
      ENDIF
      ENDIF
      WRITE(*,92) mr,r1,r,M,N
92    FORMAT(2X,'MR=',I3,', R1=',I3,',  R=',I3,',  **     M,N:',2I4)
      FM=FLOAT(M)*3.1415926/L
      FN=FLOAT(N)*3.1415926/L
      K1=15*NE-9
      DO 220 K=1,K1
220   A(K)=0.
      K1=3*NE
      DO 230 M=1,K1
      DO 230 K=1,MTT
230   B(M,K)=0.
      DO 240 K=1,NN
      C1=COS(FM*(XY1(K,1)+L/2.))
      C2=COS(FN*(XY1(K,2)+L/2.))
      S1=SIN(FM*(XY1(K,1)+L/2.))
      S2=SIN(FN*(XY1(K,2)+L/2.))
      IF(INF.EQ.1) THEN
      CC(K)=C1*C2
      ELSE
      CC(K)=S1*S2

      ENDIF
240   CONTINUE
      DO 280 I=1,NE
      S(1)=CE(I)*(D1(I)*FM*FM/3.+D5(I)*FN*FN/3.+D6(I)/CE(I)/CE(I))
      S(10)=S(1)
      S(8)=CE(I)*(D2(I)+D5(I))*FM*FN/6.
      S(11)=S(8)
      S(2)=S(8)*2.
      S(14)=S(2)
      S(3)=CE(I)*(D5(I)*FM*FM/3.+D1(I)*FN*FN/3.+D6(I)/CE(I)/CE(I))
      S(15)=S(3)
      S(4)=(-D3(I)+D6(I))*FM/2.
      S(19)=-S(4)
      S(5)=S(4)*FN/FM
      S(20)=-S(5)
      S(6)=CE(I)*(D6(I)*(FM*FM+FN*FN)/3.+D4(I)/CE(I)/CE(I))
      S(21)=S(6)
      S(7)=CE(I)*(D1(I)*FM*FM/6.+D5(I)*FN*FN/6.-D6(I)/CE(I)/CE(I))
      S(9)=-(D3(I)+D6(I))*FM/2.
      S(16)=-S(9)
      S(12)=CE(I)*(D5(I)*FM*FM/6.+D1(I)*FN*FN/6.-D6(I)/CE(I)/CE(I))
      S(13)=S(9)*FN/FM
      S(17)=-S(13)
      S(18)=CE(I)*(D6(I)*(FM*FM+FN*FN)/6.-D4(I)/CE(I)/CE(I))
      IF(INF.GT.1)  THEN
      S(4)=-S(4)
      S(5)=-S(5)
      S(9)=-S(9)
      S(13)=-S(13)
      S(16)=-S(16)
```

```
      S(17)=-S(17)
      S(19)=-S(19)
      S(20)=-S(20)
      ENDIF
      IF(I.EQ.1) THEN
      DO 250 K=1,P2
250   A(K)=S(K)
      ELSE
      II=DA(3*I-2)
      A(II)=S(1)+A(II)
      A(II+4)=S(2)+A(II+4)
      A(II+5)=S(3)+A(II+5)
      DO 260 K=1,3
260   A(DA(3*I)-3+K)=S(3+K)+A(DA(3*I)-3+K)
      IF(I.NE.NE) THEN
      DO 270 K=7,P2
270   A(DA(3*I)+K-6)=S(K)
      ENDIF
      ENDIF
280   CONTINUE
      DO 290 M=1,MTT
      IF(M.LE.LT1) THEN
      MJ=1
      IF(KP1.EQ.0) GOTO 290
      IF(INF.EQ.1) B(3,M)=16.*COS(FM*L/2.)*COS(FN*L/2.)
     * *(SIN(FM*LQA(LCO(M))/2.)*SIN(FN*LQB(LCO(M))/2.)
     * -SIN(FM*LP(LCO(M))/2.)*SIN(FN*LP(LCO(M))/2.))/L/L/FM/FN
     * /(LQA(LCO(M))*LQB(LCO(M))-LP(LCO(M))*LP(LCO(M)))
      IF(INF.EQ.2) B(3,M)=16.*SIN(FM*L/2.)*SIN(FN*L/2.)
     * *(SIN(FM*LQA(LCO(M))/2.)*SIN(FN*LQB(LCO(M))/2.)
     * -SIN(FM*LP(LCO(M))/2.)*SIN(FN*LP(LCO(M))/2.))/L/L/FM/FN
     * /(LQA(LCO(M))*LQB(LCO(M))-LP(LCO(M))*LP(LCO(M)))
      ELSE
      MI=MOD(M-LT1-1,LPT1)+1
      MJ=1+(M-LT1-1)/LPT1
      MI=KOP(MI)
      BP=LP(MI)
C     WRITE(*,286)M,MJ,INF,FM,FN,L
286   FORMAT(3X,'M=',I3,',MJ=',I3,',INF=',I2,',FM=',E10.3,',FN=',
    * E10.3,',L=',E10.4)
      CLM=COS(FM*L/2.)
      CLN=COS(FN*L/2.)
      SLM=SIN(FM*L/2.)
      SLN=SIN(FN*L/2.)
      if(mj.eq.ipl+1) goto 281
      IF(MPT.GT.0) GOTO 282
281   IF(INF.EQ.1) B(3*MJ,M)=4.*CLM*CLN/L/L
      IF(INF.EQ.2) B(3*MJ,M)=4.*SLM*SLN/L/L
      GOTO 290
282   CBM=COS(FM*BP/2.)
      CBN=COS(FN*BP/2.)
      SBM=SIN(FM*BP/2.)
      SBN=SIN(FN*BP/2.)
      IF(INF.EQ.1) THEN
      B1=16.*CLM*CLN*SBM*SBN/L/L/FM/FN/BP/BP
      B2=4.*CLM*CLN*(SBM*CBN/FM+SBN*CBM/FN)/L/L/BP
      ELSE
      B1=16.*SLM*SLN*SBM*SBN/L/L/FM/FN/BP/BP
```

```
        B2=4.*SLM*SLN*(SBM*CBN/FM+SBN*CBM/FN)/L/L/BP
        ENDIF
        GOTO (284,285,287),MPT
284     B(3*MJ,M)=B1
        GOTO 290
285     B(3*MJ,M)=B2
        GOTO 290
287     B(3*MJ,M)=.5*(B1+B2)
        ENDIF
C       WRITE(*,886)M,MJ,B(3*MJ,M)
886     FORMAT(4X,'M=',I4,', MJ=',I4,',  B=',E10.4)
290     CONTINUE
        N3=NE*3
        WRITE(*,292)
292     FORMAT(4X,'     ** SLDLT is runing **')
        CALL SLDLT(N3,1,MTT)
        WRITE(*,294)
294     FORMAT(4X,'$$$$$$ SLDLT run finished $$$$$$')
        DO 300 M=1,MTT
        DO 300 I=MF(M)+1,MF(M+1)
300     F(I)=F(I)+B(3*MW(I),M)*CC(I)

333     CONTINUE
444     CONTINUE

        DO 310 K=1,MN
310     IF(F(K).LT.0.) F(K)=0
        OPEN(6,FILE='\FLM\MD.DAT')
        WRITE(6,665) NN,((MD(I,J),I=1,NP1),J=1,NP1)
665     FORMAT(3X,I5,/(20I4))
        CLOSE(6)
        OPEN(6,FILE='\FLM\FO.DAT')
        WRITE(6,600) (F(I),I=1,NN)
600     FORMAT(2X,5E15.8)
        CLOSE(6)
        END


C   ############################

        SUBROUTINE SLDLT(N,KS,L)
        DIMENSION A(291),B(60,20),DA(0:61)
        INTEGER*2  DA
        COMMON /COM1/A,DA/COM2/B
        DA(0)=0
c       DO 10 I=1,N
c       II=N-I+1
c10    DA(II+1)=DA(II)
c       DA(1)=0
        IF(KS.EQ.0) GO TO 50
        DO 40 I=1,N
        NI=I-DA(I)+DA(I-1)+1
        IK=DA(I)-I
c       NI=I-DA(I+1)+DA(I)+1
c       IK=DA(I+1)-I
        DO 30 J=NI,I
        IJ=J-I+DA(I)
        NJ=J-DA(J)+DA(J-1)+1
```

```
          IF(NI.LE.NJ) THEN
          JI=NJ
          ELSE
          JI=NI
          ENDIF
          JK=DA(J)-J
          J1=J-1
1         FORMAT(2X,'00000000000000000000000000000000')
          DO 20 K=JI,J1
          Y=A(IK+K)
          IF(I.EQ.J) THEN
          Z=A(JK+K)/A(DA(K))
          A(JK+K)=Z
          ELSE
          Z=A(JK+K)
          ENDIF
          A(IJ)=A(IJ)-Y*Z
C         WRITE(*,1)
20        CONTINUE
C         WRITE(*,1)
30        CONTINUE
40        CONTINUE
C         WRITE(*,1)
50        DO 100 M=1,L
          DO 60 I=1,N
          NI=I-DA(I)+DA(I-1)+1
          IK=DA(I)-I
          I1=I-1
          DO 60 K=NI,I1
60        B(I,M)=B(I,M)-A(IK+K)*B(K,M)
          DO 70 I=1,N
70        B(I,M)=B(I,M)/A(DA(I))
          DO 90 II=1,N
          I=N+1-II
          NI=I-DA(I)+DA(I-1)+1
          IK=DA(I)-I
          I1=I-1
          DO 80 K=NI,I1
80        B(K,M)=B(K,M)-A(IK+K)*B(I,M)
90        CONTINUE
100       CONTINUE
c       DO 200 I=1,N
c200    DA(I)=DA(I+1)
      RETURN
      END

C###################################
$LARGE:MD,W
          SUBROUTINE SYSW
          INTEGER*2 MD,MW,MF
          COMMON  /COM4/W(212,212)/SYS/MSYB(4),MSYP(4)
     *       /COMD/MW(2646),MF(20),MD(209,209)
     *    /ABP/QA(81),QB(81),BP(81),KO(20)/COFC/F(2646),CC(2646)
     *    /CONTR/KP1,NP1,IP,IPL,MP,MFH,MTT,LT1,LPT1

          DO 100 I=1,NP1
          IF(I.LE.MSYB(3)) THEN
          I0=I
```

```
        ELSE
        K=I-MSYB(3)-1
        IXP=MOD(K,MSYP(3))+1
        IZ=K/MSYP(3)+1
        I0=KP1+(IZ-1)*IP+IXP
        ENDIF
        DO 330 J=1,NP1
        W(I,J)=.5*(F(MD(I0,J))+F(MD(J,I0)))
        IF(J.LE.MSYB(1)) THEN
        ELSE IF(J.LE.MSYB(2)) THEN
        J2=MSYB(4)-MSYB(1)+J
        W(I,J)=W(I,J)+.5*(F(MD(I0,J2))+F(MD(J2,I0)))
        ELSE IF(J.LE.MSYB(3)) THEN
         DO 334 K=1,3
         J2=J+K*(MSYB(3)-MSYB(2))
334      W(I,J)=W(I,J)+.5*(F(MD(I0,J2))+F(MD(J2,I0)))
        ELSE
        IF(IP.GT.0) THEN
        K=J-MSYB(3)-1
        JXP=MOD(K,MSYP(3))+1
        JZ=K/MSYP(3)+1
        JXB=KO(JXP)
        J0=KP1+(JZ-1)*IP+JXP
        W(I,J)=.5*( F(MD(I0,J0))+F(MD(J0,I0)) )
         IF(JXP.LE.MSYP(1)) THEN
         ELSE IF(JXP.LE.MSYP(2).OR.JXB.LE.MSYB(2)) THEN
         J2=J0+MSYP(4)-MSYP(1)
         W(I,J)=W(I,J)+.5*(F(MD(I0,J2))+F(MD(J2,I0)))
         ELSE
          DO 335 K=1,3
          J2=J0+K*(MSYP(3)-MSYP(2))
335       W(I,J)=W(I,J)+.5*(F(MD(I0,J2))+F(MD(J2,I0)))
         ENDIF
        ENDIF
        ENDIF
330     CONTINUE
100     CONTINUE
        RETURN
        END

C###################################
$LARGE: A
        SUBROUTINE MATIVT(N)
        DIMENSION A(212,212)
        INTEGER*2 INDEX(212)
        COMMON  /COM4/A
        DO 107 I=1,N
107     INDEX(I)=0
108     AMAX=-1.
        DO 111 I=1,N
        IF (INDEX(I)) 111, 109, 111
109     TEMP=ABS(A(I,I))
        IF (TEMP-AMAX) 111, 111, 110
110     ICOL=I
        AMAX=TEMP
111   CONTINUE
        IF (AMAX) 117, 120, 112
112     INDEX(ICOL)=1
```

```
        PIVOT=A(ICOL,ICOL)
        A(ICOL,ICOL)=1.0
        if (PIVOT.LE.E-20) PIVOT=E-20
        PIVOT=1.0/PIVOT
        DO 113 J=1,N
113     A(ICOL,J)=A(ICOL,J)*PIVOT
        DO 116 I=1,N
        IF (I-ICOL) 114, 116, 114
114     TEMP=A(I,ICOL)
        A(I,ICOL)=0.
        DO 115 J=1,N
115     A(I,J)=A(I,J)-A(ICOL,J)*TEMP
116     CONTINUE
        GOTO 108
117     WRITE(*,118)
118     FORMAT(/(20X,'THE INVERSE MATRIX has alread set up')/)
    GOTO 122
120     WRITE(*,121)
121     FORMAT('  ZERO PIVOT,The inverse matrix didnot set up')
122     RETURN
        END

C   *************************
$LARGE: WP
        SUBROUTINE STIFP
        DIMENSION G1(20),G2(20),WP(128,128)
        COMMON/ABP/BQA(81),BQB(81),BP(81),KO(20),
   *  /CEPM/CE(20),EP(20),AP(20)/COP/WP
   *  /CONTR/NEL,NP1,IP,IPL,MP,MFH,MTT,LT1,LPT1
        DO 100 JPD=1,IPL-MFH
        IF(JPD.EQ.1)THEN
         IF(MFH.EQ.0)THEN
          DO 5 I=1,IP
          G1(I)=0.
5         G2(I)=.5*CE(1)/(EP(I)*AP(I))
         ELSE
          DO 10 I=1,IP
          G1(I)=CE(1)/(EP(I)*AP(I))
10        G2(I)=.5*CE(2)*G1(I)/CE(1)
         ENDIF
        ELSEIF(JPD.LT.IPL-MFH)THEN
         DO 20 I=1,IP
         G1(I)=G2(I)
20       G2(I)=CE(JPD+MHS)*G2(I)/CE(JPD-1+MHS)
        ELSE
         DO 30 I=1,IP
         G1(I)=G2(I)
30       G2(I)=CE(IPL)*G2(I)*2./CE(IPL-1)
        ENDIF
        DO 90 I=1,IP
         II=(JPD-1)*IP+I
         WP(II,II)=WP(II,II)+.5*G1(I)
         DO 40 J=JPD+1,IPL+1-MFH
         JJ=(J-1)*IP+I
40       WP(II,JJ)=WP(II,JJ)+G1(I)
         DO 80 J=JPD+1,IPL+1-MFH
          II=(J-1)*IP+I
          JJ=(JPD-1)*IP+I
```

```
          WP(II,JJ)=WP(II,JJ)+.5*(G1(I)+G2(I))
          DO 50 K=JPD+1,IPL+1-MFH
          JK=(K-1)*IP+I
50        WP(II,JK)=WP(II,JK)+G1(I)+G2(I)
80       CONTINUE
90       CONTINUE
100      CONTINUE
         RETURN
         END

C   ##########################
$LARGE
         SUBROUTINE SLNPD(D,N)
         DIMENSION A(212,212),B(212)
         COMMON /COM4/A/COM5/B
         N1=N-1
         DO 100 K=1,N1
         K1=K+1
         C=A(K,K)
         IF(ABS(C)-0.000001) 1,1,3
1        DO 7 J=K1,N
         IF(ABS(A(J,K))-0.000001) 7,7,5
5        DO 6 L=K,N
         C=A(K,L)
         A(K,L)=A(J,L)
6        A(J,L)=C
         C=B(K)
         B(K)=B(J)
         B(J)=C
         C=A(K,K)
         GO TO 3
7        CONTINUE
8        WRITE(*,2) K
2        FORMAT('*** SINGULARITY IN ROW',I5)
         D=0.
C        GO TO 300
         A(K,K)=.000001
3        C=A(K,K)
         DO 4 J=K1,N
4        A(K,J)=A(K,J)/C
         B(K)=B(K)/C
         DO 10 I=K1,N
         C=A(I,K)
         DO 9 J=K1,N
9        A(I,J)=A(I,J)-C*A(K,J)
10       B(I)=B(I)-C*B(K)
100      CONTINUE
101      B(N)=B(N)/A(N,N)
         DO 200 L=1,N1
         K=N-L
         K1=K+1
         DO 200 J=K1,N
200      B(K)=B(K)-A(K,J)*B(J)
         D=1
C        DO 250 I=1,N
C250     D=D*A(I,I)
300      RETURN
         END
```

Appendix C-2: Visual Basic Code of EPWP due to Pile Driving

(For Microsoft Excell)

```
'Program for Evaluation of Mindlin Stress
Option Explicit ' All variables must be declared
' Definition of the global constants
Public Const Pi = 3.14159265359
' Variables
Public Nl As Integer '!!!!!!!!!!
Public r As Double
Public z As Double
Public p As Double
Public D As Double 'D=L
Public m As Double ' m=z/L
Public n As Double 'n=r/L
Public mu As Double 'Possion Ratio u of soil
Public A As Double 'sqrt[n^+(m-1)^]
Public B As Double 'sqrt[n^+(m+1)^]
Public F As Double 'sqrt[n^+m^]
Public Cmu As Double 'Cmu=8pi(1-mu)
Public Zu1 As Double 'zu1=2(2-mu)
Public Zu2 As Double 'Zmu2=2(1-2mu)
Public Zu5 As Double
Public Zu34 As Double
Public A2 As Double 'A^2
Public B2 As Double 'B^2
Public F2 As Double 'F^2
Public A3 As Double 'A^3
Public B3 As Double 'B^3
Public F3 As Double 'F^3
Public A5 As Double 'A^5
Public B5 As Double 'B^5
Public F5 As Double 'F^5
Public B7 As Double 'B^5
Public F7 As Double 'F^7
Public m_n As Double 'm/n
Public m_n2 As Double '(m/n)^2
Public n2_m2 As Double 'n^2-m^2
Public m2 As Double 'm^2
Public m3 As Double 'm^3
Public mn2 As Double 'm*n^2
Public n2 As Double 'n^2
Public mn6 As Double '6mn2(n2_m2)
Public m_1 As Double 'm-1
Public m1 As Double 'm+1
Public m1_2 As Double 'm1^2
Public m1_3 As Double 'm1^3
Public m1_4 As Double 'm1^4
'
Public cu0 As Double
Public Dcu As Double
Public cu As Double
Public fu0 As Double
```

```
Public ful As Double
Public qu As Double
Public r0 As Double
Public L As Double
Public E As Double  'undrained modlus
Public u2 As Double  'excess pore pressure
'
Public C As Double 'C=2pi*r0
Public Ap As Double 'Ap=pi*r0^)
'
Public i As Integer
Public j As Integer
'
Public Pu As Double
Public Pt As Double
Public Pb As Double
Public Stz As Double
Public Str As Double
Public Sto As Double
Public Stt As Double
Public SS As Double
Public TT As Double
Public Re As Double
Public Rp As Double
Public Rp3 As Double
Public af As Double

Public C1 As Double
Public C2 As Double
Public C3 As Double
Public C4 As Double
Public C5 As Double
Public C6 As Double
Public C7 As Double
Public C8 As Double
Public C9 As Double
' defining the initial values
Sub Define()
Nl = 50# * Cells(4, 1).Value
cu0 = Cells(Nl + 2, 3).Value
Dcu = Cells(Nl + 3, 3).Value
r0 = Cells(Nl + 2, 5).Value
mu = Cells(Nl + 2, 7).Value
fu0 = Cells(Nl + 3, 5).Value
ful = Cells(Nl + 3, 7).Value
qu = Cells(Nl + 3, 9).Value
E = Cells(Nl + 2, 11).Value
af = Cells(Nl + 3, 11).Value
'
C = 2# * Pi * r0
Ap = Pi * r0 * r0
Cmu = 8# * Pi * (1# - mu)
Zu1 = 2# * (2# - mu)
Zu2 = 2# * (1# - 2# * mu)
Zu5 = 2# * (5# + 2# * mu)
Zu34 = 3# * (3# - 4# * mu)
'
End Sub
```

```
'*************************************************************
Function Iz_t( ) As Double
'Define ' Initialisation
mn6 = 6# * mn2 * n2_m2
C1 = -Zu1 / A
C2 = (Zu1 * (4# * m + 1#) - Zu2 * m_n2 * m1) / B
C3 = (Zu2 * m_n2 - 4 * Zu1) * m / F
C4 = (mn2 + m_1 ^ 3) / A3
C5 = (4# * m3 + (4 * mu - 15#) * mn2 - (Zu5 * m_n2 - 1#) * m1 * m1_2) / B3
C6 = ((12# + Zu2) * mn2 - 6# * m3 + Zu5 * m_n2 * m3) / F3
C7 = (mn6 + 12# * m_n2 * m1 * m1_4) / B5
C8 = -(12# * m_n2 * m3 * m ^ 2 + mn6) / F5
C9 = -Zu1 * Log((A + m - 1#) * (B + m + 1#) / (F + m) ^ 2)
Iz_t = 2# * (C1 + C2 + C3 + C4 + C5 + C6 + C7 + C8 + C9) / Cmu
End Function
'*************************************************************
Function Ir_t( ) As Double
'Define ' Initialisation
mn6 = 6# * mn2 * n2_m2
C9 = 12# * (1# - mu) * m_n2
C1 = 0.5 * Zu2 / A
C2 = (7# - 2# * mu - 12# * m + C9 * m1) / B
C3 = (12# - C9) * m / F
C4 = -(mn2 + (m - 1#) ^ 3) / A3
C5 = 3# * m1_3 - 2# * m3 + (21# - 4# * mu) * mn2
C5 = (C5 + Zu5 * m_n2 * m1_3) / B3
C6 = -(Zu5 * m_n2 * m3 + 4# * (5# - mu) * mn2) / F3
C7 = (mn6 - 12# * m_n2 * m1 * m1_4) / B5
C8 = -(mn6 - 12 * m_n2 * m3 * m * m) / F5
C9 = 0.5 * Zu2 * Log((A + m - 1#) / (F + m))
C9 = C9 + ((0.5 * Zu2) ^ 2 - 6#) * Log((B + m + 1#) / (F + m))
C9 = C9 + (1# - mu) * Zu2 * ((m - 1) / (B + m + 1) - m / (F + m))
Ir_t = 2# * (C1 + C2 + C3 + C4 + C5 + C6 + C7 + C8 + C9) / Cmu
End Function
'*************************************************************
Function Io_t( ) As Double
'Define ' Initialisation
C9 = m_n2 * m1
C1 = 0.5 * Zu2 / A  'Zu34=3(3-4mu)
C2 = -(Zu2 * (Zu34 / 6# + 3# * C9) + 12# * m - 6#) / B
C3 = m * (3# * Zu2 * m_n2 + 12#) / F
C4 = -Zu2 * (2# * mn2 + (1# - m_n2) * m1_3) / B3
C5 = 2# * (3# * mn2 - m3 + (1# - 3# * m_n2) * m1_3) / B3
C6 = m * (Zu2 * (m2 + 2# * n2 - m2 * m_n2) - 6# * (n2 - m2 * m_n2)) / F3
C7 = 0.5 * Zu2 * Log((A + m_1) / (F + m))
C8 = (Zu2 * Zu2 / 4# - 6#) * Log((B + m1) / (F + m))
C9 = -(1# - mu) * Zu2 * (m_1 / (B + m1) - m / (F + m))
Io_t = 2# * (C1 + C2 + C3 + C4 + C5 + C6 + C7 + C8 + C9) / Cmu
End Function
'*************************************************************
Function It_t( ) As Double
'Define ' Initialisation
C9 = 0.5 * Zu2 * m / n2
C8 = 6# * m_n2 * m / n2 '6m3/n4
'
C1 = (Zu1 + C9 * m_1) / A - C8 * m / F
C2 = -(Zu1 + (C9 - C8) * m1) / B
C3 = (m * m_1 ^ 3 / n2 - n2) / A3
```

```
C9 = m * m1_3 / n2   '(m/n2)(m1^3)
C8 = C9 * m_n2       '(m3/n4)(m1^3)
'
C4 = -(Zu34 / 3# * (C9 + m2) + 17# * m2 - n2 + 12# * C8) / B3
C5 = m2 * (Zu2 * m_n2 + 4# * (5# - mu) + 12 * m_n2 * m_n2) / F3
C6 = (6# * C9 * m1_2 * (m_n2 - 1#) + 12# * m2 * n2) / B5
C7 = -6# * m2 * (m2 * m_n2 * (m_n2 - 1#) + 12# * n2) / F5
It_t = 2# * n * (C1 + C2 + C3 + C4 + C5 + C6 + C7) / Cmu
End Function
'************************************************************
Function Iz_u( ) As Double
'Define ' Initialisation
C1 = -Zu1 / A
C2 = (Zu1 + Zu2 * m_n * m1 / n) / B
C3 = -Zu2 * m_n2 / F
C4 = n2 / A3
C5 = 4# * m2 * (1# - (1# + mu) * m_n2) / F3
C6 = (4# * (1# + mu) * m * m1_3 / n2 - (4# * m2 + n2)) / B3
C7 = -6# * m_n2 * (n2 + m2) * n2_m2 / F5
C8 = 6# * m * (mn2 - m1 * m1_4 / n2) / B5
Iz_u = (C1 + C2 + C3 + C4 + C5 + C6 + C7 + C8) / Cmu
End Function

'************************************************************
Function Ir_u( ) As Double
'Define ' Initialisation
C9 = 12# * (1# - mu) * m_n
C8 = 2# * (1# + 2# * mu) * m_n
C7 = 4# * n2 - 2# * m2  '!!!!!
C1 = 0.5 * Zu2 / A
C2 = (3# + Zu1 - C9 * m1 / n) / B
C3 = -(2# * Zu1 - C9 * m_n) / F - n2 / A3
C4 = (C7 + C8 * m_n * m2) / F3
C5 = -(C7 - n2 + C8 * m1_3 / n) / B3
C6 = 6# * m2 * (n2 - m2 * m_n2) / F5
C7 = 6# * m * (m1_4 * m1 / n2 - mn2) / B5
C8 = 2# * (1# - mu) * Zu2 * (1# / (F + m) - 1# / (B + m1))
Ir_u = (C1 + C2 + C3 + C4 + C5 + C6 + C7 + C8) / Cmu
End Function
'************************************************************
Function Io_u( ) As Double
'Define ' Initialisation
C9 = 6# * (1# - 2# * mu) * m_n
C8 = 2# * (1# + 2# * mu) * m_n
C7 = 2# * m * m - 4# * mu * n2
'
C1 = 0.5 * Zu2 / A
C2 = (6# - Zu2 * Zu34 / 6# + C9 * m1 / n) / B
C3 = (Zu2 * Zu2 / 2# - C9 * m_n - 6#) / F
C4 = (C7 + C8 * m1_3 / n) / B3
C5 = -(C7 + C8 * m2 * m_n) / F3
C6 = -2# * (1 - mu) * Zu2 * (1# / (F + m) - 1# / (B + m1))
Io_u = (C1 + C2 + C3 + C4 + C5 + C6) / Cmu
End Function
'************************************************************
Function It_u( ) As Double
'Define ' Initialisation
C9 = (12# - 4# * mu) * m
```

```
C8 = m_1 / n
C7 = 0.5 * Zu2 / n
C6 = 6# * m_n2
C1 = C7 * C8 / A
C2 = m_1 * C8 * C8 / A3
C3 = (C7 - C6 / n) * m1 / n / B
C4 = (C9 + m1_3 * (1# + 12# * m_n2) / n2) / B3
C5 = -(C6 * m1 * m1_4 / n2 + 6# * mn2) / B5
C6 = (C6 - Zu2) * m_n / n / F
C7 = (-C9 - m3 * (2# + 12# * m_n2) / n2) / F3
C8 = 6# * (mn2 + m3 * m_n2 * m_n2) / F5
It_u = n * (C1 + C2 + C3 + C4 + C5 + C6 + C7 + C8) / Cmu
End Function
'************************************************************
Function Iz_p( ) As Double
'Define ' Initialisation
C9 = 0.5 * Zu2 * m_1
C1 = -C9 / A3
C2 = C9 / B3
C3 = -3# * m_1 ^ 3 / A5
C4 = -m1 * (Zu34 * m * m1 - 3# * (5# * m - 1#)) / B5
C5 = -30# * m * m1_3 / B7
Iz_p = (C1 + C2 + C3 + C4 + C5) / Cmu
End Function
'************************************************************
Function Ir_p() As Double
'Define ' Initialisation
C1 = 0.5 * Zu2 * m_1 / A3
C2 = -0.5 * Zu2 * (m + 7#) / B3
C3 = 2# * (1# - mu) * Zu2 / B / (B + m1)
C4 = -3# * n2 * m_1 / A5
C5 = ((3# * Zu2 * m1 - 6#) * m1 - Zu34 * n2 * m_1) / B5
C6 = -30# * mn2 * m1 / B7
Ir_p = (C1 + C2 + C3 + C4 + C5 + C6) / Cmu
End Function
'************************************************************
Function Io_p( ) As Double
'Define ' Initialisation
C9 = 0.5 * Zu2 * (m - 1#)
C1 = C9 / A3
C2 = (Zu34 * m1 / 6# - 3) * Zu2 / B3
C3 = -2# * (1# - mu) * Zu2 / B / (B + m1)
C4 = (3# * Zu2 * m1 - 6#) * m1 / B5
Io_p = (C1 + C2 + C3 + C4) / Cmu
End Function
'************************************************************
Function It_p( ) As Double
'Define ' Initialisation
C9 = 0.5 * Zu2
C1 = -C9 / A3
C2 = C9 / B3
C3 = -3# * (m - 1#) ^ 2 / A5
C4 = -(Zu34 * m * m1 - 3# * (3# * m - 1#)) / B5
C5 = -30# * m * m1_2 / B7
It_p = n * (C1 + C2 + C3 + C4 + C5) / Cmu
End Function
'************************************************
Function up(r, z, L) As Double
```

```
p = Sqr(r * r + (z - L) * (z - L))
cu = cu0 + Dcu * z
Re = 10# * r0
Rp = Sqr(E / 3#)
Rp3 = (E / 3#) ^ (1# / 3#)
 If (r <= Rp) Then
 C1 = 2# * Log(Rp / r) + 0.817 * af
 Else
 C1 = 0.817 * af * (Rp / r) ^ 2
 End If
 If (p <= Rp3) Then
 C2 = 4# * Log(Rp3 / p) + 0.94 * af
 Else
 C2 = 0.94 * af * (Rp3 / p) ^ 3
 End If
 C3 = 4# * Log(Rp3 / p) + 0.94 * af
If (L <= z - Re) Then
 up = 0
ElseIf (L < z) Then
 up = -C3 * (z - L) / (L - Re)
 'If (up < C1) Then up = C1
ElseIf (L >= z) Then
 up = C1
End If
up = up * cu
End Function
'*************************************************************
Function Sz(i, j) As Double
Define ' Initialisation
r = Cells(Nl + 2, 9).Value
D = Cells(Nl + j + 6, 2).Value
z = Cells(Nl + 5, i + 2).Value
'
n = r / D
m = z / D
m1 = m + 1#
m_1 = m - 1#
m2 = m * m
n2 = n * n
A2 = m_1 ^ 2 + n2
B2 = m1 ^ 2 + n2
F2 = m2 + n2
A = Sqr(A2)
B = Sqr(B2)
F = Sqr(F2)
A3 = A * A2
B3 = B * B2
F3 = F * F2
A5 = A2 * A3
B5 = B2 * B3
F5 = F2 * F3
B7 = B2 * B5
m_n = m / n
m_n2 = m_n * m_n
mn2 = m * n2
n2_m2 = n2 - m2
m3 = m * m2
m1_2 = m1 * m1 '(m+1)^2
```

```
m1_3 = m1 * m1_2 '(m+1)^3
m1_4 = m1_2 * m1_2 '(m+1)^4
'Sz = -1000 * Iz_t()   'normal
'Sz = -1000 * Iz_u()   'normal
'Sz = -1000 * Iz_p()   'normal
'Sz = -1000 * Ir_t()   'normal
'Sz = -1000 * Ir_u()   'normal
'Sz = -1000 * Ir_p()   'normal
'Sz = -1000 * Io_t()   'normal
'Sz = -1000 * Io_u()   'normal
'Sz = -1000 * Io_p()   'normal
'Sz = -1000 * It_t()   'normal
'Sz = -1000 * It_u()   'normal
'Sz = -1000 * It_p()   'normal
Pu = C * fu0 / D          'Pu=C*fu0*D/D^2
Pt = C * ful / 2
Pb = (3.67 + 3.3333 * D) / D / D
Stz = -(Pu * Iz_u() + Pt * Iz_t() + Pb * Iz_p())
Str = -(Pu * Ir_u() + Pt * Ir_t() + Pb * Ir_p())
Sto = -(Pu * Io_u() + Pt * Io_t() + Pb * Io_p())
Stt = -(Pu * It_u() + Pt * It_t() + Pb * It_p())
SS = (Stz + Str + Sto) / 3
TT = (Stz - Str) ^ 2 + (Str - Sto) ^ 2 + (Sto - Stz) ^ 2 + 4 * Stt ^ 2
TT = Sqr(TT) / 1.414

u2 = up(r, z, D)
Sz = SS
'Sz = SS + u2
End Function
```

Appendix C-3: Visual Basic Code of EPWP Dissipation Uxyz

(For Microsoft Excell)

```
'Program for Evaluation of EPWP Dissipation
Option Explicit ' All variables must be declared
' Definition of the global constants
Public Const Pi = 3.14159265359
' Variables
Public Nl As Integer '!
Public i As Integer
Public j As Integer
Public m As Integer '
Public n As Integer '
Public k As Integer
Public kk As Integer
'
Public by_bx As Double '
Public lx_bx As Double '
Public Rx_bx As Double '
Public Eta As Double '
Public bz_bx As Double '
Public y_by As Double '
Public lz_bz As Double
Public Rz_lz As Double
Public Ch_Cv As Double
```

```
Public u0_ul As Double
Public um_ul As Double
Public ub_ul As Double
'
Public x_bx As Double '
'
Public bx_Rx As Double
Public lx_Rx As Double
Public by_Ry As Double
Public ly_bx As Double '
Public ly_Ry As Double
Public Rx_Ry As Double
Public Rx_Rz As Double

Public bz_Rz As Double '
Public lz_Rz As Double 'lz/Rz
Public Bx As Double '
Public By As Double '
Public Lx As Double '
Public Ly As Double '
Public Dx As Double '
Public Dy As Double '
'
Public x_Rx As Double '
Public y_Ry As Double '
Public z_Rz As Double '

Public T As Double '
Public q As Double '
Public qz As Double '
'
Public pm As Double '
Public qn As Double '
Public hk As Double '
'
Public Mumn As Double '
Public Cmn As Double '
Public Muk As Double '
Public dk As Double '
Public Rx_Rk2 As Double '
Public Rx_Rk As Double '
Public Ck_Ch As Double '
Public Tfact As Double '
'
Public C1 As Double
Public C2 As Double
Public C3 As Double
Public C4 As Double
'*************************************************************
' defining the initial values
Sub Define( )
Nl = 40 * Cells(3, 1).Value
q = 0.5 * Cells(Nl + 5, 1).Value
qz = 0.5 * Cells(Nl + 6, 1).Value
by_bx = Cells(Nl + 2, 3).Value 'values from the cells
lx_bx = Cells(Nl + 3, 3).Value
Rx_bx = Cells(Nl + 4, 3).Value
'
```

```
Eta = Cells(Nl + 2, 5).Value
bz_bx = Cells(Nl + 3, 5).Value
y_by = Cells(Nl + 4, 5).Value
'
lz_bz = Cells(Nl + 2, 7).Value
Rz_lz = Cells(Nl + 3, 7).Value
Ch_Cv = Cells(Nl + 4, 7).Value
'
u0_ul = Cells(Nl + 2, 9).Value
um_ul = Cells(Nl + 3, 9).Value
ub_ul = um_ul
x_Rx = Cells(Nl + 7, 9).Value

bx_Rx = 1# / Rx_bx
lx_Rx = bx_Rx * lx_bx
by_Ry = 1# / (1# + ((Eta - 1#) * lx_bx - Eta + Rx_bx) / by_bx)
ly_bx = by_bx + Eta * (lx_bx - 1#)
ly_Ry = 1# / (1# + (Rx_bx - lx_bx) / ly_bx)
'
Rx_Ry = by_Ry * Rx_bx / by_bx
y_Ry = y_by * by_Ry
'
lz_Rz = 1# / Rz_lz
bz_Rz = 1# / (lz_bz * Rz_lz)
Rx_Rz = bz_Rz * Rx_bx / bz_bx
Rx_Rk2 = 1# + Rx_Ry * Rx_Ry + Rx_Rz * Rx_Rz
Rx_Rk = Sqr(Rx_Rk2)
Ck_Ch = (1# + Rx_Ry * Rx_Ry + Rx_Rz * Rx_Rz / Ch_Cv) / Rx_Rk2
Tfact = Ck_Ch * Rx_Rk2
End Sub
'************************************************************
Function u0(z_Rz) As Double
'Private z As Double
If (z_Rz <= bz_Rz) Then
u0 = u0_ul + (1 - u0_ul) * z_Rz / bz_Rz 'z_Rz
ElseIf (z_Rz <= lz_Rz) Then
u0 = 1 - (1 - um_ul) * (z_Rz - bz_Rz) / (lz_Rz - bz_Rz)
Else
u0 = 0
End If
End Function
'************************************************************
Function Umn(m, n) As Double
'Define ' Initialisation
qn = Pi * (q + n)
By = qn * by_Ry
Ly = qn * ly_Ry
Dy = Ly - By
'
Mumn = (pm * pm + qn * qn * Rx_Ry * Rx_Ry) '/ Tfact
'
If (Dx <> Dy) Then
Cmn = (Sin(By + Bx) - Sin(Ly + Lx)) / (Dx + Dy)
Cmn = Cmn - (Sin(By - Bx) - Sin(Ly - Lx)) / (Dy - Dx)
Cmn = 2# * Cmn / pm / qn
ElseIf (Dx <> 0) Then
Cmn = Cos(By - Bx) - (Sin(Ly + Lx) - Sin(By + Bx)) / (Dx + Dy)
Cmn = 2# * Cmn / pm / qn
```

```
ElseIf (Dx = 0 & Dy = 0) Then
Cmn = 4# * Sin(Bx) * Sin(By) / pm / qn
End If

Umn = Cmn * Cos(pm * x_Rx) * Cos(qn * y_Ry) * Exp(-Mumn * T)
End Function
'************************************************************************
Function Uk(k) As Double
hk = Pi * (qz + k)
Muk = (hk * hk * Rx_Rz * Rx_Rz / Ch_Cv) '/ Tfact
If (lz_bz <> 1) Then
dk = u0_ul - um_ul * Cos(hk * lz_Rz) + (1# - u0_ul) / hk / bz_Rz * Sin(hk * bz_Rz)
dk = dk + (1# - um_ul) / hk / (lz_Rz - bz_Rz) * (Sin(hk * bz_Rz) - Sin(hk * lz_Rz))
dk = 2# * dk / hk
Else
dk = u0_ul - Cos(hk * lz_Rz) + (1# - u0_ul) / hk / bz_Rz * Sin(hk * bz_Rz)
End If
Uk = dk * Sin(hk * z_Rz) * Exp(-Muk * T)
End Function
'************************************************************
Function U(i, j) As Double
Define ' Initialisation
T = Cells(Nl + j + 7, 2).Value
z_Rz = Cells(Nl + 6, i + 2).Value
C1 = 0
For m = 0 To 50
pm = Pi * (q + m)
Bx = pm * bx_Rx
Lx = pm * lx_Rx
Dx = Lx - Bx
For n = 0 To 50
C1 = C1 + Umn(m, n)
Next
Next
C2 = 0
kk = 1
If (qz > 0.01) Then kk = 0
For k = kk To 50
C2 = C2 + Uk(k)
Next k
U = 1# - C1 * C2    'u0(z_Rz)
End Function
```

Appendix C-4: Visual Basic Code of EPWP Dissipation Ur
(For Microsoft Excell)

For the 1st form of u(r,0):

```
'Program for Evaluation of EPWP Dissipation Ur for 1st form
Option Explicit ' All variables must be declared
' Definition of the global constants
Public Const Pi = 3.14159265359
' Variables
Public Nl As Integer '!!!!!!!!!!
Public i As Integer
Public j As Integer
Public m As Integer '
Public n As Integer '
Public K As Integer '
Public km As Integer '
Public kn As Integer '
Public kh As Integer '

Public by_bx As Double '
Public lx_bx As Double '
Public Rx_bx As Double '
Public Eta As Double '
Public bz_bx As Double '
'
Public ly_bx As Double '
'
Public x_bx As Double '
Public y_by As Double '
Public bx_Rx As Double
Public lx_Rx As Double
Public by_Ry As Double
Public ly_Ry As Double
Public Rx_Ry As Double

Public bz_Rz As Double '
Public lz_Rz As Double '
Public Bx As Double '
Public By As Double '
Public Lx As Double '
Public Ly As Double '
Public Dx As Double '
Public Dy As Double '
'
Public x_Rx As Double '
Public y_Ry As Double '
Public T As Double '
Public q As Double '
Public qy As Double '
'
Public u0_ul As Double '
Public um_ul As Double '
'
Public pm As Double '
Public qn As Double '
```

```
Public hk As Double '
'
Public Mumn As Double '
Public Cmn As Double '
'
Public C1 As Double
Public C2 As Double
Public C3 As Double
Public C4 As Double
Public C5 As Double
Public A As Double
Public A2 As Double
Public B As Double
Public C As Double
Public D As Double
Public E As Double
Public af As Double
Public afm As Double

' defining the initial values
Sub Define()
Nl = 40 * Cells(43, 1).Value
q = 0.5 * Cells(Nl + 4, 1).Value
qy = 0.5 * Cells(Nl + 5, 1).Value
by_bx = Cells(Nl + 2, 3).Value 'values from the cells
lx_bx = Cells(Nl + 3, 3).Value
Rx_bx = Cells(Nl + 4, 3).Value
Eta = Cells(Nl + 2, 5).Value
bz_bx = Cells(Nl + 3, 5).Value
y_by = Cells(Nl + 4, 5).Value
'x_bx = Cells(Nl + 3, 9).Value
'
bx_Rx = 1# / Rx_bx
lx_Rx = bx_Rx * lx_bx
by_Ry = 1# / (1# + ((Eta - 1#) * lx_bx - Eta + Rx_bx) / by_bx)
ly_bx = by_bx + Eta * (lx_bx - 1#)
ly_Ry = 1# / (1# + (Rx_bx - lx_bx) / ly_bx)
'
Rx_Ry = by_Ry * Rx_bx / by_bx
y_Ry = y_by * by_Ry

km = 1
If (q > 0.01) Then km = 0
kn = 1
If (qy > 0.01) Then kn = 0
End Sub
'************************************************************
Function Afo(K, j) As Double
A = 0.5 * Pi * (K - 0.5 + 2# * j)
A2 = 16 * A * A
B = 4# * K * K
C = 7# * B - 31#
D = 83# * B * B - 982# * B + 3779#
E = 6949# * B ^ 3 - 153855# * B * B + 1585743# * B - 6277237
Afo = 1 + C / 3 / A2 + D / 5 / A2 / A2 + E / 105 / A2 / A2 / A2
Afo = A - (B - 1#) / 8 / A * Afo
End Function
Function Afo1(K, j) As Double
```

```
Define
Afo1 = Pi * (K / 2# + 3# / 4# + j - 1)
End Function

'************************************************************
Function J0(K, af) As Double
'Define ' Initialisation
C3 = 0.5 * af
C5 = 1
If (af < 30#) Then
If (K > 0) Then
For j = 1 To K
C5 = C5 * C3 / j
Next
End If
C4 = C5
For i = 1 To 50
C5 = -C5 * C3 * C3 / i / (K + i)
C4 = C4 + C5
Next
J0 = C4
Else
J0 = Sqr(2# / Pi / af) * Cos(af - K * Pi / 2 - Pi / 4)
End If
End Function
Function Je2(af) As Double
If (af = 0) Then
Je2 = 0
Else
Je2 = 2 * J0(1, af) / af - J0(0, af)
End If
End Function
'************************************************************
Function Umn() As Double
'Define ' Initialisation
qn = J0(1, afm)
Bx = afm * bx_Rx
Lx = afm * lx_Rx
Dx = Lx * Lx - Bx * Bx
Mumn = afm * afm
If (Abs(Dx) >= 0.0001) Then
Cmn = lx_Rx * lx_Rx * Je2(Lx) - bx_Rx * bx_Rx * Je2(Bx)
Cmn = 4# * Cmn / Dx / qn / qn

Else
Cmn = 2# * Bx * J0(1, Bx) / Mumn / qn / qn
End If
'
Umn = Cmn * J0(0, afm * x_Rx) * Exp(-Mumn * T)
End Function
'************************************************************
Function U(i, j) As Double
Define ' Initialisation
T = Cells(Nl + j + 7, 2).Value
x_Rx = Cells(Nl + 6, i + 2).Value
C1 = 0#
For m = 1 To 32
If (m <= 16) Then
```

```
afm = Cells(m + 5, 15).Value
Else
afm = Afo1(0, m)  'Cells(m + 5, 23).Value
End If
C1 = C1 + Umn()
Next
'
U = 1# - C1
End Function
```

For the 2nd form of u(r,0)

```
'*************************************************************
'Program for Evaluation of EPWP Dissipation for u(r,0)Form 2
Option Explicit ' All variables must be declared
' Definition of the global constants
Public Const Pi = 3.14159265359
' Variables
Public Nl As Integer '!!!!!!!!!!
Public i As Integer
Public j As Integer
Public m As Integer '
Public n As Integer '
Public K As Integer '
Public km As Integer '
Public kn As Integer '
Public kh As Integer '

Public by_bx As Double '
Public lx_bx As Double '
Public Rx_bx As Double '
Public Eta As Double '
Public bz_bx As Double '
'
Public ly_bx As Double '
'
Public x_bx As Double '
Public y_by As Double '
Public bx_Rx As Double
Public lx_Rx As Double
Public by_Ry As Double
Public ly_Ry As Double
Public Rx_Ry As Double

Public bz_Rz As Double '
Public lz_Rz As Double '
Public Bx As Double '
Public By As Double '
Public Lx As Double '
Public Ly As Double '
Public Dx As Double '
Public Dy As Double '
'
Public x_Rx As Double '
Public y_Ry As Double '
Public T As Double '
```

```
Public q As Double '
Public qy As Double '
'
Public u0_ul As Double '
Public um_ul As Double '
'
Public pm As Double '
Public qn As Double '
Public hk As Double '
'
Public Mumn As Double '
Public Cmn As Double '
'
Public C1 As Double
Public C2 As Double
Public C3 As Double
Public C4 As Double
Public C5 As Double
Public A As Double
Public A2 As Double
Public B As Double
Public C As Double
Public D As Double
Public E As Double
Public af As Double
Public afm As Double

' defining the initial values
Sub Define()
Nl = 40 * Cells(43, 1).Value
q = 0.5 * Cells(Nl + 4, 1).Value
qy = 0.5 * Cells(Nl + 5, 1).Value
by_bx = Cells(Nl + 2, 3).Value 'values from the cells
lx_bx = Cells(Nl + 3, 3).Value
Rx_bx = Cells(Nl + 4, 3).Value
Eta = Cells(Nl + 2, 5).Value
bz_bx = Cells(Nl + 3, 5).Value
y_by = Cells(Nl + 4, 5).Value
'x_bx = Cells(Nl + 3, 9).Value
'
bx_Rx = 1# / Rx_bx
lx_Rx = bx_Rx * lx_bx
by_Ry = 1# / (1# + ((Eta - 1#) * lx_bx - Eta + Rx_bx) / by_bx)
ly_bx = by_bx + Eta * (lx_bx - 1#)
ly_Ry = 1# / (1# + (Rx_bx - lx_bx) / ly_bx)
'
Rx_Ry = by_Ry * Rx_bx / by_bx
y_Ry = y_by * by_Ry

km = 1
If (q > 0.01) Then km = 0
kn = 1
If (qy > 0.01) Then kn = 0
End Sub
'************************************************************
Function Afo(K, j) As Double
A = 0.5 * Pi * (K - 0.5 + 2# * j)
A2 = 16 * A * A
```

```
B = 4# * K * K
C = 7# * B - 31#
D = 83# * B * B - 982# * B + 3779#
E = 6949# * B ^ 3 - 153855# * B * B + 1585743# * B - 6277237
Afo = 1 + C / 3 / A2 + D / 5 / A2 / A2 + E / 105 / A2 / A2 / A2
Afo = A - (B - 1#) / 8 / A * Afo
End Function
Function Afo1(K, j) As Double
Define
Afo1 = Pi * (K / 2# + 3# / 4# + j - 1)
End Function

'*********************************************************
Function J0(K, af) As Double
'Define ' Initialisation
C3 = 0.5 * af
C5 = 1
If (af < 30#) Then
If (K > 0) Then
For j = 1 To K
C5 = C5 * C3 / j
Next
End If
C4 = C5
For i = 1 To 50
C5 = -C5 * C3 * C3 / i / (K + i)
C4 = C4 + C5
Next
J0 = C4
Else
J0 = Sqr(2# / Pi / af) * Cos(af - K * Pi / 2 - Pi / 4)
End If
End Function
Function Je2(af) As Double
If (af = 0) Then
Je2 = 0
Else
Je2 = 2 * J0(1, af) / af - J0(0, af)
End If
End Function
'*********************************************************
Function Umn( ) As Double
'Define ' Initialisation for (5-4a)
qn = J0(1, afm)
Bx = afm * bx_Rx
Lx = afm * lx_Rx
Dx = Lx * Lx - Bx * Bx
Mumn = afm * afm
If (Abs(Dx) >= 0.0001) Then
Cmn = lx_Rx * lx_Rx * Je2(Lx) - bx_Rx * bx_Rx * Je2(Bx)
Cmn = 4# * Cmn / Dx / qn / qn

Else
Cmn = 2# * Bx * J0(1, Bx) / Mumn / qn / qn
End If
'
Umn = Cmn * J0(0, afm * x_Rx) * Exp(-Mumn * T)
End Function
```

```
'*************************************************************
Function U(i, j) As Double
Define ' Initialisation
T = Cells(Nl + j + 7, 2).Value
x_Rx = Cells(Nl + 6, i + 2).Value
C1 = 0#
For m = 1 To 32
If (m <= 16) Then
afm = Cells(m + 5, 15).Value
Else
afm = Afo1(0, m)  'Cells(m + 5, 23).Value
End If
C1 = C1 + Umn()
Next
'
U = 1# - C1
End Function
```

Appendix C-5: Visual Basic Code of EPWP Consolidation Uz
(For Microsoft Excell)

```
'Program for Evaluation of Mindlin Stress
Option Explicit ' All variables must be declared
' Definition of the global constants
Public Const Pi = 3.14159265359
' Variables
Public Nl As Integer '!
Public i As Integer
Public j As Integer
Public m As Integer '
Public n As Integer '
Public k As Integer
Public kk As Integer
'
Public by_bx As Double '
Public lx_bx As Double '
Public Rx_bx As Double '
Public Eta As Double '
Public bz_bx As Double '
Public y_by As Double '
Public lz_bz As Double
Public Rz_lz As Double
Public Ch_Cv As Double
Public u0_ul As Double
Public um_ul As Double
Public ub_ul As Double
'
Public x_bx As Double '
'
Public bx_Rx As Double
Public lx_Rx As Double
Public by_Ry As Double
Public ly_bx As Double '
```

```
Public ly_Ry As Double
Public Rx_Ry As Double
Public Rx_Rz As Double

Public bz_Rz As Double '
Public lz_Rz As Double 'lz/Rz
Public Bx As Double '
Public By As Double '
Public Lx As Double '
Public Ly As Double '
Public Dx As Double '
Public Dy As Double '
'
Public x_Rx As Double '
Public y_Ry As Double '
Public z_Rz As Double '

Public T As Double '
Public qz As Double '
Public q As Double '
'
Public pm As Double '
Public qn As Double '
Public hk As Double '
'
Public Mumn As Double '
Public Cmn As Double '
Public Muk As Double '
Public dk As Double '
Public Rx_Rk2 As Double '
Public Rx_Rk As Double '
Public Ck_Ch As Double '
Public Tfact As Double '
'
Public C1 As Double
Public C2 As Double
Public C3 As Double
Public C4 As Double
'*************************************************************
' defining the initial values
Sub Define()
Nl = 40 * Cells(3, 1).Value
q = 0.5 * Cells(Nl + 5, 1).Value
qz = 0.5 * Cells(Nl + 6, 1).Value
by_bx = Cells(Nl + 2, 3).Value 'values from the cells
lx_bx = Cells(Nl + 3, 3).Value
Rx_bx = Cells(Nl + 4, 3).Value
'
Eta = Cells(Nl + 2, 5).Value
bz_bx = Cells(Nl + 3, 5).Value
y_by = Cells(Nl + 4, 5).Value
'
'lz_bz = Cells(Nl + 2, 7).Value
lz_Rz = Cells(Nl + 3, 7).Value   'Rz_lz
Ch_Cv = Cells(Nl + 4, 7).Value
'
u0_ul = Cells(Nl + 2, 9).Value
um_ul = Cells(Nl + 3, 9).Value
```

```
ub_ul = 1 'um_ul
x_Rx = Cells(Nl + 7, 9).Value

bx_Rx = 1# / Rx_bx
lx_Rx = bx_Rx * lx_bx
by_Ry = 1# / (1# + ((Eta - 1#) * lx_bx - Eta + Rx_bx) / by_bx)
ly_bx = by_bx + Eta * (lx_bx - 1#)
ly_Ry = 1# / (1# + (Rx_bx - lx_bx) / ly_bx)
'
'Rx_Ry = by_Ry * Rx_bx / by_bx  !!!!!!!!
Rx_Ry = 1#
y_Ry = y_by * by_Ry
'
'lz_Rz = 1# / Rz_lz
'bz_Rz = 1# / (lz_bz * Rz_lz)
Rx_Rz = bz_Rz * Rx_bx / bz_bx

Rx_Rk2 = 1# + Rx_Ry * Rx_Ry + Rx_Rz * Rx_Rz
Rx_Rk = Sqr(Rx_Rk2)
Ck_Ch = (1# + Rx_Ry * Rx_Ry + Rx_Rz * Rx_Rz / Ch_Cv) / Rx_Rk2
Tfact = Ck_Ch * Rx_Rk2
End Sub
'************************************************************
Function Umn(m, n) As Double
'Define ' Initialisation
qn = Pi * (q + n)
By = qn * by_Ry
Ly = qn * ly_Ry
Dy = Ly - By
'
Mumn = (pm * pm + qn * qn * Rx_Ry * Rx_Ry) '/ T-fact
'
If (Dx <> Dy) Then
Cmn = (Sin(By + Bx) - Sin(Ly + Lx)) / (Dx + Dy)
Cmn = Cmn - (Sin(By - Bx) - Sin(Ly - Lx)) / (Dy - Dx)
Cmn = 2# * Cmn / pm / qn
ElseIf (Dx <> 0) Then
Cmn = Cos(By - Bx) - (Sin(Ly + Lx) - Sin(By + Bx)) / (Dx + Dy)
Cmn = 2# * Cmn / pm / qn
ElseIf (Dx = 0 & Dy = 0) Then
Cmn = 4# * Sin(Bx) * Sin(By) / pm / qn
End If

Umn = Cmn * Cos(pm * x_Rx) * Cos(qn * y_Ry) * Exp(-Mumn * T)
End Function
'************************************************************************************
Function Uk(k) As Double
hk = Pi * (qz + k)
'Muk = (hk * hk * Rx_Rz * Rx_Rz / Ch_Cv) '/ Tfact
Muk = hk * hk '* Rx_Rz * Rx_Rz / Ch_Cv
If (lz_Rz <> bz_Rz) Then
dk = Cos(hk * bz_Rz) - um_ul * Cos(hk * lz_Rz) ' + (1# - u0_ul) / hk / bz_Rz * Sin(hk * bz_Rz)
dk = dk - (1# - um_ul) / hk / (lz_Rz - bz_Rz) * (Sin(hk * bz_Rz) - Sin(hk * lz_Rz))
dk = 2# * dk / hk
Else
dk = u0_ul - Cos(hk * lz_Rz) + (1# - u0_ul) / hk / bz_Rz * Sin(hk * bz_Rz)
dk = 2# * dk / hk
End If
```

```
dk = dk / hk '*Rz
'Uk = dk * Sin(hk * z_Rz) * Exp(-Muk * T)
Uk = dk * (1# - Cos(hk * lz_Rz)) * Exp(-Muk * T)
End Function
Function Uz(i, j) As Double
Define ' Initialisation
T = Cells(Nl + j + 7, 2).Value
bz_Rz = Cells(Nl + 6, i + 2).Value
'C1=(u0_ul+1)*bz_Rz/2+(um_ul+1)*(lz_Rz-bz_Rz)/2
C1 = (um_ul + 1#) * (lz_Rz - bz_Rz) / 2#
C2 = 0
kk = 1
If (qz > 0.01) Then kk = 0
For k = kk To 50
C2 = C2 + Uk(k)
Next k
Uz = 1# - C2 / C1
End Function
'************************************************************
Function U(i, j) As Double
Define ' Initialisation
T = Cells(Nl + j + 7, 2).Value
z_Rz = Cells(Nl + 6, i + 2).Value
C1 = 0
For m = 0 To 50
pm = Pi * (q + m)
Bx = pm * bx_Rx
Lx = pm * lx_Rx
Dx = Lx - Bx
For n = 0 To 50
C1 = C1 + Umn(m, n)
Next
Next
C2 = 0
kk = 1
If (qz > 0.01) Then kk = 0
For k = kk To 50
C2 = C2 + Uk(k)
Next k
U = 1# - C1 * C2    'u0(z_Rz)
End Function
```

Appendix C-6: MATLAB Code of Inversion of Laplace Transform

```
function mainGWR()
%GWR Inverse Laplace transfer
global Tau
T=10; a=0.25; Nsum=16;%aT=5~10 gave good results for Nsum=50~5000
N=Nsum; N1=N-1; Nt=N;    %L=50; Nsum/L=100
Time=zeros(N,1); ft=zeros(N,1);
ftexact=zeros(N,1); Dlt_Ft=zeros(N,1);

dt=T/Nt; T=2*T; Ot=2.*pi/T;
Time=[0:dt:dt*N1]';
for kt=1:N1
    ti=Time(kt+1);
    ft(kt+1)=GWR(ti,4);
    ftexact(kt+1)=Ftfunct(ti);
    if ftexact(kt+1)==0
        Dlt_Ft(kt+1)=ft(kt+1)-ftexact(kt+1);
    else
        Dlt_Ft(kt+1)=(ft(kt+1)-ftexact(kt+1))/ftexact(kt+1);
    end
end
%s_l=a+i*[0:Ot:Ot*(Nsum-1)]';
%fs=Fsfunct(s_l);
%ft=fft(fs,N)/N;
%ft=Fourier(-1,fs);
%ft=real(ft)-real(Fsfunct(a))/2.;
%ft=2.*ft.*exp(a*Time)/T;
%ftexact=Ftfunct(Time);
%Dlt_Ft=ft-ftexact;

fopen('LpiGWR_out.txt','w');
Mat=[Time,ft,ftexact,Dlt_Ft]
csvwrite('LpiGWR_out.txt',Mat);
fclose('all');

%-------------------------------------------------
function G=GWR(t,M0)
global Tau
M=M0+round(16*t/10);    M=M-mod(M,2);
fk=zeros(1,2*M+4);  G0=fk;Gm=fk;Gp=fk;G02=G0;
if(t==0),t=.01;end
Tau=log(2)/t;   Prec=21*M/10;  broken=0;

G0(1:2*M)=Fkfunct_1(M);
G02(1:2*M)=Fkfunct_2(M);
%Mat=[G0',G02']
Gm(1:M+1)=0.;
best=G0(M-1);

for k=0:M-2
    for n=M-2-k:-1:0
        n1=n+2;
        expr=G0(n1+1)-G0(n1);
        if(expr==0 | isnan(expr))
            broken=1; break
```

```
        end
        expr=Gm(n1+1)+(k+1)/expr;
        Gp(n1)=expr;
        if(mod(k,2)==0)
            if(n==M-2-k),best=expr;end
        end
    end
    if broken==1, break; end
    for n=0:M-k
        n1=n+1;
        Gm(n1)=G0(n1);G0(n1)=Gp(n1);
    end
    %best
end
G=best;
%-------
function b=binomial(n,k)
b=factorial(n)/factorial(k)/factorial(n-k);
%-----------------------------------------
function d=Fkfunct_1(M)
global Tau
d=zeros(1,2*M); fk=zeros(1,2*M);G0=fk;
for k=1:2*(M+2)
    fk(k)=Fsfunct(k*Tau);
end
M1=M;
for n=1:M
    sf=0.;si=-1;
    for k=0:n
        si=-si;
        sf=sf+si*binomial(n,k)*fk(n+k);
    end
    G0(n)=Tau*n*binomial(n,k)*sf;    %G0=fk(t)
    if (abs(G0(n))<1.e-6), G0(n)=0; end
    if isnan(G0(n))
        M1=n-1;
        G0(n)=0.;
        break
    end
end
d=G0(1:2*M);

function d=Fkfunct_2(M)
global Tau
d=zeros(1,2*M); fk=zeros(1,2*M+2);G0=fk;
for n=1:2*M
    fk(n)=Fsfunct(n*Tau);
    G0(n)=n*Tau*fk(n);
end
M1=M;
for k=1:2*M
    for n=k:2*M
        Gk(n)=(1+n/k)*G0(n)-n/k*G0(n+1);
    end
    for n=k:2*M
         G0(n)=Gk(n);
    end
    G0(k)=Gk(k);
     if(abs(G0(k))<1.e-6), G0(k)=0; end
```

```
 end
d=G0(1:2*M);

%-------------------------------------------------
function F=FLT(t,M0)
M=M0+round(1.6*t);  M1=M-1;
if(t>0)
    r=2.*M/(5.*t);
    %r=0.5;
else
    t=1.e-9; r=2.9e-3;
end
F=Fsfunct(r)*exp(r*t)/2.; dc=pi/M;
for cta=dc:dc:dc*M1
    s=r*cta*(cot(cta)+i);
    sgma=cta+(cta*cot(cta)-1.)*cot(cta);
    C1=Fsfunct(s); C2=exp(t*s);
    Fss=Fsfunct(s)*exp(t*s)*(1.+i*sgma);
    %sf=(1.+i*sgma)*Fss;
    F=F+real(Fss);
end
F=F*r/M;
if(abs(F)<1.e-10), F=0.; end


%-------------------------------------------------------
function Fs=Fsfunct(s)
[nsi,nsj]=size(s);Fs=zeros(nsi,nsj);f=Fs;
%
Fs=exp(-1./s)./s./sqrt(s);          %F07
%Fs=exp(-2.*sqrt(s));             %F04
%Fs=1./(sqrt(s)+sqrt(s+1.));         %F03
%f=(s.*s+1); Fs=s./(f.*f);        %------Ft1
%f=exp(-10.*s); Fs=f./s;           %------Ft2
%Fs=2./(s.*(1.0+exp(-2.0*s)));      %------Ft3

%-------------------------------------------------------
function Ft=Ftfunct(t)
[nti,ntj]=size(t); Ft=zeros(nti,ntj);
if(t<1.e-4), t=1.e-4;end;

Ft=sin(2.*sqrt(t))/sqrt(pi);         %F07
%Ft=exp(-1./t)./t./sqrt(pi*t);     %F04
%Ft=.5*(1.-exp(-t))./t./sqrt(pi*t)     %F03
%Ft=0.5*t.*sin(t);                   %------Ft1
%Ft=Ufunct(t-8);                        %------Ft2
%f=zeros(nti,ntj); g=-ones(nti,ntj);            %------Ft3
%for k=0:2000, g=-1*g; f=f+g.*Ufunct(t-2*k); end
%Ft=2*f;

%-------------------------------------------------------
function y=Ufunct(x)
[nxi,nxj]=size(x); y=zeros(nxi,nxj);
for ki=1:nxi
    for kj=1:nxj
        if(x(ki,kj)<0), y(ki,kj)=0; end
        if(x(ki,kj)==0), y(ki,kj)=0.5; end
        if(x(ki,kj)>0), y(ki,kj)=1.; end
    end
```

```
end

%-------------------------------------------------------
function g=Fourier(Kz,Y)
N=size(Y,1);
Xci=zeros(N,1)+i*zeros(N,1); g=Xci;
Xc=zeros(N,1); Xs=zeros(N,1);

if(Kz==1), Y=Y/N; end
N2=N/2; N1=N-1; J=0;
for k=0:N1-1
    if k<J
        B=Y(k+1);Y(k+1)=Y(J+1);Y(J+1)=B;
    end
    Kn=N2;
    while (J>=Kn)
        J=J-Kn; Kn=Kn/2;
    end
    J=J+Kn;
end
Xc=real(Y); Xs=imag(Y);

Dm=log2(N); M=Dm;
PI=4.0*atan(1.0);  NN=1;
for L=1:M
    K=NN;  NN=NN*2;  C=1.; S=0.; D=PI/K;
    S0=sin(D); C0=double(1.)-cos(D); D0=-double(2.)*C0;
    for jj=0:K-1
        for ii=jj+1:NN:N
            I1=ii+K;
            Tc=Xc(I1)*C+Xs(I1)*S;
            Ts=Xs(I1)*C-Xc(I1)*S;
            Xc(I1)=Xc(ii)-Tc; Xs(I1)=Xs(ii)-Ts;
            Xc(ii)=Xc(ii)+Tc; Xs(ii)=Xs(ii)+Ts;
        end
        C0=D0*C+C0; C=C+C0;
        S0=D0*S+S0; S=S+S0;
    end
end
Xci=Xc+i*Xs;
if Kz==-1
    for K=2:N2+1
        B=Xci(K); Xci(K)=Xci(N-K+2); Xci(N-K+2)=B;
    end
end
g=Xci;
```